

The University of Nottingham

UNITED KINGDOM · CHINA · MALAYSIA

Synthesis of 3-dimensional Scaffolds for Application in Medicinal Chemistry

Carolin Schwehm, Dipl.Chem.

submitted to The University of Nottingham for the degree of Doctor of Philosophy

October 2015

Declaration

This thesis is submitted to the University of Nottingham for my application of the degree of Doctor of Philosophy. Unless otherwise acknowledged the work presented has been composed by myself. It has not been submitted in any other application for any other degree at the University of Nottingham or any other institution.

The work presented has been carried out by me except for the cases outlined below:

- The biological screening against DPP-4/ DPP-8/ DPP-9 reported in chapter 4 was carried out at Hitgen/ China.
- The biological screening against $P2X_7$ reported in chapter 7 was conducted by Prof. Richard Evans at the University of Leicester.
- The screening against pi3K was carried out by James Rowidder at GSK Herts.



Carolin Schwehm

Contents

Declaration i

Abstract vi

Acknowledgements viii

Abbreviation x

1 Introduction 1

1.1 The ongoing search for new drug molecules 1

1.2 The Role of Privileged Structures in Medicinal Chemistry 6

1.3 Examples of known Privileged Structures 14

1.3.1 The classical pharmaceutical textbook example- a tricyclic diphenyl scaffolds 15

1.3.2 The biphenyl substructure- a Privileged Scaffold or only a "Frequent Hitter" . 15

1.3.3 Azo Heterocyclic Privileged Scaffolds 17

1.3.4 Oxygen containing Privileged Structures 19

1.3.5 Rhodanines: Privileged scaffold or promiscuous binder 20

1.3.6 A versatile privileged structural motif: 8- hydroxyquinoline 20

2 Aims and Objectives 26

3 Design and Synthesis of a novel tricyclic triazole-based scaffold 28

3.1 Synthesis of the [6.5.5] tricyclic scaffold 28

3.2 Synthesis of the [6.6.5] tricyclic system 36

3.3 Synthesis of [6.7.5] triazole scaffold 50

3.4 Synthesis of Heterocyclic second ring 52

3.5 Chiral synthesis of bicyclic compounds 55

3.6 Conformational analysis of newly synthesised tricyclic scaffold 67

4 Synthesis of new DPP-4 inhibitors based on a novel tricyclic scaffold 70

4.1 A global health issue: Diabetes mellitus and the role of DPP-4 70

4.2 DPP-4 inhibitors on the market 73

4.3 Docking studies in the DPP-4 active site 75

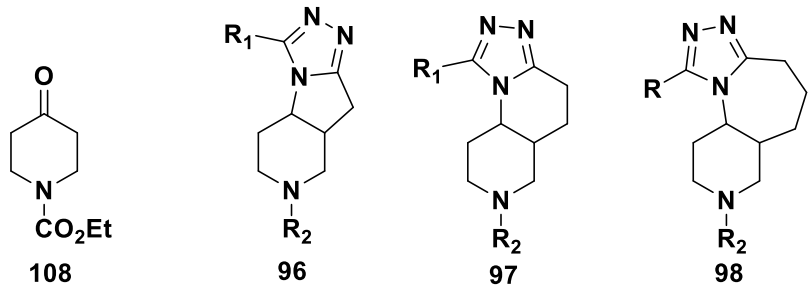
4.3.1 Docking of known marketed DPP-4 inhibitors....75
4.3.2 Docking of new Sitagliptin analogues in the DPP-4 active site....77
4.4 Synthesis of Sitagliptin Analogues....78
4.5 Enzyme inhibition by Sitagliptin analogues....84
4.5.1 Enzyme inhibition of DPP-4....84
4.5.2 Biological Screening against the enzymes DPP-8/DPP-9....85
4.6 SAR evaluation of synthesized Sitagliptin analogues....87
5 Maraviroc, a chemokine receptor (CCR-5) antagonist....91
5.1 HIV-a major global health problem....91
5.2 The chemokine receptor CCR-5 and its role in HIV....92
5.3 The chemokine receptor CXCR-4....94
5.4 The rationale behind the development of CCR-5 inhibitors....95
5.5 CXCR-4 tropism....96
5.6 Known CCR-5 receptor inhibitors....97
5.7 The Discovery of Maraviroc....99
5.7.1 The pharmacological profile of Maraviroc....100
5.8 Synthesis of Maraviroc analogues....101
5.8.1 Preliminary docking studies in the binding pocket of CCR-5....101
5.8.2 Synthesis of the amino acid part of Maraviroc....104
5.8.3 Coupling of the tricyclic triazole to the amino acid....107
5.9 Pharmacology Screen of new synthesized Maraviroc analogues....110
5.9.1 Screening against the chemokine receptor CXCR-4....110
5.9.2 Biological screen against chemokine receptor CCR-5....111
6 A versatile biological target-the PI3 kinase....116
6.1 Lung cancer, asthma and COPD....116
6.2 The target pi3 kinase- its biological role....117
6.2.1 Pi3 K α....118

6.2.2 Pi3K β 118
6.2.3 Pi3K γ 118
6.2.4 Pi3K δ 119
6.3 The selectivity profile towards pi3K δ 119
6.3.1 Docking in the pi3K δ active site 121
6.4 The rational for a new selective pi3K δ inhibitor 123
6.5 Synthesis of GDC-0941 analogues 124
6.6 Biological evaluation of new GDC-0941 analogues 126
6.6.1 Selectivity screen against pi3K α, pi3K β and pi3K γ 127
7 The purinoreceptor $P2X_7$ 129
7.1.1 Biological Background of $P2X_7$ 129
7.2 Known literature antagonists for the $P2X_7$ receptor 130
7.3 Synthesis and biological evaluation of new $P2X_7$ receptor antagonists 131
8 Conclusion 135
9 Future Studies 140
10 Experimental Part 143
10.1 Materials 143
10.1.1 Techniques 143
10.1.2 Chemical and solvents 143
10.1.3 Thin layer chromatography (TLC) 143
10.1.4 Flash Chromatography 143
10.2 Methods 144
10.2.1 Nuclear Magnetic resonance 144
10.2.2 Mass spectrometry 144
10.2.3 HPLC 144
10.3 Synthesis of [6.5.5] scaffold 145
10.4 Synthesis of [6.6.5] scaffold 151

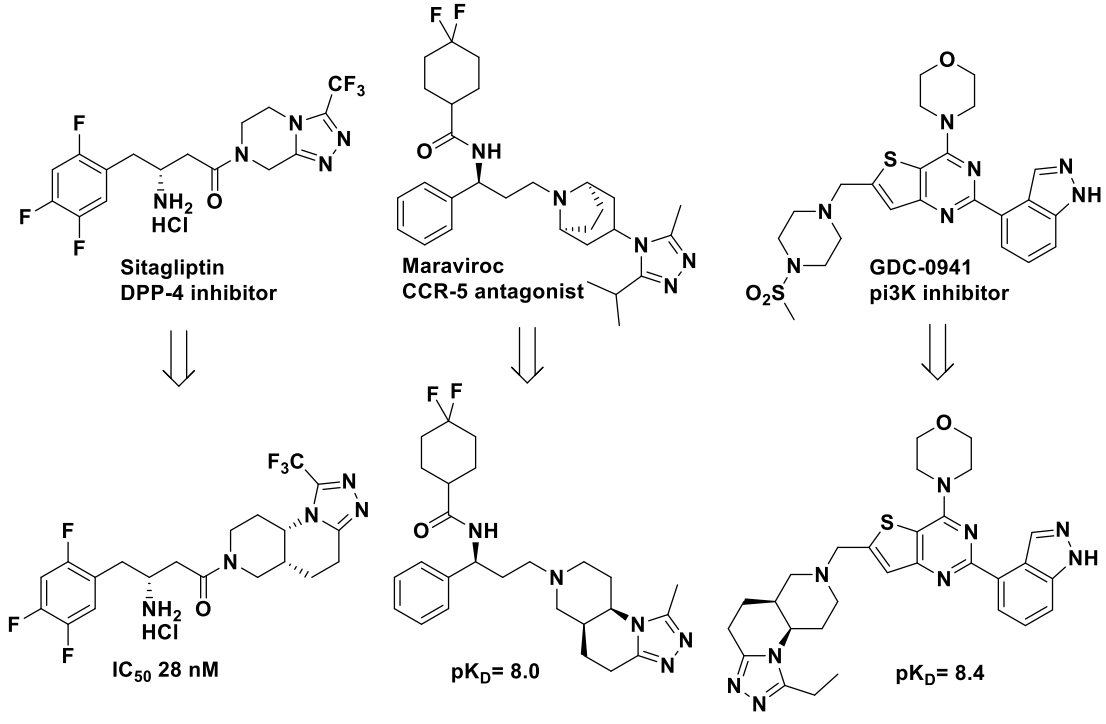
General procedure 1,2,4 triazole formation 157
General procedure for 1,2,4 triazole- amine formation deprotection of carbamate 165
10.5 Synthesis of [6.7.5] scaffold 170
10.6 Synthesis of heterocyclic scaffold 176
10.7 Synthesis of chiral [6.6.5] lactam system 178
10.8 Synthesis of Sitagliptin analogues 182
General procedure for amide coupling 182
General method for deprotection 192
10.9 Synthesis of Maraviroc analogues 207
10.10 Synthesis of pi3 Kinase inhibitors 215
General procedure for reductive amination 215
General procedure for Suzuki coupling 216
10.11 Synthesis of $P2X_7$ analogues 218
General Procedure for amide coupling 218
10.12 Pharmacology 220
10.12.1 General Material 220
10.12.2 Molecular cloning 221
10.12.3 Transformation of bacterial cells 221
10.12.4 Cell lines used 222
10.12.5 General cell culture 222
10.12.6 Passaging of cells 222
10.12.7 Generation of CCR-5 stable cell line 223
10.12.8 Seeding of cells 224
10.12.9 Assays 225
10.12.10 Data analysis 226
10.13 Molecular Docking studies 227
12 References 230

Abstract

In this thesis the successful synthesis of a novel tricyclic scaffold containing a ring fused triazole and piperidine will be discussed and furthermore its utility as a new potential privileged structure will be evaluated.

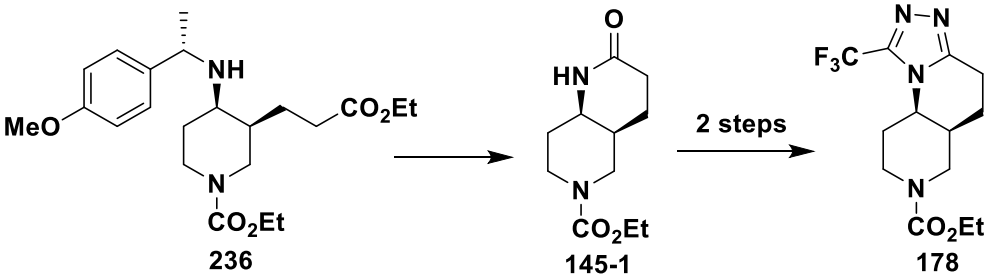


As starting material for the synthesis of the considered scaffolds the commercially available ethyl 4-oxopiperidine-1-carboxylate **108** was used. Piperidone **108** was converted into scaffolds **96**, **97** and **98** alternating the ring size (n=1, 2, 3) of the fused bicyclic ring. This tricyclic triazole scaffold was incorporated into known biologically active molecules (Sitaglitpin, a DPP-4 inhibitor, Maraviroc, a CCR-5 receptor antagonist and GDC-0941, a pi3K inhibitor) to test its potential to serve as a new possible Privileged Scaffold. Through scaffold hopping, analogues with excellent biological activity against the chosen biological targets were achieved.



Abstract

Additionally, the stereoselective synthesis of one of the four possible isomers of the tricyclic triazole **178** was obtained in 4 steps to give the synthetically access towards the synthesis of all feasible enantiomeric and diastereomeric analogues.



Acknowledgements

I would like to thank my supervisors Prof. Barrie Kellam and Dr. Michael Stocks for their support and input throughout these last three years. I am very thankful for their guidance and patience throughout this PhD project and for their continuous advice and suggestions to the successfulness of this thesis and to enable me to acquire multidisciplinary skills.

Furthermore, I would like to thank Prof. Steve Hill to give me the opportunity to work in his group to learn how to carry out my own pharmacology. Special thanks I would like to say to Dr. Leigh Stoddart for her guidance and support for accomplishing the pharmacological part of this PhD project.

I would like to thank Dr. Simon Hirst and Stephanie Barlow at SygnatureDiscovery for their help and to give me the opportunity for carrying out my chiral HPLC analysis in their labs in BioCity. Thanks, I would like to say to Prof. Richard Evans and Rebecca C. Allsop at the University of Leicester for the collaboration in the $P2X_7$ project. I would like to thank Dr. Simon MacDonald and James Rowidder at GSK for screening compounds against pi3 K. Furthermore, I would like to thank Shazad Aslam for helping me with running the NMRs of my final compounds and Huw Williams for his support using the chiral shift reagent approach. I would like to thank Dr. William Lewis for carrying out the X-ray crystallography experiments.

I would like to thank the University of Nottingham for funding.

I am very grateful to all the people who helped me to accomplish this work and to my lab colleagues in C25 and C22- Francesca Citossi, Dr. Sarah Mistry, Dr. Shailesh Mistry, Kathryn Skilling, Dr. Andrea Vernall and Dr. Fabio Rui and the people in ICS- especially to Marleen Groenen, Dr. Laura Kilpatrick and Dr. Leigh Stoddart. A big thank you I would like to say to my favorite Italians Francesca Citossi and Dario Leonardo Balacco, who were always there in the last years with a helping hand and a nice Italian discussion ☺ Another special thanks I would like to say to my family Mistry, who always adopted me in the last six weeks without any complaint- I am very grateful for your help.

Acknowledgements

A special thank you I would like to say to my friends Catha and Karla for their support by making this difficult decision and their friendship over so many years over such big distances.

I am deeply thankful to Christian, who always helped me to keep my head up and to look forward. I am thankful to his big support for all my decisions and his big patience for all my new ideas.

Zum Schluss möchte ich einen ganz besonderen Dank an meine Familie aussprechen, vorallem meiner Mutter Christiane. Gerda, Erich und Jochen moechte ich auch danken fuer ihre Hilfbereitschaft und ihrer Teilnahme an meinem Leben. Meiner Mutter möchte ich fuer Ihre grosse Unterstützung danken in allen meinen Entscheidungen, auch wenn diese nicht immer ganz einleuchtend erschienen. Ich möchte ihr danken fuer Ihr Verständnis vorallem fuer meine Entscheidung nach England zu gehen und dass sie mir durchweg zur Seite stand während meines gesamten Studiums und meiner Doktorarbeit.

Abbreviation

A	Angstrom
AcN	acetonitrile
AcOH	acetic acid
ADME	absorption, distribution, metabolism, excretion
AIDS	acquired immunodeficiency syndrome
AMC	7-amino-4-methyl coumarin
ARV	antiretroviral drugs
ART	antiretroviral therapy
ATP	adenosine triphosphate
AV	anti-viral activity
BINAP	(2,2'-bis(diphenylphosphino)-1,1'binaphtyl)
BMS	borane dimethylsulfide
Bn	benzyl
bp	base-pair
BPT	biphenyltetrazole
BzATP	2,3-(benzoyl-4-benzoyl)-ATP
°C	degree Celsius
cAMP	cyclic adenosin mono phosphate
CAN	Ammonium cerium(IV) nitrate
Cbz	carboxybenzyl
CCK	cholecystokinin
CCR-5	CC chemokine receptor 5
CD4	cluster of differentiation 4
CD8	cluster of differentiation 8
$CDCl_3$	deuterated chloroform
conc.	Concentration
COPD	chronic obstructive pulmonary disease
COSY	correlation spectroscopy
CYP	cytochrome
CXCR-4	CXC chemokine receptor 4
δ	chemical shift
d	day(s)
DAST	dimethylamino sulfurtrifluoride
DCE	1,2 dichloroethane
DCM	dichloromethane
DDQ	2,3-Dichloro-5,6-dicyano-*p*-benzoquinone
DEA	diethylamine
DIBAL-H	diisobutylaluminiumhydride
DIPEA	diisopropylethylamine
DMAP	dimethylaminopyridine
DMB	3,4-dimethoxybenzyl
DMF	dimethylformamide
DMPK	Drug Metabolism and Pharmacokinetics
DMPU	1,3-dimethyl-3,4,5,6-tetrahydro-2(1*H*)-pyrimidinone
DMSO	dimethyl sulfoxide
DPP-4	Dipeptidyl peptidase 4
EA	ethyl acetate

Abbreviation

ECL	extracellular loop
EDCI	1-ethyl-3-(3-dimethylaminopropyl)carbodiimide
Ee	*enantiomeric excess*
Et	ethyl
Et al.	and others
EtOH	ethanol
eq.	equivalents
FDA	Food and Drug Administration
FMMH	five membered multiple ring
FRET	fluorescence resonance energy transfer
FSK	forskolin
GIP	glucose dependent insulinotropic peptide
GLP-1	glycagon-like protein 1
GPCR	G protein coupled receptor
gp120	glycoprotein120
g	gram
h	hour
HAART	highly active antiretroviral therapy
Hal	halogen
HATU	O-(7-azabenzotriazol-1-yl)-N,N,N′,N′-tetramethyluronium hexafluorophosphate
HBTU	*O*-(Benzotriazol-1-yl)-*N,N,N′,N′*-tetramethyluronium hexafluorophosphate
HCl	hydrochloric acid
HEK	human embryonic kidney
hERG	human *ether a- go-go* related gene
Het	heterocyclic
Hz	hertz
HIV	human immunodeficiency virus
HMPT	Hexamethylphosphoramide
HOBt	hydroxybenzotriazole
HPLC	high performance liquid chromatography
HQ	hydroxyquinoline
HSQC	Heteronuclear single quantum correlation
HTS	High throughput screening
IL-1β	interleukin 1-β
IP_3	inositol phosphate
i-PrOH	*iso* propanol
i-Pr	*iso* propyl
K_D	dissociation constant
$KMnO_4$	potassiumpermanganate
KOH	potassium hydroxide
LCMS	Liquid chromatography-mass spectrometrie
LDA	Lithiumdiisopropylamine
LiCl	lithiumchloride
LQTS	long QT syndrome
M	Molar
Me	methyl
MeOH	methanol
MHz	Megahertz
MWt	molecular weight

Abbreviation

mL	millilitre
min	minutes
(^{125}I-)MIP-1β	(^{125}I)-macrophage inflammatory protein 1β
mol	Mol
MS	mass spectrometry
n	repetition numbers
N	normal
NaH	sodium hydride
n-BuLi	*n*-butyllithium
NBS	N-bromosuccinimide
NEt_3	triethylamine
NMR	nuclear magnetic resonance
NOESY	Nuclear Overhauser Effect Spectroscopy
NRTI	nucleoside reverse transcriptase inhibitor
NNRTI	non-nucleaoside reverse transcriptase inhibitor
OIDD	open innovation drug discovery
o.n.	overnight
$P2X_7$	purinoceptor
PAINS	pan assay interference compounds
Pdb	protein database
PE	petrolether
Pi3K	phosphoinostitol kinase 3
PG	protecting group
PMA	phosphormolybdic acid
PMB	*para*-methoxybenzyl
Ph	phenyl
$POCl_3$	phosphoroxytrichloride
PPA	polyphosphoric acid
ppm	parts per million
PSA	polar surface area
R	receptor
RANTES	regulated on activation normal T cell expressed and secreted
RAMP	(*R*)-1-amino-2-methoxymethylpyrrolidine
rac	racemic
Ref.	reference
R_f	retention factor
rf	reflux
rt	room temperature
SAMP	(S)-1-amino-2-methoxymethylpyrrolidine
SAR	structure activity relationship
SDF-1α	stromal cell-derived factor1
TB	tuberculosis
*t*Bu	*tert* butanol
TFA	trifluoroacetic acid
THF	tetrahydrofuran
TLC	thin layer chromatography
TM	trans membrane
TOS	target oriented synthesis
p-TsOH	*para* toluenesulfonic acid
UTP	uridine triphosphate

Abbreviation

UV	Ultraviolet
WHO	world health organisation

1 Introduction

1.1 The ongoing search for new drug molecules

The drug discovery process involves the ongoing search for methods to make the identification of new lead compounds as straightforward as possible. This process, established over the last century, follows a similar procedure common to most Pharma organisations (figure 1) before obtaining an appropriate lead compound which can be further optimized to give a clinical candidate.[1]



Figure 1 Timeline of the Drug Discovery Process starting with Target Discovery up to Market Registration

The first stage of the drug discovery process is the identification of a medical need and the disease and drug target associated with it, which has to be examined to become aware of all the possible therapeutic indications of this drug target.[2] In the past this process was carried out by first recognising the active drug followed by the drug target itself, which then had to be identified and analysed. The whole process was driven by a hit and miss affair rather than a rationale-driven application. Nowadays, the process starts with targeting the drug molecule for a specific organ or receptor. The rationale behind this approach is the importance to minimise the side effects outside the chosen biological target.

The first step in the target validation phase is to identify a suitable bioassay, which should be carried out *in vitro* as well as at a later stage *in vivo*. *In vitro* tests are preferred over *in vivo* tests due to the combination of cost relationship and the simplicity for performing the assay as they can often be automated. However *in vivo* tests are always essential to identify the potential drug interactions. *In vitro* screening can involve cell-based assays, enzymes or

specific tissues; where as *in vivo* tests are carried out with animals.[3] This is followed by the most crucial step for a medicinal chemist as it involves the discovery of the actual lead compounds, seeding the whole drug discovery process. Therefore different approaches to accomplish the discovery of a new lead compound were developed over recent decades. Especially, the introduction of computer based methods was developed, which allowed the prediction of the usefulness and successfulness of new lead compounds dramatically decreasing the number of screening experiments. Following these approaches lead to an effective search of compounds and an enormous cost reduction through minimizing the number of lab-based experiments.[4]

High throughput screening (HTS) is one of the major methods for finding new lead molecules in the drug discovery process.[5] In the 1990s the era of high throughput screening started and the design of new compound libraries became a big challenge for medicinal chemists. This novel screening involves a large number of compounds, which are screened against a large number of targets. One starting point for the designed compounds was the Lipinski rule of five, which is the ground breaking rule established in medicinal chemistry by the group of Lipinski. This rule is based on collected physiochemical properties of the drug compounds recommending that new drug compounds should have a maximum of 5 donor points, 10 H-bond acceptors, a molecular weight less than 500 and the clogP smaller than 5.[6] Regarding the HTS, a commentary by Maccarron in 2011 confronts the criticism against the quality of HTS with the actual accomplishments.[7] The myth that no actual drug compounds are discovered by HTS was refuted through listing the marketed drugs which came out through a discovered lead compound based on this technology (figure 2). One prominent example is the discovery of the CCR-5 entry inhibitor Maraviroc **2** launched by Pfizer in 2006, which was accomplished starting with the HTS lead compound UK-105,543 **1**.[8]

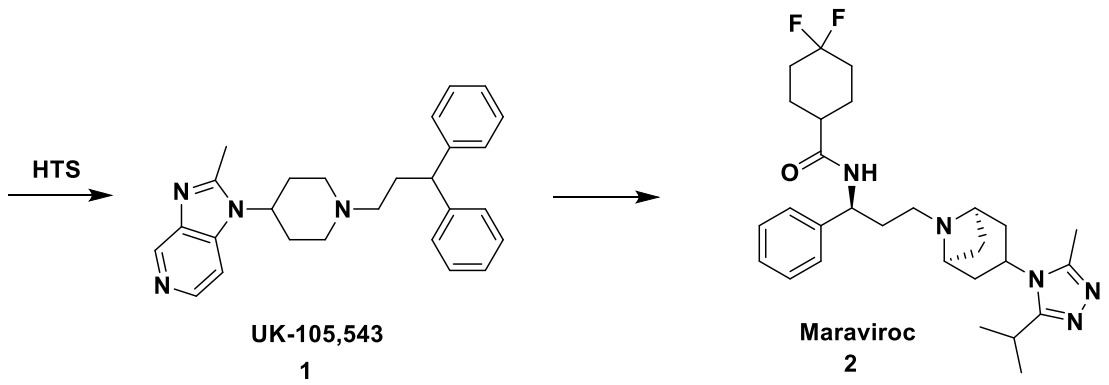


Figure 2 Example of the discovery of a drug compound after HTS: Maraviroc (**2**)

Introduction

Over the last 10 years compound libraries for HTS from large pharmaceutical companies have grown mainly due to new synthetic chemistry methods, such as combinatorial chemistry[9] or parallel synthesis[10] which accelerated the growth (figure 3) of the compound libraries enormously. This unfortunately did not achieve the considered effect in finding new lead compounds, but implicated the problem that these libraries are often not suitable anymore for new drug targets e.g. new enzymes or emerging protein-protein interactions.

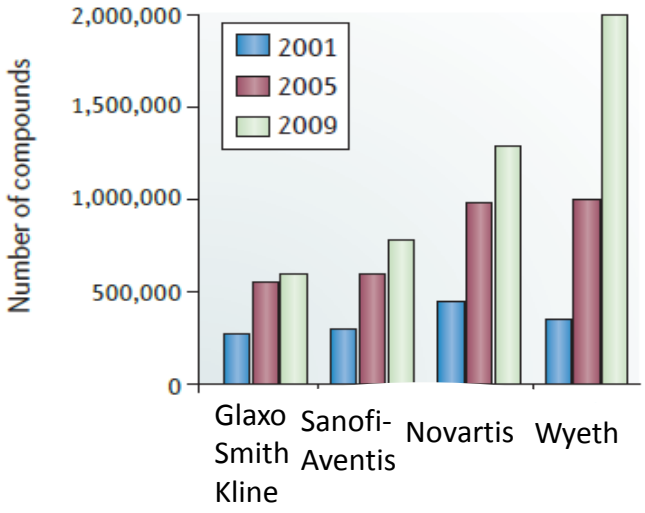


Figure 3 Growing compound numbers in HTS library in four important pharma companies, adapted from Macarron *et al*., Nature.com, 2010.

Another approach to find new lead compounds is the so-called fragment based drug discovery, which evolved over the last decade and is considered as one of the follow up methods after HTS. These so called "fragments" are initially selected considering their affinity or inhibitory effect towards a chosen target, which can later be combined to what is considered as "normal" lead compounds.[11] Therefore the fragment-based drug discovery approach on known targets can improve the affinity and selectivity of compounds for the investigated biological target. The establishment of these fragment based libraries was proposed to follow a rule of three[12] (MWT < 300, cLogP < 3, number of H-bond donors < 3, number of H-bond acceptors < 3) compared to the Lipinski rule of five and different approaches for fragment-based libraries were made including SHAPES and retrosynthetic combinatorial analysis procedure (RECAP).[13] In this context libraries with so-called privileged structures were proposed. All attempts were based on NMR, X-ray-crystallographic, high- concentration functional binding assays or mass spectrometry approaches.[14] The main challenge is the conversion of the fragments into a lead compound, which can be accomplished through fragment optimisation, fragment linking and *in situ*

fragment assembling. One representative example for fragment optimization is shown in the development of compounds targeting the Jun N-terminal kinase 3 (JNK 3) (figure 4), which was carried out by Vertex where they screened their SHAPES library using NMR-based methods. The initially detected fragments were further analysed through competition binding in the ATP pocket of JNK3 and docking studies to yield fragments which could be further explored by introducing new groups to build the actual lead compounds.[15]

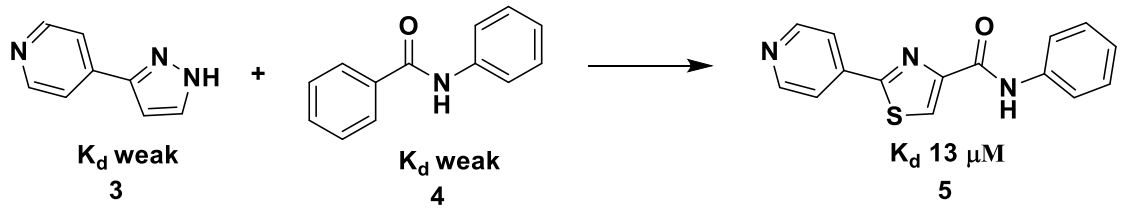


Figure 4 Fragment based drug discovery- fragment optimisation approach on the example of JNK-3

The fragment linking or merging approach is another method used to convert the fragments into lead compounds, which follows a similar principle than the optimization approach by combining two fragments to the new lead compound (figure 5). This example represents the linking approach demonstrated on the FK506 binding protein, which was achieved through linking the two fragments **6** and **7** with a small linker to yield compound **8** resulting in a compound with a K_D in the nanomolar range.[16]

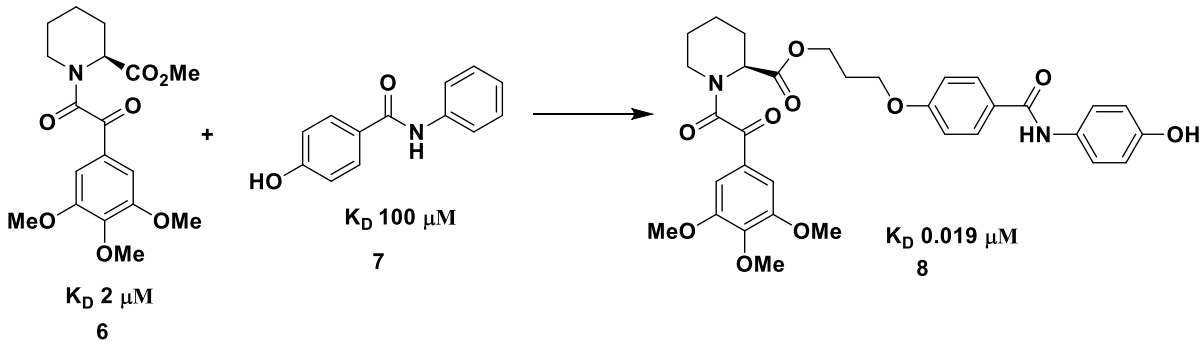


Figure 5 Fragment linking approach on the example of FK506 binding protein

In the *in situ* fragment assembly approach, the fragments individually bound to the target protein can undergo a chemical reaction to generate a compound resulting in a higher affinity. In this example (figure 6) the self-assembly approach is shown to derivative compounds of the famous neuramidase inhibitor Tamiflu (**12**) marketed by Roche which is used for the treatment of influenza.

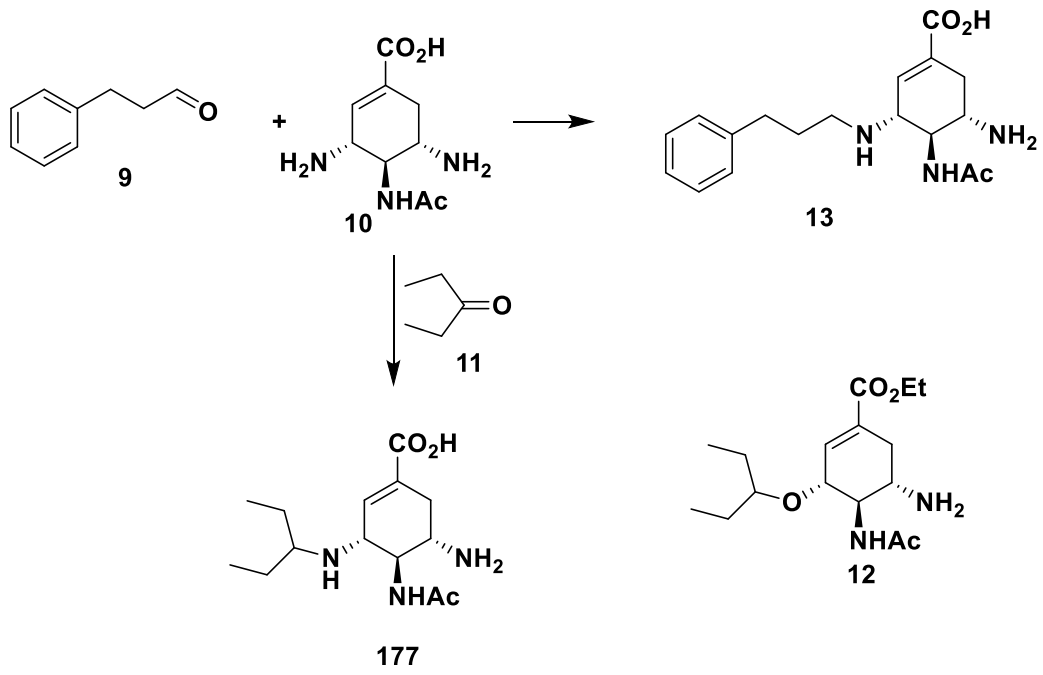


Figure 6 Fragment self-assembly through neuroamidase on the example of derivatives of Tamiflu **12**[17]

Chemogenomics is one relatively novel approach used to find new leads for new drug molecules.[18] In medicinal chemistry the phrase chemogenomics is related to a search which is aligned according to the target families rather than to a specific disease. This approach is directly related to a search for recognizable motifs which are lead structures for new biologically active compounds. The main advantages of such an approach are the know-how for a specific target class, knowledge about the mechanism of action and for example established binding modes. It is driven through a similarity orientated search, which means that the starting point is from a known biologically active compound or drug. In 2007 Klabunde evaluates the word similarity in this context and describes the criteria for a receptor or a ligand to be considered as similar.[19] The key point of the chemogenomics approach is the new procedure to rather group receptors in different common classes than to account them as individuals, for examples ion channels, G protein-coupled receptors (GPCRs) or kinases. Rognan considered in his review that the two basic assumptions for a chemogenomics approach are that compounds with chemical similarity should share the same target and as well, that targets which have similar ligands should have similar binding sites. The main difficulties are to measure or to estimate these described similarities and to find appropriate descriptors. In the review by Rognan theses descriptors are classified in different dimensions e.g. using one-dimensional descriptors such as molecular weight or atom number.[20] These descriptors are used preferably for predictions of absportion, distribution, metabolism and excretion (ADME) properties like bioavailability or solubility.[21] The most popular

comparisons using 1-D descriptor is the so-called SMILES (simplified molecular input line entry system) approach introduced by Weininger.[22] SMILES is considered to represent a facile computer language approach as an easily understood chemical language for chemists and demonstrated feasibility and utility for calculation of partition coefficients and molecular refractory in model systems, which can be furthermore applied for quantitative structure activity studies. The 2D descriptors are defined by characteristics such as the fragment or the substructure.[20] The fingerprint method is a common starting point for identifying reoccurring structural motifs. Data as atom coordinates or 3D pharmacophores are related to the 3D descriptors to search for new lead compounds in the drug discovery process. 3D information provides guidance around features such as hydrogen bond acceptors, -donors or ionisable atoms. To identify the space which is available in the target domain the most insightful attempt is the analysis of the 3D structures through X-ray crystallography or NMR studies with the focus on the ligand-binding site where the structural similarities are the most common. The term "Privileged Scaffolds" refers to such structural motifs, which are based on a similarity approach and are considered to function as useful starting points for new lead compounds by changing the functionality around the privileged structural motif.

1.2 The Role of Privileged Structures in Medicinal Chemistry

As mentioned in section 1.1, small molecules are powerful tools in the drug discovery process, but the process of building new libraries with useful molecules often remains a serendipitous approach.[23] Reaching the understanding of all necessary features of a new lead compound is still ongoing and therefore new approaches are under continuous investigation. One approach is to focus on a similarity principle, which includes the synthesis of new "Privileged Scaffolds". The term "Privileged Structure" was introduced by Evans *et al*. in their research around 1,4- benzodiazepines and finding that this scaffold served as a ligand for various biological targets (figure 7).[24]

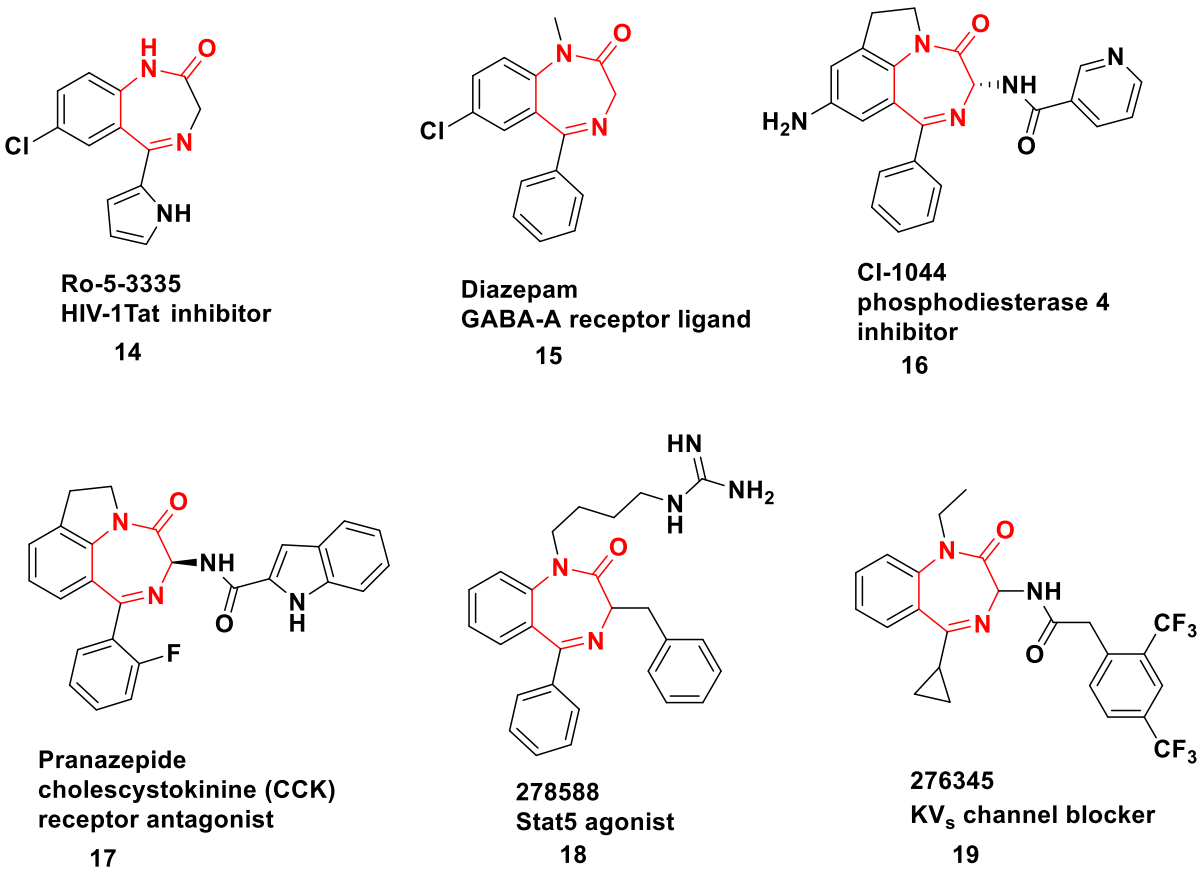


Figure 7 Drug molecules containing the benzodiazepine privileged scaffold

In their study they described the design and synthesis of novel antagonists of CCK, cholecystokinin, which is a peptide hormone of the gastrointestinal system. In their series of benzodiazepine analogues 3-acylamino compounds showed a greater (100-1000x) affinity to the CCK-A receptor than their previous reported 3-alkyl compounds (figure 8).[25] Several benzodiazepine analogues, which differ in their substitution pattern, constitution or functionality, were compared against their selectivity for either the CCK-A, CCK-B, gastrin or brain benzodiazepine-receptor. During these studies a "similarity" has been found between compound **20** reported in their search and the natural peptide CCK-7 even if this similarity is not related to its structure. Furthermore it was stated that the known benzodiazepine, Tifluodam **22** showed high affinity for the opiate receptor as well as a significant affinity for the CCK-A receptor. This lead to the first assumption that this 5-phenyl-1,4 benzodiazepine ring systems and similar examples of such molecular frameworks can serve as ligands for different receptors. In their conclusion a new approach for the drug discovery process was found considering a structural framework like the benzodiazepines as a privileged structure because of their nature to serve as a useful ligand for more than one receptor. With this statement Evans *et al.* introduced for the first time this new concept of "Privileged

Scaffolds", which could provide useful tools in the ongoing search of new drug molecules as they can provide a starting point for new agonists or antagonist for a variety of receptors.

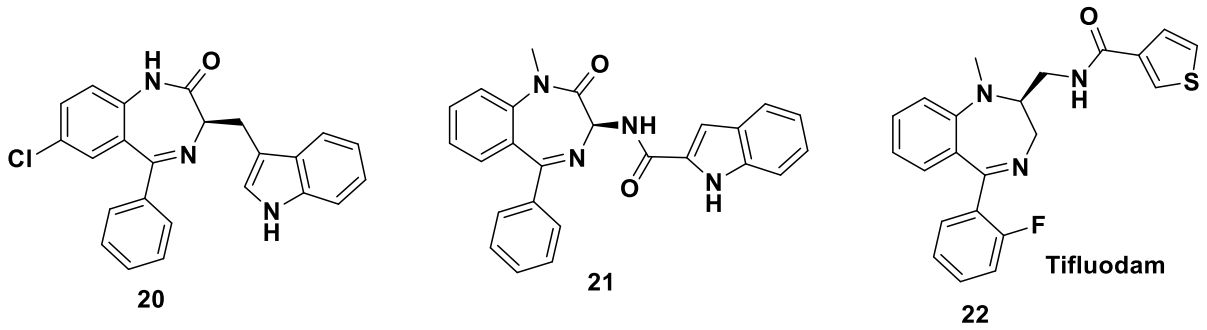


Figure 8 Examples **20** and **21** from the original statement from Evans about privileged Sctructures. Tifluodam (**22**) represents another benzodiazepine, which can serve as a ligand for more than one receptor.

Privileged structures are an important and growing topic in medicinal chemistry as they are considered as a useful concept for the design of new lead compounds for the drug discovery process. In a review about Privileged Structures in drug discovery by DeSimone in 2004 it was stated that in an analysis by the group of Murko using known drug molecules it was found that, out of the approximately 5000 drug compounds, 1100 different frameworks existed. Furthermore it was pointed out that 32 of these frameworks are found in around 50% of the drug molecules.[26] The definition of a privileged structure according to Klabunde and Hessler is a "substructure/scaffold exhibiting strong preferences for a particular area of the target space".[27] The main focus in medicinal chemistry is to design, discover and synthesise new biological active molecules as well as the analysis of the factors involved in the structure activity relationship including interpretation of the molecular recognition of the drug.[28] Understanding of the pharmacokinetics, especially absorption, distribution, metabolism, excretion and toxicity (ADMET) of a drug is of great importance in medicinal chemistry. In a review by Liu *et al*. in 2011 they investigated the corresponding ADMET data related to popular known bicyclic privileged structural motifs.[29] In conclusion they pointed out that the key factors related to the effect of absorption and metabolism are the ALogP, hydrogen donors, the polar surface area (PSA) as well as fraction of the polar surface area in respect to the total surface area (FPSA) and the number of chains assembled (Nc). The new concept of the privileged structures has had a significant impact in the development in Medicinal Chemistry, which is well illustrated by the growing number of literature articles dealing with this new concept of privileged structures. A privileged structure is not only a scaffold; it has to have a certain grade of functionalization to be considered as privileged.

But what makes a structure a "privileged scaffold"? What are the characteristic features of a privileged structure? How is a privileged structure defined and what makes it privileged?

Muller *et al.* revealed a statement in their discussion about privileged scaffolds, that this term belongs to sub-structural elements of compounds "that showed effect on more than one receptor" indifferent from the target family, which is the actual definition made by Evans *et al.*[30] Therefore the question arises how the difference between a frequent hitter and a privileged structure can be distinguished and is up to date an ongoing discussion with many attempts to clarify. For example studies for releasing reoccurring structural motifs compared to their *in silico* profile to directly target the molecular diversity space.[31] This was the starting point for finding these privileged structures in known biologically active molecules. One example is the 2- aminothiazole core structural motif which is reoccurring in several biological active molecules for clinical as well as preclinical drug candidates.[30]

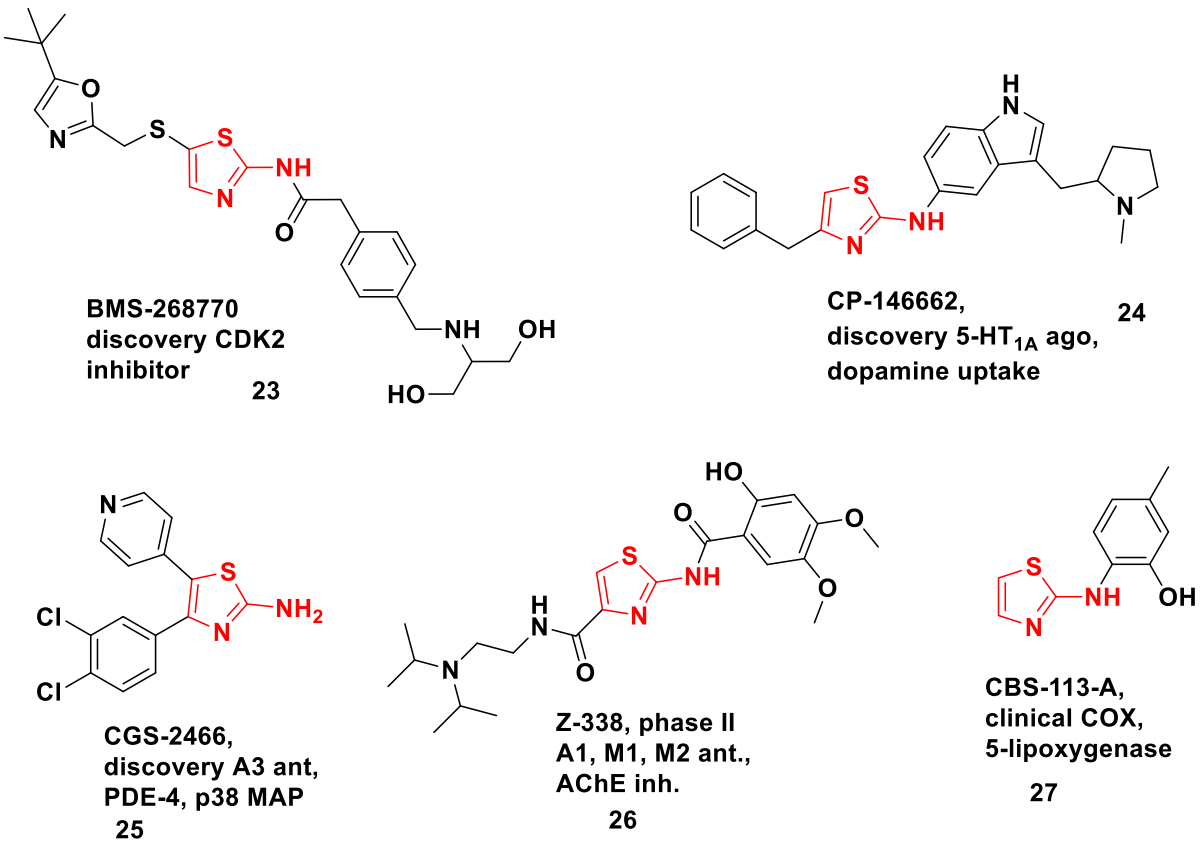


Figure 9 Biological active molecules containing the 2-aminothiazole scaffold

This 2-aminothiazole scaffold (red) (figure 9), which serves as a privileged scaffold, showed no evidence in only being active in one target family- its activity ranges from enzymes to GPCRs. In a recent paper by Gharbia *et al.* the 2-aminothiazole privilege structure was used

to find new antimicrobials targeting methicillin resistant *Straphylococcus aureus* (MRSA).[32] Their approach was based on using this known 2-aminothiazole structural motif as starting point for a new potential antimicrobial as it was seen to be successful over the last decades especially for targeting GPCRs.[33] They chose for their studies the 2-aminothiazole scaffold as it is known to reveal, amongst others, antibacterial activity.[34] In their screening assay they found promising compounds as new leads against MRSA strains, which proved the utility of a known privileged structure to be a good starting point for new lead compounds. In a review by Bondensgaard *et al*. they examined the potential of several class A family GPCRs to recognize a privileged structure motif.[35] As the GPCR family represents the largest biological target class[36] it is obvious to examine its reoccurring privileged structural motifs as it would have a major benefit to identify those privileged structure as potential starting points for targeting several GPCRs. One example for such an approach was the discovery of new ligands targeting the growth hormone secretagogue receptors starting from compounds discovered by other receptor screening programs (figure 10).[37] In their study to find new growth hormone (GH) secretagogues the starting point was the known compound **28**, where the incorporated spiropiperidine region represents a privileged structure as it functions as a ligand both for oxytocin and sigma receptors. Using this approach, they discovered their lead compound **29** by modifications of compound **28**.

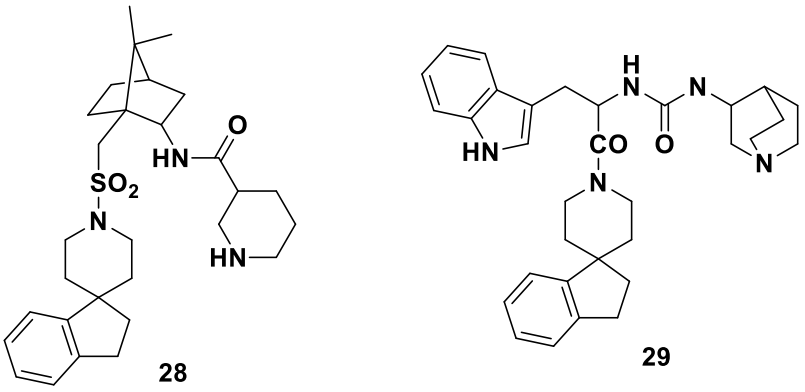


Figure 10 Example to start with a known privileged structure **28** to build a new lead compound **29**

A rational behind these reoccurring structural motifs is that the GPCRs are considered to have a common binding pocket feature which can be recognized by these privileged scaffolds. This hypothesis was investigated through analysis of pairs of privileged structures containing ligands towards different receptors regarding their binding mode. Bondensgaard *et al.* examined in their study several privileged structures targeting different GPCR receptor types

for example spiro piperidine indane analogues **32-33** and the 2-phenyl indole containing compounds **30-31** (figure 11).[35]

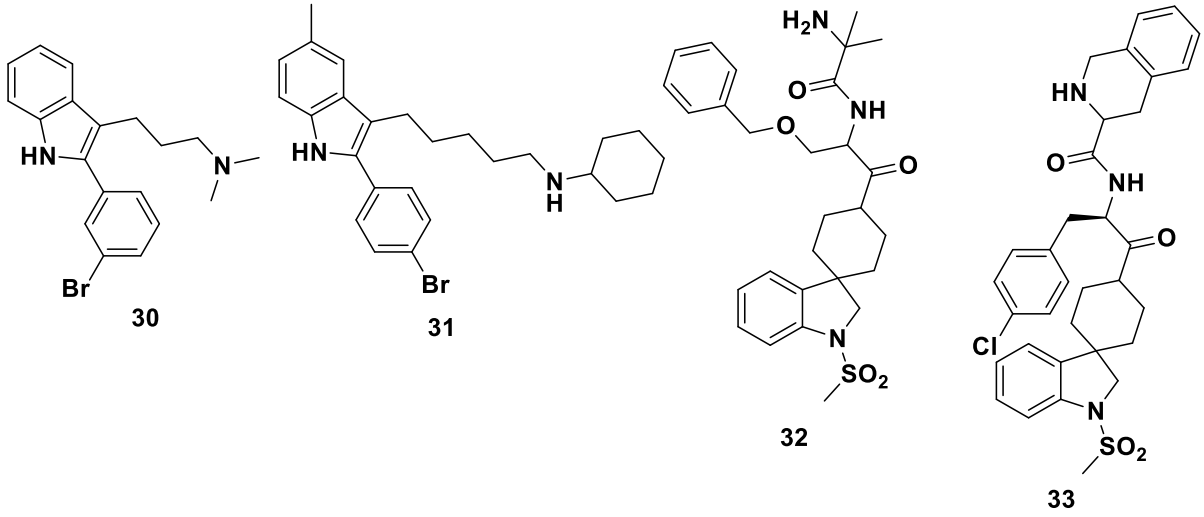


Figure 11 Structural motifs of two Privileged Structures incorporated in molecules targeting various GPCRs

Analogue **30** is a known 5HT6 inhibitor and compound **31** is targeting the MC4 receptor, both consisting of the 2 phenyl indole privileged structure. For the analysis both compounds were docked into a model of its corresponding target receptor (figure 12).

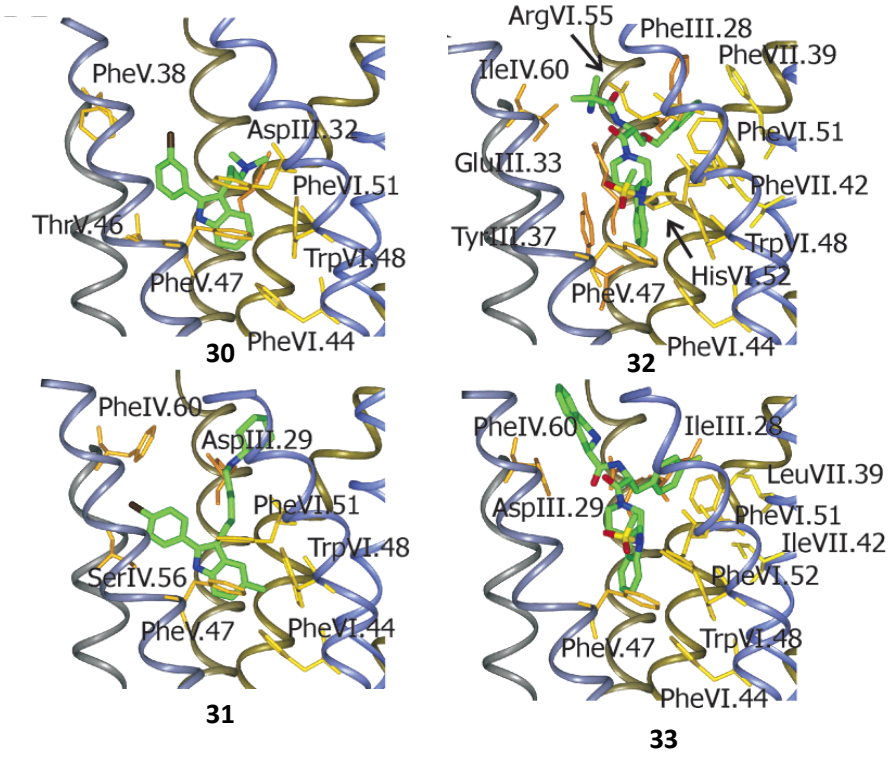


Figure 12 Analysis of the docking pose of compounds **30-33** in the corresponding GPCR binding pocket adapted from Bondensgaard *et al.* (Ref 35)

In both receptors the indole fits well in the binding pocket forming interactions with Phe V47, Phe VI 44 and Trp VI 48. In both compounds the aromatic part and the alkyl chain are pointing in the same directions within the active pocket of the receptors, which results in the same interactions and fittings in their binding pockets. Regarding the ligands bearing the spiro-piperidine-indane privileged structure motif (**32-33**) a similar docking pattern is detectable, where this moiety interacts with Phe V47, Phe V44 and Trp VI48. In most of the GPCRs the ligand binding pocket lies between the trans- membrane (TM) 3, 5, 6 and 7, which was revealed through mutagenesis studies and is a common feature.[38] Their study showed that all the docked privileged scaffolds are situated into the same region of the receptor; however some sub-pockets can only accommodate parts of a scaffold, which is the limiting factor for a privileged structure targeting the complete GPCR class A family. Nevertheless their hypothesis can aid to design new GPCR receptor agonists or antagonists for future medicinal chemistry projects. A review by Schnur et al. deals with the question if target family substructures are really privileged.[39] The rationale behind finding these so called privileged scaffolds is that they are considered to provide a more reliable starting point for new compounds in the given target family as described previous for the growth hormone segregatogues. They should include the major advantage to minimize the off target effect. In the review by Schnur *et al.* several target family classes were studied using different substructures mainly derived from GPCR databases to examine their occurrence for other target classes. As target families for example of GPCRs and ion channels are relatively similar in their structure not many of the investigated substructures were privileged for its considered target class, which could result in undesired off target effects. On the good side, the same substructures can serve for libraries to screen a variety of different targets, which results in considering the term privileged structure as Evans and Patchett described it in their early discovery.[40] Nevertheless, a substructure can be converted to a privileged structure only targeting one target family showing in the example in figure 13.

A further approach using privileged scaffolds in the design of new lead compound is the so called 4-Point Pharmacophore model. In their research towards a new method to design combinatorial libraries Mason *et al*. introduced the 4-point pharmacophore model using privileged scaffolds as starting point for library synthesis.[41] Their approach was based on known GPCR privileged structural motifs and described a novel modification of the 4-point pharmacophore model to force one point of the pharmacophore model to be associated with the privileged structure, which allows the design of new chemical libraries (figure 14).

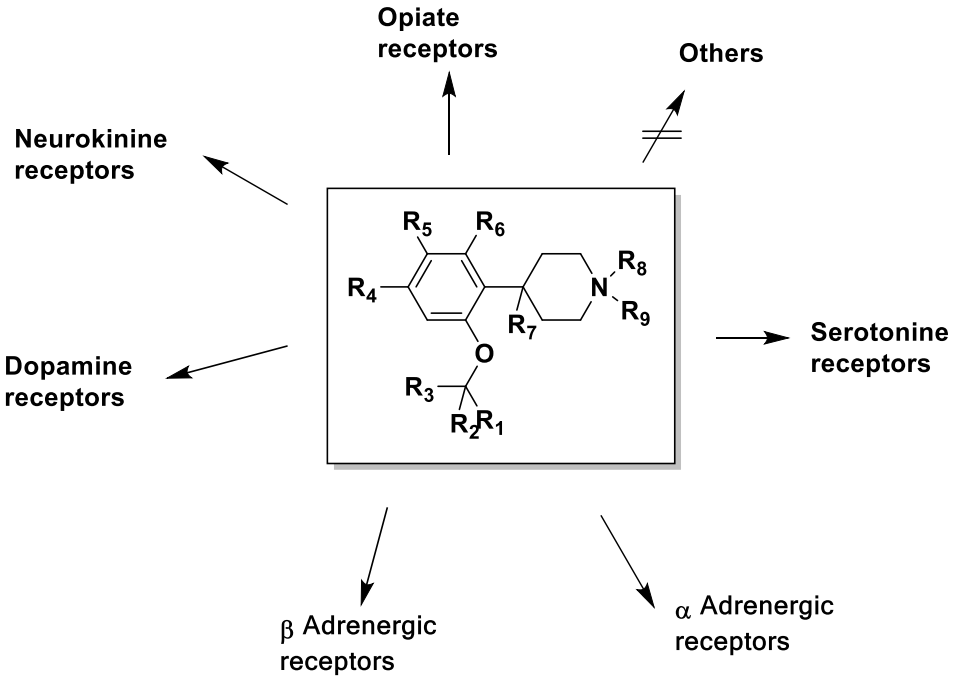


Figure 13 An example of a Privileged Scaffold which shows activity only in one target family (GPCR)

The focus was on maintaining key features, such as hydrogen bond donors or acceptors, acidic or basic centres and hydrophobic or aromatic regions in the chemical structure. The consideration of the chirality in the 4-point pharmacophore model was found to increase the selectivity for different targets.

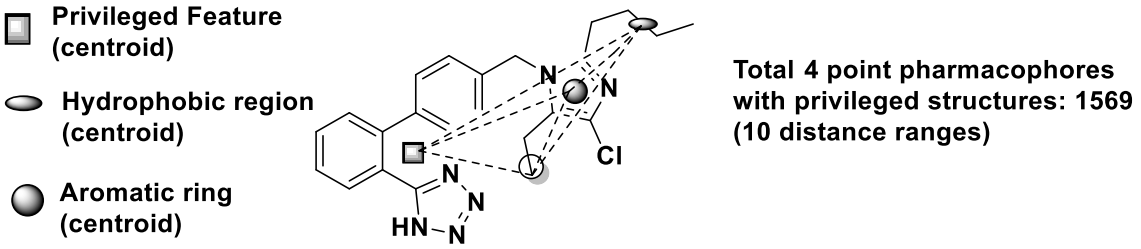


Figure 14 Example of the 4-point pharmacophore model on the compound MDDR140603 (Ref. 41)

In the example of the biphenyltetrazole privileged structural motif (compound MDDR140603) in figure 14, the privileged feature was forced to one point of the 4-point pharmacophore, where the other points are set in a relative measure for molecular similarity or diversity. The design of new compounds for a new series is no longer only based on 2D structural parameters resulting in much more structural diverse molecules. Regarding the ligand-receptor site in their study they had a closer look at the closely related serine proteases: trypsin, thrombin and factor Xa. Upon applying the 4-point pharmacophore model, an increased selectivity for one of the enzymes was observed. This approach was further

applied to building a new library of compounds based on the 4-point pharmacophore model including the privileged structural motif of biphenyltetrazole **35** (BPT). BPT was chosen as privileged structure and by applying the Ugi reaction a library of 4032 compounds was synthesised (figure 15).[41]

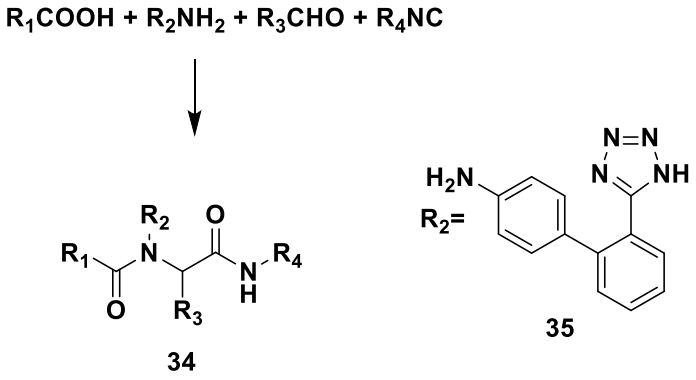


Figure 15 Schemes for building a compound library based on the 4-point pharmacophore model (Ref. 41)

With this study they could prove the usefulness and effectiveness to initiate new drug discovery projects on the basis of known privileged structural motifs.

1.3 Examples of known Privileged Structures

The closer look on known Privileged Structure libraries showed that most of the known Privileged Scaffolds are of heterocyclic nature with different ring sizes, number of heteroatoms and grades of substitution (figure 16).[18]

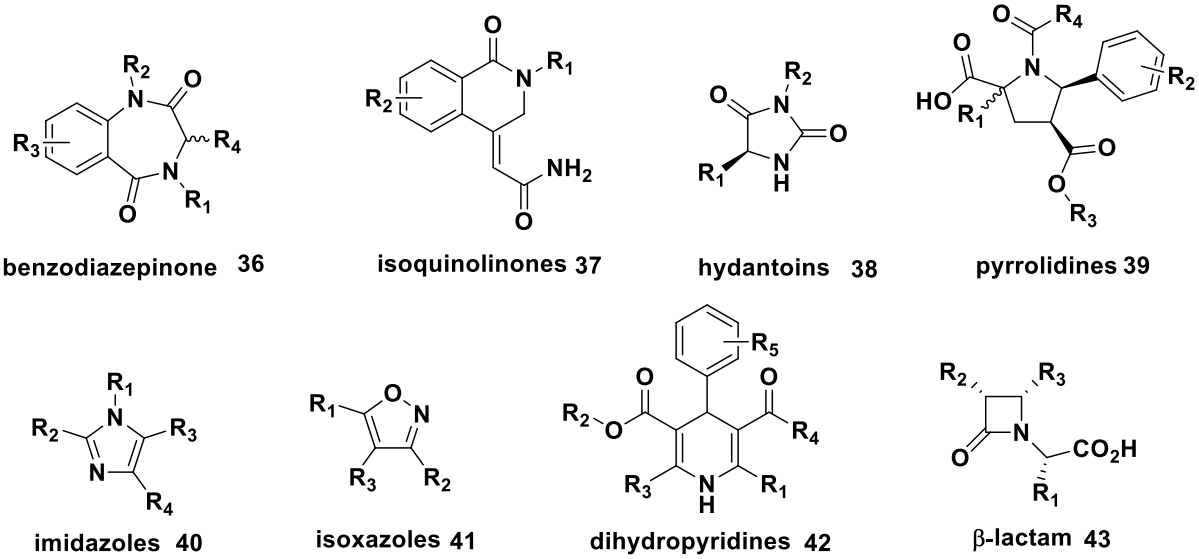


Figure 16 Known Privileged Structures, adapted from Kubinyi and Mueller, *Chemogenomics in Drugs Discovery*, 2004.

1.3.1 The classical pharmaceutical textbook example- a tricyclic diphenyl scaffolds

This tricyclic scaffold is the classical example of a privileged scaffold that targets a variety of different biological classes. It is an extraordinary example for a simple scaffold, which (when undergoing minor changes in its structural functionality and conformational substitution) can result in more than 150 drugs which were approved over the last decades.[18] Included in these drug examples is Zyprexa® **44** (figure 17), one of the blockbusters of 2001 which is a compound first marketed by Eli Lilly in 2006 for the treatment of schizophrenia and bipolar disorders.

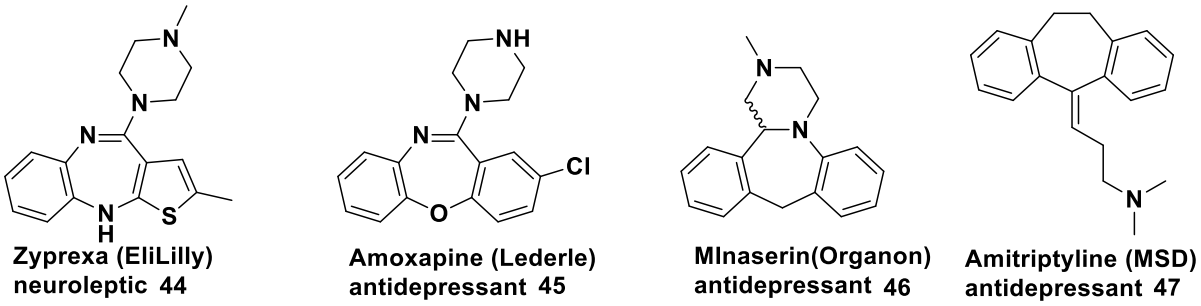


Figure 17 Examples of marketed drugs containing the tricyclic diphenyl scaffold

These four examples might lead to the conclusion that a target family correlation is emerging, due to the fact that all the compounds demonstrate biological activity towards the classical neurotransmitters binding GPCRs. This occurrence is misleading as a further investigation in the literature reveals that this privileged scaffold is presented in different structures which reach from discovery products to launched compounds for a variety of biological targets (figure 18).

1.3.2 The biphenyl substructure- a Privileged Scaffold or only a "Frequent Hitter"

One of the most discussed scaffolds is the biphenyl scaffold which is incorporated in nearly 5% of the biologically active drugs. Fesik *et al*. had a closer look at this substructure in their NMR based protein binding analysis.[42] They stated the biphenyl moiety as a privileged substructure as it was one of the 12 identified fragments in active compounds which showed binding to around 50% towards a variety of the screened proteins. It was recognised that depending on functionality the biphenyl moiety binds to different target proteins (figure 19).

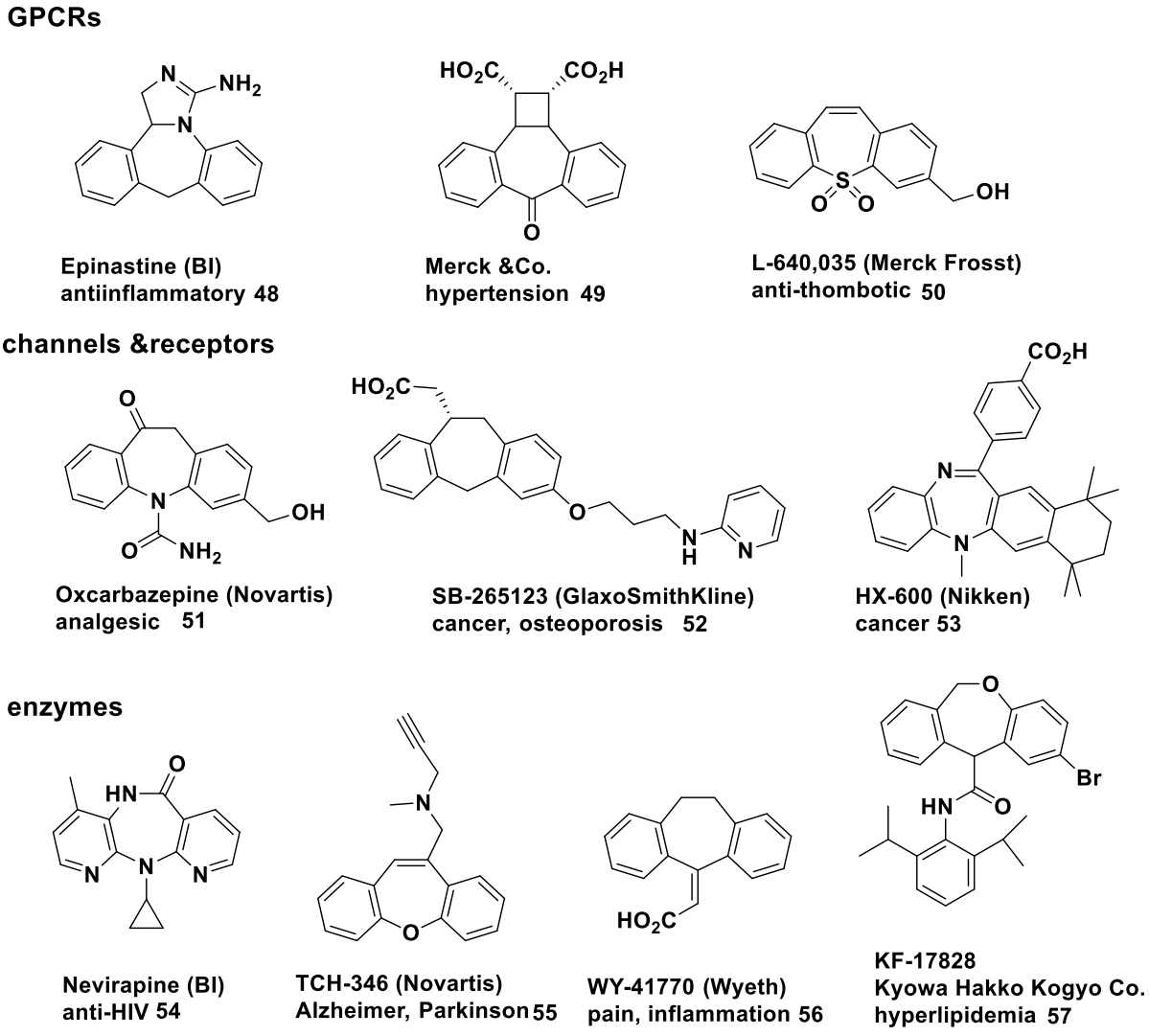


Figure 18 Examples of tricyclic biphenyl containing compounds showing biological activity towards different target classes

Fesik *et al*. explained the rationale behind the potential of the biphenyl moiety as a privileged substructure is defined by its usefulness to interact with aromatic and hydrophobic residues as a known feature and as well its capability to interact with polar groups.

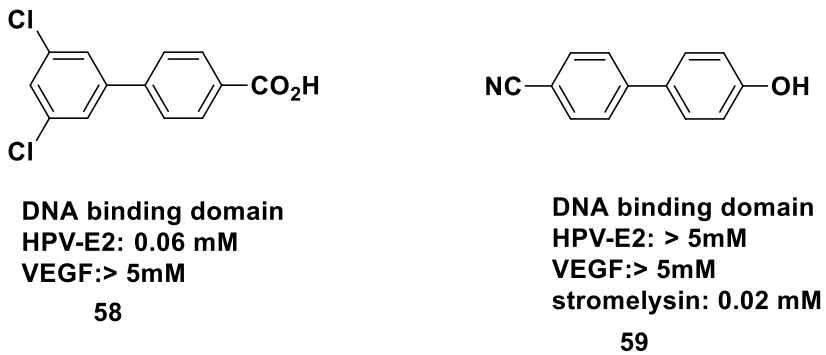


Figure 19 Effects of functionalization on a known privileged structure towards different biological targets

Only the fact that the biphenyl structure shows a higher success rate towards the chosen protein targets in comparison to other aromatic systems was suprising but could be explained through the necessary flexibility criteria, which is missing in substructures for example naphthyl due to its rigidity (figure 19).

1.3.3 Azo Heterocyclic Privileged Scaffolds

Several heterocyclic scaffolds are considered as privileged structures containing one or more nitrogens. For example the scaffolds indole **60**, quinolone **61**, isoquinoline **62** or purine **63** are well known molecules as part of highly active and structural diverse molecules (figure 20).[23]

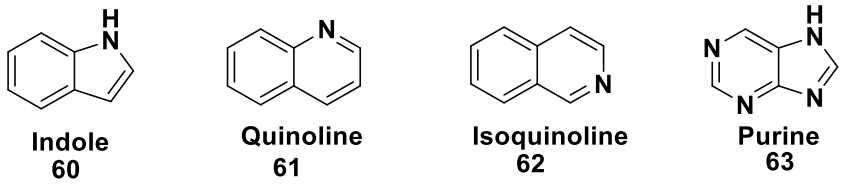


Figure 20 Example of Nitrogen containing Privileged Scaffolds

The compounds listed in figure 21 are examples of known drugs and natural products with the same incorporated privileged scaffold. The "substituents" around the privileged scaffold vary extremely and the illustrated compounds are targeting a variety of different biological targets- starting from anti-depressive to antiviral compounds. For example Oxypertine **64** is a known drug molecule bearing the indole substructure and is used as an antidepressant for the treatment of schizophrenia.[43] The natural product Nostodione A **65** consists as well of the indole scaffold and is applied as a mitotic spindle poison.[44] The possible diversity for all biological targets shown in figure 21 is demonstrated even if they all are including the same privileged structure in the drug compound as well as in the natural product.[23]

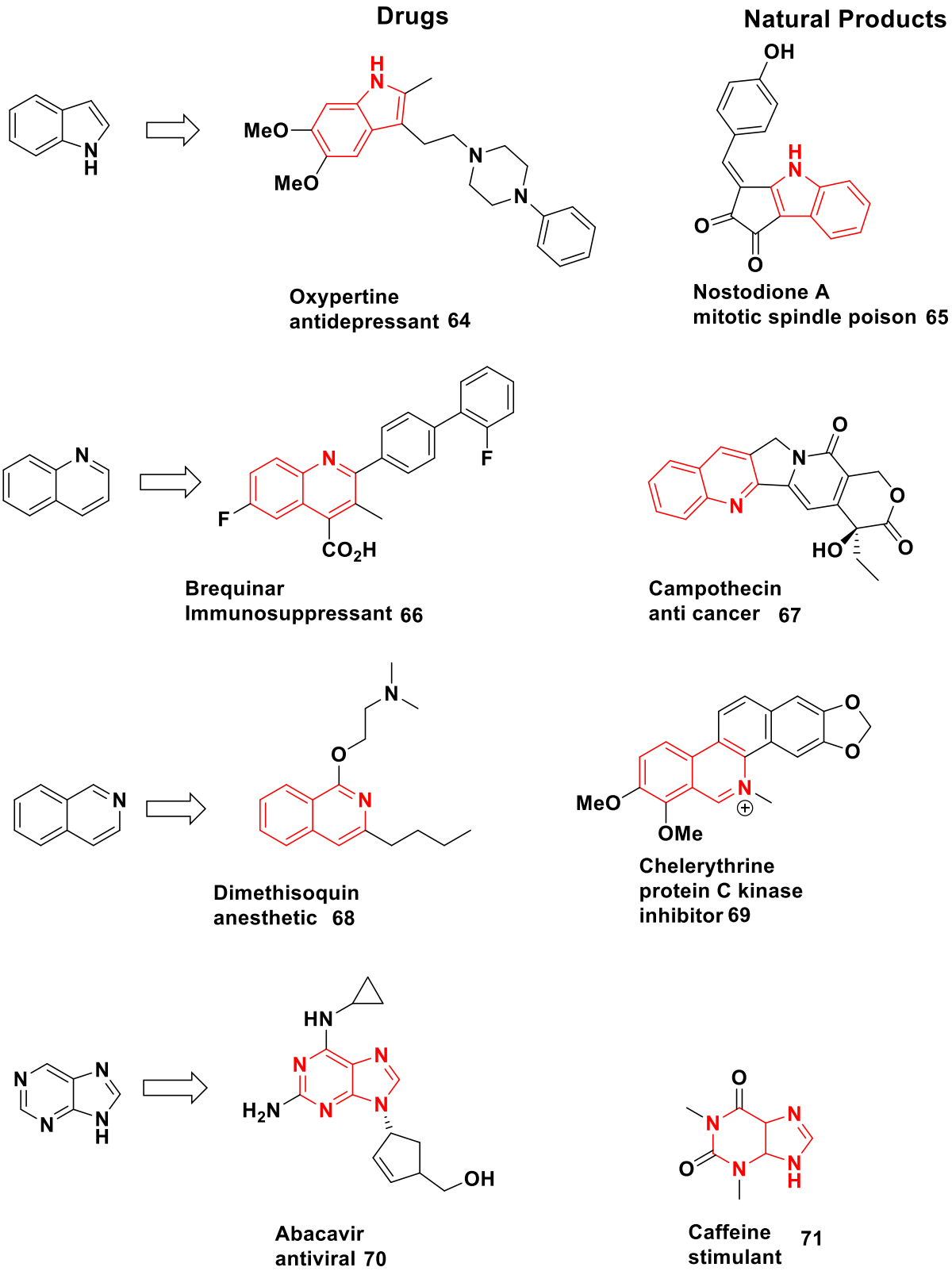


Figure 21 Examples of nitrogen containing privileged structures incorporated in biological active compounds- (drug molecules or nature derived)

1.3.4 Oxygen containing Privileged Structures

As shown for the nitrogen containing heterocyclic compounds in figure 21, there are several heterocyclic privileged scaffolds known containing oxygen atoms.[23] Once more they can be natural product derivatives or pharmaceutical drugs (figure 22). For example the coumarin substructure serves as a ligand incorporated in the structure of the drug Folescutol **79**, which is a capillary protectant. Additionally this structural motif is found in Suskudorfin **80** which is used as an anti HIV agent.

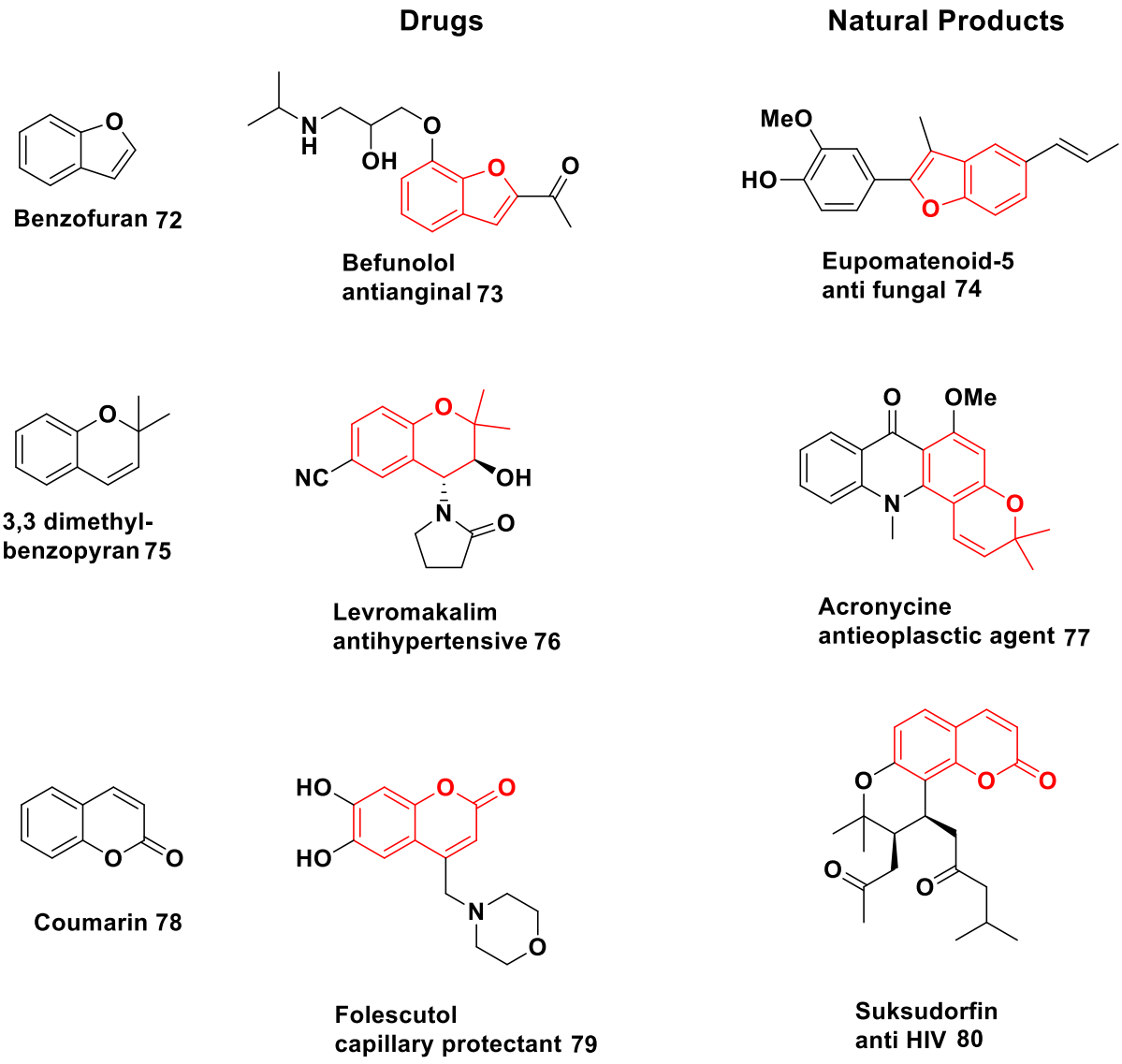


Figure 22 Examples containing privileged substructures containing oxygen atoms

1.3.5 Rhodanines: Privileged scaffold or promiscuous binder

A more recent review by Klein *et al.* is dealing with the question whether a new scaffold is a new privileged structure or a promiscuous binder is the example of rhodanine (**84**) and related 5-membered ring structures (**81-83**) (figure 23).[45]

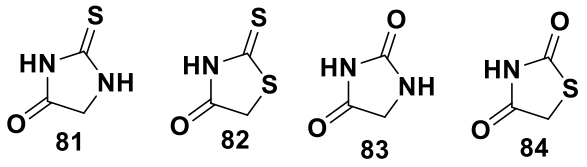


Figure 23 Structural motifs of Rhodanines and related 5 membered ring systems

The positive *versus* the negative effect of the affinity to certain targets was investigated as the structure motif of the five membered multi-heterocyclic ring compounds (FMMH) showed a relevant presence in leading medicinal chemistry publications. In the group of Klein *et al.* the rhodanine motif was tested against a variety of enzyme targets: two serine protease for dengue virus and thrombin from bovine plasma, a bacterial transferase and a metalloprotease. In their studies they came to the conclusion that these 5 membered ring structural motifs possess a distinct intramolecular interaction profile especially if an aromatic substructure is attached. They explained that the rhodanine scaffold should not be considered as a promiscuous binder and is suggested not to be regarded as an unspecific binder. Nevertheless Klein *et al.* draw the attention towards special requirements in the usefulness of the rhodanine scaffolds and to judge their eligibility as a privileged structure, whereas their affinity should be in the lower nanomolar range to be considered for the chosen target. As one of the negative aspects of rhodanines is mentioned related to an insufficient selectivity profile, which on the good side means the identification of a new lead could be accelerated.

1.3.6 A versatile privileged structural motif: 8- hydroxyquinoline

The privileged structural motif of the 8-hydroxyquinoline (8-HQ) is characterised through its broad pharmacological profile. In a review by Liu *et al.* in 2015 the 8-hydroxyquinoline was presented and its pharmacological profile was evaluated.[46] The 8-HQ motif showed excellent biological activity as a part of molecules to target a variety of biological relevant areas (figure 24).

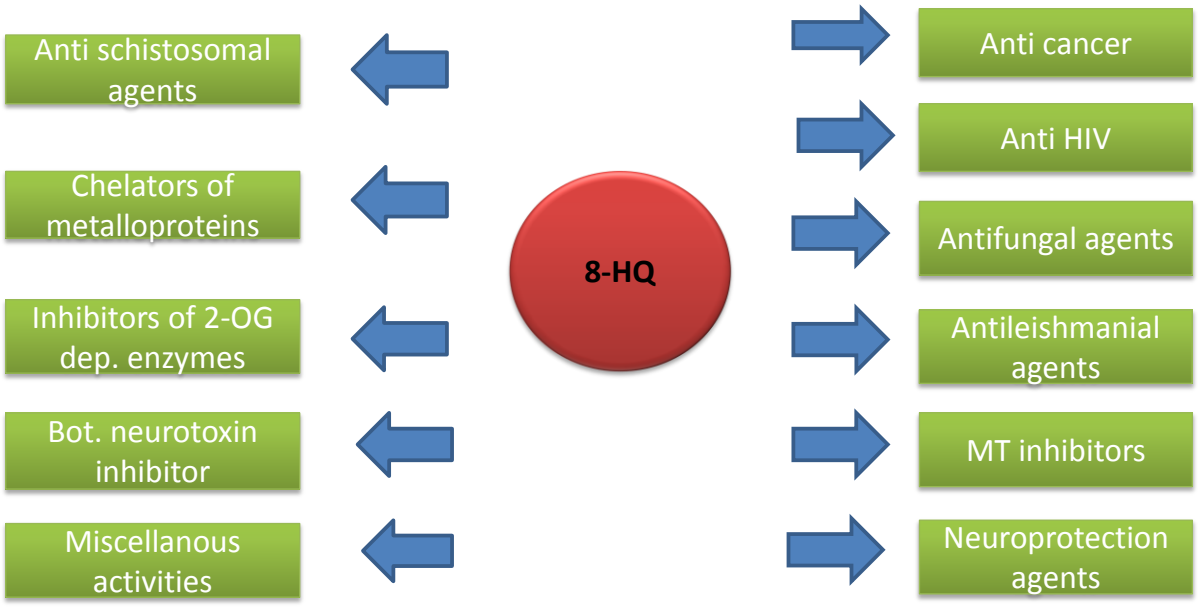


Figure 24 The broad pharmacological profile of 8-HQ

The 8-HQ was found in compounds which were used as neuroprotective agents, anticancer agents, inhibitors of 2-oxoglutarate and iron-dependent enzymes, chelators of metalloproteins, anti-HIV agents or antifungal agents. The review by Liu *et al.* showed a detailed analysis of the effect of the 8-HQ group towards the various biological targets (figure 25).

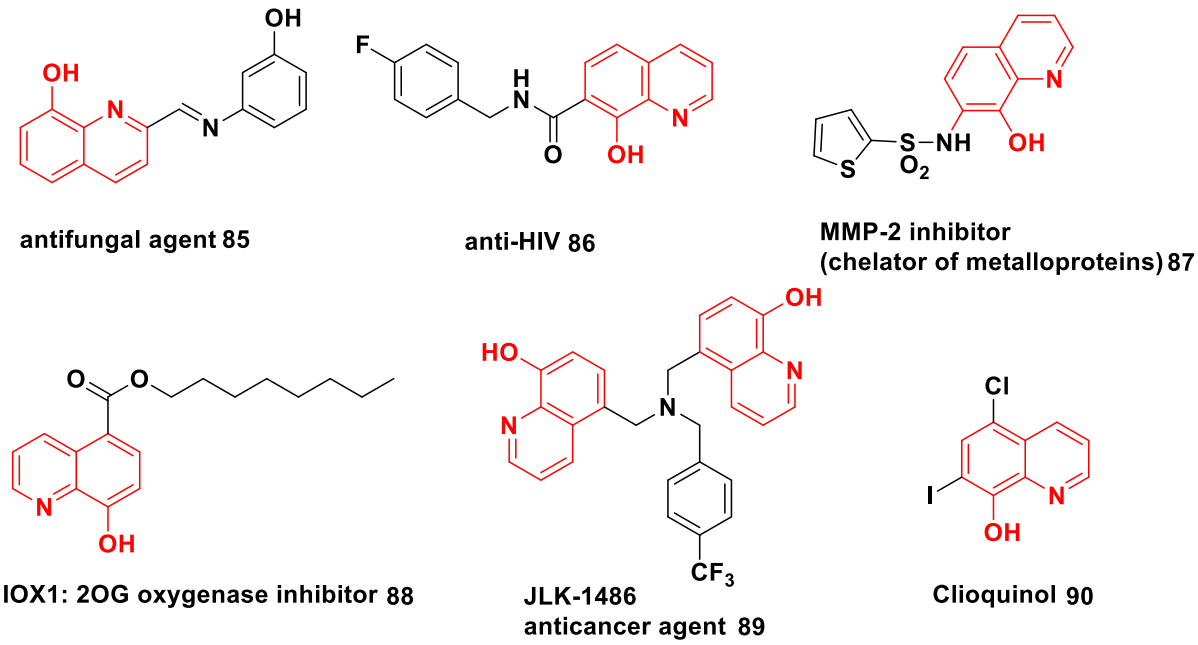


Figure 25 Compounds bearing the 8-HQ motif as a privileged structure

With unmet medical needs for conditions, such as Alzheimer and Parkinson disease, or the resistance occurring in the therapy against HIV, the 8-HQ represents a useful privileged scaffold for compounds addressing urgent medical needs. The anticancer agent JLK 1486 (**89**) was further evaluated in that review and its mode of action was shown, which follows a two steps procedure to form the alkylating species (figure 26) (**93**).[47]

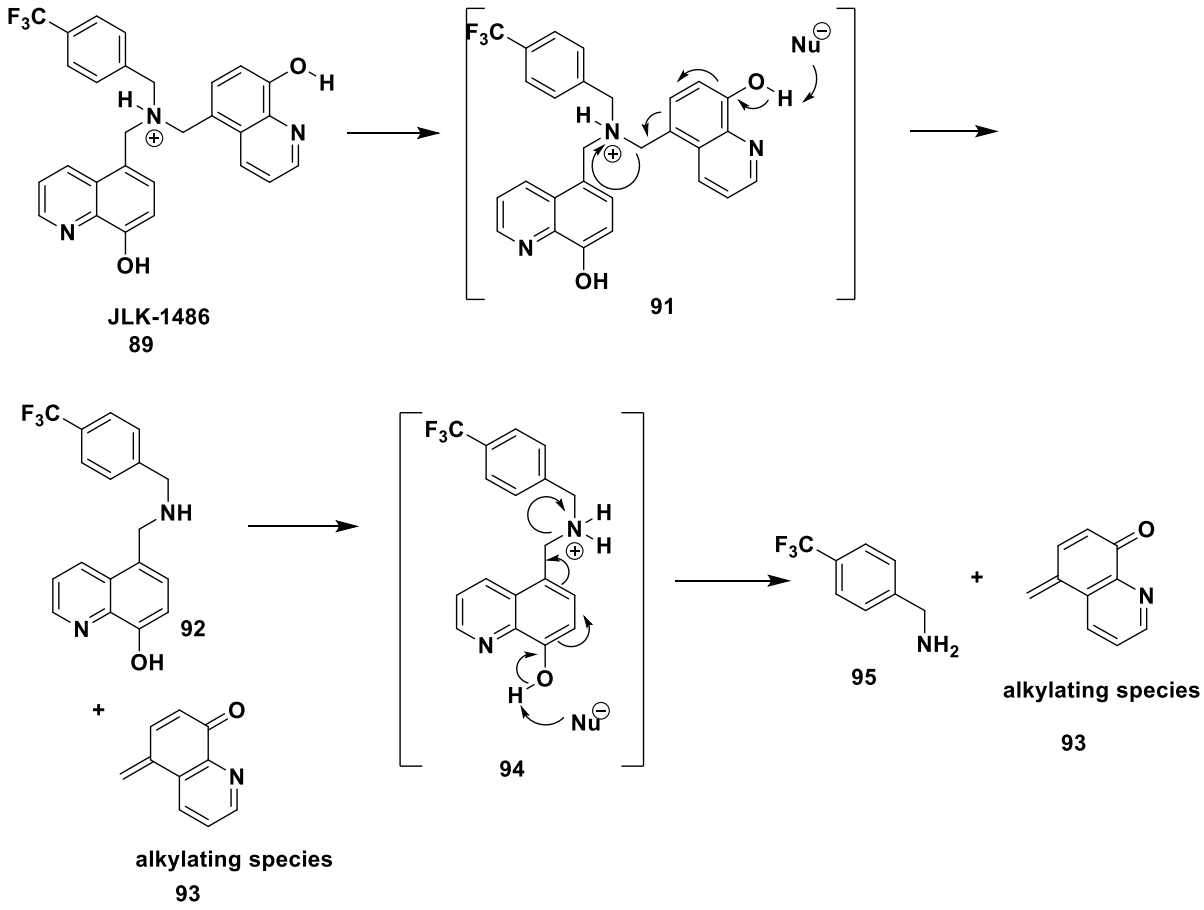


Figure 26 Mechanism of action of the anti-cancer agent JLK1486 (**89)** possessing the 8-HQ structural motif

In conclusion the 8-HQ scaffold was shown to be a starting point for introducing new functional groups for medicinal chemists for new target oriented synthesis (TOS).

The drug discovery approach using the introduced topic of the privileged structural motif opens a promising, facile and reliable starting point in finding new useful lead compounds capable of given access to a diversity of biological target classes. On the other side it is a topic under ongoing debate in the medicinal chemistry literature. As mentioned in chapter 1.3 there are several factors (promiscuity, frequent hitter etc.) why a structural motif cannot be considered as privileged as these could result in false positive hits. In articles published by Jonathan Baell the topic of PAINS (pan assay interference compounds) was introduced

referring to molecules which will give false positive biological activity due to misleading interactions with the actual biological target.[48] In his papers he described an approach towards the identification and subsequent removal of these structural motifs to receive reliable results in biological screening. He reports that the occurrence of PAINS was mostly found in academic medicinal chemistry research as the drug discovery compound design does not always take into account certain highly recommended filter criteria, such as those outlined by Lipinski.[6] The problem arising from this unguided drug discovery research is the failure in identifying an appropriate hit compound that depends on a specific interaction between a drug and a target protein. This misleading research can result in compounds that appear highly active and could therefore lead to an enormous waste of important research time and budget. In its Nature article Baell and Walters highlighted the PAINS (shown in figure 27) as the "worst offenders", and identified a selection of structural motifs which are well known to give false positive biological results.[49]

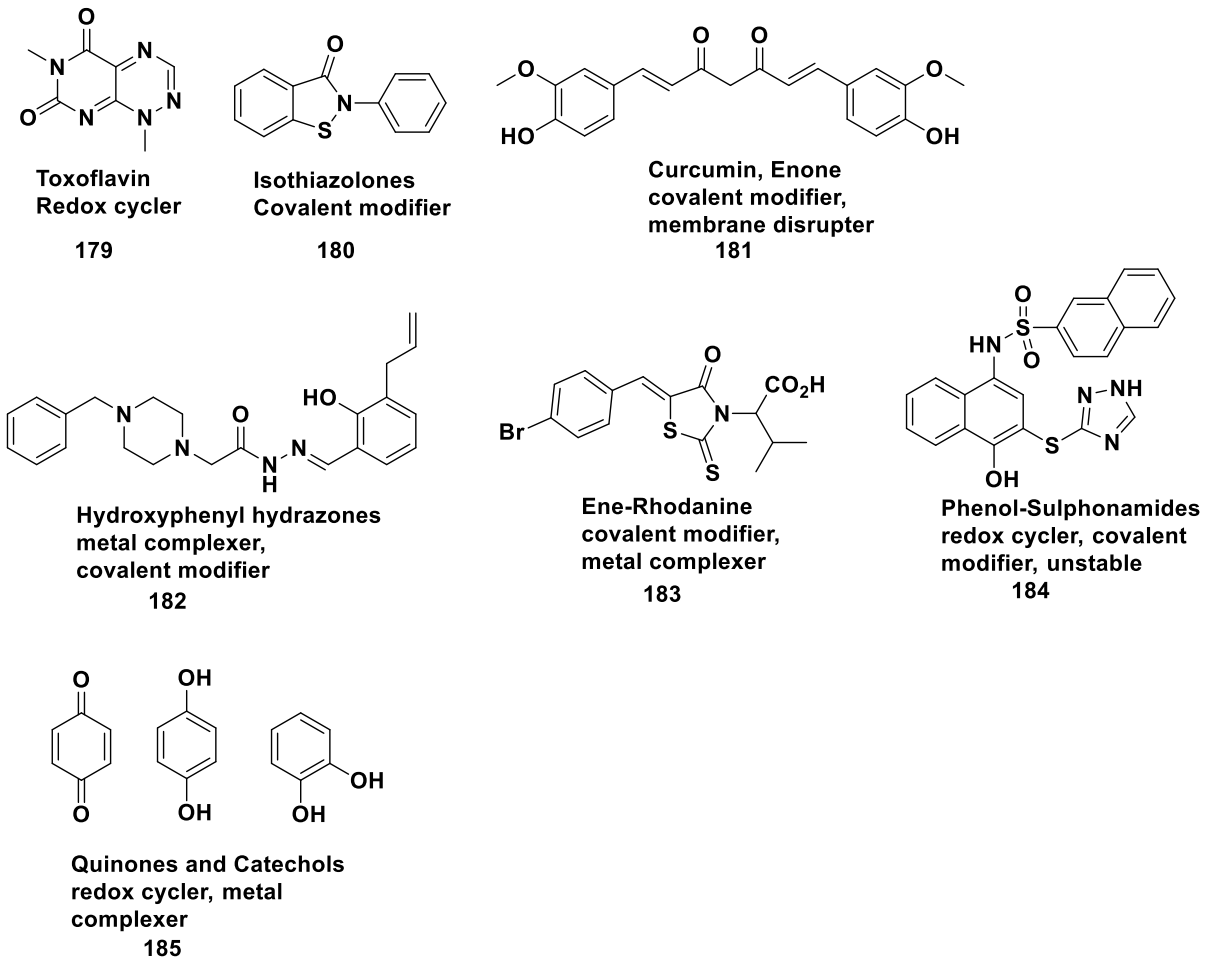


Figure 27 Known PAINS and recognised structural motifs in PAINS according to Baell *et al*.[49]

When those chemical structures shown in figure 27 appear in a new hit compound, carefulness is required as they could be considered as molecules without the required specific biological activity. As the biological screening and drug discovery process made its way into academic labs[50], the author's suggest that certain filter criteria are required to improve the quality of the research outputs, resulting mainly from a lack of drug discovery experience. There are several articles dealing with the topic of assay interfering compounds, compounds which contain certain unwanted structural motifs which are most often unrecognised leading to the pollution of the scientific literature with false promising hit compounds. False positive hit compounds can interact with proteins by forming aggregates or can show a general, non-specific activity against the target protein. Functional group filters can be applied to eliminate these compounds from assays early on in the process to increase the lead-like quality of the screening hits. Another problem which can deliver false positive compounds is their interference with the actual assay signalling, which represents one of the biggest challenges. In a review by Baell some criteria were published to identify PAINS from true active compounds, which should provide information to be able to carry out effective research and appropriate spending of research money.[48] The selection for filtering started by removing compounds, which showed around 85% similarity to another compound (measured by the Tanimoto coefficient) and furthermore applied published data to exclude certain functional groups (for example: halides substituted, alkyl sulfonates, anhydrides, peroxides, isocyanates, triflates, positively charged atoms etc. but retained certain functionalities even if they are not recommended (oximes, hydrazones, anillines etc. Only a few of the ~73000 screened compounds showed a hit in more than one assay, which resulted in the second filter criteria to exclude compounds with activity of more than 85% in four assays. They eliminated known problematic substructures like rhodanines, quinones or 2-aminothiophenes and applied further filters targeting individual occurring substructures. Furthermore his group started on the optimisation of screening assays to eliminate false positive compounds which can arise by covalent binding to the protein, binding to many sites on the protein, compounds forming aggregates and compounds which absorb light in the assay relevant wavelengths. One example of a PAIN is rhodanine, which was mentioned before in chapter 1.3.5 and its potential was evaluated to be a privileged structure. This structural motif appeared as a highly promising active compound in multiple papers from around 300 different organisations with more than 250 with from an academic background. Rhodanines are known to undergo a light induced mechanism by which they can modify proteins irreversibly, but this fact is mostly ignored in the evaluation of the rhodanine scaffold when seen in active hits. In conclusion,

the topic of a privileged scaffold is a highly discussed and a critically evaluated starting point for the drug discovery process. As mentioned in the previous chapter 1.2 many recent reviews are dealing with this topic and their advantages for good starting points for new chemical leads for drug discovery. On the other hand a critical evaluation has to be carried out about the biological dependence of certain substructures within the hit compounds. Some substructures are present in a higher number than others and, as conclusion, they have a greater chance to be recognised as positive hits and to be considered as privileged structures. As discussed, the occurrence of false positives can result in a misleading picture of certain substructures to be considered as a privileged structure. Furthermore, a critical point is the evaluation of a chemical structure to be privileged by considering more than one target family. Nevertheless, by the necessity of applying critical filters and a more critical evaluation to examine the potential of certain substructures for their ability to be a frequent hitter or to act promiscuous, the author of this thesis believes that privileged structure can exist, due to the results of this thesis by showing a new scaffold with an interesting potential against a variety of biological targets. One critical point is the diverse chemical modification of this scaffold to be able to evaluate the influence of the scaffold itself. It will be necessary to apply certain criteria evaluated and described by Baell to eliminate the chance of finding false positives. After the examination of a new scaffold described in this thesis and the occurrence of biological activity in a variety of biological targets the consideration of this scaffold to be privileged is valid. The scaffold showed that it is not promiscuous by not showing activity in biological counter screening.

.

2 Aims and Objectives

The aim of this thesis was to design and synthesize a series of new tricyclic scaffolds, that contain piperidine and substituted triazole functional groups, which are known structural motifs in many biological active molecules (figure 28).[51]

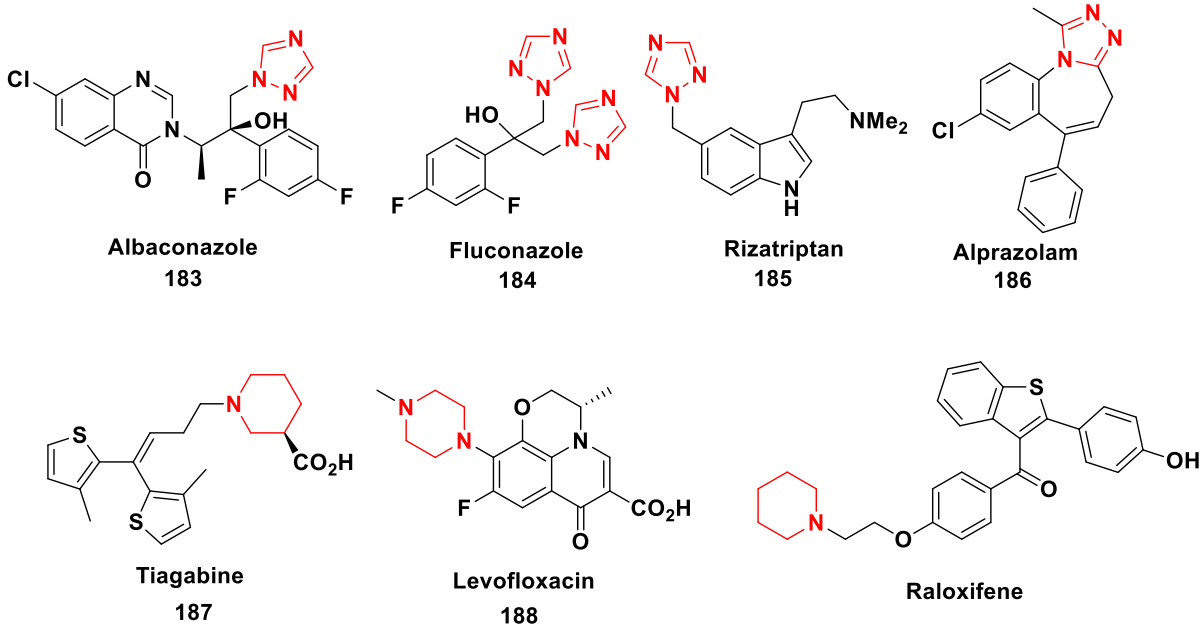


Figure 28 Examples of trizaole and piperidine containing drugs

The triazole and piperidine moiety are linked through a third ring, which will allow a decrease in flexibility of the tricyclic ring system, which furthermore enables the sysnthesis of constraint analogues of known biological drugs (figure 29).

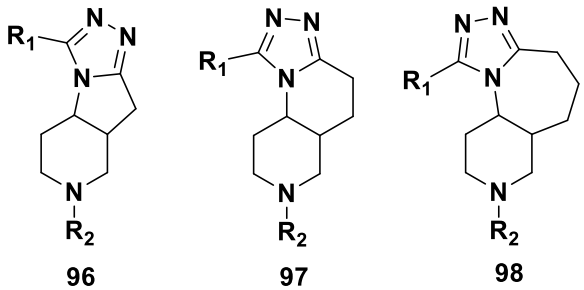
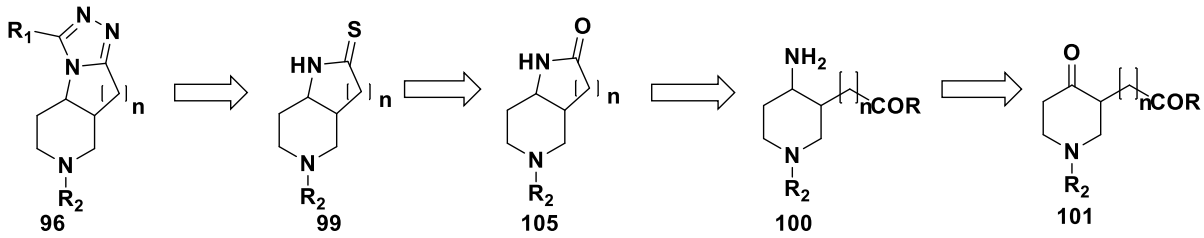


Figure 29 Tricyclic piperidine triazole scaffolds differentiating in the ring size of the connecting ring

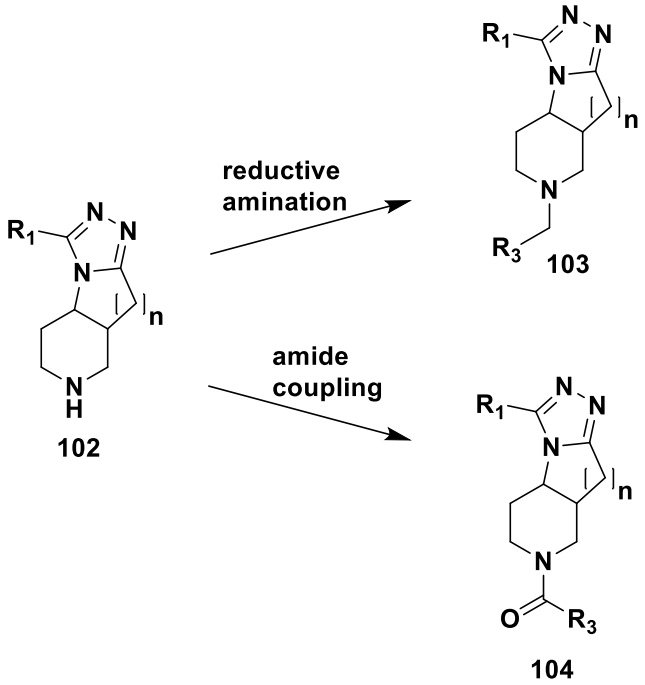
The scaffolds should be synthesized to allow functionalisation in the two positons R_1 and R_2 for introduction of a variety of substituents. Furthermore, the scaffold synthesis should be convergent to allow exploration of different ring sizes within the connecting ring between the piperidine and the triazole part of the tricyclic scaffold. The substituted triazole group should

be introduced *via* the reaction of the thiolactam **99** and the corresponding hydrazide (scheme 1). The thiolactam **99** should result through reaction of the lactam **105** with Lawessons reagent. The lactam **105** should be available through hydrogenation of the corresponding aminoester **100** precursor derived from the starting ketone **101**.



Scheme 1 Proposed retrosyntthetical plan for the synthesis of the tricyclic triazole scaffolds **96-98**

It is proposed that these scaffolds could be incorporated into known biologically active molecules or marketed drugs through scaffold hopping by attaching new residues to the nitrogen atom of the piperidine ring system. This coupling should be done through either a reductive amination or amide coupling reactions using standard reaction conditions (scheme 2).

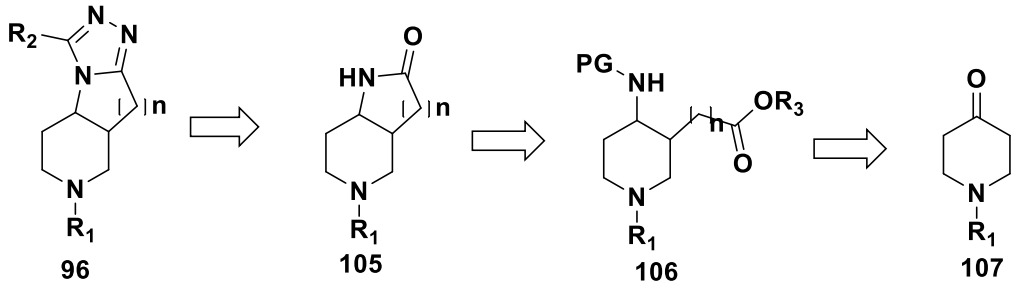


Scheme 2 Coupling approaches starting from novel tricyclic triazole **102**

Furthermore, the newly synthesised analogues should be screened against the biological target of the parent compound to test our hypothesis for the usefulness of our tricyclic scaffolds as new privileged structures.

3 Design and Synthesis of a novel tricyclic triazole-based scaffold

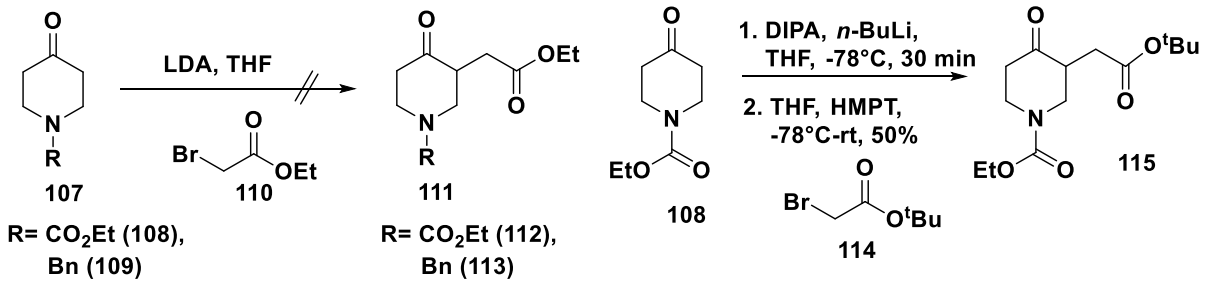
The aim of this PhD project was to establish a reliable route to synthesise a new tricyclic scaffold which could be used in the application for medicinal chemistry projects. This scaffold was designed to incorporate triazole and piperidine rings, which are common features in many known biologically active compounds.[51] The retrosynthetic plan for this scaffold was to synthesise the triazole portion of scaffold **96** ring in the final step of the sequence, through reaction of the corresponding bicylic lactam **105** with the corresponding R_2-hydrazide. The lactam **105** should be synthesised through ring closure on the alkylated amine **106** through acid or base catalysis or through direct ring closure after hydrogenation of the protected amine **106**. The sequence starts from commercially available ketone **107** (scheme 3).



Scheme 3 Retrosynthetic approach to yield triazole scaffold **96**

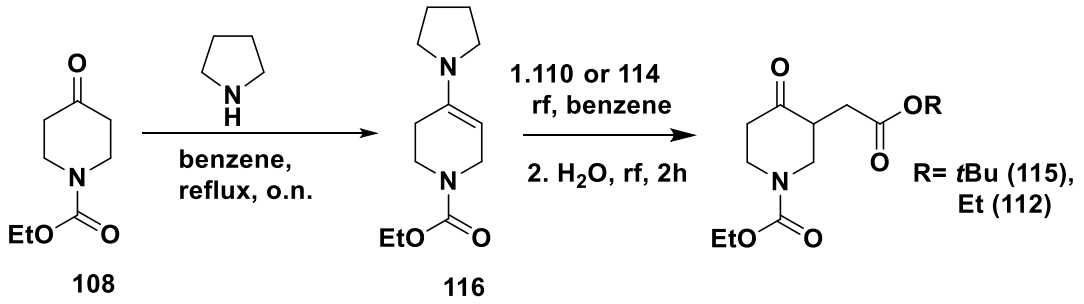
3.1 Synthesis of the [6.5.5] tricyclic scaffold

The synthesis of the [6.5.5] membered scaffold started with the commercially available ethyl 4-oxopiperidine-1-carboxylate (**108**). The first step was the conversion of piperidone **107** into alkylated ketone **111** which was more challenging than expected as this alkylation step required some optimization. The first attempt using benzylpiperidone **109** and ethylbromoacetate **110** as the alkylation reagent was carried out from a known literature procedure by Romanelli *et al.*[52] but after several attempts proved unsuccessful. The same alkylation conditions using piperidone **108** was furthermore unsuccessful. After changing the alkylating reagent to *tert*-butylbromoacetate (**114**), and using hexamethylphosphoracidtriamid (HMPT) as a solvent additive and additionally increasing the equivalents of base (LDA), a satisfactory yield (50%) of ketoester **115** was obtained.[53] (Scheme 4) HMPT is a known aprotic organic solvent for increasing the yield and the conversion rate through its solubilizing effect.



Scheme 4 Alkylation of ketoesters **108-109**

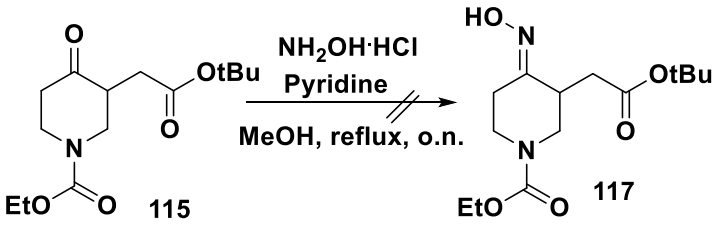
Utilising the same optimized reaction conditions, piperidone **108** and ethylbromoacetate **110** delivered the ethyl ester **112** in a moderate yield of less than 50%, as the purity was shown to be low. In the meantime, one attempt was started to synthesize the alkylation product *via* the enamine **116**, which is a compound known from a patent by Novartis on kilogram scale[54], but this approach was postponed after achieving results by using LDA as a base (Scheme 5).



Scheme 5 Synthesis route through enamine **116**

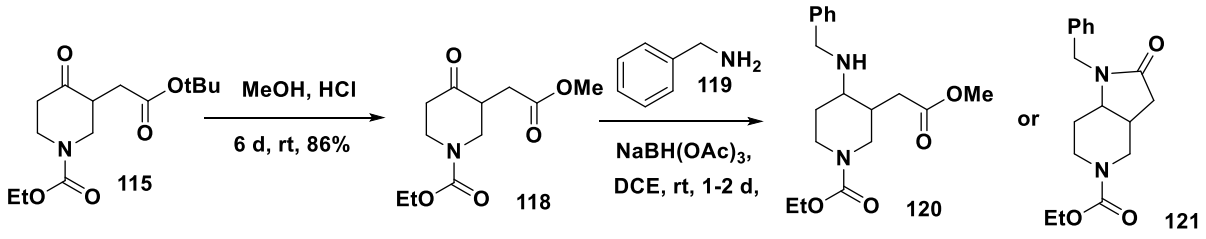
One attempt to synthesise the *tert* butyl ester **115** through the enamine route (Scheme 5) was made, but the yield was shown to be lower than with the LDA route (Scheme 4) and it was shown that the formation of an undefined by-product was dominating in this reaction sequence.

The next step was the incorporation of the nitrogen functionality, which was trialed using *tert*-butyl ester **115**, sodium triacetoxyborohydride and ammonium acetate following the procedure by the group of Romanelli.[52] Unfortunately, none of the attempts to establish the amine group directly was successful and therefore a protected amine function was introduced. The first attempt was to install a hydroxylamine using hydroxylamine hydrochloride and pyridine under refluxing conditions in methanol, but this attempt did not deliver the desired product (scheme 6).[55]



Scheme 6 Synthesis of Hydroxylamine **117**

The next approach was the trans-esterification into the methyl ester **118** starting from ketone **115** using a basic as well as an acidic method to enable access to the lactam **105** through acid-catalysed cleavage of the *tert*-butyl ester functionality. The basic variant using NaOMe and MeOH at reflux resulted in decomposition of the starting material **115**, but the acidic variant using aqueous 6N HCl in MeOH delivered the desired methyl ester **118** in a yield of 86% (Scheme 7).

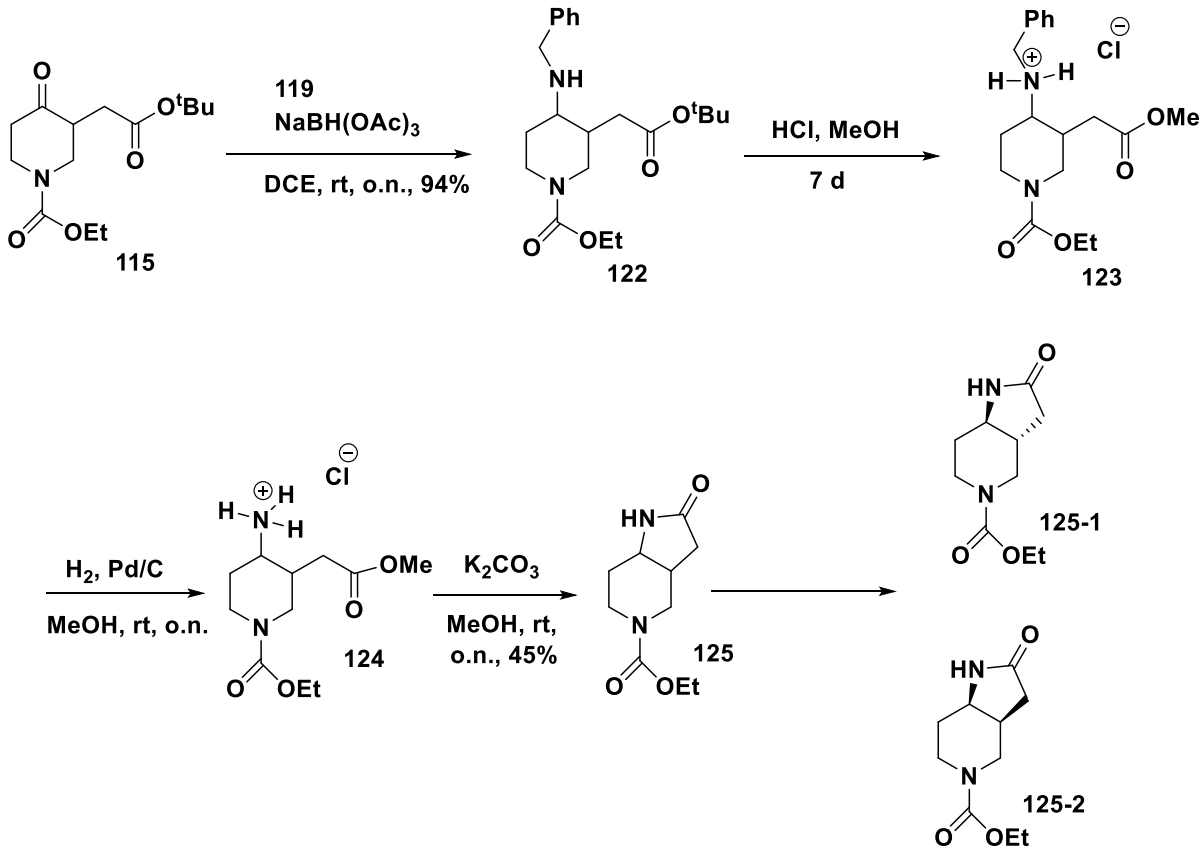


Scheme 7 Conversion of compound **115** into methylester **118** and subsequent reductive amination

It was proposed that methyl ester **118** could be converted into the lactam system **105** using ammonium acetate, however, this reaction failed. As a consequence, it was decided to try the reductive amination with an alkylated amine instead of ammonium acetate and methyl ester **118** should be used as the keto compound for the reductive amination to compounds **120** or **121** (scheme 7). The first attempt was the reductive amination using benzylamine **119** which proved successful and benzylamines **120/121** could be synthesized.[56] Unfortunately, the cyclisation was not reliable, the first attempt showed no cyclized product **121**, the second try showed mostly **120** and the third showed a nearly one to one mixture of cyclized compound **121** and the open form **120**. Some attempts (heat, acid, base) were made to accomplish the ring closure for all material, but none of the attempts delivered a desired outcome. The cyclized material **121** was used to trial the benzyl deprotection to yield lactam **125**, which was not feasible under standard hydrogenation conditions using Pd/C in methanol.[57]

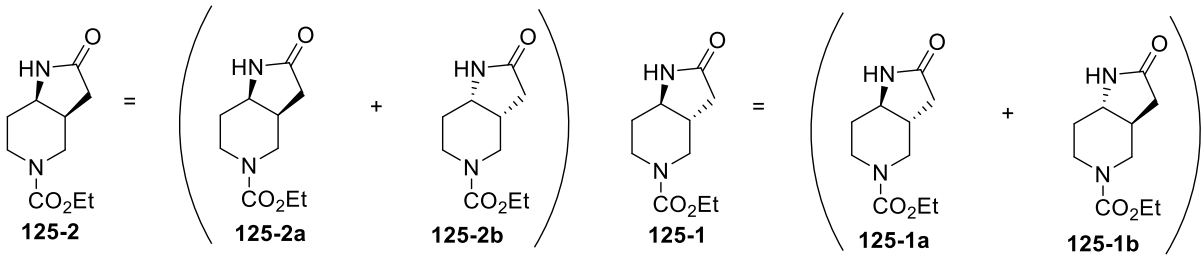
Therefore a second approach for synthesising the desired lactam **125** was used. The procedure started with *tert* butyl ester **115**, which was converted using a reductive amination

with sodium triacetoxyborohydride in 1,2 dichloroethane to the benzylamine **122**. Afterwards, the benzylamine **122** was converted into the methylester **123** as its HCl salt using MeOH and 6N HCl (Scheme 8).



Scheme 8 Synthesis route to bicyclic lactam **125**

Finally the ring closure reaction was attempted through hydrogenation using Pd/C in MeOH, which led to the isolation of compound **124** again as the HCl salt (scheme 8).



Scheme 9 Both enantiomers of each *cis*- isomer **125-2** and *trans*- isomer **125-1**

Unfortunately, during these reaction conditions the salt did not lead to ring formation, therefore compound **124** was stirred in MeOH and potassium carbonate to remove the hydrochloride acid and after purification, the clean compound **125** was obtained and both isomers (*cis*- (**125-2**) and *trans*- (**125-1**)) could be separated through column

chromatography, which are shown for simplicity as only one *cis*- and one *trans*- enantiomer (compare Scheme 9).

Unfortunately, the relative configuration for the separated geometric isomers could not be determined absolutely through 2D NMR methods using NOESY (Figure 30). This was due to the observed overlap in the NMR signals associated with H-7 and H-3, which are both coupling to H-2, masking the visible coupling constants between H-2 and H-7.

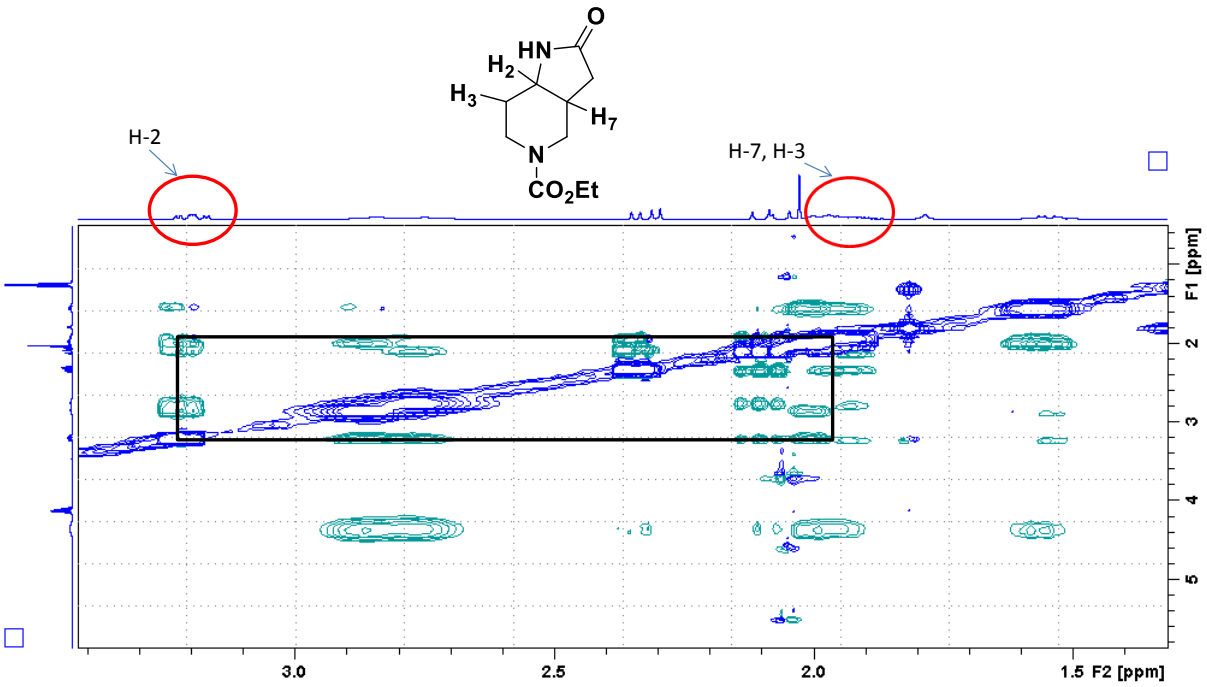


Figure 30 NOESY spectra of one isomer of **125**

As a consequence, the separated isomer was submitted for single crystal X-ray analysis demonstrating that this isomer to be the *trans*- connected isomer, therefore the other isomer was known to be the cis isomer by inference (Figure 31).

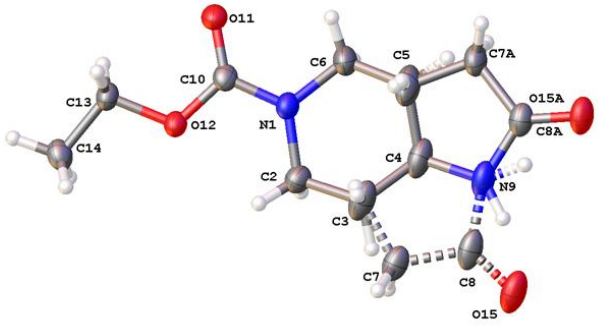


Figure 31 The contents of the asymmetric unit of isomer **125-1** showing (a) the major disorder component (with atom O15A) and (b) the minor disorder component (with atom O15) in separate views. Displacement ellipsoids are drawn at the 50% probability level.

Compound **125-1** was recrystallized slowly from ethyl acetate to afford crystals of sufficient quality for structure determination. The compound was found to crystallize in the centrosymmetric space group P_21/n, with one molecule in the asymmetric unit. Interestingly, the five-membered ring is disordered over two possible positions, so both enantiomers are represented in the asymmetric unit due to the piperidine ring flip. In this case, the overall packing of the crystal appears to be driven by the interactions of both the carbamate and the lactam functional groups. The molecules form hydrogen-bonded dimers, which pack in a classic herringbone fashion. The piperidine ring in the crystal has a chair-like conformation and the C8-O15/C8A-O15A bond lengths [1.234 (5)/1.237 (4) A°] are in the typical range. The N9-C4-C3/N9-C4-C5 bond angles are 112.06 (15)/109.21 (16) and the C7-C3-C4/C7A-C5-C4 bond angles are 98.9 (2)/100.46 (18). The torsion angles are synclinal for C7-C3-C4-N9/C7A-C5-C4-N9 [36.2 (2)/34.4 (2)] and C2-C3-C4-C5/C6-C5-C4-C3 [62.8 (2)/63.0 (2)]. With the antiperiplanar torsion angles of 158.0 (2)/157.79 (19) for C7-C3-C4-C5/C7A-C5-C4-C3 and 175.51 (15)/173.55 (16) for C2-C3-C4-N9/C6-C5-C4-N9, the antiperiplanar positon of atoms H4 and H3, and hence the relative stereochemistry of the molecule was determined.[58]

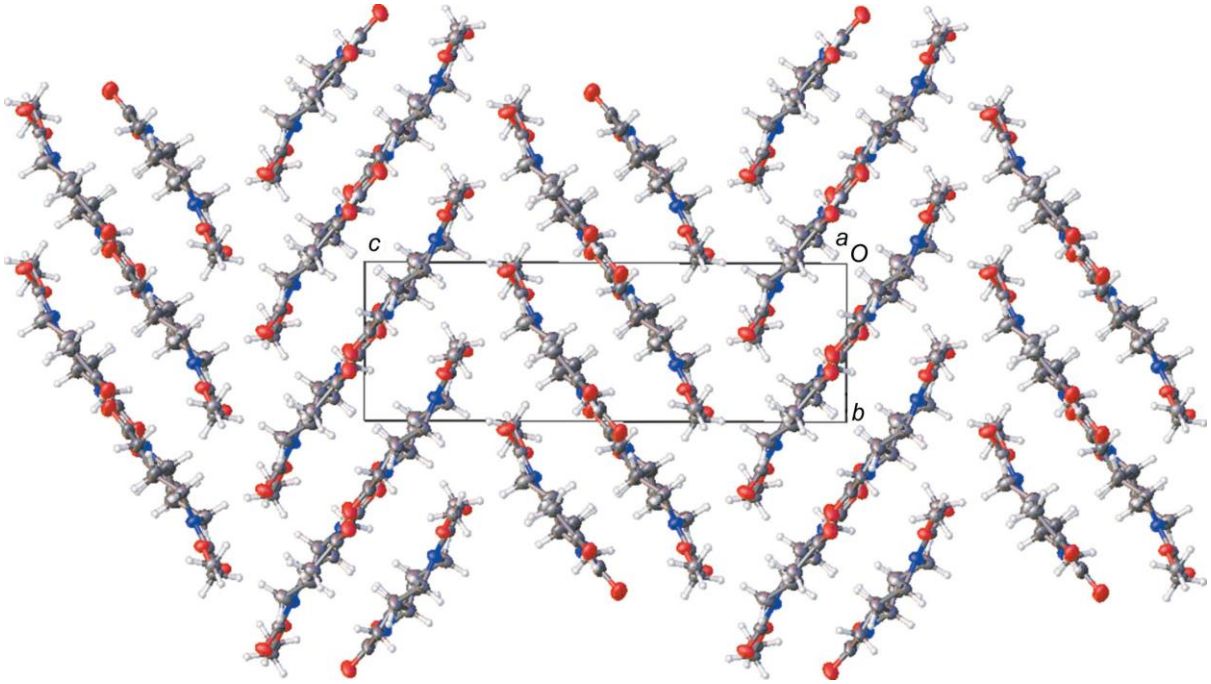
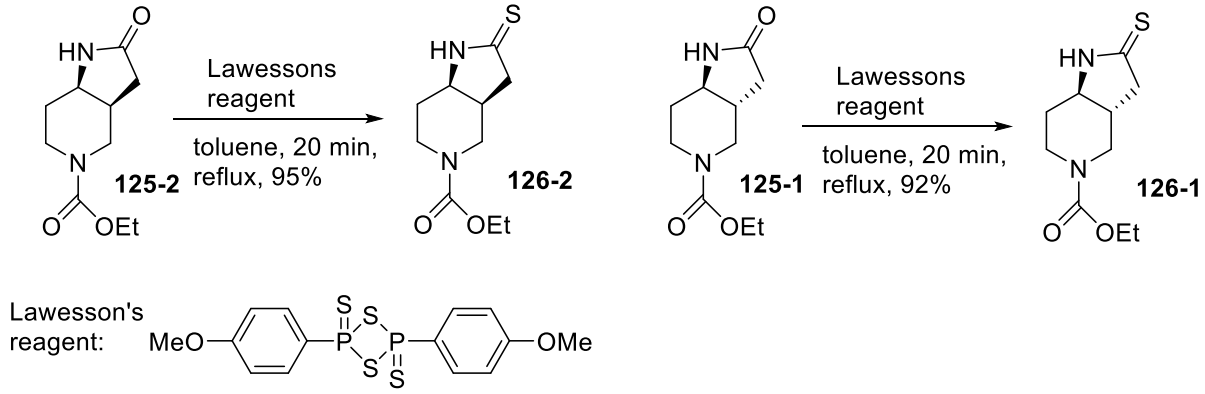


Figure 32 The herringbone packing of isomer **125-1** in the bc plane

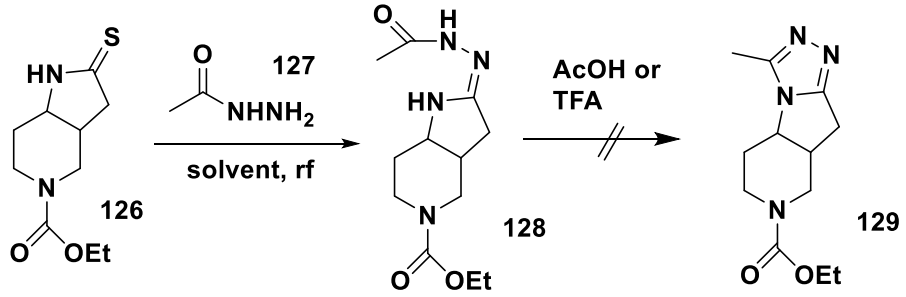
The next step was the conversion of each isomer of lactam **125** into thiolactam **126** through reaction with Lawessons reagent in an excellent yield of 92-95%.[59]



Scheme 10 Synthesis of thiolactam **126** using Lawesson's reagent

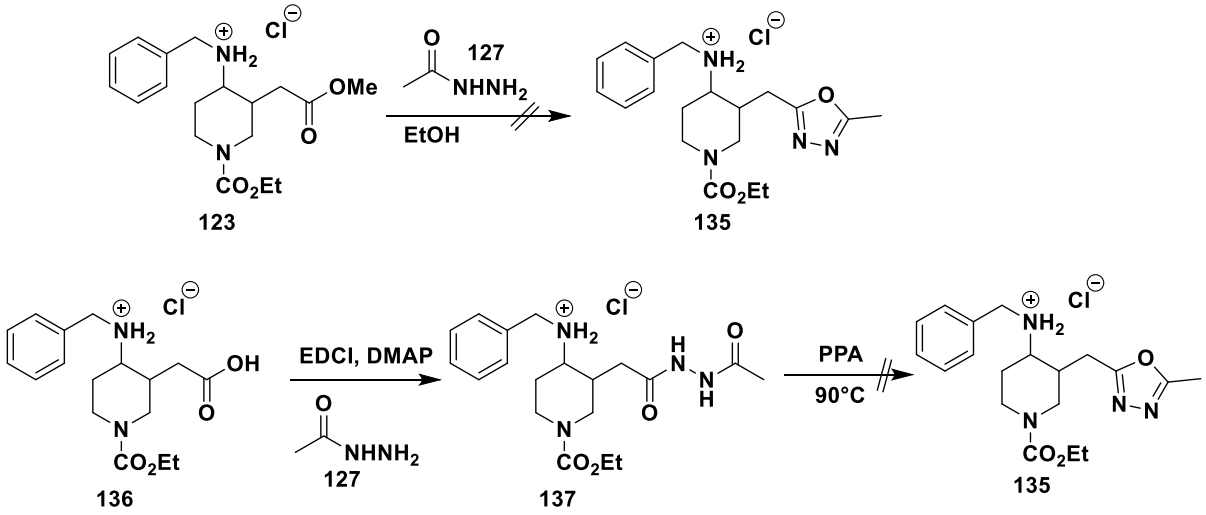
The next step was the conversion of thiolactams **126-1** and **126-2** into the triazole **129** (Scheme 11) using the high boiling solvent cyclohexanol and acethydrazide (**127**).[60] However, compound **129** could not be isolated from the reaction mixture due to the complicated removal of cyclohexanol during the purification process. The cyclisation reaction was performed using acetic acid, which showed conversion to the required product via mass spectral analysis, forming first the open non-cyclic intermediate **128** and showing finally the desired product mass of triazole **129.** Unfortunately, the crude NMR of this conversion showed no evidence of the desired compound **129**. The attempt using

acethydrazide (**127**) in toluene under reflux delivered again the open form, but the attempt through addition of TFA to accelerate the formation of triazole **129** *via* facilitating the water elimination resulted in decomposition of the intermediate **128**.



Scheme 11 Formation of triazole compound **129** starting from thiolactam **126**

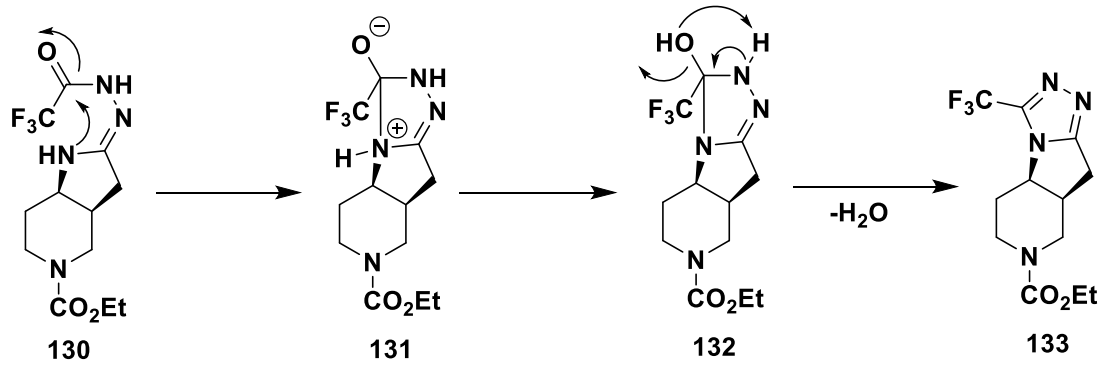
After unsuccessful direct ring closure to triazole **129** it was tried to establish an 1,3,4 oxodiazole system which should simplify the final ring closure to triazole **129** (scheme 12). This attempt used compound **123** as starting material which was treated with acethydrazide **127** in ethanol, but didn't convert into the desired 1,3,4 oxodiazole **135.** A second try was made using the corresponding acid to methylester **123** and to couple this acid to acethydrazide **127** using standard conditions EDCI and DMAP following formation of 1,3,4 oxodiazole using polyphosphoric acid (PPA) was furthermore unsuccessful in yielding compound **135**.



Scheme 12 Second approach to install triazole system

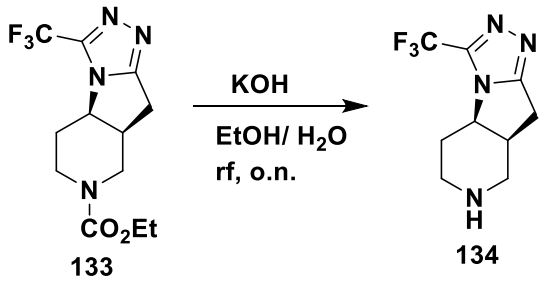
Another approach to yield triazole **129** was made by using, instead of acethydrazide **127,** the trifluoroacetic acidhydrazide under refluxing conditions in toluene, which finally lead to triazole **133**. An explanation for the failure of the acethydrazide approach compared to the

trifluoro acetic hydrazide could be that the [6.5.5] scaffold system is too constrained and therefore that the ring closure to the triazole ring, could not occur and this prevented the final ring closing reaction of the intermediate hydrazide **128**. Using the trifluoro acetic hydrazide simplifies the ring closure as the trifluoro group represents an electron withdrawing group, which triggers the nucleophilic attack of the nitrogen followed by the water elimination to form 1,2,4 triazole **133** (Scheme 13).



Scheme 13 Mechanism of triazole **133** formation using trifluoracetic acid hydrazide

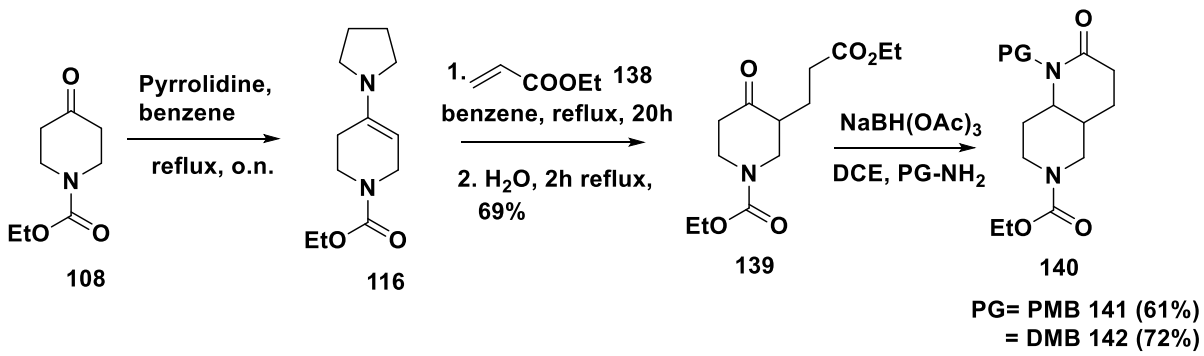
The final step was the cleavage of the carbamate group which was trialed prior for the 6.6.5 scaffold system (section 3.2) and was accomplished using potassium hydroxide under refluxing conditions in ethanol/water to yield the desired amine scaffold **134** (scheme 14).



Scheme 14 Deprotection of carbamate group to yield [6.5.5] triazole scaffold **134**

3.2 Synthesis of the [6.6.5] tricyclic system

Piperidone **108** was used as starting material for the synthesis towards the [6.6.5] scaffold system. This route started with a Dean Stark condensation building up the enamine **116** through refluxing pyrrolidine and ketone **108** in benzene overnight. This dark red mixture was dissolved in benzene and treated with ethyl acrylate **138** to yield, after hydrolysis of the intermediate enamine, the ketone **139** in 69% yield (Scheme 15).[61]



Scheme 15 Synthesis of protected lactams **141** and **142** starting from commercially available ketone **108**

It was proposed to synthesise the lactam **140** through convertion of the ketoester **139** into protected lactam **140** via a reductive amination reaction followed by a direct ring closure, which was tried with two different protecting groups. The first protecting group used was the para-methoxybenzyl (PMB) and therefore ketone **139** was treated with 4-methoxybenzylamine and $NaBH(OAc)_3$ and after stirring for 24 hours the desired bicyclic product **141** was clearly detectable and isolated in 61% yield (Scheme 15).[56] The second protecting group which was tested was the 3,4 dimethoxybenzyl (DMB), as it is known to be more easily cleaved due to the presence of the two electron donating methoxy groups and lactam **142** was obtained after treatment of ketoester **139** with 3,4 dimethoxybenzylamine and $NaBH(OAc)_3$ in 72% yield.

The next step was the deprotection of the protecting groups (PMB or DMB), the PMB deprotection was attempted using the DDQ standard conditions.[62] Unfortunately, none of the tested methods (table 1) to cleave the PMB group led to any conversion and the starting material could be isolated after work up as a pure compound, which led to the conclusion that the PMB protecting group was more stable than expected because of the lactam system. Known deprotection methods for example using TFA (neat, with anisole or in DCM), CAN, *p*-TsOH, $BF_3{\cdot}OEt_2$ or transfer hydrogenation conditions resulted in no deprotected product.

Table 1 Reaction conditions to cleave the PMB protecting group

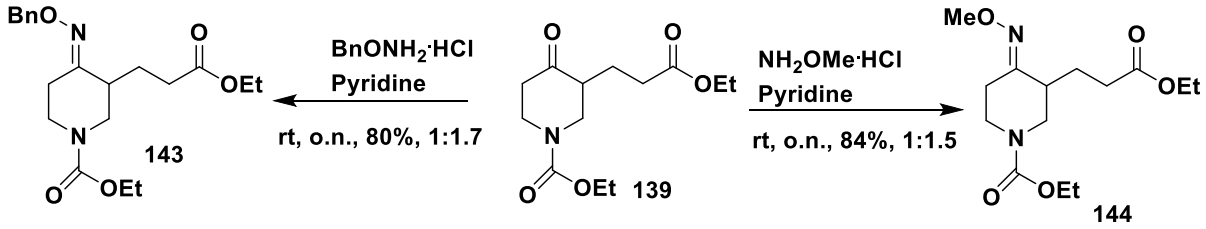
reagent	**solvent system**	**temperature**	**time**	**outcome**
DDQ	DCM/water 5:1	rt	o.n.	only starting material
TFA[63]	-	rt to 50°C	o.n.	only starting material
CAN[64]	AcN/water 3:1	rt	30 min	decomposition
TFA	DCM	50°C	o.n.	only starting material
p-TsOH[65]	toluene	reflux	o.n.	decomposition/starting material
$BF_3 \cdot Et_2O$[66]	Anisole	70°C	3h	only starting material
$Pd(OH)_2$, Ammoniumformate[67]	EtOH	rt	3h	only starting material
TFA	Anisole	rt	1h	only starting material

All attempts to cleave the 3,4 dimethoxybenzylgroup (Table 2) using DDQ, TFA or *p*-TSOH ended in a purple coloured reaction mixture, but also in the decomposition of the starting material.[68]

Table 2 Attempts to cleave the DMB protecting group

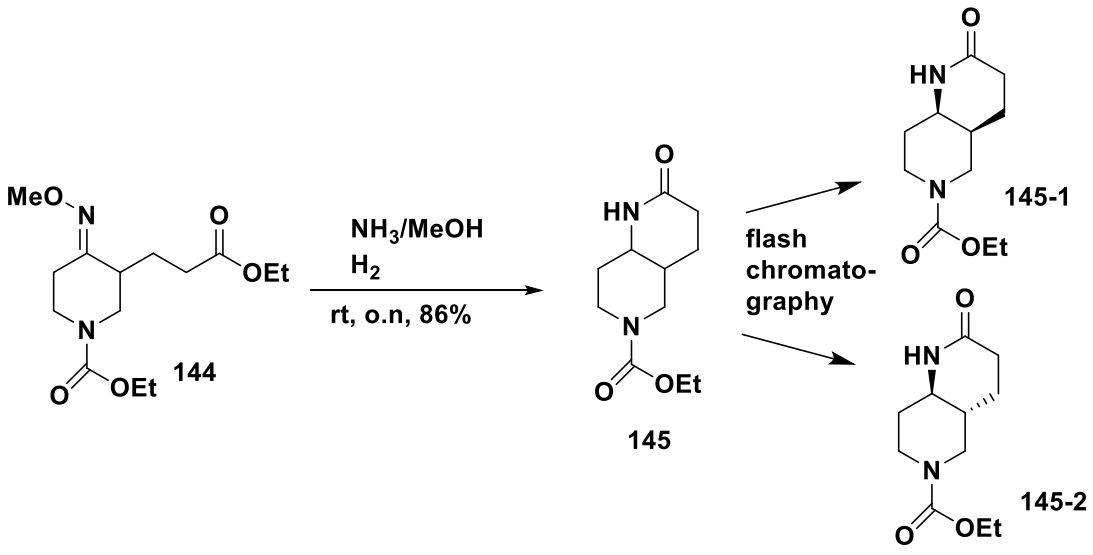
reagent	solvent system	temperature	time	outcome
DDQ	$CHCl_3$	rt	o.n.	UV active sideproducts
TFA	-	rt	o.n.	pink, decomposition
***p*-TsOH**	toluene	reflux	1h	decomposition, violet

After these unsuccessful attempts to cleave the protecting groups the ketone **139** was converted into the corresponding oximes using benzoylhydroxylamine hydrochloride and methoxyamine hydrochloride in pyridine to yield the benzyl protected compound **143** in yield of 80 % and the methoxy protected one **144** in 84 % yield[69] (scheme 16).



Scheme 16 Synthesis of oxime compounds **143** and **144**

Compound **143** was submitted for hydrogenation using Pd/C in 7N NH_3/MeOH and stirred overnight, but only a small amount of the product **145** could be obtained. The same reaction conditions were tried using compound **144** with the same outcome. Methoxime **144** was heated up to 40^{o}C with variation in time and pressure using the same hydrogenation conditions, but furthermore only a small amount (30 %) of product could be obtained. Compounds **143** and **144** were used to test the oxime cleavage using the borane-tetrahydrofuran complex (1M) at temperatures at -5°C, but without any success. Oxime **144** was furthermore treated with Pd/C only in methanol without any significant conversion and even adding $Mo(CO)_6$ didn't make any difference. Finally compound **144** was successfully hydrogenated using 7N NH_3 in MeOH with Raney Nickel catalyst to give the corresponding lactams which cyclized *in situ* (scheme 17).[70]



Scheme 17 Synthesis and separation of isomers of compound **145**

As the ring closure gave all four potential isomers (figure 33) of the lactam **145** (**145-1a**, **145-1b**, **145-2a** and **145-2b**) the diastereomers **145-1** and **145-2** of the cis- and trans- connected bicyclic rings could be separated through flash chromatography using 15% methanol in a

eluent system of ethyl acetate / petrol ether 10:1. For simplicity only one of the enantiomers of either the *cis*- or *trans*- isomers will be illustrated in the figures throughout the thesis.

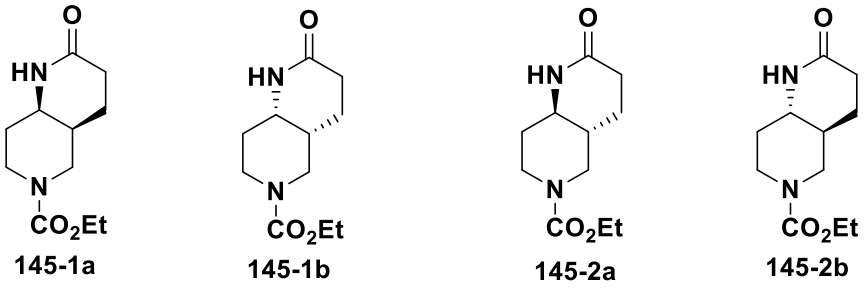


Figure 33 Illustration of all four possible isomers of compound **145**

After analysis of the 1D and 2D NMR experiments and NOESY experiments no clear assignment towards the *cis*- or *trans*- connected lactam could be made as the piperidine ring signals were shown to be once more overlapping. In figure 34 the NOESY spectra of the second isomer of compound **145** is shown, but no clear definition is assignable to the cis-isomer (H-2 and H-7 are coupling partners) as H-6 would as well couple with H-7. It was tried to crystallise compounds **145-1** and **145-2**, but no suitable crystals could be obtained.

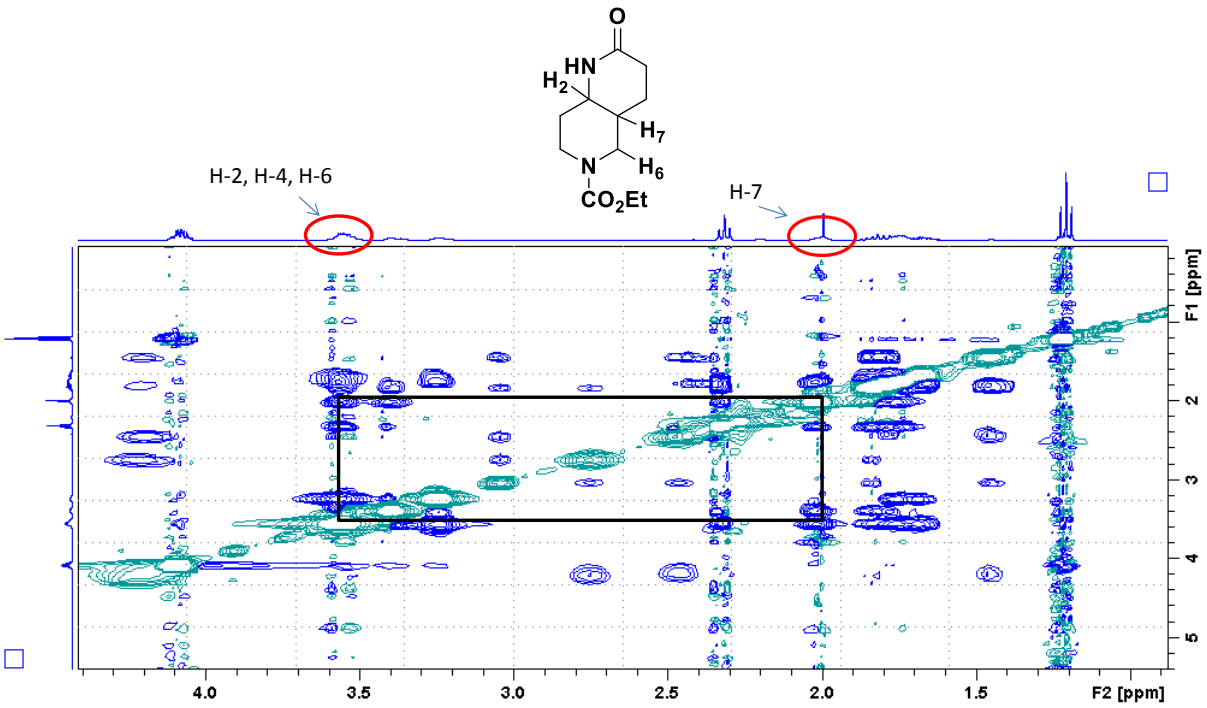
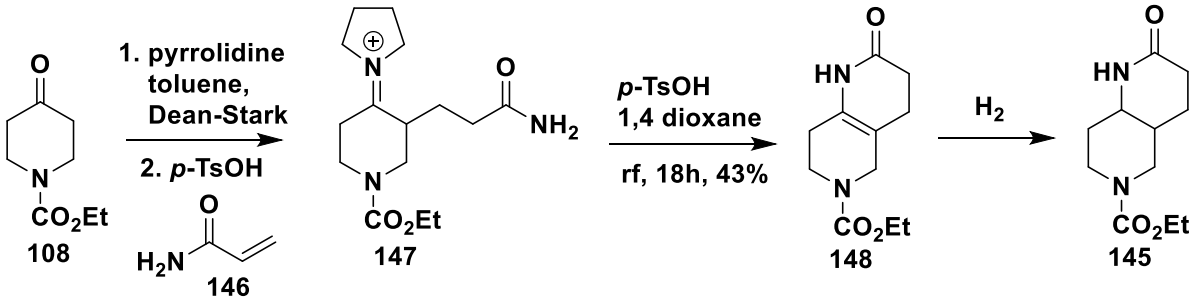


Figure 34 NOESY of second isomer of compound **145**

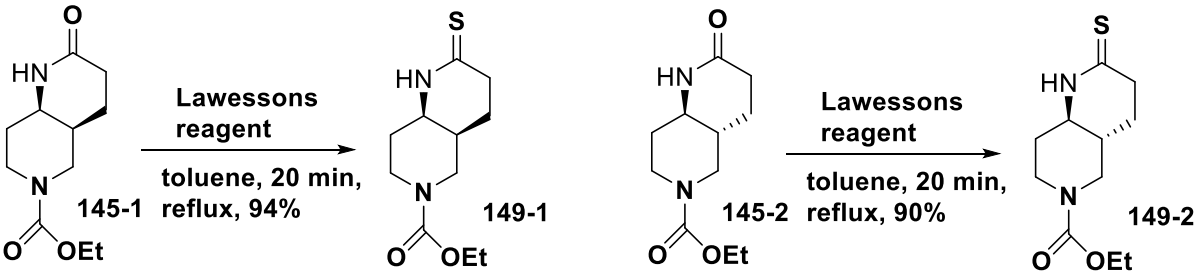
Another approach, which was reported in a patent by Gustafson *et al.*,[71] showed the direct introduction of the chiral centres at the fused bicyclic ring system starting again from ketone **108** (scheme 18)**.** Ketone **108** was treated with pyrrolidine in toluene under Dean Stark

conditions at 150°C, which resulted in a dark red mixture. *p*-Toluenesulfonic acid and acrylamide **146** were added to the mixture and heated for 4h. To the formed solid dioxane and p-toluenesulfonic acid were added and refluxed overnight to give lactam **148**. Unfortunately the conversion to the desired *cis*- lactam **145-1** resulted in a mixture or did not generate the lactam **145**.



scheme 18 Alternative synthesis of compound **145**

The next step was the conversion of the lactams **145-1** and **145-2** into the thiolactams **149-1** and **149-2** using Lawessons reagent[59] in an excellent yield of 90-94% (scheme 19).



scheme 19 Synthesis of thiolactams **149-1** and **149-2**

It was discovered that compound **149-1** was crystalline and suitable crystals could be formed by crystallising the compound in ethyl acetate/diethylether and after slow evaporation adding diisopropylether to the mixture. The X-ray crystallographic analysis showed the *cis*-connection of the bicycles and therefore the other isomer could be assumed to be the *trans*-fused lactam **145-2** (figure 35).

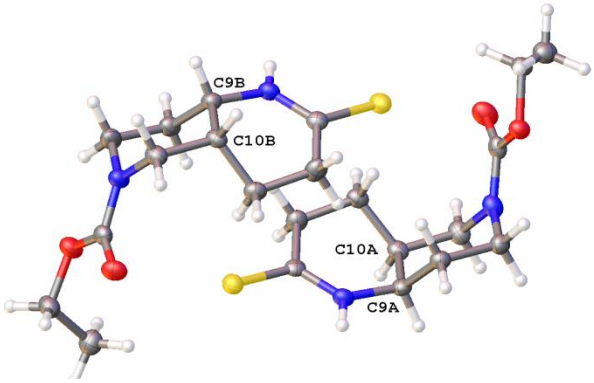


Figure 35 The molecular structures of the two rotamers of **149-1**. Displacement ellipsoids are drawn at the 50% probability level.

Thiolactam **149-1** showed two molecules in the asymmetric unit related by a noncrystallographic axis of rotation, although they have different conformations of the carbamate chain (figure 35). The overall packing of the crystal appears to be driven by the interaction of the carbamate and the lactam groups (figure 36). The crystal structure showed typical C-S bond lengths of 1.679 (2) and 1.686 (3) A° for the molecules with atom labels A and B, respectively. The piperidine ring adopts a chair conformation with the carbamate group in an equatorial position, with C5-N6-C11 angles of [119.3 (2)/ 21.5 (2)] and C7-N6-C11 angles of [123.5 (2)/123.8 (2)] for molecules A/B, respectively. The torsion angles N1-C9-C10-C4 [46.2 (3)/ 46.8 (3)], C8-C9-C10-C4 [-76.4 (2)/76.8 (3)] and C8-C9-C10-C5 [49.2 (3)/ 48.9 (3)] are all synclinal, and from the torsion angles N1-C9-C10-C5 [171.73 (19)/ 172.60 (19)] and the resulting antiperiplanar conformation it can be seen that the H atoms are arranged in a gauche conformation, giving rise to the chair-like conformation of the piperidine ring and the synclinal orientation of atoms H9 and H10.[58]

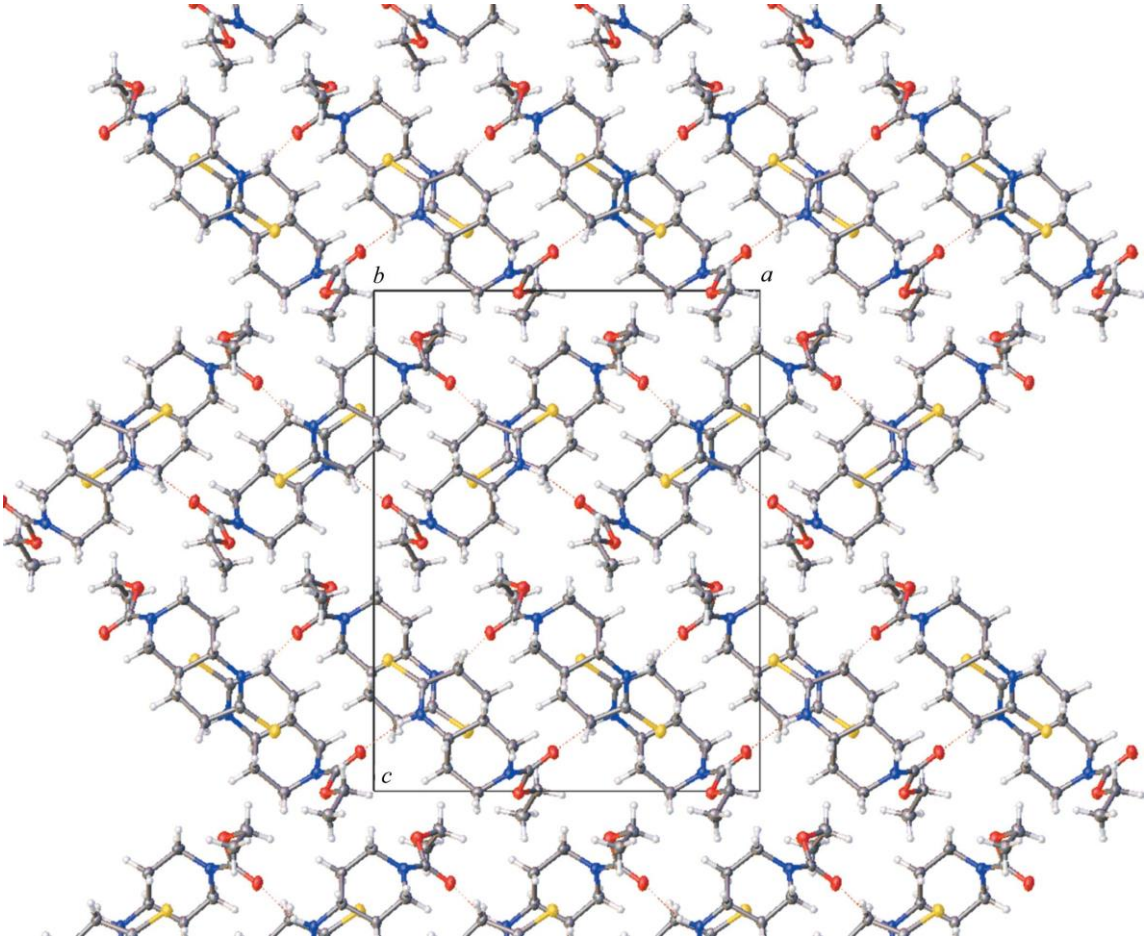
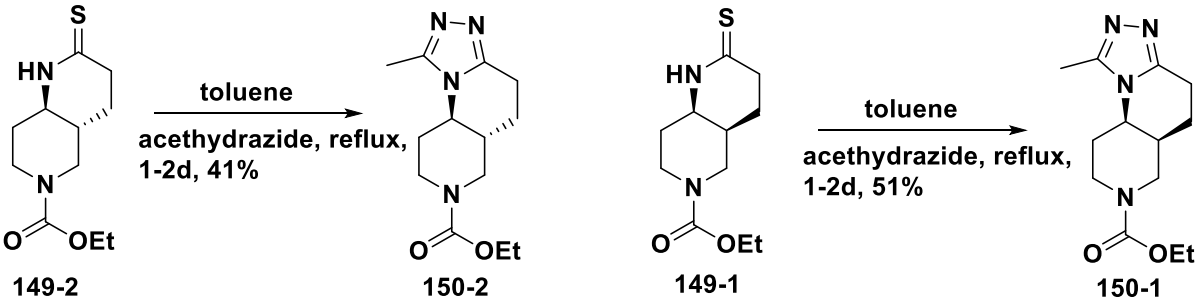


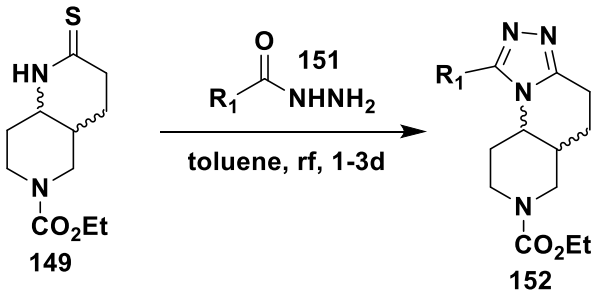
Figure 36 The herringbone packing of isomer **149-1** in the *bc* plane

In the following step, the ring closure to the triazole needed to be carried out to form the tricyclic scaffold. This conversion of thiolactam **149** into the scaffold compound was tested using the corresponding hydrazide to form the triazole ring[72] (scheme 20). As for the [6.5.5] scaffold system the literature known approach using cyclohexanol as a solvent was not feasible as no method was found to remove all the cyclohexanol from the reaction mixture. To accomplish the formation of the triazole three different solvent systems were used, which were namely ethanol, toluene and a mixture of acetonitrile and acetic acid and as hydrazide component acethydrazide **127** to start with. The reactions were checked by mass spectrometry. Using toluene as well as the acetonitrile/acetic acid approach delivered a product peak in MS, but only the toluene attempt gave only the product peak after stirring at reflux for 2 days and the crude NMR showed the methyl signal and all characteristic signals for the triazole **150**. Both isomers *cis*- and the *trans*- of thiolactam **149-1** and **149-2** were finally converted into the tricyclic triazole system **150-1** and **150-2**.



scheme 20 Synthesis of triazole compound **150**

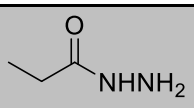
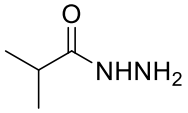
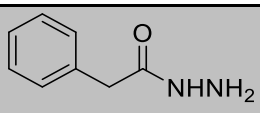
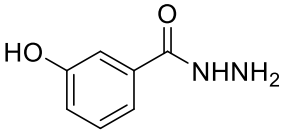
The purification of this methyl substituted triazole **150** was found to be challenging as the product is neither UV active nor stainable in any of the detection reagents (PMA, ninhydrin, $KMnO_4$). After some eluent changes it turned out that a solvent system of 10% MeOH in DCM was the most suitable for flash chromatography to yield both compounds **150-1** and **150-2**, which are visible after iodine treatment for a short time as a brown spot, which disappears very quickly after staining. Using this ring closure method several triazoles were synthesized in yields from 37%-84% (scheme 21, table 3).



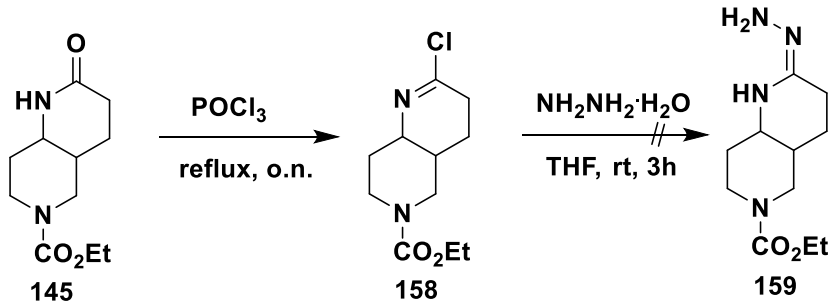
scheme 21 General synthesis of triazole **152** formation

Table 3 Triazole residues and corresponding hydrazides **151**

R_1	hydrazide	yield (cpd)	
methyl	**127**	cis: 51% (**150-1**)	trans: 41% (**150-2**)
trifluoromethyl	**151-1**	80% (**170-1**)	37% (**170-2**)

ethyl	 **151-2**	60% (**171-1**)	84% (**171-2**)
iso-propyl	 **151-3**	75% (**155-1**)	30% (**155-2**)
benzyl	 **151-4**	54% (**156**)	-
3 hydroxyphenyl	 **151-5**	„84%“ (mix with **151-5**) (**157**)	-

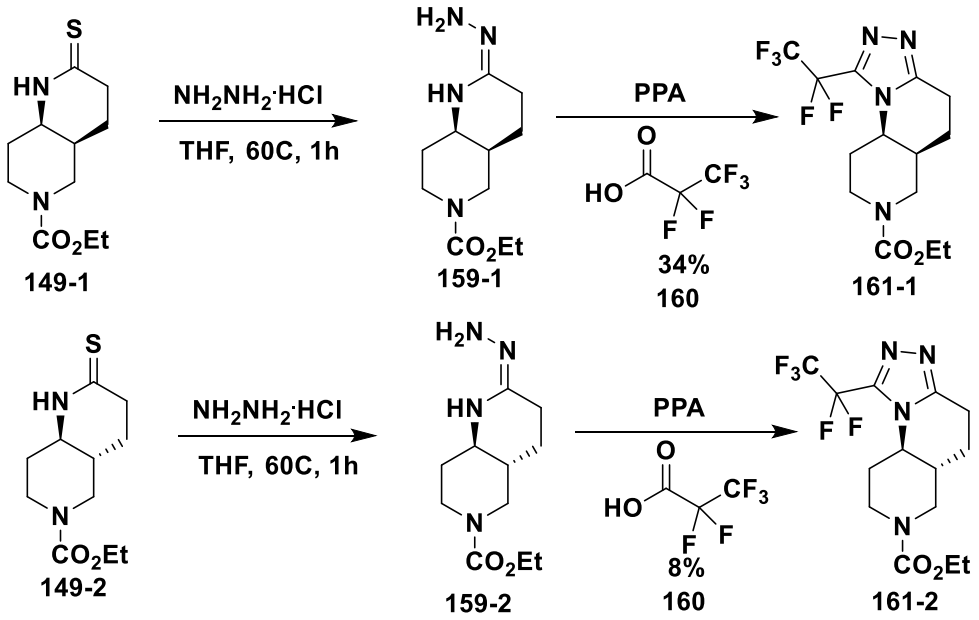
To install the -CF_2CF_3 as the side chain group on the triazole this conversion was tried using the lactam **145** which was converted into the chloroimine **158** using $POCl_3$ under refluxing conditions followed by the treatment with hydrazine hydrate, which did not result in desired hydrazine **159** (scheme 22).



scheme 22 First synthesis route towards hydrazine **159**

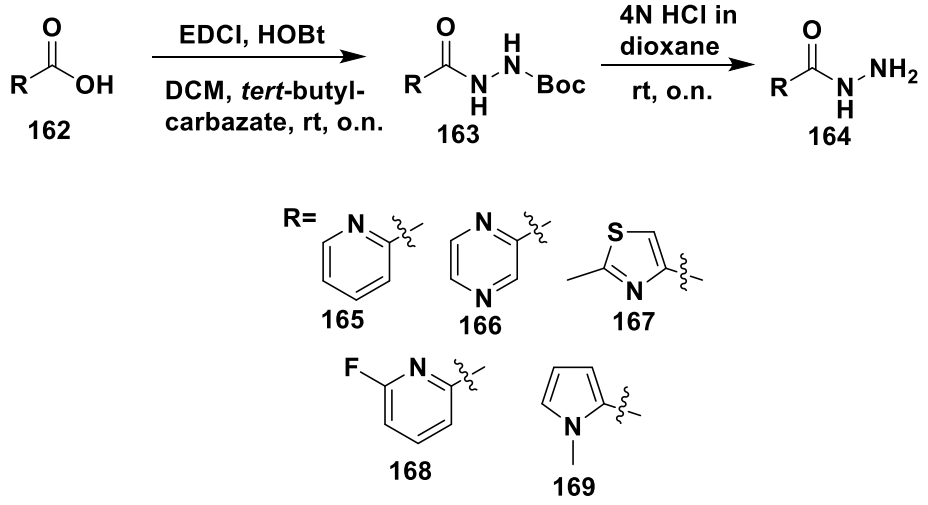
Thereafter another approach was used starting with thiolactam **149** followed by the conversion into hydrazine **159** using $NH_2NH_2{\cdot}H_2O$ in THF at 60°C, which changed the reaction mixture colour to yellow or dark greenish.[73] This hydrazine **159** was used crude and treated with pentafluoropropionic acid and polyphosphoric acid boiling at 150°C for 3 days to install the CF_2CF_3 side chain group.[74] The relative low yield is in agreement with known literature procedures and could be due to the harsh reaction conditions of the

pentafluoropropionic acid in a mixture with polyphosphoric acid which results in a very messy work up and the hydrazine **159** is used further crude (scheme 23).



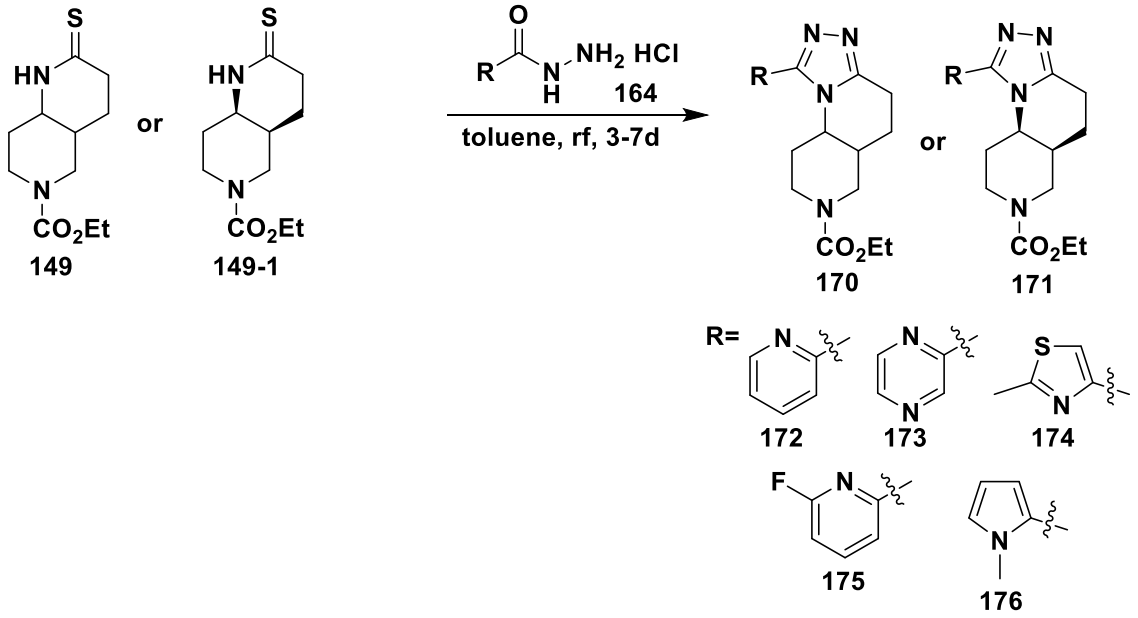
scheme 23 Synthesis of triazoles **161-1** and **161-2**

Further triazoles were synthesized containing heterocyclic side chain groups, which were synthesized as the racemate and in pure *cis*- geometry. The hydrazide component was synthesized starting with the corresponding acid **162** which was treated in an amide coupling reaction using *tert*-butylcarbazate to introduced the hydrazide functionality, followed by the cleavage of the Boc protecting group using 4M HCl in dioxane (scheme 24) to yield hydrazides **165-169**.[75]



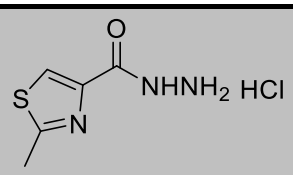
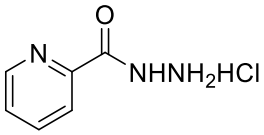
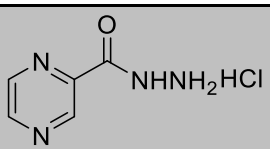
Scheme 24 Synthesis of hydrazide component **164**

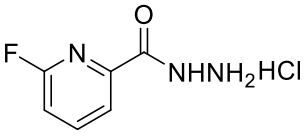
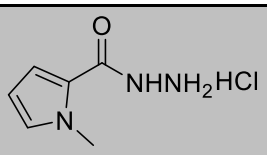
These hydrazides were reacted (scheme 25, table 4) using the racemic thiolactam **149** and the cis- fused thiolactam **149-1** to generate the triazole compound with the heterocyclic ring side chains which required longer reaction times than the previously used commercial available hydrazide **127, 151-1-151-5**, which is maybe due to the fact that the hydrazides **165-169** are HCl salts.



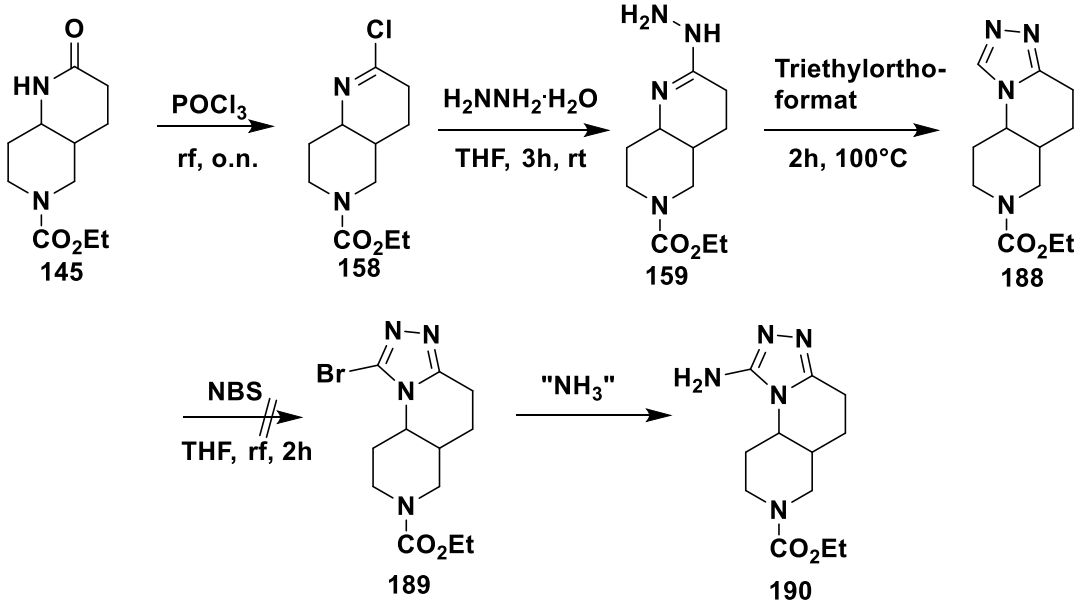
scheme 25 Synthesis of triazole compounds **170-176**

Table 4 Heterocyclic triazole compounds **172-176**

R_1	Hydrazide	Yield (*cis*)
2-methyl thiazole	 **165**	75% (**174**)
pyridyl	 **166**	31% (**172**)
pyrazinyl	 **167**	33% (**173**)

2-fluoropyridyl	 **168**	25% (**175**)
***N*-methyl-pyrrole**	 **169**	25% (**176**)

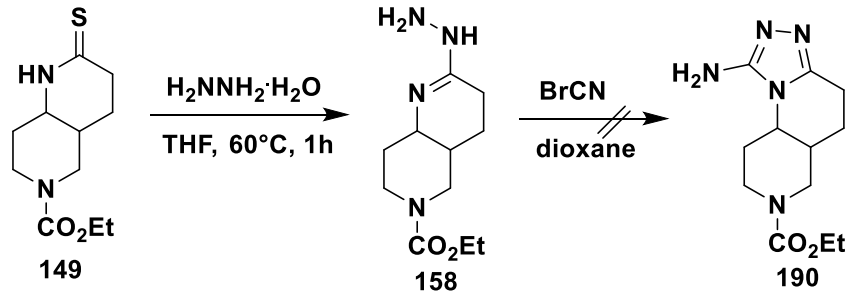
Further approaches towards different side chain groups of the newly synthesized tricyclic triazole were attempted. The first was the introduction of an aminofunction **190** (scheme 26). This approach followed two different methods. The first method was to synthesize the bromotriazole **189** using *N*-bromosuccinimide followed by amination to aminotriazole **190**.[76] This approach started with lactam **145** which was in 3 steps converted into triazole **188.** Triazole **188** was only detectable as the dimer in the mass spectrum and the compound showed a violet colour. This route was not accomplished due to the unsuccessful synthesis of bromotriazole **189** intermediate. (scheme 26)



scheme 26 Planned synthesis to amino compound **190**

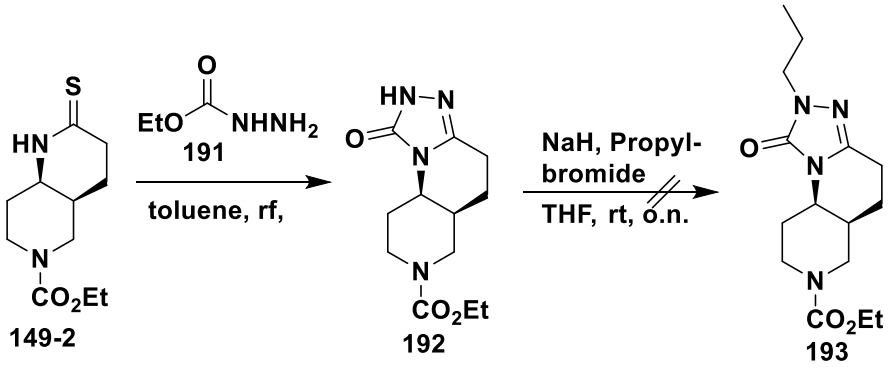
The second approach to form the aminotriazole **190** was carried out using a method starting from thiolactam **149**, which could be directly converted into hydrazine **159**. It was hoped that

the hydrazine **159** when treated with cyanogen bromide would form the aminotriazole **190**,[75] however, this route proved unsuccessful in a test scale (scheme 27).



scheme 27 Planned synthesis of compound **190** using cyanogenbromide

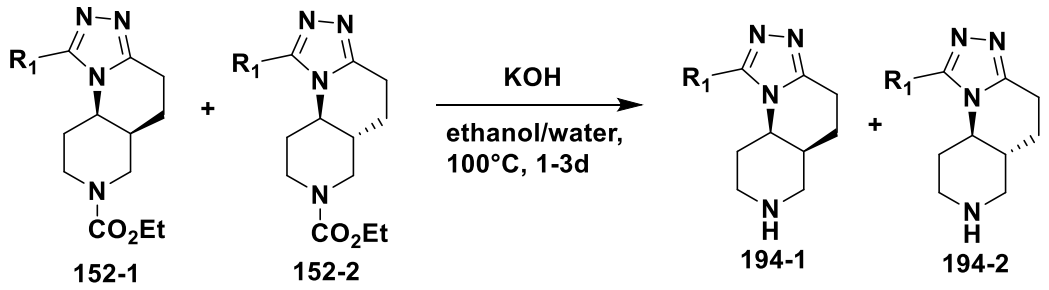
A further approach was made to synthesise the triazolone **192** through using the same method previously used for the synthesized triazoles such as **150**. Product **192** could only be obtained in a small amount as an inseparable mixture with the starting reagent, the ethylcarbazate **191**. The triazolone **192** was alkylated following a procedure published by Piao *et al.*.[77] However, no conversion to the alkylated ketotriazole **193** was achieved which was thought to be as the starting material **192** was not available in a pure form (scheme 28).



scheme 28 Synthesis route to alkylated triazolone **193**

The next step was the cleavage of the ethoxycarbamate group which was tried using an acidic as well as a basic approach. The acidic approaches using 6N aqueous HCl under refluxing conditions and 4N HCl in dioxane were not successful.[78] The basic attempt using 5M aqueous sodium hydoxide was shown to be successful as a solid was formed that showed the desired mass spectrum for the product, but unfortunately the compound could not be isolated. Therefore another basic reaction condition was tested using KOH as base in a mixture of EtOH and water as solvents under refluxing conditions.[79] This turned out to be the best method as it delivered the full conversion into the desired amine **194**. All synthesized

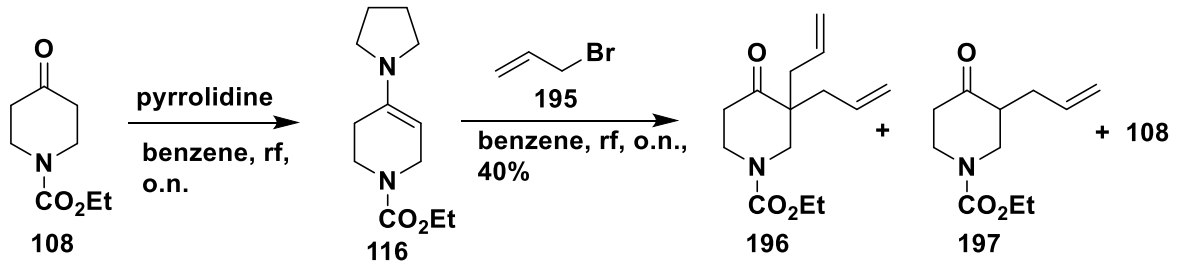
triazoles of the type as compound **152-1** and **152-2** (scheme 29) were treated following the procedure and each *cis*- and *trans*- isomer was treated separately.



scheme 29 Final cleavage of the carbamate group to amines **194-1** and **194-2**

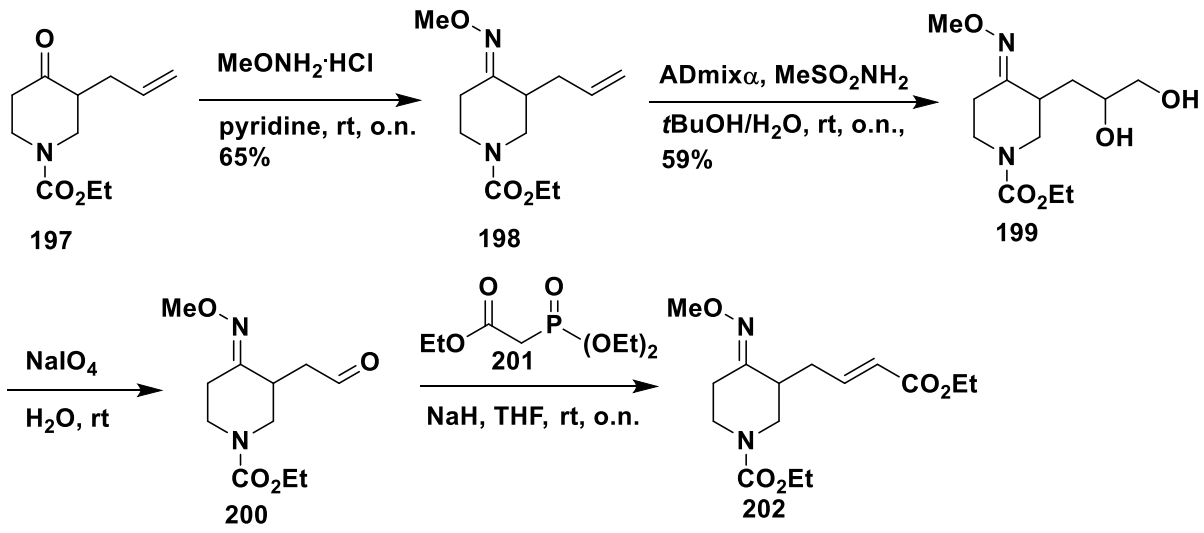
3.3 Synthesis of [6.7.5] triazole scaffold

The synthesis of the [6.7] connected bicyclic lactam started as for all previous synthesized scaffolds with ethyl-4-oxopiperidone-1-carboxylate **108**, which was alkylated using allyl bromide **195**. This was carried out under standard Dean Stark conditions using pyrrolidine to form enamine **116.** The conversion delivered a mixture of dialkylated product **196**, alkylated product **197** and starting material **108** which could be separated through flash chromatography. The desired allylated product **197** was synthesised in 40% yield (scheme 30).



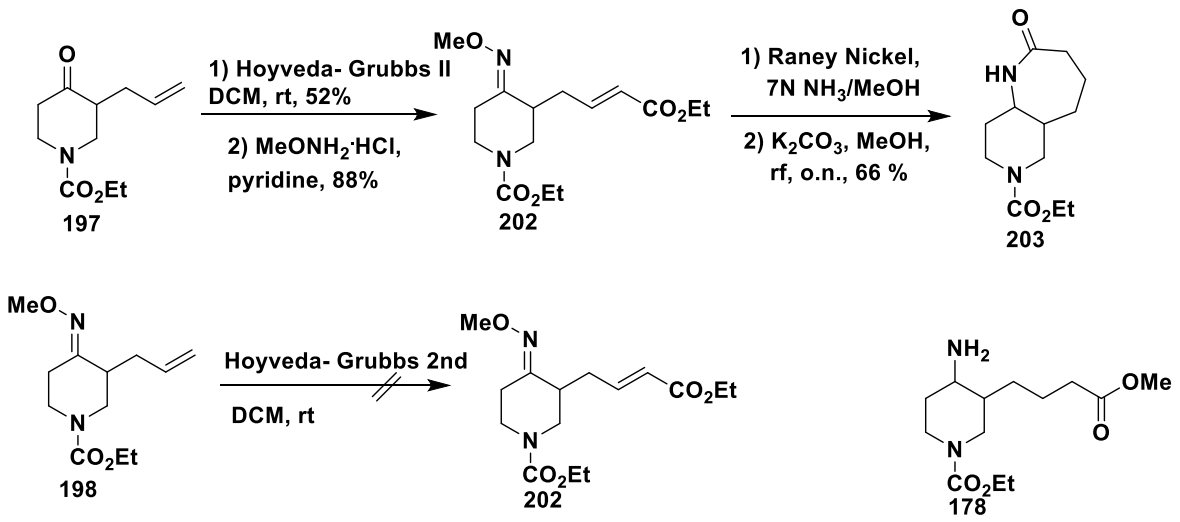
scheme 30 Synthesis of allyl compound **197**

The next step was the conversion to the methoxime **198** as previously carried out to form the [6.6] membered scaffold, which was carried out using methoxyamine hydrochloride in pyridine in 65% in a ratio of 1:4 followed by the diol formation using a Sharpless dihydroxylation.[80] The Sharpless dihydroxylation was carried out using AD mix α, $MeSO_2NH_2$ in *tert*-butanol and water to yield diol **199** in 59% (scheme 31).



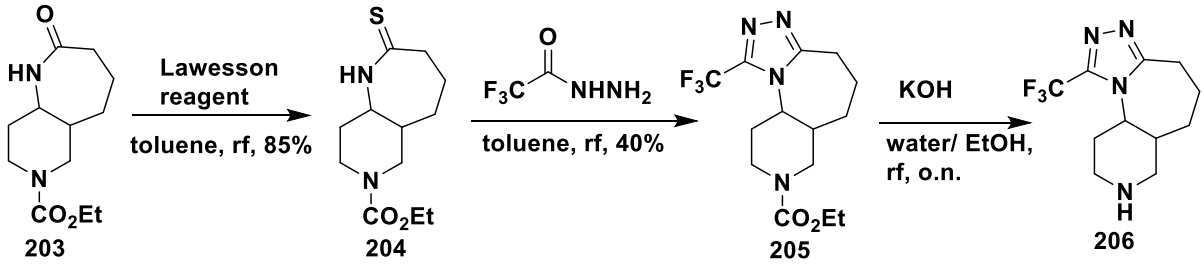
scheme 31 First approach towards compound **202**

The diol **199** was cleaved using $NaIO_4$ in water to yield aldehyde **200** followed by conversion through a Horner Wadsworth Emmons (HWE) reaction to yield ester **202** (scheme 31).[81] The aldehyde **200** was obtained in a mixture of 1.5:1 (methoxime protons: aldehyde protons) which is probably due to the harsh reaction conditions associated with sodium periodate. The HWE reaction did not deliver a clean product, the proton NMR showed an excess of phosphonate **201** which was not separable from the desired ester **202**, which led to the failure of the ring closing attempt using Raney nickel in 7N ammonia/ methanol to yield the [6.7] connected lactam **203** (scheme 32). One attempt was made using Pd/C in 7N ammonia in methanol, but no [6.7] connected lactam was yielded. Another approach was to synthesise ester **202** using a metathesis reaction to generate the double bond. The metathesis was carried out using Hoyveda Grubbs catalyst II in dichloromethane with the ketone **197** as well as methoxime **198** (scheme 32).[82]



scheme 32 synthesis of lactam **203** following a cross metathesis approach

The ketone **197** delivered ester **202** in 52% yield, however, the conversion of the oxime **198** to the desired ester **202** did not take place. The ester **202** was treated with Raney Nickel in 7N ammonia in methanol to yield amine **178**, which was directly converted into bicyclic lactam using potassium carbonate in toluene at 130^{o}C. This conversion proved slow and after 4 days only 30 % of the desired bicycles **203** was yielded. This bicycle **203** was treated with Lawesson's reagent in toluene to yield thiolactam **204** in 85% yield. Both conversions showed only one spot on TLC but the NMR showed a clear mixture of compounds. The next step was the conversion to 1, 2, 4 triazole using trifluoroacetic acid hydrazide under reflux in toluene to yield triazole **205** in 40 % yield. Final deprotection using potassium hydroxide in a water/ethanol mixture delivered amine **206** (scheme 33).

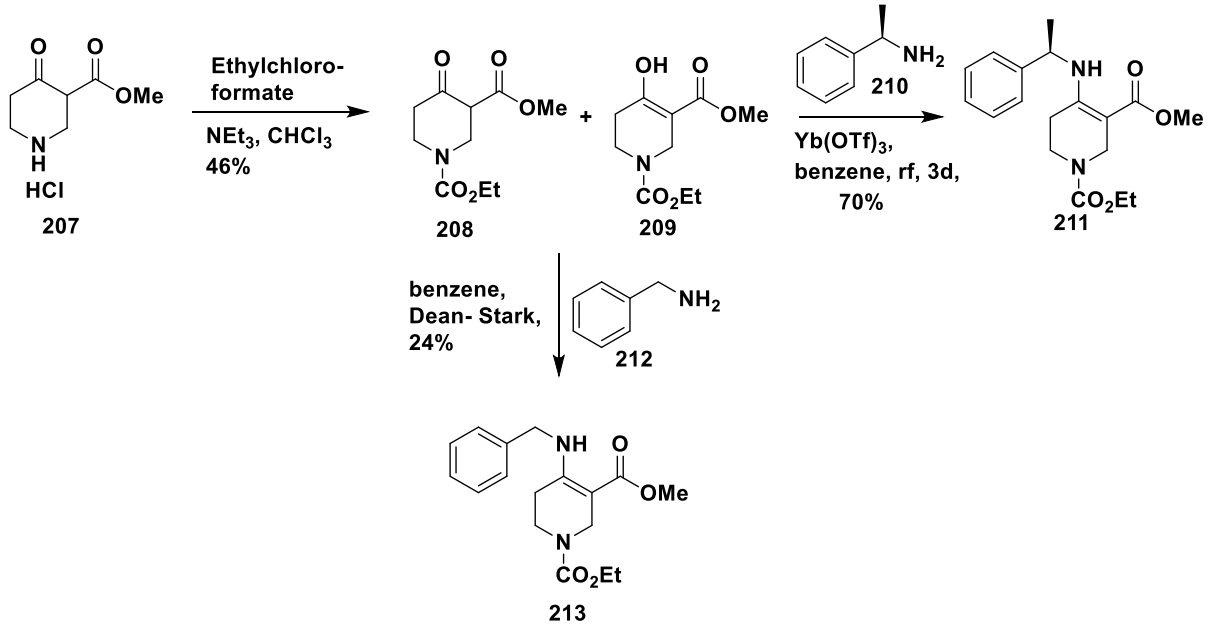


scheme 33 Synthesis of tricyclic triazole **206**

3.4 Synthesis of Heterocyclic second ring

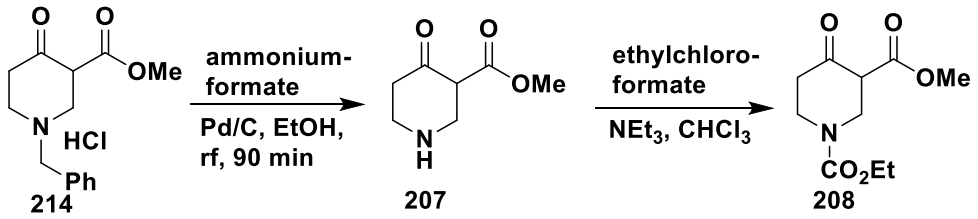
The synthesis to install a heterocyclic atom in the second attached ring started with commercially available ketoester **207**, which was protected using ethyl chloroformate to yield the ethoxycarbamate **208** and its enolic form **209** in 46% yield. The mix of **208**/**209** was treated using two different amines (**210**/**212**) to install the amine functionality- the chiral

approach using α methylbenzylamine **210** has the advantage that the absolute chiral information is directly incorporated into compound **211** (scheme 34). This approach was followed a procedure published by Duan *et al*.[83]



scheme 34 Starting sequence towards the synthesis of heterocyclic tricyclic scaffold

Alternatively another approach was started to yield carbamate **208** which used benzyl protected piperidone **214** as starting material. The first step was the deprotection of the benzyl group in a transfer hydrogenation reaction using ammonium formate and Pd/C in ethanol,[84] followed by protection to the ethoxycarbamate **208** using the same conditions as for the conversion of compound **207** (scheme 35)**.**

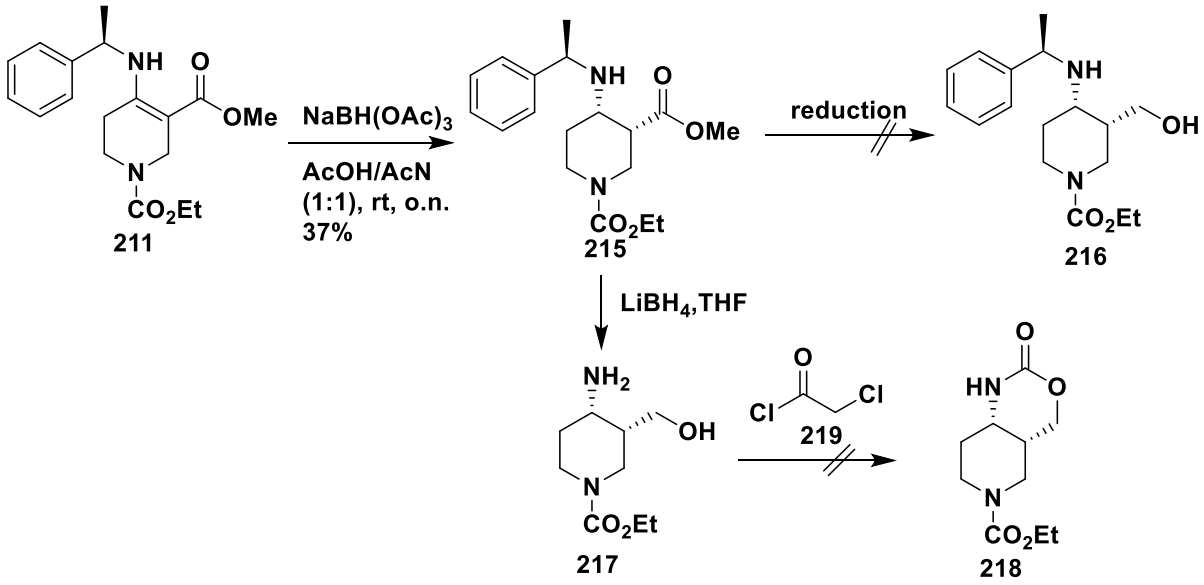


scheme 35 Alternative synthesis route towards ketone **208**

The approach in scheme 35 resulted in an impure outcome and unsatisfying yield of compound **208.**

The next step was the reduction of the formed enamine double bond between the nitrogen and the oxygen containing carbon atoms. This reduction was tested using a literature procedure described by Duan using $NaBH(OAc)_3$ in a mixture of AcOH/ AcN (1:1).[83] The product was

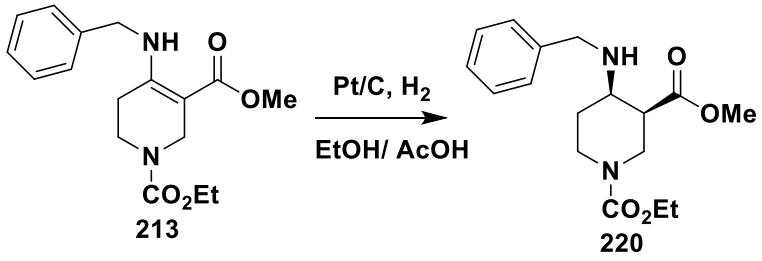
seen through the mass peak but the NMR was not clearly assignable and the isolated amount yielded not higher than 30% (scheme 36). The stereochemical outcome was reported several times in literature to be *cis*. The absolute *cis*- configuration should be introduced due to the before installed chiral center using α methylbenzylamine **210**. Nevertheless the amount yielded was tested further to establish a route towards heterocyclic compound **218.**



scheme 36 Planned and tested route towards heterocyclic compound **218**

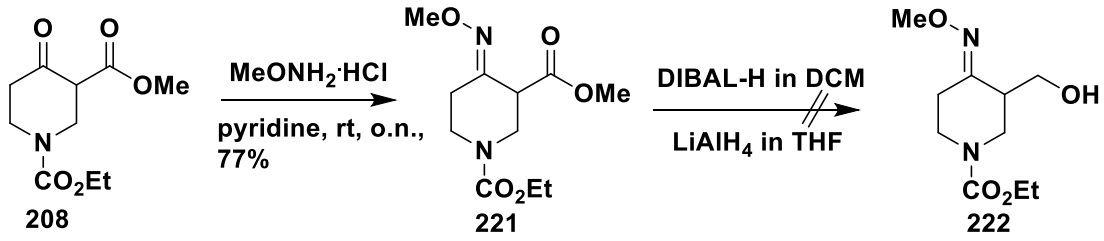
The reduction to alcohol **216** was more challenging than expected and none of the tested approaches ($LiAlH_4$, DIBAL-H) delivered a satisfying outcome and in most cases only the starting material **215** was recovered. Lithium borohydride was the only reagent, which reduced the ester function, but did not deliver a reliable outcome as one attempt directly cleaved the amine protecting group, which was not reproducible. Nevertheless the small amount of the double deprotected product **217** was used in a test reaction towards the desired oxygen containing heterocyclic ring **218** using chloroacetylchoride **219**, which showed the desired mass, but no product could be isolated (scheme 36).

In the meantime another approach starting with compound **213** was tested using Pd/C or Pt under hydrogenation conditions to receive the reduction of the enamine double bond yielding in a *cis*- stereoselectivity and yielded compound **220** in 3% yield. In this approach the stereochemical outcome could only be predicted to be the *cis*- compound but no absolute assignment was possible as no defined stereo centre is included (scheme 37).



scheme 37 Another approach using compound **213** to reduce the enamine double bond

As the reduction turned out to be difficult a racemic approach was started using compound **208**, which was converted into oxime **221** in 77% and the ester reduction was attempted using DIBAL-H or $LiAlH_4$, but neither of the approaches resulted in the desired reduced product **222** (scheme 38).



scheme 38 Approach towards a racemic compound **222**

The approach towards the synthesis of the heterocyclic compound **220** was stopped at this point as it took more time than expected without useful and reliable results and the focus had to be on the chiral synthesis of the tricyclic scaffold (explained in chapter 3.5). As the chiral approach is based in some attempts on the heterocyclic approach it probably can be applied in the future to get an easy access to the heterocyclic scaffold.

3.5 Chiral synthesis of bicyclic compounds

All so far synthesized bicyclic lactam systems **145** as well as all tricyclic triazole compounds **152** consist of both enantiomers of each *cis*- or each *trans* isomer (Figure 37).

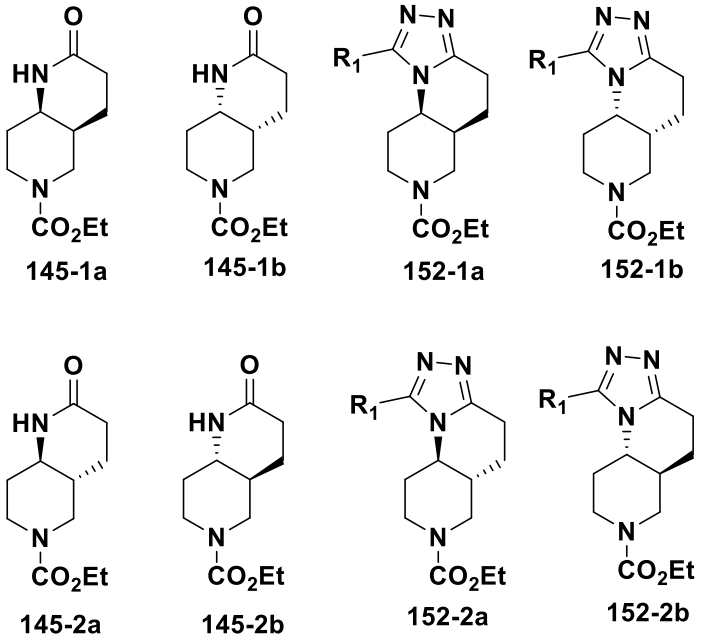
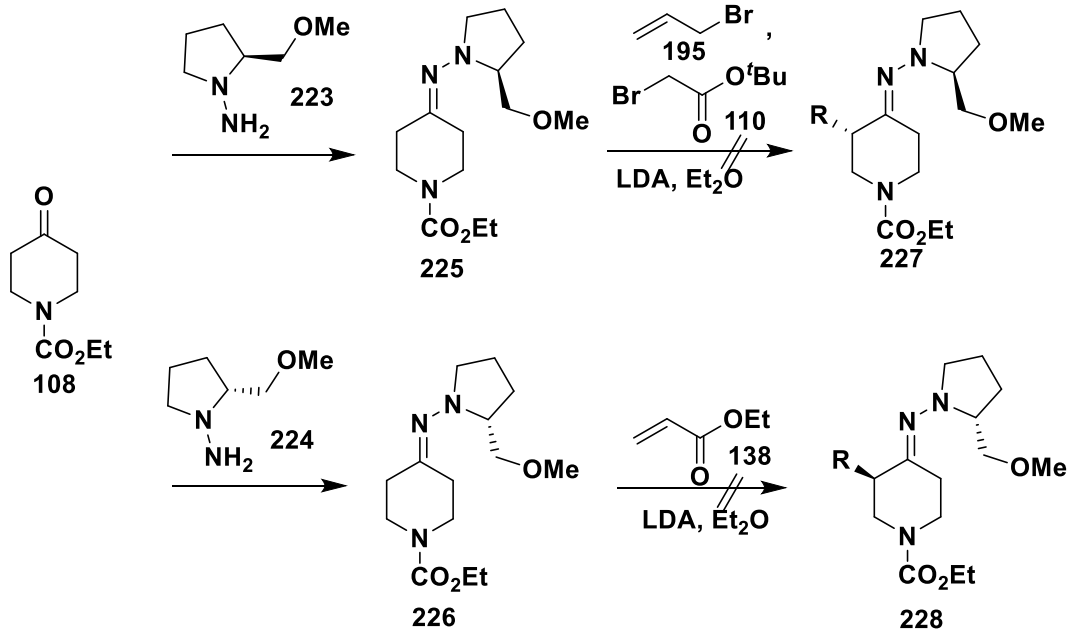


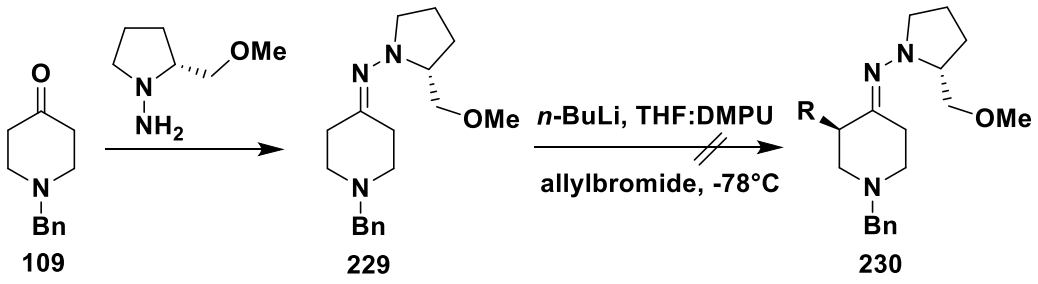
Figure 37 All possible enantiomeric forms of the bicyclic and tricyclic compounds

Therefore, a chiral synthesis of the bicyclic compounds **145-1 and 145-2** is crucial to accomplish the synthesis of a single enantiomeric compound. According to the literature, the only reliable route to install a single chiral center in the α-position to a keto functionality is the Enders alkylation method using (depending on the required isomer) the chiral auxiliaries SAMP ((*S*)-1-amino-2-methoxymethylpyrrolidine) **223** or RAMP ((*R*)-1-amino-2-methoxymethylpyrrolidine) **224**, which are commercially available (scheme 39). The first step was the conversion of the known ethyloxo-piperidone carboxylate **108** into hydrazones **225** and **226,** illustrating the two possible chiral compounds using both Enders chiral auxiliaries.[85] This conversion was carried at 60°C to yield both hydrazones **225** and **226** in an assumed yield of 100%, which were used crude due to their reported instability on silica. The conversion of hydrazones **225** and **226** into alkylated compounds **227** and **228** was tested using the standard reaction conditions described by Enders by treating hydrazones **225** and **226** with LDA *in situ* for deprotonation in α-position to the carbonyl function of compounds **225** and **226.**[86] The alkylation was tested using both hydrazones **225** and **226** with several alkylating agents (*tert*-butylbromoacetate **110**, allyl bromide **195** and ethyl acrylate **138**), but unfortunately none of the alkylating reagents gave any desired product. This was expected for *tert*-butyl bromoacetate **110** and ethyl acrylate **138** because of the electron withdrawing groups present in the reagents. Surprisingly allyl bromide **195,** known as a good electrophile did not show any conversion at the low temperature (-78°C), which was needed for stereoselectivity in the Enders alkylation (Scheme 39).



Scheme 39 Synthesis route using Enders chiral auxiliaries SAMP **223** and RAMP **224**

Another attempt using the Enders alkylation approach was carried out using ketone **109** to form hydrazone **229**, which was tested by alkylation using allyl bromide **195** following a procedure by Horenstein *et al.*,[87] which seemed to form the allylated product **230**, but only in low yield. The main issue with this publication is the reliability of the diastereoselectivity of the reaction as it was reported as an assumption. Therefore this synthesis route was not progressed due to the unsuccessful outcome of the alkylation step (Scheme 40).

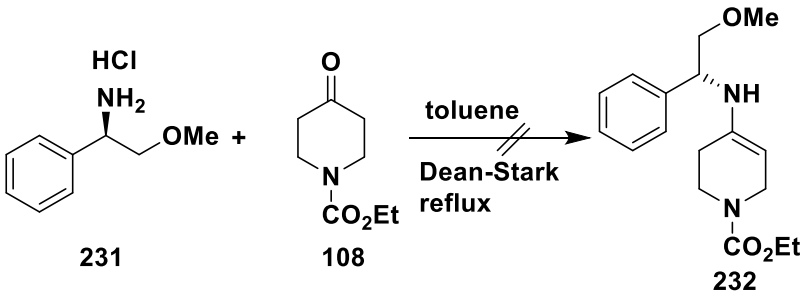


Scheme 40 Synthesis route to allylation product **230**

The same reaction conditions were tried using hydrazone **225** but without obtaining any allylated product.

The next attempt was carried out by following the procedure of Meyers *et al.* who used amine **231** as the chiral auxiliary.[88] Unfortunately, the condensation of amine **231** with ketone **108** didn't proceed to imine **232** under the reported conditions using a Dean Stark trap (Scheme

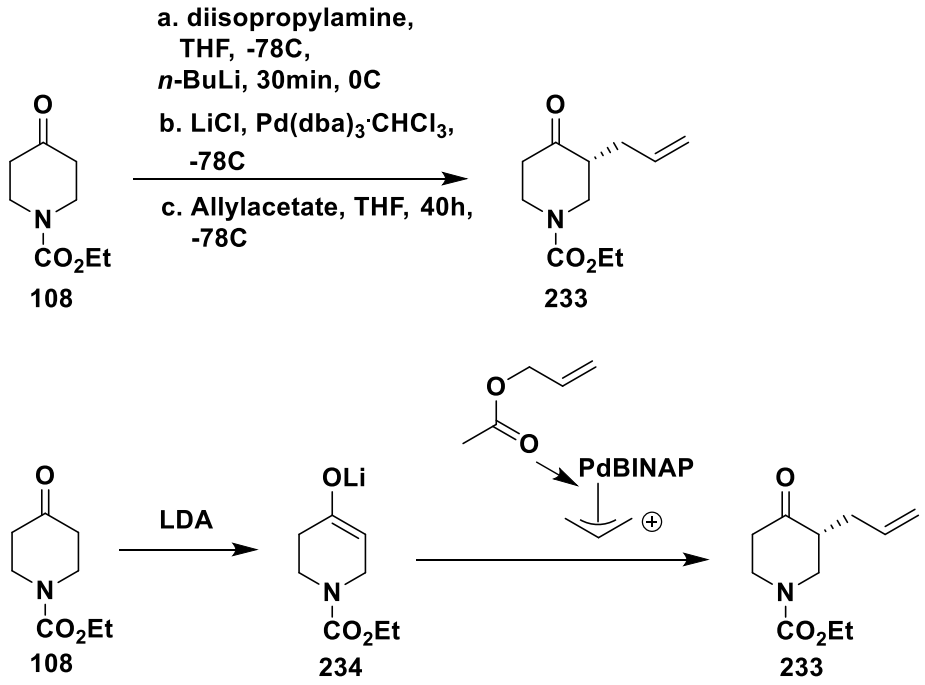
41). Even the condensation using the free base, which resulted from treating **231** with triethylamine, didn't deliver any product **232**. Therefore this approach was abandoned.



Scheme 41 Condensation attempt to compound **232**

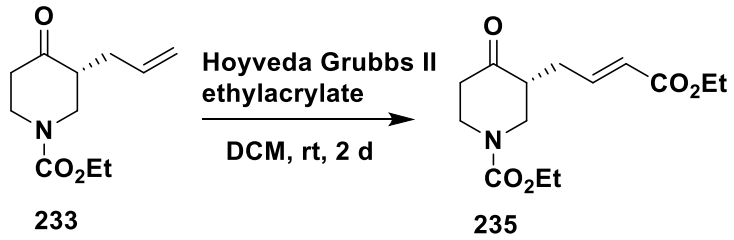
In 2005 the group of Meier reported a stereo selective allylation approach of cyclic ketones in high enantiomeric excess.[89] This attempt using ketone **108** yielded in a clean allylation product **233** after stirring the reaction mixture at -78°C for 40h using allyl acetate **256** and a mixture of $Pd(dba)_3{\cdot}CHCl_3$, LiCl and *(R)*-BINAP (scheme 42). The deprotonation was achieved using *in situ* generated LDA at 0°C. The major difficulty was to maintain the constant low temperature as no equipment to carry out reactions at -78°C over a longer period of time is available in the medicinal chemistry laboratories. As the low temperature was reported to be crucial for high enantioselectivity, this was a major concern regarding the stereoselective outcome of this allylation reaction (Scheme 42).

The stereoselective outcome of the reaction was proposed to be the result of a mechanism over a Pd- allyl complex intermediate (Scheme 42). The nucleophile was prepared using LDA to deprotonate ketone **108**, which forms the lithium enolate species **234**. The enantioselectivity in this example was introduced through a chiral BINAP ligand which was used to generate a complex with palladium and allyl acetate **256**. This complex allows the nucleophilic attack of the lithium enolate **234** from the least hindered side, which should result in the highly enantioselective product **233**. Unfortunately, the determination of the enantiomeric excess for the reaction was not straight forward. Therefore, the product **233** was converted into a diastereomeric mixture to confirm the *ee* of the synthesized compound (Scheme 43).



Scheme 42 Synthesis of compound **233** and suggested reaction mechanism by the group of Meier

Compound **233** was further converted following the [6.7.5] scaffold route to form the diastereomeric compound **235,** which would allow the determination of the enantiomeric excess. Therefore, compound **233** was treated with Hoyveda Grubbs catalyst and ethyl acrylate **138** to synthesize compound **235** (Scheme 43)**.**



Scheme 43 Synthesis of α. β– unsaturated ester **235**

Unfortunately, this approach towards compound **235** didn't give any evidence regarding the stereoselective outcome of compound **233**. It was clearly detectable that only the *E*-double bond was formed, but no clarification of the enantiomeric excess of compound **233** was possible.

A chiral shift reagent approach was followed to estimate the enantiomeric purity of compound **233.** Three chiral shift reagents were tested to determine the enantiomeric excess by splitting and shifting the proton NMR signals by first investigating racemic allylated product **197**, followed by product **233**. The chiral shift reagents are lanthanide-based

compounds, which were in the past frequently used in organic synthesis to determine the enantiomeric purity of a synthesized compound. Through their paramagnetic properties the chiral shift reagent is able to increase the magnitudes in the resulting shift differences ($\Delta\ \delta$). These shift differences are larger than with, for example, diastereomeric auxiliary compounds. The principle behind this method is that the lanthanide complex can coordinate to the Lewis base centre of the compound (**233** or **197** in our case), which results in a magnetic interaction between the lanthanide complex and the nearby protons, which induces an anisotropic magnetic field next to the lanthanide. Through this anisotropic magnetic field of the chiral shift reagent, the protons in the vicinity undergo a change in their chemical shift, which leads to the larger magnitude and the splitting of a "single" peak if two compounds are present.[90] The chiral shift reagents used were Europium(III) *tris*[3-(heptafluoropropylhydroxymethylene)-d-camphorate] $Eu(hfc)_3$ **181**, *tris*(6,6,7,7,8,8,8-heptafluoro-2,2-dimethyl-3,5-octanedionato)ytterbium YbFOD **180** and europium(III)-*tris*(1,1,1,2,2,3,3-heptafluoro-7,7-dimethyl-4,6-octanedionate) EuFOD **179**, which are shown in Figure 38.

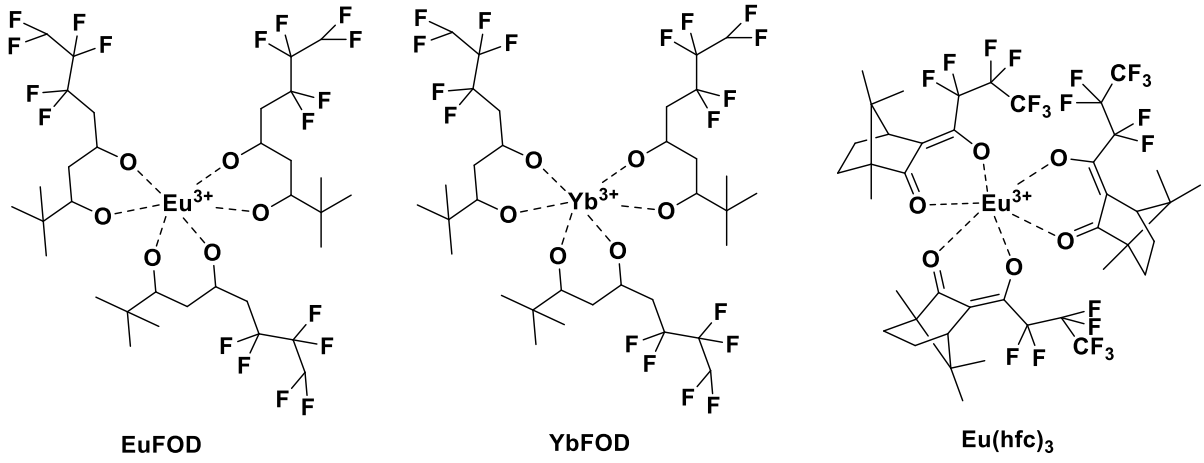


Figure 38 Chiral shift reagents EuFOD **179**, YbFOD **180**, $Eu(hfc)_3$ **181**

The chiral shift reagents (Figure 39) were added to the racemic and the enantiomeric compound **233** in different concentrations to find the best concentration for achieving the optimal shift and splitting in the proton NMR spectra according to known literature procedures.[91] Samples in ratios of 1:10-1:20 were prepared using the racemic compound in a concentration of 5mM in $CDCl_3$.

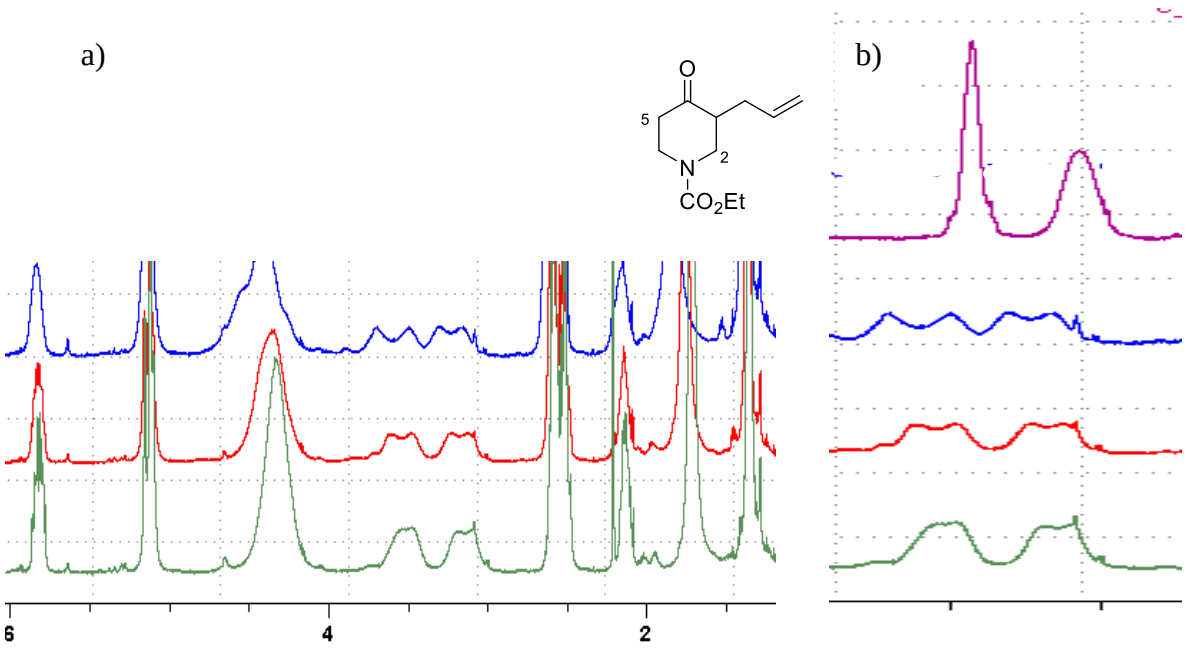


Figure 39 a) spectra of the racemic compound **197** in different dilutions of the chiral shift reagent **181** b) comparison of the line broadening compared to the neat compound **197** (green: ratio 1:20, red: ratio 1:15, blue: ratio: 1:10, violet: neat compound) using chiral shift reagent **181**

Figure 39 shows the effect resulting from the addition of different concentrations of the chiral shift reagent. In this approach the chiral shift reagent $Eu(hfc)_3$ **181** gave the best results. The best splitting was achieved by a broadening of signals for H-2 and H-5, which showed a splitting towards a double peak (blue spectra, figure 39) compared to the original compound (lilac spectra). This splitting was achieved using a 5 mM concentration of the racemic product **197** by adding the chiral shift reagent to yield a final dilution of 1:10. Regarding the dilutions of 1:15 (red) and 1:20 (green) a slight broadening as well as a splitting for the signals H-2 and H-5 in the 1:15 concentration was seen. As reported, the best splitting was achieved with a 1: 10 dilution (Figure 40), which showed two signals, unfortunately without baseline separation.

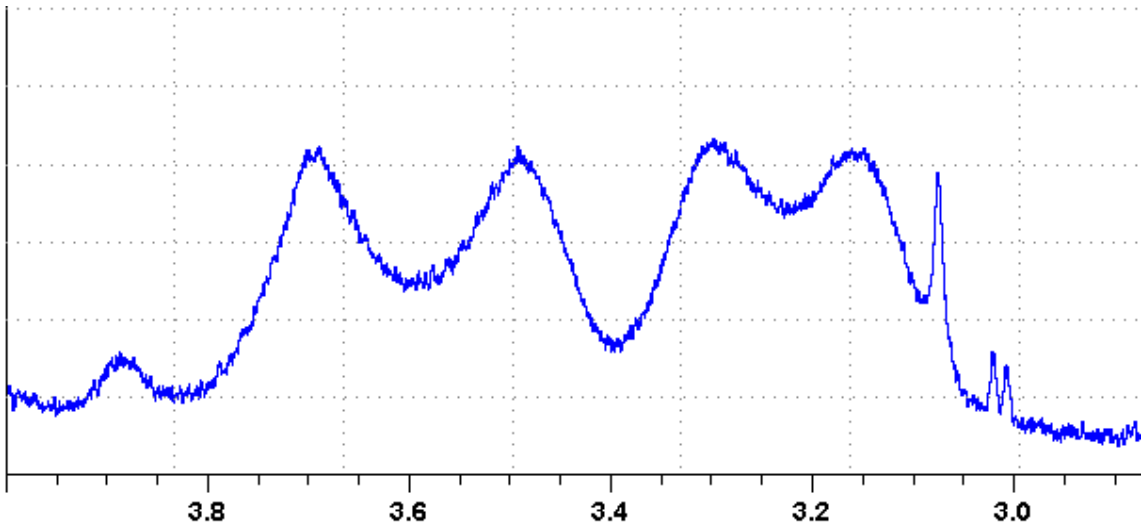


Figure 40 Splitting of the peaks of protons H-2 and H-5 in a dilution ratio of 1:10 using chiral shift reagent **259**

The validation of this approach was to test compound **233** using the chiral shift reagent $Eu(hfc)_3$ **181** as no reliable results compared to racemic compound **197** could be found (Figure 41). In this attempt, only a large broadening was seen in all the concentrations studied (1:10 (red), 1;15 (green) and 1:25 (blue)). The dilutions 1:10 and 1:15 showed a large peak broadening of signals H-2 and H-5, which didn't result in any analyzable NMR spectra. The ratio 1:25 showed no significant difference for the signals H-2 and H-5 compared to the original NMR of compound **233** (lilac).

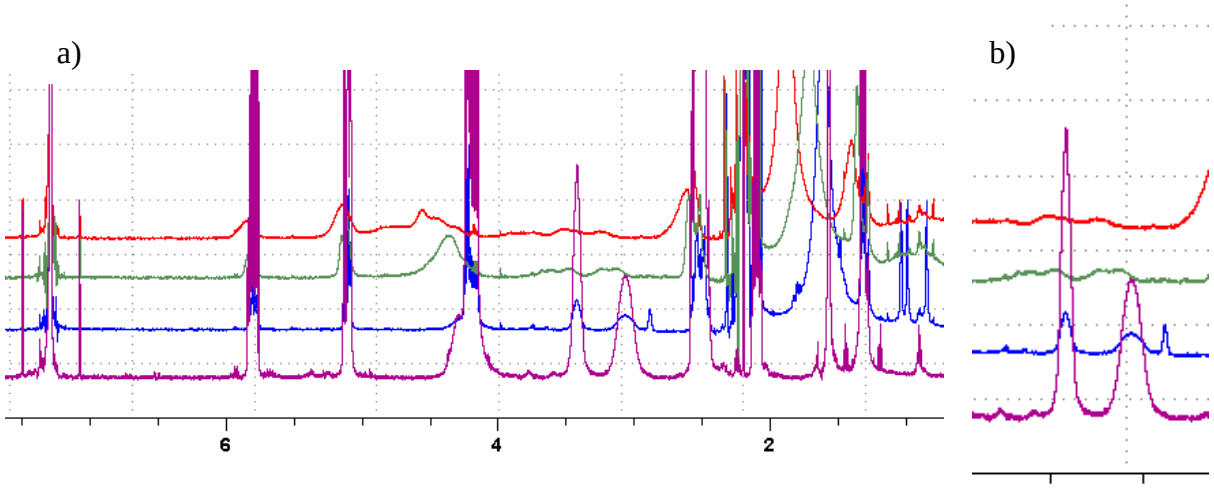
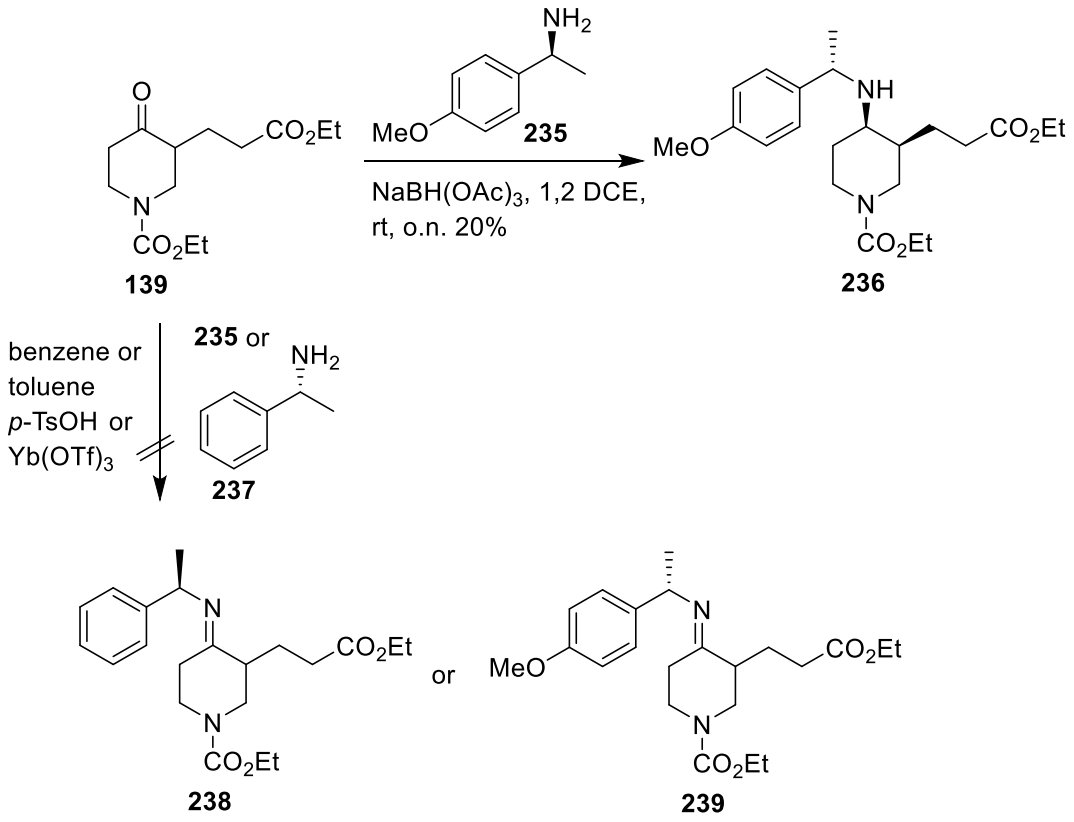


Figure 41 a) spectra of compound **233** in dilution with the chiral shift reagent **181** b) comparison of the line broadening of signals for H-2 and H-5 with the neat compound **233** (red: ratio 1:10, green: ratio 1:15, blue: ratio: 1:25, violet: neat compound)

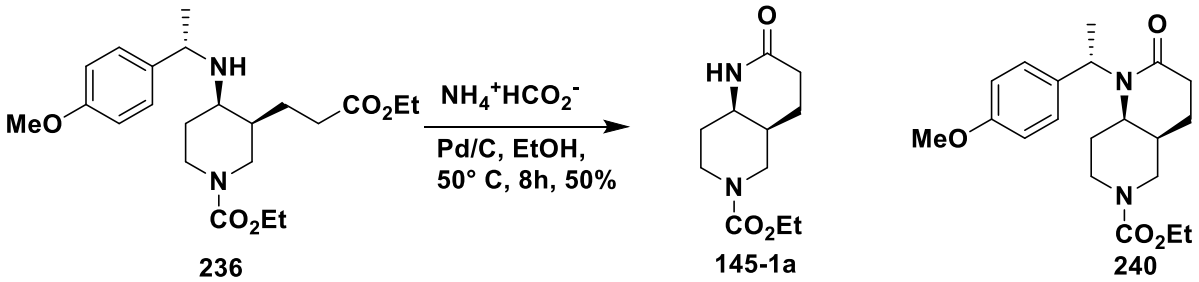
This approach was therefore stopped as it was not possible to find a method to analyse the enantiomeric purity through a reliable quantification of the ratio of the enantiomers.

A further approach, to induce the stereochemical outcome around the bicyclic ring connection, was shown to afford only the *cis*- connected isomer **145-1**. This approach started using a similar route tried for the heterocyclic scaffold system. The procedure was adapted from a paper published by Catalano *et al.* in their synthesis towards a novel tricyclic CXCR-4 receptor antagonist starting with a similar δ–ketoester as in our [6.6.5] approach.[92] In our attempt, the previously synthesized δ–ketoester **139** was treated with (*S*)-(-)-1-(4-methoxyphenyl) ethylamine **235** to form amine **236** (Scheme 44). The first attempt towards compound **236** was made using a standard condensation approach using a Dean-Stark condensation with chiral amine **235** and (*R*)-(+)-α-methylbenzylamine **237**. Surprisingly, this classical condensation to imines **238** and **239** didn't deliver the desired products even by using additives as *p*-toluensulphonic acid (*p*-TsOH) or ytterbium triflate ($Yb(OTf)_3$). This was thought to be because of the sterically-demanding ester side chain, which didn't allow the attack of the amines **235** or **237**. It was further proposed that the imines **238** and **239** would be sterical demanding leading in the non- preferred axial configuration of the ester side chain. Therefore, the reductive amination step, which normally would be the second step to reduce the imine function to the desired *cis*- connected amino ester **236**, was directly carried out using the δ–ketoester **139**. No precedent was known that this reductive amination would give directly the desired *cis*- connected compound **236**. Even though, the yield of this step is unoptimised (with 20% conversion to date, n=1 experiment), it was decided to progress with this new synthetic methodology. Unfortunately, the proton NMR of compound **236** couldn't be clearly assigned to be only one isomer. Therefore, **236** was converted through to the final product **249**, to allow a chiral HPLC determination of the optical purity.



Scheme 44 Synthesis route towards imines **238** and **239** and synthesis of compound **236**

Deprotection of the 1-(4-methoxyphenyl) ethyl protecting group to yield the free amine functionality was carried out according to the procedure of Catalano *et al.*[92] using TFA following a procedure by Davis *et al.*,[93] which did not cleave the protecting group. Therefore a transfer hydrogenation approach was employed using Pd/C and ammonium formate in ethanol, which readily gave bicyclic lactam **145-1** in 50% yield (Scheme 45).



scheme 45 Conversion of compound **236** into bicyclic compound **145-1a**

Through comparing the previous synthesised bicyclic lactam compounds **145-1** and **145-2**, either through the comparison of that TLC analysis and the proton NMR spectra, showed that the reaction delivered mainly the *cis*- connected compound with only a less than 5% amount

of the *trans*- isomer **145-2**. The crude NMR spectra of the newly synthesised compound **145-1** through this new chiral approach showed only one *cis*- isomer present (Figure 42).

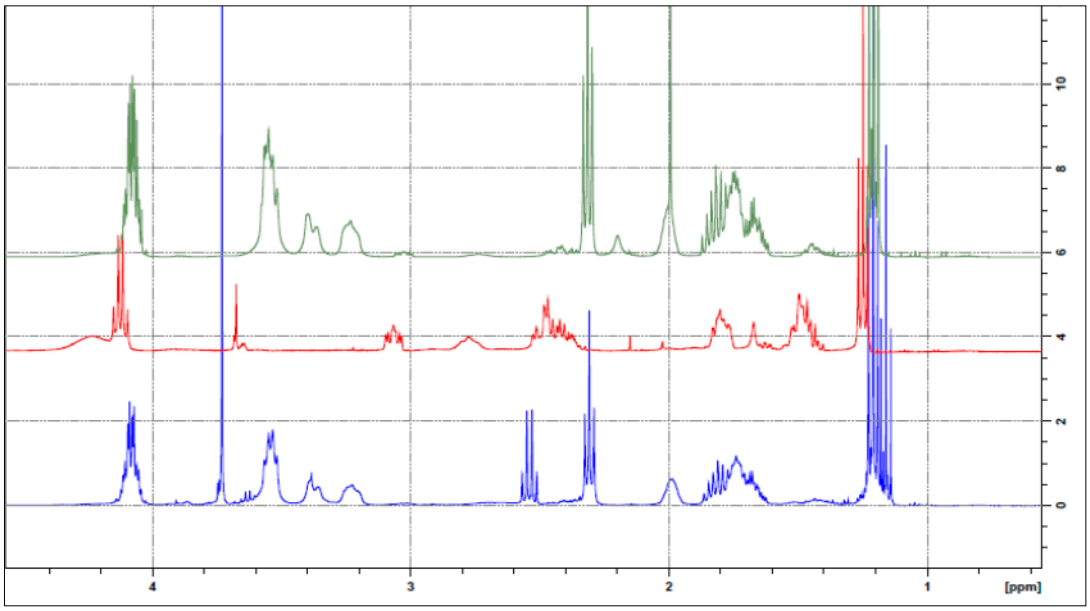
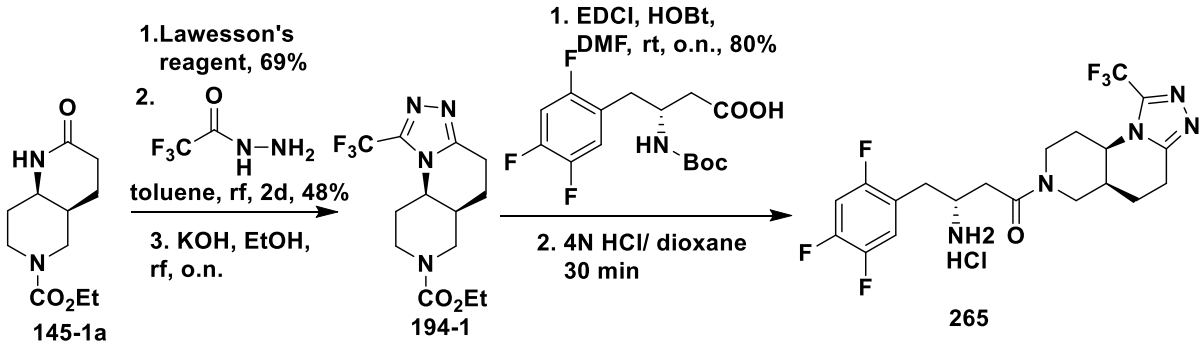


Figure 42 Overlay of both separated isomers **145-1 (**green) and **145-2 (**red**)** compared with crude newly synthesised **145-1a** (blue)

The crude NMR spectrum of compound **145-1a** (blue) showed no evidence of the *trans*-isomer (red spectra), therefore all signals present in the *cis*- compound (green) are detectable. From an examination of the mass spectrum, no evidence for the protected lactam **240** (scheme 45) was found, which was seen in the approach to compound **141/142** (Section 3.2**)**. The further synthesis followed the same route carried out to scaffold system **194-1** (Section 3.2), which was followed by the conversion into Sitagliptin analogue **265** (detailed explanation in section 4.4) (scheme 46).



scheme 46 Final steps to compound **265/266**

The next step was to determine the stereoselective outcome of this new approach to deliver either compound **265** or **266**. The new chiral analogue was tested through chiral HPLC and

compared with the outcome of the chiral separation (explained in chapter 4.4) of the previously synthesised analogues **265** and **266.** The determination of the purity resulted in a ratio of 93:7 in favour of isomer **265** (Figure 43**).** The assumption of the stereochemical assignment derived from previous literature precedent (Figure 44).

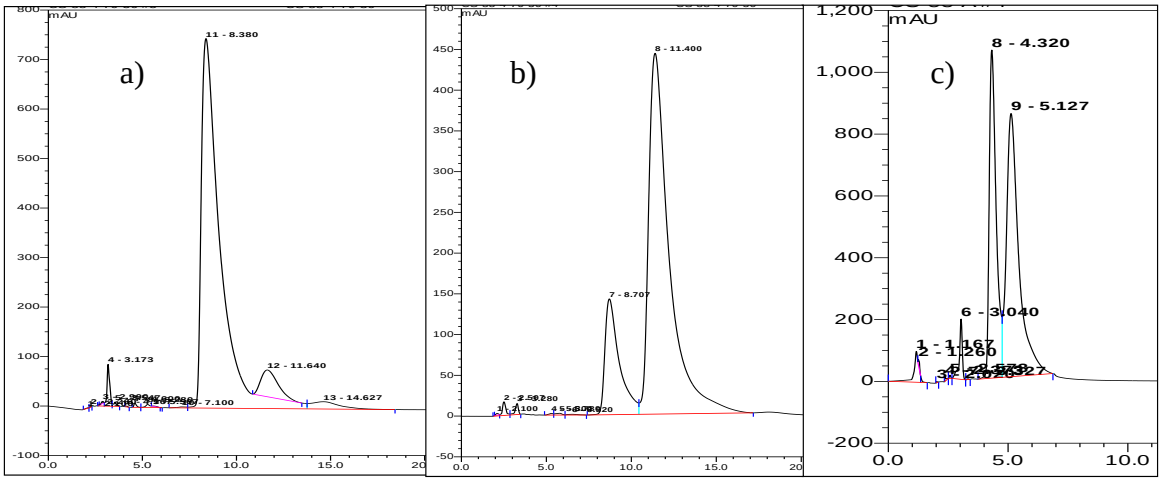


Figure 43 Comparison of a) new synthesised compound **265**, b) overlay of compound **265** with one of the separated *cis*-isomers, (both in a ratio Hex: EtOH 70:30 with 0.2% DEA) c) mixture of *cis*- connected compounds **265**/**266** (ratio Hex: EtOH 60:40 with 0.2% DEA)

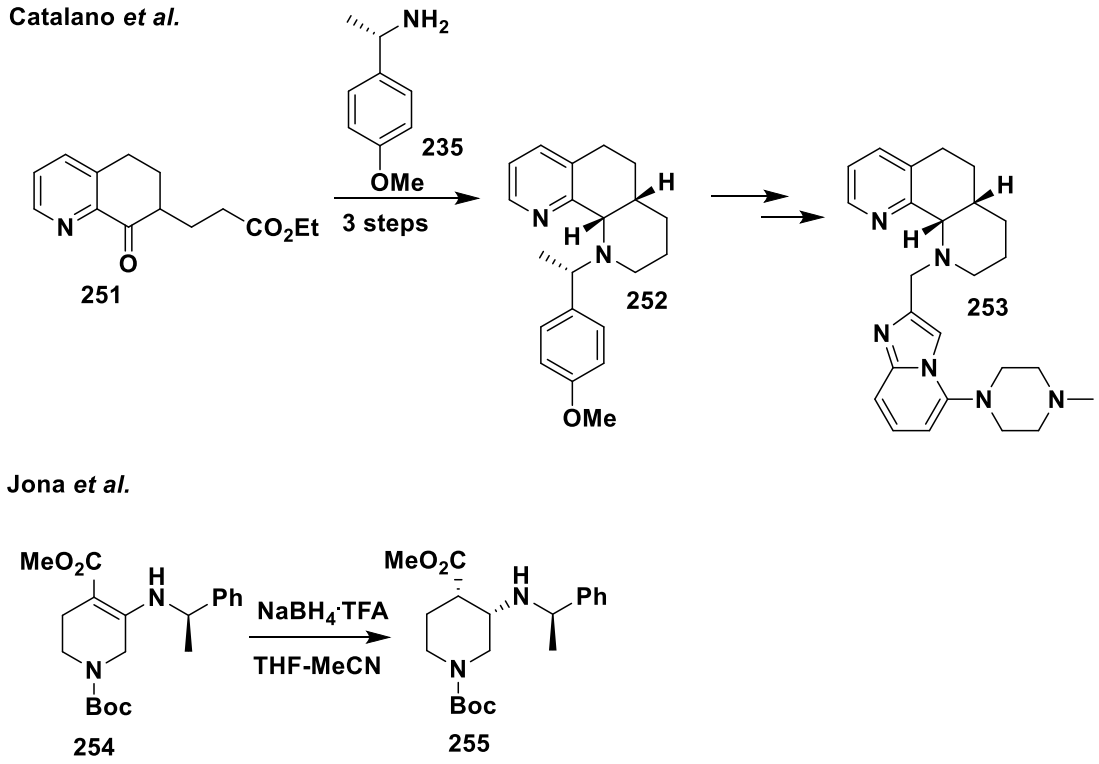


Figure 44 Known literature examples by the groups of Catalano and Jona to install the *cis* oriented groups on the piperidine

In the paper by Catalano it is shown that the use of (*S*)-(-)-1-(4-methoxyphenyl) ethylamine **235** resulted in compound **252,** from which the stereochemical outcome was finally

determined through X-ray analysis of compound **253**.[92] Furthermore, another known approach to the selective *cis*- connection on the cyclohexane ring is known through treating compound **254** with sodium borohydride and TFA to yield the stereoselective compound **255.** This was reported by Jona *et al.* in their synthesis towards analogues of J-113397, a nociceptin receptor antagonist.[94] The stereochemical outcome was proved using X-ray crystallography.

In this approach, the synthesis of the three remaining bicyclic lactam enantiomers is still incomplete, which should be carried out following the same procedure reported in the paper by Catalano by changing the chiral amine to the (*R*)-(-)-1-(4-methoxyphenyl) ethylamine to yield **145-1b** and by treating the *cis*- connected enantiomers with sodium carbonate in methanol to yield the *trans*- connected analogues **145-2a** and **145-2b** (figure 45).

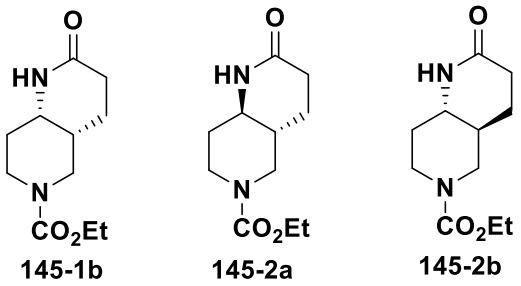


Figure 45 Remaining possible enantiomers of bicyclic compound **145**

The enantio pure bicycles could be further incorporated into the desired drug molecules, which would allow the determination of their purity and absolute chirality. Furthermore, a crystal structure of compound **236** is required to prove its absolute configuration.

3.6 Conformational analysis of newly synthesised tricyclic scaffold

In this thesis three novel tricyclic chemical scaffolds have been synthesized consisting of a piperidine ring joined to a triazole part. The piperdine and the triazole parts are connected through a third ring varied in the ring size from five to seven carbon atoms. The 6.6.5 system was synthesized in the *trans*- as well in the *cis*- connected versions. From the 6.5.5 system only the *cis*- connected ring was synthesized. For the 6.7.5 system a mixture of all four possible isomers was still present and no separation was accomplished. The analysis of the conformation of the synthesised tricyclic scaffolds showed the conformation of the 6-membered rings in the 6.6.5 system in the energy favoured chair like conformation as no eclipsed hydrogen atoms are present (figure 46).

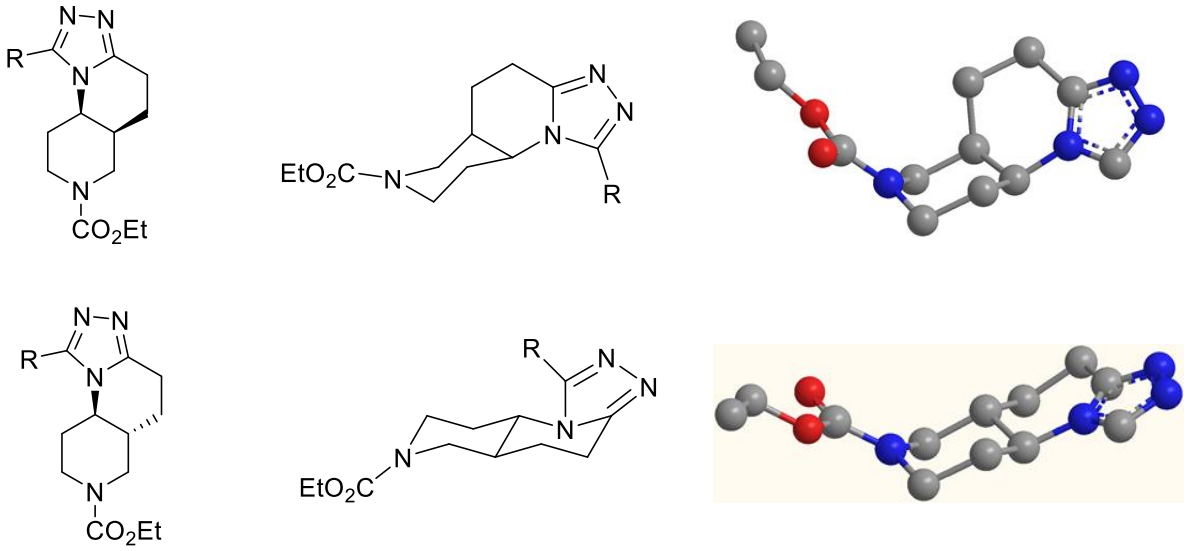


Figure 46 Conformational analysis of the *cis* and *trans* connected 6.6.5 tricyclic triazole system using ChemBio3D (Software ChemBioDraw Ultra 14.0)

Looking at the ring strain in cyclopentanes and cyclohexanes, the ring strain for cyclopentane is 6 kcal/mol and for cyclohexane is 0 kcal/mol, which explained the problems arising from the synthesis of the 6.5.5 compared to the 6.6.5 analogues. The formation of the 6.6 system compared to the 6.5 system didn't afford harsh conditions and was carried out in a one-step procedure compared to the 6.5 system, which needed a second step using a base (K_2CO_3) to force the final ring closure.

Analysing the conformation of the fused 6.5.5 tricyclic scaffold and the 6.7.5 tricyclic system shows that both scaffolds are present in the energy favoured chair conformation of the six-membered piperidine ring. In the 6.5.5 system the 5-membered ring adapts a rigid envelope conformation due to the presence of the fused triazole ring system. The cycloheptane ring in the 6.7.5 system has the same ring strain energy as the cyclopentane with 6 kcal/mol, which could explain the difficulties for forming the 6.7 ring system. The low yield of this formation can be explained by the faster formation of the *cis*- connected 6.7 system compared to the *trans*- connected ring 6.7 system due to the favoured ring closing from the same side of the ring (figure 47). The 6.7.5 system shows furthermore the chair conformation of the piperidine ring and the energy favoured twist conformation of the cycloheptane ring. In the case of the seven-membered ring system the chair like conformation is not the favoured ring orientation of the cycloheptane ring as it would result in two eclipsed hydrogen atoms.

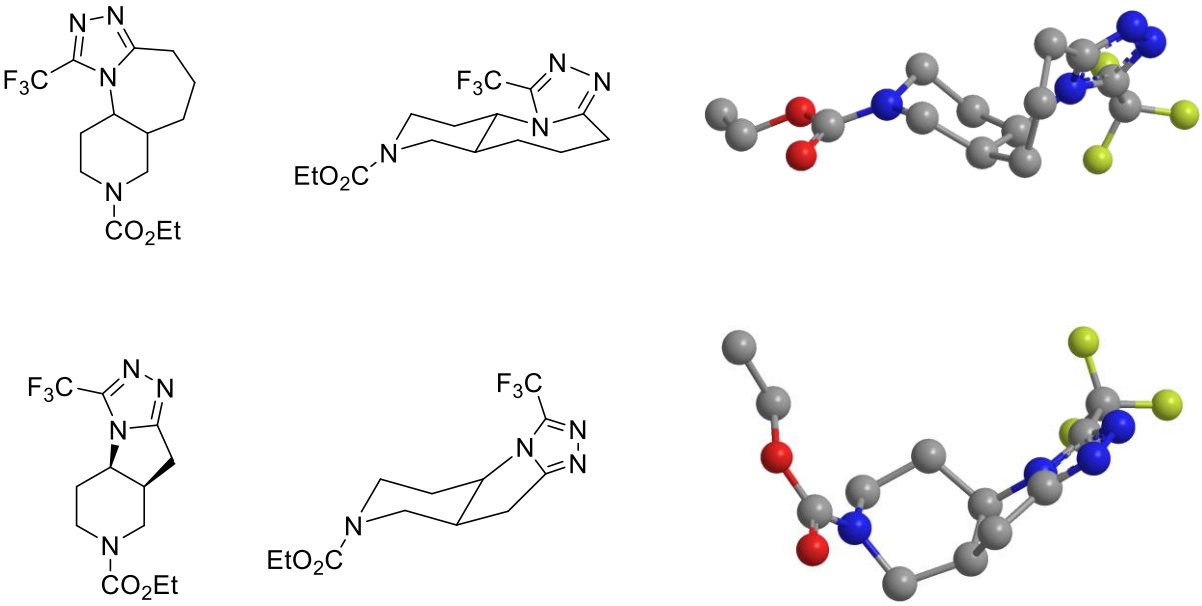


Figure 47 Conformational analysis of the *cis* connected 6.5.5 tricyclic triazole system and the racemic 6.7.5 tricyclic triazole system using ChemBio3D (Software ChemBioDraw Ultra 14.0)

4 Synthesis of new DPP-4 inhibitors based on a novel tricyclic scaffold

4.1 A global health issue: Diabetes mellitus and the role of DPP-4

Diabetes is one of the major health issues, affecting 382 million people in 2013 with 1.5 million deaths in 2012, in addition to an increasing and alarming number of new cases reported over the last decades (figure 48)[95]. More than 80% of the reported cases appear in the low and middle income countries, which lead to the fact that diabetes has become a major global health care issue.

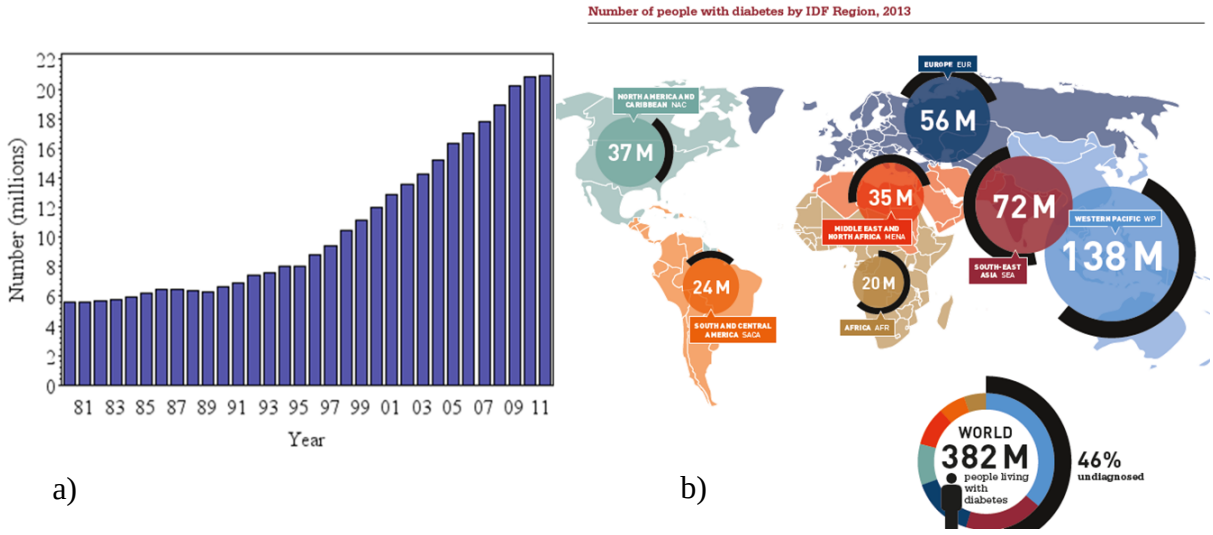


Figure 48 a)Increasing number in millions of diabetes cases in the US from 1981to 2011, adapted from www.cdc.gov/diabetes/statistics/prev/national/figpersons.htm, b) Distribution of diabetes cases in the world (people/country) in 2013 according to WHO, adapted from 6th edition of diabetes atlas.

Diabetes mellitus is a chronic disease that is divided into two sub-types. Type-1 diabetes is a result of an autoimmune process and it is characterized through the body's insufficient production of insulin. This autoimmune reaction is caused where the system attacks β-cells in the pancreas. Insulin, which is produced in β–cells in the pancreas, enables the body to use glucose from the carbohydrates after food intake. Furthermore, it helps the body to maintain blood glucose levels to avoid sugar levels getting too high (hyperglycemia) or too low (hypoglycemia) by controlling the storage and release of glucose in the liver (Figure 49).[96]

Type-2 diabetes, which affects more than 80% of all the diabetes cases, is characterized by the body's ineffective use of insulin. The body still produces insulin, however it is not able to use it effectively or respond in the appropriate manner. Most people with type-2 diabetes aren't aware of being affected until the symptoms become severe. Diabetes itself, when under

control is not a necessarily fatal, but untreated it can lead to severe health consequences (Figure 49).

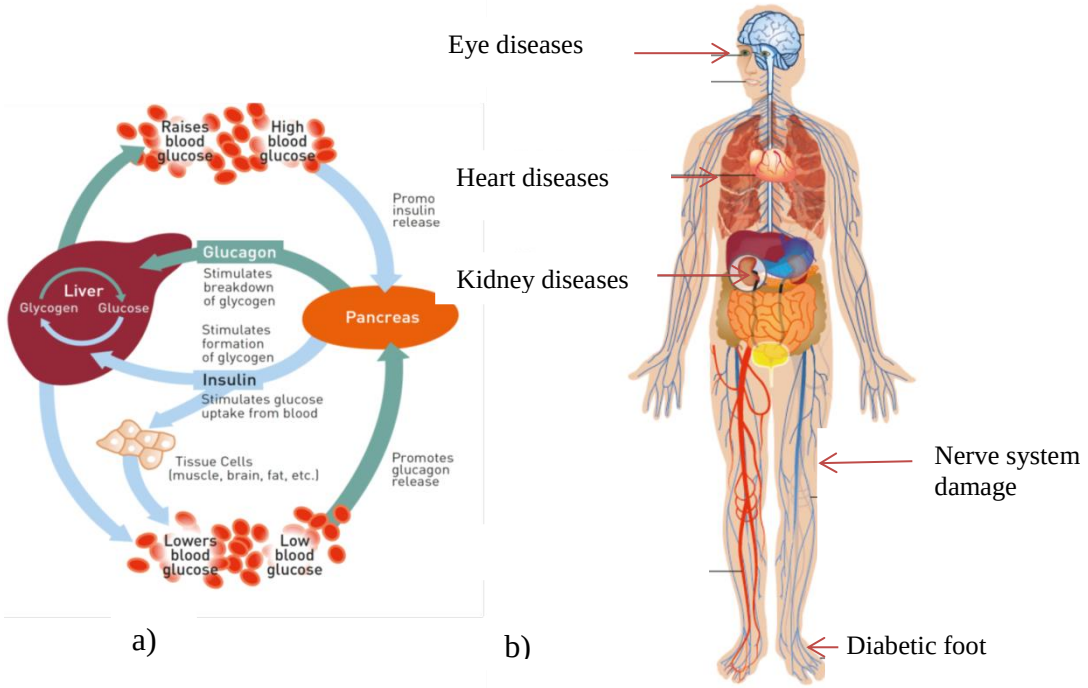


Figure 49 a) Circuit of the tasks and production of insulin b) Health issues related to diabetes, both adapted: by www.idf.org/node/23538

Complications, that can occur related to diabetes mellitus, can affect the whole body and are often disabling or life-threatening diseases. For example the heart, the blood vessels or the nervous system can be affected. Diabetes mellitus is still a major factor for the risk of a heart disease and 50% of the diabetes patients die of cardiovascular diseases for example through angina, myocardial infarction, stroke or congestive heart failure. Nephropathy (kidney disease) is another condition which is more common to diabetes patients, which can occur due to the damage of small blood vessels and the inefficient function of the kidney. Furthermore, retinopathy (eye disease) and neuropathy (nerve damage) are known to be related to patients with diabetes. One consequence of diabetes mellitus leads to the so called “diabetic foot”, which is a consequence of nerve damage and blood vessel damage. This can lead to ulceration and infections and can result in a limb amputation through severe nerve damage in the feet.[97]

A relatively new approach in the therapeutic field of type-2 diabetes is to target the enzyme DPP-4 (dipeptidyl peptidase 4). DPP-4 is a serine protease which is indirectly involved in insulin biosynthesis (Figure 50).

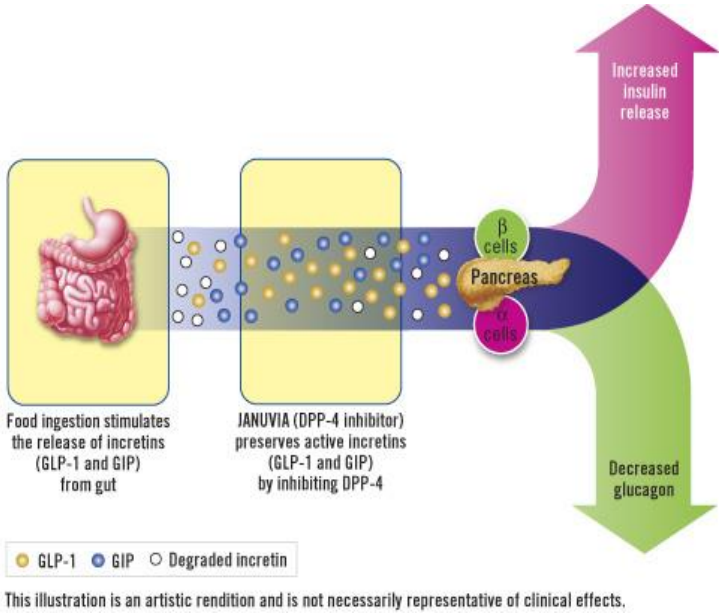


Figure 50 Mechanism of action of DPP-4 towards GLP-1 and GIP, adapted from januvia.com

This protein is a ubiquitous enzyme which is found on the surface of most cell types and also solubilized in blood with a measurable enzymatic activity in plasma. Glucaregulatory peptide hormones in the gut, which are known as incretins (namely GIP, glucose dependent insulinotropic peptide and GLP-1, glucagon like peptide-1) are involved in the biosynthesis of insulin (Figure 50).[98] The biosynthesis of insulin is regulated by these incretins after food intake.[99] Both active hormones are secreted into the circulation shortly after food consumption and bind to the specific G protein-coupled receptor present on the β cells followed by activation of the incretin receptor. This activation induces a glucose-dependent insulin secretion and furthermore stimulates the insulin biosynthesis. Another function of GLP-1 is to lower the plasma glucose level by inhibition of glucagon secretion. These incretin hormones, GLP-1 and GIP, are directly inactivated through the enzyme DPP-4 by degradation within minutes resulting in the elimination of incretin hormones.[100] DPP-4 cleaves the hormones preferably in the position-2 of the *N*-terminus, which means that for GLP-1 the dipeptide (His-Ala) and GLP-1 (9-36) amide are degradation products from GLP-1 (7-36) amide.[101] The main principle behind targeting DPP-4 in type-2 diabetes is that the inhibition of this enzyme should assist to control the blood glucose level and an increased level of biologically active GLP-1. Furthermore, this approach gives new perspectives of an improved safety and tolerance profile over known oral agents. The strict glucose-dependent insulin release and glucagon inhibition through GLP-1 results in a low risk of hypoglycemia (low blood sugar levels) and weight gain through the treatment of type-2 diabetes with a DPP-4 inhibitor.

4.2 DPP-4 inhibitors on the market

Extensive structure activity studies were carried out in many major pharmaceutical companies, and have resulted in a number of new competitive DPP-4 inhibitors over the last decade.[102] The pharmacological profile and the mechanism of action of the DPP-4 inhibitors were studied intensively and an increased level of GLP-1, GIP and glucose tolerance was observed.[103] A major issue related to the DPP-4 inhibitors is their selectivity towards other closely-related serine proteases. DPP-4 is a member of a protease family, which includes the structurally similar enzymes DPP-8 and DPP-9. DPP-8 and DPP-9 are cytosolic enzymes and to date no endogenous substrate has been identified for them.[104] It was shown that the selectivity towards DPP-4 was crucial, as inhibition of DPP-8 and DPP-9 resulted in increased toxicity in preclinical studies.[105] Sitagliptin **256** was the first DPP-4 inhibitor launched in 2006 by Merck and there has been a succession of further inhibitors launched over the following years (Figure 51).[106]

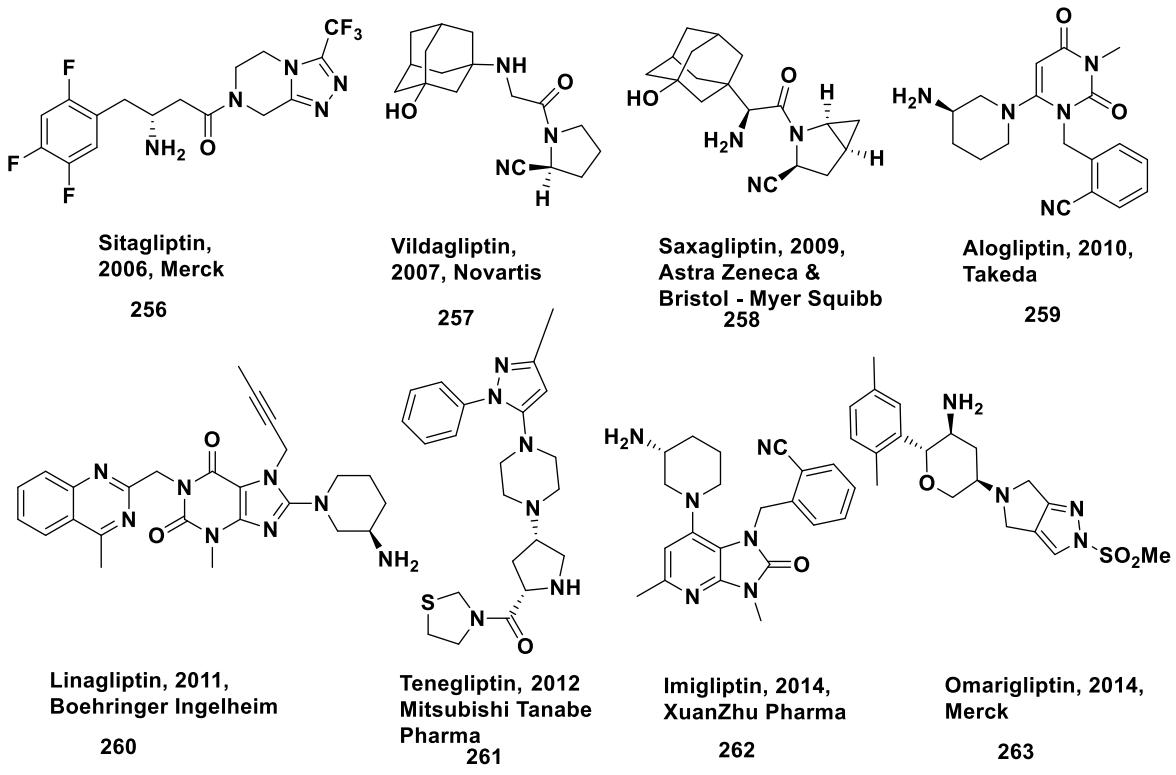


Figure 51 Known DPP-4 inhibitors (marketed or in clinical trials)

All of the so called “gliptins” are orally bioavailable and demonstrate enzyme inhibition in the low nanomolar range. Sitagliptin **256** is a potent triazolopiperazine-based DPP-4 inhibitor with excellent selectivity and efficacy profile. It is a reversible inhibitor and is administered once daily.

Vildagliptin **257** was developed by Novartis and was launched in 2008[107], and was the first drug of a series of "gliptins" with nitrile function that forms a covalent bond with the serine residue (Ser 630) in the active site of DPP-4. However, due to its rapid clearance, this drug has to be administered twice daily.

The need for an improvement in the metabolic stability resulted in saxagliptin **258**, a DPP-4 inhibitor launched by Bristol Meyer Squibb and AstraZeneca in 2009.[108]

Another covalent binding inhibitor, Alogliptin **259** from Takeda, was launched 2010 in Japan and 2013 in the US. It was discovered during the studies towards an inhibitor with increased metabolic stability including the chemical functionality of a pyrimidinone moiety.[109]

Linagliptin **260,** a DPP-4 inhibitor by Boehringer Ingelheim and Eli Lilly marketed in 2011 is based on a methylxanthine moiety and showed a good selectivity towards DPP-4,[110] followed by Tenegliptin **261,** which is to date the last launched compound by Mitsubishi Tanabe Pharma in 2012.[111]

Recent publications in 2014 showed that there is still an ongoing search and need for new DPP-4 inhibitors to improve mainly in patient compliance.[112] Imigliptin **262** was developed by XuanZhu Pharma after scaffold hopping from Alogliptin **259**. After extensive studies and variation in the core and both side chains of Alogliptin, Imigliptin **262** showed the optimal activity and selectivity profile and this compound is currently in clinical trials in China.

Omarigliptin **263** is a follow up compound of sitagliptin **256** developed by Merck.[112] Omarigliptin **263** is a new long-acting once a week DPP-4 inhibitor. The rationale behind the development of a new follow up compound to sitagliptin **256** was to minimise the side effects related to all antidiabetic drugs, including weight gain, hypoglycaemia and gastrointestinal intolerance. These side effects are all related to insufficient patient reliability by taking the necessary amount of pills each day. As all known DPP-4 inhibitors are once or twice a day therapy, omarigliptin **263**, which is currently in phase 3 clinical trials, would be a desirable alternative with the same pharmacology profile as sitagliptin **256** and an improvement in patient compliance due to the once a week administration.

4.3 Docking studies in the DPP-4 active site

4.3.1 Docking of known marketed DPP-4 inhibitors

The structure of the DPP-4 active site is well known due to the availability of the co-crystal structures from all marketed DPP-4 inhibitors through the pdb-database. A comparison of all co-crystal structure complexes was published by Nabeno *et al*. which points out the interaction of the inhibitors in the DPP-4 active site (figure 52).[113]

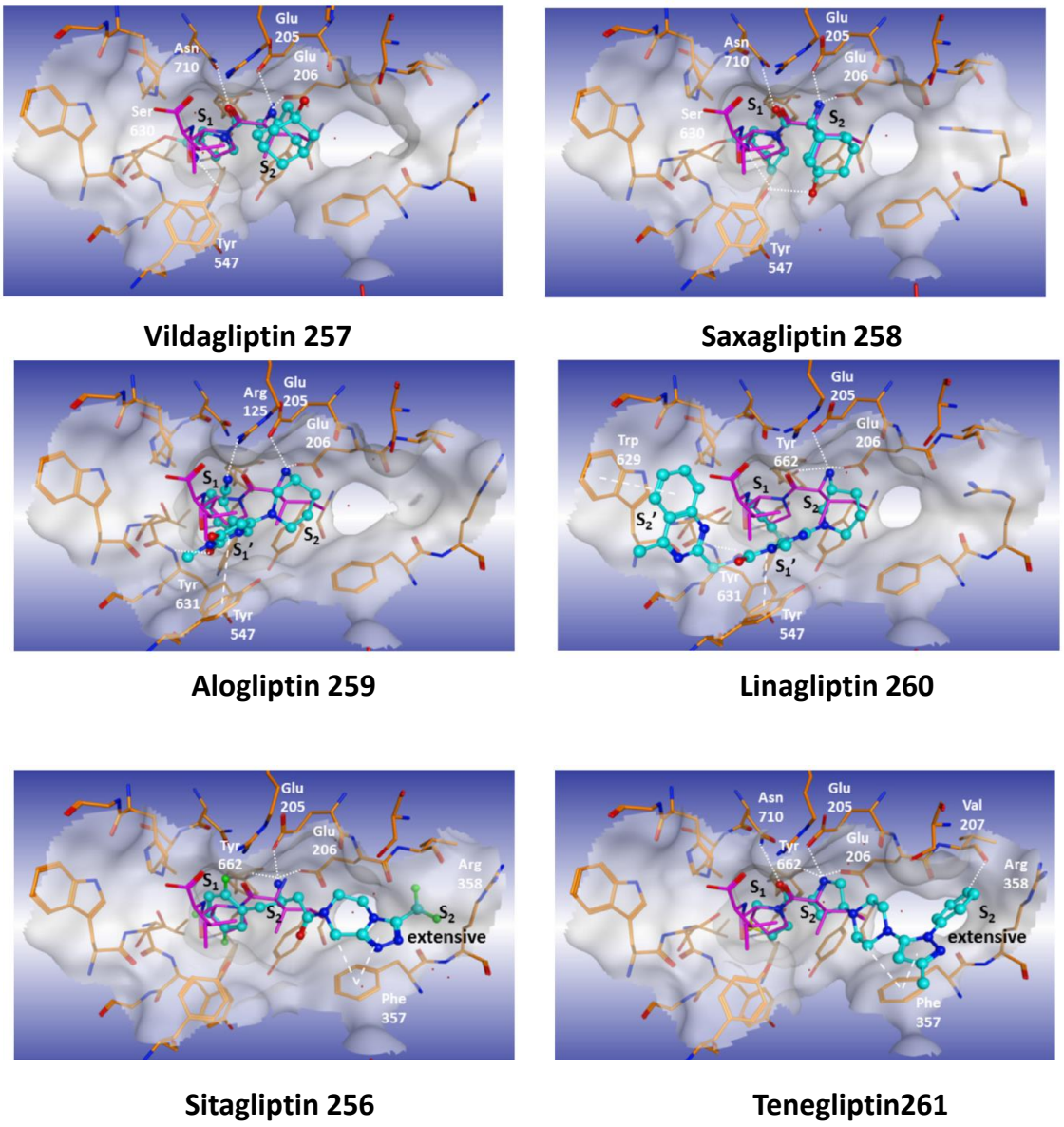


Figure 52 Co-crystal structure of the six marketed DPP-4 inhibitors in the DPP-4 active site [pdb code: 1X70 (sitagliptin **256**), 3BJM (saxagliptin **258**), 3G0B (alogliptin **259**), 2RGU (linagliptin **260**), and 3VJK (teneligliptin **261**)].) adapted and modified from Nabeno *et al.* (Ref 113)

In Figure 52 all six marketed DPP-4 inhibitors are shown in the DPP-4 active site overlaid to the substrate peptide. In the review by Nabeno *et al.* the known DPP-4 inhibitors are

classified into different groups according to their binding mode in the DPP-4 active site. The sub-sites in the DPP-4 active site are defined through the binding site of the substrate peptide (diprotin A, Ile-Pro-Ile),[114] which means that the amino acids are numbered starting from the point of cleavage and the protein sub-sites occupied by the corresponding amino acid are numbered in the same order. In the case of the DPP-4 active site Ser 630 cleaves the *N*-terminus of the substrate peptide at the penultimate position (P1), which is related to the sub-site (S1). No sub-site in the DPP-4 pocket is defined after S2, but some inhibitors bind well behind the defined sub-site S2, which therefore is named "S2 extensive sub-site".

Vildagliptin **257** and saxagliptin **256** (figure 51, 52) belong to the same class regarding their binding mode in the DPP-4 active site and both inhibitors are limited to binding to the S1 and S2 sub sites. Both of these inhibitors are designed as peptide mimetics forming a covalent bond through the cyanopyrrolidine moiety with the Ser630 in the S1 pocket.

Linagliptin **260** and alogliptin **259** contain a uracil moiety that is involved in π–π stacking with Tyr547 in the S_1' sub-site. The binding to the S_1 sub-site in the case of linagliptin **260** is represented by its butynyl group and alogliptin by its cyanobenzyl group. Linagliptin **260** is eight times more potent than alogliptin **259,** which could be a result of Linagliptin's **260** occupation of the S_2' sub-site.

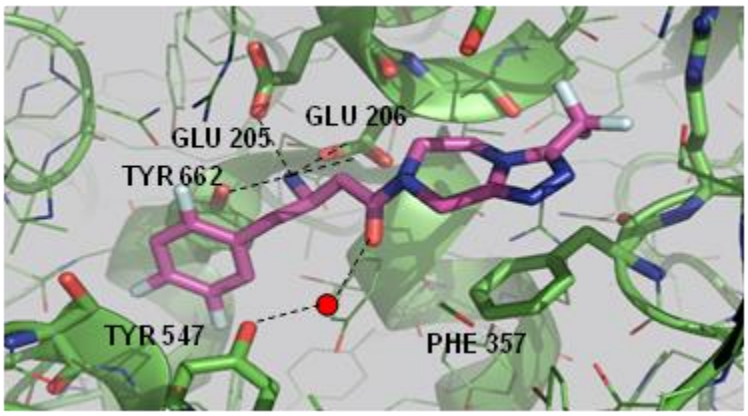


Figure 53 Sitagliptin **256** docked using OpenEye in the DPP-4 active site (1X70) showing the second best pose in agreement with the co-crystal structure of Sitagliptin

The binding of the last two marketed inhibitors, Sitagliptin **256** and Tenegliptin **261,** demonstrate binding to the S_2 extensive site, which is referred to as the anchor lock domain. The S_2 extensive site is occupied by Sitagliptin's trifluorotriazolopiperazine part and by tenegliptin **261** with its (1-phenylpyrazol-5-yl) piperazine moiety. The co-crystal structure of Sitagliptin **256** in the DPP-4 active site showed eight significant interactions (figure 53). The

2,4,5 trifluorophenyl moiety fully occupies the S1 pocket. The β amino group shows four hydrogen interactions with Tyr662 and Glu (205 and 206). The carboxylic oxygen forms a water bridge to Tyr547 and the triazole part undergoes a π–π stacking with Phe357 (Figure 53).[106]

4.3.2 Docking of new Sitagliptin analogues in the DPP-4 active site

Our project aim was to incorporate our novel scaffold (**194**) into known biological-active drug molecules, to test for the scaffold's ability to serve as a privileged scaffold. In this case, the four stereochemical isomers of the Sitagliptin analogues **265-268** (figure 54) were docked into the DPP-4 active site and are shown overlaid with Sitagliptin **256** (figure 55).

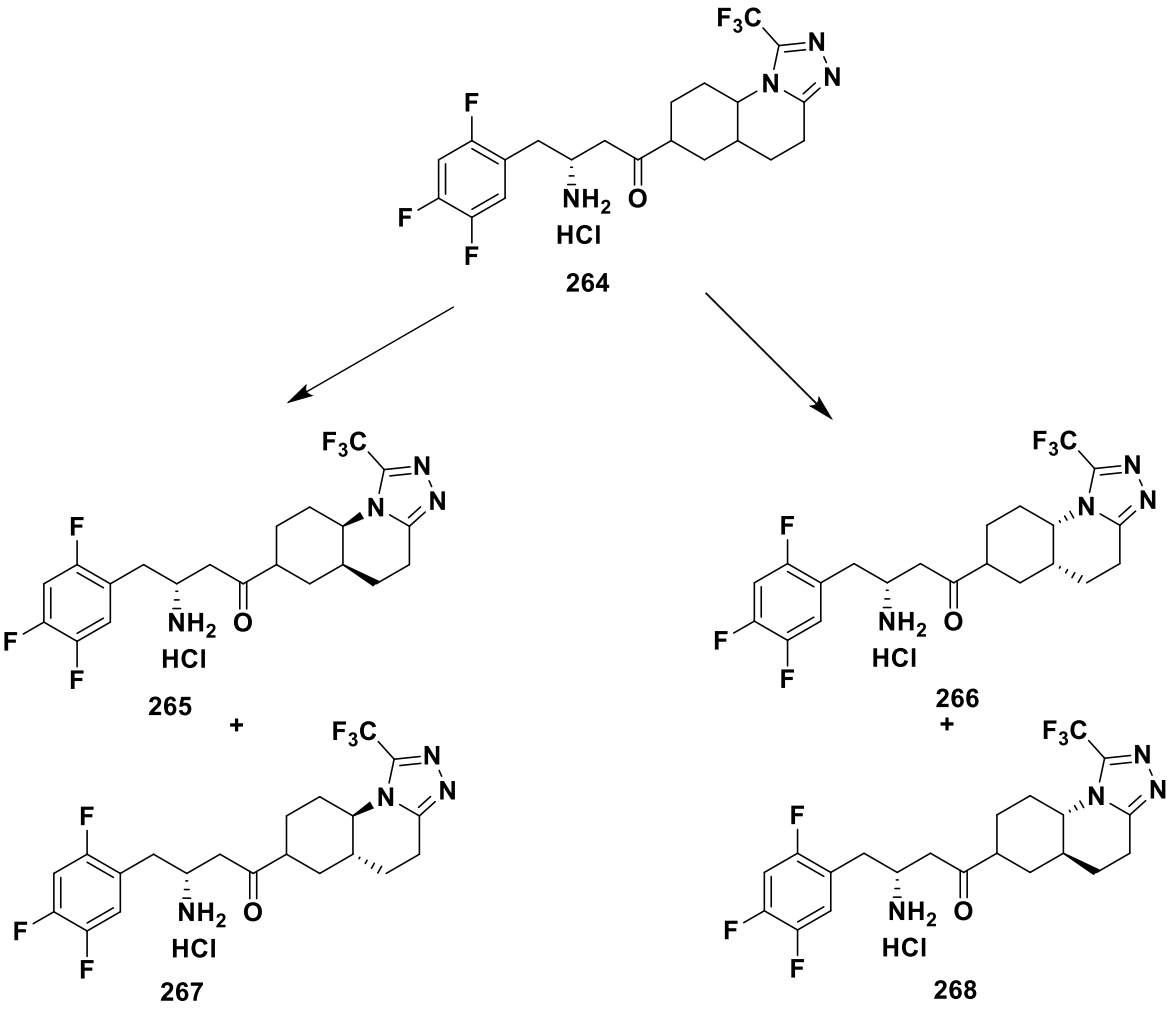


Figure 54 Suggested Sitagliptin analogue **264** and its single isomers **265-268**

The docking into the DPP-4 active site showed complementary overlay of the aromatic region of all four isomers **265-268** compared to Sitagliptin **256** (figure 55). The *cis*- isomer **266** and *trans*- isomer **267** showed further overlay in the region of the carbonyl function and

the amino group. The other two isomers **265** and **268** showed poor overlap with the amino group of Sitagliptin **256**. Interestingly, all four isomers overlay nicely in the triazolo part whereas compound **265** is the only isomer with the CF_3 group occupying the same space and directionality of the Sitagliptin CF_3 group.

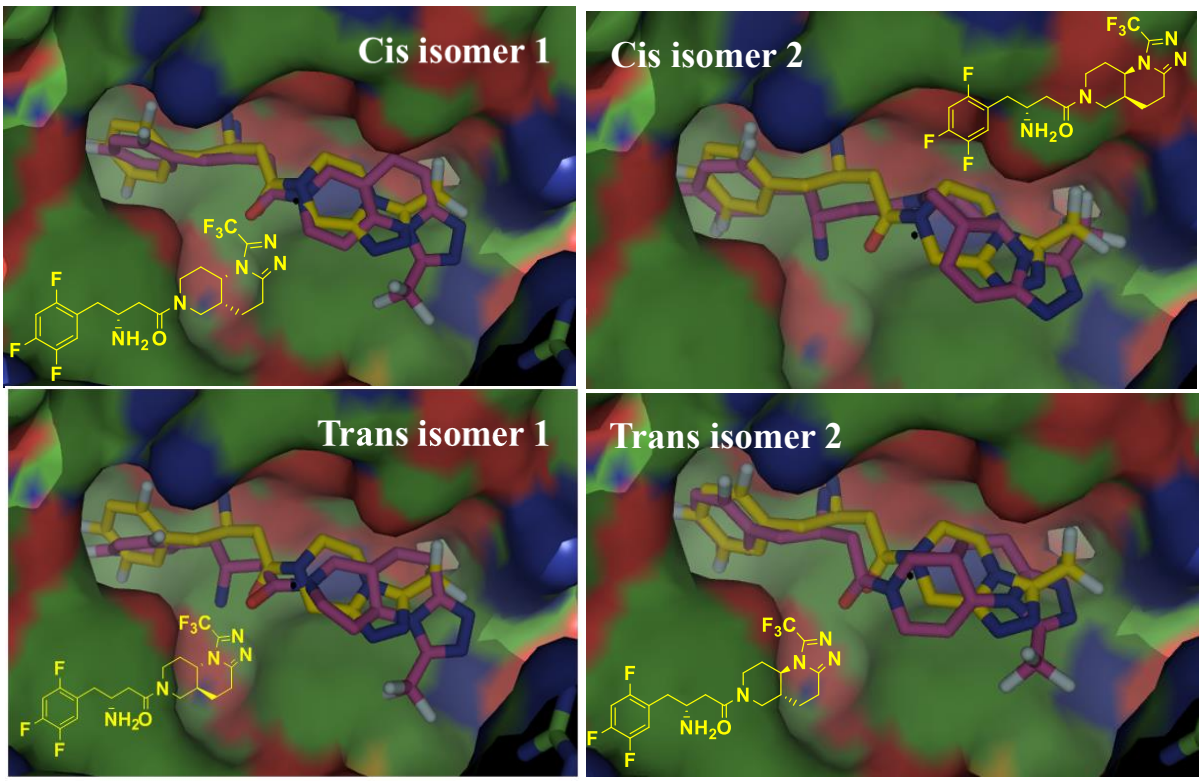


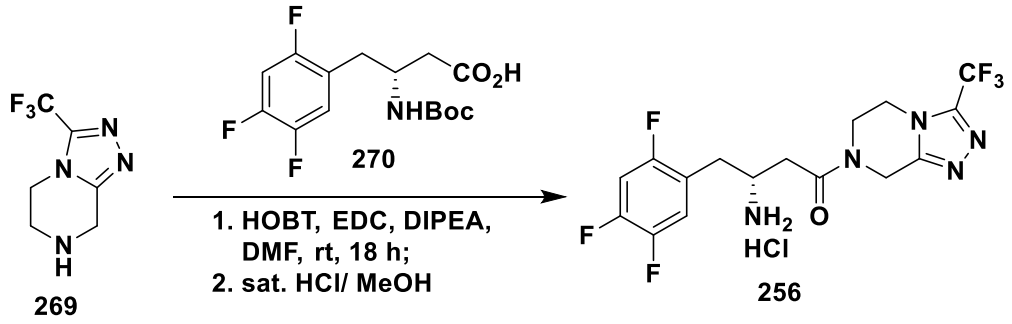
Figure 55 Isomers **265-268** docked in the DPP-4 active site overlaid with Sitagliptin (yellow) **256,** surface colouring shown according to the atoms

This docking study offered confidence for the synthesis of the Sitagliptin analogues, which will be discussed in chapter 4.4.

4.4 Synthesis of Sitagliptin Analogues

In this work the synthesis of new Sitagliptin analogues **265-268** was carried out due to the chemical structure similarity of the new tricyclic scaffold compared to the triazolopiperazine part in Sitagliptin **256**. The confidence for the synthesis of the analogues came from initial docking studies and the potential for the discovery of new DPP-4 inhibitors, which can serve to clarify the ability of the new tricyclic scaffold to function as a Privileged Structure. In addition, the discovery of such inhibitors designed based on our novel scaffold would add evidence to our hypothesis that the scaffold could act as a privileged structure. Sitagliptin **256** was synthesized by the group of Merck and the last steps to couple the amino acid part **270** with the triazopiperazine part **269** was carried out under standard amide coupling conditions

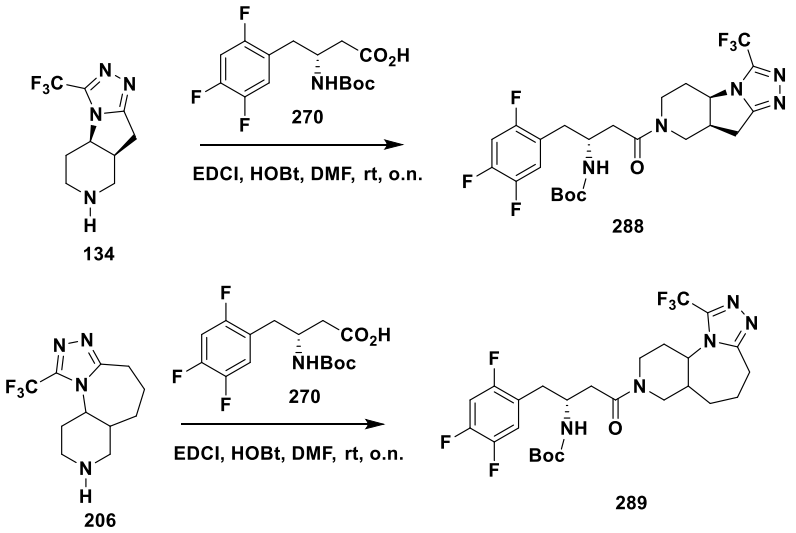
(Scheme 47).[115] The previously described [6.6.5] tricyclic scaffolds (**194**) were coupled with the commercially available (*R*)-3-((*tert*-butoxycarbonyl)amino)-4-(2,4,5-trifluorophenyl)butanoic acid **270** and (*R*)-3-((*tert*-butoxycarbonyl)amino)-4-phenylbutanoic acid **271**. This conversion was carried out following the procedure described by Merck using HOBt and EDCI in DMF stirring overnight at room temperature resulting in amides (**288-306**). The yields for the amide coupling were between 31-99 % (scheme 49).



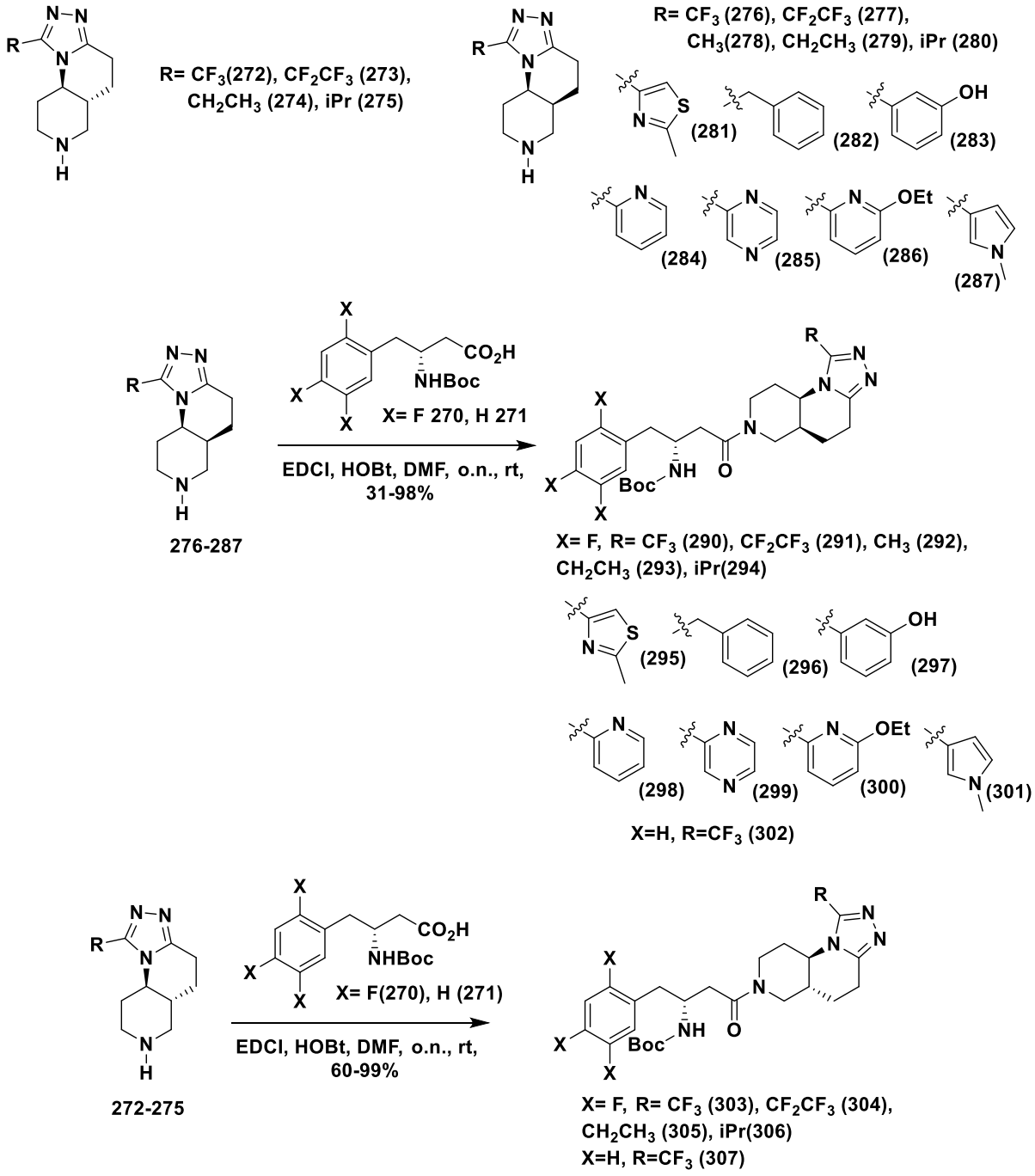
Scheme 47 Final steps in the synthesis of Sitagliptin **256** in the discovery synthesis route by Merck

In the case of the synthesis to compound **302** and **307** using acid **271** only the triazoles **272** and **276**, bearing the trifluoromethyl side group, was coupled using the same procedure as for the [6.6.5] Sitagliptin analogues.

Furthermore, the amide coupling was carried out using the synthesized [6.5.5] tricyclic scaffold **134** to yield compound **288** as the mixture of both possible *cis* isomers. The same procedure was applied additionally to the [6.7.5] membered tricyclic system (**206**), unfortunately still consisting of all four inseparable *cis- and trans-* isomers (scheme 48).



Scheme 48 Synthesis of analogues **288** and **289**

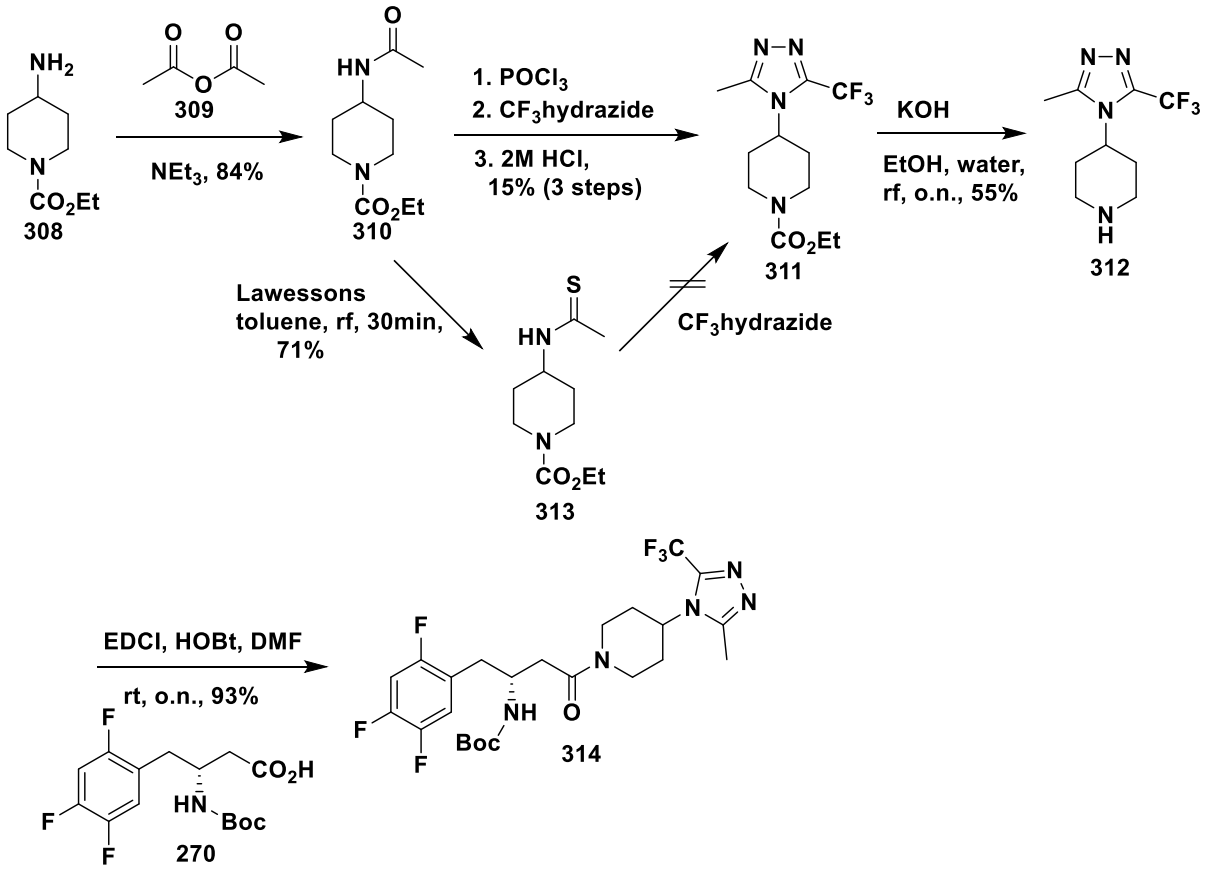


Scheme 49 Synthesis of Sitagliptin analogues **290** -**307** incorporating the [6.6.5] scaffold **272-287**

A further Sitagliptin analogue was synthesized using a bicyclic triazole piperidine system **311** to investigate the activity of such a system in comparison to our novel tricyclic scaffold. This bicycle **311** was prepared starting from amine **308**. The conversion to the acetyl protected amine **310** was carried out using acetic anhydride **309** followed by the conversion to chloroimidate using phosphorous oxytrichloride. The crude product was further converted using trifluoroacetic acid hydrazide which was treated using 2N hydrochloric acid to give

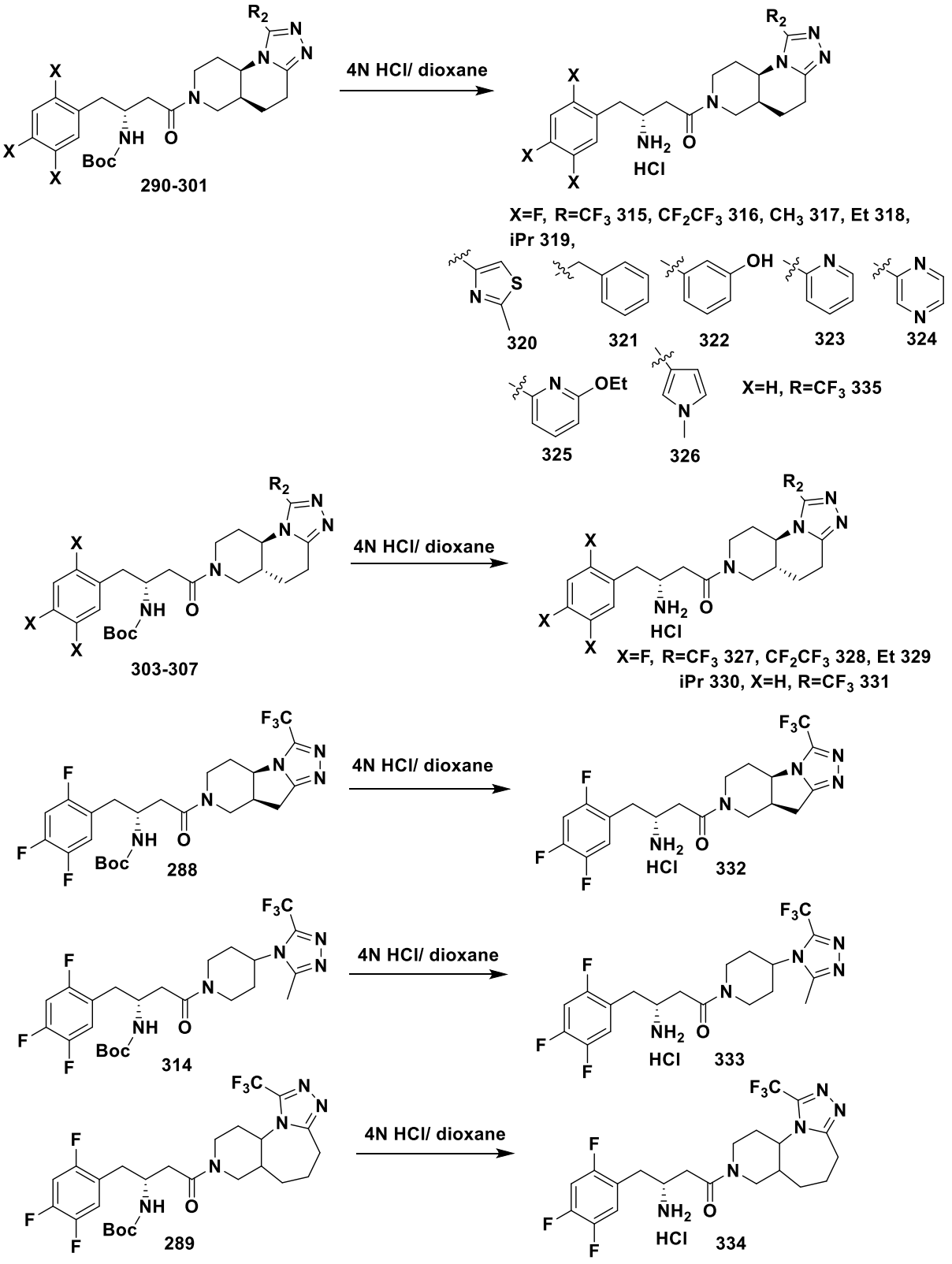
triazole **311** in 15% overall yield. The final deprotection using potassium hydroxide in water/ ethanol delivered amine **312** (scheme 50).

The final coupling to the bicyclic analogue **314** was carried out using the same amide coupling procedure shown for the [6.5.5], [6.6.5] and [6.7.5] scaffold triazole system to yield bicyclic analogue **314** in 93% yield (Scheme 50). Disappointingly, although compound **310** was cleanly converted to thiolactam **313** using Lawesson's reagent, the thioamide **313** could not be converted into the desired bicyclic triazole **311**.



Scheme 50 Synthesis of Sitagliptin analogue **314**

Amides (**288-307, 314**) were purified and deprotected using 4N HCl in dioxane. The HCl / dioxane mixture was evaporated under N_2 atmosphere to give the corresponding hydrochloride salts **315-335**, which were analysed through HPLC (Scheme 51).



Scheme 51 Deprotection strategy through to final Sitagliptin analogues **315-335**

Each of the *cis*- or *trans*- connected scaffolds **315** and **331** are still consisting of a mixture of two *cis*- or *trans*- diastereosiomers **265-266** and **267-268**. The separation was first tried using flash chromatography and classical reverse phase HPLC, but both methods were unsuccessful

and therefore the CF_3 substituted compounds **315** and **327** were purified by chiral HPLC. This work was carried out by the author at the Sygnature Discovery laboratories in Nottingham under the supervision of Stephanie Barlow and all four isomers **265-268** could be separated to allow for biological evaluation (Figure 56).

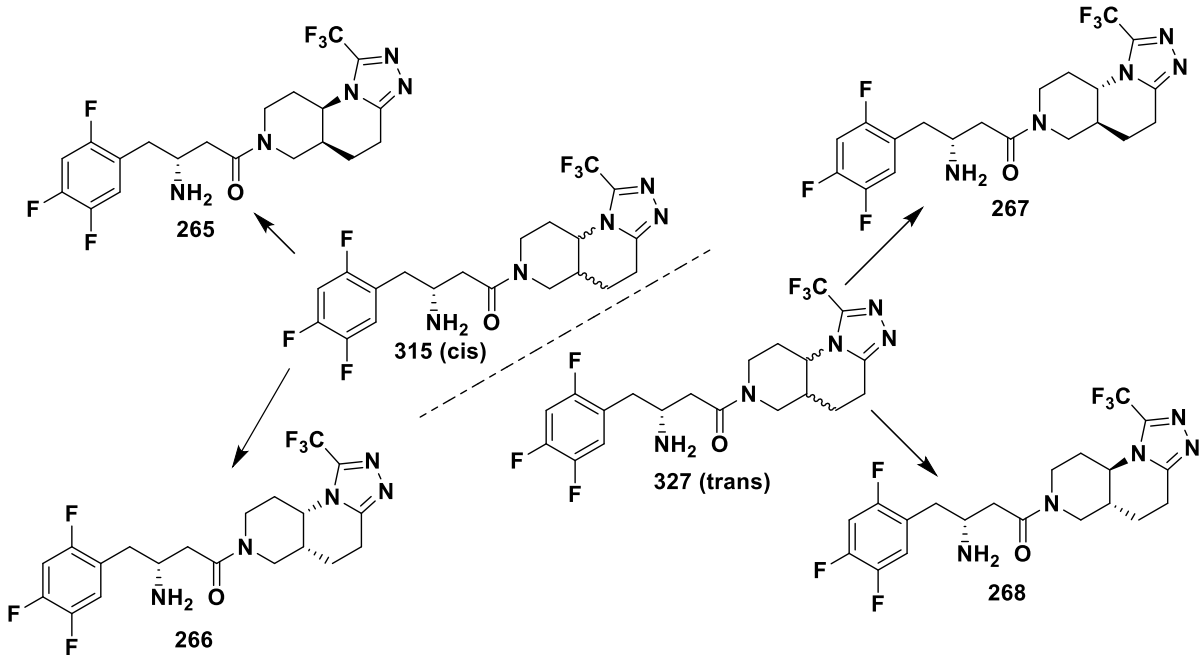


Figure 56 Seperation of diastereomeric *trans*- and *cis*- compounds **315** and **327**

Both enantiomers **265/266-267/268** were resolved from a 1:1 mixture for each *cis*- or *trans*-diastereoisomers **315** and **327** (Figure 57).

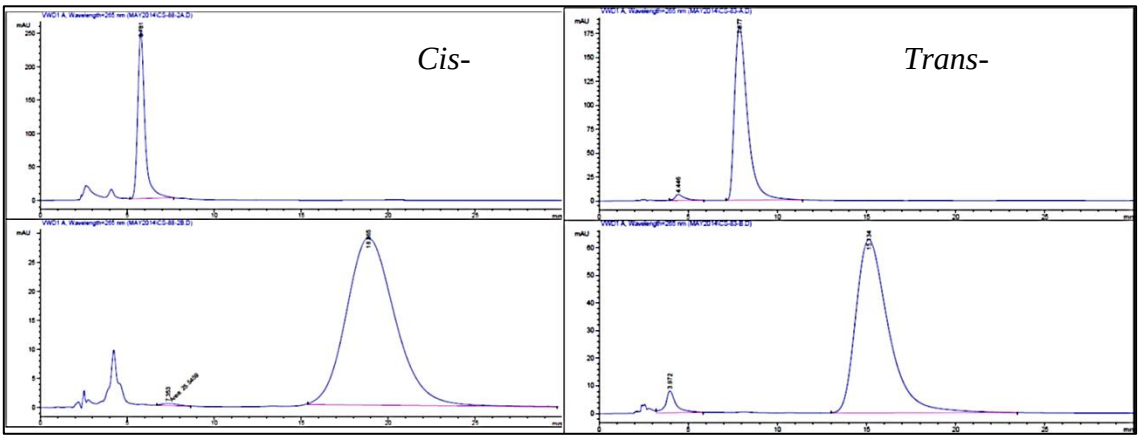


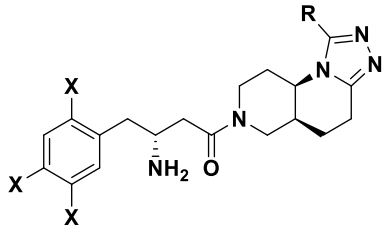
Figure 57 Spectra of separated *trans*- enantiomers **267-268** and *cis*- enantiomers **265-266**

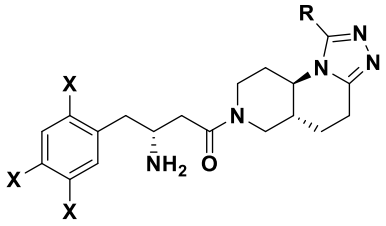
4.5 Enzyme inhibition by Sitagliptin analogues

4.5.1 Enzyme inhibition of DPP-4

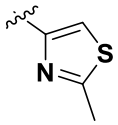
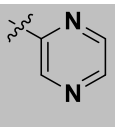
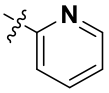
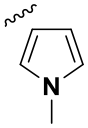
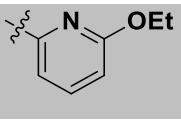
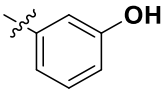
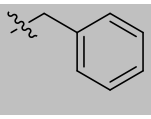
The synthesized analogues **315-335** reported in Chapter 4.4 were submitted to the biopharmaceutical company Hitgen in China for biological screening against the serine protease DPP-4.[116] In this functional assay the remaining activity of the enzyme DPP-4 was determined through measuring the fluorescence observed (ex/em=360/460 nm) as the active DPP-4 cleaves a non-fluorescent substrate (H-Gly-Pro-AMC) to release a fluorescent substrate (7-amino-4-methyl coumarin (AMC)). The IC_{50} values from all analogues are listed in Table 5.

Table 5 IC_{50} values after enzyme DPP-4 inhibition by the Sitagliptin analogues **265-268, 315-335** (n=2), Data are presented as Mean ± SD., Plasma DPP-IV activity was measured using a continuous fluorometric assay with the substrate Gly-Pro-AMC, which is cleaved by DPP-IV to release the fluorescent AMC leaving group and the fluorescent change (ex/em=360/460 nm) was monitored.

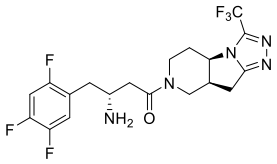
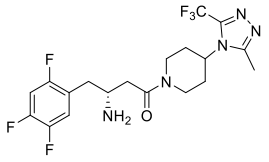
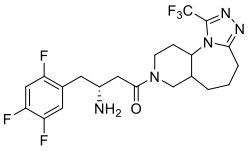
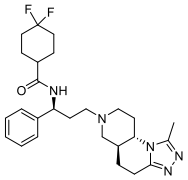




compound	cis or trans	X	R	DPP-4 inhibitory activity [nM]
265/266	*cis*	F	CF_3	27.9± 1.3*
265/266	*cis*	F	CF_3	70.0±2.3*
267/268	*trans*	F	CF_3	527.4±22.5#
267/268	*trans*	F	CF_3	145.1±4.6#
335	*cis*	H	CF_3	694.7+30.5
331	*trans*	H	CF_3	2801.7±85.7
318	*cis*	F	Et	85.4±3.2
329	*trans*	F	Et	107.5±5.6
316	*cis*	F	CF_2CF_3	66.6±1.5
328	*trans*	F	CF_2CF_3	257.7±11.0
319	*cis*	F	*i*Pr	31.8+0.8
330	*trans*	F	*i*Pr	151.7±9.4

320	*cis*	F		50.2±1.0
324	*cis*	F		60.0±2.1
323	*cis*	F		43.4±1.3
317	*cis*	F	CH_3	27.6±0.9
326	*cis*	F		49.5±1.4
325	*cis*	F		139.0±4.1
322	*cis*	F		81.8±4.7
321	*cis*	F		123.3±6.8

Sitagliptin IC_{50} 22±2 (n=20), **cis*- connected single diastereomers, #*trans*- connected single diastereomer; all remaining compounds consisting of a mixture of both diastereoisomers

			
332	333	334	371
93.6±3.7	100.4±3.6	134.4±4.3[+]	>100,000.00^

[+] mix of four isomers, ^ *trans*- connected isomer

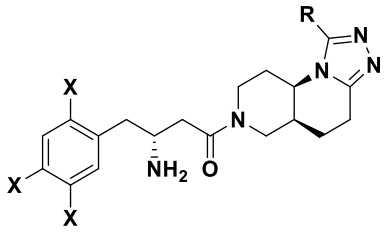
Compound **371** was used as a negative control for evaluation of the selectivity profile of the Sitagpliptin analogues (structure will be shown in chapter 5).

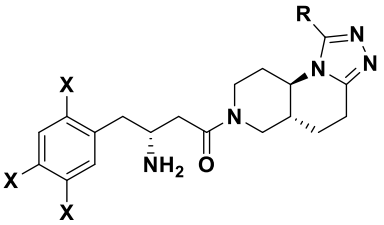
4.5.2 Biological Screening against the enzymes DPP-8/DPP-9

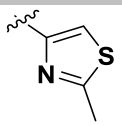
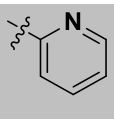
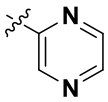
As mentioned in Chapter 4.2, selectivity for the serine protease DPP-4 is crucial for finding a new safe DPP-4 inhibitor. To test the usefulness of our new potential DPP-4 inhibitors towards type-2 diabetes, the compounds were further evaluated for their selectivity profile

against the enzymes DPP-8/DPP-9 (table 6). This biological screen utilized the same protocol as for the DPP-4 screen and was carried out within the Hitgen screening laboratories in China.

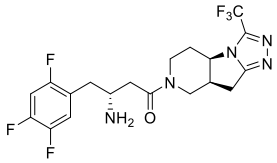
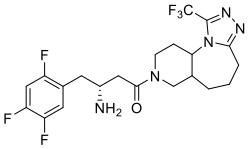
Table 6 IC_{50} values showing the inhibitory effect of the new Sitagliptin analogues against DPP-8/ DPP-9 (n=2). Data are presented as Mean ± SD., Plasma DPP-IV activity was measured using a continuous fluorometric assay with the substrate Gly-Pro-AMC, which is cleaved by DPP-IV to release the fluorescent AMC leaving group and the fluorescent change (ex/em=360/460 nm) was monitored.





compound	cis or trans	X	R	DPP-8 inhibitory activity [nM]	DPP-9 inhibitory activity [nM]
265/266	*cis*	F	CF_3	2247± 261.7*	179.1± 261.7*
265/266	*cis*	F	CF_3	18099±2603.1*	10454.3±659.3*
267/268	*trans*	F	CF_3	5771.5±942.6[#]	3956.1±149.7[#]
319	*cis*	F	*i*Pr	878.9±39.1	38.5±2.7
320	*cis*	F		1518.4±81.4	120.5±6.0
323	*cis*	F		1053.1±34.8	144.7±8.5
324	*cis*	F		1188.9±84.0	138.2±13.0

Sitagliptin (DPP-8) IC_{50} 65±2.5 μM(n=9), Sitagliptin (DPP-9) IC_{50} 71±6 (n=9), **cis*- connected single diastereomers, [#]*trans*-connected single diastereomer; all remaining isomers are consisting of both diastereoisomers

		
	332	334[+]
DPP-8 inhibitory activity [nM]	14787.6±2298.5	5256.8±555.3
DPP-9 inhibitory activity [nM]	4711.9±311.3	557.8±19.5

[+] mix of four isomers

4.6 SAR evaluation of synthesized Sitagliptin analogues

In total 25 compounds were submitted for biological screening against DPP-4 and a further nine compounds were tested against DPP-8/DPP-9 to evaluate their selectivity for DPP-4 over DPP-8 and DPP-9.

Comparing the analogues **315/327, 332, 333** and **334,** which are different in the size/absence of the second ring, showed a trend to increasing biological activity through increasing the ring size and gratifyingly the analogue **315** was slightly more potent than the bicyclic compound **333** (Figure 58).

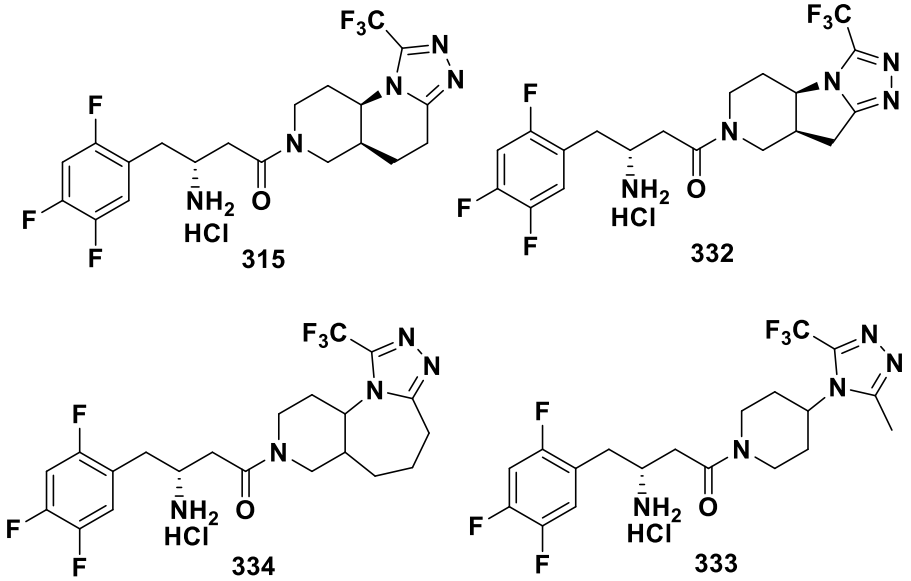


Figure 58 Differences in compounds **315 (**single diastereoisomer**), 332 (**mix of *cis* diastereoisomers**), 333** and **334 (**mix of four isomers**)**

Unfortunately, the seven-membered ring compound **334** was still a mixture of four isomers and the five-membered ring compound **332** was still a mixture of two enantiomers of the *cis*-

connected bicycle. Only the six membered compounds were tested as two single diastereoisomers **266/ 265** with one isomer three times more active compared to the second isomer, which shows no significant difference in the biological activity of these intermediates. This concludes in the trend that the ring size matters in increasing the potency of the sitagliptin analogues which is consistent with the comparison of the analogues in the DPP-4 active site. This docking study was carried out using the scientific software docking program OpenEye and analogues **315, 332-334** were overlaid with the co-crystal structure of sitagliptin **256** (pdb code:1X70) (figure 59).

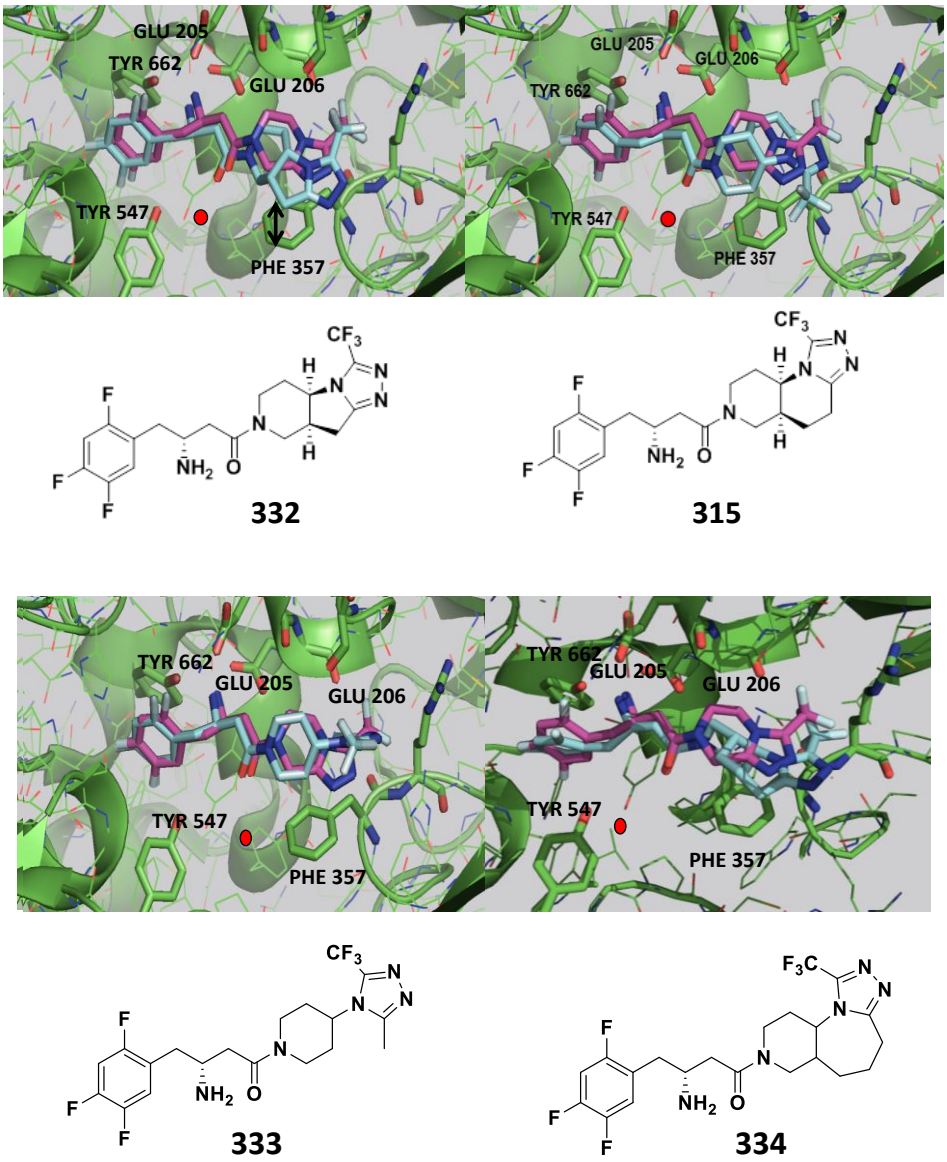


Figure 59 Docking of analogues **315, 332-334** (light blue) in the DPP-4 active site overlaid with Sitagliptin **256** (magenta)

All of the four compounds (**315, 332-334** shown in turquoise) showed a good overlay in the aromatic region compared with Sitagliptin (**256**, shown in magenta) (figure 59). The [6.5.5] membered analogue **332** showed, in its energy minimized docking pose, a clash in the region of Phe 357, which could be the explanation for the lower activity compared to the single diastereoisomer of **315**. The [6.6.5] membered analogue **315** showed a good overall topographical fit with Sitagliptin **256**, with the exception that both CF_3 groups are pointing in the opposite direction to that observed in Sitagliptin. The bicyclic compound **333** showed a twist of 90 degrees in the triazole part compared to Sitagliptin **256.** The [6.7.5] membered connected analogue **334** showed a good overall fit compared to Sitagliptin **256**, where the aromatic part, the amino group as well as the amide group were overlaying well with these groups in Sitagliptin **256**. In the region of the tricyclic scaffold a twist between the six membered and seven membered rings was detected, where the seven membered ring is occupying the S2 extensive pocket. In this analogue **334** the CF_3 group is pointing in the same direction as the CF_3 group in Sitagliptin **256**. The opposite direction of the CF_3 group in the Sitagliptin analogues **315** and **333** could give opportunities to discover new interaction in the DPP-4 sub-pocket.

In all the tested analogues the *cis*- isomers (**315-326, 335**) were more potent than the corresponding *trans*- isomers (**327-331**). The most potent compounds were the methyl (**317**) and *iso*-propyl (**319**) substituted compounds which showed a similar potency compared to Sitagliptin **256,** whilst they still consist of a mixture of diastereoisomers. Furthermore, one single diastereoisomer of the CF_3-substituted compound (**265/266**) demonstrated an IC_{50} of 28 nM, which is a similar level of activity to Sitagliptin (IC_{50} 22 nM). The fluorine incorporated analogues (**316/328,** 67 nM and 258 nM) were in the same activity range than the corresponding ethyl side chain compounds **318/329** (86 nM and 108 nM), regarding the assay variations.

The tested heterocyclic substituted compounds **320** and **323-326** showed a similar activity in the low nanomolar range (between 44 nM-140 nM) as a mixture of two diastereoisomers of the *cis*- fused ring compounds. Whereas only the ethoxypyridino substituted compound (**325**) showed an activity greater than 100 nM. The increase in size through the introduction of benzyl and hydroxyphenyl groups resulting in compounds **321** and **322** with a greater steric demand in the S2 pocket didn't result in any significant changes in the biological activity and are in the range of 100 nM (124 nM and 82 nM). By elimination of the fluorine on the

aromatic ring system in analogues **335** and **331** the activity was decreased by 5-and 23-fold compared to analogues **315** and **327**.

Compound **371** was synthesized for screening the new scaffold against the chemokine receptor CCR5 (explanation in Chapter 5) and was tested against DPP-4 to prove the selectivity of the new scaffold towards different biological targets. Gratifyingly, compound **371** showed no activity towards the enzyme DPP-4 (> 100,000 nM).

The selectivity screen with compounds **265** or **266, 267** or **268, 332, 334, 319, 323, 320** and **324** against the enzymes DPP-8/DPP-9 gave unfortunate results as all promising DPP-4 inhibitors **265/266** and **319** resulted in highly potent DPP-8/DPP-9 inhibitors. Only three compounds were obtained which gave an inhibitory activity against DPP-8/ DPP-9 in the low micromolar range. One of the single diastereoisomeric compounds of **265/266 (**18 μM/10 μM) showed a selectivity towards DPP-4 in the range of 140- to 260-fold and the [6.5.5] connected compound **332** (15 μM/5 μM) resulted in a reasonable selectivity towards DPP-8 in the range of 160-fold compared to Sitagliptin **256** (66 μM/70 μM) which has selectivity of 3000-3100 fold. Interestingly, the less DPP-4 active analogue from the diastereoisomer mixture of **265/266** had better selectivity profile against DPP-8/DPP-9 and is a result that is worth further investigation to tease out the structural requirements for selectivity in this new class of DPP-4 inhibitors

In conclusion, 25 new analogues of the known DPP-4 inhbitor Sitagliptin were synthesized and screened against DPP-4. Furthermore, the biological activity of the best DPP-4 inhibitors was tested against DPP-8 and DPP-9. So far, the trifluoromethyl side chain containing analogues showed comparable biological activity against DPP-4, compared to Sitagliptin, with the *cis*- connection of the rings demonstrating increased levels of DPP-4 inhibitory activity compared to the *trans*- analogues. Only compound **265/266** showed a reasonable selectivity profile towards DPP-4 in a range of 140-260 folds, which was the slightly less active compound of the single diastereoisomers in the DPP-4 screens. Nevertheless, it is a promising starting point with first SAR studies for a new series of Sitagliptin analogues bearing a novel tricyclic triazole system.[116]

5 Maraviroc, a chemokine receptor (CCR-5) antagonist

5.1 HIV-a major global health problem

According to the world health organization (WHO) 35 million people were affected by the human immunodeficiency virus (HIV) in 2013 with 2.1 million new infections and 1.5 million deaths.[117] Over 70% of the new infections occurred in the Sub-Saharan region and this region accounts for around 25 million HIV patients. The Acquired Autoimmune Syndrome (AIDS) was identified as a disease in 1981 with the discovery of the causative viral pathogen[118], later known as human immunodeficiency virus (HIV). From this time on HIV-1 infection and AIDS became a worldwide pandemic and one of the major infectious diseases worldwide.[119] There are two known HIV types (HIV-1 and HIV-2) and both have different viral strains and show different symptoms during the development of the disease. There is still no therapy to cure HIV infection; however medications in the form of antiretroviral drugs (ARV) allow people infected with HIV to live a more unburdened life. The HIV virus targets the immune system and weakens affected patients by destroying the function of their immune cells. As a result the patient is more exposed to variety of infectious diseases and as a result, death often occurs through infectious pathogens, such as TB.

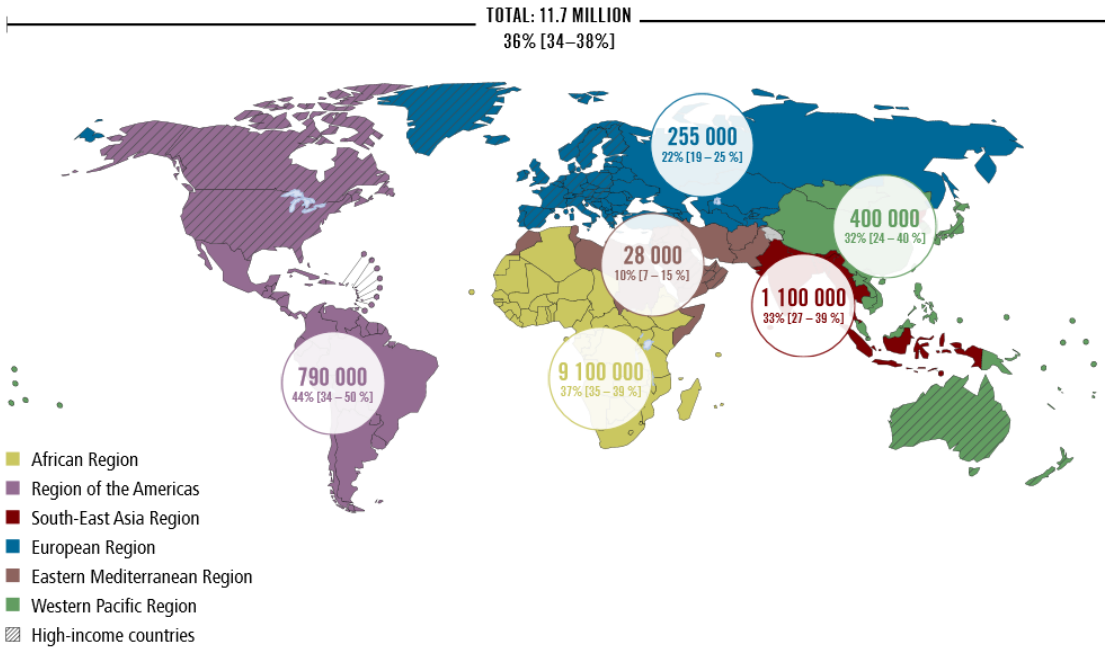


Figure 60 Number of people affected of HIV around the globe, adapted from www.who.int/HIV

Unfortunately, only around 36% of the HIV patients are eligible for a suitable ART (anti-retroviral therapy), which means that only a third of the infected patients are under controlled

medication (Figure 60). The first available treatment for HIV was the nucleoside reverse transcriptase inhibitors [NRTI], which required a complex dosing schedule. This therapy was followed by non-nucleoside reverse transferase inhibitors [NNRTI] which were later substituted by the HAART treatment (highly active antiretroviral therapy), which include a combination of at least three drugs from different HIV drug classes.[120] However the HAART treatment has its limitations due to toxicity issues and the development of resistance. Therefore the search for new effective treatment option for HIV is a continuing ongoing.[121]

5.2 The chemokine receptor CCR-5 and its role in HIV

The CCR-5 receptor is a chemokine receptor, which is located on the cell surface of T cells and can bind peptide ligands called chemokines. Chemokine receptors belong to a large family of the seven transmembrane G protein-coupled receptors (GPCR). GPCRs as therapeutic targets are well-known, as more than 60% of prescribed drugs are GPCR modulators.[122] The human CCR-5 receptor itself is a 352 amino acid protein and consists of seven transmembrane spanning helices connected through 3 extracellular loops (ECL1, ECL2 and ECL3) three intracellular loops, an extracellular N-terminus and an intracellular C-terminus and N-terminus functionality (Figure 61). The extracellular loops and transmembrane helices are responsible for binding ligands and the intracellular regions are responsible for signal transduction. The activation of the chemokine receptor CCR-5 through its binding of endogenously expressed chemokines (macrophage inflammatory proteins MIP-1α and MIP-1β as well as “regulated on activation, normal T cell expressed and secreted” RANTES) can cause typical cellular responses including inhibition of cAMP production or stimulation of intracellular Ca^{2+}.[123]

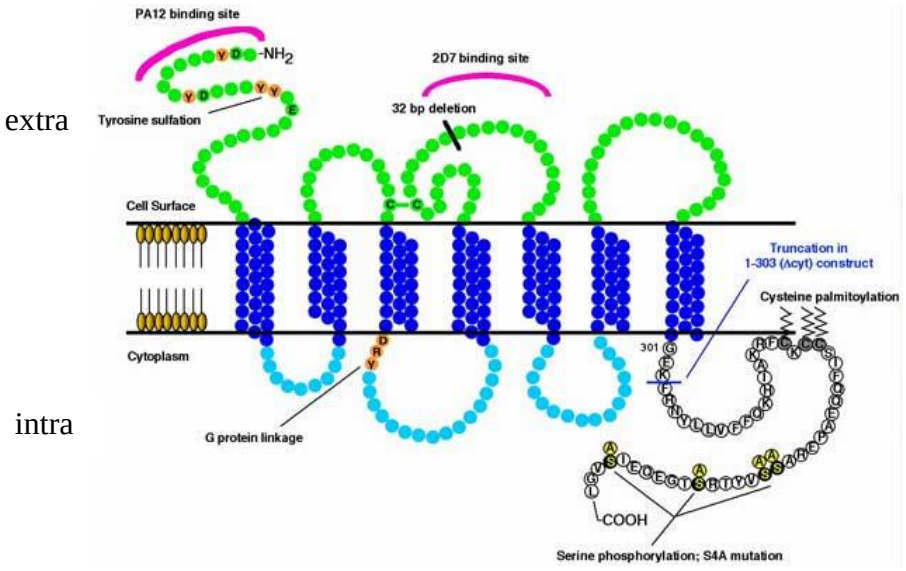


Figure 61 Structure of CCR-5 receptor showing extracellular loops in green and intracellular loops in light blue, adapted from: News and Views: Only weekly of the Scripps Research Institute Vol 3. Issue 31 / October 18, 2004

If an agonist binds to a GPCR it causes a change in conformation within the receptor resulting in activation of heterotrimeric G-proteins.[2] These proteins act as signalling proteins which can activate or deactivate a variety of membrane bound enzymes.

The entry of the HIV into a human cell is a multi-step process starting with the attachment of the gp120 (figure 62), located on the surface of the virus, to the CD4 receptor of the T cells. The interaction between the CD4 receptor and the gp120 leads to a conformational change in gp120, which enables the formation of the co- receptor binding site in the glycoprotein. The chemokine receptors CXCR-4 and CCR-5 are known to be co-receptors for HIV entry into T cells. After binding of the gp120 to the corresponding co-receptor another glycoprotein gp41 is released. In the next step the gp41 N-terminus inserts into the cell membrane, which leads to the approximation of the two membranes to each other and finally to the fusion of the membranes and the entry of the virus into the cell.[124] Whereas the known fusion inhibitor enfuvirtide targets the fusion of gp41, the inhibition point for entry inhibitors is the gp120, which causes the binding to the co-receptor.[125]

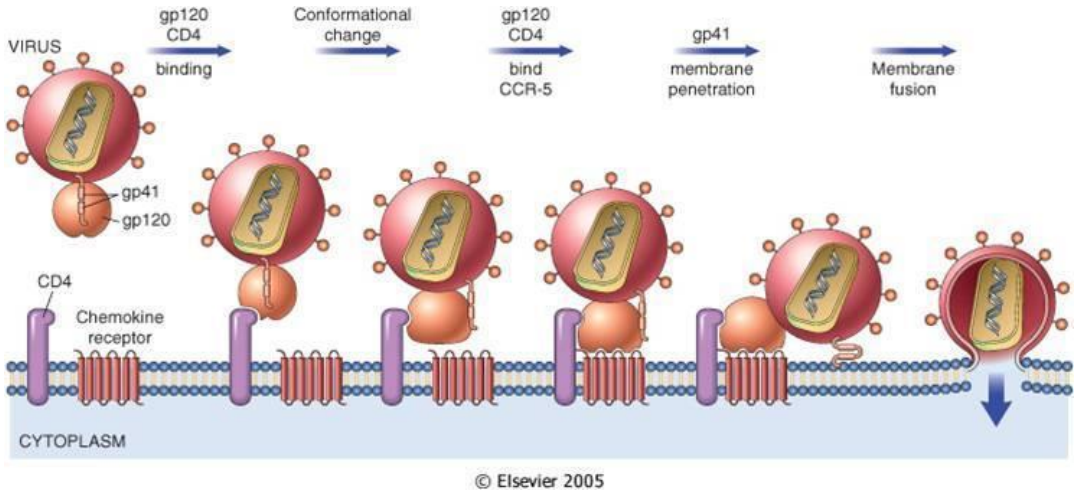


Figure 62 Schematic HIV entry into the cell, adapted from studyblue.com, Elsevier, 2005.

In natural HIV infection, CCR-5 is the primary co-receptor when compared to CXCR-4 as it has a greater affinity to solubilised gp120 (K_d 200-500nM) resulting from the essential binding of the tyrosine sulphated N-terminus of CCR-5 to gp 120.

5.3 The chemokine receptor CXCR-4

CXCR-4 is a structurally related chemokine receptor to CCR-5 belonging to the GPCR superfamily. It was originally identified as an orphan receptor and received its first real attention when its potential as a co-receptor for HIV-1 was discovered with its natural agonist SDF-1.[126] CXL12 (SDF-1α) has a potent virus blocking activity which correlates with the potential internalization of the CXCR-4 receptor. CXCR-4 itself is expressed on the cell surface of various cancer cells and plays a role in cell proliferation. CXCR-4 can be used in the same way for HIV entry as the co-receptor CCR-5. The chemokine receptor CXCR-4 is known to regulate cell migration during immune system control and development of cardiovascular processes and is found the central nervous system.[126] Additionally to its important role in HIV, CXCR-4 plays an important role in the treatment of cancer. To clarify the structural features of the CXCR-4 the group around Qin was able to crystallize the chemokine receptor with a viral chemokine vMIP-II, which allowed further insights into the interactions of CXCR-4 with its endogenous ligand CXCL12 through homology molecular modelling (Figure 63).[127]

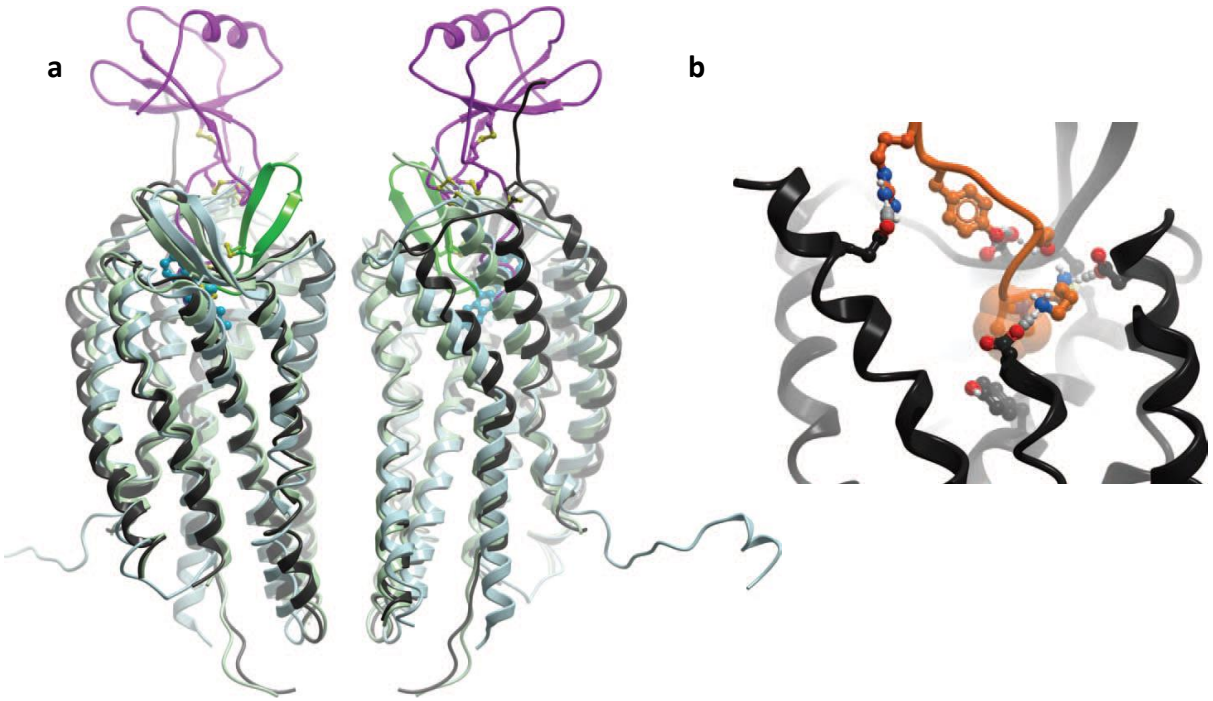


Figure 63 a) Overall crystal structure of the CXCR-4:vMIPII (gray, magenta) complex in comparison with the CXCR-4:IT1t (pdb code: 3ODU, light blue) and CXCR-4: CVX15 (pdb code: 3OE0, green); b) Homologues models of the CXCR-4 R with its ligand CXCL12, adapted from: Qin *et al.*, *Science*, **2015**, *347*, 1117-1122.

This crystal structure complex reveals that CX chemokine receptor bind their ligands as dimers compared to CC chemokines which form β-sheet interactions within the CC chemokine motif and the N- terminal.

5.4 The rationale behind the development of CCR-5 inhibitors

The rationale for developing CCR-5 receptor antagonists followed the observation of resistance of HIV-1 infection of individuals caused by a mutation in their CCR-5 gene.[128] Because of the discovery of the natural base pair 32 deletion (32-bp, CCR-5Δ32) it was possible to identify the absence of CCR-5 on the T-cell surface of this population. This mutation is found in around 1% of Northern European Caucasians. Individuals who are homozygotes for this 32-bp deletion are genetically protected against HIV-1 infection and those who are heterozygotes will experience a huge delay in the disease progression.[129] This CCR-5Δ32 is called a natural human knockout, which allows the confidence in safety, which was observed by CCR-5 promoter polymorphism, which showed resistance against HIV-1 progression. Receptor internalization was caused through cognate agonist ligands which makes the receptor unavailable for HIV-1 strains and therefore for infection. It was also observed that these natural agonists can furthermore inhibit HIV-1 entry which affects the identification of CCR-5 as a co-receptor.[130] This inhibition is thought to take place because

the chemokine induced internalization results in a reduced cell surface exposure of the receptor on the cell surface.[131] More than 50% of the patients who are infected by HIV carry only the R5 strains (see section 5.4).

One major disadvantage mentioned by Westby and van der Rist, resulting from targeting the extracellular host receptors (CCR-5 or CXCR-4), is the blockade of their natural function, which could result in severe unwanted pharmacological effects.[132] One major concern in targeting the CCR-5 co-receptor is its potential to develop a resistance after CCR-5 blockade, for example through a CXCR-4 tropic virus (see chapter 5.5) or through changes in the HIV gp120, which can bind to the CCR5- antagonist complex and continues using the CCR-5 co-receptor.[133]

5.5 CXCR-4 tropism

As the CCR-5 receptor is the essential receptor for HIV infection, CXCR-4 was later identified as a further co-receptor for HIV infected people (Figure 64). The CD4 receptor was rapidly discovered as the primary receptor for the HIV- virus, but it was clear that there must be another receptor involved.[134] Finally, the CXCR-4 receptor was identified as the co-receptor for the X4 HIV-1 in addition to the co-receptor CCR-5. The CX chemokines are characterized by the separation of the two N-terminal cysteines by one amino acid. The discovery of the HIV co-receptors provides a logical explanation for the observed tropism. The definition of tropism is the affinity or specify for a certain target, which mean in the special case for HIV-1 tropism, that it is defined by the differential co-receptor usage of the different HIV strains. There is a nomenclature for the different HIV strains categorized as R5 (CCR-5 tropic), X4 (CXCR-4 tropic) or R5X4 (dual tropic). The CXCR-4 using strains are able to infect cells in the absence and the presence of CCR-5 antagonists. In some individuals, the CXCR-4 R tropism evolves over time and is associated with the rapid CD4 T lymphocyte decline and faster disease progression. In the end there are two different ways a R5 virus can develop resistance against a CCR-5 R antagonist. The virus can use CXCR-4 R, which is called a true co-receptor “switch” by mutating in the viral envelope or expansion of the population which already uses CXCR-4 R. The increase of the population is only possible after the introduction of a CCR-5 R antagonist. A second option is that the virus still uses the CCR-5 receptor, but the virus has the ability of using receptors occupied by a ligand or the affinity for unbound CCR-5 molecules is higher.

Studies by the groups of Agrawal and Alkathib proposed that HIV resistance in CCR-5Δ32 homozygote might result from either a genetic loss of CCR-5 R on the cell surface or an active down regulation of CXCR-4 R expression by the mutant CCR-5Δ32 protein.[135]

This study supports the hypothesis that the CCR-5Δ32 protein acts as a HIV suppressing factor by changing the amount of molecules involved in HIV-1 entry and furthermore the search for drugs that mimic the CCR-5Δ32 protein interaction.

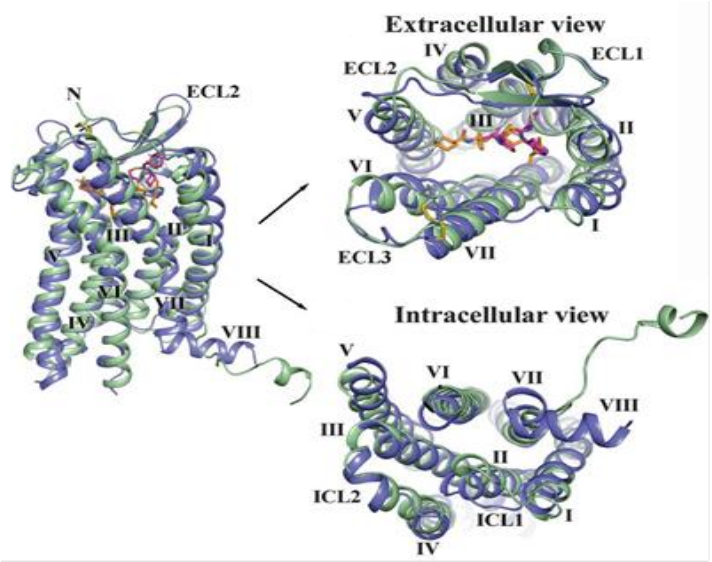


Figure 64 Structural comparison and overlay of the co-receptors CCR-5 (blue) and CXCR-4 (green) in the extracellular and intracellular view, adapted from Tan *et al*., *Science*, **2015,** *341*, 1387-1390.

5.6 Known CCR-5 receptor inhibitors

CCR-5 receptor antagonists inhibit HIV-1 entry by blocking the interaction between HIV-1 gp120 and the CCR-5 cellular receptor. To date, Maraviroc **339** (Figure 65) is the only CCR-5 receptor antagonist which reached the market for the treatment of HIV.[136] As stated before, the co-receptor binding of gp120 to CCR-5 is essential in the entry of the virus. The CCR-5 receptor inhibitors alter the conformation of the extracellular loop which is required for the virus to enter.[137] Multiple pharmaceutical companies embarked on drug discovery programs to search for potent and selective CCR-5 receptor antagonists for anti-HIV indications, as well as for other therapeutic disease areas[138] and several late stage CCR-5 receptor antagonists are shown (Figure 65). The ending "viroc" is an abbreviation for "viral receptor occupancy".

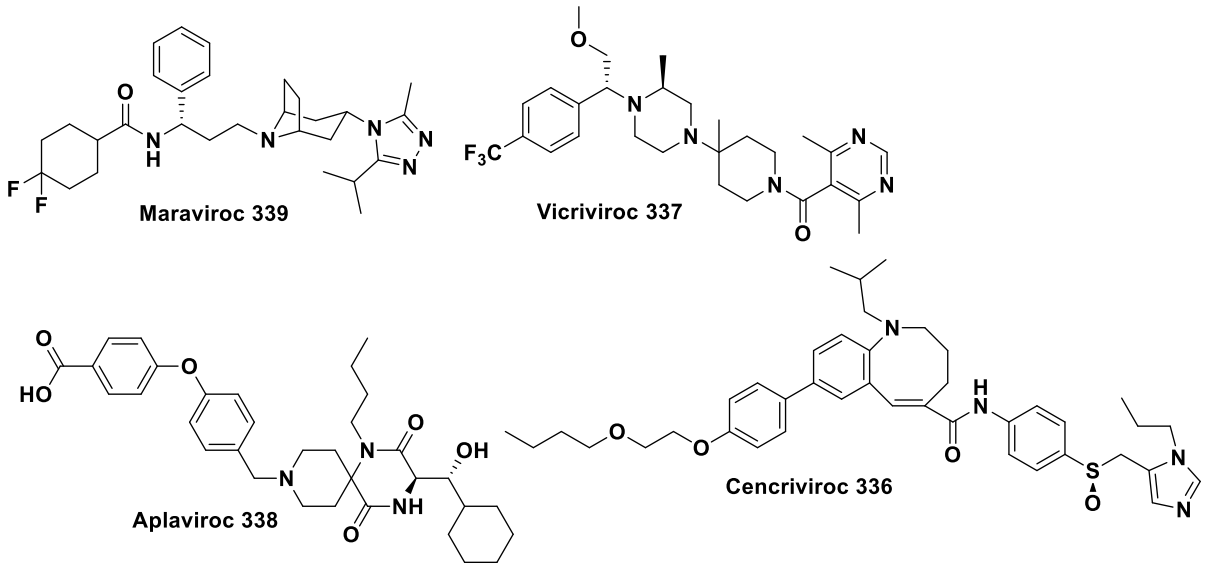


Figure 65 Known CCR-5 R antagonists, Cencriviroc **336**, Vicriviroc **337**, Aplaviroc **338** and Maraviroc **339**

5.6.1 Aplaviroc

Aplaviroc **338** (AK 602, GSK-873140) is a small molecule CCR-5 inhibitor developed by GlaxoSmithKline and is effective due to the inhibition of laboratory adapted and primary R5 HIV-1 isolates *in vitro* in the low nanomolar range. It was discontinued as severe hepatotoxicity occurred during the clinical evaluation.

5.6.2 Vicriviroc

Vicriviroc **337** (Sch-417690/Sch-D) is a piperazine-based CCR-5 antagonist developed by Schering-Plough, which is proceeding in clinical trials, but QT prolongation lead to the reversal of further studies.[136] This compound binds specifically to the CCR-5 receptor and prevents infection of target cells by CCR-5-tropic HIV-1 isolates.[139] The compound passed testing in phase III clinical studies, but was subsequently withdrawn from further clinical development.[140] The studies were stopped for the compound as two phase III studies with recruited treatment-experienced patients failed.

5.6.3 Cenicrivoc

Cenicriviroc **336** (TBR-652) is a small molecule CCR-5 receptor antagonist developed by Takeda Pharmaceutics and Tobira Therapeutics as a follow up of their previous compound TAK-779, which showed a lack in oral bioavailability.[136] TBR-652 can also act as a CCR-2 receptor antagonist which means that it has the potential to decrease inflammation.[121] This compound showed short term virology activity in HIV R5 infected patients and Phase II studies are currently ongoing.

5.7 The Discovery of Maraviroc

The Pfizer CCR-5 receptor antagonist program began with a high throughput screening based on inhibition of radiolabeled ^{125}I-MIP-1β binding to the human CCR-5 receptor. From this screen UK-107543 was shown to have reasonable inhibitory activity against ^{125}I-MIP-1β (IC_{50} = 0.6 μM) in whole cells (Figure 66). Unfortunately, UK-107543 showed no antiviral activity and was shown to be an agonist instead of an antagonist. Another issue was its potency towards the polymorphic human CYP2D6 enzyme, putative *via* coordination of the pyridine N atom to the haem group. Cytochrome P450 enzymes are involved in drug metabolism and the synthesis of steroids and lipids and many other processes.[119,141]

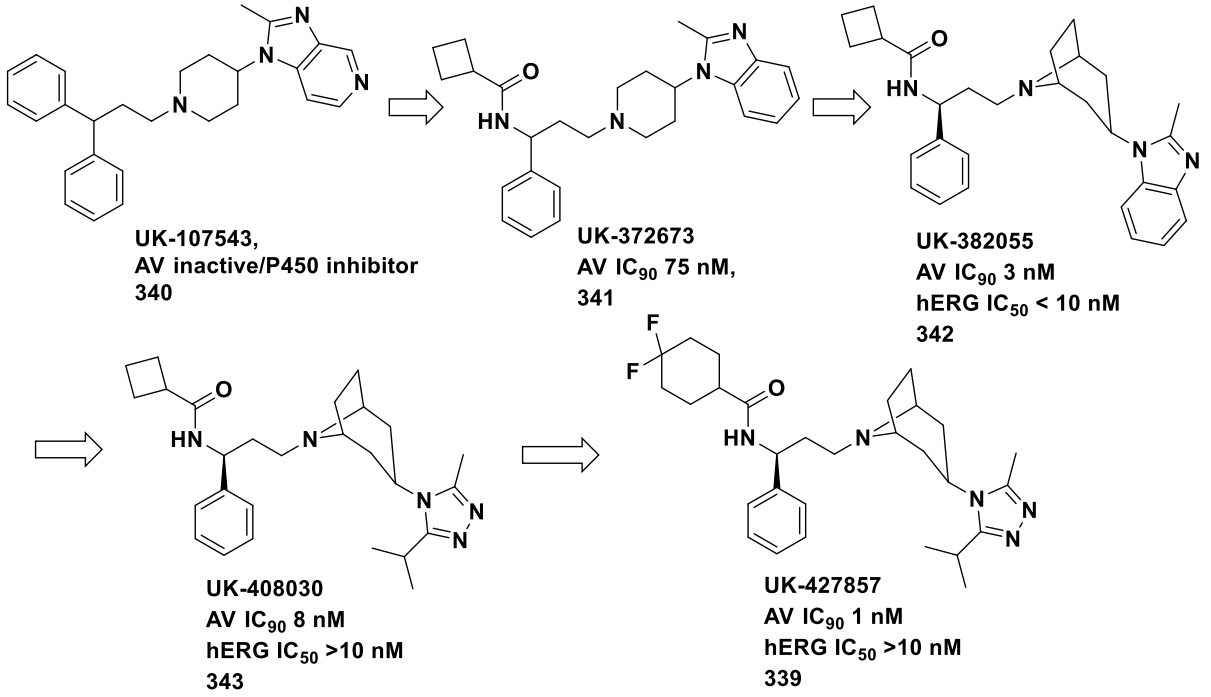


Figure 66 The Pfizer route to Maraviroc (AV= anti-viral activity)

For this reason two changes were made to prevent CYP2D6 inhibition. First, the replacement of azabenzimidazole by a benzimidazole resulted in a potent CCR-5 receptor inhibitor **341** (UK 372673) with significant reduction of CYP inhibition. Furthermore, an additional replacement of one phenyl group from the benzhydryl moiety by an amide was made, which reduced the lipophilicity significantly and, in combination with the tropane ring, R5-HIV-1 specific antiviral activity was obtained with compound **341** (UK-372673). The steric hindrance of the piperidine N atom was increased by substitution with a tropane ring, which gave further improvements in terms of potency in CCR-5 receptor binding and in the receptor signaling assays and led to compound **342** (UK 382055). The enhanced activity was

proposed to result from the reduction of the conformational flexibility of the piperidine ring by the tropane moiety. Further SAR studies showed higher activity of the (*S)*-phenyl analogues, here represented by compound **342**, while the *endo* as well as the *exo* benzimidazole diastereoisomers showed similar equivalent receptor binding and antiviral activities.

The next challenge was to overcome the high and unacceptable affinity for the hERG potassium ion channel. hERG is expressed especially in heart tissue, where overregulation can cause fatal and life-threatening dysfunction.

After inherited mutations were found to cause long QT syndrome (LQTS), which is a cardiac repolarization disorder, the role of human *ether-a-go-go* related gene (hERG)-channel became important in normal human cardiac electrical activity.[142] This cardiac repolarization disorder affects predisposed individuals to cardiac arrhythmia, which is an irregular rapid heartbeat that can lead to fainting and death. The LQTS syndrome is the prolongation of the QT interval, which is the time required for repolarization during a cardiac cycle.

Synthetic effort led then to the triazole **343 (**UK-408030), a compound of the series in which the antiviral activity began to favour the *exo* diastereomer. This compound compromised the profile for favorable absorption, stability, hERG affinity and CCR-5 receptor mediated antiviral activity. The change from the cyclobutyl group to the difluorocyclohexyl group to compound **339** (UK-427857) finally delivered a compound which showed excellent antiviral potency, as well as low activity against hERG. UK-427857 **339** (Maraviroc) was extensively characterized in pharmacology based assays, which highlighted the potent and selective CCR-5 receptor inhibitory activity in a low nanomolar range and finally Maraviroc was approved by the FDA as the first CCR-5 receptor antagonist in August 2007.[143]

5.7.1 The pharmacological profile of Maraviroc

To measure the activity of Maraviroc **339** against chemokine binding to CCR-5 a radioligand competition binding assay was used and Maraviroc **339** inhibited the chemokine MIP-1 α (IC_{50}= 3.3 nM), MIP-1 β (IC_{50}= 7.2 nM) and Rantes (IC_{50}= 5.2 nM) in the low nanomolar range.[144] Maraviroc **339** did not trigger the release of intracellular calcium up to concentrations of 10 μM which proved that no agonist effect was measured. Furthermore the activity of Maraviroc **339** against HIV-1 envelope binding and fusion was tested. This was tested in binding competition experiments against the subunit of the HIV-1 envelope

glycoprotein gp120. The IC_{50} was measured to be 11 nM and in the following fusion cell based assay Maraviroc **339** gave an IC_{50} of 0.22 nM. Maraviroc **339** showed no activity when it was assayed against the chemokine receptor CXCR-4.

5.8 Synthesis of Maraviroc analogues

5.8.1 Preliminary docking studies in the binding pocket of CCR-5

In 2013 the co-crystal structure of Maraviroc **339** in the active site of the CCR-5 receptor was released and could be considered for docking studies of our designed Maraviroc analogues (Figure 67).[145]

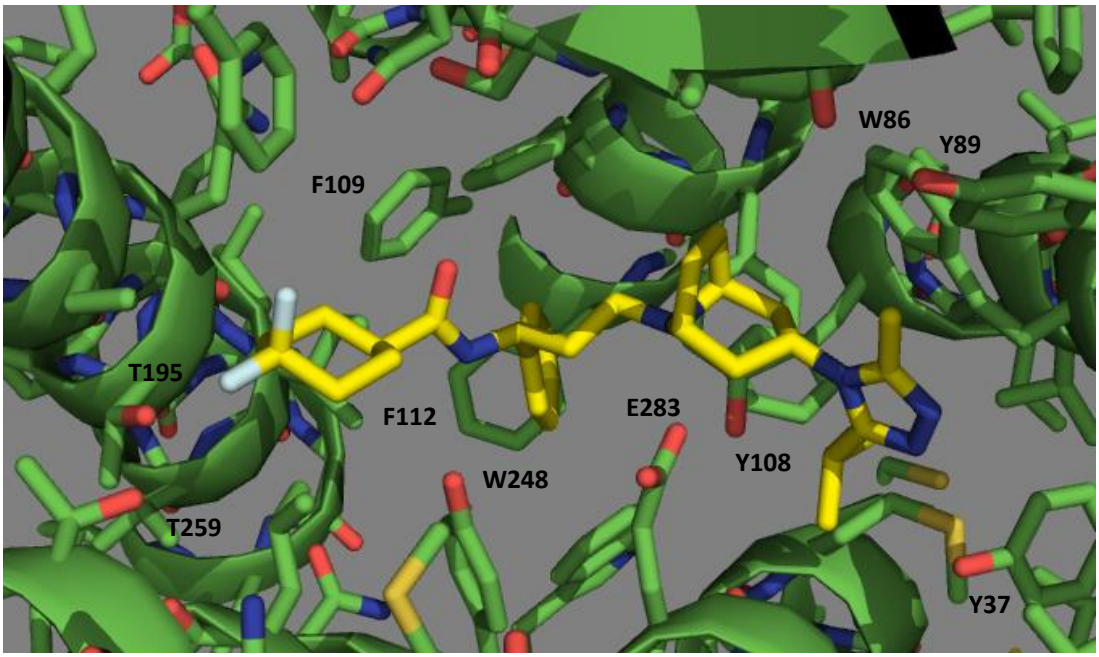


Figure 67 Maraviroc docked in the CCR-5 active site showing the necessary interaction of Maraviroc for activity. Showing the highest scored pose in agreement with the co-crystal structure of Maraviroc (Docked using openeye, pdb code 4MBS, visualised with pymol)

Maraviroc **339** in the CCR-5 receptor active site forms hydrogen bonding to the residues T195, T259, Y251, Y89 and Y37. Furthermore the co-crystal structure revealed the salt bridge of the piperidine N atom to E283 and the aromatic residue of Maraviroc **339** is surrounded by the residues Y251, W248, F112 and F109 to form π–π interactions (Figure 68).

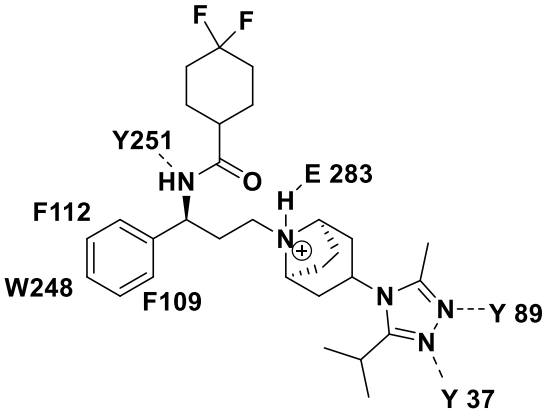


Figure 68 Interactions of Maraviroc **339** in the CCR-5 active site

In this approach we applied the same scaffold hopping concept shown in chapter 4 by changing the piperidine triazole part in Maraviroc with our newly synthesised scaffold **194** to yield four possible diastereoisomers **344-347** (figure 69).

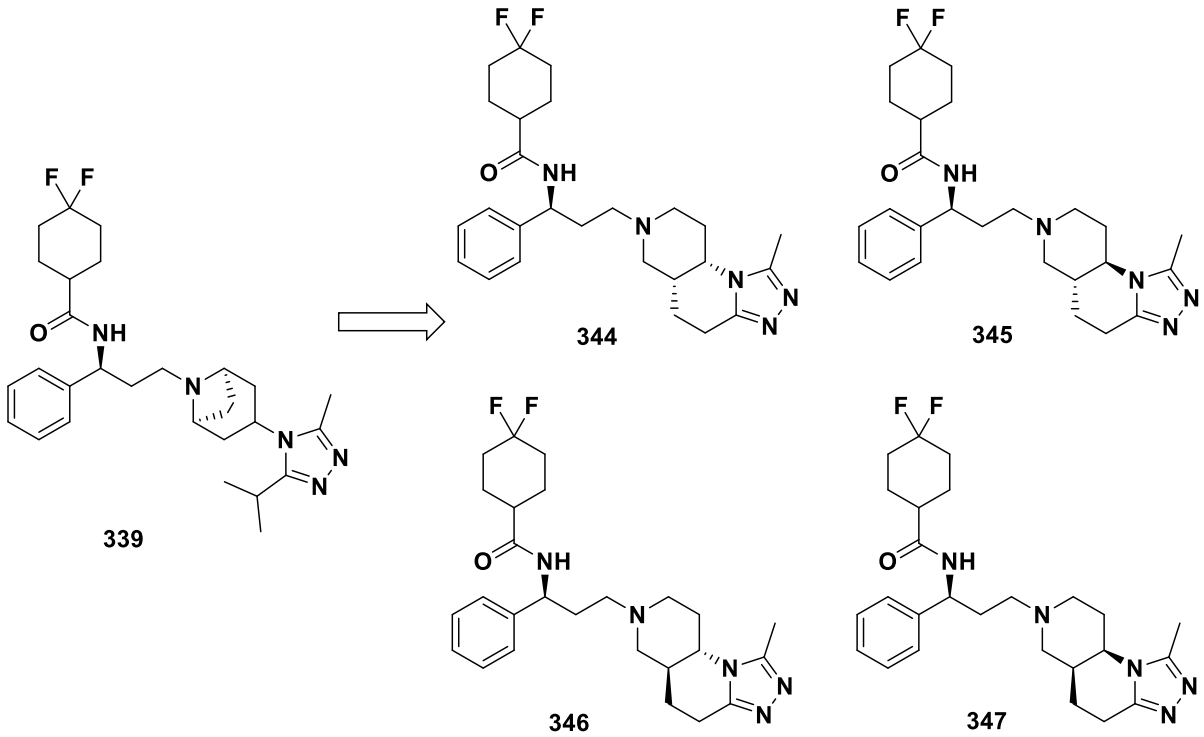


Figure 69 Maraviroc analogues **344-347**

All four diastereoisomers of the Maraviroc analogues **344-347** fitted well into the active site of the CCR-5 receptor binding pocket (figure 70). The overlay with Maraviroc itself is topographically matching with both *cis*- isomers (**344**/**347**) showing a good overlay of the aromatic part as well as the difluorocyclohexane part with Maraviroc itself. The *cis*- analogue **344** matches perfectly with Maraviroc **339**, whereas the space occupied by the tropane bridge

of Maraviroc **339** remains unoccupied. The second *cis*- analogue **347** presents a 90 degree twist in the tricyclic system compared to the first analogue **344**, which allows for interactions in the tropane ring region.

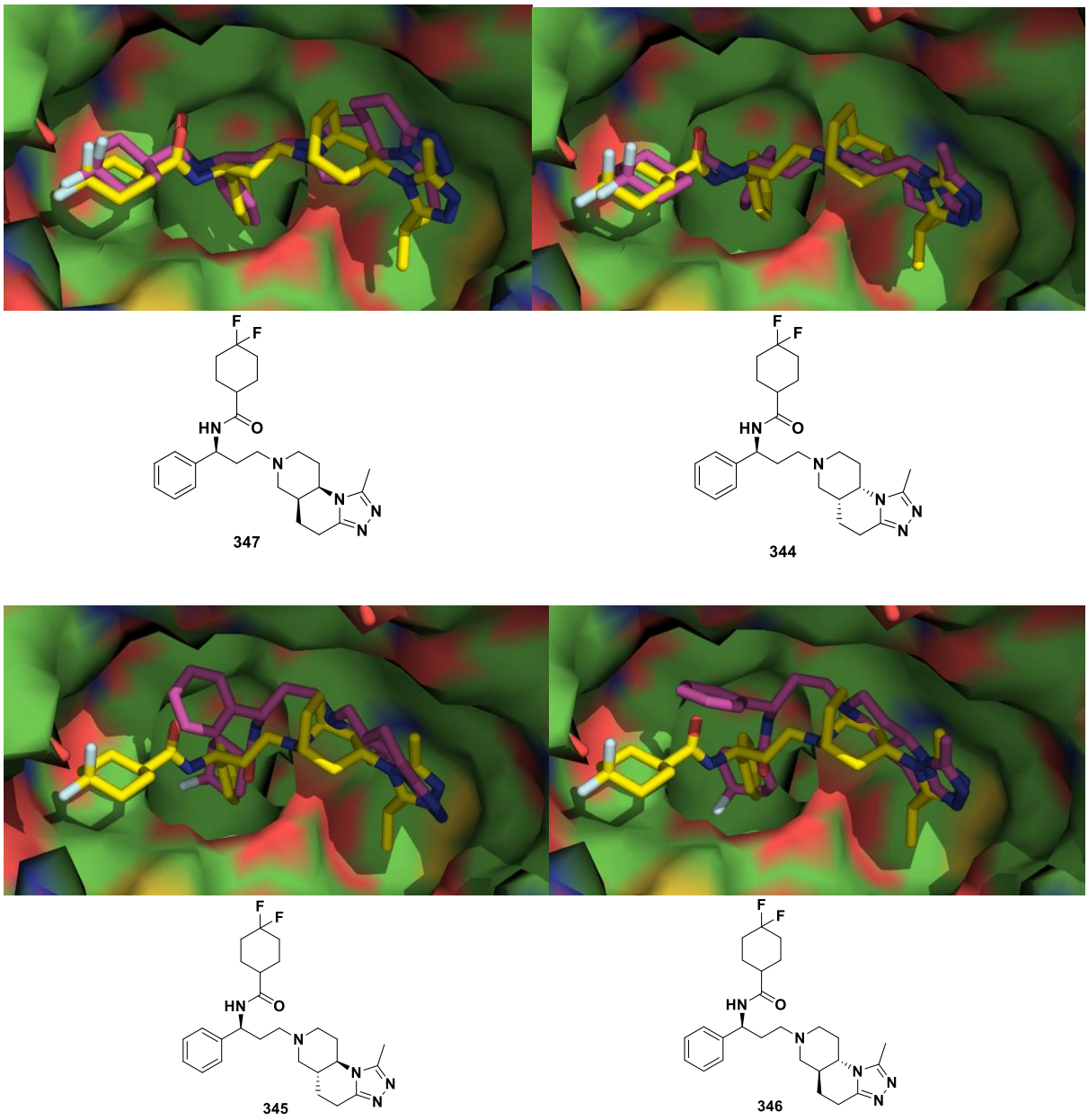


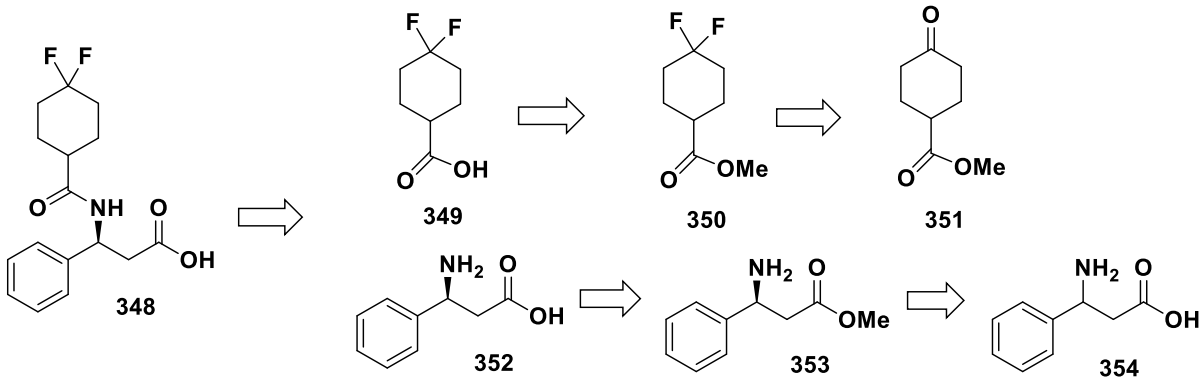
Figure 70 Maraviroc analogues **344-347** (magenta) docked in the CCR-5 active overlaid with Maraviroc (yellow), (Docked using Openeye, pdb code 4MBS, visualised using pymol), surface colouring shown according to the atoms

The fitting of the tricyclic piperdine-triazole part of Maraviroc **339** and the newly synthesised tricyclic part of the Maraviroc analogues **346-347** were shown to be matching well through our initial receptor docking studies. Regarding the *trans*- fused tricyclic analogues **346** and **347** the aromatic as well the difluorocyclohexane part are twisted compared to Maraviroc **339**, which results in an overlay of the difluorocyclohexane part of the analogues **346-347**

with the aromatic region of Maraviroc **339**. The aromatic region of **346-347** points in another direction compared to Maraviroc **339.**

5.8.2 Synthesis of the amino acid part of Maraviroc

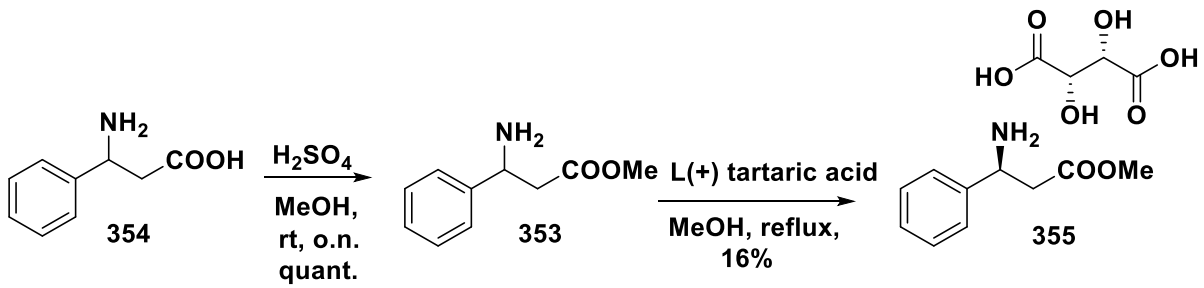
The synthesis of the amino acid part of the Maraviroc **339** should be carried out following the published process route by Pfizer (scheme 52).[146]



Scheme 52 Retrosynthetic approach to amino acid **352** and ester **349**

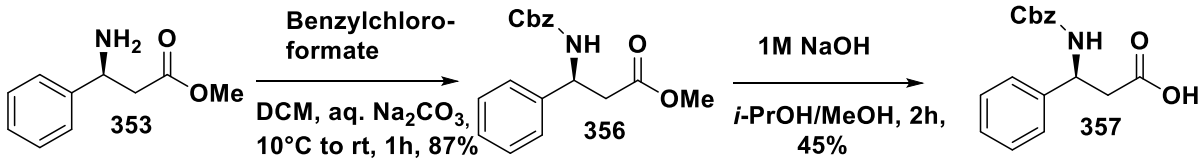
The amino acid part **348** for the synthesis of the Maraviroc analogue **344-347** could be synthesized by the two building blocks **352** and **349.** The amino acid **352** should be synthesized from methyl ester **353,** which can be obtained after diastereomeric resolution with L(+) tartrate out of racemic acid **354**. The second building block (difluoro compound **349)** can be synthesised from methylester **350.** The fluorination should be carried out using ketone **351** and DAST (diethylaminosulfur trifluoride) as the fluorinating reagent (scheme 52).

The second building block of the amino acid part, the amino acid **352** was synthesized starting from commercially available β-phenylalanine **(354)**. This amino acid **354** was converted into the methyl ester **353**, which was resolved using L(+) tartaric acid resulting in the desired amino acid **355**. The crystallisation of this acid **355** required optimization due to the unsuccessful first attempt but immediate precipitation occurred while running the process at low temperatures (Scheme 53).



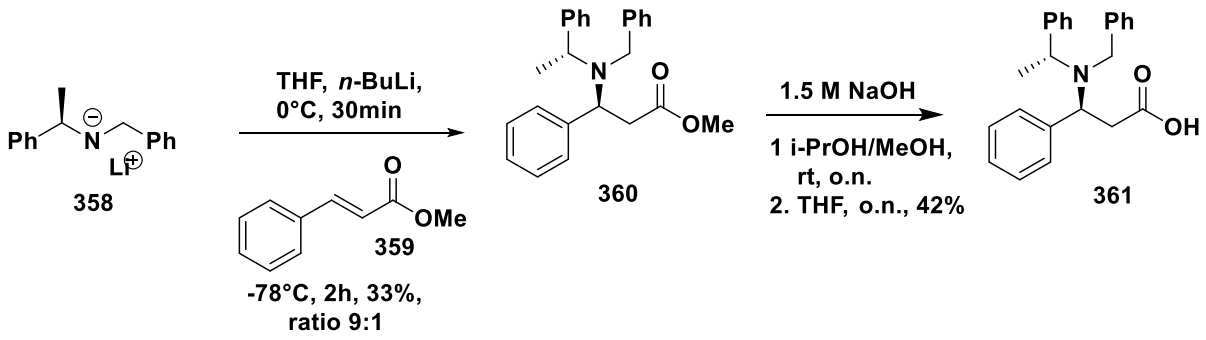
Scheme 53 Synthesis route towards amino acid **355**

The crystallization with tartaric acid yielded the amino acid salt **355**, which was accomplished by crystallizing the compound out of methanol at 0 °C overnight and the optical rotation proved the correct configuration of the amino acid **355**. All subsequent crystallizations were achieved without further problems and compound **355** could be obtained in the desired chirally pure form. The next step was the introduction of the Cbz protecting group using benzyl chloroformate to yield amine **356**, followed by the cleavage of the methyl ester resulting in the desired acid **357**, which was carried out using aqueous sodium hydroxide solution. The resulting NMR data matched well with the data of the Pfizer procedure, proving that the correct compound **357** was synthesized (Scheme 54).



Scheme 54 Synthesis of acid **357**

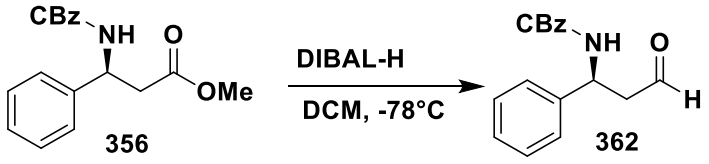
As this synthetic route involves too many steps towards the amino acid **357** another promising procedure was found in the literature which was first reported by the group of Davies.[147] In this two-step procedure, the first step involved a Michael addition of chiral amine **358** to methyl cinnamate (**359**), leading to the direct incorporation of the chiral stereocenter. This reaction was carried out in high diastereoselectivity and in the proton NMR spectrum showed a diastereomeric ratio of 9:1, showing only traces of starting material. The second step was the cleavage of the methyl ester to yield acid **361**. A slight variation regarding the protecting groups was made, staying with both benzyl protecting groups instead of a conversion into the Cbz group, because all groups have to be removed using $Pd(OH)_2$ under hydrogenation conditions (Scheme 55).



Scheme 55 Synthesis of acid **361** following a procedure by Davies *et al.*

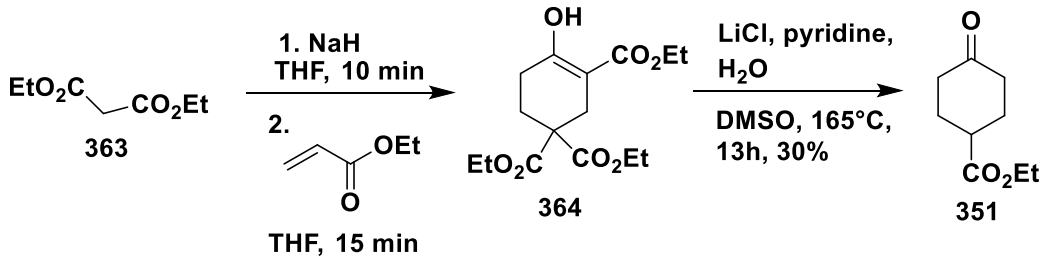
The conversion into acid **361** was challenging as the methyl ester **360** turned out to be highly insoluble in MeOH. Different solvent systems were tested and only THF/ MeOH/ *i*-PrOH dissolved the methyl ester **360** completely and in the following reaction full conversion could be detected. The work up required some optimization and the acid **361** was isolated in a reasonable 42% yield. Despite the low yield this approach was much cleaner and faster than the process route outlined by Pfizer.

As the coupling using amino acid **361** was not successful, amino acid **356** was converted into the aldehyde **362** (Scheme 56) by treating the before synthesized ester **356** with DIBAL-H. By variation of the reported procedure, changing two eq. of DIBAL-H to 1.2 eq. the over-reduction to alcohol was minimized yielding in aldehyde **362** which could be used crude for the reductive amination. All attempts using ester **360** to form the aldehyde functionality failed due to over reduction to the corresponding alcohol, which could not be oxidized back to the desired aldehyde. Furthermore the failure of removing the two benzyl protecting groups using hydrogenation conditions required a stepwise approach to remove the protecting groups. An unexpected observation was the order of reductive cleavage starting with the benzyl protecting group removal instead of the methyl benzyl group cleavage, which was carried out using CAN in a yield of 35%.



Scheme 56 Reduction of the ester function to aldehyde **362**

For the synthesis of acid **349** a literature procedure was found, which used ethyl acrylate and diethylmalonate **(363)** as starting materials to form the desired starting material **351** in a two-step synthesis**.**[148] (Scheme 57).

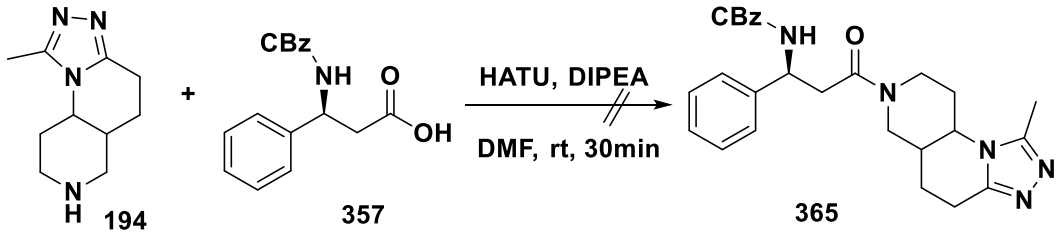


Scheme 57 Synthesis towards starting material **351**

In small scale the reaction proceeded without problems, to give triester **364,** which was used further without purification to yield pure compound **351** in a low yield of around 30%. During the scale up problems occurred, especially during the purification. Therefore, difluoro acid **349** was eventually purchased.

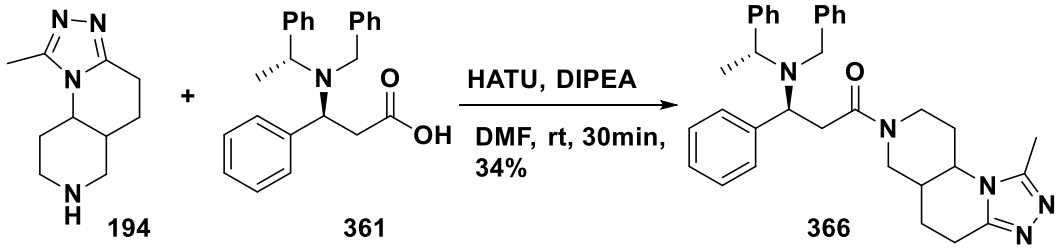
5.8.3 Coupling of the tricyclic triazole to the amino acid

Amine **194** was used directly to couple with either acid **357** or **361.** The reaction with acid **357** was first tried following the Pfizer protocol, which means converting acid **357** into the corresponding acid chloride *in situ* followed by treating with amine **194**. The product seems to be formed according to mass spectrometry, but only in a low conversion. Therefore the previously used coupling method with HATU was used again and MS showed complete conversion to amide **365** (Scheme 58). Unfortunately, the amide **365** could not be isolated during flash chromatography.



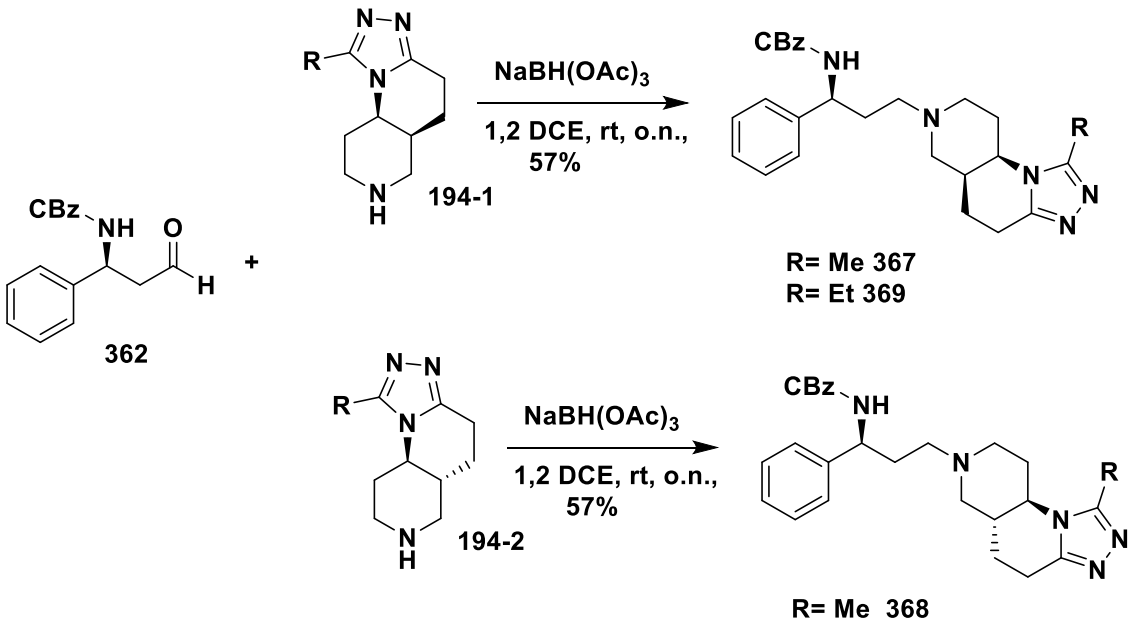
Scheme 58 Synthesis towards amide **365**

In the meantime acid **361** was synthesized featuring the two benzyl protecting groups and another coupling approach was made, using the standard conditions of HATU, DIPEA in DMF and amide **366** was yielded in 34% in a 2:1 mixture of the formed *cis-/trans*-diastereoisomers (Scheme 59).



Scheme 59 Synthesis to amide **366** using acid **361**

As all attempts to reduce the carbonyl function failed by using BH_3·THF, lithiumaluminumhydride in Et_2O, lithiumaluminumhydride in THF or BMS in THF, the next approach was to couple aldehyde **362** using $NaBH(OAc)_3$ in DCE with amines **194-1** and **194-2** in a reductive amination to form amine **367-369**. To improve the yield, acetic acid was added to promote the formation of the amine product in the reductive amination (Scheme 60, figure 71).



Scheme 60 Reductive amination towards amines **367-368**

This reaction was carried out using methyl and ethyl substituted analogues, whereas the methyl analogue was incorporated in tricyclic compounds bearing either the bicyclic *cis*-configured compound **367** or the *trans*- configured compound **368**. The ethyl compound **369** was only synthesised in its *cis*- connected form.

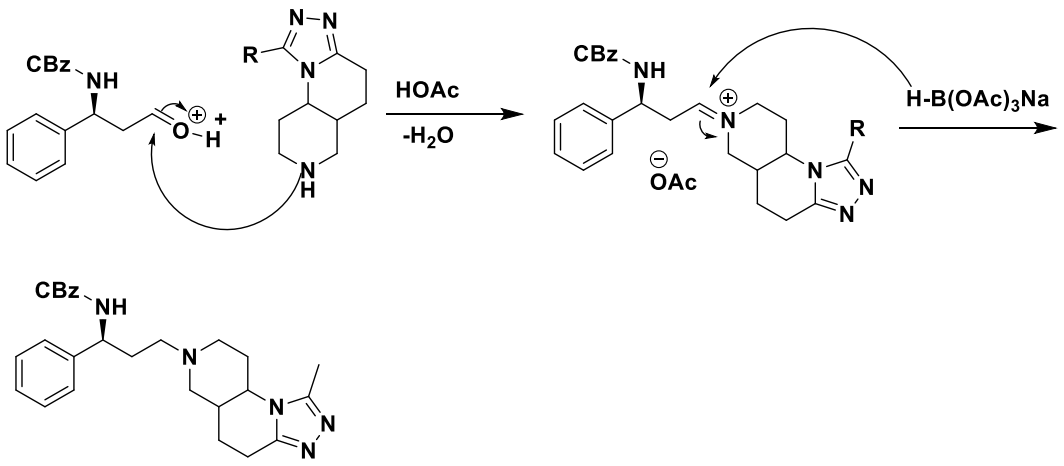
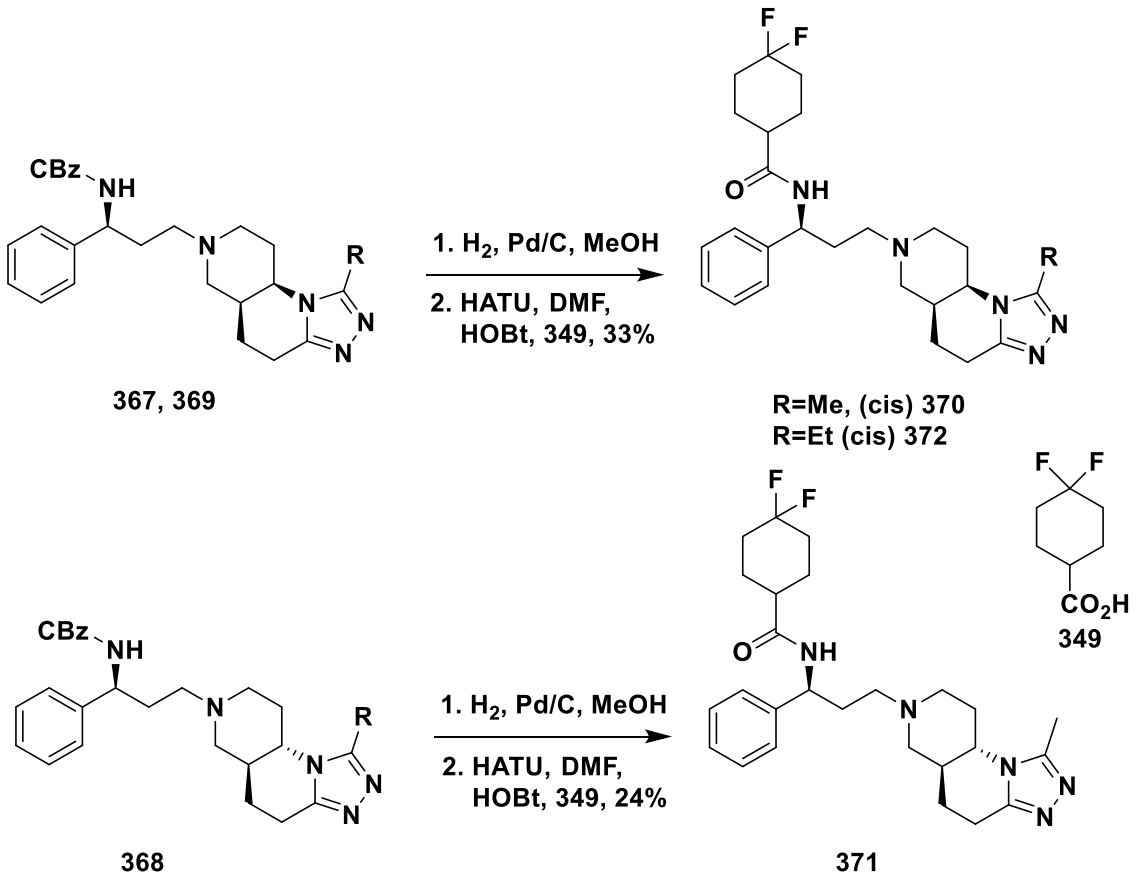


Figure 71 Reaction mechanism of the reductive amination using amine **194** and aldehyde **362**

The next step was the removal of the CBz protecting group followed by the amide coupling with acid **349** to yield Maraviroc analogues **370-372** in low yields of 24-33% following the procedure published by the group of Pfizer in the discovery route towards Maraviroc **339** (scheme 61).



Scheme 61 Synthesis of Maraviroc analogues **370-372**

Three compounds were synthesised for the screen against the chemokine receptor CCR-5 to evaluate the potential of the new synthesised scaffold as a new privileged structure, whereas compound **372** was synthesised by one of my project students (figure 72).

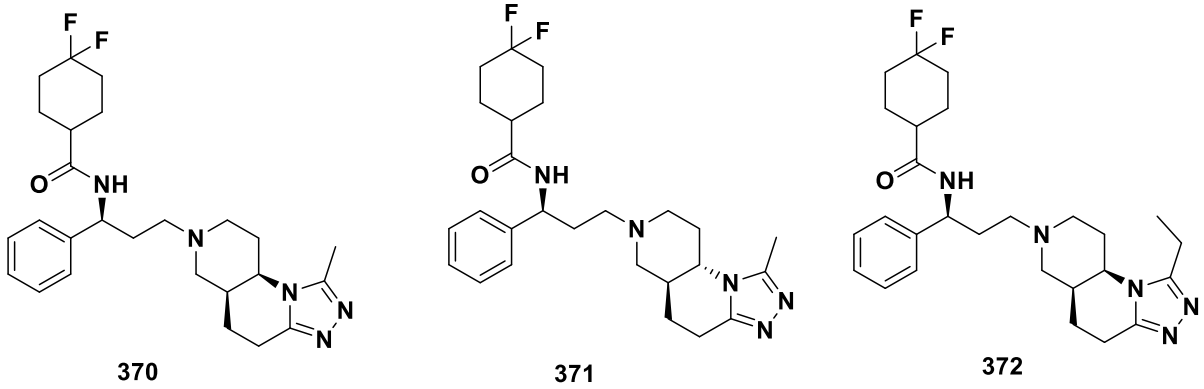


Figure 72 Synthesised analogues **370-372**

5.9 Pharmacology Screen of new synthesized Maraviroc analogues

5.9.1 Screening against the chemokine receptor CXCR-4

Due to the co-receptor tropism, it is necessary to evaluate the potential of the newly synthesized analogues **370-372** to function as potential CXCR-4 agonists. To screen for this, HEK293 glosensor cells expressing the CXCR-4 receptor were used. The cells were grown and plated using white walled plates (see section 11.12.9.1). The assay to evaluate the potential of the new synthesized compounds **370-372** as agonists for CXCR-4 was a cAMP based assay, where the luminescence was decreased if agonism was present. cAMP (cyclic 3',5' adenosine monophosphate) is a second messenger and its role was first reported by Sutherland in the 1950's.[149] cAMP is involved in signal transduction and is a nucleotide which is produced within the cell from ATP which can be inactivated by hydrolysis to 5' AMP by phosphodiesterase enzymes. cAMP regulates many aspects of cellular function, such as metabolism, cell division and cell differentiation. Furthermore it is involved in the ion transport. cAMP activates a variety of protein kinases which catalyze the phosphorylation of serine and threonine residues, which results in activation and inhibition of target enzymes and ion channels. As the CXCR-4 receptor is a G_i coupled receptor it results in reducing cAMP by inhibiting adenylate cyclase, which can be directly activated by forskolin.[149]

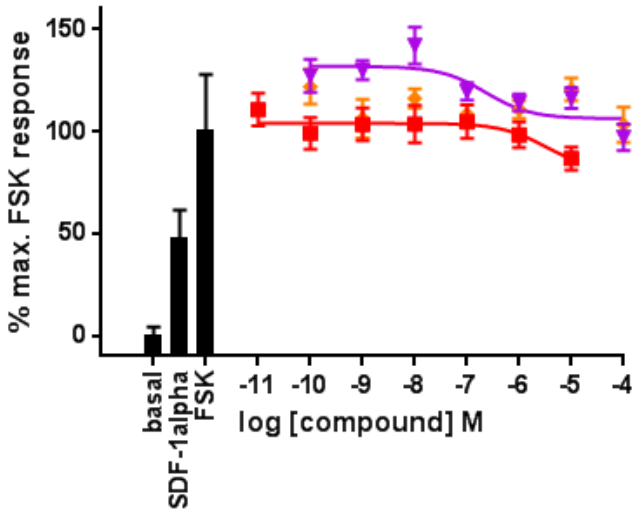


Figure 73 cAMP based assay screening Maraviroc (orange), **370** (lilac) and **372** (red) against CXCR-4 (n=3), Data represented as mean±SEM. Hek Glosensor cells expressing the CXCR-4 receptor were treated with cAMP reagent and cAMP was stimulated with FSK (10 μM) to give a maximum luminescence response of cAMP. The compounds **370-372** were screened in relation to the natural agonist SDF-1α, whereas no agonist effect was seen as the full FSK response is still present.

None of the tested analogues **370-372** showed any agonistic activity towards CXCR4 (figure 73), which is the requirement for the usefulness of the compound **370** and **372** as potential CCR-5 antagonists. No agonism was seen comparing with the agonistic effect of the natural agonist SDF-1a (second bar), which resulted in a decrease in luminescence compared to forskolin (FSK). FSK is responsible for the full activity of cAMP and therefore is producing the maximal luminescence.

5.9.2 Biological screen against chemokine receptor CCR-5

For the screen against the CCR-5 receptor first a new CCR-5 expressing cell line had to be developed starting with HEK 293 Glosensor cells, which were transfected using the corresponding CCR-5 DNA (detailed explanation in chapter 11.12.7). First the transfected cell line was tested in the in section 5.9.1 described cAMP reporter assay and Ca^{2+} assays to test the quality of the developed cell line using the chemokine MIP-1 α, which is the natural agonist of the CCR-5 receptor (figure 74). Intracellular Ca^{2+} is a further second messenger, which can routinely be measured through fluorescent dyes. The intracellular Ca^{2+} is stored in vesicles and its free concentration in the cytosol will be released by activation of inositol phosphate (IP_3).

Unfortunately, the quality of the cell line turned out to be insufficient and a dilution cloning of the cell line had to be carried out as no saturation was achieved and no sufficient response was seen by screening against MIP-1α.

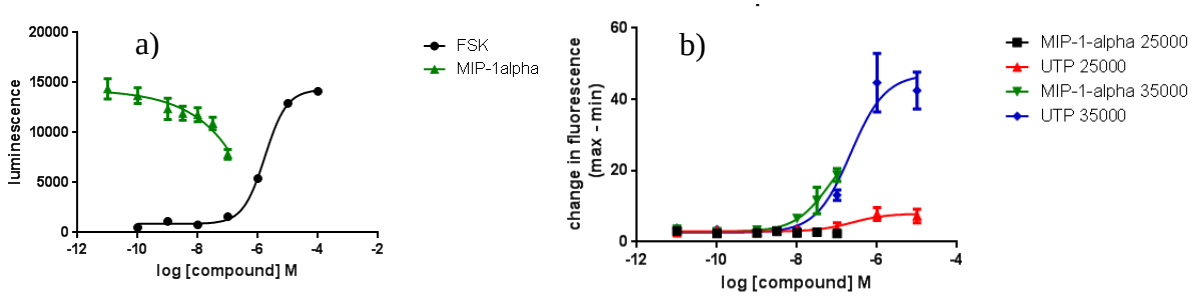


Figure 74 a) Biological screen against CCR-5 receptor using a cAMP based assay, showing the concentration response curve of FSK (10 μM) stimulating the cAMP response to the maximum of luminescence (black) and in green the concentration response curve of natural agonist MIP-1α. By screening against a dose response curve of MIP-1α [1 μM to 0.1 nM] no saturation was accomplished. b) Biological screen against CCR-5 in a Ca^{2+} signalling assay (n=2). Data are represented as mean± SEM. Screening CCR-5 against the natural agonist MIP-1α using different densities of cells/mL (black curve 25000 and green curve 35000 cells/mL, n=2). In this assay no saturation of the concentration response curve of the agonist was obtained compared to UTP (red: 25000, blue:35000)

In figure 74 it is clearly visible that the CCR-5 receptor is not highly expressed in HEK 293 Glosensor cells as only a small response was achieved in the Ca^{2+} signaling assay (b). By increasing the density of cells (25000 to 35000 cells/well) in the assay the signal strength increased and a higher change in fluorescence was measured. However in both assays (a and b) no saturation of the concentration response curve was accomplished, even using a 1 μM concentration of the agonist MIP-1α. As mentioned, no saturation is seen using a cAMP based assay (a)) by treating the cells with the natural agonist MIP-1α (final concentration of 1 μM to 0.1 nM). Another evaluation through the use of single cell imaging of calcium release was carried out to estimate the successfulness of the transfection, but this showed only a small fraction of the cells responding to MIP 1α in comparison to 100 % of cells responding to UTP which acts on endogenously expressed P2Y receptors, indicating that although the CCR5 is present the number of cells expressing the receptor is low and prevents the response being detected in a population assay. Therefore the following step was the dilution cloning of the before established CCR-5 cell line to obtain a cell line resulting from a single cell and ensuring higher proportion of the cells expressing the receptor (details in chapter 11.12.7). The best clone showed a good range of response in the change in fluorescence and the synthesized compounds were tested against the natural agonist MIP-1α (figure 75).

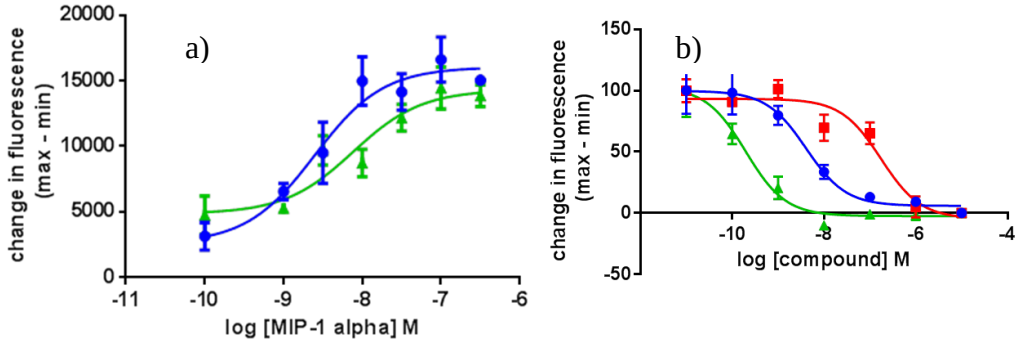
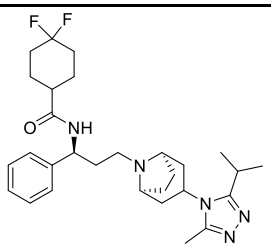
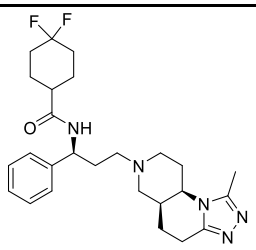
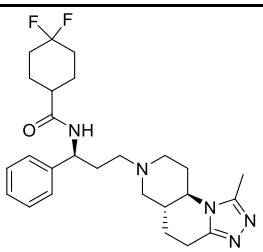


Figure 75 a) Best clone by screening against a concentration response of agonist MIP-1α. Both clones showing a good dose response curve of the natural agonist MIP-1α in a good range of change in fluorescence after stimulation of Ca^{2+} release (n=2). Data are shown as mean±SEM. b) Maraviroc (green) and analogues **370** (blue) and **371** (red) screened against a fixed concentration of MIP-1α [1 μM] (n=2) in a Ca^{2+} signalling assay measuring the change in fluorescence (min-max) after stimulation of the Ca^{2+} release. Both compounds show a good biological activity with IC_{50} values in the low nanomolar range. Data are represented as mean±SEM.

In figure 75 b) the biological activity of compounds **370** and **371** compared to Maraviroc **339** itself is shown at a fixed concentration of agonist. Both compounds showed a good activity against CCR-5 with IC_{50} values of 4 nM and 175 nM compared to Maraviroc **339** with an IC_{50} of 0.2nM (table 7).

Table 7 Biological activity of Maraviroc analogues **370** and **371** at a fixed concentration of MIP-1α [1 μM]. Data are shown as mean± SEM.

compound	 **339**	 **370**	 **371**
IC_{50} (MIP-1α[1 μM])	0.2 nM±0.15	4.1 nM±0.6	175.0 nM±36.4
pIC_{50}	9.7±0.13	8.4±0.5	6.7±0.8

In this screen both analogues **370** and **371** showed good activity as antagonist for the CCR-5 receptor in a nanomolar range. Compound **370** as a mixture of diastereomers was around 20 fold less active than Maraviroc **339** itself and **370**, which is the *trans* fused isomer, showed a 900 fold drop in activity compared to **339**.

Unfortunately after this successful start of the screening program no reliable results could be obtained using MIP-1-α whilst screening against the CCR-5 receptor. Therefore a switch to a

further natural agonist of CCR-5 was necessary. This biological screen was carried out using again the Ca^{2+} signalling assay at a single concentration of antagonist (3-1000 nM, final concentration) in comparison to the dose response curve of the agonist RANTES (figure 76).

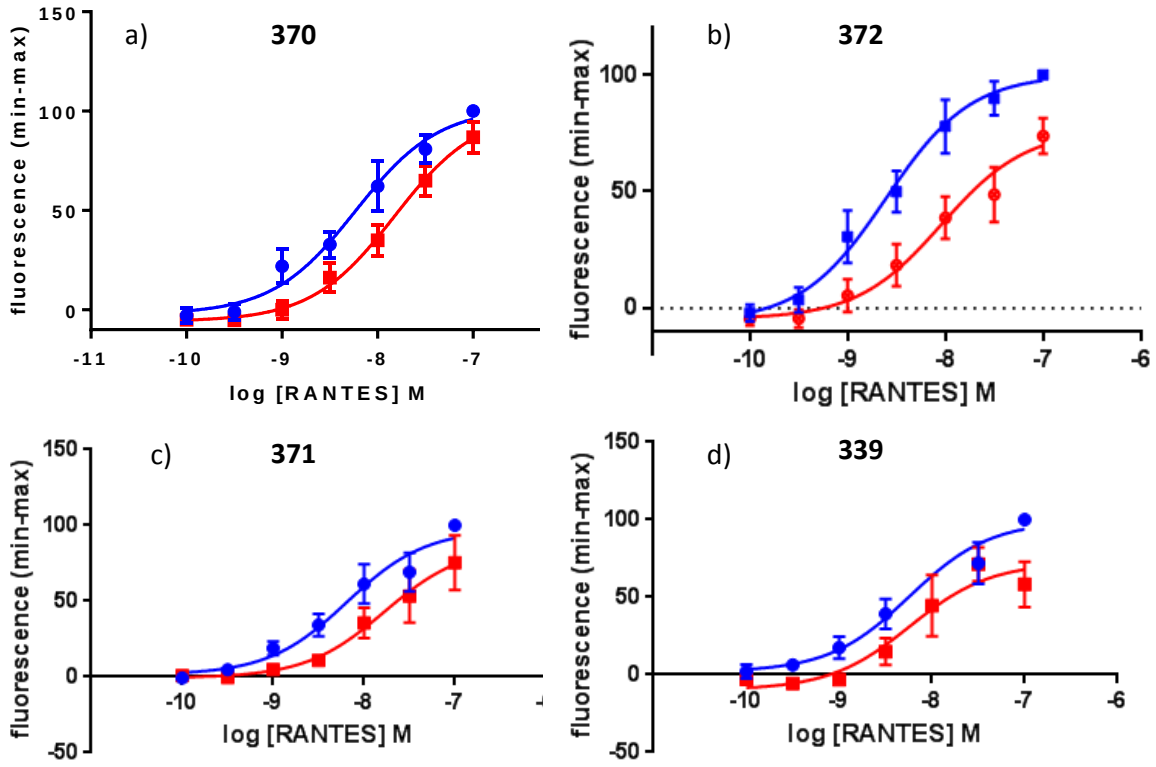
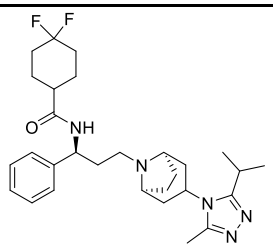
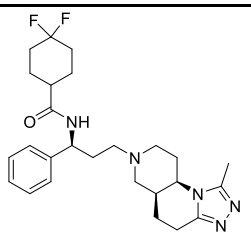
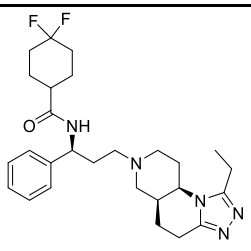
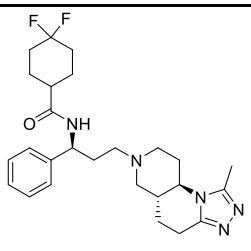


Figure 76 Ca^{2+} signalling screen against CCR-5 in a dose response curve of agonist RANTES using Fluo-4 as fluorescent dye- a) **370** at 30nM (n=6), b) **372** at 30 nM (n=6), c) **371** at 1000 nM (n=3) and d) **339** at 3 nM (n=3) showing the change in fluorescence after stimulation of the Ca^{2+} release.

All three tested analogues (**370**-**372**) showed a good affinity towards the CCR-5 receptor by screening against a concentration response curve of the natural agonist RANTES. Compounds **370**-**372** resulted in pK_D values of 6.5-8.0 (table 8).

Table 8 pK_D and K_D values of Maraviroc analogues **370**-**372** compared to Maraviroc **339**

Compound	 **339**	 **370**	 **372**	 **371**
K_D	**1.6 nM± 0.3**	**10.0 nM ±0.6**	**15.8 nM ± 0.8**	**316.2 nM ± 1.6**
pK_D	**8.8 ± 0.2**	**8.0 ±0.2**	**7.8 ± 0.2**	**6.5 ± 0.1**

In this screen compound **370** showed a 6-fold decrease as a mixture of diastereoisomers compared to Maraviroc **339**, whereas the ethyl analogue **371** showed a 10 fold decrease in activity to Maraviroc. Therefore the change of the side chain group on the triazole didn't show any remarkable difference by replacing the methyl group with an ethyl. The *trans* isomer **371** showed as a mixture of isomers 200 fold less active than Maraviroc **339** and compared to its corresponding cis isomer **370** 32 fold decrease in activity. This finding is in agreement with the previous docking of compounds **370** and **371** in the CCR-5 active site, where the *trans* isomer **371** showed a twist in the region of the aromatic system and the cyclohexane moiety, where in contrast the cis isomer **370** showed an excellent overlay with Maraviroc itself **339**.

In this project three potential new CCR-5 inhibitors could be synthesised with good biological affinity towards the CCR-5 receptor in the low nanomolar range with no agonist activity seen towards CXCR-4. In this project the next step would be to separate the four possible diastereoisomers **344-347** either by chiral HPLC or through a synthetically approach. Combined with the previous reported biological results from the DPP-4 screening (chapter 4) the potential of the scaffold as a new Privileged scaffold is shown and will be further evaluated.

6 A versatile biological target-the PI3 kinase

6.1 Lung cancer, asthma and COPD

Through targeting the respiratory tract, the major clinical focus is on treating diseases such as lung cancer, asthma and COPD. Asthma affects around 235 million people worldwide and is characterized as a chronic disease which dilates the lung airways resulting in acute inflammation, resulting in breathing difficulties. Asthma is a non-communicable condition and can be triggered by allergens, air pollution, tobacco smoke and chemical irritants.[150] Through the appropriate management of medication and by avoiding these triggers, people can live a normal and enjoyable life style. In contrast, lung cancer and chronic obstructive pulmonary disease (COPD) are life-threatening diseases associated with, for example, tobacco consumption.[151] COPD is at this time not curable and has the same risk factors known for asthma patients. More than 90% of the COPD cases are occurring in the low and middle income countries. Pi3K inhibition has a potential therapeutic benefit as pi3K is involved in many important signaling pathways its main focus for therapeutic use on the four class 1 pi3K. Pi3K α and pi3K β are mainly involved in the progression of lung cancer, whereas in contrast pi3K γ and pi3K δ are playing a major role in asthma and COPD (Figure 77).

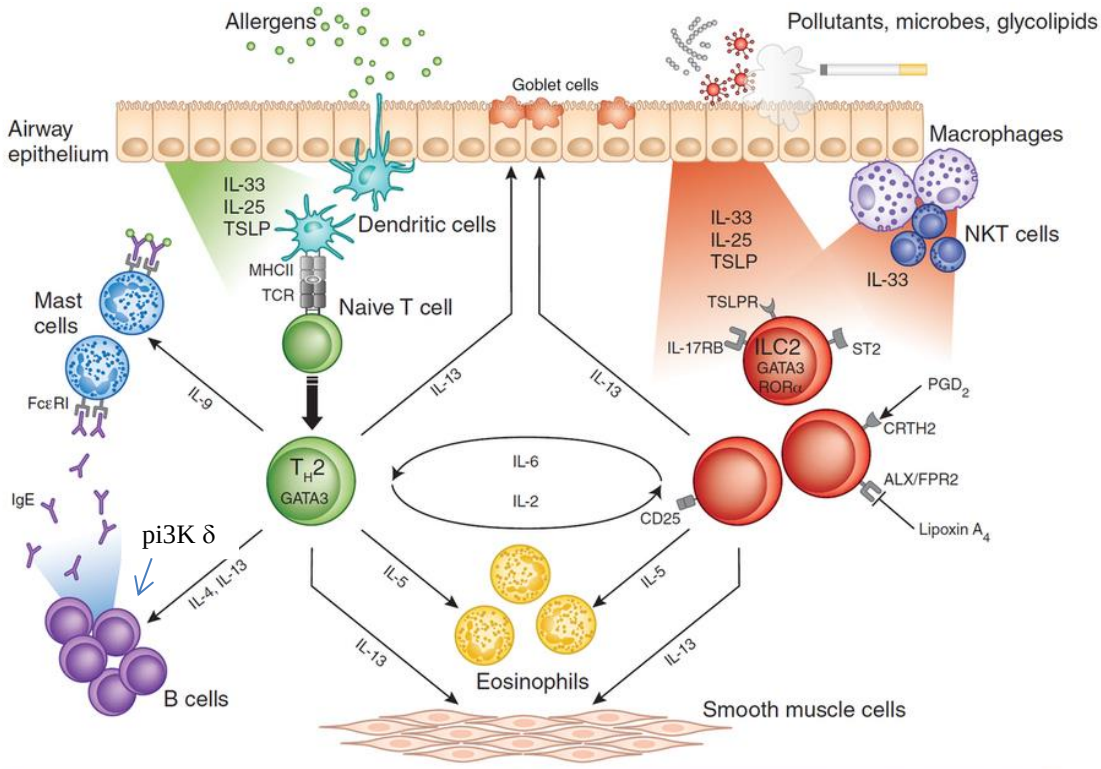


Figure 77 schematic illustrations of triggers to develop asthma adapted by Nature Medicine 19, 977–979, (2013) and slightly modified.

Pi3K inhibition was shown to be important to treat asthma, whereas no beneficial responses are reported by targeting inhibition of pi3K in the treatment of COPD.[152] It has been shown that increased levels of the interleukins (IL-4 and IL-5) are seen in asthma patients, which could be significantly reduced by treatment with a pi3K inhibitor. Furthermore, inhibition of pi3K was shown to inhibit the pathological pathways known in asthma, such as eosinophil count or eotaxin levels. Myou *et al*. first demonstrated the importance of class1 pi3K inhibition in airway inflammation and hyper responsiveness. Furthermore, class1 pi3K δ was classified as key mediator in asthmatic disease by mainly targeting B cells.[153] This was shown in studies were p110δ–inactivated mice had diminished airway inflammation and mucus production.[152]

6.2 The target pi3 kinase- its biological role

The phosphoinositol-3 kinase (pi3K) plays a central role in cellular functioning including growth, proliferation or migration and therefore it plays a major role in diseases related to the respiratory tract ranging from asthma to cancer.[154] These lipid kinases catalyze phosphorylation, which leads to the production of phosphatidylinositol ($PI(3,4,5)P_3$) through the isoforms α,β and δ. ($PI(3,4,5)P_3$) is involved in the signalling of kinase Akt (protein

kinase B), which is a serine/threonine protease involved in cell growth, survival, proliferation and angiogenesis. The phosphoinositol system (PIP_3) is an important intracellular second messenger, whose biological action occurs through stimulating increase of the intracellular calcium concentration. The pi3 kinase family can be divided into three different classes depending on their domain structure. The main focus in current research is on the class 1 pi3Ks, which consists of four members. The majority of research is concentrated on the class 1A sub-unit isoforms pi3K α, pi3K β and pi3K δ, and furthermore class 1B subunit pi3K γ. The selectivity profile for inhibition is important to consider, as non-selective compounds could result in toxicity. This is why several factors have to be evaluated in considering pi3K as the drug target for respiratory diseases.

6.2.1 Pi3 K α

Pi3K α is ubiquitously expressed and its amplification is known in carcinomas and lung diseases.[155] A major feature of pi3K α is its PKB/Akt phosphorylation in dysregulated tumorigenesis and it is known that PKB possess strong proliferation and anti-apoptotic effects. Due to its central role in cell growth and cell proliferation, a rising toxicity effect in foetal development is a major concern accompanied by a major metabolic effect.[156] Therefore pi3K α inhibition has a legitimate consideration in the treatment of cancer therapy.

6.2.2 Pi3K β

Pi3K β is also ubiquitously expressed and plays a significant role in the area of thrombosis, which is associated to the lung by evolving pulmonary arterial hypertension (PAH). The thrombus formation occurs in the signaling process of platelet formation. Pi3K β is known to play an important role in the processes of downstream regulation of GPCR-mediated thrombin and ADP signaling.[157] The effect of inhibition of pi3K β in tumorigenesis is known more in relation to colon cancer than to lung cancer.

6.2.3 Pi3K γ

Pi3K γ expression is limited to neutrophils, eosinophils, macrophage and T cells and in low levels it is found in the endothelium and the heart. Firstly, pi3K γ inhibition has received attention in the drug discovery industry, where early research focused on the lack of GPCR-mediated stimuli. The rationale behind inhibiting the pi3K γ is the influx of inflammatory effector cells, which play a major role in the pathology.[158] Allergic inflammation is characterized through activation and degranulation of tissue mast cells and the influx of

eosinophils. The recruitment of the eosinophils to the site of inflammation results in activation of a variety of molecules acting through GPCRs to stimulate pi3Kγ. It is known that asthmatics have impaired lung response through infection resulted in a severity and progression of obstructive pulmonary diseases, which would be a major concern in developing a pi3 K γ antagonist for the treatment of lung diseases.

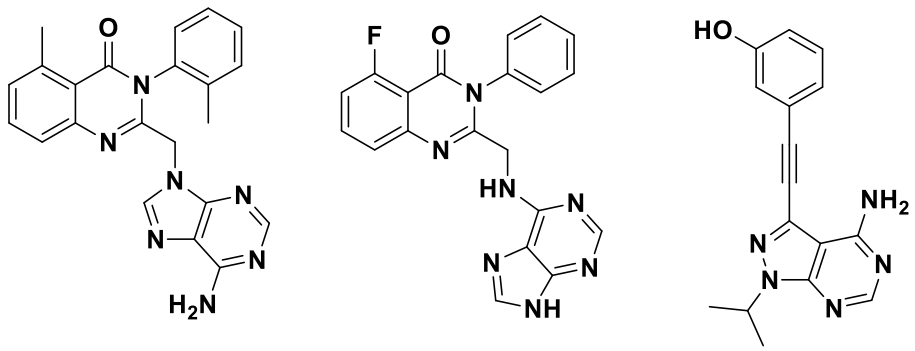
6.2.4 Pi3K δ

As the expression of pi3K δ is limited to leukocytes, its inhibition has a great potential for the treatment of respiratory diseases. The reduction of response in pi3K δ knock in (KI) mice and animals was seen after treatment with a pi3K δ specific inhibitor, which is demonstrated by reduced clonal expansion of CD4 cells and diminished pathology in asthma models.[159] The inactivation of pi3K δ also affects mast cell function, which play an important role in allergic responses and asthma.

6.3 The selectivity profile towards pi3K δ

The fact, that the isoforms γ and δ are almost exclusively expressed in leukocytes gives the opportunity to target inflammatory diseases specifically. It is known that pi3K δ signals downstreams in B-cells, which is important for antigen recognition.[160] Pi3K δ is furthermore signaling downstream in a number of receptors known in a variety of leukocytes important in immune function. Therefore pi3K δ inhibition became an interesting target for leukemia, asthma and rheumatoid arthritis, as the cell types where pi3K δ is linked are responsible for the pathogenesis in inflammatory diseases. Regarding the selectivity towards pi3K δ over the other three isoforms, it is known that the selective inhibitors IC87114 **373** and Idelalisib (Cal-101) **374** adopts a propeller shape position in the pi3K δ active site (Figure 78).

a)



IC 87114
373

Cal-101
374

DL07
375

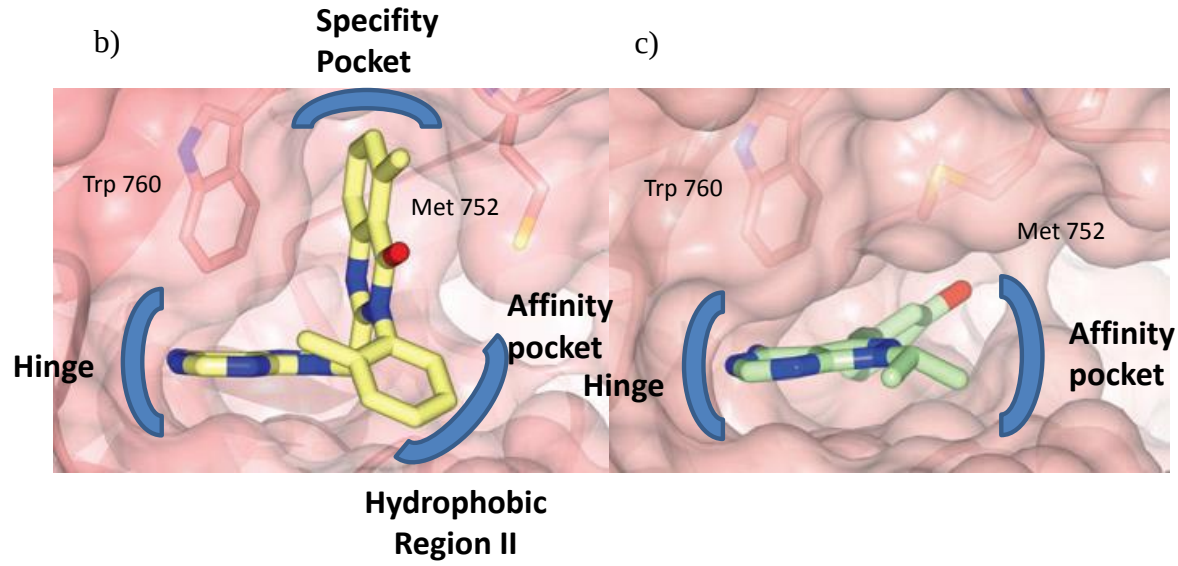


Figure 78 a) Known selective pi3k δ inhibitors IC 87114 (**373**) and Cal 101 (**374**), Docking picture of b) **373** in the active site of pi3K δ (pdb code 2X38) showing the propeller shape and opening of the specificity pocket, c) DL07 **375** in the active site, showing its planar arrangement, adapted by Workman *et al*. (NatChem. Biol. 2010, 6, 81-83) and modified.

Through the propeller shape orientation, a change in conformation occurs which opens a specificity pocket between Trp812 and Met804.[161] Therefore, the important design concept is to allow more flexibility in the inhibitors to enable the inhibitor to bind into the specificity pocket present in the pi3K δ (Figure 78). Whereas inhibitors which adopt a planar structure can't reach this specificity pocket and no selectivity is achieved towards pi3K δ. Following the compound class typified by the known inhibitor GDC-0941 **376**, which is a non-selective pi3K inhibitor developed by Genentech in 2008 for the treatment of cancer[162] and GDC-0980 **377**, a non-selective pi3K/mTOR kinase inhibitor[163], in 2012 Sutherlin *et al*. published a potent selective pi3K δ inhibitor- **378** (Figure 79)[164].

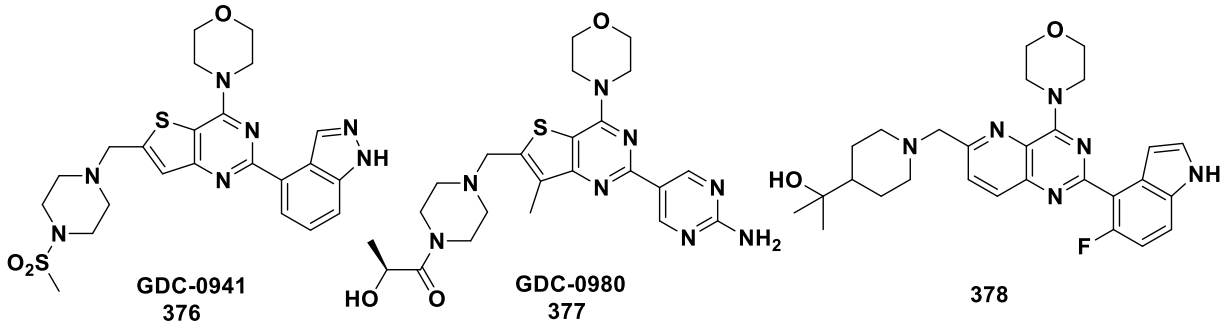


Figure 79 Non-selective pi3K inhibitors GDC-0941 (**376**) and GDC-0980 (**377**) and the selective pi3K δ inhibitor (**378)**

Compound **378** shows 200- to 400-fold selectivity towards pi3K δ over the three isoforms α, β and γ. This compound was initially achieved by developing isosters for the phenolic compound **379**, which was shown improved the selectivity towards pi3K δ (Figure 80).

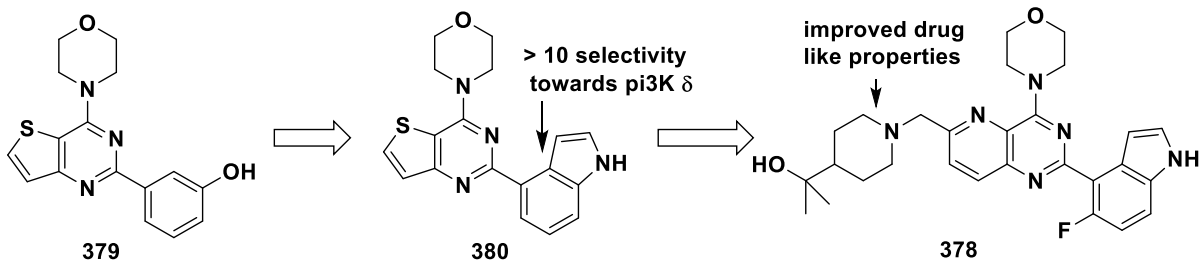


Figure 80 Establishment route to pi3K δ–selective compound **378**

The introduction of the basic amine group resulted in an improved drug profile with improved potency, solubility and ADME properties. Compound **378** showed furthermore a selectivity profile towards other kinases, which was reported by Genentech using the Invitrogen Select Screen service (0/239 kinases showed > 50% at 1μM).

6.3.1 Docking in the pi3K δ active site

The rationale for the improved selectivity profile was evaluated through the co-crystal structure of compound **378** to illustrate the important interactions in the active site. One of the major differences of the active site of pi3K δ compared to the other three isoforms is the presence of the threonine 802 residue in pi3K δ (γ numbering), whereas this space is occupied by larger charged lysine or arginine residues in the other three isoforms. These residues are directly located over the tryptophan 812 (numbering of pi3 K γ) where the amine substituent would be located (Figure 81). This gives insight into a so called tryptophan shelf, which is thought to play the important role regarding the selectivity of inhibitors towards the δ isoform.

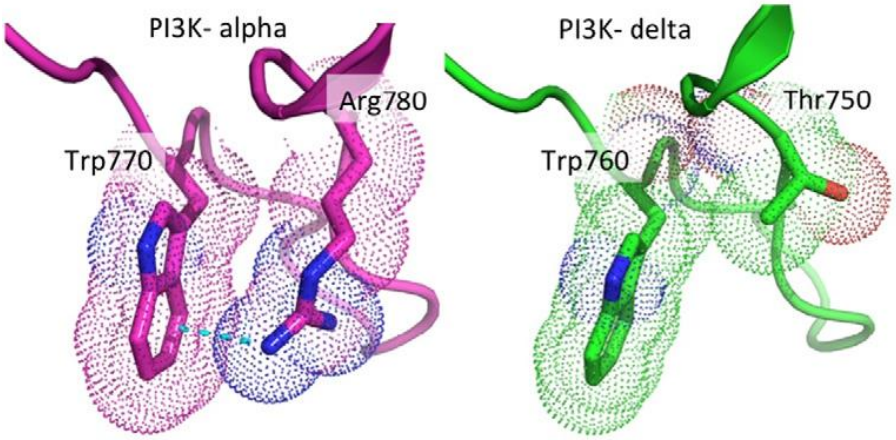


Figure 81 Differences in the active site in pi3K α (PDB code 3HHM) and pi3K δ (PDB code 2WXP), numbering according to the active site, adapted by Sutherlin, Bioorganic & Medicinal Chemistry Letters 22 (2012) 4296–4302.

Genentech used in their co-crystal structure the (K802T) pi3K γ mutant, where compound **378** bound in a similar way as it was known for the inhibitors GDC-0941 **376** and GDC-0980 **377** (figure 79, 82). The morpholine ring interacts with the hinge region of the active site and the indole substituent forms a hydrogen bond to Asp 841 (Figure 82). The tryptophan shelf available in the mutation K802T pi3K γ allows the tertiary methyl groups to interact with the face of the tryptophan 812, which is the major difference compared to the other three isoforms. Furthermore, the planar quinazolone part is known from the previous inhibitor IC87114 **373** to allow insertion into the pocket of threonine 802 and the methionine 804 (pi3Kγ numbering), which allows the favourable interaction with the edge of tryptophan 812.

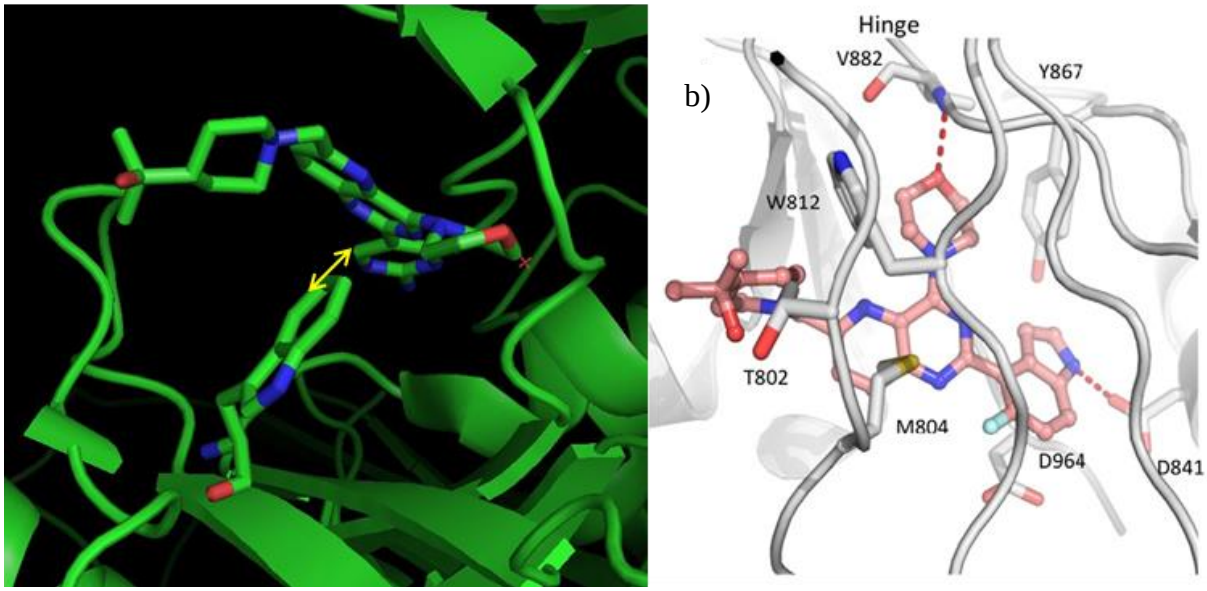


Figure 82 a) Docking studies using the K802T mutation of pi3K γ (pdb code: 4EZL) showing the interaction with the edge of tryptophan 812 with the quinazolone part of **378** and b) the fit of compound **378** into the active site showing the interactions, b) adapted from Sutherlin, Bioorganic & Medicinal Chemistry Letters 22 (2012) 4296–4302.

Regarding the affinity pocket, the indole interacts with the tyrosine 867 to form a strong hydrogen bond interaction in the affinity site which is considered to play a further significant role in the selectivity towards the pi3K δ isoform.

6.4 The rational for a new selective pi3K δ inhibitor

Considering the work by Genentech towards the pi3K δ-selective compound **378,** the scaffold synthesised in chapter 3 was introduced in the core structure of GDC-0941 **376** to establish new analogues **381-382** of the pi3K antagonist **376**. The analogues **381-382** were docked into the active site of the K802T mutation of the pi3K γ to evaluate their potential as new selective pi3K δ antagonists (figure 83, 84).

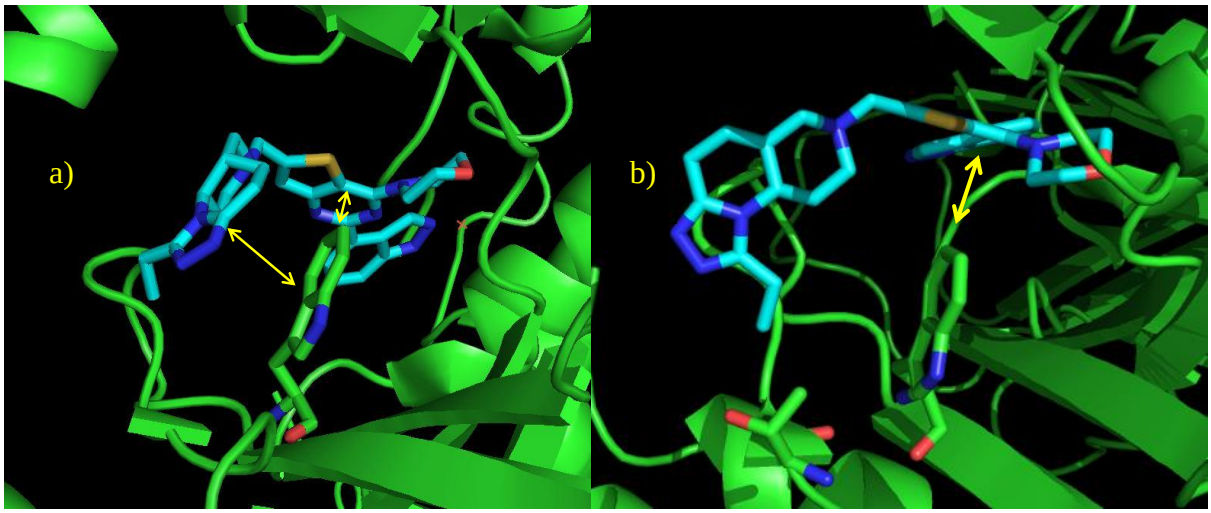


Figure 83 a)Docking of compound **381** into the active site of mutant K802T pi3K γ (PDB code 4EZL) to form a face-edge interaction with Trp 812, showing the additional π–π interaction with the tricyclic triazole part. b) the trans isomer **382** showing its planar structure in the mutant of pi3K γ active site not able to form any π–π interaction with Trp 812

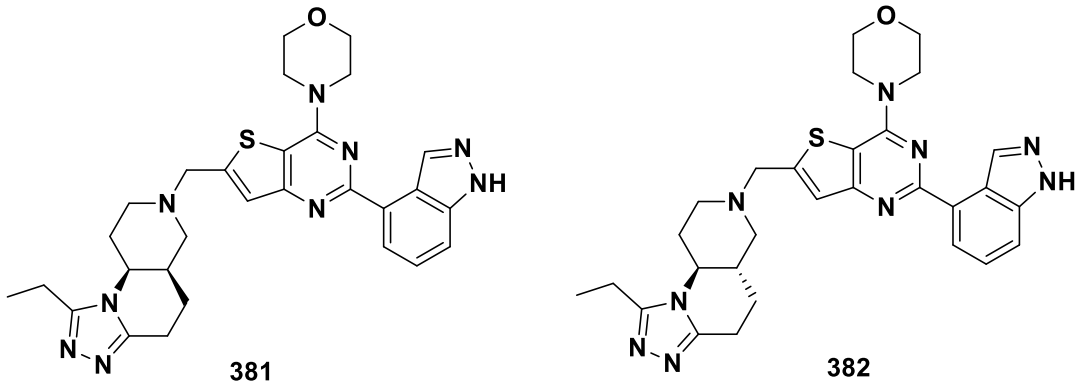


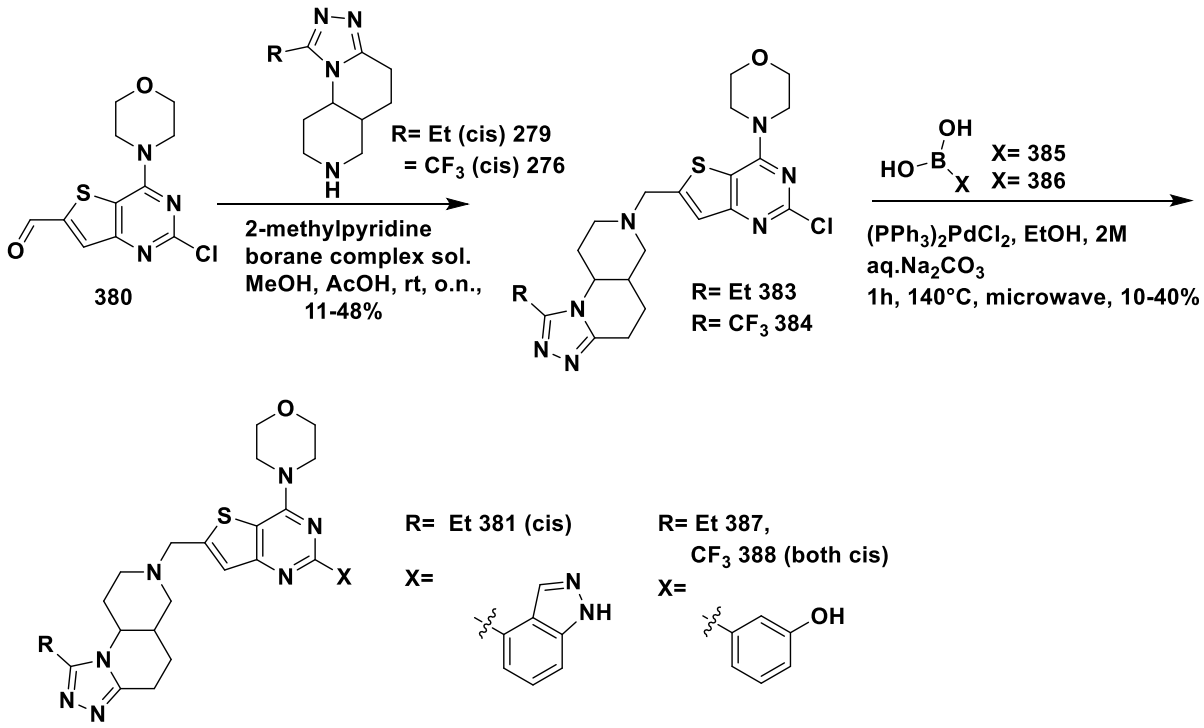
Figure 84 Suggested compounds **381** and **382** for targeting pi3K δ (each cis and trans compound still consisting of both enantiomeric compounds)

The *cis*- connected scaffold **381** showed the expected torsional angle of 90°, which allows the π–π interaction of the scaffold structure with the face of tryptophan 812, and the interaction

with the edge of tryptophan 812. The *trans*- compound **382** is oriented in a planar fashion which didn't show the face interaction with tryptophan 812, which is considered to be crucial for the selectivity towards the pi3K δ.

6.5 Synthesis of GDC-0941 analogues

The synthesis of the GDC-0941 analogues **381-382** followed the known route established by Genentech to synthesize GDC-0941 **376** starting with aldehyde **382** provided by GSK (Scheme 61).[162]



Scheme 61 Synthesis of GDC-0941 analogues **381, 387-388**

The aldehyde **382** was converted using 2-picoline borane complex and acetic acid in a reductive amination reaction to intermediates **383-384** in a yield of 26-48%. The yield was thought to be low due to required intensive purification of a mixture with the corresponding alcohol of aldehyde **382**. The aldehyde **382** was used in excess as amine supply **276** and **279** was limited, which resulted in the presence of a significant amount of the highly-insoluble alcohol. The intermediates were further converted in a Suzuki reaction using $PdCl_2(PPh_3)_2$ and the corresponding boronic acid (**385-386**) under microwave conditions to yield analogues **381, 387-388** in low yields of 10-40%. The purification of intermediates **385-386** as well as the final analogues **381, 387-388** turned out to be difficult as the proximity of the spots on TLC from product, side product as well as starting materials needed several purifications to

separate the desired compound with the necessary purity (>85% - the limit set by GSK). Another reason for the low yields was the mixture of the starting material for the final Suzuki coupling which still showed impurities of the reduced alcohol. Nevertheless, in total four new GDC-0941 analogues **381**-**382, 387**-**388** were synthesised bearing a CF_3 and ethyl side chain group on the triazole part and consisting of two different X substituents- 3-hydroxylphenyl and indazole (Figure 85).

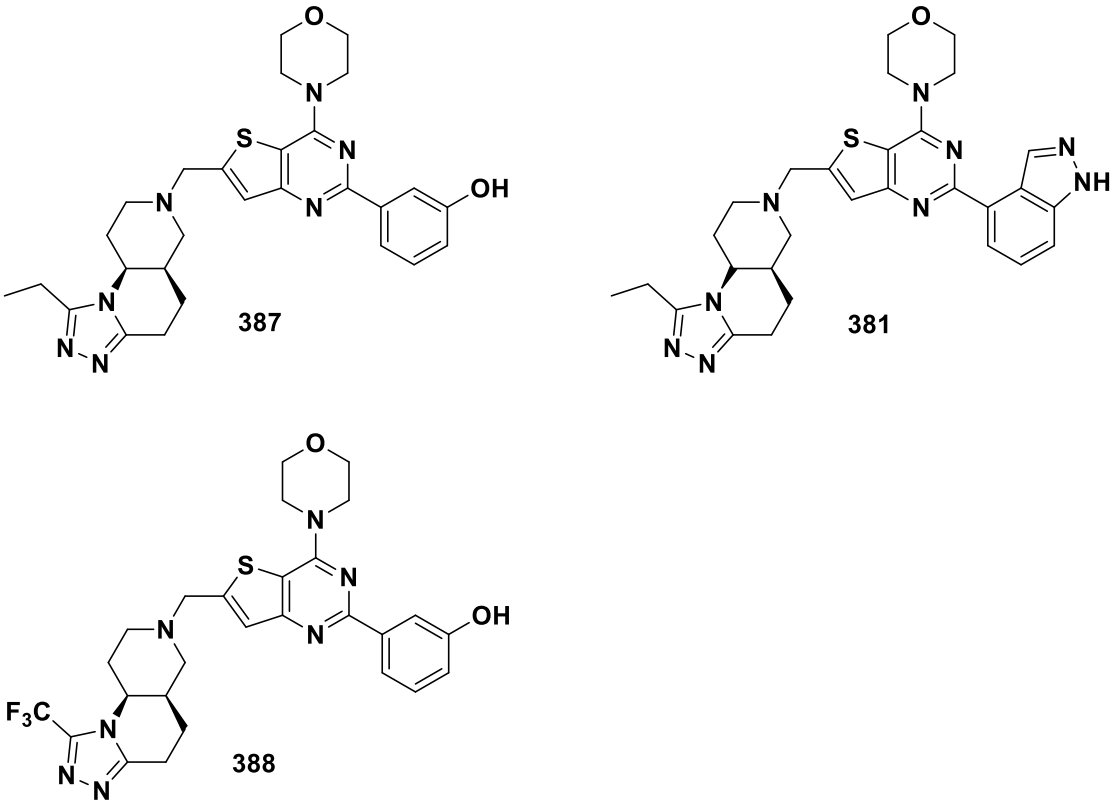


Figure 85 Synthesised GDC-0941 analogues **381, 387-388**

The series of compound bearing the 3-hydroxyphenyl side group was synthesised for comparison to the known GDC-0941 **376** derivative **389** previously synthesised as part of the GSK-UoN teaching collaboration (Figure 86).

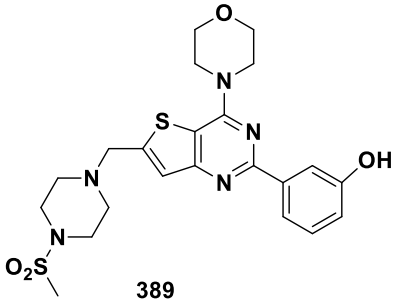
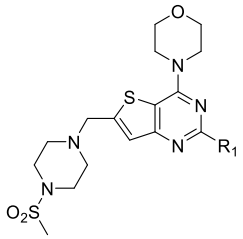
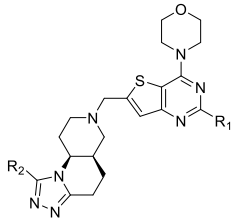
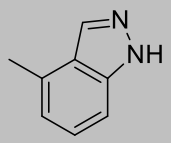
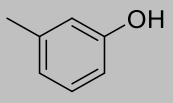
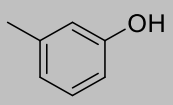
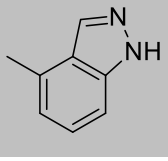
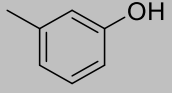


Figure 86 Potent pi3K inhibitor analogue **389** of GDC-0941

6.6 Biological evaluation of new GDC-0941 analogues

The three *cis*- connected compounds **381, 387-388** were tested by GSK for their biological activity towards pi3k δ. The screen against pi3 Kδ was carried out at GSK using a FRET (fluorescence resonance energy transfer) assay. In this assay the PIP3 (product of the pi3K δ reaction) is tagged with a fluorophore, which will emit light when bound to a europium complex. By carrying out a phosphorylation reaction untagged PIP3 will be produced, which decreases the fluorescence as it will compete with the tagged PIP3 to bind to the europium complex. By adding increasing concentrations of an inhibitor less untagged PIP_3 will be available, which will result in a decrease of fluorescence. All cis connected compounds **381, 387-388** showed an excellent biological activity towards pi3K δ in comparison to the known compounds **376** and **389** with K_D values in the low nanomolar range (table 9).

Table 9 pK_D values of GDC-0941 analogues by screening against pi3K δ (n=1) using a competitive FRET assay. pK_D measured through the decrease of fluorescence by an increasing availability of more untagged PIP_3.

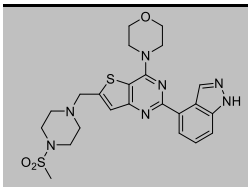
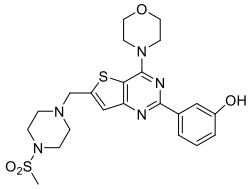
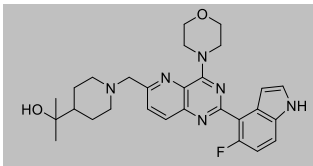
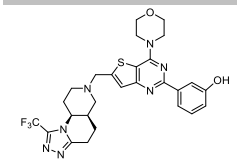
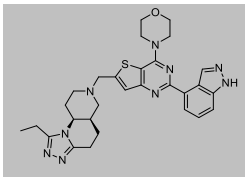
cpd					
	R_1= 	R_1= 	R_2=CF_3 R_1= 	R_2=Et R_1= 	R_2=Et R_1= 
	376	**389**	**388**	**381**	**387**
pK_D (δ)	7.9	8.0	9.2	8.5	9.4

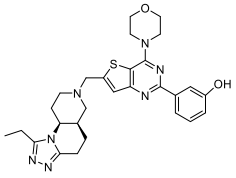
This biological activity is in good agreement with the previous docking studies in the pi3K δ active site (Figure 83), where the tricyclic triazole part forms a significant edge-face interaction with tryptophan 812 and represents an excellent start in this screening program.

6.6.1 Selectivity screen against pi3K α, pi3K β and pi3K γ

The compounds were tested for their selectivity profile against the pi3K isoforms α, β and γ. Compounds **381, 387-388** were tested for their biological activity against the other three isoforms of class 1 pi3K as the selectivity is crucial for their toxicity profile. This was carried out using the described FRET assay. Both compounds GCD-0941 **376** and **389** showed similar activity towards the four isoforms of pi3K, whereas in comparison compound **378** from Genentech showed a good selectivity profile with 200-400 fold selectivity towards the δ isoform (Table 10).

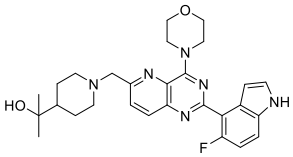
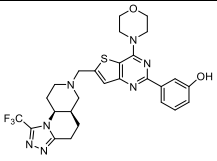
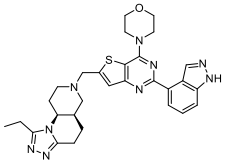
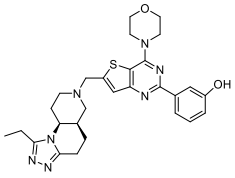
Table 10 pK_D values of all pi3 K isoforms (n=1) using a competitive FRET assay. pK_D calculated through the decrease of fluorescence by an increasing availability of more untagged PIP_3.

	α	β	γ	δ
 **GDC-0941**	7.2	6.6	6.4	7.9
 **389**	8.4	7.7	7.3	8.6
 **378**	340-fold	200-fold	400-fold	IC_{50} 3.8 nM
 **388**	7.4	7.0	in progress	9.2
 **381**	6.6	5.8	in progress	8.5

 **387**	7.2	7.2	in progress	9.4

Compounds **381, 387-388** showed a promising selectivity profile by showing selectivity in the range of 70- to 500 fold (Table 11)

Table 11 Selectivity profile of the screened GDC-0941 analogues **381, 387-388** towards pi3K δ (n=1)

pi3K isoform	 **378**	 **388**	 **381**	 **387**
α	340-fold	100 fold	70 fold	100 fold
β	200-fold	250 fold	500 fold	100 fold
γ	400-fold	in progress	in progress	in progress

This approach towards a new selective pi3K δ antagonist for the treatment of asthma resulted in highly potent compounds, which are still under biological screening against all four isoforms. As this project is in an early stage further compounds for SAR studies have to be considered by evaluating the biological activity and selectivity of the *trans*- connected compound and by changing the side chain on the triazole. The *trans* connected system could not be evaluated in this primary screens as these compounds could not be synthesised in the required purity. So far the side chain groups (Et or CF_3) didn't result in any remarkable difference in activity. By introducing the phenolic part into the analogues compared to the indazole part a slight increase in activity was seen, whereas the selectivity was higher keeping the indazole moiety. In summary this project revealed new and highly-potent analogues of GDC-0941 **376** with a good selectivity profile to target pi3K δ.

7 The purinoreceptor $P2X_7$

The $P2X_7$ receptor is a purinoreceptor, which is a family of ligand-gated membrane ionotropic channels. These ion channels are activated through extracellular ATP.[165] The $P2X_7$ receptor is expressed in most of the cell types and can trigger cell death during certain neurodegenerative disorders.

7.1.1 Biological Background of $P2X_7$

ATP is found as a stimulating transmitter in the peripheral as well as central nervous system.[166] It acts on cell surface receptors such as P2X or as well P2Y, which are ion channel gated. The P2X gene family is subdivided in 7 different subunits (P_2X_1 to P_2X_7) and those receptors are widely found in most cell types. The individual subunits are 384 to 595 amino acids long and each has two hydrophobic parts to be able to cross the plasma membrane. The P2X receptors form trimers with two domains in every subunit. A unique feature is that by activating the $P2X_7$ receptor it forms large plasma membrane pores which allow the non-selective flux of ions as well as hydrophilic molecules up to 900 Da.[165] It can trigger cell death and is known to play an important role in many neurodegenerative disorders (Figure 87).

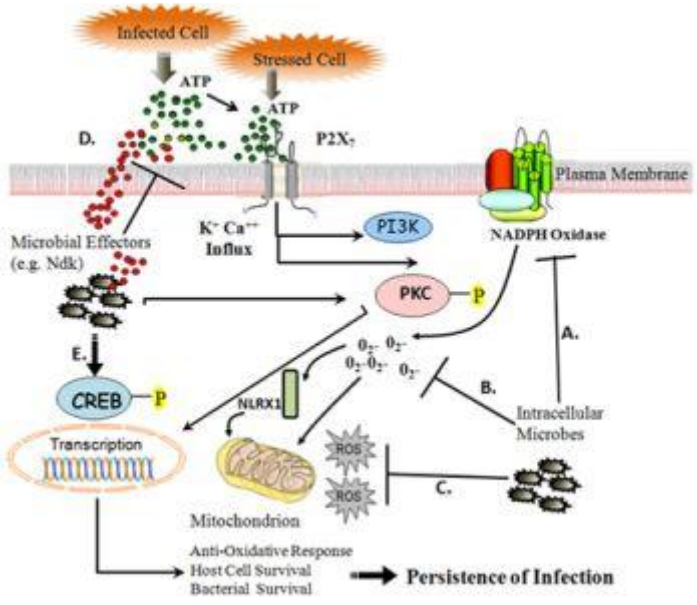


Figure 87 Schematic illustration of the pathways where the $P2X_7$ ion channel is involved, adapted from *Int. J. Mol. Sci.* **2011**, *12*

The $P2X_7$ receptor is predominantly expressed in macrophages and monocytes in the periphery and astrocytes as well as in the microglia in the central nervous system.[167] The

receptor plays a role in neurodegenerative processes such as Alzheimer's disease, Parkinson's disease or multiple sclerosis.[168] Furthermore, the expression of the $P2X_7$ has been demonstrated to be found on most cell types in the retina. In a paper by Suguyiama[165] it was stated that there is a relation between activation of the $P2X_7$ receptor in the retina and the release of inflammatory cytokines such as interleukin and tumour necrosis factor. The $P2X_7$ purinoceptor is one of the three present ionotropic receptors which can control the ion flux.[169] In a study by Illes *et al.*,[169] in which they investigated the role of the $P2X_7$ receptor in astroglia in the central and peripheral nervous system, they found this receptor to be the main entry point for Ca^{2+} and shows to be its activation point. It is known that the astrocyclic $P2X_7$ receptor activate neuronal effects through signalling at nearby neurons. One of the key points of the activity of the $P2X_7$ receptor is its release of pro-inflammatory interleukin (IL-1β), which is an important factor in inflammation, mood disorders, neurogenerative disorders and pain. There is a high interest in studying its role in the brain due to the relation to depression and bipolar disorder.[170]

7.2 Known literature antagonists for the $P2X_7$ receptor

Several antagonists are known to be active on the $P2X_7$ receptor subunit. For biological evaluation 2, 3–(benzoyl-4-benzoyl)-ATP (BzATP) is used by replacing the natural agonist ATP as it is 10-30 times more potent (figure 88).

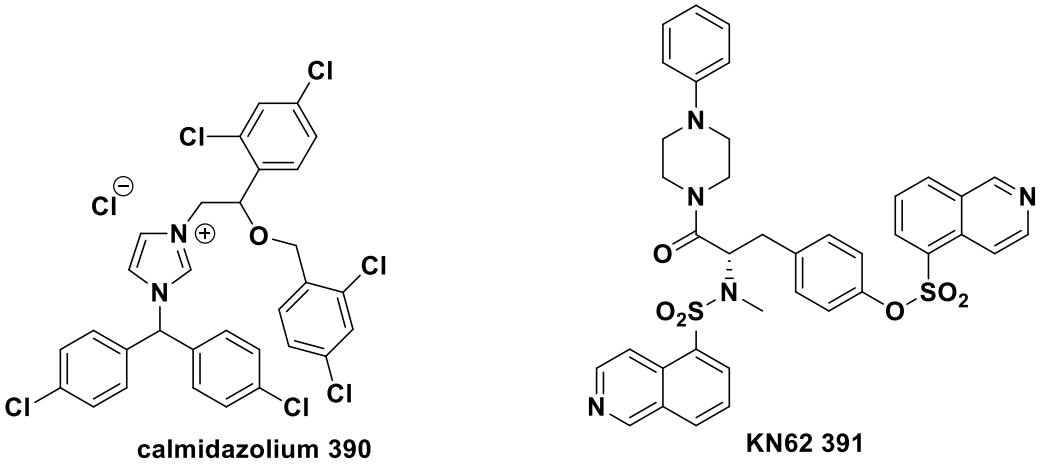


Figure 88 Organic cations calmidazolium **390** and KN62 **391** functioning as antagonists for $P2X_7$

Up to date no $P2X_7$ inhibitor reached to the market, but the search for a potential antagonist is an ongoing process and they can be divided in different classes. One group is represented by several ions (magnesium, calcium, zinc or copper) which act as antagonists and have the potential to inhibit ATP.[171] Another group is the generic blockers represented by brilliant

BlueG as the most useful blocker in this class, which blocks human P2X$_7$ at 200 nM.[172]The next class is characterized through large organic cations as calmidazolium and KN-62 (Figure 88). KN-62 is a piperazine based inhibitor, which blocks currents in cells expressing the human P2X$_7$ receptor. Furthermore, small molecules **392-397** are known to have a great potential as antagonists for the P2X$_7$ receptor (Figure 89).

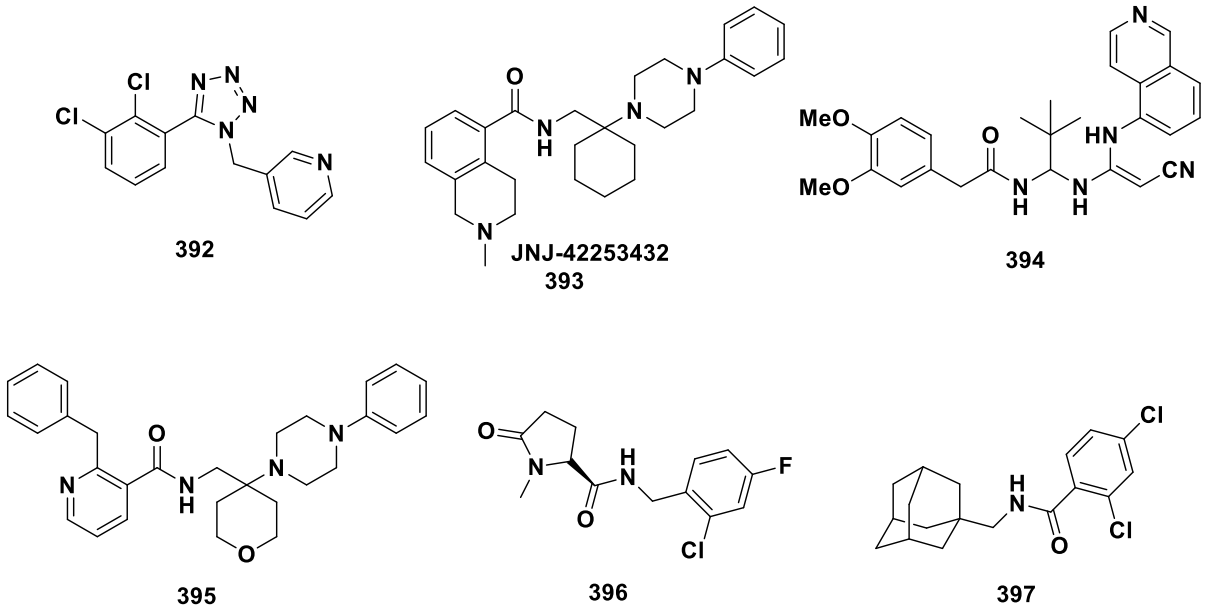


Figure 89 Small molecules known as P2X$_7$ receptor antagonists

In Figure 89, the compounds **392** and **394** represent competitive, selective and reversible antagonists of the P2X$_7$ receptor.[173] The potent antagonists **393** and **395** were found by Janssen in the discovery of novel brain penetrating P2X$_7$ receptor antagonists.[174] Compound **397** was established by AstraZeneca and is a potent inhibitor of agonist-induced IL-1β release (pA$_2$ 8.0).[175] Another interesting small molecule is the P2X$_7$ receptor antagonist **396**, which is a compound discovered by GlaxoSmithKline and was effective in preclinical studies. Additionally it showed similar activity towards the rat P2X$_7$ receptors (hP2X$_7$ pIC$_{50}$ 8.5, rP2X$_7$ pIC$_{50}$ 6.5), which is stated as another major issue for finding P2X$_7$ receptor antagonists for obtaining a reliable animal model, even if the activity shows still a great difference.[176]

7.3 Synthesis and biological evaluation of new P2X$_7$ receptor antagonists

The newly synthesised analogues, targeting the ion channel P$_2$X$_7$, were designed based on known antagonists from a patent by GSK.[177] Therefore the synthesised tricyclic scaffolds **194** were incorporated into the template of GSK compound **398** (figure 90). Due to the lack of a

crystal structure of the ion channel P2X$_7$, the rationale behind the synthesis of analogues of the structure **399** was its structural similarity to the chosen antagonist **398** published by GSK by bearing a piperazine and a triazole structural part. A similar strategy was used by designing the new potent analogues **315-335** of the DPP-4 inhibitor Sitagliptin **256** (chapter 4).

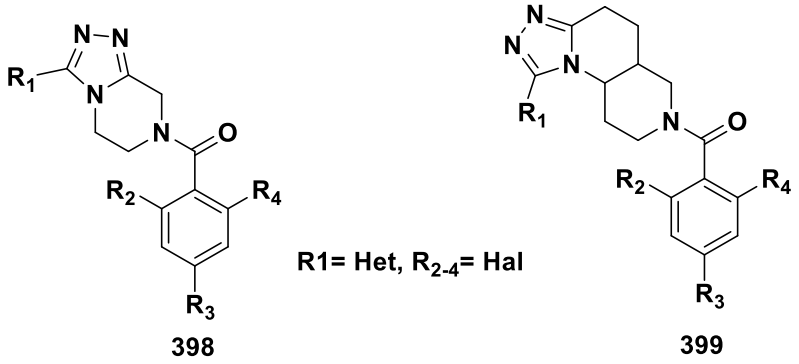
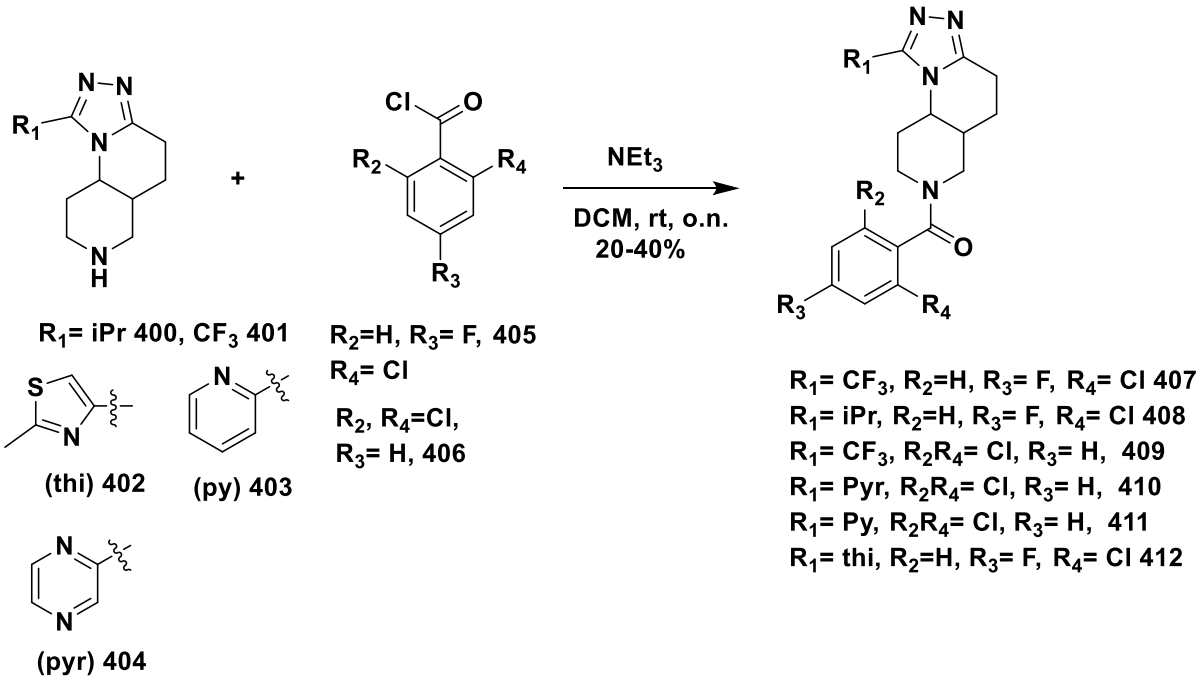


Figure 90 Proposed analogues **399** of known GSK antagonists **398**

The first approach was the conversion of scaffold **400-404** through an amide coupling of the corresponding acid chlorides **405** and **406** to amides **407-412** in yield between 20-45%. This was carried out using standard coupling conditions by deprotonating the amine with trimethylamine to form the amide bond. (scheme 62).



Scheme 62 Synthesis route to potential P2X$_7$ receptor analogues **407-412** consisting of the tricyclic scaffold

The synthesised analogues **407-412** are all racemic as the main aim in this approach was to rapidly establish the utility of our scaffold as part of a potential $P2X_7$ receptor antagonist. Nevertheless, through preparative HPLC purification of the final compounds two isomers from each compound could be separated for most of the analogues, which would allow us to assign the *cis*- or *trans*- geometry after successful biological results by screening against the ion channel $P2X_7$.

The biological screen was carried out at the University of Leicester in the group of Prof. Richard Evans. The remaining activity of the agonist BzATP was tested against the newly synthesised compounds **407-412**. The screen was carried out using a Ca^{2+} signalling assay by showing the BzATP (10 μM) induced ethidium bromide (20 μM) uptake through the human $P2X_7$ receptor in the absence or presence of the new $P2X_7$ analogues **407-412** (30 μM, 30-minute pre-incubation). As control AZ106 (AZ10606120 (**413**) at 100nM) was used (Figure 91), which is a known $P2X_7$ antagonist discovered by AstraZeneca.

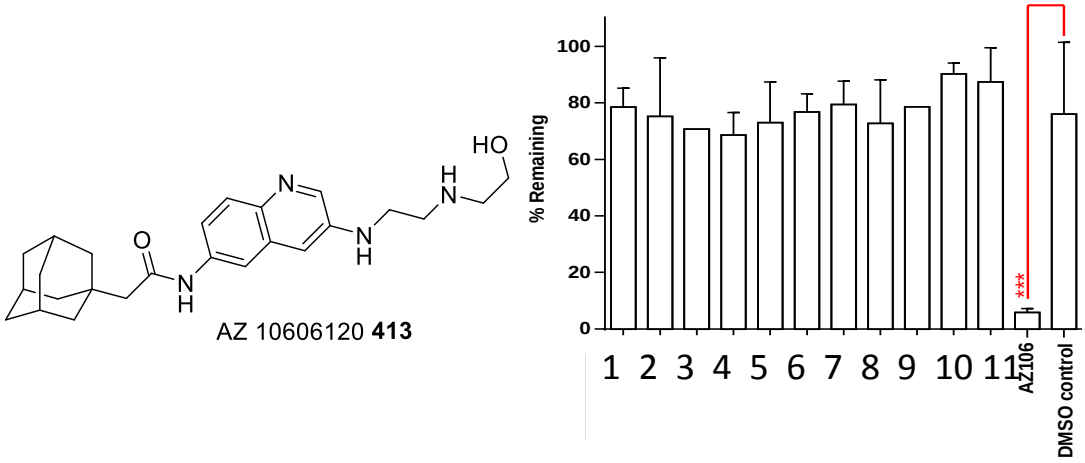


Figure 91 a) Structure of AZ10606120 **413;** b**)** Effect of **407-412 (1-11) (**figure 92**)** on ethidium bromide dye uptake through the human $P2X_7$ receptor pore (n=2). Histogram summary showing the % response remaining at the end of the FlexStation recording compared to DMSO control. Ethidium bromide (20 μM) and compounds **407-412** (30 μM) were pre-incubated for 30-minutes prior to agonist-induced (10μM BzATP) dye uptake recording. Data presented as mean ± S.E.M, statistical differences between the means determined by one-way analysis of variance followed by Bonferroni's post-test. ***, $p < 0.001$

Unfortunately, none of the synthesised compounds **407-412** bearing the novel tricyclic scaffold showed any activity against $P2X_7$ at a concentration of 30 μM (Figure 91 and Figure 92). Due to the failure of antagonist potency of analogues **407-412** by simple scaffold hopping, this project was not further conducted as no rational through 3-D overlay (using ChemBioDraw 3D) could be achieved for the design of new $P2X_7$ analogues comprsising the tricyclic triazole part.

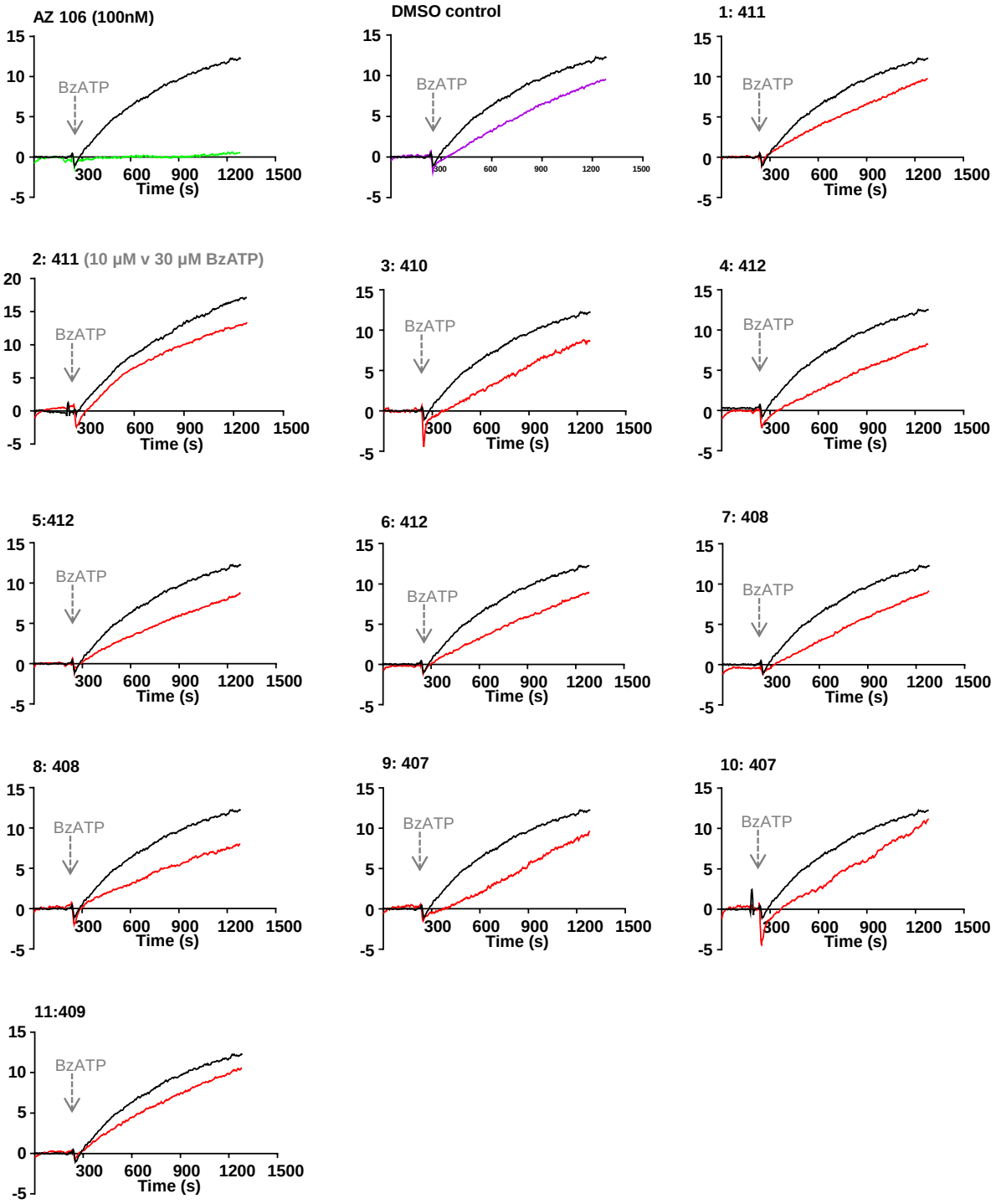


Figure 92 Representative FlexStation responses showing BzATP (10 µM) induced ethidium bromide (20 µM) uptake through the human P2X7 receptor in the absence (black trace) or presence (red trace) of **407-412** (30 µM, 30-minute pre-incubation). The effect of 30-minute pre-incubation with 100 nM AZ106, and effect of pre-incubation in DMSO-only is also shown (green trace and purple trace respectively). Agonist addition (at 240 s) is indicated by the grey arrow.

8 Conclusion

In this thesis, the successful racemic synthesis of a new tricyclic scaffold was described. Recently, a new chiral approach has been evolved leading to the exciting possibility of generating the tricyclic scaffold in an enantiopure form (Figure 93) starting from a commercially available ketone **108** in a robust 5 steps procedure.

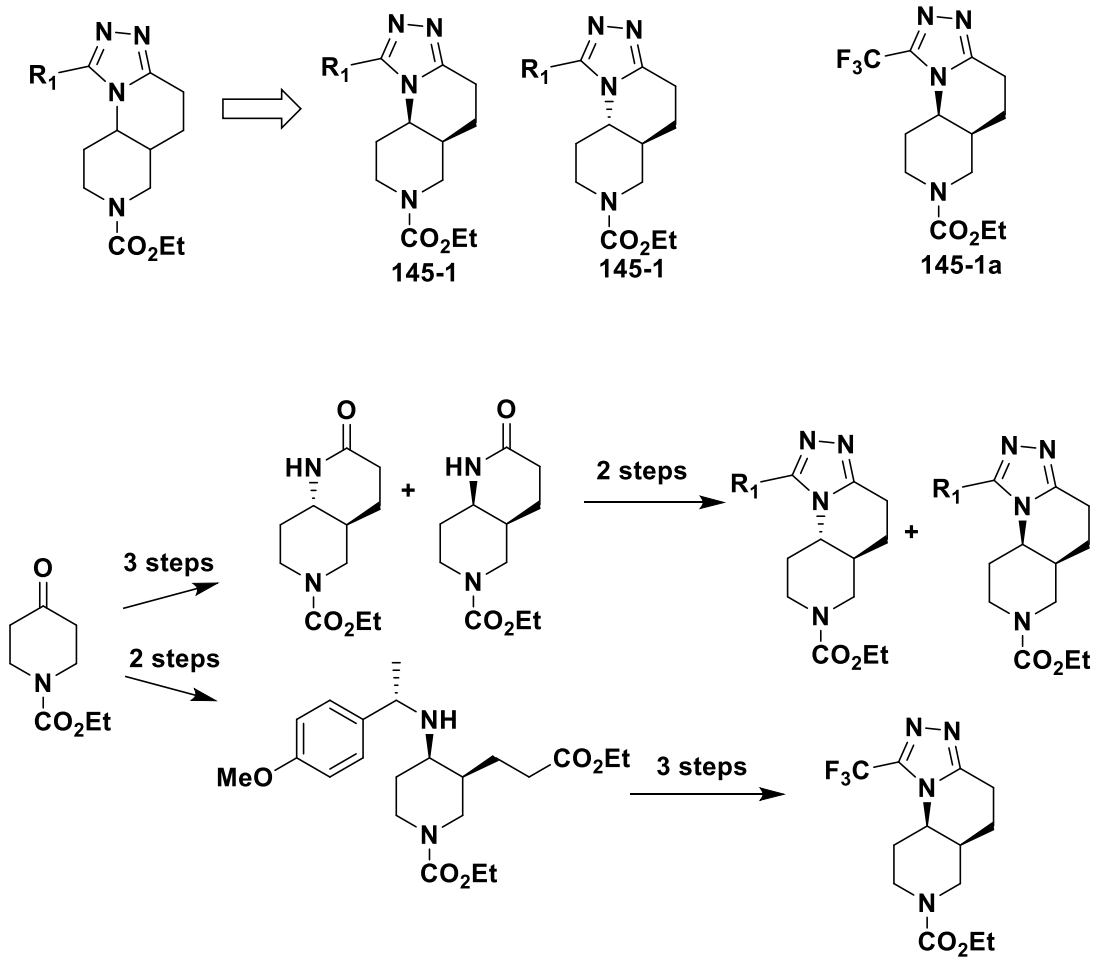


Figure 93 Tricyclic triazole scaffold **145-1** and **145-2** and enantiomeric pure compound **145-1a** and their corresponding synthetic route

In summary, a small library of 17 6.6.5 tricyclic triazole containing ring systems could be synthesised with a variety of side groups R1 attached to the triazole part. The side groups ranged from alkyl groups to more electron withdrawing groups, such as CF_3, CF_2CF_3 and finally to heterocyclic rings. In the synthesis it was noted that the reactivity of the groups increased from the electron withdrawing groups attached to the acyl hydrazide (CF_3 and CF_2CF_3) being the most reactive and the heterocyclic groups being the least reactive. By using heterocyclic group a more demanding sterical hindrance was introduced, which could

be an explanation of the decrease of reactivity. In the series to the 6.6.5 tricyclic ring system all the triazoles could be synthesised by using the corresponding hydrazide (figure 94). By applying the known methods to generate the hydrogen substituted, bromo substituted, amino substituted triazole or amido triazolone system no desired product could be obtained. Furthermore no difference in reactivity in the triazole formation of the *cis*- connected thiolactam system compared to the *trans*- connected thiolactam system could be detected.

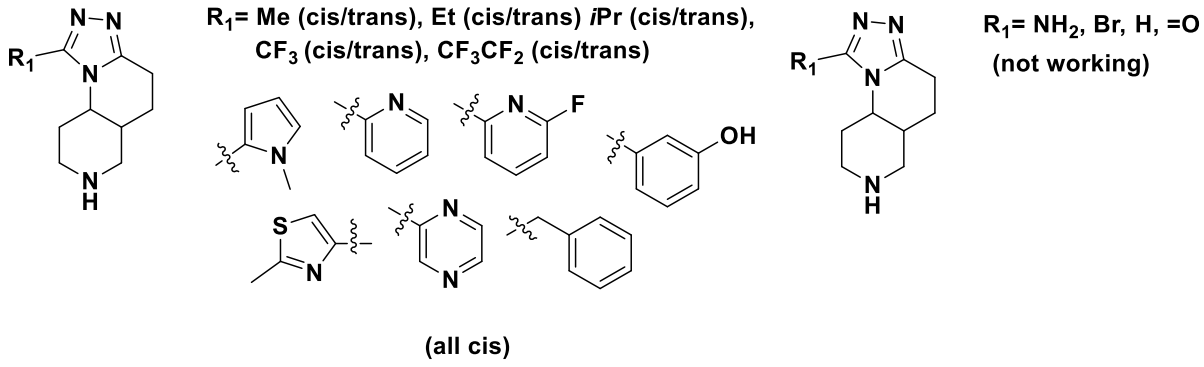


Figure 94 All feasible 6.6.5 tricyclic triazole systems

Looking at the 6.5.5 triazole ring system, the synthesis bearing the methyl side chain on the triazole system could not be accomplished in this thesis, but the synthesis of the 6.5.5 ring system bearing an electron withdrawing side chain group, namely the CF_3 group was established and no formation of the triazole could be obtained by using a simple methyl group. This was thought to be the case as the CF_3 group produces a greater electrophilic carbonyl functionality and the nucleophilic attack is more readily occuring. Due to the resources of the available material only the *cis*- connected thiolactam system was used to try the final triazole formation, therefore no information is available if there would be a difference in the ring formation between the *cis*- and the *trans*- connected system. For the 6.7.5 system, only one attempt was carried out using the CF_3 side chain, which was accomplished, in a system containing all four possible isomers (figure 95).

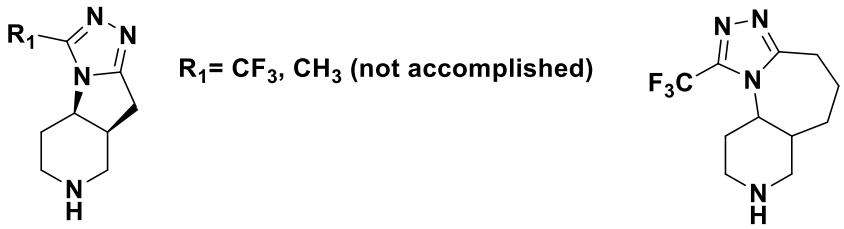


Figure 95 Accesible 6.5.5 and 6.7.5 tricyclic triazole scaffolds

Conclusion

Regarding the stereoelectronic effect in the actual triazole formation reaction by applying Baldwin's rules the favoured process of a ring closing via a 5-exo trig process is followed in all three synthesised tricyclic triazole systems (figure 96). Another stereoelectronic effect to consider is the angle of the actual nucleophilic attack. One major criterion is known as the Buergi-Dunitz angle, which would be in this case the angle in which the amine is attacking the carbonyl functionality.

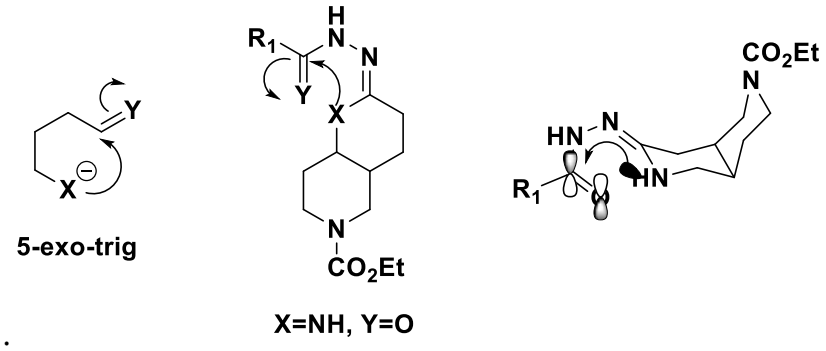


Figure 96 Stereoelectronic effects present in the formation of the tricyclic triazole systems (mainly shown at the model of the 6.6.5 tricyclic system)

As shown in figure 96 for the 6.6.5 connected ring system the nucleophilic attack of the amine functionality has to occur in an angle of 107° as this would allow the minimum repulsion between of its HOMO of the amine and the carbonyl π bond. This angle is achieved more readily in the larger ring systems (6.6 and 6.7) than in the more constraint 6.5 system.

The aim to develop a new privileged scaffold was investigated by incorporating this scaffold into known biologically-active drugs molecules and evaluating its usefulness towards a variety of biological targets (Figure 97).

Conclusion

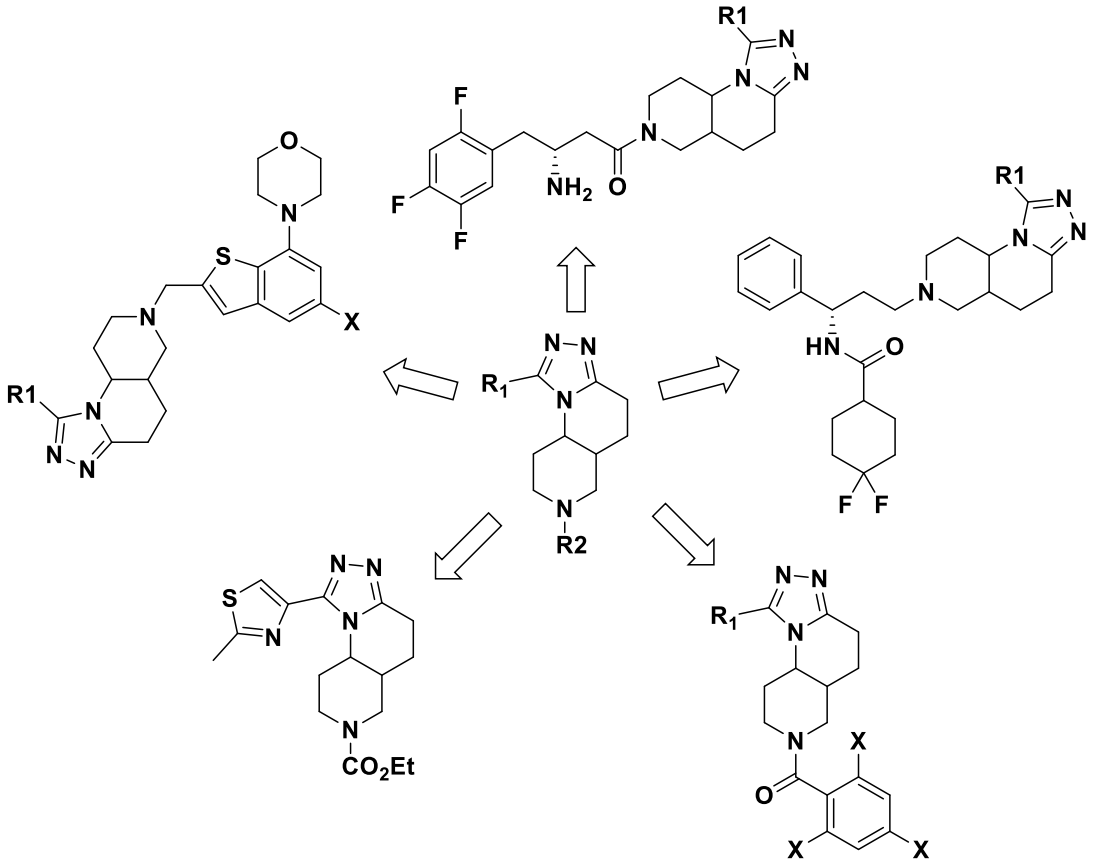


Figure 97 Target molecules after incorporation of the tricyclic scaffold

The new analogues demonstrated excellent biological activity by screening against the several biological targets: the serine protease DPP-4; the chemokine receptor CCR-5 and the kinase pi3K δ isoform (figure 97 and figure 98). High potency was obtained across the three biological classes, which was rationalized through co-crystal structure docking studies.

Whilst the lack of activity observed for the tested analogues against the ion channel $P2X_7$ and the first screens in the Eli Lilly OIDD program, it should be noted that these negative results demonstrate that the scaffolds should not be considered as promiscuous inhibitors either through the unselective reaction with proteins or through interfering with biological assays.

In conclusion, these findings demonstrate that the tricyclic scaffolds are promising new potential privileged structures for use in future medicinal chemistry lead generation exercises and this thesis presents a useful starting point for further evaluation of these new scaffolds.

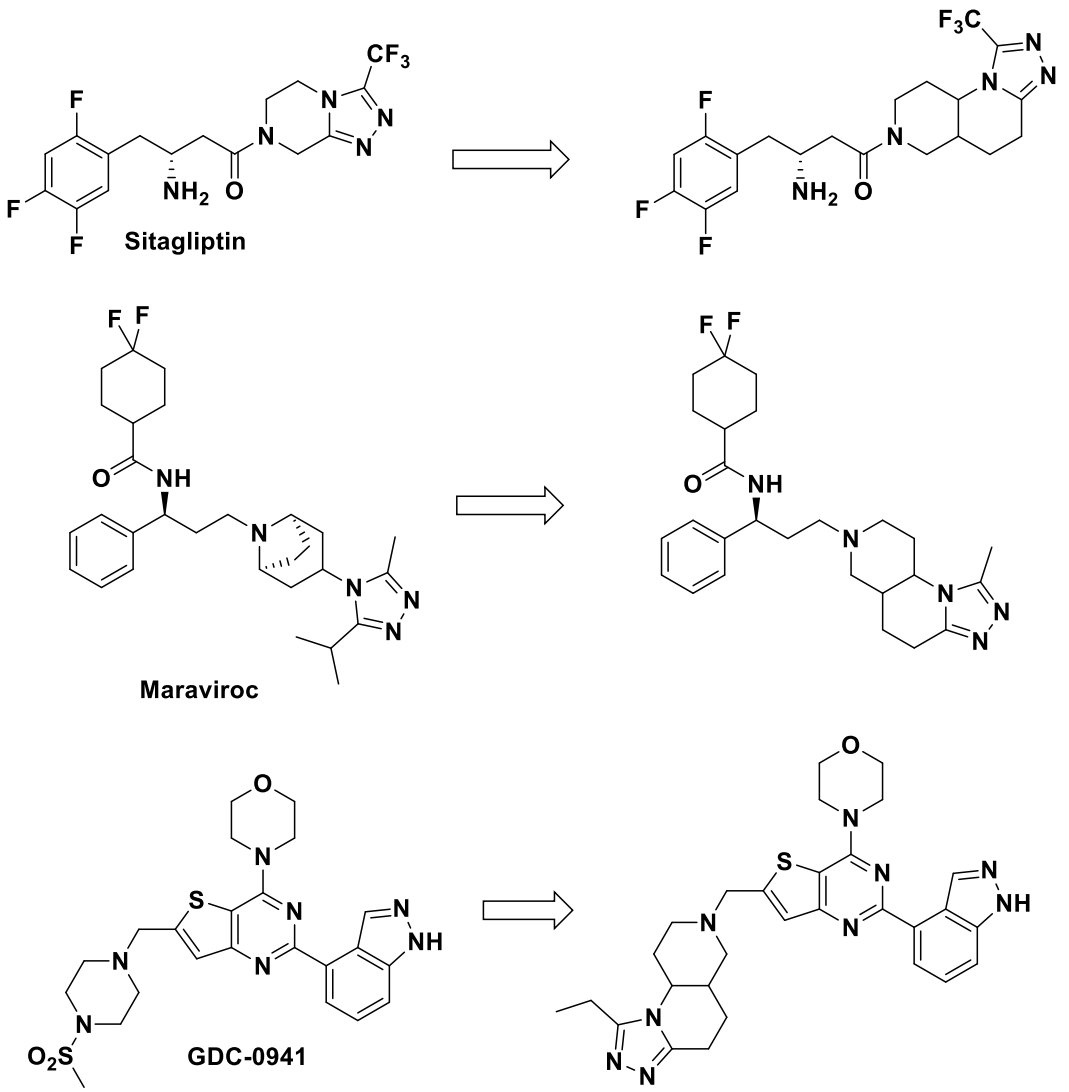


Figure 98 Scaffold hopping to Analogues of the known drug molecules Sitagliptin, Maraviroc and GDC-0941

9 Future Studies

As an outcome of this thesis valuable information about the interactions of the scaffold with the chemokine receptor CCR-5, the enzyme DPP-4 and the kinase pi3K, were obtained and a good starting point was achieved for further SAR studies in this three biological targets. The screen against the pi3K δ is still in an early stage of the project and showed a great potential to be further investigated by the discovery of highly potent analogues of the known drug molecule GDC-0941. In the future work, further analogues bearing new side chain groups, *trans*- connection of the bicyclic ring system and changing the phenolic site group should be considered for synthesis and docking in the active site of pi3K δ. A scale up process should be carried out to obtain more material for further analytical clarification and for further biological testing (Figure 99).

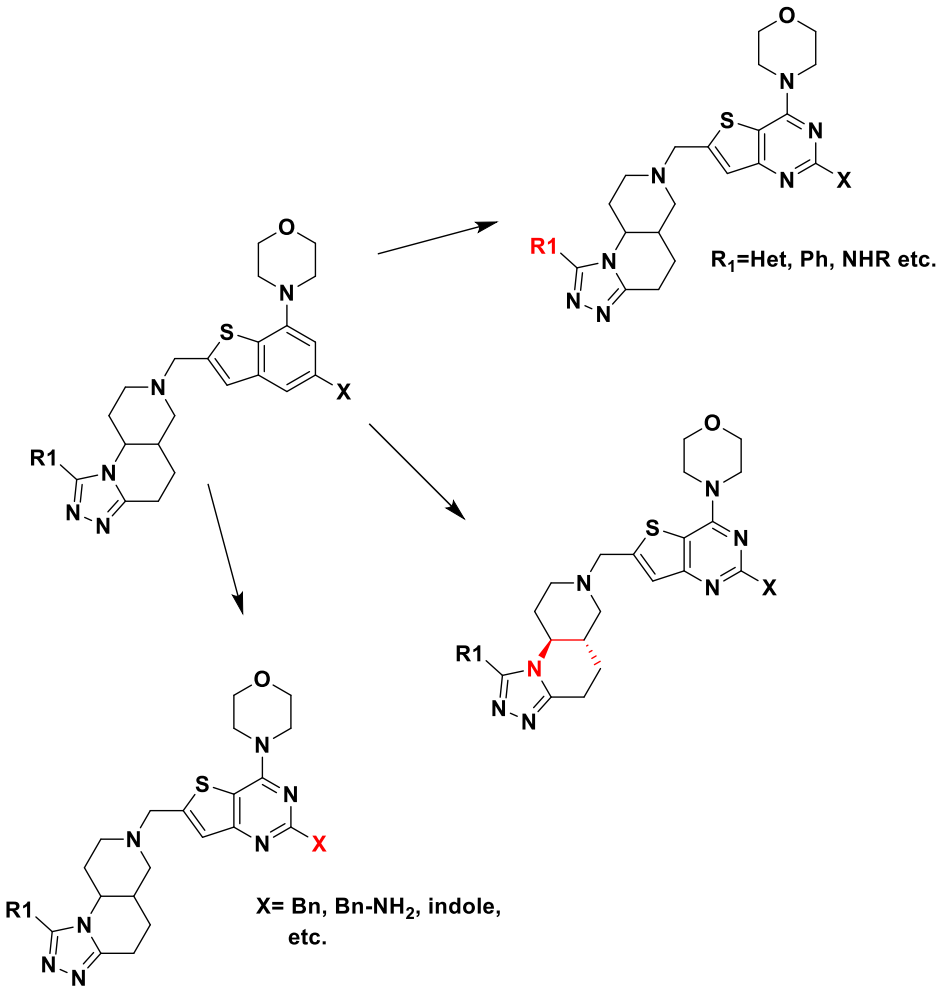


Figure 99 Proposed synthesis plan for new analogues of GDC-0941

The chiral synthesis of the scaffold should be further investigated by proving the outcome through resynthesis of compound **145-1a** and synthesis of the enantiomeric compound **145-1b**. Furthermore the *trans*- connected compounds **145-2a** and **145-2b** should be synthesized by changing one chiral center of the *cis*- connected compound using a base catalyzed approach (figure 100).

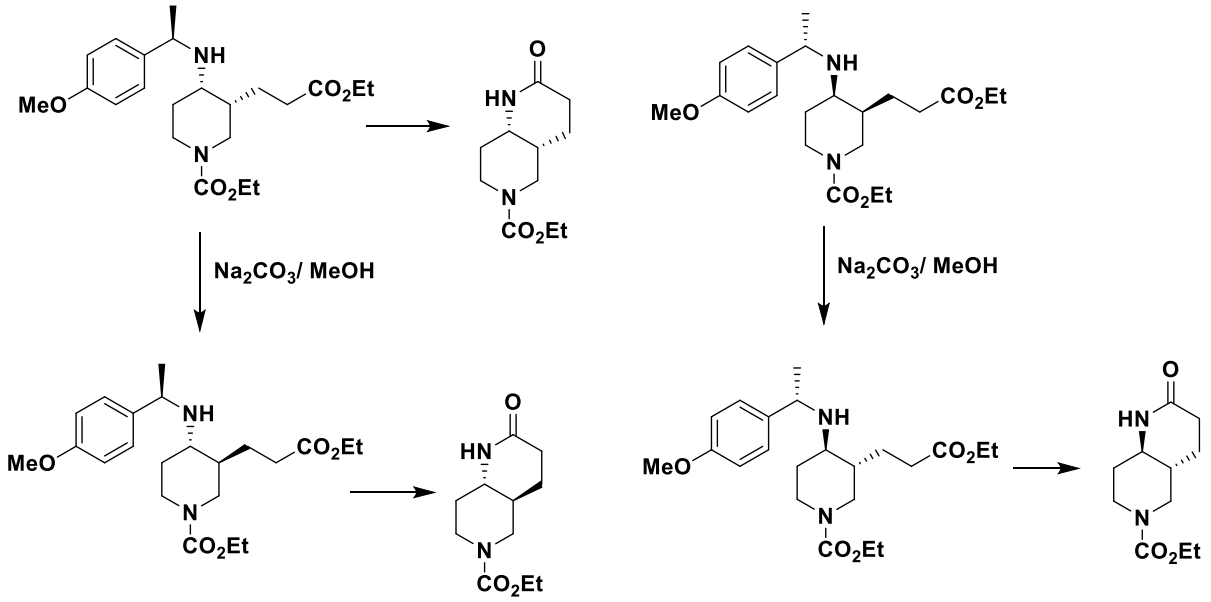


Figure 100 Suggested synthesis towards the remaining enantiomeric bicyclic compounds **145-1b, 145-2a and 145-2b** following the previous synthesis route for the other enantiomer

All four enantiomers could be incorporated in the next step in the previous synthesised diastereomeric compounds targeting the chemokine receptor CCR-5 (Figure 101). This resynthesis could be followed by further analogues bearing the *cis*- connectivity of the scaffold system. The single diastereomers should be screened afterwards against CCR-5 to evaluate the difference in their biological activity.

This project could be further expanded by looking at new biological targets to evaluate the potential of the new synthesised scaffold as a privileged scaffold. Targets for consideration in future work could be the β– adrenoceptors or polo like kinase.

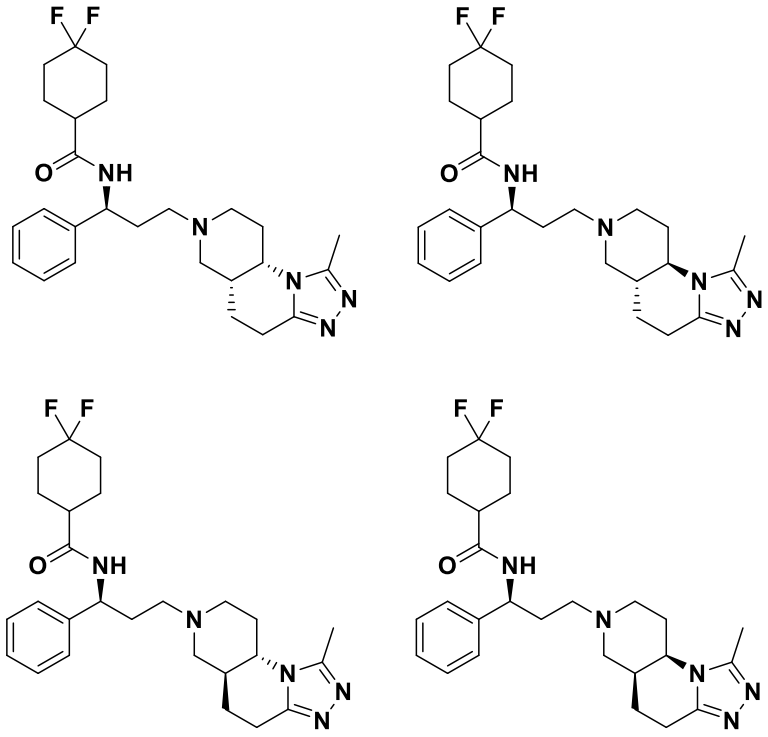


Figure 101 All four possible single diastereoisomer of Maraviroc analogues

10 Experimental Part

10.1 Materials

10.1.1 Techniques

All reactions with air- and humidity- sensitive reagents were carried out under an atmosphere of nitrogen. The flasks were pre-dried in the oven and flushed with nitrogen. The liquids were added using plastic syringes.

10.1.2 Chemical and solvents

All raw materials, reagents and solvents were purchased from commercial suppliers e.g. Acros, Sigma Aldrich, Fluorochem, KeyOrganics and Merck. All solvents were either analytical reagent or HPLC grade and were supplied by Fisher Scientific. Dry solvents were used for all reactions and were purchased from Sigma Aldrich and VWR. The Petrolether had a boiling point of 40 to 60°C. $CDCl_3$ was supplied by Cambridge Isotope Laboratories, Inc., $MeOD_4$ was obtained from SigmaAldrich.

10.1.3 Thin layer chromatography (TLC)

All reactions were monitored for completion using TLC. Therefore commercially available pre-coated silica gel 60 F_{254} aluminium plates from Merck were used. Visualisation of the spots was carried using the UV-lamp (λ=254 nm) and stained with $KMnO_4$, iodine, Ninhydrin or PMA stain and subsequently heated with a heatgun.

10.1.4 Flash Chromatography

Flash column chromatography was carried out using silica gel, technical grade, pore size 60A, 230-400 mesh particle size, 40-60 μm particle size from Sigma Aldrich.

10.2 Methods

10.2.1 Nuclear Magnetic resonance

The ^{13}C- and ^{1}H-NMR spectra were recorded using a *Bruker 400 Ultrashield* spectrometer with a magnetic field strength of 9.4T. This is corresponding to a resonance frequency of 400 MHz for protons and around 100 MHz for the ^{13}C nucleus. Final ^{13}C-NMR spectra were recorded using a *Bruker AV (II) 500* spectrometer with a magnetic field strength of 9.4T. All ^{13}C-NMR are ^{1}H-broadband-decoupled. The chemical shifts δ are given in [ppm] and all coupling constants *J* are given in [Hz]. The spectra are referenced to the signal of the deuterated solvent: $CDCl_3$ (δ_H= 7.26, δ_C=77.16 ppm), $MeOD_4$ (δ_H= 3.31, δ_C=49.00 ppm). The following abbreviations were used to describe signalshapes and multiplicity: s (singlet), bs (broad singulet), d (doublet), dd (doublet of doublet), ddd (doublet of doublet of a doublet), dddd (doublet of a doublet of a doublet of a doublet), t (triplet), dt (doublet of a triplet), q (quartet), dq (doublet of a quartet), quint. (quintet), and m (multiplet). Furthermore 2D-NMR experiments: COSY, HSQC and NOESY were used for the assignment of the signals and the processing of the NMR data was carried out using the NMR software TopSpin 3.0.

10.2.2 Mass spectrometry

All high-resolution mass spectra (HRMS)- time to flight electrospray were recorded on a Waters 2795 spectrometer by electrospray ionization (TOF ES) and the LC-MS spectra were performed on a Shimadzu UFLCXR system coupled to an Applied Biosystems API2000, and visualized at 220 nm (channel 2) and 254 nm (channel 1). LC-MS was carried out using a Phenomenex Gemini-NX C18 110A, column (50 mm x 2 mm x 3μm) at a flow rate 0.5 ml/min.

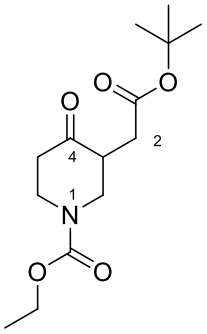
10.2.3 HPLC

RP-HPLC was performed using a Waters 2767 sample manager, Waters 2525 binary gradient module, and visualised at 220 nm with a Waters 2487 dual wavelength absorbance detector. Spectra were analysed using MassLynx. Preparative HPLC was performed using a Phenomenex Gemini-NX 5u C18 110A, AXIA packed column (160 mm x 21.2 mm) at a flow rate of 20 mL/min, typically starting with 90% water/ 10% acetonitrile and progressing to 100% acetonitrile over 30 min. The water phase contained 0.01% ammonia. Preparative HPLC gradient method reported doesn't include requilibration time. Chiral analytical HPLC was performed using a Phenomenex LC Lux 5u Amylose-2 packed column (250 x 4.6 mm) at

a flow rate of 1.5 mL/min, isocratically using 70% hexane: 30% ethanol supplemented with 0.2% DEA over 30 min.

10.3 Synthesis of [6.5.5] scaffold

Ethyl 3-(2-(*tert*-butoxy) 2-oxyethyl)-4-oxopiperidine-1-carboxylate (115)

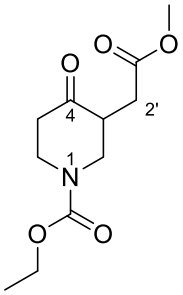


To a solution of diisopropylamine (5.6 g, 7.8 mL, 55.6 mmol, 1.9 eq.) in THF (175 mL) at 0°C was added *n*-BuLi (18.5 mL, 2.5M in hexane, 46.2 mmol, 1.6 eq.) and the mixture was stirred for 30 min. The mixture was cooled to -78°C, ethyl 4-oxopiperidine-1-carboxylate (**108**) (5.0 g, 4.4 mL, 29.2 mmol, 1 eq.) was added and the mixture was stirred for additional 30 min at -78°C. A solution of *tert*-bromoethylacetate (9.2 g, 7.0 mL, 47.2 mmol, 1.6 eq.) in THF (17.5 mL) and HMPT (2.9 mL) was added and the yellow reaction mixture was warmed gradually to room temperature overnight. The mixture was quenched with saturated aqueous NH_4Cl (200 mL), the phases were separated and the aqueous phase was extracted with ethyl acetate (3 x 200 mL). The combined organic layers were dried over $MgSO_4$, filtered and the solvent was evaporated under reduced pressure. The crude product was purified by flash chromatography (petrol ether / ethyl acetate: 3:1) to yield *tert* butyl ester (**115**) in 50% yield as a yellow oil.

^{1}H-NMR (400 MHz, $CDCl_3$) δ/ppm 4.34 (bs, H-6, H-2, 2H), 4.13 (q, *J*= 7.0, 14.5 Hz, $CO_2\mathbf{CH_2}CH_3$, 2H), 3.21 (m, H-2, 1H), 2.94-2.80 (m, $\mathbf{CH_2}CO_2t$Bu, 2H), 2.64-2.50 (m, H-6, H-5, 2H), 2.39 (t, *J*= 3.9 Hz, H-3, 0.68 H), 2.35 (t, *J*= 4.3 Hz, H-3, 0.32 H), 2.25-2.18 (m, H-5, 1H), 1.45 (s, CO_2***t*Bu,** 9H), 1.28 (t, *J*= 7.1 Hz, $CO_2CH_2\mathbf{CH_3}$, 3H)

^{13}C-NMR (100 MHz, $CDCl_3$) δ/ppm 207.2 (C=O), 170.6 ($\mathbf{C}O_2t$Bu), 155.2 ($\mathbf{C}O_2$Et), 80.9 (CO_2***t*Bu**), 61.9 ($CO_2\mathbf{C}H_2CH_3$), 47.9 (C-2), 46.5 (C-6), 43.6 (C-3), 40.7 (C-5), 32.7 (C-2'), 28.0 (CO_2***t*Bu**), 14.6 ($CO_2CH_2\mathbf{C}H_3$)

Ethyl 3-(2-methoxy-2-ethoxyethyl)-4-oxopiperidine-1-carboxylate (118)



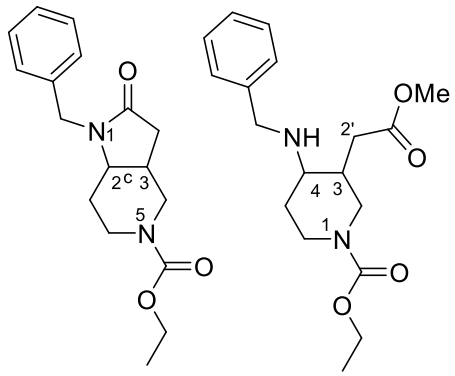
Tert butylester (**115**) (300 mg, 1.05 mmol, 1 eq.) was dissolved in MeOH (9 mL) and HCl (0.75 mL) was added before the mixture was stirred at rt for 6 days. The solvent was evaporated under N_2 atmosphere and the crude product was purified by flash chromatography (petrol ether/ethyl acetate: 2:1) to yield methyl ester (**118**) as a colorless oil in 220 mg, 86% yield as a

yellowish oil.

^{1}H-NMR (400 MHz, $CDCl_3$) δ/ppm 4.27 (bs, H-2, H-6, 2H), 4.08 (q, *J*= 7.2, 14.3 Hz, O**C**$\mathbf{H_2}$$CH_3$, 2H), 3.58 (s, OC$\mathbf{H_3}$, 3H), 3.12 (dt, *J*= 3.4, 12.6 Hz, H-6, 1H), 2.86 (m, H-3, H-2, 2H), 2.59 (d, *J*= 17.3 Hz, H-2', 1H), 2.50-2.42 (m, H-5, 1H), 2.35-2.31 (2 x t, *J*= 3.3 Hz, H-5, 1H), 2.19 (d, *J*= 16.6 Hz, H-2', 1H), 1.19 (t, *J*= 7.1 Hz, $OCH_2C\mathbf{H_3}$, 3H)

^{13}C-NMR (100 MHz, $CDCl_3$) δ/ppm 207.3 (C=O), 172.1(**C**O_2Me), 155.1 (**C**O_2Et), 62.3 (**C**O_2**Et**), 52.2 (O**C**H_3), 47.9 (C-2), 46.4 (C-6), 43.8 (C-3), 40.7 (C-5), 31.1 (**C**-2'**)**, 14.6 (**C**O_2**E**t)

Ethyl 4-(benzylamino)-3-(2-methoxy-2-oxoethyl)piperidine-1-carboxylate 120 and ethyl 1-benzyl-2-oxooctahydro-5H-pyrrolo[3,2-c]pyridine-5-carboxylate (121)



To a solution of methyl ester (**118**) (1.0 g, 4.1 mmol, 1.0 eq.) in 1,2 dichloroethane (DCE) (18 mL) was added $NaBH(OAc)_3$ (1.26 g, 6.0 mmol, 1.4 eq.) and benzylamine (0.46 mL, 4.1 mmol, 1.0 eq.) and the mixture was stirred at rt for two days. The reaction mixture was quenched by the addition of saturated aqueous $NaHCO_3$ (100 mL). The aqueous phase was extracted with ethyl acetate (3 x 100 mL). The combined organic layers were dried over $MgSO_4$, filtered and the solvent was evaporated under reduced pressure. The crude product was purified by flash chromatography (petrol ether/ethyl acetate: 1:3, 1% NH_4OH) to yield amides **120** and **121** in a 3:1 mixture as colorless oils.

(**120**):

^{1}H-NMR (400 MHz, $CDCl_3$) δ/ppm 7.33-7.22 (m, Ph, 5H), 4.13 (q, *J*= 6.9Hz, O**C**$\mathbf{H_2}$$CH_3$, 2H), 4.06 (bs, H-2, H-6, 2H), 3.91 (dd, *J*= 13.3 Hz, C$\mathbf{H_2}$Ph, 1H,), 3.70 (dd, *J*= 13.3 Hz, C$\mathbf{H_2}$Ph, 1H), 3.65 (s, OC$\mathbf{H_3}$, 3H), 2.89 (dt, *J*= 2.7, 10.9 Hz, H-6, 1H), 2.73-2.62 (m, H-2, H-4, 2H), 2.37 (dt, *J*= 3.9, 9.6 Hz, H-2', 1H), 2.21-2.08 (m, H-2', H-5, 3H), 1.93 (bs, H-3, 1H), 1.26 (t, *J*= 6.9 Hz, $OCH_2C\mathbf{H_3}$, 3H)

HRMS *m/z*: $C_{18}H_{27}N_2O_4$ calculated 335.1965 $[M+H]^+$, found 335.2058.

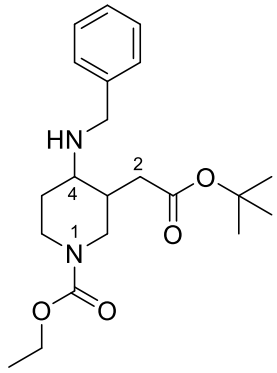
(**121**):

^{1}H-NMR (400 MHz, $CDCl_3$) δ/ppm 7.36-7.24 (m, Ph, 5H), 4.92 (d, *J*= 15.4 Hz, C**H**$_2$Ph, 1H), 4.14 (q, *J*= 6.8, 14.5 Hz, OC**H**$_2$CH$_3$, 2H), 4.06 (d, *J*= 14.9 Hz, C**H**$_2$Ph, 1H), 3.64-3.52 (m, H-2, H-6, 2H), 3.39-3.27 (m, H-6, H-4, 2H), 2.59-2.49 (m, H-3, H-4, 2H), 2.29-2.21 (m, H-4, 1H), 1.89-1.81 (m, H-3, 1H), 1.76-1.68 (m, H-3, 1H), 1.26 (t, *J*= 7.3 Hz, OCH$_2$C**H**$_3$, 3H)

^{13}C-NMR (100 MHz, $CDCl_3$) δ/ppm 174.0 (C=O), 155.4 (**C**O$_2$Et), 136.3 (Ph), 128.2 (2) (Ph), 127.4 (2) (Ph), 61.1 (O**C**H$_2$CH$_3$), 54.0 (C-2), 44.0 (**C**H$_2$Ph), 43.2 (C-6), 39.1 (C-4), 34.1 (C-4), 30.9 (C-3), 25.2 (C-3), 14.4 (OCH$_2$**C**H$_3$)

HRMS *m/z*: $C_{17}H_{22}N_2O_3$ calculated 302.1751 $[M+H]^+$, found 302.1782.

Ethyl 4-(benzylamino)-3-(2-(tert-butoxy)-2-oxoethyl)piperidine-1-carboxylate (**122**)



To a solution of ethyl 3-(2-(*tert*-butoxy)-2-oxoethyl)-4-oxopiperidine-1-carboxylate (**115**) (1.43 g, 5.01 mmol, 1.0 eq.) in 1,2 dichloroethane (22 mL) was added benzylamine (0.65 mL, 0.63 g, 5.90 mmol, 1.17 eq.) and sodium triacetoxyborohydride (1.80 g, 8.53 mmol, 1.70 eq.) and the resulting mixture was stirred overnight. The reaction mixture was quenched with saturated aqueous $NaHCO_3$ (150 mL) and the aqueous phase was extracted with ethyl acetate (3 x 150 mL). The combined organic layers were dried over $MgSO_4$, filtered and the solvent was evaporated under reduced pressure. The crude product was purified by flash chromatography (petrol ether /ethylacetate, 1:5) to yield ethyl 4-(benzylamino)-3-(2-(*tert*-butoxy)-2-oxoethyl)piperidine-1-carboxylate (**122**) as a yellowish oil (1.77g, 94%).

^{1}H-NMR (400 MHz, $CDCl_3$) δ/ppm 7.34-7.31,7.29-7.23 (m, Ph, 5H), 4.12 (q, *J*= 7.1Hz, CO_2Et, 2H), 4.04-3.69 (m, H-2, H-6, H-4, CH_2-Ph, 5H), 3.11-2.89 (m, H-2, 1H), 2.86-2.81 (m, H-6, 1H), 2.74-2.46 (m, H-2', NH, 2H), 2.37-2.30 (m, H-3, 1H), 2.18-2.12 (m, H-2', 1H), 1.91-1.76 (m, H-5, 1H), 1.56-1.46 (m, H-5, 1H), 1.45 (s,CO_2*t*Bu, 9H), 1.24 (t, *J*= 6.8 Hz, CO_2Et, 3H)

^{13}C-NMR (100 MHz, $CDCl_3$) δ/ppm 172.5, 155.8, 155.4, 140.6, 140.4, 128.4, 128.3 (2), 128.1 (2), 126.9 (2), 82.6, 80.4, 80.3, 62.2, 61.5, 61.2, 59.2, 50.9, 50.4, 45.9, 42.5, 42.4, 28.2, 14.7 (2),

HRMS *m/z***:** $C_{22}H_{33}N_2O_4$ calculated 377.2435 $[M+H]^+$, found 377.2422.

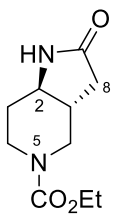
Ethyl 2-oxohexahydro-1H-pyrrolo[3,2-c]pyridine-5(6H)-carboxylate (**125**)

To a solution of ethyl 4-(benzylamino)-3-(2-(*tert*-butoxy)-2-oxoethyl)piperidine-1-carboxylate (**122**) (1.70 g, 4.52 mmol, 1.0 eq.) in MeOH (50 mL) was added hydrochloric acid (0.6 M, 4 mL) and the reaction mixture was stirred for 4 days at rt. A further additional aliquot of hydrochloric acid (conc., 1 mL) was added and the mixture was stirred for a further two days. The reaction mixture was evaporated under reduced pressure and subsequently diluted in MeOH (30 mL) and hydrochloric acid (0.5M, 2 mL) was added. The reaction was stirred for 48 hours at room temperature. After evaporation, the crude product was obtained as the hydrochloride salt and was used without further purification.

To a solution of the hydrochloride salt (**123**) (550 mg, 1.49 mmol, 1.0 eq.) in MeOH (15 mL) was added Pd/C (10% w/w, 100 mg) and the reaction mixture was stirred at room temperature overnight under an atmosphere of hydrogen. The reaction mixture was filtered through Celite and the filter cake was washed with MeOH (3 x 10 mL). The filtrate was evaporated to yield ethyl 4-amino-3-(2-methoxy-2-oxoethyl)piperidine-1-carboxylate hydrochloride (**124**) which was used without further purification in the next step.

To a solution of crude product (1-(ethoxycarbonyl)-3-(2-methoxy-2-oxoethyl)piperidine-4-aminium chloride (**124**) in MeOH (6 mL) was added anhydrous K_2CO_3 (200 mg, 1.4 mmol, 1.4 eq.) and the reaction mixture was stirred overnight at room temperature. The reaction mixture was quenched with water (30 mL) and the aqueous phase was extracted with ethyl acetate (3 x 30 mL). The combined organic layers were dried over $MgSO_4$, filtered and the solvent was evaporated under reduced pressure. The crude product was purified by flash chromatography (ethyl acetate/ petrol ether/ methanol: 10:1:1) to yield ethyl 2-oxohexahydro-1*H*-pyrrolo[3,2-*c*]pyridine-5(6*H*)-carboxylate (**125**) which was separated by flash column chromatography to afford two isomers: isomer 1 (168 mg, 37%) and isomer 2 (286 mg, 63%), combined: 454 mg, 45%).

1.isomer (**125-1**)



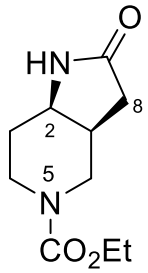
^{1}H-NMR (400 MHz, $CDCl_3$) δ/ppm 6.29 (bs, NH, 1H), 4.34 (m, H-4, H-6, 2H), 4.12 (q, *J*= 7.4 Hz, $CO_2\mathbf{CH_2}CH_3$, 2H), 3.19 (ddd, *J*= 3.7, 10.2 Hz, H-2, 1H), 2.84-2.74 (m, H-4, H-6, 2H), 2.32 (dd, *J*= 6.7, 15.7 Hz, H-8, 1H), 2.08 (dd, *J*= 12.9, 15.7 Hz, H-8, 1H), 2.01-1.87 (m, H-7, H-3, 2H), 1.54 (ddd, *J*=

4.4, 12.9, 24.5 Hz, H-3, 1H), 1.25 (t, *J*= 7.4 Hz, $CO_2CH_2\mathbf{CH_3}$, 3H)

^{13}C-NMR (100 MHz, $CDCl_3$) δ/ppm 178.2 (C=O), 156.2 ($\mathbf{C}O_2Et$), 61.5 ($CO_2\mathbf{C}H_2CH_3$), 60.4 (C-2), 59.5 (C-4), 46.4 (C-7), 43.8 (C-6), 42.5 (C-8), 34.9 (C-3), 14.7 ($CO_2CH_2\mathbf{C}H_3$)

m.p. 104-105 °C,

HRMS *m/z*: $C_{10}H_{17}N_2O_3$ calculated 213.1234 $[M+H]^+$, found 213.0807.



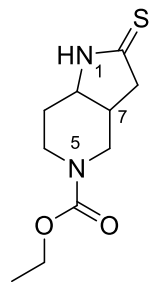
2.isomer (**125-2**)

^{1}H-NMR (400 MHz, $CDCl_3$) δ/ppm 7.22 (bs, NH, 1H), 4.05 (q, *J*= 7.4 Hz, $CO_2C\mathbf{H_2}CH_3$, 2H), 3.80 (q, *J*= 4.8 Hz, H-2, 1H), 3.60 (dd, *J*= 5.1, 13.9 Hz, H-6, 1H), 3.46-3.41 (m, H-4, 1H), 3.24 (ddd, *J*= 3.6, 9.7, 13.4 Hz, H-4, 1H), 3.15 (dd, *J*= 7.1, 13.8 Hz, H-6, 1H), 2.52 (bs, H-7, 1H), 2.38 (dd, *J*= 10.6, 17.9 Hz, H-8, 1H), 1.97 (dd, *J*= 4.7, 16.6 Hz, H-8, 1H), 1.87-1.78 (m, H-3, 1H), 1.70-1.62 (m, H-3, 1H), 1.18 (t, *J*= 7.0 Hz, $CO_2CH_2C\mathbf{H_3}$, 3H)

^{13}C-NMR (100 MHz, $CDCl_3$) δ/ppm 178.4 (C=O), 155.5 ($\mathbf{C}O_2Et$), 61.5 ($CO_2\mathbf{C}H_2CH_3$), 51.1 (C-2), 43.6 (C-6), 39.3 (C-4), 34.9 (C-8), 27.6 (C-7), 21.2 (C-3), 14.7 ($CO_2CH_2\mathbf{C}H_3$)

HRMS *m/z*: $C_{10}H_{16}KN_2O_3$ calculated 251.0793 $[M+K]^+$, found 251.0761.

Ethyl 2-thioxohexahydro-1*H*-pyrrolo[3,2-c]pyridine-5(6*H*)-carboxylate (126)



To a solution of amide (**125**) (74 mg, 0.35 mmol, 1.0 eq.) in toluene (1.5 mL) was added Lawessons reagent (70 mg, 0.17 mmol, 0.5 eq.) and the mixture was refluxed for 20 min. The solvent was evaporated under reduced pressure and the residue was purified by flash chromatography (ethyl acetate/petrol ether: 10:1 +5% MeOH) to yield thioamide (**126**) (75 mg, 95%) as a colorless oil.

1.isomer (**126-1**)

^{1}H-NMR (400 MHz, $CDCl_3$) δ/ppm 8.15 (bs, NH, 1H), 4.39 (m, H-4, H-6, 2H), 4.14 (q, *J*= 7.4 Hz, $CO_2C\mathbf{H_2}CH_3$, 2H), 3.44 (dt, *J*= 3.3, 11.2 Hz, H-2, 1H), 2.97 (dd, *J*= 7.1, 16.5 Hz, H-8, 1H), 2.82 (m, H-4, H-6, 2H), 2.50 (dd, *J*= 13.3, 16.9 Hz, H-8, 1H), 2.09-1.97 (m, H-7, H-3, 2H), 1.67-1.58 (m, H-3, 1H), 1.26 (t, *J*= 7.2 Hz, $CO_2C\mathbf{H_2}CH_3$, 3H)

^{13}C-NMR (100 MHz, $CDCl_3$) δ/ppm 206.7 (C=S), 155.7 (CO_2Et), 65.6 (C-2), 61.9 ($CO_2\mathbf{C}H_2CH_3$), 46.6 (C-8), 46.3 (C-6), 45.7 (C-7), 42.3 (C-4), 29.4 (C-3), 14.7 ($CO_2CH_2\mathbf{C}H_3$)

LCMS *m/z* 229.2 $[M+H]^+$, 270.1 $[M+AcN]^+$, 2.21 min.

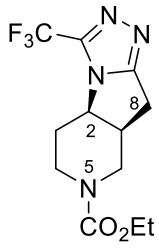
2.isomer (**126-2**)

^{1}H-NMR (400 MHz, $CDCl_3$) δ/ppm 9.14 (bs, NH, 1H), 4.13-4.08 (m, $CO_2C\mathbf{H_2}CH_3$, 2H), 3.80-3.63 (m, H-2, 1H), 3.59-3.50 (m, H-6, 1H), 3.23 (ddd, *J*= 4.1, 9.7, 13.3 Hz, H-4 1H), 3.12 (dd, *J*= 8.2, 14.3 Hz, H-4, 1H), 2.95 (d, *J*= 7.4Hz, H-6, 1H), 2.67-2.62 (m, H-8, 1H), 2.59 (m, H-3, 1H), 1.97-1.78 (m, H-8, 2H), 1.22 (t, *J*= 7.2 Hz, $CO_2CH_2C\mathbf{H_3}$, 3H)

^{13}C-NMR (100 MHz, $CDCl_3$) δ/ppm 204.9 (C=S), 155.8 ($\mathbf{C}O_2Et$), 61.6 ($CO_2C\mathbf{H_2}CH_3$), 47.5 (C-2), 42.7 (C-8), 39.3 (C-6), 35.2 (C-4), 26.1 (C-7), 14.8 ($CO_2CH_2C\mathbf{H_3}$)

LCMS *m/z* 229.2 $[M+H]^+$, 2.21 min.

Ethyl (4aR,8aS)-3-(trifluoromethyl)-4a,5,8a,9-tetrahydro-6H [1,2,4] triazolo [4',3':1,5] pyrrolo[3,2-c]pyridine-7(8H)-carboxylate (133)



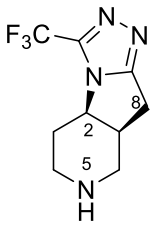
To a solution of ethyl (3a*S*,7a*R*)-2-thioxooctahydro-5H-pyrrolo[3,2-c]pyridine-5-carboxylate (**126**) (54 mg, 0.26 mmol, 1 eq.) in toluene (2 mL) was added trifluoroacetic acid hydrazide (61 mg, 0.47 mmol, 2 eq.) and the solution/mixture/suspension was refluxed for 3 nights. The solvent mixture was evaporated under reduced pressure and the crude product was purified by intensive flash chromatography (dichlormethane/methanol 10:1) to yield, ethyl (4aR,8aS)-3-(trifluoromethyl)-4a,5,8a,9-tetrahydro-6H-[1,2,4]triazolo[4',3':1,5]pyrrolo[3,2-c]pyridine-7(8H)-carboxylate (**133)** (55 mg, 70%) as a yellowish oil.

^{1}H-NMR (400 MHz, $CDCl_3$) δ/ppm 4.60 (q, *J*= 7.0 Hz, H-2, 1H), 4.17-4.11 (dq, *J*= 2.0, 7.1, Hz, $CO_2C\mathbf{H_2}CH_3$, 2H), 3.91 (m, H-6, 1H), 3.80 (m, H-4, 1H), 3.45 (d, *J*= 13.4 Hz, H-6, 1H), 3.33 (m, H-7, 1H), 3.13 (dd, *J*= 8.2, 16.7 Hz, H-4, H-8, 2H), 2.82 (dd, *J*= 8.8, 17.1 Hz, H-8, 1H), 2.30-2.22 (m, H-3, 1H), 1.84-1.73 (m, H-3, 1H), 1.24 (t, *J*= 6.8 Hz, $CO_2CH_2C\mathbf{H}_3$, 3H)

^{13}C-NMR (100 MHz, $CDCl_3$) δ/ppm 162.8 (C-9), 157.9 (C-12), 141.2 (q, CF_3), 62.0 ($CO_2\mathbf{C}H_2CH_3$), 55.5 (C-2), 43.1 (C-6), 42.3 (C-7), 39.6 (C-4) 27.7 (C-3), 24.3 (C-8), 14.6 ($CO_2CH_2\mathbf{C}H_3$)

HRMS *m/z*: $C_{12}H_{15}N_4O_2F_3$ calculated 305.1220 $[M+H]^+$, found 305.1240.

(4a*R*,8a*S*)-3-(Trifluoromethyl)-4a,5,7,8,8a,9-hexahydro-6H-[1,2,4]triazolo [4',3':1,5] pyrrolo [3,2-c]pyridine (**134**)

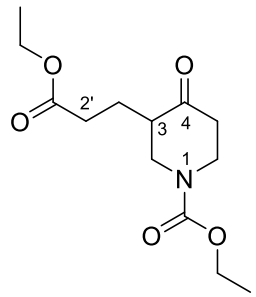


To a solution of triazole (**133**) (0.24 mmol, 1eq.) in a mixture of ethanol (0.22 ml) and water (1.25 mL) was added potassiumhydroxide (100 mg, 0.7 mmol, 3 eq.) and the reaction mixture was refluxed for overnight. The reaction mixture was extracted with dichloromethane (6 x 10 mL) and the combined organic layers were dried over Na_2SO_4, filtered and the solvent was removed under reduced pressure to yield amine (**134**) (23 mg, 42 %) as a colorless oil which was used crude without further purification.

^{1}H-NMR (400 MHz, $CDCl_3$) δ/ppm 4.43 (ddd, *J*= 6.3, 9.9, 12.2 Hz, H-2, 1H), 3.09-3.04 (m, H-4, H-6, H-8, 3H), 3.00-2.92 (m, H-4, H-6, H-8, 3H), 2.61 (dddd, *J*= 3.1, 10.8, 12.5, 23.3 Hz, H-7, 1H), 2.21-2.16 (m, H-5, 1H), 1.79 (m, NH, 1H), 1.63-1.54 (m, H-5, 1H)

10.4 Synthesis of [6.6.5] scaffold

Ethyl 3-(3-ethoxy-3-oxopropyl)-4-oxopiperidine-1-carboxylate (139)



To a solution of ethyl-oxo-piperidone (**108**) (20.0 g, 17.6 mL, 116 mmol, 1.0 eq.) in benzene (240 mL) was added pyrrolidine (11.2 g, 13 mL, 158 mmol, 1.35 eq.) and the mixture was refluxed overnight using a Dean-Stark trap. The excess of benzene and pyrrolidine was reduced under reduced pressure. The dark red residue was again dissolved in benzene (240 mL), ethyl acrylate (23.2 g, 25.2 mL, 232 mmol, 2.0 eq.) was added and the mixture was refluxed for 20h. Afterwards water (88 mL) was added to the black red solution and the mixture was refluxed for another 2h. The phases were separated and the organic phase was dried over $MgSO_4$, filtered and the solvent was evaporated under reduced pressure. The crude product was purified by flash chromatography (ethyl acetate/ petrol ether: 1:4) to yield ethyl 3-(3-ethoxy-3-oxopropyl)-4-oxopiperidine-1-carboxylate **139** as a slightly yellow oil (22 g, 69%).

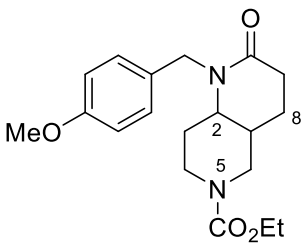
^{1}H-NMR (400 MHz, $CDCl_3$) δ/ppm 4.19 (q, *J*= 7.1, Hz, $CO_2C\mathbf{H}_2CH_3$, 2H), 4.12 (q, *J*= 7.0 Hz, $CO_2C\mathbf{H}_2CH_3$, H-2, H-6, 4H), 3.38 (ddd, *J*= 5.5, 9.0, 14.3 Hz, H-2, 1H), 3.04 (bs, H-6,

1H), 2.51-2.32 (m, H-3, H-2', H-5, 5H), 2.06 (m, H-3', 1H), 1.64-1.55 (m, H-3', 1H), 1.29 (t, *J*= 7.1 Hz, $CO_2CH_2C\mathbf{H}_3$, 3H), 1.25 (t, *J*= 7.2 Hz, $CO_2CH_2C\mathbf{H}_3$, 3H)

^{13}C-NMR (100 MHz, $CDCl_3$) δ/ppm 208.7 (C=O), 173.1 ($\mathbf{C}O_2Et$), 155.4 ($\mathbf{C}O_2Et$), 62.1 ($\mathbf{C}O_2Et$), 60.6 ($\mathbf{C}O_2Et$), 49.3 (C-6), 48.4 (C-4), 43.9, 31.7, 22.4, 14.8 ($\mathbf{C}O_2Et$), 14.3 ($\mathbf{C}O_2Et$)

LCMS *m/z* 272.2 $[M+H]^+$, 2.49 min.

Ethyl 1-(4-methoxybenzyl)-2-oxooctahydro-1,6-naphthyridine-6(2H)carboxylate (141)



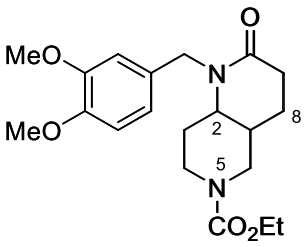
To a solution of ethyl ester **139** (3.0 g, 11.1 mmol, 1.0 eq.) in DCE (39 mL) was added $NaBH(OAc)_3$ (3.3 g, 15.5 mmol, 1.4 eq.) and $PMBNH_2$ (1.7 mL, 11.6 mmol, 1.05 eq.) and the mixture was stirred overnight at rt.. The reaction mixture was quenched with saturated aqueous $NaHCO_3$ (300 mL) and the aqueous phase was extracted with ethylacetate (3 x 300 mL). The combined organic layers were dried over $MgSO_4$, filtered and the solvent was evaporated under reduced pressure. The crude product was purified by flash chromatography (ethylacetate/petrolether 3:1-> 5:1 + 0.5% NH_4OH) to yield amide (**141**) as a colorless sticky oil (3.82 g, 82%, in a 10:1 mixture).

^{1}H-NMR (400 MHz, $CDCl_3$) δ/ppm 7.15 (d, *J*= 11.3 Hz, CH-PMB, 2H), 6.84 (d, *J*= 6.2 Hz, CH-PMB, 2H), 5.24 (d, *J*= 14.4 Hz, CH_2-PMB, 1H), 4.36-3.96 (m, $CO_2C\mathbf{H_2}CH_3$, H-4, H-6, 4H), 3.88 (d, *J*= 14.3 Hz, CH_2-PMB, 1H), 3.78 (s, OMe, 3H), 3.28 (m, H-2, 1H), 3.00-2.87 (m, H-6, 1H), 2.69-2.45 (m, H-9, H-4, 3H), 2.02- 1.87 (m, H-8, 2H), 1.77-1.57 (m, H-7, H-3, 3H), 1.26-1.21 (m, $CO_2CH_2C\mathbf{H_3}$, 3H)

^{13}C-NMR (100 MHz, $CDCl_3$) δ/ppm 169.1, 159.1, 155.8, 129.7, 129.2, 114.2, 61.6, 55.4, 47.4, 46.8, 42.9, 34.4, 31.1, 26.9, 20.5, 14.8

HRMS *m/z*: $C_{19}H_{27}N_2O_4$ calculated 347.1965 $[M+H]^+$, found 347.2143.

Ethyl 1-(3,4-dimethoxybenzyl)-2-oxooctahydro-1,6-naphthyridine-6(2*H*)-carboxylate (142)

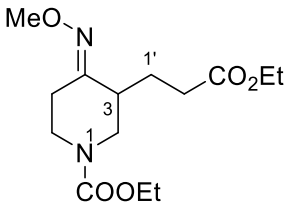


To a stirred solution of ketoester **139** (1.0 g, 3.7 mmol, 1 eq.) in 1,2 dichloroethane (13 mL) was added $DMBNH_2$ (0.57 mL, 3.88 mL,

1.15 eq.) and sodiumtriacetoxyborohydride (1.09 g, 5.14 mmol, 1.4 eq.) and the reaction mixture was stirred overnight at rt. The mixture was quenched with saturated aqueous $NaHCO_3$ (50 mL) and the aqueous phase was extracted with ethylacetate (3 x 50 mL). The combined organic layers were dried over $MgSO_4$, filtered and the solvents were removed under reduced pressure. The crude product was purified by flash chromatography (petrol ether/ ethyl acetate 1:10) to yield amide (**142**) (1.0 g, 72%, mixture: 8.4:1) as a red liquid.

^{1}H-NMR (400 MHz, $CDCl_3$) δ/ppm 7.10 (d, *J*= 9.2 Hz, CH-DMB, 1H), 6.44-6.41 (m, CH-DMB, 2H), 5.04 (d, *J*=15.4 Hz, 1H), 4.14-4.06 (m, 5H), 3.78 (s, 3H), 3.78 (s, 3H), 3.34-3.19 (dt, *J*= 3.5, 11.5 Hz, 1H), 3.00-2.86 (m, 1H), 2.69-2.56, 2.52-2.42 (m, 3H), 2.0-1.95 (m, 3H), 1.72-1.57 (m, 2H), 1.26 (2t, *J*= 7.1 Hz, 3H)

Ethyl 3-(3-ethoxy-3-oxopropyl)-4-(methoxyimino) piperidine-1-carboxylate (144)



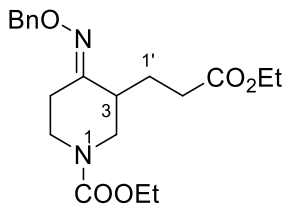
To a solution of ethyl 3-(1-((ethylperoxy)-2-methyl)-4-oxopiperidin-3-yl)propanoate (**139**) (3.0 g, 11.0 mmol, 1.0 eq.) in pyridine (21 mL) was added *o*-methylhydroxylamine hydrochloride (1.11 g, 13.3 mmol, 1.2 eq.) and the reaction was stirred at room temperature overnight. The solvent was evaporated and diluted with diethyl ether (150 mL) and water (150 mL). The organic phase was washed with hydrochloric acid (1M, 60 mL) and brine (150 mL). The combined organic layers were dried over $MgSO_4$, filtered and the solvent was evaporated under reduced pressure to yield ethyl 3-(3-ethoxy-3-oxopropyl)-4-(methoxyimino)piperidine-1-carboxylate (**144**) as a yellow/orange oil (2.80 g, 84%, 1:1.5 diastereomeric mixture).

^{1}H-NMR (400 MHz, $CDCl_3$) δ/ppm 4.16-4.08 (m, $CO_2C\mathbf{H_2}CH_3$, 4H), 3.85 (s, OMe, 2H), 3.78 (s, OMe, 1H), 3.61 (m, H-2, 1H), 3.39 (m, H-2, 1H), 3.23 (m, H-6, 1H), 2.92-2.67 (m, H-2', H-6, 2H), 2.43-2.21 (m, H-3, H-2', H-5, 4H), 1.95 (m, H-1', 1H), 1.82-1.72 (m, H-1', 1H), 1.26, 1.25 (2t, *J*= 7.47 Hz, $CO_2CH_2C\mathbf{H}_3$, 6H)

^{13}C-NMR (100 MHz, $CDCl_3$) δ/ppm 173.2 (CO_2Et), 173.0 (CO_2Et), 157.1 (CO_2Et), 155.7 (CO_2Et), 61.7 ($CO_2\mathbf{C}H_2CH_3$), 61.5 ($CO_2\mathbf{C}H_2CH_3$), 61.3 ($CO_2\mathbf{C}H_2CH_3$), 60.5, 48.4 (C-2), 44.3 (C-6), 42.7, 40.6 (C-3), 31.9 (C-5), 24.9(C-1'), 24.8 (C-2'), 14.7 ($CO_2CH_2\mathbf{C}H_3$), 14.3 ($CO_2CH_2\mathbf{C}H_3$)

HRMS *m/z*: $C_{14}H_{24}N_2O_5$ calculated 301.1758 $[M+H]^+$, found 301.1699.

Ethyl (E)-4-((benzyloxy)imino)-3-(3-ethoxy-3-oxopropyl)piperidine-1-carboxylate (143)

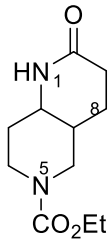


To a solution of ketone (**139**) (1.0 g, 3.7 mmol, 1.0 eq.) in pyridine (7 mL) was added benzyloxyamine hydrochloride (0.71 g, 4.43 mmol, 1.2 eq.) and stirred at rt overnight. The reaction mixture was evaporated and diluted with diethylether (50 mL) and water (50 mL). The organic phase was extracted with 1N HCl (20 mL) and washed with brine (50 mL). The combined organic phases were dried over $MgSO_4$, filtered and the solvent was evaporated under reduced pressure to yield benzyloxime (**143**) as yellowish oil (1.10 g, 80%, 1:1.7 mixture).

^{1}H-NMR (400 MHz, $CDCl_3$) δ/ppm 7.34-7.33 (m, Ph, 5H), 5.06 (s, CH_2-Ph, 1.2 H), 5.04 (s, CH_2-Ph, 0.8H), 4.19-3.99 (m, $CO_2C\mathbf{H}_2CH_3$, 4H), 3.64-3.59 (m, 1H), 3.49-3.42 (m, 1H), 3.31-3.22 (m, 1H), 2.92-2.68 (m, 2H), 2.48-2.21 (m, 4H), 1.95- 1.71 (m, 2H), 1.28-1.19 (m, $CO_2CH_2C\mathbf{H}_3$, 6H)

HRMS *m/z*: $C_{20}H_{29}H_2O_5$ calculated 377.2071 $[M+H]^+$, found 377.2054.

Ethyl 2-oxooctahydro-1,6-naphthyridine-6(2H)-carboxylate (**145**)



To a stirred solution of ethyl 3-(3-ethoxy-3-oxopropyl)-4-(methoxyimino)piperidine-1-carboxylate (**144**) (200 mg, 0.66 mmol, 1.0 eq.) in methanolic NH_3 (7N, 5 mL) was added Raney nickel (50 mg, 50% slurry in water) and the resulting mixture was stirred under an hydrogen atmosphere overnight. The reaction mixture was filtered through Celite and the filter cake was washed with methanol (3 x 10 mL). The solvent was evaporated under reduced pressure and the crude product was purified by flash chromatography (ethyl acetate / petrol ether / methanol 9:1:2) to yield the two isomers of ethyl 2-oxooctahydro-1,6-naphthyridine-6(2*H*)-carboxylate (**145**): isomer 1: 40 mg, 30%; isomer 2: 90 mg, 70%, combined yield: 130 mg, 86%, isomer 1 as a white solid and isomer 2 as a colorless oil).

1.isomer (**145-2**)

^{1}H-NMR (400 MHz, $CDCl_3$) δ/ppm 6.20 (bs, NH, 1H), 4.24 (m, H-4, H-6, 2H), 4.12 (q, *J*= 7.6 Hz, $CO_2C\mathbf{H}_2CH_3$, 2H), 3.06 (ddd, *J*= 4.0, 9.8, 12.3 Hz, H-2, 1H), 2.81-2.74 (m, H-4, 1H), 2.52-2.34 (m, H-6, H-9, 3H), 1.83-1.76 (m, H-7, H-8, 2H), 1.55-1.41 (m, H-3, H-8, 3H), 1.24 (t, *J*= 7.4 Hz, $CO_2CH_2C\mathbf{H}_3$, 3H)

^{13}C-NMR (100 MHz, $CDCl_3$) δ/ppm 172.2 (C=O), 155.4 (CO_2Et), 61.7 ($CO_2CH_2CH_3$), 56.4 (C-2), 47.3 (C-6), 42.3 (C-4), 38.9 (C-7), 32.2 (C-8), 30.9 (C-9), 24.5 (C-3), 14.7 ($CO_2CH_2CH_3$)

m.p.: 141°C

HMRS *m/z*: $C_{14}H_{19}N_2O_3$ calculated 227.1390 $[M+H]^+$, found 227.1365.

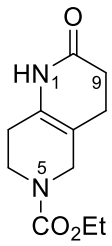
2.isomer (**145-1**)

^{1}H-NMR (400 MHz, $CDCl_3$) δ/ppm 7.33 (bs, NH, 1H), 4.11-4.04 (m, $CO_2CH_2CH_3$, 2H), 3.57-3.51 (m, H-2, H-4, H-6, 3H), 3.40-3.36 (m, H-6, 1H), 3.26-3.20 (m, H-4, 1H), 3.15 (t, *J*= 6.9 Hz, H-9, 2H), 2.03-1.98 (m, H-7, 1H), 1.86-1.62 (m, H-3, H-8, 4H), 1.20 (t, *J*= 7.2 Hz, $CO_2CH_2CH_3$, 3H)

^{13}C-NMR (100 MHz, $CDCl_3$) δ/ppm 172.6 (C=O), 155.6 (**C**O_2Et), 61.7 (CO_2**C**H_2CH_3), 50.6 (C-2), 44.7 (C-6), 40.5 (C-4), 32.7 (C-7), 30.5 (C-8), 28.9(C-9), 22.0 (C-3), 14.9 (CO_2CH_2**C**H_3)

HRMS *m/z*: $C_{14}H_{19}N_2O_3$ calculated 227.1390 $[M+H]^+$, found 227.1229.

Ethyl 2-oxo-1,3,4,5,7,8-hexahydro-1,6-naphthyridine-6(2H)-carboxylate (**148**)



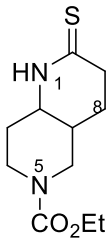
To a solution of ketone (5 g, 29 mmol, 1eq.) in toluene (18 mL) was added pyrrolidine (4.8 mL, 4.1 g, 58 mmol, 2 eq.) and the reaction mixture was heated to 150 °C using a Dean Stark trap for 25h. The red reaction mixture was cooled down to rt and the solvent was evaporated under reduced pressure. To the residue was added *p*-toluenesulphonic acid (102 mg) and acrylamide (4.1 g, 57 mmol, 2 eq.) and the mixture was heated to 90 °C for 30 min. The reaction mixture was afterwards heated to 150 °C for 2h, cooled down to rt and stirred at rt overnight. To the clumpy solid was added 1, 4-dioxane (10 mL) and *p*-toluenesulphonic acid (234 mg) and this mixture was heated at reflux for 18h. The solvent mix was evaporated under reduced pressure and the crude product was purified by flash chromatography (petrol ether/ ethyl acetate 1:10) to yield lactam **148** (2.8 g, 43 %) as an orange oil.

^{1}H-NMR (400 MHz, $CDCl_3$) δ/ppm 9.53 (bs, NH, 0.5H), 8.79 (bs, NH, 0.5H), 4.85-4.77 (m, H-6 or H-2, 0.5H), 4.12 (m, H-4 or H-6, 1H), 3.93 (q, *J*= 6.7Hz, $CO_2CH_2CH_3$, 2H), 3.67 (s, H-4 or H-6, 1H), 3.38 (t, *J*= 5.8 Hz, H-4 or H-6, 1.5H), 2.47-2.21 (m, H-9, H-3, 3H), 2.05-

1.95 (m, H-8, H-9, 2H), 1.72-1.64 (m, H-8, 0.5H), 1.24 (ddd, *J*= 6.7, 12.3, 24.5 Hz, H-8, 0.5 H), 1.05 (t, *J*= 7.0 Hz, CO_2 CH_2CH_3, 3H)

LCMS *m/z* 225.2 $[M+H]^+$, 2.14 min.

Ethyl 2-thioxooctahydro-1,6-naphthyridine-6(2H)-carboxylate (149)



To a solution of ethyl 2-oxooctahydro-1,6-naphthyridine-6(2H)-carboxylate (**145**) (80 mg, 0.35 mmol, 1.0 eq.) in toluene (1 mL) was added Lawesson's reagent (71 mg, 0.17 mmol, 0.5 eq.) and the mixture was refluxed for 20 min. The solvent was evaporated under reduced pressure and purified by flash chromatography (ethyl acetate/ petrol ether: 10:1) to yield ethyl 2-thioxooctahydro-1,6-naphthyridine-6(2H)-carboxylate (**149**) as a colorless waxy oil.

1.isomer (**149-2**) (90%)

^{1}H-NMR (400 MHz, $CDCl_3$) δ/ppm 9.25 (bs, NH, 1H), 4.22 (bs, H-4, H-6, 2H), 4.08 (q, *J*= 7.2 Hz, $CO_2C\mathbf{H_2}CH_3$, 2H), 3.09-3.02 (m, H-2, H-9, 2H), 2.89-2.70 (m, H-4, H-9, 2H), 2.44 (bs, H-6, 1H), 1.96 (dq, *J*= 2.4, 5.5 Hz, H-8, 1H), 1.74-1.69 (m, H-3, 1H), 1.54-1.34 (m, H-3, H-7, H-8, 3H), 1.21 (t, *J*= 7.0 Hz, $CO_2CH_2C\mathbf{H}_3$, 3H),

^{13}C-NMR (100 MHz, $CDCl_3$) δ/ppm 202.3 (C=S), 155.3 ($\mathbf{C}O_2Et$), 61.7 ($CO_2\mathbf{C}\mathbf{H_2}CH_3$), 58.9 (C-2), 47.4 (C-6), 42.4 (C-4), 39.0 (C-9), 37.7 (C-7), 30.8 (C-8), 24.2 (C-3), 14.6 ($CO_2CH_2\mathbf{C}H_3$)

LCMS *m/z* 243.2 $[M+H]^+$, 2.16 min.

2.isomer (**149-1**) (94%)

^{1}H-NMR (400 MHz, $CDCl_3$) δ/ppm 8.34 (bs, NH, 1H), 4.12 (dq, *J*= 2.3, 7.2 Hz, $CO_2C\mathbf{H}_2CH_3$, 2H), 3.64-3.52 (m, H-2, H-4, H-6, 3H), 3.46-3.42 (m, H-4, 1H), 3.33-3.27 (m, H-6, 1H), 2.93 (qt, *J*= 7.1, 19.6Hz, H-9, 2H), 2.19-2.06 (m, H-7, H-8, 2H), 1.88-1.72 (m, H-3, H-8, 3H), 1.25 (t, *J*= 7.0 Hz, 3H),

^{13}C-NMR (100 MHz, $CDCl_3$) δ/ppm 202.3 (C=S), 155.6 ($\mathbf{C}O_2Et$), 61.7 ($CO_2\mathbf{C}H_2CH_3$), 53.3 (C-7), 44.9 (C-4), 40.6 (C-6), 37.6 (C-9), 31.7 (C-7), 29.3 (C-3), 21.4 (C-8), 14.9 ($CO_2CH_2\mathbf{C}H_3$)

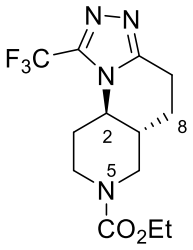
m.p. 401–403 K

HRMS m/z: $C_{11}H_{19}H_2O_2S$ calculated 243.1162 $[M+H]^+$, found 243.1003.

General procedure 1,2,4 triazole formation

To a solution of ethyl 2-thioxooctahydro-1,6-naphthyridine-6(2H)-carboxylate (**149**) (2.43 mmol, 1 eq.) in toluene (20 mL) was added the corresponding hydrazide (4.86 mmol, 2 eq.) and the mixture was refluxed at 110 °C for two nights. The solvent was evaporated and the crude product was purified by flash chromatography (dichloromethane/ methanol 10:1) to yield triazoles **150-1, 150-2, 155-1, 155-2, 156, 157, 161-1, 161-2**, **170-1, 170-2, 171-1, 171-2, 172-1-176-1**.

Ethyl 1-(trifluoromethyl)-4,5,5a,8,9,9a-hexahydro-[1,2,4]triazolo[4,3-a] [1,6] naphthyridine-7(6H)-carboxylate (170)

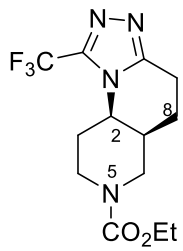


1.isomer (**170-2**): (40 %)

^{1}H-NMR (400 MHz, $CDCl_3$) δ/ppm 4.35 (bs, H-4, H-6, 2H), 4.12 (q, *J*= 7.2Hz, $CO_2C\mathbf{H_2}CH_3$, 2H), 3.82 (dt, *J*= 3.3, 11.7 Hz, H-2, 1H), 3.30-3.24 (ddd, *J*= 1.49, 5.06, 17.15 Hz, H-9, 1H), 2.97-2.87 (m, H-4, H-9, 2H), 2.70 (bs, H-6, 1H), 2.55 (d, *J*= 11.91 Hz, H-3, 1H), 1.97 (ddt, *J*= 1.42, 6.31, 13.19 Hz, H-8, 1H), 1.87-1.78 (dq, *J*= 2.34, 12.31 Hz, H-7, 1H), 1.70 (dq, *J*= 5.05, 12.42 Hz, H-3, 1H), 1.56 (dq, *J*= 5.05, 12.84 Hz, H-8, 1H), 1.24 (t, *J*= 7.11 Hz, $CO_2CH_2C\mathbf{H_3}$, 3H),

^{13}C-NMR (100 MHz, $CDCl_3$) δ/ppm 155.2, 154.9, 117.9, 114.9, 62.0 ($CO_2\mathbf{C}H_2CH_3$), 61.0 (C-2), 47.6 (C-6), 42.5 (C-4), 41.0 (C-7), 30.8 (C-3), 23.5 (C-8), 22.9 (C-9), 14.7 ($CO_2CH_2\mathbf{C}H_3$)

HRMS *m/z*: $C_{13}H_{18}F_3N_4O_2$ calculated 319.1376 $[M+H]^+$, found 319.1376.



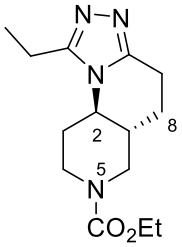
2.isomer (**170-1**) (80 %)

^{1}H-NMR (400 MHz, $CDCl_3$) δ/ppm 4.45 (dt, *J*= 4.3, 11.5 Hz, H-2, 1H), 4.32 (bs, H-4, H-6, 2H), 4.12 (m, $CO_2CH_2CH_3$, 2H), 3.27 (dd, *J*= 7.4, 17.7 Hz, H-9, 1H), 3.10 (bs, H-4, 1H), 2.96 (ddd, *J*= 7.6, 12.2, 18.9 Hz, H-9, 1H), 2.84 (bs, H-6, 1H), 2.22 (m, H-7, 1H), 2.15 (dd, *J*= 5.4, 12.6 Hz, H-8, H-3, 2H), 1.97 (m, H-8, 1H), 1.79 (dq, *J*= 5.4, 12.6 Hz, H-3, 1H), 1.25 (t, *J*= 6.9 Hz, $CO_2CH_2C\mathbf{H}_3$ 3H)

^{13}C-NMR (100 MHz, $CDCl_3$) δ/ppm 155.6 (CO_2Et), 153.0, 119.9 (q), 61.8 ($CO_2\mathbf{C}H_2CH_3$), 54.3 (C-2), 47.0 (C-4), 42.2 (C-6), 33.5 C-7), 28.9 (C-3), 20.8 (C-9), 18.7 (C-8), 14.5 ($CO_2CH_2\mathbf{C}H_3$)

HRMS *m/z*: $C_{13}H_{18}F_3N_4O_2$ calculated 319.1376 $[M+H]^+$, found 319.1045.

Ethyl 1-ethyl-4,5,5a,8,9,9a-hexahydro-[1,2,4]triazolo[4,3-a][1,6]naphthyridine-7(6*H*)-carboxylate (171)

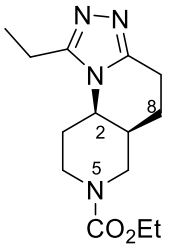


1.isomer (**171-2**) (84 %)

^{1}H-NMR (400 MHz, $CDCl_3$) δ/ppm 4.36 (bs, H-4, H-6, 2H), 4.16 (q, *J*= 7.5Hz, $CO_2C\mathbf{H_2}CH_3$, 2H), 3.65 (td, *J*= 3.3, 10.9 Hz, H-2, 1H), 3.21 (ddd, *J*= 1.6, 5.0, 16.7 Hz, H-9, 1H), 2.96-2.70 (m, H-9, H-4, H-6, $C\mathbf{H_2}CH_3$, 5H), 2.61 (m, H-3, 1H), 1.94 (dd, *J*= 5.7, 13.1 Hz, H-8, 1H), 1.83-1.76 (m, H-7, 1H), 1.73 (dq, *J*= 4.6, 12.4 Hz, H-3, 1H), 1.57 (dq, *J*= 5.3, 12.9 Hz, H-8, 1H), 1.39 (t, *J*= 7.6 Hz, $CH_2C\mathbf{H_3}$, 3H), 1.27 (t, *J*= 7.3 Hz, $CO_2CH_2C\mathbf{H_3}$, 3H)

^{13}C-NMR (100 MHz, $CDCl_3$) δ/ppm 171.9, 155.0, 154.4, 151.7, 61.6 ($CO_2\mathbf{C}H_2CH_3$), 59.1 (C-2), 47.5 (C-6), 42.2 (C-4), 40.8 (C-7), 30.3 (C-3), 24.1 (C-8), 22.5 (C-9), 21.1 ($\mathbf{C}H_2CH_3$), 14.4($CO_2CH_2\mathbf{C}H_3$), 11.3 ($CH_2\mathbf{C}H_3$)

HRMS *m/z*: $C_{14}H_{22}N_4O_2$ calculated 279.1816 $[M+H]^+$, found 279.1758.



2.isomer (**171-1**) (60%)

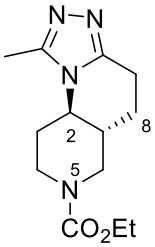
^{1}H-NMR (400 MHz, $CDCl_3$) δ/ppm 4.29 (bs, H-4, H-6, 2H), 4.16-4.10 (m,$CO_2C\mathbf{H_2}CH_3$,H-2, 3H), 3.18-3.11 (dd, *J*= 6.5, 17.8 Hz, H-9, H-6, 2H), 2.90 (m, H-4, H-9, 2H), 2.73-2.63 (dq, *J*= 8.0, 15.4Hz, $C\mathbf{H_2}CH_3$, 2H), 2.16 (bd, *J*= 12.5 Hz, H-7, 1H), 1.97 (dq, *J*= 6.25, 15.1Hz, H-8, 1H), 1.80 (bd, *J*= 11.6 Hz, H-3, H-8, 2H), 1.76 (dq, *J*= 5.3, 13.4 Hz, H-3, 1H), 1.43 (t, *J*= 7.1 Hz, $CH_2C\mathbf{H_3}$, 3H), 1.26 (t, *J*= 8.0, $CO_2CH_2C\mathbf{H_3}$, 3H)

^{13}C-NMR (100 MHz, $CDCl_3$) δ/ppm 171.1, 155.7, 153.7, 150.0, 61.8 ($CO_2\mathbf{C}H_2CH_3$), 52.2 (C-2), 47.5 (C-6), 42.4 (C-4), 34.1 (C-7), 28.7 (C-3), 21.3 (C-9), 19.7 ($\mathbf{C}H_2CH_3$), 18.4 (C-8), 14.7 ($CH_2\mathbf{C}H_3$), 11.5 ($CO_2CH_2\mathbf{C}H_3$)

HRMS *m/z*: $C_{14}H_{22}N_4O_2$ calculated 279.1816 $[M+H]^+$, found 279.2073.

Ethyl 1-methyl-4,5,5a,8,9,9a-hexahydro-[1,2,4]triazolo[4,3a][1,6]naphthyridine-7(6H)-carboxylate (150)

1.isomer (**150-2**) (41 %)

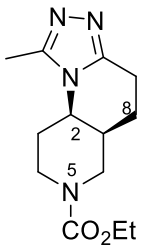


^{1}H-NMR (400 MHz, $CDCl_3$) δ/ppm 4.32 (bs, H-4, H-6, 2H), 4.11 (q, *J*= 7.5Hz, $CO_2C\mathbf{H_2}CH_3$, 2H), 3.65 (dt, *J*= 4.0, 11.1 Hz, H-2, 1H), 3.14 (ddd, *J*= 1.9, 5.6, 16.9 Hz, H-9, 1H), 2.92-2.78 (m, H-4, H-9, 2H), 2.70-2.59 (m, H-6, H-3, 2H), 2.47 (s, Me, 3H), 1.91 (dd, *J*= 5.3, 13.0 Hz, H-8, 1H), 1.80-1.71 (m, H-7, 1H), 1.66 (qd, *J*= 4.8, 12.8 Hz, H-3, 1H), 1.52 (qd, *J*= 5.5, 13.0Hz, H-8, 1H), 1.24 (t, *J*= 6.8 Hz, $CO_2CH_2C\mathbf{H_3}$, 3H)

^{13}C-NMR (100 MHz, $CDCl_3$) δ/ppm 155.3, 152.1, 150.0, 61.9 ($CO_2\mathbf{C}H_2CH_3$**)**, 59.3 (C-2), 47.8 (C-6), 42.5 (C-4), 40.9 (C-7), 30.4 (C-3), 24.6 (C-8), 22.8 (C-9), 14.8 (Me), 14.3 ($CO_2CH_2\mathbf{C}H_3$)

HRMS *m/z*: $C_{13}H_{21}N_4O_2$ calculated 265.1659 $[M+H]^+$, found 265.5332.

2.isomer (**150-1**) (51 %)

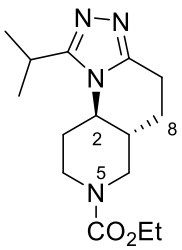


^{1}H-NMR (400 MHz, $CDCl_3$) δ/ppm 4.20 (bs, H-4, H-6, 2H), 4.11-4.00 (m, H-2, $CO_2C\mathbf{H_2}CH_3$, 3H), 3.08-2.96 (m, H-9, H-4, 2H), 2.78-2.67 (m, H-9, H-6, 2H), 2.31 (s, Me, 3H), 2.12-2.08 (m, H-7, 1H), 1.95-1.75 (m, H-8, H-3, 3H), 1.60 (qd, *J*= 5.6, 13.3Hz, H-3, 1H), 1.16 (t, *J*= 7.1 Hz, $CO_2CH_2C\mathbf{H_3}$, 3H)

^{13}C-NMR (100 MHz, $CDCl_3$) δ/ppm 155.5, 149.8, 148.9, 61.6 ($CO_2\mathbf{C}H_2CH_3$), 51.8 (C-2), 47.2 (C-4), 42.1 (C-6), 33.7 (C-7), 28.1 (C-3), 20.9 (C-9), 19.3 (C-8), 14.5 ($CO_2CH_2\mathbf{C}H_3$), 10.3 (Me)

HRMS *m/z*: $C_{13}H_{21}N_4O_2$ calculated 265.1659 $[M+H]^+$, found 265.2795.

Ethyl 1-isopropyl-4,5,5a,8,9,9a-hexahydro-[1,2,4]triazolo[4,3-a] [1,6] naphthyridine-7(6*H*)-carboxylate



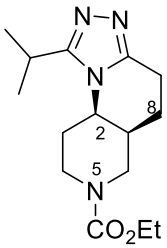
1.isomer (**155-2**): (30 %)

^{1}H-NMR (400 MHz, $CDCl_3$) δ/ppm 4.31(m, H-4, H-6, 2H), 4.09 (q, *J*= 6.8 Hz, CO_2Et, 2H), 3.66 (dt, *J*= 3.8, 11.1 Hz, 1H), 3.14 (ddd, *J*= 1.5, 4.1, 16.0 Hz, H-9, 1H), 3.03 (sept, *J*= 6.7 Hz, CH-*i*Pr, 1H), 2.91 (bs, H-6, 1H), 2.79

(ddd, *J*= 6.0, 13.1, 19.5 Hz, H-9, 1H), 2.66 (bs, H-4, 1H), 2.59 (bs, H-3, 1H, mix) 1.87 (dd, *J*= 6.1, 13.3 Hz, H-8, 1H), 1.78-1.62 (m, H-7, H-3, 2H), 1.49 (ddd, *J*= 4.6, 12.7, 25.0 Hz, H-8), 1.38 (d, *J*= 6.6 Hz, CH_3-iPr, 3H), 1.28 (d, *J*= 7.1 Hz, CH_3-*i*Pr, 3H), 1.21 (t, *J*= 6.1 Hz, $CO_2CH_2C\mathbf{H}_3$, 3H)

^{13}C-NMR (100 MHz, $CDCl_3$) δ/ppm 174.1, 158.3, 155.2, 151.1, 61.8 (CO_2Et), 59.6 (C-2), 47.8 (C-4), 42.5 (C-6), 41.3 (C-7), 33.4 (C-3), 30.8 (CH-*i*Pr), 24.2 (C-8), 22.8 (C-9), 21.5 (CH_3-*i*Pr), 21.1 (CH_3-*i*Pr)

HRMS *m/z*: $C_{15}H_{25}N_4O_2$ calculated 293.1972 $[M+H]^+$, found 293.1517, **LCMS** *m/z*: 293.3, 2.82 min.



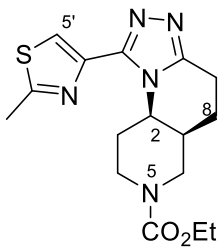
2.isomer (**155-1**) (75%)

^{1}H-NMR (400 MHz, $CDCl_3$) δ/ppm 4.26 (bs, H-4, H-6, 2H), 4.18-4.07 (m, H-2, CO_2Et), 3.13 (dd, *J*= 5.6, 17.0 Hz, H-9, 1H), 3.08 (bs, H-4, 1H), 2.91-2.77 (m, H-9, H-6, CH-*i*Pr, 4H), 2.16 (d, *J*= 11.1 Hz, H-7, 1H), 2.03-1.92 (m, H-8, 1H), 1.90-1.84 (m, H-3, H-8, 2H), 1.70 (ddd, *J*= 3.9, 12.5, 26.1 Hz, H-3, 1H), 1.40 (d, *J*= 6.6 Hz, CH_3-*i*Pr, 3H), 1.30 (d, *J*= 6.9 Hz, CH_3-*i*Pr, 3H), 1.22 (t, *J*= 7.3 Hz, CO_2Et, 3H)

^{13}C-NMR (100 MHz, $CDCl_3$) δ/ppm 174.1, 157.7, 155.7, 149.4, 61.8 ($CO_2\mathbf{C}H_2CH_3$), 52.2 (CH-*i*Pr), 42.8 (C-4), 33.9 (C-6), 29.1 (C-3), 22.7 (C-9), 21.3 (C-8), 21.1 (CH_3-*i*Pr), 19.7 (CH_3-*i*Pr), 14.6 ($CO_2CH_2\mathbf{C}H_3$)

HRMS *m/z*: $C_{15}H_{25}N_4O_2$ calculated 293.1972 $[M+H]^{++}$, found 293.1961.

Ethyl (5aS,9aR)-1-(2-methylthiazol-4-yl)-4,5,5a,8,9,9a-hexahydro-[1,2,4] triazolo [4,3-a][1,6]naphthyridine-7(6H)-carboxylate (174-1)



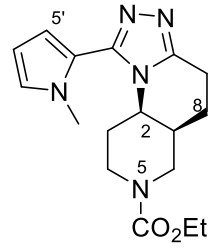
(75 %)

^{1}H-NMR (400 MHz, $CDCl_3$) δ/ppm 8.11 (s, H-5', 1H), 5.22 (dt, *J*= 4.2, 11.9 Hz, H-2, 1H), 4.26 (bs, H-4, H-6, 2H), 4.17-4.09 (m, $CO_2C\mathbf{H_2}CH_3$, 2H), 3.24 (dd, *J*= 5.1, 16.7 Hz, H-9, 1H), 3.15 (bs, H-6, 1H), 2.92 (ddd, *J*= 7.2, 12.4, 20.1 Hz, H-9, 1H), 2.80 (bs, H-4, 1H), 2.75 (s, Me, 3H), 2.25 (d, *J*= 11.2 Hz, H-7, 1H), 2.09-2.05 (m, H-8, H-3, 2H), 1.92 (bs, H-8, 1H), 1.60 (dq, *J*= 5.4, 12.5 Hz, H-3, 1H), 1.24 (t, *J*= 7.1 Hz, $CO_2CH_2C\mathbf{H_3}$, 3H)

^{13}C-NMR (100 MHz, $CDCl_3$) δ/ppm 166.7, 155.9, 150.8, 147.5, 142.6, 120.2 (C-5'), 61.8 (CO_2**C**H_2CH_3), 54.1 (C-2), 47.5 (C-6), 42.7 (C-4), 34.0 (C-7), 28.9 (C-3), 21.5 (C-9), 19.7 (Me), 19.5 (C-8), 14.8 (CO_2CH_2**C**H_3)

LCMS *m/z* 348.2 $[M+H]^+$, 2.33 min.

Ethyl (5aS,9aR)-1-(1-methyl-1H-pyrrol-2-yl)-4,5,5a,8,9,9a-hexahydro-[1,2,4]triazolo[4,3-a][1,6]naphthyridine-7(6H)-carboxylate (176-1)

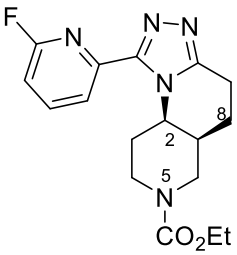


(28 %, brownish oil)

^{1}H-NMR (400 MHz, $CDCl_3$) δ/ppm (minor mix with thiolactam) 6.79 (dd, *J*= 1.6, 2.6 Hz, 1H), 6.42 (dd, *J*= 1.6, 4.1 Hz, 1H), 6.21 (dd, *J*= 2.6, 3.8 Hz, 1H), 4.47 (dt, *J*= 4.4, 10.8 Hz, 1H), 4.29 (bs, 2H), 4.16-4.07 (m, 2H), 3.78 (s, Me, 3H), 3.54 (dd, *J*= 5.8, 13.8 Hz, 0.5H), 3.42 (bd, *J*= 12.5 Hz, 0.5H), 3.26 (dd, *J*= 5.8, 16.6 Hz, 1H), 3.10 (bs, 1H), 3.05- 2.87 (m, 2H), 2.71 (bs, 1H), 2.27 (bs, 1H), 2.02-1.73 (m, 2H), 1.71-1.66 (m, 1H), 1.57 (m, 1H), 1.24 (t, *J*= 7.0 Hz, 3H)

LCMS m/z 330.4 $[M+H]^+$, 2.10 min.

Ethyl (5aS,9aR)-1-(6-fluoropyridin-2-yl)-4,5,5a,8,9,9a-hexahydro-[1,2,4] triazolo [4,3-a][1,6]naphthyridine-7(6H)-carboxylate (175-1)

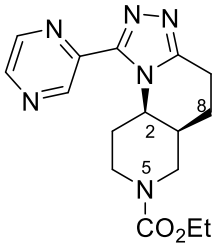


(25 %)

^{1}H-NMR (400 MHz, $CDCl_3$) δ/ppm 8.20 (dd, *J*= 1.9, 7.5 Hz, 1H), 7.13 (dddd, *J*= 0.8, 2.6, 8.1, 22.8 Hz, 1H), 6.94 (dd, *J*= 3.2, 8.4 Hz, 1H), 5.37 (m, 1H), 4.37-4.08 (m, 4H), 3.26 (dd, *J*= 7.5, 16.5 Hz, 1H), 3.16 (bs, 1H), 3.00-2.90 (m, 1H), 2.58 (bd, *J*= 14.1 Hz, 1H), 2.15 (bd, 1H), 2.05 (ddd, *J*= 6.3, 13.4, 26.1 Hz, 1H), 1.92 (m, 1H), 1.61 (ddd, *J*= 4.2, 13.7, 24.0 Hz, 1H), 1.23 (t, *J*= 7.1 Hz, 3H)

LCMS m/z 346.2 $[M+H]^+$, 2.43, 2.50 min.

Ethyl (5aS,9aR)-1-(pyrazin-2-yl)-4,5,5a,8,9,9a-hexahydro-[1,2,4]triazolo[4,3-a] [1,6]naphthyridine-7(6H)-carboxylate (173-1)



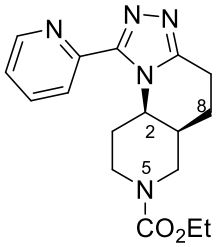
(33 %)

^{1}H-NMR (400 MHz, $CDCl_3$) δ/ppm 9.56 (s, Het, 0.7 H), (s, Het, 0.3 H), 8.56, 8.54, 8.53, 8.50, 8.49 (ms, Het, 2H), 5.28 (dt, *J*= 4.2, 11.3 Hz, H-2, 1H), 4.26 (bs, H-4, H-6, 2H), 4.15-4.07 (m, $CO_2C\mathbf{H_2}CH_3$, 2H), 3.29 (dd, *J*= 6.1, 17.5 Hz, H-9,1H), 3.13 (bs, H-4, 1H), 2.96 (ddd, *J*= 8.1, 12.3, 19.7 Hz, H-9, 1H), 2.84 (m, H-6, 1H), 2.27 (d, *J*= 13.5 Hz, H-7, 1H), 2.09-2.02 (m, H-8, H-3, 2H), 1.93 (bs, H-8, 1H), 1.63 (dq, *J*= 4.5, 12.2Hz, H-8, 1H), 1.22 (t, *J*= 6.7 Hz, $CO_2CH_2C\mathbf{H_3}$, 3H)

^{13}C-NMR (100 MHz, $CDCl_3$) δ/ppm 163.3, 155.7, 152.6, 148.3, 147.7, 144.8, 144.2, 144.1, 143.8, 142.9, 142.8 (Het), 61.7 ($CO_2\mathbf{C}H_2CH_3$), 54.5 (C-2), 47.4 (C-4), 42.6 (C-6), 34.0 (C-7), 28.9 (C-3), 21.5 (C-9), 19.3 (C-8), 14.7 ($CO_2CH_2\mathbf{C}H_3$)

LCMS *m/z* 329.1 $[M+H]^+$, 2.23 min.

Ethyl (5a*S*,9a*R*)-1-(pyridin-2-yl)-4,5,5a,8,9,9a-hexahydro-[1,2,4]triazolo[4,3-a] [1,6]naphthyridine-7(6H)-carboxylate (172-1)



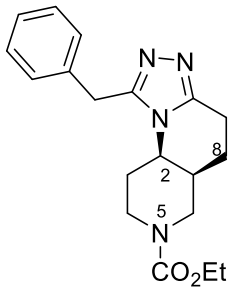
(31 %)

^{1}H-NMR (400 MHz, $CDCl_3$) δ/ppm 8.54 (d, CH-Ar, 0.67 H), 8.47 (m, CH-Ar, 0.33 H), 8.24 (d, *J*= 8.0 Hz, CH-Ar, 0.67H), 8.0 (d, *J*= 9.0Hz, CH-Ar, 0.33H), 7.82-7.71 (m, CH-Ar, 1H), 7.36 (t, *J*= 6.5 Hz, CH- Ar, 0.33 H), 7.26 (t, *J*= 5.2 Hz, CH-Ar, 0.67H), 5.43 (dt, *J*= 2.9, 10.4 Hz, H-2, 1H), 4.22 (bs, H-4, H-6, 2H), 4.11-4.04 (m, $CO_2C\mathbf{H}_2CH_3$, 2H), 3.28 (bd, *J*= 15.0 Hz, H-4, 1H), 3.12 (bs, H-9, 1H), 2.94-2.78 (m, H-9, H-6, 2H), 2.32 (d, *J*= 15.0 Hz, H-7, 1H), 2.08-1.96 (m, H-3, H-8, 2H), 1.87 (bs, H-3, 1H), 1.55 (ddd, *J*= 4.6, 12.8, 24.5 Hz, H-8, 1H), 1.19 (t, *J*= 6.8 Hz, $CO_2CH_2C\mathbf{H}_3$, 3H)

^{13}C-NMR (100 MHz, $CDCl_3$) δ/ppm 155.8, 148.8, 148.5, 148.4, 126.9, 126.7 (2), 125.5, 122.8, 122.6, 122.2, 61.7 ($CO_2\mathbf{C}H_2CH_3$), 54.4 (C-2), 50.5 (C-4), 47.4 (C-6), 42.6 (C-7), 40.4 (C-3), 21.4 (C-8), 19.2 (C-9), 14.7 ($CO_2CH_2\mathbf{C}H_3$)

LCMS *m/z* 328.2$[M+H]^+$, 2.27 min.

Ethyl (5aS,9aR)-1-benzyl-4,5,5a,8,9,9a-hexahydro-[1,2,4]triazolo[4,3-a] [1,6] naphthyridine-7(6H)-carboxylate (156)



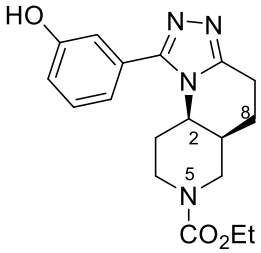
(54 %)

^{1}H-NMR (400 MHz, $MeOD_4$) δ/ppm 7.32-7.17 (m, Ph, 5H), 4.25-4.03 (m, CH_2-1', $CO_2C\mathbf{H_2}CH_3$, H-2, H-4, H-6, 7H), 3.11-3.03 (dd, *J*= 6.0, 17.0, H-6, H-9, 2H), 2.87-2.75 (ddd, *J*= 7.7, 12.1, 19.8 Hz, H-4. H-9, 2H), 2.09 (d, *J*= 10.9 Hz, H-7, 1H), 1.89-1.83 (m, H-8, 1H), 1.79 (dq, *J*= 4.8, 12.1 Hz, H-8, 1H), 1.67-156 (m, H-3, 2H), 1.22 (t, *J*= 7.4 Hz, $CO_2CH_2C\mathbf{H_3}$, 3H)

^{13}C-NMR (100 MHz, $MeOD_4$) δ/ppm 173.0, 157.3, 153.3, 136.5, 129.9, 129.4, 127.8, 62.7 ($CO_2\mathbf{C}H_2CH_3$), 53.4 (C-2), 43.1 (C-6), 41.4 (C-4), 34.7 (C-7), 31.2, (CH_2), 28.9 (C-3), 21.5 (C-9), 19.9 (C-8), 14.8 ($CO_2\mathbf{C}H_2CH_3$)

LCMS *m/z*: 341.4 $[M+H]^+$, 2.66 min.

Ethyl (5a*S*,9a*R*)-1-(3-hydroxyphenyl)-4,5,5a,8,9,9a-hexahydro-[1,2,4]triazolo[4,3-a][1,6]naphthyridine-7(6*H*)-carboxylate (157)



(mix with hydrazide) (65 %)

^{1}H-NMR (400 MHz, $MeOD_4$) δ/ppm 7.11 (dt, *J*= 1.0, 7.9 Hz, 1H), 7.07 (t, *J*= 2.2 Hz, 1H), 6.98 (ddd, *J*= 1.0, 2.4, 8.8 Hz, 1H), 4.71 (dt, *J*= 4.6, 11.4 Hz, H-2, 1H), 4.24 (d, *J*= 13.5 Hz, H-4, 1H), 4.10 (m, $CO_2C\mathbf{H_2}CH_3$, 2H), 4.00 (d, *J*= 15.0 Hz, H-6, 1H), 3.15 (bs and dd, *J*= 6.3, 17.4 Hz, H-4, H-9, 2H), 2.98-2.88 (ddd, *J*= 7.3, 12.2, 16.8 Hz, H-9, 1H), 2.71 (bs, H-6, 1H), 2.40 (bs, H-7, 1H), 2.00 (ddd, *J*= 5.9, 13.2, 26.9 Hz, H-8, 1H), 1.95-1.87 (m, H-8, 1H), 1.57 (ddd, *J*= 4.2, 11.2, 25.7 Hz, H-3, 1H), 1.51-1.44 (m, H-3, 1H), 1.26-1.21 (m, $CO_2CH_2C\mathbf{H_3}$, 3H)

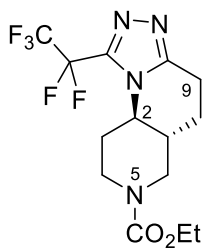
^{13}C-NMR (100 MHz, $MeOD_4$) δ/ppm 169.7, 154.4, 152.8, 135.6, 131.5, 120.3, 118.6, 116.4, 62.8 ($CO_2\mathbf{C}H_2CH_3$), 54.5 (C-2), 43.1 (C-4), 34.9 (C-6), 29.1 (C-7), 22.0 (C-3), 20.6 (C-8/C-9), 14.8 ($CO_2CH_2\mathbf{C}H_3$)

LCMS *m/z* 343.2 $[M+H]^+$, 2.15 min.

Ethyl 1-(perfluoroethyl)-4,5,5a,8,9,9a-hexahydro-[1,2,4]triazolo[4,3-a] [1,6] naphthyridine-7(6*H*)-carboxylate (**161**)

To a solution of ethyl 2-thioxooctahydro-1,6-naphthyridine-6(2H)-carboxylate (**149**) (380 mg, 1.57 mmol, 1 eq.) in THF (16 mL) was added hydrazine hydrate (0.64 mL, 50-60%) and the mixture was heated to 60°C for one hour. The reaction was cooled to rt and the solvent was removed under an nitrogen atmosphere. To the greenish oil pentafluoro propionic acid (0.46 mL, 0.71 g, 4.37 mmol, 2.8 eq.) was added followed by polyphosphoric acid and the mixture was refluxed for 2 days at 150°C. The reaction mixture was neutralized with NH_4OH and the aqueous phase was extracted with ethyl acetate (3 x 40 mL). The combined organic phases were dried over Na_2SO_4, filtered and the solvent evaporated under reduced pressure. The crude product was purified by flash chromatography (dichloromethane/ methanol 10:1) to yield ethyl 1-(perfluoroethyl)-4,5,5a,8,9,9a-hexahydro-[1,2,4]triazolo[4,3-a][1,6]naphthyridine-7(6H)-carboxylate (**161**) as a yellowish oil.

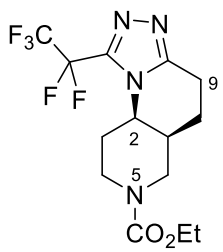
1.isomer (**161-2**) (8 %),



^{1}H-NMR (400 MHz, $CDCl_3$) δ/ppm 4.39 (bs, 2H), 4.15 (q, *J*= 7.60, 14.03 Hz, 2H), 3.86 (td, *J*= 2.9, 11.6 Hz, 1H), 3.32 (dd, *J*= 5.2, 16.9 Hz, 1H), 3.01-2.90 (m, 2H), 2.75 (bs, 1H), 2.66 (d, *J*= 14.0 Hz, 1H), 2.03-1.98 (m, 1H), 1.90- 1.81 (m, 1H), 1.74 (ddd, *J*= 4.8, 12.7, 23.8 Hz, 1H), 1.59, (ddd, *J*= 4.8, 13.8, 26.1 Hz, 1H), 1.27 (t, *J*= 7.1 Hz, 3H)

HRMS *m/z* $C_{14}H_{17}F_5N_4O_2$ calculated 369.1344 $[M+H]^+$, found 369.1207.

2.isomer (**161-1**) (34 %)



^{1}H-NMR (400 MHz, $CDCl_3$) δ/ppm 4.45 (dt, *J*= 5.14, 12.17 Hz, H-2, 1H), 4.20 (bs, H-4, H-6, 2H), 4.07-3.99 (m, $CO_2C\mathbf{H_2}CH_3$, 2H), 3.16 (dd, *J*= 6.1, 18.1 Hz, H-9, 1H), 3.05 (bs, H-6, 1H), 2.87-2.79 (m, H-9, H-4, 2H), 2.19 (bd, *J*= 12.6 Hz, H-7, 1H), 2.05-1.93 (m, H-3, H-8, 2H), 1.89-1.83 (m, H-8, 1H), 1.72 (ddd, *J*= 4.4, 11.9, 23.9 Hz, H-3, 1H), 1.15 (t, *J*= 7.1 Hz, $CO_2CH_2C\mathbf{H_3}$, 3H),

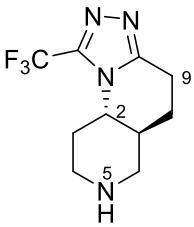
^{13}C-NMR (100 MHz, $CDCl_3$) δ/ppm 155.5 (**C**O_2Et), 153.1 (C-10), 141.4 (t, C-13), 123.1 (t), 122.2 (t), 119.4 (t), 116.5 (t), 113.5 (t), 111.8 (t), 109.4 (t), 106.8 (t), 61.7 (CO_2**C**H_2CH_3), 54.7 (C-2), 46.9 (C-6), 42.2 (C-4), 33.5 C-7), 29.1 (C-3), 20.1 (C-9), 18.5 (C-8), 14.4 (CO_2CH_2**C**H_3)

LC/MS *m/z*: 369.0 $[M+H]^+$, 3.81 min.

General procedure for 1,2,4 triazole- amine formation deprotection of carbamate

To a solution of triazole (**150-1, 150-2, 155-1, 155-2, 156, 157, 161-1, 161-2**, **170-1, 170-2, 171-1, 171-2, 172-1-176-1**) (0.41 mmol, 1 eq.) in ethanol (0.44 mL) and water (2.50 mL) was added KOH (1.80 mmol, 2.0-4.4 eq.) and the mixture was refluxed at 110 °C for one night. The reaction mixture was extracted with DCM (10 mL). The organic phase was dried over $MgSO_4$, filtered and the solvent was evaporated and the crude product (**194-1** and **194-2**) was used further as it is.

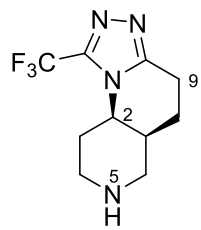
1-(trifluoromethyl)-4,5,5a,6,7,8,9,9a-octahydro-[1,2,4]triazolo[4,3-a] [1,6] naphthyridine



(65 %)

^{1}H-NMR (400 MHz, $CDCl_3$) δ/ppm 3.83 (dq, *J*= 3.3, 10.7 Hz, 1H), 3.33 (ddd, *J*= 1.5, 3.8, 16.6, 1H), 3.28 (ddd, *J*= 1.4, 3.4, 12.3 Hz, 1H), 2.98 (dddd, *J*= 6.1, 12.7, 19.1, 1H), 2.87 (dt, *J*=2.8, 12.3 Hz, 1H), 2.64 (dd, *J*= 10.9, 12.7 Hz, 1H), 2.61 (bs, 1H), 1.97-1.83 (m, 2H), 1.73 (ddd, *J*= 4.0, 11.7, 24.1, 1H), 1.60 (m, 1H)

HRMS *m/z*: $C_{12}H_{17}F_3N_5$ calculated 288.1431 $[M+AcN]^+$, found 288.1369.

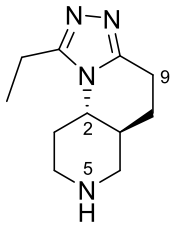


(80 %)

^{1}H-NMR (400 MHz, $CDCl_3$) δ/ppm 4.41 (dt, *J*= 4.8, 11.8 Hz, 1H), 3.31 (dd, *J*= 6.5, 17.3 Hz, 1H), 3.20-3.13 (m, 1H), 3.02 (dd, *J*= 3.0, 12.1 Hz, 1H), 2.99- 2.91 (m, 1H), 2.72 (dt, *J*= 2.4, 12.5 Hz, 1H), 2.45 (ddd, *J*= 6.2, 13.0, 26.6 Hz, 1H), 2.18-2.04 (m, 2H), 1.90-1.73 (m, 2H)

HRMS *m/z*: $C_{12}H_{17}F_3N_5$ calculated 288.2431 $[M+AcN]^+$, found 288.2346.

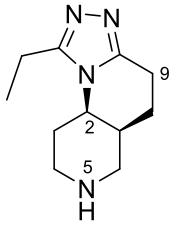
1-Ethyl-4,5,5a,6,7,8,9,9a-octahydro-[1,2,4]triazolo[4,3-a][1,6]naphthyridine



(50 %)

^{1}H-NMR (400 MHz, $CDCl_3$) δ/ppm 3.63 (td, *J*= 3.5, 10.9 Hz, 1H), 3.28 (m, 1H), 3.20-3.15 (m, 2H), 2.95-2.72 (m, 4H), 2.62-2.56 (m, 2H), 1.88-1.75 (m, 2H), 1.68 (ddd, *J*= 4.5, 12.5, 24.0 Hz, 1H), 1.51 (ddd, *J*= 5.8, 12.1, 25.2 Hz, 1H), 1.37 (t, *J*= 7.0 Hz, 3H)

HRMS *m/z*: $C_{11}H_{19}N_4$ calculated 207.1604 $[M+H]^+$, found 206. 8772.

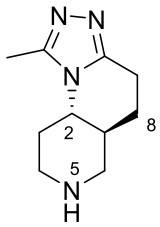


(73 %)

^{1}H-NMR (400 MHz, $CDCl_3$) δ/ppm 4.02 (dt, *J*= 4.8, 11.8 Hz, 1H), 3.14-3.04 (m, 3H), 2.94 (dd, *J*= 3.2, 12.1 Hz, 1H), 2.81-2.69 (m, 2H), 2.67-2.56 (m, 3H), 2.31-2.17 (m, 3H), 2.00 (bd, *J*= 13.0 Hz, 1H), 1.84-1.79 (m, 1H), 1.75-1.69 (m, 1H), 1.61 (ddd, *J*= 4.5, 12.9, 25.8 Hz, 1H), 1.34 (t, *J*= 7.5 Hz, 3H)

HRMS *m/z*: $C_{11}H_{19}N_4$ calculated 207.1604 $[M+H]^+$, found 207.1317.

1-methyl-4,5,5a,6,7,8,9,9a-octahydro-[1,2,4]triazolo[4,3-a][1,6]naphthyridine

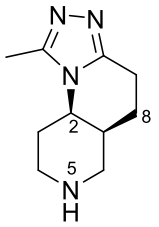


(76 %)

^{1}H-NMR (400 MHz, $CDCl_3$) δ/ppm 3.61 (dt, *J*= 4.2, 11.2 Hz, H-2, 1H), 3.26 (m, H-6, 1H), 3.18-3.12 (m, H-4, H-9, 2H), 2.89-2.77 (m, H-6, H-4, 2H), 2.63-2.54 (m, H-9, H-3, 2H), 2.48 (s, Me, 3H), 1.87-1.74 (m, H-7, NH, H-8, 3H), 1.66 (qd, *J*= 3.7, 11.5Hz, H-3, 1H), 1.50 (qd, *J*= 5.2, 12.6, Hz, H-8, 1H)

^{13}C-NMR (100 MHz, $CDCl_3$) δ/ppm 152.2, 150.0, 59.9 (C-2), 51.0 (C-4), 45.4 (C-6), 42.5 (C-7), 31.9 (C-3), 25.0 (C-8), 23.0 (C-9), 14.3 (Me)

HRMS *m/z*: $C_{10}H_{17}N_4$ calculated 193.1448 $[M+H]^+$ found 193.1389.



(65 %)

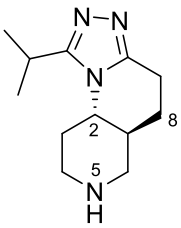
^{1}H-NMR (400 MHz, $CDCl_3$) δ/ppm 4.03 (dt, *J*= 5.1, 11.7 Hz, H-2, 1H), 3.17-3.07 (m, H-4, H-6, H-9, 3H), 2.98 (dd, *J*= 4.1, 12.7 Hz, 1H), 2.83-2.73 (qd, *J*=

6.5, 12.7 Hz, H-4, 1H), 2.67 (dt, *J*= 3.1, 13.1 Hz, H-6, 1H), 2.36 (s, Me, 3H), 2.28 (ddd, *J*= 7.6, 13.8, 23.8 Hz, H-8, 1H), 2.06-2.01 (m, H-7, 1H), 1.94 (bs, NH, 1H), 1.88-1.82 (m, H-3, 1H), 1.79-1.73 (m, H-9, 1H), 1.63 (ddd, *J*= 4.8, 12.6, 25.3 Hz, H-3, 1H)

^{13}C-NMR (100 MHz, $CDCl_3$) δ/ppm 150.5, 149.2, 52.6 (C-2), 50.6 (C-4), 45.2 (C-6), 34.1 (C-7), 29.7 (C-3), 21.6 (C-9), 20.2 (C-8), 10.5 (Me)

HRMS *m/z*: $C_{10}H_{17}N_4$ calculated 193.1448 $[M+H]^+$, found 193.1507.

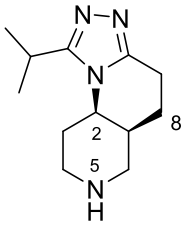
1-isopropyl-4,5,5a,6,7,8,9,9a-octahydro-[1,2,4]triazolo[4,3-a][1,6]naphthyridine



(48 %)

^{1}H-NMR (400 MHz, $CDCl_3$) δ/ppm 3.64 (dt, *J*=3.3, 11.2 Hz, 1H), 3.25-3.17 (m, 1H), 3.17-3.04 (m, 3H), 2.86-2.78 (m, 2H), 2.61-2.54 (m, 2H), 2.03 (bs, 1H), 1.83-1.64 (m, 3H), 1.54-1.46 (ddd, *J*= 4.3, 11.1, 23.2 Hz, 1H), 1.42 (d, *J*= 6.7 Hz, 3H), 1.30 (d, *J*= 6.7 Hz, 3H)

HRMS *m/z*: $C_{12}H_{21}N_4$ calculated 221.1761 $[M+H]^+$, found 221.1684.

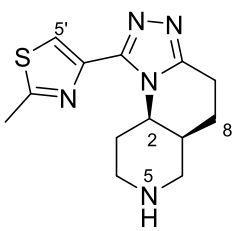


(68 %)

^{1}H-NMR (400 MHz, $CDCl_3$) δ/ppm 4.07 (dt, *J*= 4.8, 10.2 Hz, 1H), 3.18-3.07 (m, 3H), 3.00-2.97 (dd, *J*= 3.7, 12.8 Hz, 1H), 2.91-2.75 (m, 2H), 2.67 (dt, *J*= 3.3, 12.8 Hz, 1H), 2.36-2.23 (m, 1H), 2.04 (bd, *J*= 13.7 Hz, 1H), 1.85- 1.82 (m, 1H), 1.78-1.71 (m, 2H), 1.67 (ddd, *J*= 4.4, 12.8, 24.9 Hz, 1H), 1.39 (d, *J*= 6.7 Hz, 3H), 1.30 (d, *J*= 6.7 Hz, 3H)

HRMS *m/z*: $C_{12}H_{21}N_4$ calculated 221.1761 $[M+H]^+$, found 221.1447.

2-Methyl-4-((5a*S*,9a*R*)-4,5,5a,6,7,8,9,9a-octahydro-[1,2,4]triazolo[4,3-a] [1,6] naphthyridin-1-yl)thiazole



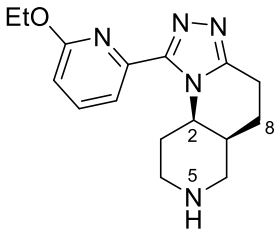
(87 %)

^{1}H-NMR (400 MHz, $CDCl_3$) δ/ppm 7.91 (s, 1H), 5.16-5.10 (m, 1H), 3.26 (dd, *J*= 6.1, 16.9 Hz, 1H), 3.14 (m, 1H), 3.07-3.02 (m, 2H), 2.94-2.84 (m, 1H), 2.73 (s, Me, 3H), 2.69-2.62 (t, *J*= 11.2 Hz, 1H), 2.36 (ddd,

J= 5.1, 12.7, 25.9 Hz, 1H), 2.16 (d, *J*= 14.1 Hz, 1H), 1.94 (d, *J*= 12.5 Hz, 1H), 1.83-1.77 (m, 2H), 1.60-1.50 (m, 1H)

LC/MS *m/z*: 276.2 $[M+H]^+$, 2.71 min.

(5a*S*,9a*R*)-1-(6-ethoxypyridin-2-yl)-4,5,5a,6,7,8,9,9a-octahydro-[1,2,4] triazolo [4,3-a][1,6]naphthyridine

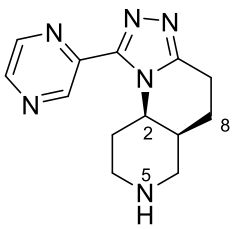


(67 %)

^{1}H-NMR (400 MHz, $CDCl_3$) δ/ppm 7.90 (dd, *J*= 0.8, 7.6 Hz, 1H), 7.66 (dd, *J*= 6.8, 8.2 Hz, 1H), 6.74 (dd, *J*= 0.8, 8.2 Hz, 1H), 5.36 (dt, *J*= 5.0, 11.7 Hz, 1H), 4.42-4.24 (m, 2H), 3.31 (ddd, *J*= 1.0, 5.6, 17.4 Hz, 1H), 3.23 (t, *J*= 13.1 Hz, 1H), 3.13 (m, 1H), 3.04 (dd, *J*= 3.3, 12.4 Hz, 1H), 2.95 (ddd, *J*= 6.0, 12.5, 17.2 Hz, 1H), 2.66 (td, *J*= 3.0, 13.0 Hz, 3H), 2.41 (ddd, *J*= 5.6, 13.0, 25.9 Hz, 1H), 2.27-2.22 (m, 1H), 2.14-2.09 (m, 1H), 1.88-1.81 (m, 1H), 1.68 (ddd, *J*= 4.1, 12.5, 24.5 Hz, 1H), 1.42 (t, *J*= 7.1 Hz, 3H)

HRMS *m/z*: $C_{16}H_{22}N_5O$ calculated 300.1819 $[M+H]^+$, found 300.4049.

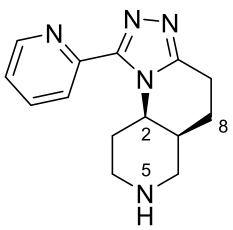
(5a*S*,9a*R*)-1-(pyrazin-2-yl)-4,5,5a,6,7,8,9,9a-octahydro-[1,2,4]triazolo[4,3-a] [1,6] naphthyridine



(54 %)

^{1}H-NMR (400 MHz, $CDCl_3$) δ/ppm 9.55 (d, *J*= 1.3 Hz, 1H), 8.56-8.55 (m, 2H), 5.24 (dt, *J*= 4.8, 11.0 Hz, 1H), 3.33 (ddd, *J*= 1.0, 5.8, 17.0 Hz, 1H), 3.17 (dt, *J*= 1.6, 13.0 Hz, 1H), 3.10-3.03 (m, 2H), 2.96 (ddd, *J*= 7.0, 12.6, 17.3 Hz, 1H), 2.71 (dt, *J*= 2.6, 12.6 Hz, 1H), 2.40 (ddd, *J*= 5.8, 12.6, 25.8 Hz, 1H), 2.19-2.03 (m, 1H), 1.90-1.80 (m, 4H), 1.60 (ddd, *J*= 4.7, 12.4, 24.2 Hz, 1H)

(5aS,9aR)-1-(pyridin-2-yl)-4,5,5a,6,7,8,9,9a-octahydro-[1,2,4]triazolo[4,3-a] [1,6] naphthyridine



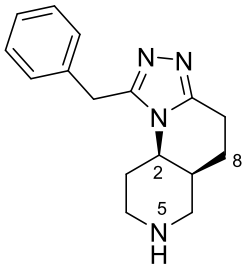
(59 %, 4:1 mix with reagent)

^{1}H-NMR (400 MHz, $CDCl_3$) δ/ppm 8.57 (dq, *J*= 0.8, 4.4 Hz, 1H), 8.25 (dt, *J*= 1.0, 8.1 Hz, 1H), 7.75 (dt, *J*= 1.9, 7.9 Hz, 1H), 7.26 (dd, *J*= 1.2,

4.2Hz, 1H), 5.38 (dt, *J*= 5.3, 12.2 Hz, 1H), 3.28 (ddd, *J*= 1.3, 5.9, 17.0 Hz, 1H), 3.13 (m, 1H), 3.06-2.99 (m, 2H), 2.91 (ddd, *J*= 6.8, 12.1, 17.6 Hz, 1H), 2.68 (dt, *J*= 2.8, 12.7 Hz, 1H), 2.35 (ddd, *J*= 5.8, 13.1, 26.2 Hz, 1H), 2.21-2.15 (m, 1H), 2.10-1.94 (m, 2H), 1.83-1.76 (m, 1H), 1.53 (ddd, *J*= 4.3, 12.5, 25.5 Hz, 1H)

LCMS *m/z*: 256.0 $[M+H]^+$, 0.42 min.

(5aS,9aR)-1-benzyl-4,5,5a,6,7,8,9,9a-octahydro-[1,2,4]triazolo[4,3-a] [1,6] naphthyridine

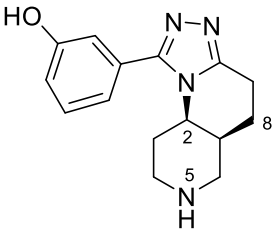


(80 %)

^{1}H-NMR (400 MHz, $CDCl_3$) δ/ppm 7.30-7.20 (m, 5H), 4.25 (d, *J*= 16.3 Hz, 1H), 4.02 (d, *J*= 16.3 Hz, 1H), 3.83 (dt, *J*= 5.3, 11.4 Hz, 1H), 3.18 (ddd, *J*= 1.7, 6.5, 17.1 Hz, 1H), 3.09-3.00 (m, 2H), 2.53 (dt, *J*= 3.4, 12.3 Hz, 1H), 2.29 (ddd, *J*= 5.9, 12.9, 26.0 Hz, 1H), 1.94 (m, 1H), 1.77-1.56 (m, 2H)

HRMS *m/z*: $C_{16}H_{21}N_4$ calculated 269.1761 $[M+H]^+$, found 269.2529.

3-((5aS,9aR)-4,5,5a,6,7,8,9,9a-octahydro-[1,2,4]triazolo[4,3-a] [1,6] naphthyridin-1-yl) phenol

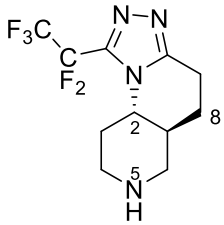


(mix with reagent, 50 %)

^{1}H-NMR (400 MHz, $CDCl_3$) δ/ppm 7.22-6.62 (m, undefined as mix with reagent), 4.66-4.63 (m, 1H), 4.45 (s, 1H), 3.16-3.05 (m, 2H), 2.97-2.80 (m, 3H), 2.44-2.38 (m, 1H), 2.29-2.23 (m, 2H), 1.84-1.78 (m, 1H), 1.54-1.41 (m, 2H)

LC/MS *m/z*: 271.2 $[M+H]^+$, 1.88 min.

1-(perfluoroethyl)-4,5,5a,6,7,8,9,9a-octahydro-[1,2,4]triazolo[4,3-a][1,6]naphthyridine

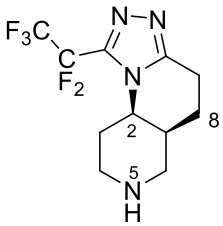


(42 %)

^{1}H-NMR (400 MHz, $CDCl_3$) δ/ppm 3.85 (dt, *J*= 3.4, 10.9 Hz, 1H), 3.33-3.27 (m, 2H), 3.22 (ddd, *J*= 1.3, 3.0, 12.1 Hz, 1H), 2.95 (ddd, *J*= 5.6, 12.5, 18.5 Hz, 1H), 2.85 (dt, *J*=2.7, 12.3 Hz, 1H), 2.67-2.60 (m, 2H),

1.94-1.81 (m, 2H), 1.72-1.56 (m, 4H)

HRMS *m/z*: $C_{11}H_{17}F_5N_5$ calculated 338.1399 $[M+AcN]^+$, found 338.1397.



(35 %)

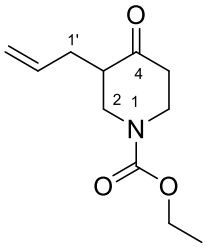
^{1}H-NMR (400 MHz, $CDCl_3$) δ/ppm 4.46 (dt, *J*= 4.6, 12.0 Hz, H-2, 1H), 3.33 (dd, *J*= 5.8, 17.4 Hz, H-9, 1H), 3.19-3.13 (m, H-4, H-6, 2H), 3.01 (dd, *J*= 3.7, 12.1 Hz, H-4, 1H), 2.98-2.93 (m, H-4, 1H), 2.72 (dt, *J*= 3.1, 12.1 Hz, H-4, 1H), 2.52-2.40 (ddd, *J*= 6.6, 13.4, 26.6 Hz, H-8, 1H), 2.19-2.07 (m, H-7, H-3, 2H), 1.89-1.74 (m, H-3, H-8, 2H), 1.48 (bs, NH, 1H)

^{13}C-NMR (100 MHz, $CDCl_3$) δ/ppm 153.7, 55.5, 50.5, 45.5, 34.1, 30.7, 21.5, 19.5

HRMS *m/z*: $C_{11}H_{13}F_5KN_4$ calculated 335.0692 $[M+K]^+$, found 335.1224.

10.5 Synthesis of [6.7.5] scaffold

Ethyl 3-allyl-4-oxopiperidine-1-carboxylate (197)

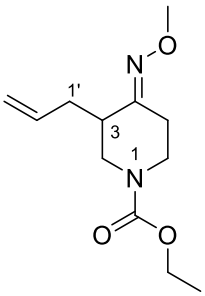


To ethyl-4-oxopiperidone-1-carboxylate **108** (10g, 58 mmol, 1 eq.) in benzene (120 mL) was added pyrrolidine (6.5 mL, 78 mmol, 1.35 eq.) and refluxed under Dean Stark conditions for one night. The excess solvent was evaporated and the crude material was suspended in benzene (120 mL) and allylbromide (10 mL, 116 mmol, 2eq.) was added and the mixture was refluxed for overnight. Water (44 mL) was added and refluxed for 2h. The phases were separated and the organic phase was dried over $MgSO_4$, filtered and the solvent was evaporated under reduced pressure. The crude material was purified through flash chromatography (petrol ether/ ethyl acetate: 3:1) to yield ketone (5g, 40%) as yellowish oil.

^{1}H-NMR (400 MHz, $CDCl_3$) δ/ppm 5.82-5.72 (m, H-2', 1H), 5.10-5.05 (m, H-3', 2H), 4.21 (q, *J*= 7.1Hz, $CO_2\mathbf{CH_2}CH_3$, 2H), 4.18-4.09 (m, H-6, H-2, 2H), 3.38 (m, H-2, 1H), 3.03 (bs, H-5, 1H), 2.56-2.41 (m, H-1', H-5, H-3, H-6, 4H), 2.10-2.04 (m, H-1', 2H), 1.29 (t, *J*= 7.0 Hz, $CO_2CH_2\mathbf{CH_3}$, 3H)

^{13}C-NMR (100 MHz, $CDCl_3$) δ/ppm 208.8 (C=O), 155.7 (COOEt), 135.0 ($CHCH_2$), 117.5 ($CHCH_2$), 61.1 ($CO_2\mathbf{C}H_2CH_3$), 49.9 (C-1'), 47.9 (C-2), 43.8 (C-6), 41.0 (C-3) 31.4 (C-5) 14.8 ($CO_2CH_2\mathbf{C}H_3$)

Ethyl -3-allyl-4-(methoxyimino)piperidine-1-carboxylate (198)

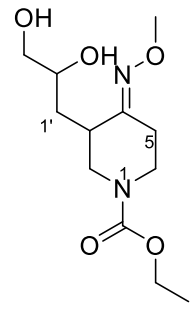


To a solution of Ethyl 3-allyl-4-oxopiperidine-1-carboxylate **197** (4.5 g, 21.3 mmol, 1 eq.) in pyridine (35 mL) was added methoxyamine hydrochloride (1.85 g, 22.3 mmol, 1.04 eq.) and stirred overnight at room temperature. The reaction mixture was diluted with diethylether (100 mL) and water (100 mL). The phases were separated and the organic phase was washed with 1N HCl (40 mL) and saturated aqueous sodiumchloride (50 mL). The organic phase was dried over Na_2SO_4, filtered and the solvent was evaporated under reduced pressure to yield methoxyoxime (3.3 g, 65%, ratio: 1:1) as yellowish oil.

^{1}H-NMR (400 MHz, $CDCl_3$) δ/ppm 5.85-5.68 (m, H-2', 1H), 5.09-5.04 (m, H-3', 2H), 4.15 (q, *J*= 6.9, 14.2 Hz, $CO_2\mathbf{CH_2}CH_3$, 2H), 3.83 (2s, OMe, 2.4H), 3.80 (2s, OMe, 0.6H), 3.05 (dd, *J*= 4.3, 13.6 Hz, 1H), 2.93 (dd, *J*= 3.6, 12.9 Hz, 4H), 2.76-2.15 (m, H-1', H-5, 4H), 1.26 (t, *J*= 7.2 Hz, $CO_2CH_2\mathbf{CH_3}$, 3H)

LC/MS *m/z*: 242.3 $[M+H]^+$, 2.77 min.

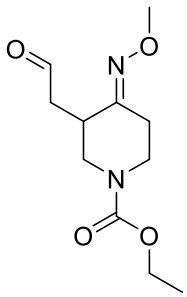
Ethyl -3-(2,3-dihydroxypropyl)-4-(methoxyimino)piperidine-1-carboxylate (199)



To a suspension of AD mix alpha (5 g) in *t*-BuOH/ water (1:1, 40 mL) was added methane sulphonamide (1.8 g, 19 mmol) and stirred for 30 min. Ethyl -3-allyl-4-(methoxyimino)piperidine-1-carboxylate **198** (1.8 g, 7.5 mmol, 2.5 eq.) in *t*BuOH/ water (1:1, 40 mL) was added and the orange suspension was stirred overnight. To the suspension sodiumsulfite (14 g) was added and stirred for 30 min. The reaction mixture was extracted with dichloromethane (2 x 150 mL). The separated organic phase was washed with aqueous saturated sodiumbicarbonate (150 mL) and saturated aqueous sodiumchloride (150 mL). The phase was dried over Na_2SO_4, filtered and the solvent was evaporated under reduced pressure. The crude product was purified by flash chromatography (ethyl acetate/ methanol 4:1) to yield diol **199** (1.2 g, 60%) as yellowish oil.

^{1}H-NMR (400 MHz, $CDCl_3$) δ/ppm 4.35-4.09 (m, 3H), 3.82, 3.81 (2s, OMe, 3H), 3.79-3.67 (m, 1H), 3.61- 3.41 (m, 4H), 3.34-3.19 (m, 1H), 3.00-2.57 (m, 5H), 2.49-2.19 (m, 2H), 1.81-1.68 (m, 1H), 1.63-1.48 (m, 1H), 1.25 (t, *J*= 6.6 Hz, 3H)

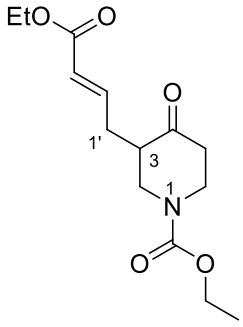
Ethyl (E)-4-(methoxyimino)-3-(2-oxoethyl)piperidine-1-carboxylate (200)



To diol (500 mg, 2.33 mmol, 1 eq.) in water (3 mL) was added sodium periodate (496 mg, 2.33 mmol, 1 eq.) in water (3 mL) and stirred overnight at rt. The crude reaction mixture was extracted with dichloromethane (3 x 50 mL). The combined organic phases were washed with sodiumbicarbonate (50 mL) and dried over Na_2SO_4, filtered and the solvent was evaporated under reduced pressure. The crude product was purified by flash chromatography (ethyl acetate/petrol ether 9:1) to yield aldehyde (170 mg, 60%; 3:1 mix with cleaved methoxy compound) as a colorless oil.

^{1}H-NMR (400 MHz, $CDCl_3$) δ/ppm 9.79 (s, CHO, 1H), 4.36 (bs, H-4, H-6, 2H), 4.19 (q, *J*= 7.0 Hz, $CO_2C\mathbf{H_2}CH_3$, 2H), 3.86 (s, 0.5H), 3.79 (s, 0.5H), 3.26-3.16 (m, 1H), 3.10-3.02 (m, 1H), 2.94-2.86 (m, 2H), 2.77-2.36 (m, 3H), 1.29 (t, *J*= 7.1 Hz, $CO_2CH_2C\mathbf{H_3}$, 3H)

Ethyl (*E*)-3-(4-ethoxy-4-oxobut-2-en-1-yl)-4-oxopiperidine-1-carboxylate



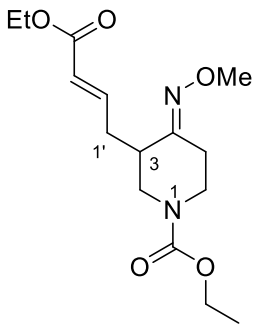
To allylproduct **197** (200 mg, 0.94 mmol, 1 eq.) in dichlormethane (7 mL) was added ethylacrylate (1.88 mmol, 2 eq.) and Hoyveda Grubbs catalyst II (20 mg, 5 mol%) and the greenish brown reaction mixture was stirred overnight at rt. The solvent was evaporated and the crude product was purified by flash chromatography (ethyl acetate/ petrol ether 1:1) and to yield α,β unsaturated ester (140 mg, 52%) as a light yellow oil.

^{1}H-NMR (400 MHz, $CDCl_3$) δ/ppm 6.88 (dt, *J*=7.4, 14.9 Hz, H-2', 1H), 5.87 (d, *J*=15.6 Hz, H-3', 1H), 4.26-4.14 (m, 2 x $CO_2C\mathbf{H_2}CH_3$, H-2, H-6, 6H), 3.30 (m, H-2, 1H), 2.93 (bs, H-6, 1H), 2.70-2.55 (m, H-1', H-5, 2H), 2.52-2.40 (m, H-3, H-5, 2H), 2.19 (dt, *J*= 7.0, 14.1 Hz, H-1', 1H), 1.30-1.25 (m, 2 x $CO_2CH_2C\mathbf{H_3}$, 6H)

^{13}C-NMR (100 MHz, $CDCl_3$) δ/ppm 207.4 (C=O), 166.1 ($\mathbf{C}O_2Et$), 155.3 ($\mathbf{C}O_2Et$), 144.8 ($\mathbf{C}HCH_2$), 123.7 ($CH\mathbf{C}H_2$), 62.0 ($CO_2\mathbf{C}H_2CH_3$), 60.4 ($CO_2\mathbf{C}H_2CH_3$), 48.7 (C-1'), 48.0 (C-3), 43.7 (C-2), 43.7 (C-6), 29.4 (C-5), 14.7 ($CO_2CH_2\mathbf{C}H_3$), 14.2 ($CO_2CH_2\mathbf{C}H_3$)

LC/MS *m/z*: 284.0 $[M+H]^+$, 2.67 min.

Ethyl (*E*)-3-((*E*)-4-ethoxy-4-oxobut-2-en-1-yl)-4-(methoxyimino)piperidine-1-carboxylate (202)



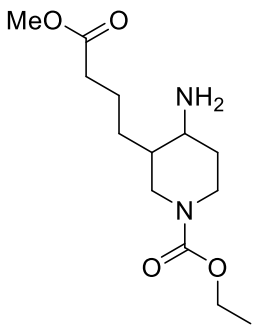
To ethyl (*E*)-3-(4-ethoxy-4-oxobut-2-en-1-yl)-4-oxopiperidine-1-carboxylate (140 mg, 0.49 mmol, 1.0 eq) in pyridine (1 mL) was added *O*-methylhydroxylamine hydrochloride (80 mg, 0.82 mmol, 1.7 eq.) and stirred at rt overnight. The reaction mixture was diluted with water and diethylether. The organic phase was washed with 1N HCl and saturated aqueous sodium chloride solution. The organic phase was dried over Na_2SO_4, filtered and the solvents were evaporated under reduced pressure to yield oxime **202** (154 mg, 88%) as a yellow oil in a 1:2 mixture.

^{1}H-NMR (400 MHz, $CDCl_3$) δ/ppm 6.94-6.80 (m, H-2', 1H), 5.84 (d, *J*= 15.9 Hz, H-3', 1H), 4.19-4.10 (m, H-6, 2x $CO_2C\mathbf{H_2}CH_3$, 5H), 3.81 (s, OMe, 1.7H), 3.79 (s, OMe, 1.3H), 3.44 (m, H-3, H-2, 3H), 2.94 (dd, *J*= 3.9, 13.8 Hz, H-2, 1H), 2.62-2.44 (m, H-1', 2H), 2.40-2.24 (m, H-1', H-5, 3H), 1.28-1.23 (m, 2x $CO_2CH_2C\mathbf{H_3}$, 6H)

^{13}C-NMR (100 MHz, $CDCl_3$) δ/ppm 166.3 (2), 157.1, 156.4, 155.8, 155.6, 145.6, 145.1 (C-2'), 123.6 (C-3'), 61.8 (OMe), 61.5 (OMe), 61.4 (CO_2Et), 60.3 (CO_2Et), 42.6 (C-6), 40.3 (C-2),33.9 (C-3), 32.1 (C-1'), 28.4 (C-5), 14.7 (CO_2Et), 14.3 (CO_2Et)

LC/MS *m/z*: 313.3 $[M+H]^+$, 2.62, 2.80 min.

Ethyl 4-amino-3-(4-ethoxy-4-oxobutyl)piperidine-1-carboxylate

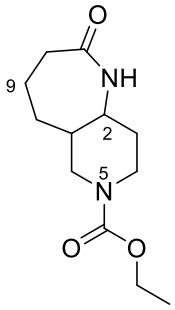


To ester **202** (100 mg, 0.32 mmol, 1 eq.) in a mixture of 7N NH_3 in methanol (5 mL) was hydrogenated using Raney Nickel overnight. The reaction mixture was filtered through celite and the filtrate was evaporated under reduced pressure. The crude product was purified by flash chromatography (ethyl acetate/ petrol ether/ 7N ammonia in methanol 10:1 + 40 %) to yield amine as a colorless oil.

^{1}H-NMR (400 MHz, $CDCl_3$) δ/ppm 4.10-4.03 (m, 3H), 3.62 (s, OMe, 3H), 3.52-3.24 (m, 3H), 2.48-2.40 (m, 1H), 2.34-2.23 (m, 2H), 1.78-1.47 (m, 7H), 1.35-1.23 (m, 2H), 1.20 (t, *J*= 7.0 Hz, $CO_2CH_2C\mathbf{H_3}$, 3H)

LC/MS *m/z*: 273.2 $[M+H]^+$, 2.93 min.

Ethyl 2-oxodecahydro-7*H*-pyrido[4,3-b]azepine-7-carboxylate (203)



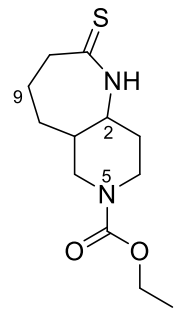
Amine (0.32 mmol, 1 eq.) in toluene was heated to 70°C and continuously to reflux overnight. Potassiumcarbonate (50 mg, 0.36 mmol, 1.1 eq.) was added and heated overnight. The solide was filtered and the solvent was evaporated under reduced pressure. The crude product was purified by flash chromatography (ethyl acetate/ petrol ether/ 7N ammonia in methanol: 10:1: 30%) to yield lactam **203** (50 mg, 66 %) as a colorless oil.

^{1}H-NMR (400 MHz, $CDCl_3$) δ/ppm 5.62 (bs, NH, 0.5H), 5.38 (bs, NH, 0.5H), 4.12 (q, *J*=6.9, Hz, $CO_2C\mathbf{H}_2CH_3$, H-4, H-6, 4H), 3.22-3.14 (m, 1H), 2.54-2.26 (m, H-2, 3H), 2.75 (m, H-4, 1H), 2.44-2.47 (m, H-10, 1H), 2.43-2.36 (m, H-3, H-10, 2H), 1.96-1.83 (m, H-8, H-9, 2H), 1.82-1.73 (m, H-7, 1H), 1.70-1.59 (m, H-3, H-9, 2H), 1.49-1.33 (m, H-8, 1H), 1.24 (t, *J*= 7.5 Hz, $CO_2CH_2C\mathbf{H}_3$, 3H)

^{13}C-NMR (100 MHz, $CDCl_3$) δ/ppm 177.8, 155.2, 61.7(2) ($CO_2\mathbf{C}H_2CH_3$), 54.6 (C-2), 48.4 (C-4), 42.6 (C-6), 41.8 (C-3), 37.0 (2) (C-8), 35.3 (C-7), 22.4 (C-9), 14.8 ($CO_2CH_2\mathbf{C}H_3$)

LC/MS *m/z*: 241.2 $[M+H]^+$, 2.89 min.

Ethyl 2-thioxodecahydro-7*H*-pyrido[4,3-b]azepine-7-carboxylate (204)



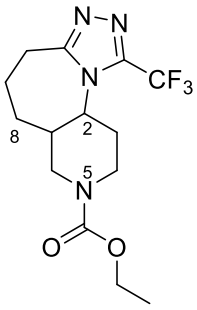
To lactam **202** (50 mg, 0.21 mmol, 1 eq.) in toluene (1 mL) was added Lawessons reagent (50 mg, 0.10 mmol, 0.5 eq.) and refluxed for 1 hour. The solvent mixture was evaporated under reduced pressure and the crude product purified by flash chromatography (ethyl acetate/ petrol ether 10:1) to yield thiolactam **204** (45 mg, 85%) as yellow oil.

^{1}H-NMR (400 MHz, $CDCl_3$) δ/ppm 7.86 (bs, NH, 1H), 4.27-4.03 (m, H-4, H-6, $CO_2C\mathbf{H}_2CH_3$, 4H), 3.42-3.35 (m, 1H), 3.28-3.16 (m, 2H), 2.87-2.79 (m, 0.5H), 2.72-2.65 (m, H-4, 1.5H), 2.40-2.30 (m, H-6, 1H), 1.99-1.82 (m, 3H), 1.80-1.46 (m, 5H), 1.23 (t, *J*= 6.8 Hz, $CO_2CH_2C\mathbf{H}_3$, 3H)

^{13}C-NMR (100 MHz, $CDCl_3$) δ/ppm 171.2, 114.2, 61.7 (2) ($CO_2\mathbf{C}H_2CH_3$), 60.5, 58.2, 55.6, 48.4 (C-4), 42.2 (C-6), 41.0, 35.0, 32.0, 31.2, 24.6, 21.1, 14.7 (2) ($CO_2CH_2\mathbf{C}H_3$)

LC/MS *m/z*: 257.3 $[M+H]^+$, 2.41 min.

Ethyl 1-(trifluoromethyl)-5,6,6a,9,10,10a-hexahydro-4H-pyrido [3,4f] [1,2,4] triazolo[4,3-a]azepine-8(7*H*)-carboxylate (205)

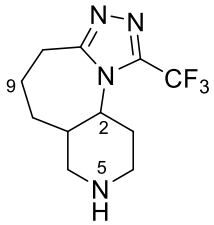


To thiolactam **204** (40 mg, 0.16 1 eq.) in toluene (1 mL) was added trifluoroacetic acidhydrazide (40 mg, 0.31 mmol, 1.9 eq.) and refluxed overnight. The crude reaction mixture was evaporated and purified by flash chromatography (dichloromethane/ methanol 10:1) to yield triazole as a colorless oil in 40% yield.

^{1}H-NMR (400 MHz, $CDCl_3$) δ/ppm 4.47 (dt, *J*= 3.7, 13.1 Hz, 1H), 4.34 (bs, 2H), 4.20-4.10 (m, 3H), 3.99 (dt, *J*= 2.4, 11.0 Hz, 1H), 3.52 (dd, *J*= 5.1, 15.3 Hz, 0.5H), 3.32 (ddd, *J*= 2.6, 5.4, 15.3 Hz, 1H), 3.06-2.61 (m, 5H), 2.30-2.20 (m, 2H), 2.15-1.92 (m, 4H), 1.82 (ddd, *J*= 4.7, 11.0, 23.5 Hz, 1H), 1.73-1.66 (m, 1H), 1.60-1.39 (m, 2H), 1.30-1.23 (m, 4H)

LC/MS *m/z*: 333.1 $[M+H]^+$, 2.82 min.

1-(trifluoromethyl)-5,6,6a,7,8,9,10,10a-octahydro-4H-pyrido[3,4-f] [1,2,4] triazolo[4,3-a]azepine



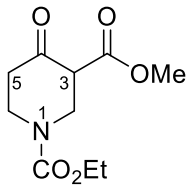
To triazole (10 mg, 0.03 mmol, 1 eq.) in an ethanol/ water mix (0.2 mL/ 1.2 mL) was added potassium hydroxide (1 piece) and refluxed overnight. The crude product was diluted with dichloromethane and extracted with dichloromethane (4 x 10 mL). The combined organic phases were dried over Na_2SO_4, filtered and the solvent was evaporated under reduced pressure to yield amine (4 mg, 50%).

^{1}H-NMR (400 MHz, $CDCl_3$) δ/ppm 4.44 (dt, *J*= 3.5, 13.0 Hz, 0.5H), 4.17 (m, 0.5H), 3.95 (td, *J*= 3.5, 11.8 Hz, 1H), 3.50 (ddt, *J*= 1.6, 7.6, 15.6 Hz, 0.5H), 3.30-3.23 (m, 2H), 3.18 (m, 0.5H), 3.10-2.98 (m, 2H), 2.85-2.74 (m, 1H), 2.72-2.58 (m, 1H), 2.53-2.43 (m, 1H), 2.34-2.20 (m, 2H), 2.18-2.03 (m, 1H), 1.99-1.92 (m, 2H), 1.86-1.77 (m, 2H), 1.65-1.56 (m, 2H), 1.44-1.36 (m, 1H)

LC/MS *m/z*: 261.2 $[M+H]^+$, 2.82 min.

10.6 Synthesis of heterocyclic scaffold

1-Ethyl 3-methyl 4-oxopiperidine-1,3-dicarboxylate (208)



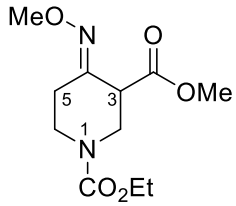
To hydrochloride **207** (3.0 g, 13 mmol, 1 eq.) in chloroform (30 mL) was added triethylamine (4.5 mL, 32 mmol, 2.5 eq.) and was stirred for 20min at rt. Afterwards ethylchloroformate (1.62 mL, 16 mmol, 1.2 eq.) was added at 0°C and the reaction mixture was warmed up to rt and stirred for 2.5h. The reaction mixture was diluted with aqueous saturated sodiumbicarbonate (20 mL) and the aqueous phase was extracted with ethylacetate (50 mL). The organic phase was dried over Na_2SO_4, filtered and the solvent evaporated under reduced pressure to yield ester **208 (**2 g, 46%) as a yellow oil.

^{1}H-NMR (400 MHz, $CDCl_3$) δ/ppm 11.96 (s, OH, 1H), 4.15 (q, *J*= 7.4, 14.1 Hz, $CO_2C\mathbf{H_2}CH_3$, 2H), 4.09 (bs, H-2, H-6, 2H), 3.77 (s, OMe, 3H), 3.60 (t, *J*= 5.7 Hz, H-6, H-2, 2H), 2.37 (t, *J*= 5.6 Hz, H-5, 2H), 1.26 (t, *J*= 6.8 Hz, $CO_2CH_2C\mathbf{H_3}$, 3H)

^{13}C-NMR (100 MHz, $CDCl_3$) δ/ppm 170.1 ($\mathbf{C}O_2CH_2CH_3$), 61.9 ($CO_2\mathbf{C}H_2CH_3$), 51.8 (OMe), 40.5 (C-2), 40.4 (C-6), 28.9 (C-5), 15.1 ($CO_2CH_2\mathbf{C}H_3$)

LC/MS *m/z*: 230.2 $[M+H]^+$, 2.62 min.

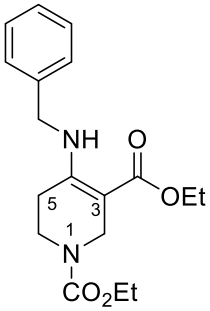
1-Ethyl 3-methyl (*E*)-4-(methoxyimino)piperidine-1,3-dicarboxylate (221)



To ester **208** (2.0 g, 8.7 mmol, 1.0 eq.) in pyridine (17 mL) was added $MeONH_2{\cdot}HCl$ (873 mg, 9.0 mmol, 1.0 eq.) and stirred at rt overnight. The reaction mixture was diluted water (120 mL) and diethylether (120 mL). The organic phase was washed with 1N HCl (47 mL) and saturated aqueous sodiumchloride (120 mL) and dried over Na_2SO_4, filtered and the solvent evaporated under reduced pressure to yield oxime **221** (1.71 g, 77%) as yellowish oil.

^{1}H-NMR (400 MHz, $CDCl_3$) δ/ppm 4.49 (dt, *J*= 2.8, 14.8 Hz, 0.5H), 4.32 (dd, *J*= 4.6, 13.3 Hz, 0.5H), 4.15-4.07 (m, 2H), 3.81 (2s, Me, 3H), 3.68 (2s, OMe, 3H), 3.36 (dd, *J*= 4.5, 13.3 Hz, 0.5H), 3.30 (bs, 0.5 H), 3.08 (dd, *J*= 4.5, 13.4 Hz, 1H), 2.77-2.45 (m, 2H), 2.36 (d, 0.5H), 1.22 (2t, *J*= 7.3/ 7.1 Hz, 3H)

1-Ethyl 3-methyl 4-(benzylamino)-5,6-dihydropyridine-1,3(2*H*)-dicarboxylate (213)

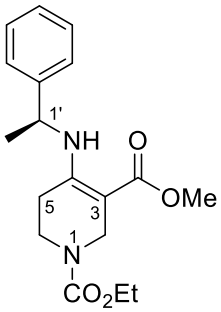


To ester **208** (7.0 g, 28.8 mmol, 1.0 eq.) in toluene (105 mL) was added benzylamine (3.5 g, 32.0 mmol, 1.1 eq.) and was refluxed under Dean Stark conditions. The crude reaction mixture was evaporated under reduced pressure and the crude product was purified by flash chromatography (dichloromethane/ ethylacetate 1:4) and the product **213** (2.3 g, 24%) was yielded as a yellow oil.

^{1}H-NMR (400 MHz, $CDCl_3$) δ/ppm 9.24 (t, *J*= 6.2 Hz, NH, 1H), 7.34-7.22 (m, Ph, 5H), 4.38 (d, *J*= 5.9 Hz, CH_2, 2H), 4.18-4.11 (m, 2 x $CO_2C\mathbf{H_2}CH_3$, H-2, H-6, 6H), 3.51 (t, *J*= 6.0 Hz, H-6, H-2, 2H), 2.37 (t, *J*= 5.8 Hz, 2H), 1.28 (m, 2 x $CO_2CH_2C\mathbf{H_3}$, 6H)

HRMS *m/z*: $C_{17}H_{22}N_2O_4$ calculated 333.1809 [M+H]+, found 333.1981.

1-Ethyl 3-methyl (*S*)-4-((1-phenylethyl)amino)-5,6-dihydropyridine-1,3(2*H*)-dicarboxylate (211)



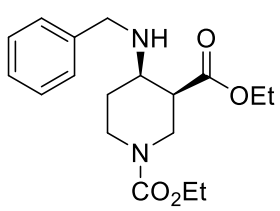
To ester (1.0 g, 4.1 mmol, 1.0 eq.) in benzene (14 mL) was added $Yb(OTf)_3$ (83 mg) and methylbenzylamine (0.6 mL, 4.8 mmol, 1.2 eq.) and refluxed under Dean-Stark conditions. The crude solvent was evaporated under reduced pressure and the crude product was purified by flash chromatography (petrol ether/ ethylacetate 9:1) to yield amine **211** (0.95g, 70%) as a yellow oil.

^{1}H-NMR (400 MHz, $CDCl_3$) δ/ppm 9.26 (d, *J*= 6.9 Hz, NH, 1H), 7.34-7.20 (m, Ph, 5H), 4.60 (dt, *J*= 6.4, 13.8 Hz, H-1', 1H), 4.14-4.08 (m, H-2, $CO_2C\mathbf{H_2}CH_3$, 4H), 3.72 (s, OMe, 3H), 3.49-3.42 (m, H-6, 1H), 3.39-3.32 (m, H-6, 1H), 2.40 (dt, *J*= 5.3, 16.3 Hz, H-5, 1H), 2.09-2.05 (m, H-5, 1H), 1.49 (d, *J*= 6.7 Hz, Me, 3H), 1.25 (t, *J*= 7.3 Hz, $CO_2CH_2C\mathbf{H_3}$, 3H)

^{13}C-NMR (100 MHz, $CDCl_3$) δ/ppm 129.0, 127.3, 125.5, 61.5 ($CO_2\mathbf{C}H_2CH_3$), 52.4 (C-1'), 50.6 (OMe), 41.5 (C-2), 39.5 (C-6), 25.3 (C-5), 21.8 (Me), 14.8 ($CO_2CH_2\mathbf{C}H_3$)

LC/MS *m/z*: 333.2 $[M+H]^+$, 3.01 min.

1-Diethyl (3*S*,4*R*)-4-(benzylamino)piperidine-1,3-dicarboxylate (220)



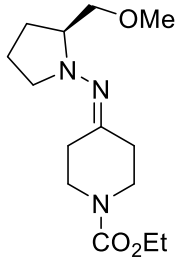
To methylester **213** (3.7 g, 1 eq.) in ethanol/ acetic acid (2 mL, 1:1) was treated with Pt/C (1.39 g) and was stirred at rt overnight under a hydrogen atmosphere. The reaction mixture was filtered through celite and the filtrate was evaporated under reduced pressure. The crude product was purified by flash chromatography (dichloromethane/ ethylacetate 1:4) and the amine **220** was yielded as colorless oil.

^{1}H-NMR (400 MHz, $CDCl_3$) δ/ppm 7.34-7.21 (m, 5H, Ph), 4.21-4.08 (m, 2H), 3.89-3.82 (m, 1H), 3.79 (dd, *J*= 13.3, 35.6 Hz, 2H), 3.64 (ddd, *J*= 3.9, 8.8, 13.6 Hz, 1H), 3.55 (bd, *J*= 13.9 Hz, 1H), 3.39-3.32 (m, 1H), 3.09 (quint., *J*= 3.6, 7.5 Hz, 1H), 2.74 (bs, 1H), 1.94-1.85 (m, 1H), 1.76-1.63 (m, 3H), 1.30-1.20 (m, ~5H)

LC/MS *m/z*: 335.4 $[M+H]^+$, 2.79 min.

10.7 Synthesis of chiral [6.6.5] lactam system

Ethyl (*S*)-4-((2-(methoxymethyl)pyrrolidin-1-yl)imino)piperidine-1-carboxylate (225)

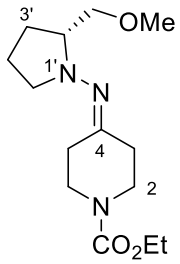


To ketone **108** (1.0 g, 5.8 mmol, 1.0 eq) was added SAMP (0.5 mL, 5.8 mmol, 1.0 eq.) and the mixture was stirred at 60°C overnight. The reaction mixture was diluted with diethylether (10mL) and the organic phase was washed with water (10 mL). The phases were separated and the organic phase was evaporated under reduced pressure to yield hydrazone an assumed yield of 100%, which was used further without purification.

^{1}H-NMR (400 MHz, $CDCl_3$) δ/ppm 4.18-4.11 (m, 3H), 3.80- 3.72 (m, 3H), 3.43 (m, 2H), 3.33 (s, OMe, 3H), 3.29-3.17 (m, 2H), 3.06 (m, 1H), 2.78 (m, 1H), 2.46-2.36 (m, 4H), 1.98 (m, 1H), 1.81 (m, 2H), 1.64 (m, 1H), 1.26 (t, *J*= 6.9 Hz, 3H)

LC/MS *m/z*: 284.2 $[M+H]^+$, 0.65 min and 0.82 min.

Ethyl (*R*)-4-((2-(methoxymethyl)pyrrolidin-1-yl)imino)piperidine-1-carboxylate (226)

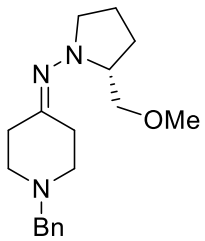


To ketone **108** (1.0 g, 5.8 mmol, 1.0 eq.) was added RAMP (0.5 mL, 5.8 mmol, 1.0 eq.) and the mixture was stirred at 60°C overnight. The reaction mixture was diluted with diethylether (10 mL) and the organic phase was washed with water (10 mL). The phases were separated and the organic phase was evaporated under reduced pressure to yield hydrazone in an assumed yield of 100%, which was used further without purification.

^{1}H-NMR (400 MHz, $CDCl_3$) δ/ppm 4.21-4.11 (m, H-2, H-6, 2H), 3.81-3.71 (m, 2H), 3.40-338 (m, $CO_2CH_2C\mathbf{H}_3$, 2H), 3.33 (s, OMe, 3H), 3.24 (m, 2H), 3.07 (m, 1H), 2.79 (bd, *J*= 13.9 Hz, 1H), 2.44 (t, *J*= 7.36 Hz, 1H), 2.39 (bs, 2H), 2.04-1.96 (m, H-3' or H-4', 1H), 1.84-1.77 (m, H-3' or H-4', 2H), 1.68-1.60 (m, H-3' or H-4', 1H), 1.26 (t, *J*= 7.1 Hz, $CO_2CH_2C\mathbf{H}_3$, 3H)

LC/MS *m/z*: 285.2 $[M+H]^+$, 0.73 min.

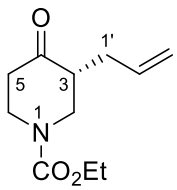
(*R*)-1-benzyl-*N*-(2-(methoxymethyl)pyrrolidin-1-yl)piperidin-4-imine (229)



To ketone **109** (1.0 g, 5.3 mmol, 1.0 eq.) was added RAMP (0.5 mL, 5.8 mmol, 1.1 eq.) and the mixture was stirred at 60°C overnight. The reaction mixture was diluted with diethylether (10 mL) and the organic phase was washed with water (10 mL). The phases were separated and the organic phase was dried over Na_2SO_4, filtered and the solvent was evaporated under reduced pressure to yield hydrazone in an assumed 100% yield.

^{1}H-NMR (400 MHz, $CDCl_3$) δ/ppm 7.35-7.26 (m, Ph, 5H), 3.53 (s, CH_2-Bn, 2H), 3.41 (dd, *J*= 4.2, 9.6 Hz, 1H), 3.33 (s, OMe, 3H), 3.23, *J*= 7.1, 9.9 Hz, 1H), 3.19-3.13 (m, 1H), 3.04 (dt, *J*= 5.5, 11.6 Hz, 1H), 2.82-2.63 (m, 4H), 2.49-2.32 (m, 2H), 2.03-1.94 (m, 1H), 1.83-1.76 (m, 2H), 1.69-1.60 (m, 1H)

Ethyl (*R*)-3-allyl-4-oxopiperidine-1-carboxylate (233)

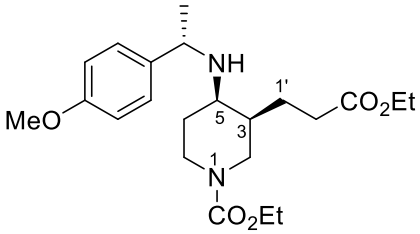


A mixture of LiCl (1.1 g, 26.0 mmol, 2.4 eq.), $[Pd(dba)_3]\cdot CHCl_3$ (100mg) and R-BINAP (134 mg, 21.6 mmol, 1.9 eq.) were added in a flask and allylacetate (1.3 mL, 13.0 mmol, 1.2 eq.) inTHF (25 mL) was added to the solids and this brownish mixture was stirred at rt. In a second flask, diisopropylamine (1.5 mL, 11.0 mmol, 1.0 eq.) in THF (8 mL) were cooled to -78°C and *n*-BuLi (6.8 mL, 11.0 mmol, 1.6 M, 1.0 eq.) was added and the yellowish reaction mixture was stirred for 30 min at

0°C. Ketone **108** (2.0 g, 11.0 mmol, 1.0 eq.) was added in THF (6.4 mL) and the mixture was stirred for 60 min at 0°C. This enolate mixture was added to the prepared mixture of LiCl, R-BINAP, $[Pd_2(dba)_3]\cdot CHCl_3$ and allylacetate in THF at -78°C and stirred at this temperature for 48 h. The reaction mixture was quenched with 100 mL phosphate buffer (pH 7.4) and stirred for 30min at rt. The phases were separated and the aqueous layer was extracted with dichloromethane (3 x 50 mL). The organic phases were combined and washed with saturated aqueous NaCl (50 mL) and dried over Na_2SO_4, filtered and the solvent was removed under reduced pressure. The crude product was purified using flash chromatography (petrol ether/ ethyl acetate 3:1) to yield allylic product **233** as a slight yellowish oil.

^{1}H-NMR (400 MHz, $CDCl_3$) δ/ppm 5.81-5.73 (m, H-2', 1H), 5.11-5.06 (m, H-3', 2H), 4.19 (q, *J*= 6.9, 14.0 Hz, $CO_2C\mathbf{H}_2CH_3$, 2H), 4.17-4.11 (m, H-2, H-6, 2H), 3.39 (bs, H-2, 1H), 3.04 (bs, H-6, 1H), 2.55-2.44 (m, H-3, H-5, H-1', 4H), 1.29 (t, *J*= 7.0 Hz, $CO_2CH_2C\mathbf{H}_3$, 3H)

Ethyl (3*R*,4*S*)-3-(3-ethoxy-3-oxopropyl)-4-(((R)-1-(4-methoxyphenyl) ethyl) amino) piperidine-1-carboxylate (236)



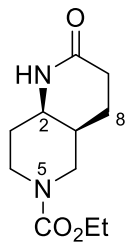
To ketoester **139** (2.0 g, 7.4 mmol, 1.0 eq.) in 1,2 dichlorethane (32 mL) was added (*S*)-1-1(4-methoxy-phenyl) ethylamine (1.2 mL, 7.9 mmol, 1.1 eq.) and $NaBH(OAc)_3$ (2.2 g, 10.4 mmol, 1.4 eq.) and stirred at rt overnight. The reaction mixture was diluted wit saturated aqueous $NaHCO_3$ (50 mL) and the aqueous phase was extracted with ethylacetate (3 x 50 mL). The combined organic phases were dried over Na_2SO_4, filtered and the solvent was evaporated under reduced pressure. The crude product was purified using flash chromatography (ethyl acetate/ petrolether+ NH_4OH, 10:1) to yield amine **236** (600 mg, 20%)

^{1}H-NMR (400 MHz, $CDCl_3$) δ/ppm 7.19 (d, *J*= 9.2 Hz, CH_{Ar}, 2H), 6.84 (d, *J*= 8.1 Hz,CH_{Ar}, 2H), 4.18-4.04 (m, 2 x $CO_2C\mathbf{H}_2CH_3$, H-2, H-6, 6H), 3.78 (s, OMe, H-2, H-6, 5H), 2.83- 2.74 (m, CH-Me, H-4, 2H), 2.61-2.57 (m, H-2', 1H), 2.51-2.28 (m, H-2', 1H), 1.83-1.68 (m, H-3, 2H), 1.48-1.37 (m, H-5, H-1', 4H), 1.30-1.20 (m, 2x $CO_2CH_2C\mathbf{H}_3$, Me, 9H)

^{13}C-NMR (100 MHz, $CDCl_3$) δ/ppm 173.8, 158.6, 155.9, 137.9, 127.6 (CH_{Ar}), 113.9 (CH_{Ar}), 61.3 ($CO_2\mathbf{C}H_2CH_3$), 60.4 (C-2, C-6), 55.4 (OMe), 54.0 (C-4), 44.9 (C-H-Me), 40.8 (C-3), 36.6 (C-2'), 32.2 (C-1'), 25.1 (Me), 19.1 (C-5), 14.7 (2, $CO_2CH_2\mathbf{C}H_3$)

LC/MS *m/z*: 407.6 $[M+H]^+$, 2.16 min.

Ethyl (4a*R*,8a*S*)-2-oxooctahydro-1,6-naphthyridine-6(2*H*)-carboxylate (145-1a)



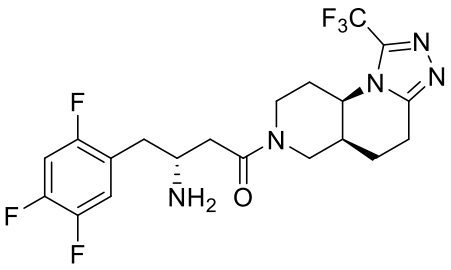
To amine (600 mg, 1.5 mmol, 1.0 eq.) in ethanol was added ammoniumformate (400 mg, 6.3 mmol, 4.2 eq.) and Pd/C (small spatula) and heated to 50°C for 8h. The reaction mixture was filtered over celite and the filtrate was evaporated under reduced pressure. The crude product was purified by flash chromatography (ethyl actetate/ petrol ether 10:1 +10 % methanol) to yield lactam **145-1a** (150 mg, 51%) as colorless oil.

^{1}H-NMR (400 MHz, $CDCl_3$) δ/ppm 4.50 (dt, *J*= 4.9, 12.0 Hz, 1H), 4.35 (bs, 2H), 4.19-4.10 (m, 2H), 3.64-3.55 (m, 1H), 3.34 (dd, *J*= 6.0, 17.0 Hz, 1H), 3.14 (bs, 1H), 3.07-2.87 (m, 2H), 2.33-2.24 (m, 2H), 2.14-2.06 (m, 2H), 2.00 (bs, 1H), 1.89-1.76 (m, 2H), 1.27 (t, *J*= 7.0 Hz, 3H)

LC/MS *m/z*: 268.2 $[M+H]^+$, 2.92 min.

All spectra were compared with previous compounds **145-1** and **170-1**.

(*R*)-3-amino-1-((5a*R*,9a*S*)-1-(trifluoromethyl)-4,5,5a,8,9,9a-hexahydro-[1,2,4]triazolo[4,3-a][1,6]naphthyridin-7(6*H*)-yl)-4-(2,4,5-trifluorophenyl)butan-1-one hydrochloride (249)



Procedure will be found in section 11.8 and all spectra were compared.

^{1}H-NMR (400 MHz, $MeOD_4$) δ/ppm 7.46-7.36 (m, 1H), 7.27-7.18 (m, 1H), 4.68 (t, *J*= 17.5 Hz, 1H), 4.01 (dd, *J*= 15.7, 30.6 Hz, 1H), 3.86 (bs, 1H), 3.76-3.50 (m, 1H), 3.39-3.25 (m, 2H), 3.22-3.07 (m, 3H), 2.92-2.81 (m, 3H), 2.49 (m, 1H), 2.18-2.10 (m, 2H), 2.02-1.94 (m, 2H)

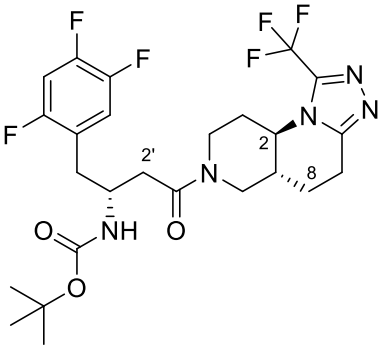
LC/MS *m/z*: 462.2 $[M+H]^+$, 2.02 min.

10.8 Synthesis of Sitagliptin analogues

General procedure for amide coupling

To a solution of amine **194-1/ 194-2** (0.33 mmol, 1.0 eq.) in DMF (1 mL) was added (*R*)-3-((*tert*-butoxycarbonyl)amino)-4-(2,4,5-trifluorophenyl)butanoic acid (**270**)/ (*R*)-3-((*tert*-butoxycarbonyl)amino)-4-phenylbutanoic acid (**271**) (0.34 mmol, 1.05 eq), EDCI (0.38 mmol, 1.2 eq) and HOBt (0.38 mmol, 1.2 eq.) and the mixture was stirred at rt overnight. The reaction mixture was diluted with ethyl acetate (20 mL) and saturated aqueous $NaHCO_3$ (20 mL). The water phase was extracted with ethyl acetate (3 x 20 mL). The combined organic phases were washed with saturated aqueous sodiumchloride (20 mL), dried over Na_2SO_4, filtered and the crude product was purified by flash chromatography (dichloromethane/ methanol: 10:1) to yield amide **288-307, 314**. All compounds are still consisting of a mixture of diastereoisomers.

***tert*-Butyl ((2*R*)-4-oxo-4-(1-(trifluoromethyl)-4,5,5a,8,9,9a-hexahydro-[1,2,4]triazolo[4,3-a][1,6]naphthyridin-7(6*H*)-yl)-1-(2,4,5-trifluorophenyl)butan-2-yl)carbamate (303** and **290)**



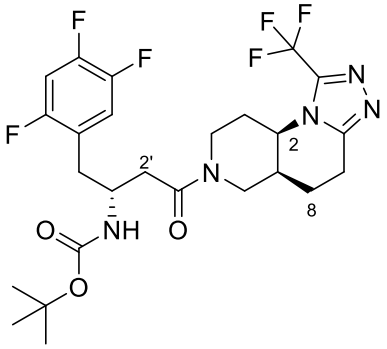
1 .isomer (**303**) (91%)

HPLC (t_R= 11.17 min, 100%)

^{1}H-NMR (400 MHz, $CDCl_3$) δ/ppm 7.06 (m, CH_{Ar}, 1H), 6.88 (m, CH_{Ar}, 1H), 5.33 (m, NH, 1H), 4.87 (m, H-2, 1H), 4.01 (m, H-3', H-6, 2H), 3.91 (dt, *J*= 4.1, 11.3 Hz, H-4, 2H), 3.33 (m, H-6, 1H), 3.22 (m, H-9, 1H), 2.99-2.93. (m, H-2', H-9, 3H), 2.74-2.46 (m, H-4', H-7, H-3, 4H), 2.07-1.63 (m, H-3, H-8, 3H), 1.35 (s, Boc, 9H)

^{13}C-NMR (100 MHz, $CDCl_3$) δ/ppm 169.2, 157.4, 155.4, 154.9, 154.6, 150.0 (3), 147.9 (2), 147.6 (2), 145.5 (2), 143.3, 142.9, 122.0, 121.7, 120.3, 119.3, 119.1, 105.6 (2), 105.3 (2), 79.6 (Boc), 60.8 (2) (C-3'), 49.3 (C-4), 48.4 (C-4), 45.2 (C-2), 44.2 (2), 41.5 (2) (C-7), 40.8 (2) (C-6), 40.2 (C-6), 36.5 (C-2'), 33.1 (C-4'), 31.3 (C-3), 30.5 (C-3), 28.3 (Boc), 23.6 (C-8), 22.7 (2) (C-9)

HRMS *m/z*: $C_{25}H_{30}N_5F_6O_3$ calculated 562.2247 $[M+H]^+$, found 562.2310, calculated 506.1621 $[M-t\text{Bu}]^+$, found 506.1642, calculated 462.1723 $[M\text{-Boc}]^+$, found 462.1769.



2.isomer (**290**) (77 %)

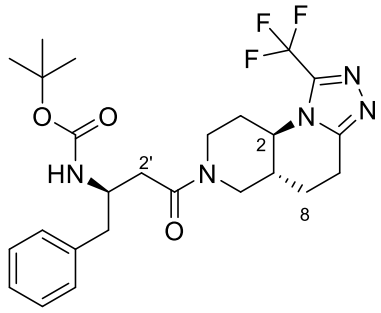
HPLC (t_R=11.20 min, 100%)

^{1}H-NMR (400 MHz, $CDCl_3$) δ/ppm 7.03 (m, CH_{Ar}, 1H), 6.85 (m, CH_{Ar}, 1H), 5.42 (dt, *J*= 8.3, 40.3 Hz, NH, 1H), 4.84-4.75 (m, H-3', 1H), 4.51 (m, H-2, 1H), 4.11-4.01 (m, H-4 or H-6, 1H), 3.97-3.86 (m, H-4 or H-6, 1H), 3.40 (m, H-4 or H-6, 1H), 3.28-3.11 (m, H-4 or H-6, 1H), 2.97-2.84 (m, H-9, H-4', 4H), 2.72-2.47 (m, H-2', 2H), 2.31 (bs, H-7, 1H), 2.14 (m, H-3, 1H), 2.02-1.72 (m, H-8, H-3, 3H), 1.34-1.31 (2m, Boc, 9H),

^{13}C-NMR (100 MHz, $CDCl_3$) δ/ppm 169.2, 155.4, 152.9, 152.5, 142.8, 119.3, 119.1, 117.7, 105.7, 105.5, 105.3, 79.7, 54.2, 48.8 (3), 48.4, 44.8, 44.2, 40.1 (2), 36.7, 36.1, 33.8 (2), 33.7 (2), 33.5, 33.0, 31.1, 29.7, 28.4, 21.1, 20.9, 19.1, 18.9

HRMS *m/z*: $C_{25}H_{30}N_5F_6O_3$ calculated 562.2247 $[M+H]^+$ found 562.2108, calculated 506.1621 $[M-t\text{Bu}]^+$, found 506.1627, calculated 462.1723 $[M\text{-Boc}]^+$, found 462.1449.

***tert*-Butyl ((2*R*)-4-oxo-1-phenyl-4-(1-(trifluoromethyl)-4,5,5a,8,9,9a-hexahydro-[1,2,4]triazolo[4,3-a][1,6]naphthyridin-7(6*H*)-yl)butan-2-yl)carbamate (307** and **302)**



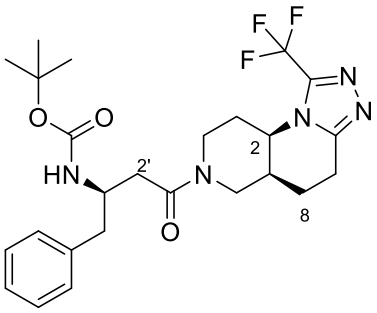
1.isomer (**307**) (75%)

HPLC (t_R= 10.53 min, 100%)

^{1}H-NMR (400 MHz, $CDCl_3$) δ/ppm 7.25-7.14 (m, Ph, 5H), 5.44-5.20 (m, NH, 1H), 4.80 (t, *J*= 16.8 Hz, H-2, 1H), 4.12-4.05 (m, H-3', 1H), 3.93-3.76 (m, H-4, H-6, 2H), 3.28-3.06 (m, H-4 or H-6, H-9, 2H), 3.00-2.75 (m, H-2', H-9, H-4 or H-6, H-4', 5H), 2.61-2.40 (m, H-3, H-7, H-4', 3H), 2.03-1.50 (m, H-8, H-3, 3H), 1.35, 1.34 (2s, Boc, 9H)

^{13}C-NMR (100 MHz, $CDCl_3$) δ/ppm 169.6, 155.5, 154.9, 138.2 (4), 129.4, 129.2, 128.5, 128.4, 126.6, 126.4, 79.4 (Boc), 60.7 (4-C-2), 49.3 (2- C-4 or C-6), 45.2 (2- C-3'), 44.2 (2-C-6 or C-4), 41.3 (C-4' or C-2'), 40.8 (C-7), 40.5 (C-4' or C-2'), 40.3 (C-2), 40.1 (C-3), 28.3 (Boc), 23.4 (C-8), 23.3 (C-8), 22.7 (C-9), 22.6 (C-9)

HRMS *m/z*: $C_{25}H_{32}N_5F_3O_3$ calculated 508.2530 $[M+H]^+$, found 508.2567, calculated 452.1965 $[M-tBu]^+$, found 452.1946, calculated 408.2006 $[M-Boc]^+$, found 408.2015.



2.isomer (**302**) (80%)

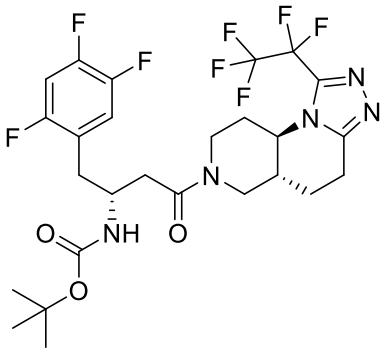
HPLC (t_R=10.50 min, 100%)

^{1}H-NMR (400 MHz, $CDCl_3$) δ/ppm 7.26-7.16 (m, Ph, 5H), 5.49 (m, NH, 0.5 H), 5.4 (m, NH, 0.5 H), 4.83-4.73 (m, H-3' 1H), 4.51-4.44 (m, H-2, 1H), 4.15-4.05 (m, H-4 or H-6, 1H), 3.89-3.67 (m, H-4 or H-6, 1H), 3.32-2.78 (m, H-4, H-6, H-3, H-9, H-4', H-2',7H), 2.64-2.40 (m, H-7, H-4' or H-2', 2H), 2.40-2.13 (m, H-3, H-8, 3H), 1.54-1.34 (m, Boc, 9H),

^{13}C-NMR (100 MHz, $CDCl_3$) δ/ppm 170.4, 155.5, 138.2, 129.4 (3), 128.6 (3), 126.6 (4-CH-Ph), 79.4 (Boc), 54.1 (C-2), 48.7 (2- C-4 or C-6), 44.7 (2- C-4 or C-6), 44.1 (2-C-3'), 40.1 (C-2' or C-4'), 39.9 (C-2' or C-4'), 33.8 (C-7), 33.6 (2- C-3), 28.4 (Boc), 20.9 (2-C-9),18.8 (2-C-8)

HRMS *m/z*: $C_{25}H_{32}N_5F_3O_3$ calculated 508.2530 $[M+H]^+$, found 508.2540, calculated 452.1904 $[M-tBu]^+$, found 452.1946.

***tert*-Butyl ((2*R*)-4-oxo-4-(1-(perfluoroethyl)-4,5,5a,8,9,9a-hexahydro-[1,2,4]triazolo[4,3-a][1,6]naphthyridin-7(6*H*)-yl)-1-(2,4,5-trifluorophenyl)butan-2-yl)carbamate (258** and **271**)



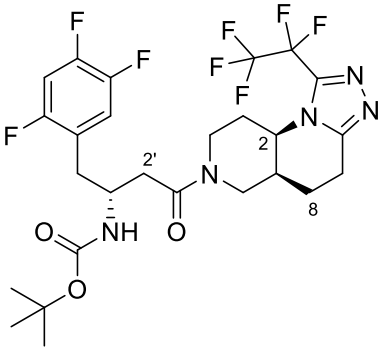
1. isomer (**304**) (99 %)

HPLC (t_R =19.43 min, 90 %)

^{1}H-NMR (400 MHz, $CDCl_3$) δ/ppm 7.06 (m, 1H), 6.88 (m, 1H), 5.38 (m, 1H), 4.87 (m, 1H), 4.10 (m, 1H), 4.01 (m, 1H), 3.35-3.25 (m, 2H), 3.03-2.87 (m, 5H), 2.75-2.45 (m, 3H), 2.08-1.94 (m, 1H), 1.85-1.60 (m, 3H), 1.40-1.32 (m, 9H),

LC/MS 612.3 $[M+H]^+$, 2.92 min.

2. isomer (**291**) (98 %)



HPLC (t_R =18.85 min) (98 %)

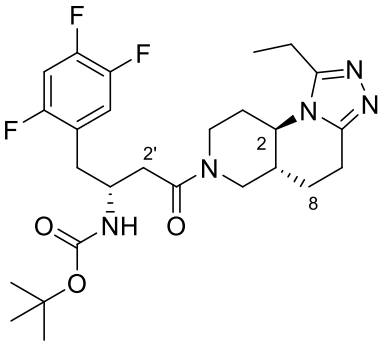
^{1}H-NMR (400 MHz, $CDCl_3$) δ/ppm 7.05 (m, CH_{Ar}, 1H), 6.85 (m, CH_{Ar}, 1H), 5.65-5.20 (m, NH, 1H), 4.86-4.73 (m, C-3', 0.5H), 4.59-4.48 (m, C-2, 0.5H), 4.44-4.24 (m, C-2, 0.5H), 4.17- 4.01 (m, H-3', H-4 or H-6, 1.5H), 3.96-3.84 (m, H-4 or H-6, 1H), 3.41 (m, H-4, H-6, 2H), 3.09-2.75 (m, H-9, H-4', H-6', 6H), 2.72-2.43 (m, H-3, 1H), 2.36-2.16 (m, H-7, 1H), 2.11-1.77 (m, H-8, H-3, 2H), 1.38-1.30 (m, Boc, 9H)

^{13}C-NMR (100 MHz, $CDCl_3$) δ/ppm 169.8, 169.6, 155.4, 155.0, 153.2, 152.8, 150.1, 147.6 (3), 141.6, 119. 5(m CH_{Ar}), 105.6 (m, CH_{Ar}), 79.6 (Boc), 54.6 (C-2), 48.7 (2-C-4 or C-6), 44.8 (C-3'), 44.2 (2- C-4 or C-6), 40.1 (2- C-4' or C-2'), 36.8 (C-4' or C-2'), 33.7 (3-C-3), 29.8 (C-7), 29.0 (Boc), 28.3 (Boc), 20.9 (2-C-9), 18.6 (C-8)

HRMS *m/z* $C_{26}H_{28}F_8N_5O_3$ calculated 612.2215 $[M+H]^+$, found 612.2228, calculated 556.1589 $[M-t\text{Bu}]^+$, found 556.1579, calculated 512.1691 $[M\text{-Boc}]^+$, found 512.1726.

***tert*-Butyl ((2*R*)-4-(1-ethyl-4,5,5a,8,9,9a-hexahydro-[1,2,4]triazolo[4,3-a][1,6]naphthyridin-7(6*H*)-yl)-4-oxo-1-(2,4,5-trifluorophenyl)butan-2-yl)carbamate (293** and **305**)

1.isomer **(305)** (60 %)



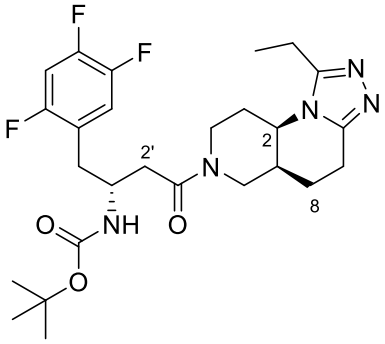
^{1}H-NMR (400 MHz, $CDCl_3$) δ/ppm 6.99 (m, CH_{Ar}, 1H), 6.80 (m, CH_{Ar}, 1H), 5.54 (m, NH, 1H), 4.73 (2d, *J*= 14.0, 15.2 Hz, H-2, 1H), 4.03-3.83 (m, H-3', H-6, 2H), 3.69 (dt, *J*= 3.5, 11.2 Hz, H-4, 1H), 3.22- 3.06 (m, H-4, H-9, 2H), 2.94-2.37 (m, H-9, H-7, C**H**$_2$CH$_3$, H-4', H-2', 8H), 1.92 (m, H-3, 1H), 1.75-1.40 (m, H-8, H-3, 3H), 1.26 (m, Boc, $CH_2C\mathbf{H}_3$, 12H)

^{13}C-NMR (100 MHz, $CDCl_3$) δ/ ppm 169.1, 157.4, 155.4, 154.9, 154.6, 154.4, 151.8 (2), 150.0, 147.6 (2), 143.2, 122.2 (2), 119.0 (m, CH_{Ar}), 105.3 (m, CH_{Ar}), 79.4 (Boc), 59.2 (2-C-

4), 49.4 (2-C-6), 48.2 (C-2), 45.2 (C-3'), 44.0 (C-4'), 41.4 (C-2'), 40.8 (C-3), 40.0 (**C**H_2CH_3), 33.0, 31.0 , 30.2 (Boc), 28.2 (Boc), 24.3 (C-8), 22.6, 21.2 (C-9), 11.4 (CH_2**C**H_3)

HRMS *m/z*: $C_{26}H_{34}N_5F_3O_3$ calculated 522.2687 $[M+H]^+$, found 522.4608.

2.isomer (**279**) (31 %)



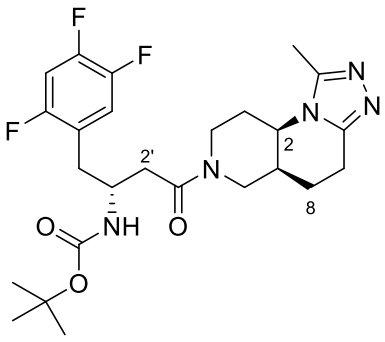
^{1}H-NMR (400 MHz, $CDCl_3$) δ/ppm 7.05-6.97 (m, CH_{Ar}, 1H), 6.87- 6.79 (m, CH_{Ar}, 1H), 5.60-5.43 (ddd, *J*= 9.9, 13.4, 37.4 Hz, NH, 1H), 4.76 (d, *J*= 14.2 Hz, H-3', 0.5H), 4.70 (d, *J*= 14.2 Hz, H-3', 0.5 H), 4.20 (m, H-2, 1H), 4.07 (m, H-4 or H-6, 1H), 3.89 (m, H-4 or H-6, 1H), 3.37 (m, H-4 or H-6, 0.5 H), 3.16 (m, H-9, H-4 or H-6, 1.5H), 2.95-2.73 (m, H-9, C**H**$_2$CH$_3$, 3H), 2.70-2.49 (m, H-2', H-4', 5H), 2.20 (m, H-7, 1H), 1.97-1.59 (m, H-3, H-8, 4H), 1.36 (t, *J*= 7.9 Hz, CH_2C**H**$_3$, 3H), 1.30, 1.28 (2s, Boc, 9H)

^{13}C-NMR (100 MHz, $CDCl_3$) δ/ppm 169.6, 169.5, 157.4 (2), 155.4, 155.0, 154.9, 153.6(2), 150.0, 149.7, 149.4, 119.1 (m, CH_{Ar}), 105.3 (m, CH_{Ar}), 79.4 (Boc), 51.8 (C-2), 48.9 (C-4), 45.0 (C-3'), 44.0 (C-6), 39.9 (C-4'), 34.1 (2) (C-7), 33.9 (2) (C-2'), 32.8 (**C**H_2CH_3) , 29.1 (Boc), 28.3 (Boc), 21.0 (C-9), 20.9 (C-8), 18.2 (C-4'), 11.4 (2, CH_2**C**H_3)

HRMS *m/z*: $C_{26}H_{34}N_5F_3O_3$ calculated 522.2687 $[M+H]^+$, found 522.2607, calculated 466.2061 $[M-t\text{Bu}]^+$, found 466.1626.

***tert*-Butyl ((*R*)-4-((5a*S*,9a*R*)-1-methyl-4,5,5a,8,9,9a-hexahydro-[1,2,4]triazolo[4,3-a][1,6]naphthyridin-7(6*H*)-yl)-4-oxo-1-(2,4,5-trifluorophenyl)butan-2-yl)carbamate (292)**

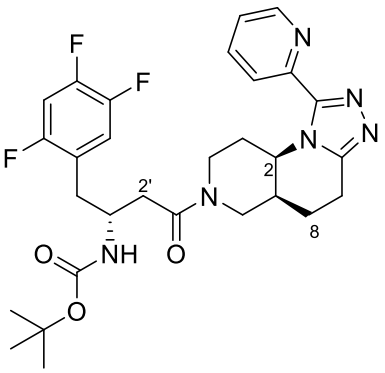
(45 %)



^{1}H-NMR (400 MHz, $MeOD_4$) δ/ppm 7.22-7.16 (m, CH_{Ar}, 1H), 7.14-7.04 (m, CH_{Ar}, 1H), 6.68-6.56 (m, 1H), 4.72 (t, *J*= 13.8 Hz, 0.5H), 4.63 (m, 0.5H), 4.54-4.46 (m, 1H), 4.23-4.01 (m, 2H), 3.56-3.48 (m, 0.5H), 3.35-3.24 (m, 3H), 3.14-2.47 (m, 6H), 2.44 (s, Me, 3H), 2.35-2.27 (m, 1H), 2.14-1.63 (m, 3H), 1.34-1.24 (3s, Boc, 9H)

HRMS *m/z*: $C_{25}H_{33}N_5F_3O_3$ calculated 508.2530 $[M+H]^+$, found 508.3067.

***tert*-butyl ((*R*)-4-oxo-4-((5a*S*,9a*R*)-1-(pyridin-2-yl)-4,5,5a,8,9,9a-hexahydro-[1,2,4]triazolo[4,3-a][1,6]naphthyridin-7(6*H*)-yl)-1-(2,4,5-trifluorophenyl)butan-2-yl)carbamate (298)**



(37 %)

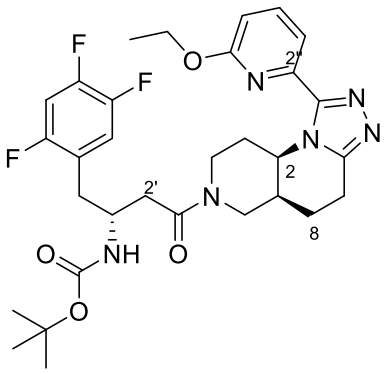
^{1}H-NMR (400 MHz, $CDCl_3$) δ/ppm 8.60-8.57 (m, CH-pyridine, 1H), 8.29 (d, *J*= 7.9 Hz, CH-pyridine, 1H), 7.79 (dt, *J*= 1.3, 7.8 Hz, CH-pyridine, 1H), 7.32-7.28 (m, CH-pyridine, 1H), 7.08-7.00 (m, CH_{Ar}, 1H), 6.89-6.80 (m, CH_{Ar}, 1H), 5.60-5.40 (m, H-2, NH, 2H), 4.83 (d, *J*= 14.0 Hz, H-4 or H-6, 0.5 H), 4.72-4.65 (m, H-4 or H-6, 0.5H), 4.13-4.01 (m, H-3', 1H), 3.92 (t, *J*= 15.1 Hz, H-4 or H-6, 0.5H), 3.83-3.76 (m, H-4 or H-6, 0.5H), 3.47-3.41 (m, H-4 or H-6, 0.5H), 3.34-3.23 (m, H-9, 1H), 3.15 (dt, *J*= 2.7, 13.0 Hz, H-4 or H-6, 0.5H), 3.03-2.85 (m, H-9, H-2' or H-4', H-4 or H-6, 4H), 2.70-2.47 (m, H-2' or H-4', H-3, 3H), 2.40-2.32 (m, H-7, 1H), 2.27-2.15 (m, H-3, 1H), 2.10-1.91 (m, H-8, 1H), 1.66-1.48 (m, H-8, 1H), 1.35-1.33 (m, Boc, 9H)

^{13}C-NMR (100 MHz, $CDCl_3$) δ/ppm 169.6, 169.4, 157.6, 155.4, 155.0, 151.9, 151.6, 150.4, 150.1, 148.8 (2-CH-pyridine), 148.1 (2-CH-pyridine), 147.8, 147.7, 145.4, 137.2 (CH-pyridine), 124.0 (2-CH-pyridine), 123.3 (CH-pyridine), 119.3 (4- CH_{Ar}), 105.4 (4-CH_{Ar}), 79.5 (Boc), 54.2 (C-2), 49.3 (C-4 or C-6), 49.1 (C-4 or C-6), 48.5 (C-3'), 44.5 (2-C-4 or C-6), 40.5 (2-C-4 or C-6), 34.3 (C-2' or C-4'), 34.2 (C-2' or C-4'), 34.1 (C-7), 34.0 (C-7), 33.4 (C-2' or C-4'), 33.1 (2- C-2' or C-4'), 29.4 (C-3), 28.3 (Boc), 21.6 (C-9), 21.5 (C-9), 19.6 (C-8), 19.4 (C-8)

LC/MS *m/z*: 571.2 $[M+H]^+$, 2.53 min.

***tert*-Butyl ((*R*)-4-((5a*S*,9a*R*)-1-(6-ethoxypyridin-2-yl)-4,5,5a,8,9,9a-hexahydro-[1,2,4]triazolo[4,3-a][1,6]naphthyridin-7(6*H*)-yl)-4-oxo-1-(2,4,5-trifluorophenyl)butan-2-yl)carbamate (300)**

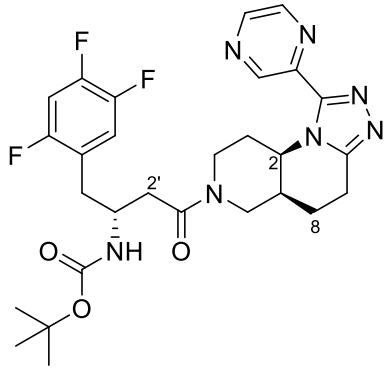
(50 %)



<u>^{1}H-NMR (400 MHz, $CDCl_3$)</u> δ/ppm 8.07-7.95 (m, CH-pyridine, 1H), 7.82-7.72 (m, CH-pyridine, 1H), 7.61-7.51 (m, CH-pyridine, 0.5H), 7.50-7.40 (m, CH-pyridine, 0.5H), 7.13-7.02 (m, CH_{Ar}, 1H), 6.98-6.86 (m, CH_{Ar}, 1H), 5.70-5.34 (m, 1H), 5.00-4.75 (m, 1H), 4.43-4.33 (m, 1H), 4.29-4.22 (m, 0.5H), 4.14-3.87 (m, 1.5H), 3.61-3.45 (m, 3H), 3.16-2.82 (m, 6H), 2.74-2.41 (m, 2H), 2.38-2.26 (m, 1H), 2.16-1.90 (m, 2H), 1.81-1.69 (m, 1H), 1.48-1.30 (m, 12H)

<u>LC/MS</u> *m/z*: 615.3 $[M+H]^+$, 2.88 min.

***tert*-butyl ((*R*)-4-oxo-4-((5a*S*,9a*R*)-1-(pyrazin-2-yl)-4,5,5a,8,9,9a-hexahydro-[1,2,4]triazolo[4,3-a][1,6]naphthyridin-7(6*H*)-yl)-1-(2,4,5-trifluorophenyl)butan-2-yl)carbamate (299)**



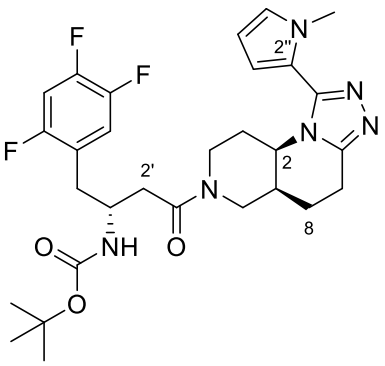
(44 %)

<u>^{1}H-NMR (400 MHz, $CDCl_3$)</u> δ/ppm 8.68 (m, 1H, CH_{Ar}, 1H), 7.80 (dd, *J*= 9.4 Hz, CH_{Ar}, 1H), 7.43 (m, CH_{Ar}, 1H), 7.09-7.01 (m, CH_{Ar}, 1H), 6.90-6.86 (m, CH_{Ar}, 1H), 5.51 (m, H-2, 1H), 4.86 (d, *J*= 12.5 Hz, H-4 or H-6, 0.5H), 4.75 (m, H-4 or H-6, 0.5H), 4.15-3.35 (m, H-2, H-4, H-6, H-3', H-9, 6H), 3.19-3.10 (m, H-9, 1H), 2.97-2.80 (m, H-2', H-3, NH, 5H), 2.70-2.48 (m, H-7, H-4', 3H), 2.14-1.89 (m, H-8, 2H), 1.35-1.31 (m, *t*-Bu, 9H)

<u>^{13}C-NMR (100 MHz, $CDCl_3$)</u> δ/ppm 173.6, 159.9, 157.3, 155.3, 145.8, 145.3, 145.2, 143.3, 142.8, 128.7, 127.0, 126.8, 119.2, 117.0, 111.6, 105.7, 105.4, 105.3, 79.8 (**C**$(CH_3)_3$), 55.9 (C-2), 55.1 (C-2), 49.1, 48.9, 47.7, 45.0, 44.3, 37.8, 36.6, 35.5, 33.6, 33.2, 29.4, 28.4, 25.4, 21.2 (2), 18.8, 18.6

<u>HRMS</u> *m/z*: $C_{28}H_{33}N_7F_3O_3$ calculated 572.2591 $[M+H]^+$, found 572.2415.

***tert*-butyl ((*R*)-4-((5a*S*,9a*R*)-1-(1-methyl-1H-pyrrol-2-yl)-4,5,5a,8,9,9a-hexahydro-[1,2,4]triazolo[4,3-a][1,6]naphthyridin-7(6*H*)-yl)-4-oxo-1-(2,4,5-trifluorophenyl)butan-2-yl)carbamate (301)**

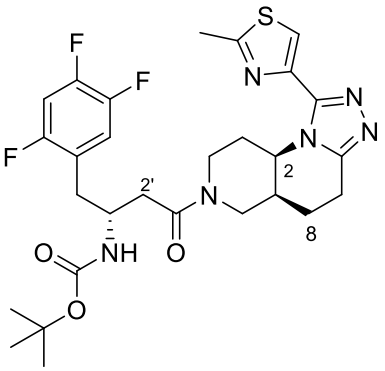


(42 %)

<u>^{1}H-NMR (400 MHz, CDCl$_3$)</u> δ/ppm 7.08-7.00 (m, CH_{Ar}, 1H), 6.92-6.84 (m, CH_{Ar}, 1H), 6.80 (s, CH-pyrrol), 6.44 (s, CH-pyrrol, 1H), 6.23-6.20 (m, CH-pyrrol, 1H), 5.54-5.32 (m, 1H), 4.08 (d, *J*= 14.1 Hz, 0.5H), 4.62 (d, *J*= 13.4 Hz, 0.5H), 4.56-4.51 (m, 1H), 4.13-3.99 (m, 1H), 3.99 (t, *J*= 16.6 Hz, 0.5H), 3.79 (s, Me, 3H), 3.75-3.69 (m, 0.5H), 3.42-3.34 (m, 0.5H), 3.31-3.19 (m, 1H), 3.02-2.83 (m, 4H), 2.72-2.42 (m, 3H), 2.39-2.31 (m, 1H), 2.02-1.85 (m, 2H), 1.77-1.73 (m, 1H), 1.62-1.49 (m, 1H), 1.36-1.31 (4s, Boc, 9H)

<u>LC/MS</u> *m/z*: 573.3 $[M+H]^+$, 2.53 min.

***tert*-butyl ((*R*)-4-((5a*S*,9a*R*)-1-(2-methylthiazol-4-yl)-4,5,5a,8,9,9a-hexahydro-[1,2,4]triazolo[4,3-a][1,6]naphthyridin-7(6*H*)-yl)-4-oxo-1-(2,4,5-trifluorophenyl)butan-2-yl)carbamate (295)**

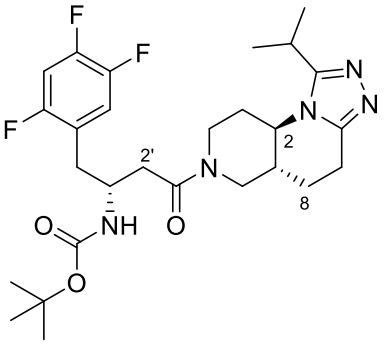


(69 %)

<u>^{1}H-NMR (400 MHz, CDCl$_3$)</u> δ/ppm 8.01 (s, CH-thiazole, 0.5H), 7.97 (s, CH-thiazole, 0.5H), 7.07-6.99 (m, CH_{Ar}, 1H), 6.90-6.81 (m, CH_{Ar}, 1H), 5.62-5.40 (m, 1H), 5.33-5.24 (m, 1H), 4.81-4.64 (m, 0.5H), 4.14 (bm, 1H), 3.98-3.77 (m, 0.5H), 3.46-3.04 (3t, 1H), 2.98-2.82 (m, 6H), 2.74 (s, Me, 3H), 2.67-2.45 (m, 2H), 2.33 (m, 1H), 2.21-2.09 (m, 1H), 2.06-1.74 (m, 1H), 1.67-1.49 (m, 1H), 1.34-1.30 (2s, Boc, 9H)

<u>HRMS</u> *m/z*: $C_{28}H_{34}N_6F_3O_3S$ calculated 591.2360 $[M+H]^+$, found 591.2156.

***tert*-butyl ((2*R*)-4-(1-isopropyl-4,5,5a,8,9,9a-hexahydro-[1,2,4]triazolo[4,3-a][1,6]naphthyridin-7(6*H*)-yl)-4-oxo-1-(2,4,5-trifluorophenyl)butan-2-yl)carbamate (306** and **294)**

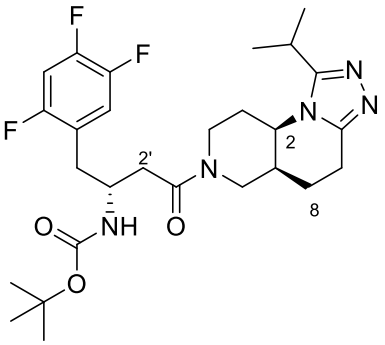


1.isomer (**306**) (77 %)

^{1}H-NMR (400 MHz, $CDCl_3$) δ/ppm 7.10-7.04 (m, CH_{Ar}, 1H), 6.92-6.86 (m, CH_{Ar}, 1H), 5.48-5.42 (m, NH, 1H), 4.82 (dd, *J*= 13.2, 29.9 Hz, H-2, 1H), 4.14-3.93 (m, H-6, 1H), 3.79 (dt, *J*= 3.0, 10.9 Hz, H-4, 1H), 3.27-3.16 (m, H-9, 1H), 3.12-2.46, m, H-2', H-4, H-6, CH-*i*Pr, H-4', H-9, 9H), 2.00-1.87 (m, H-8, 1H), 1.84-1.67 (m, H-3, 2H), 1.64-1.51 (m, H-8, 1H), 1.45, 1.43 (2s, *i*Pr, 3H), 1.35 (s, Boc, 9H), 1.33, 1.32 (2s, *i*Pr, 3H)

^{13}C-NMR (100 MHz, $CDCl_3$) δ/ppm 169.2, 158.5, 158.4, 157.5, 155.4, 155.0, 151.7, 151.5, 150.1 (3), 147.8 (2), 147.5, 145.5, 143.3, 128.7, 126.5, 124.4, 122.0, 121.8, 119.3 (C-16), 119. 0 (C-16), 105.6 (C-18), 105.4 (2-C-18), 105.1 (C-18), 79.6 (Boc), 59.7 (C-4), 59.5 (C-4), 49.5 (C-6), 48.4 (C-12), 45.5 (C-7), 44.3 (2, C-6, C-12), 41.8 (2-C-12), 41.2 (C-3), 41.1 (C-3), 36.6 (2, C-11), 33.2 (C-13), 31.4 (2, C-3), 28.4 (Boc), 27.0, 24.3 (C-8), 22.8 (C-9), 21.5 (*i*Pr), 21.2 (*i*Pr)

HRMS *m/z*: $C_{27}H_{37}N_5F_3O_3$ calculated 536.2843 $[M+H]^+$, found 536.2926.



2.isomer (**294**) (64 %)

^{1}H-NMR (400 MHz, $CDCl_3$) δ/ppm 7.07-7.00 (m, CH_{Ar}), 6.89 (m, CH_{Ar}, 1H), 5.56-5.37 (m NH, 1H), 4.82-4.72 (m, H-3', 1H), 4.24-4.20 (m, H-2, 1H), 4.10 (bs, H-6, 1H), 4.00-3.89 (m, H-4, 1H), 3.38 (dt, H-4, 0.5H), 3.17-3.08 (m, H-9, H-4, 1.5H), 2.97-2.80 (m, H-2', C**H**-iPr, H-6, 4H), 2.71-2.47 (m, H-4', H-9, 3H), 2.23 (bs, H-7, 1H), 1.99-1.62 (m, H-8, H-3, 4H), 1.42-1.39 (m, C**H**$_3$iPr, 3H), 1.32-1.30 (m, C**H**$_3$iPr, Boc, 12H)

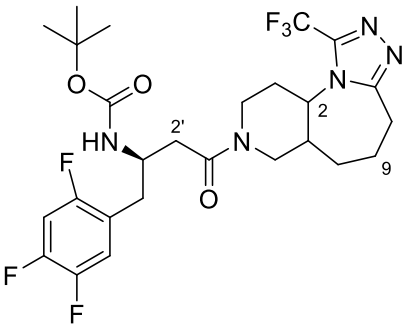
^{13}CNMR(100MHz,$CDCl_3$)δ/ppm169.7, 157.7 (2), 157.4, 155.0, 149.4, 149.1, 147.9, 147.7

(2), 145.4, 143.2, 128.6, 126.5, 124.4, 121.8, 119.2 (m, CH_{Ar}), 112.1, 110.3, 105.1 (m, CH_{Ar}), 79.6 (Boc), 52.1 (2-C-2), 49.2 (2-C-4), 48.4 (C-4), 45.1 (C-6), 44.2 (C-6), 44.1 (C-6), 40.1

(2), 34.0 (2-C-4'), 33.9 (C-7), 33.8 (C-3'), 28.9 (C-3), 26.4 (Boc), 24.5 (CH-*i*Pr), 21.7 (*i*Pr), 21.2 (*i*Pr), 19.6 (C-9), 19.4 (C-8)

HRMS *m/z*: $C_{27}H_{37}N_5F_3O_3$ calculated 536.2843 $[M+H]^+$, found 536.2856.

***tert*-butyl ((2*R*)-4-oxo-1-phenyl-4-(1-(trifluoromethyl)-5,6,6a,9,10,10a-hexahydro-4*H*-pyrido[3,4-f][1,2,4]triazolo[4,3-a]azepin-8(7*H*)-yl)butan-2-yl)carbamate (289)**

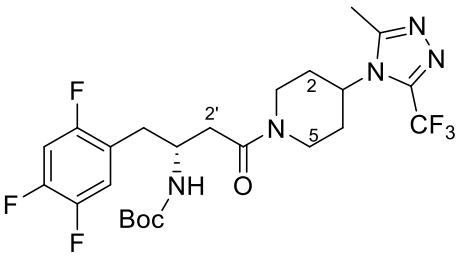


(45 %)

^{1}H-NMR (400 MHz, $CDCl_3$) δ/ppm 7.11-7.01 (m, 1H), 6.93-6.84 (m, 1H), 5.81 (m, 0.5H), 5.55-5.27 (m, 1H), 5.11-5.03 (m, 0.5H), 4.89-4.73 (m, 1H), 4.53-4.47 (m, 0.5H), 4.18-3.74 (m, 3H), 3.56-3.14 (m, 2H), 3.03-3.84 (m, 2.5H), 2.75-2.41 (m, 4H), 2.34-2.15 (m, 2H), 2.09-1.95 (m, 2H), 1.81-1.73 (m, 1H), 1.38-1.33 (m, Boc, 9H)

LC/MS *m/z*: 576.2 $[M+H]^+$, 2.85 min.

***tert*-Butyl (*R*)-(4-(4-(3-methyl-5-(trifluoromethyl)-4*H*-1,2,4-triazol-4-yl)piperidin-1-yl)-4-oxo-1-(2,4,5-trifluorophenyl)butan-2-yl)carbamate (314)**



(93%)

^{1}H-NMR (400 MHz, $CDCl_3$) δ/ppm 7.08-6.99 (m, CH_{Ar}, 1H), 6.88-6.81 (m, CH_{Ar}, 1H), 5.52 (d, *J*= 9.0 Hz, NH, 0.5H), 5.42 (d, *J*= 9.1 Hz, NH, 0.5H), 4.86 (d, *J*= 14.0 Hz, H-1, 1H), 4.38-4.29 (m, H-3, 1H), 4.12-3.96 (m, H-3', H-5, 2H), 3.12 (dt, *J*= 3.1, 14.3 Hz, H-5, 1H), 2.90-2.82 (m, H-4', H-3, 3H), 2.69-2.49 (m, H-2', H-2, Me, 6H), 2.15-1.92 (m, H-6, 2H), 1.31 (s, Boc, 9H)

^{13}C-NMR (100 MHz, $CDCl_3$) δ/ppm 169.2, 169.0, 155.4, 153.9 (2), 144.6 (q, CF_3), 119.9 (m, CH_{Ar}), 105.3 (m, CH_{Ar}), 79.5 (Boc), 55.7 (C-3), 48.3 (C-3'), 45.0 (C-5), 41.0 (C-2), 37.2, 33.3 (2) (C-2'), 31.0 (2) (C-4'), 30.2 (C-6), 28.3(Boc), 13.4 (Me)

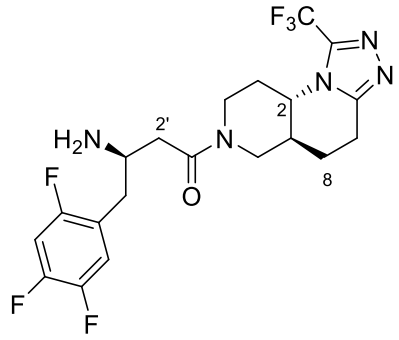
LCMS m/z 550.3 $[M+H]^+$, 2.84 min.

General method for deprotection

To amide (**288-289, 290-307, 314**) (0.08 mmol, 1 eq.) was added 4N HCl in dioxane (0.5 mL) and stirred at rt for 30 min. The HCl solution was evaporated under N_2 gas to yield HCl salt of amine (**315-335**) as oils.

(3*R*)-3-Amino-1-(1-(trifluoromethyl)-4,5,5a,8,9,9a-hexahydro-[1,2,4]triazolo[4,3-a][1,6]naphthyridin-7(6*H*)-yl)-4-(2,4,5-trifluorophenyl)butan-1-one hydrochloride (327 and **315)**

Compounds were separated using chiral HPLC using Diacel Chiralpak IC, 5 µm, 20x250 mm at 15 ml/min at 265 nm over 30 min. The solvents were *iso*-hexane containing 0.2% diethylamine and ethanol in a 30:70 ratio to give two separated compounds per isomer.



1.isomer (**267/268**)

A: <u>HPLC</u> (t_R= 7.87 min, 100%)

<u>^{1}H-NMR (400 MHz, MeOD$_4$)</u> δ/ppm 7.10-7.03 (m, CH_{Ar}, 1H), 6.93-6.87 (m, CH_{Ar}, 1H), 4.91-4.82 (m, H-3', 1H), 4.04 (2 d, *J*= 13.7, 14.8 Hz, H-2, 1H), 3.89 (dt, *J*= 3.8, 11.1 Hz, H-4, 1H), 3.56 (m, H-6, 1H), 3.36-3.29 (m, H-4, 1H), 3.23 -2.91 (m, H-2', H-9, H-6, 4H), 2.81-2.68 (m, H-4', H-2', 2H), 2.63-2.33 (m, H-7, H-4', 2H), 2.07-1.58 (m, H-3, H-8, 4H)

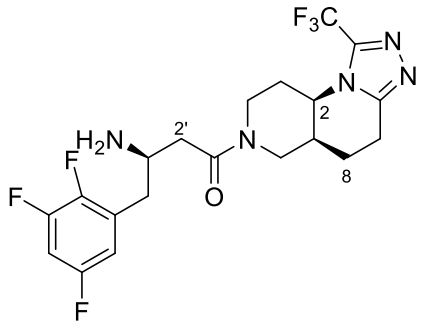
(267/268)

B: **<u>HPLC</u>** (t_R= 15.13 min, 100%)

<u>^{1}H-NMR (400 MHz, CDCl$_3$)</u> δ/ppm 7.11-7.03 (m, CH_{Ar}, 1H), 6.95-6.88 (m, CH_{Ar}, 1H), 4.93-4.83 (m, H-3', 1H), 4.07 (d, *J*= 14.0 Hz, H-2, 1H), 3.96-3.87 (m, H-4, 1H), 3.58-3.52 (m, H-6, 1H), 3.38-3.30 (m, H-4, 1H), 3.21 (dt, *J*= 2.5, 13.3 Hz, H-6, 1H), 3.05-2.91 (m, H-9, 2H), 2.82-2.74 (m, H-2',1H), 2.70-2.62 (m, H-2', H-4', 3H), 2.52- 2.35 (m, H-7, H-4', H-3, 3H), 2.08-1.97 (m, H-3, 1H), 1.83-1.58 (m, H-8, 2H)

<u>^{13}C-NMR (100 MHz, MeOD$_4$)</u> δ/ppm 169.8 (2), 169.7, 163.4, 159.2, 157.9, 156.8, 152.1 (2), 149.6, 149.3, 146.9, 144.5, 144.1, 120.5 (m, CH_{Ar}), 107.0 (m, CH_{Ar}) 73.5, 72.4, 63.1, 63.0, 62.1, 45.9, 44.7, 43.7, 41.2 (2), 40.6, 35.1 (2-C2'), 34.9 (2-C-3), 32.3, 31.3, 30.7, 22.7 (2, C-9), 22.6 (C-8)

LC/MS (A) m/z: 462.2 $[M+H]^+$ 1.95 min, (B) m/z: 462.2 $[M+H]^+$, 1.97 min.



2. isomer **(264/266**)

A: HPLC (t_R= 5.78 min, 100%)

^{1}H-NMR (400 MHz, $CDCl_3$) δ/ppm 7.10-7.03 (m, CH_{Ar}, 1H), 6.95-6.88 (m, CH_{Ar}, 1H), 4.87 (dd, *J*= 1.8, 14.8 Hz, H-3', 1H), 4.53 (dt, *J*= 4.8, 11.3 Hz, H-2, 1H), 3.94 (t, *J*= 15.0 Hz, H-6, 1H), 3.58-3.51 (m, H-4, 1H), 3.43-3.13 (m, H-4, H-6, 2H), 3.04-2.74 (m, H-9, 2H), 2.67-2.39 (m, H-2' or H-4', 2H), 2.29-2.22 (m, H-2' or H-4', 2H), 2.09-2.01 (m, H-7, 1H), 1.89-1.84 (m, H-3, 2H), 1.74 (m, H-8, 2H)

^{13}C-NMR (100 MHz, $MeOD_4$) δ/ppm 170.2, 169.9, 159.0, 157.1, 155.3, 155.1, 152.0,150.0, 144.16 (q, CF_3),126.1, 120.6 (m, CH_{Ar}), 107.1 (m, CH_{Ar}), 55.4 (C-3'), 45.8 (C-2), 41.1 (C-4), 34.8 (C-6), 34.6 (2, C-4'), 32.5 (C-7), 30.9 (C-2'), 30.0 (C-3), 21.5 (C-9), 19.6 (C-8)

HRMS *m/z*: $C_{20}H_{22}N_5F_6O$ calculated 462.1723 $[M+H]^+$, found 462.1732.

(**264/266**)

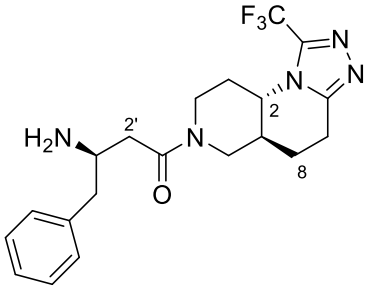
B: **HPLC** (t_R= 18.86 min, 99%)

^{1}H-NMR (400 MHz, $CDCl_3$) δ/ppm 7.10-7.01 (m, CH_{Ar}, 1H), 6.95-6.87 (m, CH_{Ar}, 1H), 4.86 (dt, *J*= 1.5, 13.4 Hz, d, *J*= 14.0 Hz, H-3', H-4' or H-2', 2H), 4.52 (dt, *J*= 4.7, 14.9 Hz, H-2, H-4 or H-6, 2H), 3.95 (t, *J*= 14.3 Hz, H-4 or H-6, 1H), 3.59 (m, H-4, or H-6, 1H), 3.49-3.10 (m, H-6 or H-4, H-9, 2H), 3.04-2.93 (m, H-4' or H-2', H-9, 3H), 2.87 (dd, *J*= 2.8, 13.7 Hz, H-2' or H-4', 1H), 2.78 (dd, *J*= 5.7, 13.1 Hz, H-2' or H-4', 1H), 2.67-2.59 (m, H-7, 1H), 2.20-1.95 (m, H-3, H-8, 4H), 1.88-1.68 (m, NH_2, 2H)

^{13}C-NMR (100 MHz, $MeOD_4$) δ/ppm 170.4 (2), 159.2, 156.5, 156.3, 149.7, 149.3, 147.0 (q), 144.3, 143.9, 120.5 (m, CH_{Ar}), 107.2 (m, CH_{Ar}), 55.4 (C-3'), 45.8 (C-2), 41.0 (C-4), 35.4 (C-6), 34.6 (2, C-4'), 32.4 (C-7), 30.2 (C-2'), 29.4 (C-3), 21.5 (C-9), 19.5 (C-8)

LCMS *m/z*: 462.2 $[M+H]^+$ 1.95 min.

(3*R*)-3-Amino-4-phenyl-1-(1-(trifluoromethyl)-4,5,5a,8,9,9a-hexahydro-[1,2,4] triazolo [4,3-a][1,6]naphthyridin-7(6*H*)-yl)butan-1-one hydrochloride (331 and **335)**



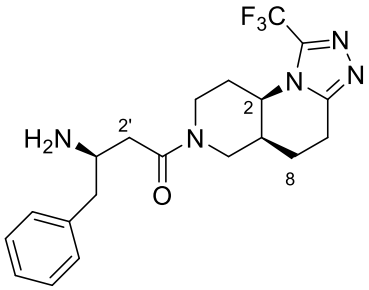
1.isomer (**331**)

HPLC (t_R= 7.80 min, 100%)

^{1}H-NMR (400 MHz, MeOD$_4$) δ/ppm 7.40-7.29 (m, CH_{Ar}, 5H), 4.80-4.64 (m, H-3', 1H), 4.19 (m, H-2, 1H), 4.05 (m, H-4, 1H), 3.93-3.83 (m, H-6, 1H), 3.35-3.19 (m, H-6, 1H), 3.09-2.92 (m, H-4, H-9, H-2', 4H), 2.89-2.53 (m, H-9, H-2', H-3, H-7, 5H), 1.82 (m, H-8, H-3, 3H)

^{13}C-NMR (100 MHz, CDCl$_3$) δ/ppm 170.5 (4), 136.9 (3), 130.4 (4), 130.2 (2), 128.6, 121.1, 118.9, 55.4, 51.5 (4), 45.8, 44.6 (2), 41.1, 40.9, 39.6, 39.4 (3), 34.7, 34.6 (3), 34.2, 30.2, 30.0, 29.5, 24.2, 21.6 (4), 19.7, 19.5 (2), 19.3

HRMS *m/z*: $C_{20}H_{24}N_5F_3O$ calculated 408.2006 $[M+H]^+$, found 408.1962.



2. isomer (**335**)

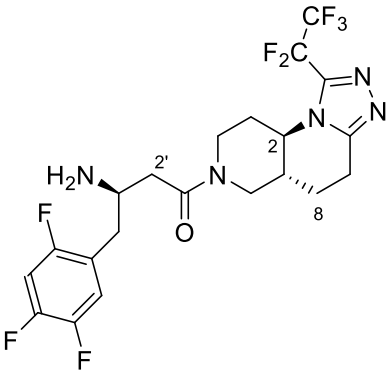
HPLC (t_R= 7.85 min, 100%)

^{1}H-NMR (400 MHz, MeOD$_4$) δ/ppm 7.39-7.26 (m, CH_{Ar}, 5H), 4.80-4.70 (m, H-3', 1H), 4.19 (t, *J*= 10.3 Hz, H-2, 1H), 4.05 (dd, *J*= 13.6, 26.7 Hz, H-6, 1H), 3.93-3.83 (m, H-4, 1H), 3.25-3.19 (m, H-2', H-4, H-6, 4H), 3.09-2.53 (m, H-7, H-4', H-9, H-3, 6H), 2.07-1.65 (m, H-8, H-3, 3H),

^{13}C-NMR (100 MHz, MeOD$_4$) δ/ppm 170.1, 136.8, 130.4, 130.1, 128.6, 61.8, 59.9, 51.5, 46.2, 44.7, 41.9, 41.7, 41.4, 41.3, 39.5, 34.8, 34.6, 23.9, 23.7, 23.3

LC/MS *m/z*: 408.3 $[M+H]^+$, 1.87 min.

(3*R*)-3-amino-1-(1-(perfluoroethyl)-4,5,5a,8,9,9a-hexahydro-[1,2,4]triazolo[4,3-a][1,6]naphthyridin-7(6*H*)-yl)-4-(2,4,5-trifluorophenyl)butan-1-one hydrochloride (316 and **328**)

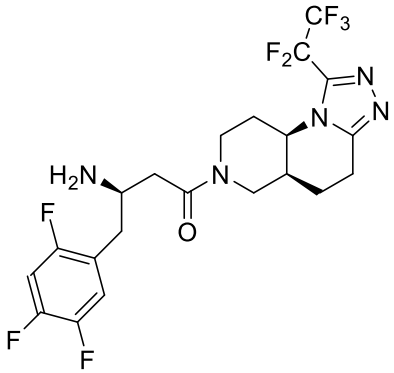


1.isomer (**328**)

^{1}H-NMR (400 MHz, MeOD$_4$) δ/ppm 7.39-7.32 (m, CH_{Ar}, 1H), 7.28-7.21 (m, CH_{Ar}, 1H), 4.78-4.70 (m, H-3', 1H), 4.22 (m, H-2, 1H), 4.04 (m, H-4, 1H), 3.87-3.81 (m, H-6, 1H), 3.71 (m, H-4, 1H), 3.21-3.18 (m, H-9, 1H), 3.13-2.93 (m, H-9, H-6, H-2', 4H), 2.90-2.78 (m, H-4', 2H), 2.73-2.60 (m, H-7, H-3, 2H), 2.06-1.94 (m, H-8, 1H), 1.92-1.83 (m, H-3, 1H), 1.80-1.66 (m, H-8, 1H),

^{13}C-NMR (100 MHz, MeOD$_4$) δ/ppm 169.9, 169.7, 157.3 (2), 120.6 (2), 120.4, 107.3, 107.1, 107.0, 106.9, 62.0, 46.3, 44.6, 42.3, 41.7 (2), 41.3, 35.2, 32.7, 23.9, 23.8, 23.4

LC/MS m/z 512.2 $[M+H]^+$, 2.09 min.



2.isomer (**316**)

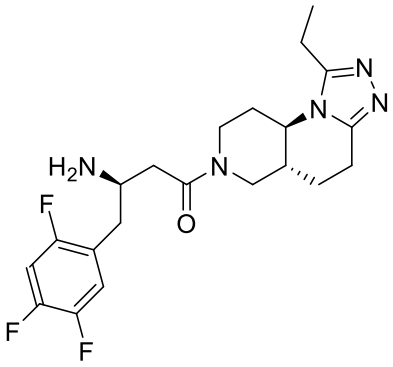
^{1}H-NMR (400 MHz, MeOD$_4$) δ/ppm 7.40-7.31 (m, CH_{Ar}, 1H), 7.27-7.19 (m, CH_{Ar}, 1H), 4.77-4.66 (m, H-3', 1H), 4.01 (m, H-2, 1H), 3.90-3.81 (m, H-4, 1H), 3.56-3.47 (m, H-6, 1H), 3.27-3.02 (m, H-4, H-6, H-9, H-4', 6H), 2.95-2.65 (m, H-2', 2H), 2.50-2.41 (m, H-7, 1H), 2.22-1.86 (m, H-3, H-8, 4H)

^{13}C-NMR (100 MHz, MeOD$_4$) δ/ppm 170.4 (2), 170.1, 165.0, 159.2 (2), 156.8, 156.6, 152.1, 151.9, 149.6, 149.5, 149.3, 147.0 (2), 147.0, 146.9, 142.9, 120.7, 120.5, 107.2, 107.1 (2), 106.7, 92.2, 73.5,72.4, 63.5, 62.1, 60.6, 57.7, 45.4, 44.5, 43.8, 40.1, 37.4, 34.8 (2), 34.0, 33.9, 32.4, 32.3, 29.8, 29.1, 21.0, 18.1 (2), 17.9

m.p: 243.5

LC/MS *m/z* 512.2 $[M+H]^+$, 2.08 min.

(3*R*)-3-Amino-1-(1-ethyl-4,5,5a,8,9,9a-hexahydro-[1,2,4]triazolo[4,3-a][1,6]naphthyridin-7(6*H*)-yl)-4-phenylbutan-1-one hydrochloride (318 and **329)**



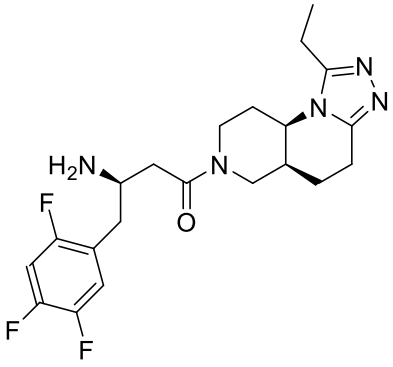
1.isomer (**329**):

HPLC (t_R= 7.30 min, 100%)

^{1}H-NMR (400 MHz, MeOD$_4$) δ/ppm 7.31-7.23 (m, 1H), 7.18-7.10 (m, 1H), 4.71 (m, 1H), 4.28 (m, 1H), 4.11-4.00 (m, 2H), 3.87 (m, 1H), 3.38-2.62 (m, 12H), 2.01-1.59 (m, 4H), 1.35 (m, 3H)

^{13}C-NMR (100 MHz, MeOD$_4$) δ/ppm 170.2, 170.0, 156.8, 120.6, 120.5, 107.2, 107.1 (2), 106.8, 54.4, 45.6 (2), 44.5, 41.0, 40.9, 34.8, 34.7 (2), 34.2, 34.0, 32.4, 32.3, 32.2, 28.8 (2), 28.1, 20.8 (2), 18.9, 18.8 (2), 18.6, 10.2 (2)

HRMS *m/z*: $C_{21}H_{26}N_5F_3O$ calculated 422.2166 $[M+H]^+$, found 422.1171.



2.isomer (**318**)

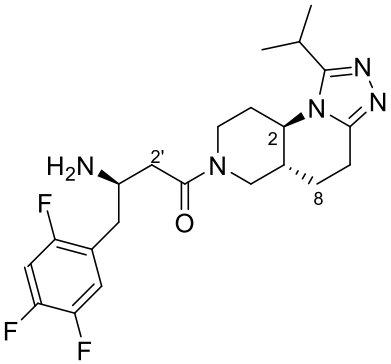
HPLC (t_R= 7.22 min, 100%)

^{1}H-NMR (400 MHz, MeOD$_4$) δ/ppm 7.43-7.34 (m, 1H), 7.28-7.19 (m, 1H), 4.81-4.65 (m, 2H), 4.10 (m, 0.5H), 3.91 (m, 0.5H), 3.89-3.79 (m, 1H), 3.29-3.19 (m, 3H), 3.14-2.45 (m, 8H), 2.37 (m, 1H), 2.17-1.81 (m, 5H), 1.45 (t, *J*= 7.3 Hz, 3H)

^{13}C-NMR (100 MHz, MeOD$_4$) δ/ppm 169.8, 169.7, 169.6, 120.6, 120.4, 107.3, 107.1, 107.0, 106.8, 61.0 (2), 46.2, 44.7, 41.6 (2), 41.2 (2), 34.9 (3), 34.7, 32.4, 31.3 (2), 30.7, 24.1, 23.8 (2), 22.7, 21.7, 11.1 (2),

HRMS *m/z*: $C_{21}H_{26}N_5F_3O$ calculated 422.2166 $[M+H]^+$, found 422.2016.

(3*R*)-3-amino-1-(1-isopropyl-4,5,5a,8,9,9a-hexahydro-[1,2,4]triazolo[4,3-a] [1,6] naphthyridin -7(6H)-yl)-4-(2,4,5-trifluorophenyl)butan-1-one hydrochloride (319 and **331)**



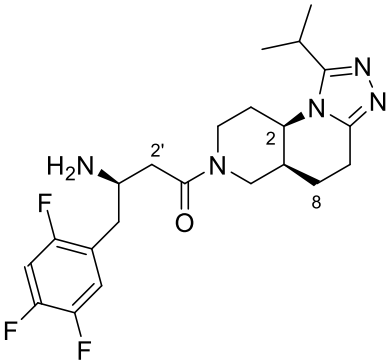
1.isomer (**331**)

HPLC (t_R= 7.64 min)

^{1}H-NMR (400 MHz, MeOD$_4$) δ/ppm 7.42-7.36 (m, CH_{Ar}, 1H), 7.27-7.21 (m, CH_{Ar}, 1H), 4.75 (dd, *J*=14.4, 15.6 Hz, H-4 or H-6), 4.34-4.26 (m, H-2, 1H), 4.10-4.04 (m, H-6 or H-4, 1H), 3.89-3.82 (m, H-3', 1H), 3.51-3.43 (m, CH-*i*Pr, 1H), 3.27-3.21 (m, H-9, 1H), 3.16-3.02 (m, H-9, H-2' or H-4', H-4 or H-6, 4H), 2.96-2.64 (m, H-2' or H-4', H-3, H-7, 4H), 2.13-1.74 (m, H-3, H-8), 1.44 (2d, CH_3-*i*Pr, 3H), 1.41 (2d, CH_3-*i*Pr, 3H)

^{13}C-NMR (100 MHz, MeOD$_4$) δ/ppm 169.8 (2), 169.6, 161.1, 154.5, 120.6 (CH_{Ar}), 107.2, 107.0 (2, CH_{Ar}), 106.8 (CH_{Ar}), 61.7 (C-2), 50.2 (C-3'), 46.1 (CH-*i*Pr), 44.8 (C-4 or C-6), 41.5 (2) (C-4 or C-6), 41.2 (C-4 or C-6), 41.0 (C-7), 34.9 (C-4' or C-2'), 34.8 (C-4' or C-2'), 32.4 (C-4' or C-2'), 31.4 (2, C-4' or C-2'), 27.8 (C-3), 23.3 (C-9), 23.1 (C-9), 21.2 (2, C-8), 20.8 (CH_3-*i*Pr)

LC/MS *m/z* 436.2 $[M+H]^+$, 1.84 min.



2.isomer (**319**)

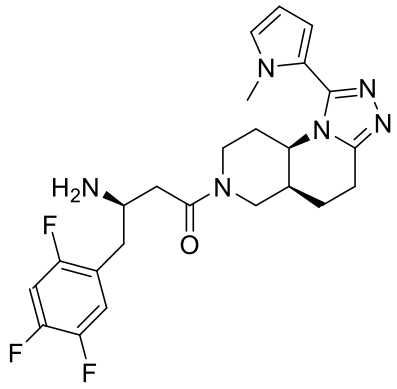
HPLC (t_R= 7.60 min)

^{1}H-NMR (400 MHz, MeOD$_4$) δ/ppm 7.40-7.32 (m, CH_{Ar}, 1H), 7.30-7.21 (m, CH_{Ar}, 1H), 4.69-4.62 (m, H-2, H-4 or H-6, 3H), 4.02-3.96 (m, H-4 or H-6, 0.5H), 3.93-3.80 (m, H-3', H-4 or H-6, 2H), 3.55-3.48 (dt, *J*= 3.6, 11.6 Hz, H-4 or H-6, 0.5H), 3.28-3.21 (m, CH-*i*Pr, 1H), 3.17-3.10 (m, H-4 or H-6, 1H), 3.08-3.03 (m, H-4 or H-6, H-9, H-2' or H-4', 3H), 3.00-2.66 (m, H-9, H-2' or H-4', 4H), 2.38 (d, *J*= 12.7 Hz, H-7, 1H), 2.09-1.74 (m, H-3, H-8, 4H), 1.42 (2d, *J*= 6.7 Hz, 6.7 Hz, CH_3-*i*Pr, 3H), 1.37 (2d, *J*= 6.7 Hz, 6.7 Hz, CH_3-*i*Pr, 3H)

^{13}C-NMR (100 MHz, MeOD$_4$) δ/ppm 170.4. 170.3, 170.0, 160.5, 152.7 (2), 152.5 (2), 128.8, 127.9, 120.7 (CH_{Ar}), 120.5 (2, CH_{Ar}), 118.3, 111.6, 107.2 (CH_{Ar}), 107.0 (2, CH_{Ar}), 106.8 (CH_{Ar})73.5, 72.4, 62.2, 54.7 (C-2), 50.2 (C-3'), 45.6 (2, C-4 or C-6), 44.6 (CH-*i*Pr), 41.0 (C-4 or C-6), 40.9 (C-4 or C-6), 34.9 (2, C-7), 34.1 (C-2' or C-4'), 33.9 (2, C-2' or C-4'), 32.4 (2, C-2' or C-4'), 29.6 (2, C-3), 28.8 (C-3), 21.9 (CH_3-*i*Pr), 21.1 (2, C-9), 20.7 (CH_3-*i*Pr), 18.8 (3, C-8)

LC/MS *m/z* 436.5 $[M+H]^+$, 1.85 min.

(*R*)-3-amino-1-((5a*S*,9aR)-1-(1-methyl-1H-pyrrol-2-yl)-4,5,5a,8,9,9a-hexahydro-[1,2,4]triazolo[4,3-a][1,6]naphthyridin-7(6H)-yl)-4-(2,4,5-trifluorophenyl)butan-1-one hydrochloride (326)



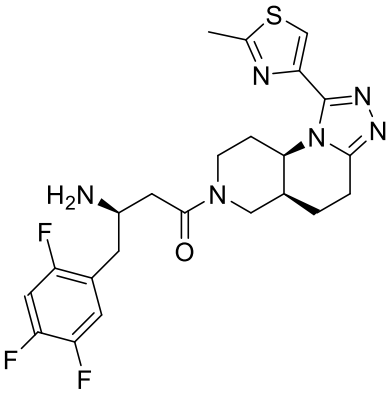
HPLC (t_R= 12.05 min)

^{1}H-NMR (400 MHz, MeOD$_4$) δ/ppm 7.41-7.33 (m, CH_{Ar}, 1H), 7.27-7.19 (m, CH_{Ar}, 1H), 7.08 (s, CH-pyrrol, 1H), 6.93 (s, CH-pyrrol, 1H), 6.32 (t, *J*= 3.1 Hz, CH-pyrrol, 1H), 5.03-4.98 (m, H-2, 1H), 4.75-4.69 (m, H-4 or H-6, 0.5H), 4.55 (d, *J*= 12.9 Hz, H-4 or H-6, 0.5H), 4.06-4.01 (m, H-4 or H-6, 0.5H), 3.88-3.81 (m, H-3', 1H), 3.80 (t, *J*= 3.2, Hz, Me, 3H), 3.75-3.64 (m, H-9, 1H), 3.22-3.02 (m, H-9, H-2' or H-4', 3H), 2.92-2.62 (m, H-2' or H-4', 2H), 2.55-2.51 (m, H-7, 1H), 2.12-1.97 (m, H-8, 2H), 1.89-1.69 (m, H-3, 2H)

^{13}C-NMR (100 MHz, MeOD$_4$) δ/ppm 170.3, 170.2, 169.9, 129.6 (CH-pyrrol), 120.6 (CH-pyrrol)m 120.5 (CH-pyrrol), 115.8, 115.1 (CH_{Ar}), 110.2 (CH_{Ar}), 107.1 (CH-pyrrol), 106.8 (CH-pyrrol), 73.5, 72.4, 62.2, 55.6 (C-2), 49.8 (C-3'), 45.6 (2, C-4 or C-6), 44.5 (C-4 or C-6), 43.7 (C-4 or C-6), 40.9 (2, C-4 or C-6), 36.2 (2, C-4 or C-6), 34.9 (2, Me), 34.3 (C-2' or C-4'), 32.4 (2, C-7), 30.7 (2, C-4' or C-2'), 28.7, 24.2 (C-3), 21.0 (C-9), 19.1 (2, C-8), 19.0 (C-8)

HRMS *m/z*: $C_{24}H_{28}N_6F_3O$ calculated 473.2271 $[M+H]^+$, found 473.2134.

(R)-3-amino-1-((5aS,9aR)-1-(2-methylthiazol-4-yl)-4,5,5a,8,9,9a-hexahydro-[1,2,4]triazolo[4,3-a][1,6]naphthyridin-7(6H)-yl)-4-(2,4,5-trifluorophenyl)butan-1-one hydrochloride (320)



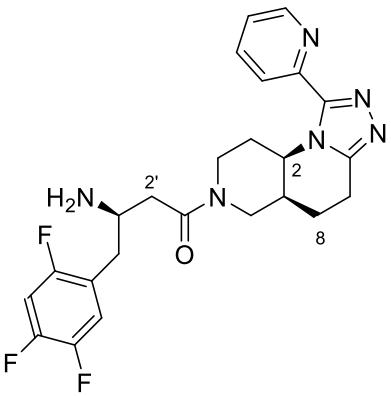
HPLC (t_R= 11.94 min, 100%)

^{1}H-NMR (400 MHz, MeOD$_4$) δ/ppm 8.23-8.22 (m, CH-thiazole, 1H), 7.42-7.34 (m, CH_{Ar}, 1H), 7.30-7.20 (m, CH_{Ar}, 1H), 5.49-5.43 (m, H-2, 1H), 4.75 (dd, *J*= 8.7, 14.1 Hz, H-4 or H-6, 0.5H), 4.64 (d, *J*= 13.0 Hz, H-4 or H-6, 0.5H), 4.06-4.00 (m, H-4 or H-6, 0.5H), 3.95-3.52 (m, H-3', H-4 or H-6, 1.5H), 3.59-3.52 (m, H-4 or H-6, 1H), 3.29-3.19 (m, H-4 or H-6, 0.5H), 3.17-3.05 (m, H-2' or H-4', H-9, 3H), 2.96-2.83 (m, H-4 or H-6, H-9, 2H), 2.81 (s, Me, 3H), 2.80-2.69 (m, H-2' or H-4', 2H), 2.49 (d, *J*= 13.5 Hz, H-7, 1H), 2.30-2.19 (m, H-3, 1H), 2.14-1.84 (m, H-8, 2H), 1.76 (ddd, *J*= 5.8, 12.8, 25.5 Hz, H-3, 1H)

^{13}C-NMR (100 MHz, MeOD$_4$) δ/ppm 170.3, 170.2, 169.9, 159.0, 157.0, 153.2, 153.0, 149.0, 148.7, 147.2, 141.1, 124.0 (CH-thiazole), 120.6 (2-CH_{Ar}), 107.0 (3- CH_{Ar}), 56.6 (C-2), 56.1 (C-2), 50.2 (C-3'), 45.9 (2-C-4 or C-6), 44.8 (C-4 or C-6), 41.3 (C-4 or C-6), 41.2 (C-4 or C-6), 34.8 (C-4' or C-2'), 34.7 C-4' or C-2'), 34.6 (C-4' or C-2'), 34.5 (C-4' or C-2'), 32.4 (C-7), 32.3 (C-7), 29.6 (2- C-4' or C-2'), 28.9 (C-3), 24.2 (C-9), 21.3 (C-3), 19.3 (4-Me)

HRMS *m/z*: $C_{23}H_{26}N_6F_3OS$ calculated 491.1835 $[M+H]^+$, found 491.2482.

(*R*)-3-amino-1-((5a*S*,9a*R*)-1-(pyridin-2-yl)-4,5,5a,8,9,9a-hexahydro-[1,2,4]triazolo[4,3-a][1,6]naphthyridin-7(6*H*)-yl)-4-(2,4,5-trifluorophenyl)butan-1-one hydrochloride (323)



HPLC (t_R= 10.75 min, 100%)

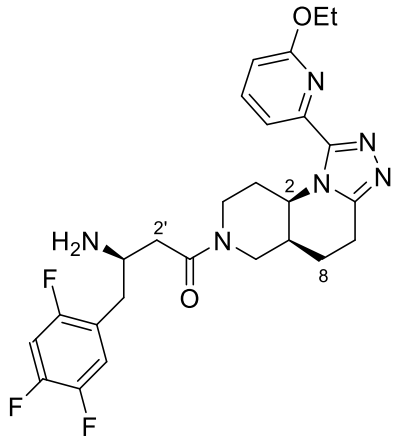
^{1}H-NMR (400 MHz, MeOD$_4$) δ/ppm 8.81 (s, CH-pyridine, 1H), 8.26 (d, *J*= 7.4 Hz, CH-pyridine, 1H), 8.06 (t, *J*= 8.5 Hz, CH-pyridine, 1H), 7.64-7.61 (m, CH-pyridine, 1H), 7.46-7.39 (m, CH_{Ar}, 1H), 7.29-7.19 (m, CH_{Ar}, 1H), 5.81-5.73 (m, H-2, 1H), 4.76 (t, *J*= 11.9 Hz, H-4 or H-6, 0.5H), 4.65 (d, *J*= 14.8 Hz, H-4 or H-6, 0.5H), 4.32-4.21 (m, H-4 or H-6, 0.5H), 4.17-4.06 (m, H-4 or H-6, 1H), 3.96 (t, *J*= 12.9 Hz, H-4 or H-6, 0.5H), 3.90-3.82 (m, H-3', 1H), 3.61-3.53 (m, H-4 or H-6, 0.5H), 3.46-3.36 (m, H-9, 1H), 3.31-3.21 (m, H-9,

H-4 or H-6, 2H), 3.15-3.05 (m, H-2' or H-4', 2H), 2.96-2.75 (m, H-2'or H-4', 2H), 2.59-2.50 (m, H-7, 1H), 2.36 (t, *J*= 11.9 Hz, H-3, 1H), 2.24-2.09 (m, H-8, 1H), 2.07-1.96 (m, H-8, 1H), 1.92-1.80 (m, H-3, 1H)

^{13}C-NMR (100 MHz, MeOD$_4$) δ/ppm 170.4, 170.3, 170.0 (2), 154.5, 151.5, 150.9 (CH-pyridine), 146.1, 139.2 (CH-pyridine), 127.4 (CH-pyridine), 120.7 (3- CH_{Ar}), 107.2 (2- CH_{Ar}), 106.9 (2- CH_{Ar}), 57.2 (C-2), 49.8 (C-3'), 45.8 (2-C-4 or C-6), 44.9 (C-4 or C-6), 41.3 (2, C-4 or C-6), 34.8 (2, C-4'or C-2'), 34.3 (C-4' or C-2'), 34.2 (C-4 or C-2'), 32.4 (C-7), 32.2 (C-7), 29.4 (2, C-4' or C-2'), 28.7 (C-3), 21.4 (2, C-9), 18.6 (C-8), 18.5 (C-8)

HRMS *m/z*: $C_{24}H_{26}N_6F_3O$ calculated 471.2115 $[M+H]^+$, found 471.2754.

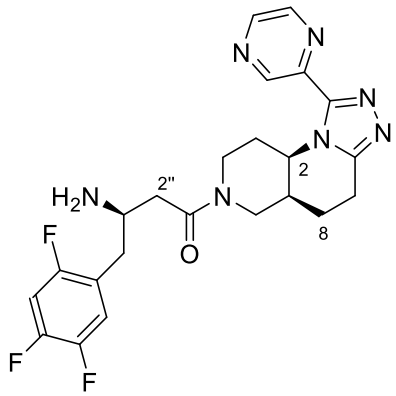
(*R*)-3-amino-1-((5a*S*,9a*R*)-1-(6-ethoxypyridin-2-yl)-4,5,5a,8,9,9a-hexahydro-[1,2,4]triazolo[4,3-a][1,6]naphthyridin-7(6*H*)-yl)-4-(2,4,5-trifluorophenyl)butan-1-one hydrochloride (325)



^{1}H-NMR (400 MHz, MeOD$_4$) δ/ppm 7.80-7.75 (m, 1H), 7.47-7.38 (m, 1H), 7.36-7.29 (m, 1H), 7.27-7.20 (m, 1H), 6.89 (d, *J*= 8.1 Hz, 1H), 5.59-5.54 (m, 1H), 4.67-4.56 (m, 1H), 4.50-4.43 (m, 1H), 4.38-4.30 (m, 1H), 3.94-3.79 (m, 3H), 3.68-3.61 (m, 1H), 3.22-3.13 (m, 2H), 3.10-2.95 (m, 4H), 2.83-2.60 (m, 2H), 2.52-2.45 (m, 2H), 2.29-2.21 (m, 1H), 2.07-1.58 (m, 2H), 1.29 (s, 3H)

HRMS *m/z*: $C_{26}H_{30}N_6F_3O_2$ calculated 515.2377 $[M+H]^+$, found 515.2961.

(*R*)-3-amino-1-((5a*S*,9a*R*)-1-(pyrazin-2-yl)-4,5,5a,8,9,9a-hexahydro-[1,2,4]triazolo[4,3-a][1,6]naphthyridin-7(6*H*)-yl)-4-(2,4,5-trifluorophenyl)butan-1-one hydrochloride (324)



HPLC (t_R= 11.87 min)

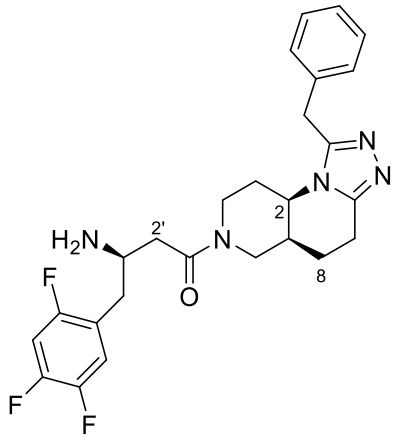
^{1}H-NMR (400 MHz, MeOD$_4$) δ/ppm 9.42 (s, CH-pyrazine, 1H), 8.81 (s, CH-pyrazine, 1H), 8.78 (s, CH-pyrazine, 1H), 7.44-7.31 (m, CH_{Ar}, 1H), 7.29-7.20 (m, CH_{Ar}, 1H), 5.59-5.55 (m, H-2, 1H), 4.76 (dd, *J*= 8.0, 13.6 Hz, H-4 or H-6, 0.5H), 4.65 (dd, *J*= 12.5 Hz, H-4 or H-6,

0.5H), 4.09-4.03 (m, H-4 or H-6, 0.5H), 3.96-3.80 (m, H-3', H-4 or H-6, 2H), 3.28-3.16 (m, H-9, H-4 or H-6, 2H), 3.13-3.01 (m, H-9, H4' or H-2', 3H), 2.88-2.59 (m, H-4' or H-2', 2H), 2.55-2.49 (m, H-7, 1H), 2.32 (t, *J*= 12.9 Hz, H-3, 1H), 2.19-2.05 (m, H-8, 1H), 2.03-1.92 (m, H-8, 1H), 1.86-1.76 (m, H-3, 1H)

^{13}C-NMR (100 MHz, MeOD$_4$) δ/ppm 173.1, 170.3, 170.2, , 170.0, 147.0 (CH-pyrazine), 145.5, 145.3 (CH-pyrazine), 128.4, 20.6 (2, CH_{Ar}), 120.5 (2, CH_{Ar}), 107.2 (CH_{Ar}), 107.0 (2, CH_{Ar}), 56.9 (2, C-2), 49.8 (C-3), 45.8 (2, C-4 or C-6), 44.9 (C-4 or C-6), 41.3 (2, C-4 or C-6), 34.8 (2, C-4' or C-2'), 34.7 (2, C-4' or C-2'), 34.5 (2, C-2' or C-4'), 32.4 (2, C-7), 29.6 (2, C-4'or C-2'), 28.9 (C-4' or C-2'), 24.2 (C-3), 21.3 (C-9), 19.0 (3, C-8)

HRMS *m/z*: $C_{23}H_{24}N_7F_3O$ calculated 472.2067 $[M+H]^+$, found 472.2714.

(*R*)-3-amino-1-((5a*S*,9a*R*)-1-benzyl-4,5,5a,8,9,9a-hexahydro-[1,2,4]triazolo[4,3-a][1,6]naphthyridin-7(6*H*)-yl)-4-(2,4,5-trifluorophenyl)butan-1-one hydrochloride (321)



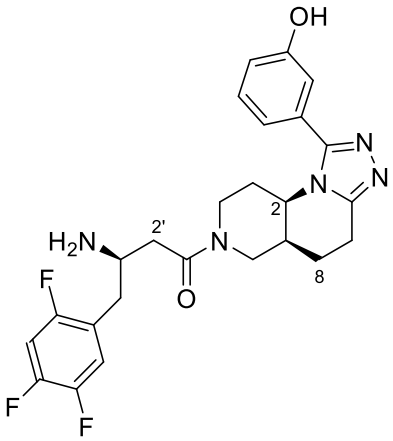
HPLC (t_R= 11.01 min)

^{1}H-NMR (400 MHz, MeOD$_4$) δ/ppm 7.41-7.29 (m, Ph, CH_{Ar}, 5H), 7.26-7.20 (m, CH_{Ar}, 2H), 4.75-4.64 (m, H-2, 1H), 4.39 (q, CH_2-Ph, 2H), 3.89-3.76 (m, H-3', H-9, H-4 or H-6, 3H), 3.13-2.99 (m, H-9, H-4' or H-2', H-4 or H-6, 4H), 2.79-2.55 (m, H-7, H-4' or H-2', H-3, 4H), 2.09-1.67 (m, H-8, H-3, 3H)

^{13}C-NMR (100 MHz, MeOD$_4$) δ/ppm 173.1, 170.4, 169.9, 159.0 (2), 157.0 (2), 152.1 (2), 151.9, 150.1 (2), 149.9, 149.3 (2), 149.1 (2), 147.3 (3), 130.2, 130.1 (2), 128.9, 120.4 (CH_{Ar}), 107.0 (4, CH_{Ar}), 54.6 (C-2), 45.7 (C-3'), 44.7 (C-4 or C-6), 36.4 (C-4 or C-6), 36.3 (C-4 or C-6), 34.8 (2, C-4' or C-2'), 34.2 (2, C-2' or C-4'), 32.4 (C-7), 32.3 (C-7), 30.9 (2, C-2' or C-4'), 30.7 (CH_2-Ph), 29.0 (2, C-3), 28.4 (C-3), 20.8 (C-9), 18.7 (C-8)

HRMS *m/z*: $C_{26}H_{29}N_5F_3O$ calculated 484.2389 $[M+H]^+$, found 484.2330, **LCMS** *m/z*: 484.3, 2.01 min.

(*R*)-3-amino-1-((5a*S*,9a*R*)-1-(3-hydroxyphenyl)-4,5,5a,8,9,9a-hexahydro-[1,2,4]triazolo[4,3-a][1,6]naphthyridin-7(6*H*)-yl)-4-(2,4,5-trifluorophenyl)butan-1-one hydrochloride (322)



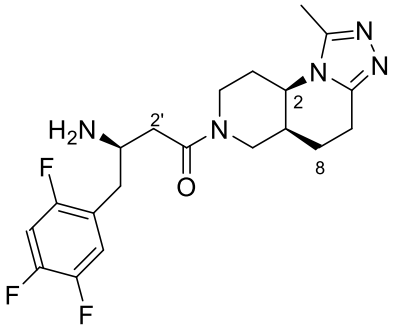
HPLC (t_R= 8.73 min, 100%)

^{1}H-NMR (400 MHz, MeOD$_4$) δ/ppm 7.99 (s, CH_{Ar}, 1H), 7.93 (dt, *J*= 1.1, 7.7 Hz, CH_{Ar}, 1H), 7.76 (t, *J*= 1.8 Hz, CH_{Ar}, 1H), 7.52 (t, *J*= 7.8 Hz, CH_{Ar}, 1H), 7.46-7.40 (m, CH_{Ar}, 1H), 7.39-7.33 (m, CH_{Ar}, 1H), 7.28-7.19 (m, CH_{Ar}, 1H), 4.03-3.96 (m, H-2, 1H), 3.88-3.78 (m, H-3', 1H), 3.74-3.58 (m, H-4, H-6, 2H), 3.20-3.03 (m, H-4, H-6, H-7, H-4', H-2, H-9, 7H), 2.74-2.62 (m, H-3, H-8, 4H)

^{13}C-NMR (100 MHz, MeOD$_4$) δ/ppm 173.1, 171.9, 170.1, 168.5, 164.9, 158.9 (2), 157.0 (2), 151.9, 151.7, 149.9, 147.2, 133.6, 130.7, 128.4, 127.2, 123.8, 120.8 (m), 107.0 (m), 73.5, 72.4,62.1, 43.7, 37.0, 36.7, 36.4, 36.2, 32.3, 32.2 (2), 31.7

HRMS *m/z*: $C_{25}H_{27}N_5F_3O_2$ calculated 486.2111 $[M+H]^+$, found 486.2972.

(*R*)-3-amino-1-((5a*S*,9a*R*)-1-methyl-4,5,5a,8,9,9a-hexahydro-[1,2,4]triazolo[4,3-a][1,6]naphthyridin-7(6*H*)-yl)-4-(2,4,5-trifluorophenyl)butan-1-one hydrochloride (317)



HPLC (t_R= 9.60 min, 100%)

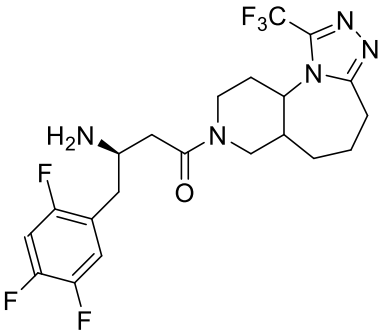
^{1}H-NMR (400 MHz, MeOD$_4$) δ/ppm 7.45-7.38 (m, CH_{Ar}, 1H), 7.29-7.21 (m, CH_{Ar}, 1H), 4.81-4.66 (m, H-2, H-4 or H-6, 2H), 4.08-4.02 (m, H-4 or H-6, 0.5H), 3.99-3.94 (m, H-4 or H-6, 0.5H), 3.89-3.82 (m, H-3', 1H), 3.57-3.49 (m, H-4 or H-6, 0.5H), 3.31-3.18 (m, H-9, H-4 or H-6, 1.5H), 3.15-3.03 (m, H-4' or H-2', H9, 3H), 2.94-2.73 (m, H-4' or H-2', 2H), 2.64 (s, Me, 3H), 2.44-2.40 (m, H-7, 1H), 2.20-1.87 (m, H-3, H-8, 4H)

^{13}C-NMR (100 MHz, MeOD$_4$) δ/ppm 170.3 (2), 170.0 (2), 153.0, 152.6, 120.7 (CH_{Ar}), 107.2 (CH_{Ar}), 107.0 (CH_{Ar}), 106.8 (CH_{Ar}), 54.4 (C-2), 49.8 (C-3'), 45.7 (2, C-4 or C-6), 44.6 (C-4 or C-6), 41.0 (2, C-4 or C-6), 34.9 (C-4 or C-6), 34.8 (C-4 or C-6), 34.2 (C-4 or C-6), 34.0

(C-4 or C-6), 32.4(C-4' or C-2'), 28.8 (2, C-7), 28.0 (C-4' or C-2'), 24.2 (C-3), 20.9 (C-9), 19.0 (C-8), 18.9 (C-8), 9.8 (2, Me)

LCMS *m/z*: 408.2 $[M+H]^+$, 2.43 min.

(3*R*)-3-amino-1-(1-(trifluoromethyl)-5,6,6a,9,10,10a-hexahydro-4H-pyrido[3,4-f] [1,2,4] triazolo[4,3-a]azepin-8(7*H*)-yl)-4-(2,4,5-trifluorophenyl)butan-1-one hydrochloride (334)



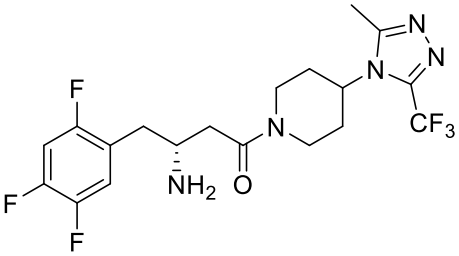
HPLC (t_R= 13.30 min)

^{1}H-NMR (400 MHz, MeOD$_4$) δ/ppm 7.42-7.35 (m, 1H), 7.28-7.22 (m, 1H), 4.75-4.70 (m, 0.5H), 4.66-4.62 (m, 0.5H), 4.38 (t, *J*= 11.7 Hz, 0.5H), 4.00 (dd, *J*= 13.3, 33.3 Hz, 1.5H), 3.39-3.26 (m, 5H), 3.20-3.14 (m, 0.5H), 3.11-3.02 (m, 2H), 3.00-2.79 (m, 2H), 2.74-2.63 (m, 1H), 2.54-2.45 (m, 0.5H), 2.35-2.26 (m, 1.5H), 2.17-2.05 (m, 2H), 2.00-1.92 (m, 1H), 1.86-1.78 (m, 1H), 1.75-1.71 (m, 0.5H), 1.65-1.57 (m, 1.5H)

^{13}C-NMR (100 MHz, MeOD$_4$) δ/ppm 169.9 (2), 169.8, 159.2, 120.6, 120.5, 107.2, 107.1, 107.0, 106.8, 73.6, 72.4, 65.7 (2), 62.6, 62.2, 60.3, 50.3, 45.7, 45.1, 43.7, 42.2, 41.6 (2), 39.0 (2), 38.9, 38.8, 38.5, 38.4, 35.1 (2), 34.9, 34.7, 34.0, 33.3, 32.4, 31.6, 30.7, 29.6 (2), 27.9, 27.8, 27.4, 27.3, 26.3, 26.2, 24.5, 24.2, 23.7, 23.5 (2), 23.4 (2), 23.3 (2)

HRMS *m/z*: $C_{21}H_{24}N_5F_6O$ calculated 476.1880 $[M+H]^+$, found 475.7235.

(*R*)-3-Amino-1-(4-(3-methyl-5-(trifluoromethyl)-4*H*-1,2,4-triazol-4-yl)piperidin-1-yl)-4-(2,4,5-trifluorophenyl)butan-1-one hydrochloride (333)



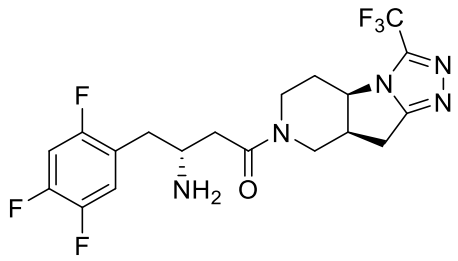
HPLC (t_R= 8.37 min, 8.48 min)

^{1}H-NMR (400 MHz, CDCl$_3$) δ/ppm 7.41-7.34 (m, 1H), 7.27-7.20 (m, 1H), 4.78 (d, *J*= 13.9 Hz, 1H), 4.57 (bs, 1H), 4.05 (d, *J*= 13.5 Hz, 1H), 3.86 (bs, 1H), 3.33-3.26 (m, 4H), 3.08 (m, 2H), 2.95 (d, *J*= 16.9 Hz, 1H), 2.84- 2.67 (m, 2H), 2.64, 2.62 (2s, 3H), 2.19-2.04 (m, 3H)

^{13}C-NMR (100 MHz, $CDCl_3$) δ/ppm 169.8, 169.7, 165.2, 163.4, 158.9 (2), 156.9 (3), 151,8, 151,7, 151.6, 149.8 (2), 149.7, 149.1 (2), 149.0 (2), 147.2 (2), 147.1 (2), 145.7, 145.3, 145.0, 144.7, 129.6, 121.7, 120.8 (2), 120.6, 119. 6, 117.4, 117.2, 115.3, 112.3, 107.1 106.9 (2), 106.7, 73.4, 72.3, 64.2, 62.0, 59.8, 50.3, 45.3, 41.7 (2), 37.7, 35.4, 34.9 (3), 32.3 (3), 31.4, 31.3, 30.7 (2), 12.7 (2)

LCMS m/z 450.2 $[M+H]^+$, 1.96 min.

(*R*)-3-Amino-1-((4a*R*,8a*S*)-3-(trifluoromethyl)-4a,5,8a,9-tetrahydro-6H-[1,2,4] triazolo[4',3':1,5]pyrrolo[3,2-c]pyridin-7(8*H*)-yl)-4-(2,4,5-trifluorophenyl)butan-1-one hydrochloride (**332**)



HPLC (t_R= 8.47 min, 100%)

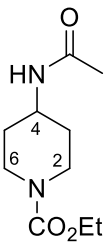
^{1}H-NMR (400 MHz, $MeOD_4$) δ/ppm 7.40-7.30 (m, 1H), 7.27-7.17 (m, 1H), 4.29- 4.22 (m, 1H), 3.89-3.80 (m, 2H), 3.76-3.65 (m, 2H), 3.60-3.35 (m, 2H), 3.26-3.14 (m, 1H), 3.08-3.00 (m, 2H), 2.88-2.58 (m, 3H), 2.36 (m, 1H), 1.88 (m, 1H)

^{13}C-NMR (100 MHz, $CDCl_3$) δ/ppm 173.4, 171.9, 171.1, 170.9, 170.5, 170.4, 165.1, 159.0, 158.9, 157.0, 156.9, 151.9, 149.9, 149.2 (2), 147.3 (2), 129.6, 128.3, 127.2, 120.8, 120.6, 120.5, 118.7, 11.5, 107.2 (3), 106.9, 106.8, 73.5, 72.4, 62.1, 57.2 (2), 56.9, 52.7, 45.2 (2), 43.7, 43.5 (2), 41.8 (2), 39.2, 36.4 (2), 35.2, 35.0, 34.9 (2), 32.3 (2), 28.6, 27.7 (2), 24.9, 24.8 (2)

HRMS m/z: $C_{19}H_{19}N_5OF_6$ calculated 448.1567 $[M+H]^+$, found 448.1568.

Ethyl 4-acetamidopiperidine-1-carboxylate (310)

To ethyl 4-aminopiperidine-1-carboxylate (**308**) (500 mg, 0.5 mL, 2.9 mmol, 1 eq.) in dichloromethane (12 mL) was added acetic acid anhydride (0.3 mL, 3.2 mmol, 1.1 eq.) and triethylamine (1.2 mL, 8.7 mmol, 3.0 eq.) and the reaction mixture was stirred overnight. The mixture was diluted with dichloromethane and the organic phases were washed with water. The organic phases were dried over Na_2SO_4, filtered and the solvent evaporated under reduced pressure to yield ethyl 4-acetamidopiperidine-1-carboxylate (**310**) (520 mg, 84%) as a white solide.



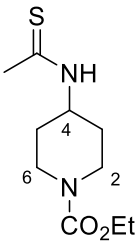
^{1}H-NMR (400 MHz, $CDCl_3$) δ/ppm 5.49 (bs, NH, 1H), 4.12 (q, *J*= 7.5, 14.6 Hz, $CO_2C\mathbf{H}_2CH_3$, H-2, H-6, 4H), 3.93 (m, H-4, 1H), 2.89 (t, *J*= 12.6 Hz, H-2, H-6, 2H), 1.97 (s, Me, 3H), 1.91 (d, *J*= 14.2 Hz, H-5, H-3, 2H), 1.34-1.27 (m, H-5, H-3, 2H), 1.25 (t, *J*= 7.1 Hz, $CO_2CH_2C\mathbf{H}_3$, 3H),

^{13}C-NMR (100 MHz, $CDCl_3$) δ/ppm 169.5 (C=O), 155.6 (CO_2Et), 61.5 ($CO_2\mathbf{C}H_2CH_3$), 46.7 (C-4), 42.9 (C-2, C-6), 32.1 (C-3, C-5), 23.6 (Me), 14.8 ($CO_2CH_2\mathbf{C}H_3$)

m.p. 156.3°C

Ethyl 4-ethanethioamidopiperidine-1-carboxylate (313)

To amide **310** (133 mg, 0.6 mmol, 1.0 eq.) in toluene (3 mL) was added Lawessons reagent (125 mg, 0.3 mmol, 0.5 eq.) and the reaction mixture was refluxed for 30 min. The solvent was evaporated and the crude mixture was purified by flash chromatography (ethyl acetate/ petrol ether 4:1) to yield thioamide **313** (100 mg, 71%).

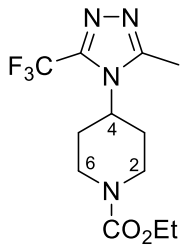


^{1}H-NMR (400 MHz, $CDCl_3$) δ/ppm 7.00 (m, NH, 1H), 4.59-4.50 (m, H-4, 1H), 4.21-4.09 (m, NH-2, H-6, 2H), 4.12 (q, *J*= 7.4 Hz, $CO_2C\mathbf{H}_2CH_3$, 2H), 2.90 (t, *J*= 11.7 Hz, H-2, H-6, 2H), 2.53 (s, Me, 3H), 2.10 (d, *J*= 12.7 Hz, H-5, H-3, 2H), 1.37 (m, H-3, H-5, 2H), 1.25 (t, *J*= 6.9 Hz, $CO_2CH_2C\mathbf{H}_3$, 3H)

Ethyl 4-(3-methyl-5-(trifluoromethyl)-4H-1,2,4-triazol-4-yl)piperidine-1-carboxylate (311)

$POCl_3$ (0.39 g, 0.24 mL, 2.6 mmol, 3 eq.) was added to ethyl 4-acetamidopiperidine-1-carboxylate (**310**) (180 mg, 0.84 mmol, 1 eq.) in a mixture of chloroform (0.55 mL) and pyridine (0.41 mL) at 0°C. The solvent was evaporated under nitrogen using toluene and leave standing overnight. To the brownish slurry in chloroform (0.5 mL) trifluoroacetic acid hydrazide (164 mg, 1.3 mmol, 1.5 eq.) was added and the mixture was refluxed for 5h. The reaction mixture was quenched with saturated aqueous $NaHCO_3$ (20 mL). The aqueous phase was extracted with dichloromethane (3 x 20 mL) and the combined organic phases were dried over Na_2SO_4, filtered and the solvent was evaporated under reduced pressure. To the residue was added 2M HCl (1.2 mL) and the mixture was refluxed for 4h. The reaction mixture was evaporated under nitrogen and diluted with saturated aqueous $NaHCO_3$ (20 mL) and

dichloromethane (20 mL). The aqueous phase was extracted with dichloromethane (2 x 20 mL), dried over Na_2SO_4, filtered and the solvent evaporated under reduced pressure. The crude product was purified by flash chromatography (dichloromethane/ methanol 10:1) to yield ethyl 4-(3-methyl-5-(trifluoromethyl)-4H-1,2,4-triazol-4-yl)piperidine-1-carboxylate (**311**) (30 mg, 15%) as a white solid.



^{1}H-NMR (400 MHz, $CDCl_3$) δ/ppm 4.26-4.19 (m, H-4, H-6, H-2, 3H), 4.02 (q, *J*= 6.7, 14.4 Hz, $CO_2C\mathbf{H}_2CH_3$, 2H), 2.81-2.68 (bt, *J*= 11.7 Hz, H-2, H-6, 2H), 2.47 (s, Me, 3H), 1.95 (dq, *J*= 5.0, 12.7 Hz, H-3, H-5, 2H), 1.84 (m, H-3, H-5, 2H), 1.15 (t, *J*= 7.2 Hz, $CO_2CH_2C\mathbf{H}_3$, 3H)

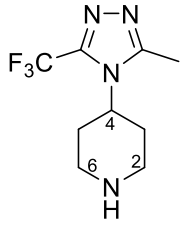
^{13}C-NMR (100 MHz, $CDCl_3$) δ/ppm 154.9, 153.7, 119.7 (q, CF_3), 61.6 ($CO_2CH_2C\mathbf{H}_3$), 55.7 (C-4), 49.9 (C-2, C-6), 43.1 (C-2, C-6), 30.4 (C-3, C-5), 14.4 ($CO_2CH_2C\mathbf{H}_3$), 13.2 (Me)

m.p.: 126.9

LCMS *m/z*: 307.1 $[M+H]^+$, 2.41 min.

4-(3-Methyl-5-(trifluoromethyl)-4*H*-1,2,4-triazol-4-yl)piperidine (312)

To triazole **311** (30 mg, 0.1 mmol, 1.0 eq.) in ethanol (84 µL) and water (0.48 mL) was added KOH (38 mg, 0.3 mmol, 2.7 eq.) and the mixture was heated to 110°C overnight. The mixture was diluted with dichloromethane and the aqueous phase was extracted with dichloromethane (6 x 10 mL). The combined organic phases were dried over Na_2SO_4, filtered and the solvent was evaporated under reduced pressure to yield amine **312** (12 mg, 55%) as an oil, which was used further without purification.



^{1}H-NMR (400 MHz, $CDCl_3$) δ/ppm 4.15 (tt, *J*= 4.4, 12.5 Hz, H-4, 1H), 3.19 (dt, *J*= 2.3, 12.5 Hz, H-6, H-2, 2H), 2.65 (dt, *J*= 2.5, 12.7 Hz, H-6, H-2, 2H), 2.57 (s, Me, 3H), 2.02 (dq, *J*= 4.1, 12.4 Hz, H-3, H-5, 2H), 1.86-1.80 (m, H-3, H-5, 2H)

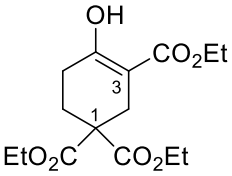
^{13}C-NMR (100 MHz, $CDCl_3$) δ/ppm 154.9, 144.4 (q, CF_3), 118.4 (q, CF_3), 56.4 (C-4), 45.9 (C-2, C-6), 31.8 (C-3, C-5), 13.5 (Me)

m.p.: 102.4°C

HRMS *m/z*: $C_9H_{14}N_4F_3$ calculated 275.1358 $[M+AcN]^+$, found 275.1470.

10.9 Synthesis of Maraviroc analogues

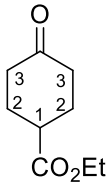
Triethyl 4-hydroxycyclohex-3-ene-1,1,3-tricarboxylate (364)



A solution of diethylmalonate (**363**) (1.88 mL, 2.00 g, 12.48 mmol, 1.0 eq.) in THF (4 mL) was added dropwise over 10 min to a suspension of NaH (1.24 g, 31.20 mmol, 2.5 eq., 60% in paraffinoil) in THF (13.3 mL) at 40°C. After 15 min of stirring a solution of ethylacrylate (2.85 mL, 2.62 g, 26.2 mmol, 2.1 eq.) in THF (4 mL) was added slowly over 10 min. The resulting mixture is allowed to stir for another 15 min and poured afterwards into ice water (25 mL) and extracted with ethylacetate (3 x 30 mL). The combined organic layers were dried over Na_2SO_4 and the solvent was evaporated under reduced pressure to yield a brown oil which was used crude in the next step.

^{1}H-NMR (400 MHz, $CDCl_3$) δ/ppm 12.21 (s, OH, 1H), 4.25-4.17 (m, OEt, 6H), 2.79 (s, H-2, 2H), 2.37 (t, *J*= 6.1 Hz, H-5, 2H), 2.20 (t, *J*= 6.1 Hz, H-6, 2H), 1.33-1.23 (m, OEt, 9H)

Ethyl 4-oxocyclohexanecarboxylate (351)



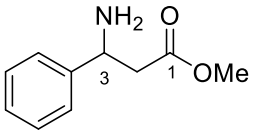
A mixture of triester (**364**) (500 mg, 1.59 mmol, 1.0 eq.), LiCl (202 mg, 4.77 mmol, 3 eq.), water (86 µL), pyridine (0.12 mL) and DMSO (5 mL) was heated to 165 °C and stirred for 13h under N_2 atmosphere. The solution was poured into 25 g sodium chloride in water (100 mL). The aqueous phase was extracted with ethylacetate (6 x 20 mL). The combined organic layers were dried over Na_2SO_4 and purified by flash chromatography (PE/EA: 2:1) to yield ketone (**351**) (60 mg, 30%) as a yellow oil.

^{1}H-NMR (400 MHz, $CDCl_3$) δ/ppm 4.17 (q, *J*= 7.1, 14.1 Hz, $CO_2C\mathbf{H}_2CH_3$, 2H), 2.77-2.70 (m, H-1, 1H), 2.51-2.44 (m, H-3, 2H), 2.39-2.31 (m, H-3, 2H), 2.24-2.17 (m, H-2, 2H), 2.07-1.97 (m, H-2, 2H), 1.28 (t, *J*= 7.6 Hz, $CO_2CH_2C\mathbf{H}_3$, 3H)

^{13}C-NMR (100 MHz, $CDCl_3$) δ/ppm 210.5 (C=O), 174.5 (CO_2Et), 61.0 ($CO_2\mathbf{C}H_2CH_3$), 41.0 (C-3), 39.9 (C-1), 29.1 (C-2), 14.5 ($CO_2CH_2\mathbf{C}H_3$)

LCMS *m/z* 171.0 $[M+H]^+$, 2.28 min.

Methyl 3-amino-3-phenylpropanoate (353)

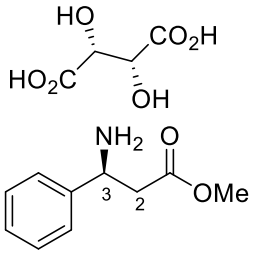


D,L phenylalanine (**354**) (5.0 g, 30 mmol, 1.0 eq.) was slurried in MeOH (60 mL) and cooled to -10°C and conc. H_2SO_4 (6.3 mL) was added over 5 min. The reaction mixture was warmed to rt and stirred overnight. The reaction mixture was evaporated with N_2. To the solution DCM (60 mL) was added and it was adjusted to pH=10 with 2M NaOH (50 mL) (under ice). The aqueous phase was extracted with DCM (20 mL). The combined organic layers were washed with water (10 mL), dried, filtered and the solvent was evaporated under N_2 to yield **353** (assumed as 100%) a yellow white slurry which was used without further purification.

^{1}H-NMR (400 MHz, $CDCl_3$) δ/ppm 7.38-7.28 (m, Ph, 5H), 4.42 (t, *J*= 7.9 Hz, H-3, 1H), 3.68 (s, OMe, 3H), 2.67 (d, *J*= 7.9 Hz, H-2, 2H), 1.70 (bs, NH_2, 2H)

HRMS *m/z*: $C_{10}H_{13}NO_2$ calculated 179.0946 $[M+H]^+$, found 178.9419.

Methyl (S)-3-amino-3-phenylpropanoate (2S,3S)-2,3-dihydroxysuccinate (355)

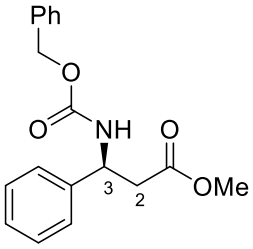


To a solution of L(+) tartaric acid (7.0 g, 46.6 mmol) in MeOH (54 mL) was added methylester (**353**) (5.4 g, 30.0 mmol, 1.0 eq.) in MeOH (15 mL) and refluxed until a clear solution is formed. The reaction mixture was cooled down and kept in the coldroom. The formed orange white slurry was dissolved in MeOH, then washed with MeOH and filtered and the obtained white solide (**355**) (880 mg, 16%) was dried under vacuum.

^{1}H-NMR (400 MHz, $CDCl_3$) δ/ppm 7.33-7.18 (m, Ph, 5H), 4.38 (t, *J*= 7.8 Hz, H-3, 1H), 3.40 (s, OMe, 3H), 2.89 (dd, *J*= 6.9, 16.1 Hz, H-2, 1H), 2.74 (dd, *J*= 7.8, 15.9 Hz, H-2, 1H), 2.36 (q, *J*= 2.2, 3.9 Hz, NH_2, 2H)

m.p.: 176.3.

Methyl (*S*)-3-(((benzyloxy)carbonyl)amino)-3-phenylpropanoate (356)



Tartrate **355** (800 mg, 1.0 eq.) was slurried in dichloromethane (4 mL) and was treated with a solution of sodiumcarbonate (868 mg) in water (3.1 mL). The reaction was cooled to 0°C and benzylchloroformate (0.41 mL, 1.2 eq) was added while maintaining the temperature below 10°C. The reaction mixture was stirred at rt for 1 hour and afterwards

diluted with dichlormethane (10 mL) and water (20 mL). The phases were separated and the water phase was extracted with dichloromethane (10 mL). The organic phase was washed with a sodiumcarbonate/ water mix (10 mL) and water (10 mL), dried over Na_2SO_4,filtered and the solvent was evaporated under reduced pressure to yield CBz ester **356** (87%) as a crystalline white solide after standing at rt.

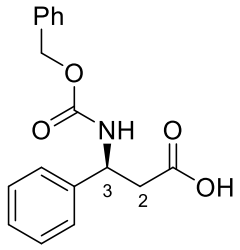
^{1}H-NMR (400 MHz, $CDCl_3$) δ/ppm 7.35-7.27 (m, 2 x Ph, 10H), 5.17 (m, NH, H-3, 2H), 5.09 (dd, *J*= 12.2, 18.0 Hz, C**H**$_2$Ph, 2H), 3.60 (s, OMe, 3H), 2.87 (m, H-2, 2H)

LCMS *m/z* 314.2 $[M+H]^+$, 3.53 min

m.p. 71°C

$[\alpha]^{20}$ c=1.0, - 12.1, Lit: (c=1.0, -13.4)[178]

(*S*)-3-(((benzyloxy)carbonyl)amino)-3-phenylpropanoic acid (357)

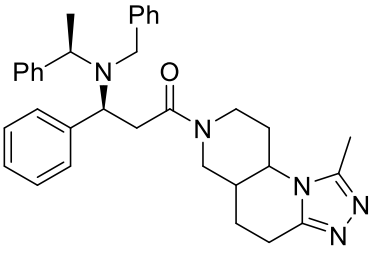


To a solution of methylester (**356**) (760 mg, 2.4 mmol, 1.0 eq.) in *i*-PrOH/MeOH (0.16 mL/ 0.56 mL) was added aqueous NaOH (6 mL, 1M) and stirred for 2 hours. The reaction mixture turns into a big slurry. DCM was added and the mixture was stirred for 20 min until both phases became clear. The phases were separated and the aqueous phase was extracted with DCM (20 mL). The organic phase was washed with water (20 mL) and evaporated under reduced pressure. The resulting slurry was treated with heptane and put into the coldroom for crystallisation to yield acid (**357**) (330 mg, 45 %) as a white oily solide.

^{1}H-NMR (400 MHz, $CDCl_3$) δ/ppm 7.37-7.28 (m, 2x Ph, 10H), 5.73 (m, H-3, 1H), 5.20 (bs, NH, 1H), 5.12 (m, 2H), 2.91 (m, H-2, 2H)

LCMS *m/z* 301.2 $[M+H]^+$, 2.62 min.

(3*S*)-3-(benzyl((*R*)-1-phenylethyl)amino)-1-(1-methyl-4,5,5a,6,9,9a-hexahydro-[1,2,4]triazolo[4,3-a][1,6]naphthyridin-7(8*H*)-yl)-3-phenylpropan-1-one (366)



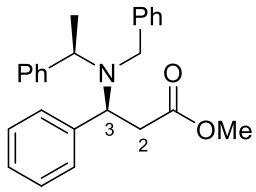
To acid (**361**) (70 mg, 0.2 mmol, 1.8 eq.) in DMF (1 mL) was added DIPEA (40.2 mg, 52 µL, 0.3 mmol, 3.0 eq.), HATU (47 mg, 0.1 mmol, 1.2 eq.) and finally amine (**194**) (20 mg, 0.1 mmol, 1.0 eq.) in DMF (0.5 mL) and the resulting yellow

mixture was stirred for 30 min. The reaction mixture was diluted with water (10 mL). The aqueous phase was extracted with ethylacetate (3 x 10 mL). The combined organic layers were washed with saturated aqueous NH_4Cl (10 mL), dried over $MgSO_4$, filtered and the solvents were evaporated under reduced pressure. The crude product was purified by flash chromatography (DCM + 10% MeOH) to yield amide (**366**) (18 mg, 34 %, mixture: 2:1) as a colorless oil.

^{1}H-NMR (400 MHz, $CDCl_3$) δ/ppm 7.49-7.12 (m, 15H), 4.63-4.47 (m, 2H), 4.05-3.87 (m, 2H), 3.84-3.73 (m, 1H), 3.70-3.62 (m, 1H), 3.48-3.20 (m, 1H), 3.05-2.74 (m, 2H), 2.73-2.61 (m, 2H), 2.59-2.47 (m, 2H), 2.43-2.38 (m, 1H), 2.34 (s, 2H), 2.31 (s, 1H), 2.09-1.77 (m, 2H), 1.59-1.39 (m, 2H), 1.36-1.16 (m, 4H)

HRMS *m/z*: $C_{34}H_{40}N_5O$ calculated 534.3227 $[M+H]^+$, found 534.3446.

(*S*)-methyl 3-(benzyl(*R*-1-phenylethyl)amino)-3-phenylpropanoate (360)



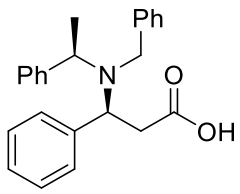
To a solution of amine (**358**) (2.85 g, 2.82 mL, 13.5 mmol, 1.1 eq.) in THF (27 mL) was added at 0°C *n*-BuLi (5.9 mL, 2.5 M in hexane, 1.2 eq.) dropwise and the solution turns to a violet coloured solution. The resultant mixture was stirred at this temperature for 30 min and cooled to -78°C before the dropwise addition of methylcinnamate (**359**) (2.0 g, 2.3 mmol, 1.0 eq.) in THF (19 mL) and the colour of the reaction gets orange. The reaction mixture was stirred at -78°C for 2h. The mixture was quenched with saturated aqueous NH_4Cl (20 mL) and warmed to rt. The aqueous phase was extracted with ethylacetate (3 x 20 mL) and the combined organic layers were dried over $MgSO_4$, filtered and the solvents were evaporated under reduced pressure. The crude product was purified by flash chromatography (petrolether/ ehtylacetate 10:1) to yield methylester (**360**) as a yellow oil (1.5 g, 33%).

^{1}H-NMR (400 MHz, $CDCl_3$) 7.42-7.17 (m, 3 x Ph, 15H), 4.44 (dd, *J*= 5.9, 9.3 Hz, H-3, 1H), 4.00 (q, *J*= 7.3, 13.7 Hz, C**H**-Ph, 1H), 3.70 (dd, *J*= 14.8, 34.8 Hz, C**H**$_2$-Ph, 2H), 3.46 (s, OMe, 3H), 2.68 (dd, *J*= 5.8, 15.0 Hz, H-2, 1H), 2.50 (dd, *J*= 9.3, 15.0 Hz, H-2, 1H), 1.21 (d, *J*= 7.0 Hz, Me, 3H)

^{13}C-NMR (100 MHz, $CDCl_3$) δ/ppm 172.3, 144.1, 141.8, 141.4, 128.4, 128.2 (2), 128.1, 127.9, 127.3, 126.9, 126.7, 59.3, 56.8, 51.5, 50.8, 37.6, 15.9

HRMS *m/z*: $C_{25}H_{28}NO_2$ 374.2115 $[M+H]^+$, found 374.1536.

(*S*)-3-(benzyl(R-1-phenylethyl)amino)-3-phenylpropanoic acid (361)



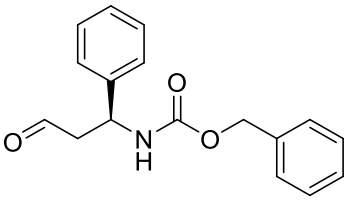
To a solution of methylester (**360**) (0.2 g, 0.5 mmol, 1.0 eq.) in a mixture of MeOH /i-PrOH (0.15 mL, 0.05 mL) was added aqueous NaOH (1.5 mL, 1.5 M) and stirred at rt overnight. After one night THF (0.5 mL) was added to dissolve all starting material and the reaction mixture was stirred for a further night. The reaction mixture was diluted with DCM (10 mL) and water (10 mL). The phases were separated and the aqueous phase was adjusted to pH=2 with 1N HCl. The aqueous phase was washed extracted with ethylacetate (10 mL) and the combined organic layers were washed with brine (2 x 10 mL), dried over MgSO4, filtered and the solvent was evaporated under reduced pressure. The crude product was purified by flash chromatography (petrolether/ ethylacetate: 5:1) to yield acid (**361**) (70 mg, 42%) as a colorless oil.

^{1}H-NMR (400 MHz, $CDCl_3$) δ/ppm 7.39-7.21 (m, 3x Ph, 15H), 4.47 (dd, *J*= 6.8, 8.5 Hz, H-3, 1H), 4.12 (q, *J*= 6.9, 14.2 Hz, CH-Ph, 1H), 3.90 (d, *J*= 14.2 Hz, CH_2-Ph, 1H), 3.68 (d, *J*= 17.1 Hz, CH_2-Ph, 1H), 2.28 (dd, *J*= 9.2, 16.3 Hz, H-2, 1H), 2.51 (dd, *J*= 5.7, 14.9 Hz, H-2, 1H), 1.25 (d, *J*= 6.3 Hz, Me, 3H)

^{13}C-NMR (100 MHz, $CDCl_3$) δ/ppm 174.9, 141.8, 139.0, 138.5, 128.8, 128.7, 128.6 (2), 128.5, 128.2, 128.1, 127.7, 127.5, 60.5, 58.5, 57.7, 50.7, 36.3, 30.9, 15.8

HRMS m/z $C_{24}H_{26}NO_2$ calculated, 360.1958 $[M+H]^+$, found 360.1990.

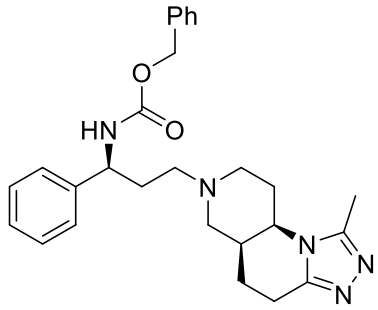
Benzyl (*S*)-(3-oxo-1-phenylpropyl)carbamate (362)



To a solution of ester **356** (250 mg, 0.79 mmol, 1 eq.) was added in dichlormethane (2.5 mL) at -78°C DIBAL-H (0.9 mL, 1.1 eq) and stirred at this temperature for 30 min. The reaction mixture was diluted with saturated aqueous Rochelles salt/ diethylether (2:1, 100 mL: 50 mL). The aqueous phase was extracted with diethylether (3 x 50 mL). The combined organic phases were washed with saturated aqueous sodiumchloride (50 mL). The combined organic phases were dried over Na_2SO_4, filtered and the solvent evaporated under reduced pressure to yield aldehyde **338** (133 mg, 60%) which was used further without purification.

^{1}H-NMR (400 MHz, $CDCl_3$) δ/ppm 9.74 (s, CHO, 1H), 7.39-7.29 (m, 2x Ph, 10H), 5.40 (bs, NH, 1H), 5.29 (m, H-3, 1H), 5.10-5.08 (m, CH_2-Ph, 2H), 3.07-2.84 (m, H-2, 2H)

Benzyl ((*S*)-3-((5a*S*,9a*R*)-1-methyl-4,5,5a,8,9,9a-hexahydro-[1,2,4]triazolo[4,3-a][1,6]naphthyridin-7(6*H*)-yl)-1-phenylpropyl)carbamate (367)



To a solution of aldehyde **362** (530 mg, 1.5 mmol, 1.4 eq.) in 1,2 dichloroethane (6.3 mL) was added sodiumtriactetoxyborohydride (386 mg, 1.8 mmol, 1.2 eq.) and amine **194** (200 mg, 1.0 mmol, 1.7 eq.) and stirred for overnight at rt. The crude reaction mixture was diluted with saturated aqueous sodiumbicarbonate (25 mL). The aqueous phase was extracted with ethylacetate (3 x 25 mL). The combined organic phases were dried over Na_2SO_4, filtered and the solvent was evaporated under reduced pressure. The crude product was purified by flash chromatography (dichloromethane/ methanol, 10:1) and amine **367** (40 mg, 57 %) was yielded as a colorless oil, which was further purified by preparative HPLC.

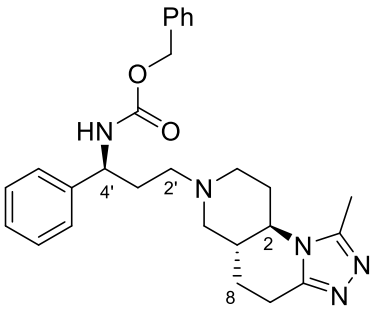
HPLC: (t_R= 15.2 min, 97%)

^{1}H-NMR (400 MHz, $CDCl_3$) δ/ppm 7.37-7.22 (m, 10H), 7.13 (m, 1H), 5.16-5.03 (m, 1H), 4.96-4.83 (m, 2H), 3.97-3.91 (m, 1H), 3.11-2.53 (m, 4H), 2.40 (s, Me, 4H), 2.39-2.19 (m, 3H), 2.11-1.69 (m, 9H)

^{13}C-NMR (100 MHz, $CDCl_3$) δ/ppm 156.0 (2), 150.4, 149.3, 136.6, 136.5, 128.7 (2), 127.4, 126.2, 67.7, 66.9, 66.8, 54.9, 54.4, 52.1, 42.5, 34.5, 34.0, 32.2, 21.5, 21.2, 19.7, 10.6

HRMS *m/z* $C_{27}H_{34}N_5O_2$ calculated, 460.2707 $[M+H]^+$, found 460.2319.

Benzyl ((*S*)-3-((5a*R*,9a*R*)-1-methyl-4,5,5a,8,9,9a-hexahydro-[1,2,4]triazolo[4,3-a][1,6]naphthyridin-7(6*H*)-yl)-1-phenylpropyl)carbamate (368)



To a solution of aldehyde **362** (331 mg, 0.9 mmol, 1.1 eq.) in 1,2 dichloroethane (5 mL) was added sodiumtriactetoxyborohydride (244 mg, 1.15 mmol), acetic acid (47 µL) and amine **194** (170 mg, 0.8 mmol, 1.4 eq.) in 1,2 dichloroethane (2 mL) and stirred for overnight at rt. The

crude reaction mixture was diluted with saturated aqueous sodiumbicarbonate (10 mL). The aqueous phase was extracted with ethylacetate (3 x 25 mL). The combined organic phases were dried over Na_2SO_4, filtered and the solvent was evaporated. The crude product was purified by flash chromatography (petrol ether/ ethyl acetate, 2:1) and amine **368** (217 mg, 57 %) was yielded as colorless oil, which was further purified by preparative HPLC.

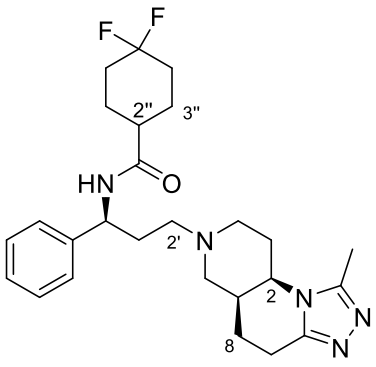
HPLC (t_R= 14.41 min, 98%)

^{1}H-NMR (400 MHz, $CDCl_3$) δ/ppm 7.36-7.21 (m, 2 x Ph, 10H), 6.90-6.77 (2 x bs, NH, 1 H), 5.17-5.06 (m, H-4 or H-6, 1H), 5.01-4.93 (m, H-4 or H-6, 1H), 4.90-4.81 (m, H-4', 1H), 3.49-3.17 (m, CH_2-CBz, H-2, 2H), 3.15-2.86 (m, H-9, H-4, H-6, 3H), 2.78-2.67 (m, H-9, 1H), 2.52-2.46 (m, H-3, 1H), 2.44 (2s, Me, 3H), 2.41-2.30 (m, H-2', 2H), 2.14-1.99 (m, H-3'. 2H), 1.93-1.69 (m, H-8, H-3, H-7, 5H), 1.55-1.42 (m, H-8, 1H)

^{13}C-NMR (100 MHz, $CDCl_3$) δ/ppm 155.9, 152.1, 149.9, 136.6, 128.5, 128.3, 127.9, 127.1, 126.1, 66.4, 59.2, 58.9, 57.8, 54.5, 52.3, 51.6, 42.4, 40.8, 40.7, 32.8, 30.5, 30.3, 24.9, 22.6, 14.0

LCMS *m/z* 460.2 $[M+H]^+$, 1.99 min.

4,4-difluoro-*N*-((*S*)-3-((5a*S*,9a*R*)-1-methyl-4,5,5a,8,9,9a-hexahydro-[1,2,4]triazolo[4,3-a][1,6]naphthyridin-7(6*H*)-yl)-1-phenylpropyl)cyclohexane-1-carboxamide (**370**)



To a solution of CBz protected amine **367** (200 mg, 0.4 mmol, 1 eq.) in methanol (7 mL) was added Pd/C and stirred under an atmosphere of hydrogen overnight. The crude product was filtered through celite and the solvent was evaporated under reduced pressure. The crude product was used further in the next step.

To acid **349** (38 mg, 0.2 mmol, 1.5 eq.) in DMF (3.5 mL) was added DIPEA (56 µL, 0.3 mmol, 3.0 eq.), HATU (50 mg, 0.13 mmol, 1.2 eq) and amine **194** (50 mg, 0.15 mmol, 1.0 eq.) and stirred at rt for 2h. The reaction mixture was diluted with water (10 mL). The aqueous phase was extracted with ethylacetate (3 x 10 mL) and the combined organic phases were washed with saturated aqueous ammoniumchloride (10 mL), dried over Na_2SO_4, filtered and the solvent was evaporated under reduced pressure. The crude product was purified by flash chromatography (dichloromethane/ methanol 20:1) to

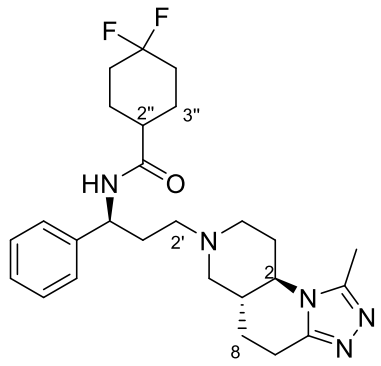
yield amine **370** (68 mg, 33%) as a white solid after further purification using preparative HPLC.

HPLC (t_R 12.64 min, 100%)

^{1}H-NMR (400 MHz, $CDCl_3$) δ/ppm 7.39-7.26 (m, 5H), 6.37 (dd, *J*= 8.2 Hz, NH, 0.5H), 6.22 (d, *J*= 7.5 Hz, NH, 0.5H), 5.15-5.05 (2q, *J*= 7.55 Hz; 6.92 Hz, 1H), 4.02-3.96 (m, 1H), 3.26-3.16 (m, 1H), 3.12-3.09 (m, 0.5H), 3.02-2.98 (m, 0.5H), 2.94-2.91 (m, 0.5H), 2.88-2.83 (m, 1.5H), 2.42 (s, Me, 3H), 2.34-2.12 (m, 6H), 2.06-1.76 (m, 13H)

HRMS *m/z* $C_{26}H_{36}F_2N_5O$ calculated, 472.2882 $[M+H]^+$, found 472.2845.

4,4-difluoro-*N*-((*S*)-3-((5aR,9aR)-1-methyl-4,5,5a,8,9,9a-hexahydro-[1,2,4]triazolo[4,3-a][1,6]naphthyridin-7(6H)-yl)-1-phenylpropyl)cyclohexane-1-carboxamide (372)



To a solution of CBz protected amine **368** (97 mg, 0.2 mmol, 1.0 eq.) in methanol (1 mL) was added Pd/C and stirred under an atmosphere of hydrogen overnight. The crude product was filtered through celite and the solvent was evaporated under reduced pressure. The crude product was used further in the next step.

To acid **349** (20 mg, 0.12 mmol, 1.5 eq.) in DMF (2.5 mL) was added DIPEA (33 µL, 0.24 mmol, 3.0 eq.), HATU (37 mg, 0.1 mmol, 1.2eq) and amine (26 mg, 0.1 mmol, 1.0 eq.) and stirred at rt for 2h. The reaction mixture was diluted with water (10 mL). The aqueous phase was extracted with ethylacetate (3 x 10 mL) and the combined organic phases were washed with saturated aqueous ammoniumchloride (10 mL), dired over Na_2SO_4, filtered and the solvent was evaporated under reduced pressure. The crude product was purified by flash chromatography (dichloromethane/ methanol 20:1) and SCX column chromatography (dichloromethane → methanol →7N ammonia in methanol) to yield amine **372** (9 mg, 24%) as a white solide after further purification using preparative HPLC.

HPLC (t_R 12.17 min, 98 %)

^{1}H-NMR (400 MHz, $CDCl_3$) δ/ppm 7.36-7.24 (m, Ph, 5H), 6.89-6.84 (m, NH, 1H), 5.05 (q, *J*= 7.0 Hz, H-4', 1H), 3.55 (t, *J*= 10.8 Hz, H-2, 1H), 3.26 (d, *J*= 11.3 Hz, H-4 or H-6, 1H), 3.20-3.15 (m, H-9, H-4 or H-6, 2H), 2.92-2.83 (m, H-9, 1H), 2.68 (dt, *J*= 2.5, 12.6 Hz, H-2', 1H), 2.49 (d, OMe, 3H), 2.34-2.24 (m, H-4 or H-6, 1H), 2.22-1.66 (m, H-7, H-4, H-6, H-2', H-3'', H-4'', H-2'', H-8, H-3, H-3', 18H), 1.62-1.52 (m, H-8, 1H)

^{13}C-NMR (100 MHz, $CDCl_3$) δ/ppm 173.6, 151.9, 149.9, 141.4, 128.8, 127.6, 124.4, 120.6 (q, C-5''), 58.8 (C-2), 57.4 (C-4 or C-6), 54.5, 52.1 (C-4'), 42.9 (C-2''), 40.2 (C-7), 32.9 (C-3'', C-4'' or C-3'), 32.6 (C-3'', C-4'' or C-3'), 32.2 (C-3'', C-4''or C-3'), 29.9 (C-2'), 26.0 (C-3), 25.0 (C-8), 22.7 (C-9), 14.1 (Me)

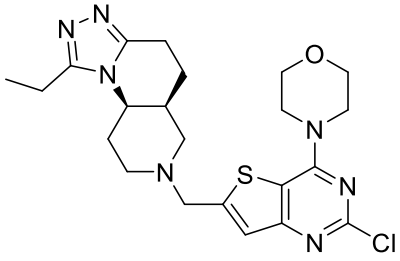
HRMS m/z $C_{26}H_{36}NF_2O_2$ calculated, 472.2882 $[M+H]^+$, found 472.2924.

10.10 Synthesis of pi3 Kinase inhibitors

General procedure for reductive amination

To amine **194** (0.2 mmol, 1.0 eq.) in a mixture of methanol/ acetic acid (10:1, 4.5 mL: 0.5 mL) was added aldehyde **382** (0.3 mmol, 1.5 eq.) and the suspension was heated to 40°C for 30 min. Picolinoborane (0.3 mmol, 1.5 eq.) was added to the yellow suspension and stirred overnight at rt. The suspension was diluted with saturated aqueous sodiumbicarbonate (15 mL) and the aqueous phase was extracted with ethylacetate (3 x 15 mL). The combined organic phases were dried over Na_2SO_4, filtered and the solvent was evaporated under reduced pressure. The crude product was purified by extensive flash chromatography (dichloromethane/ methanol 10:1) and SCX column purification (DCM→ MeOH → 7N ammonia/ MeOH) to yield compound **383-384** as an oil (still as mixture of both enantiomers).

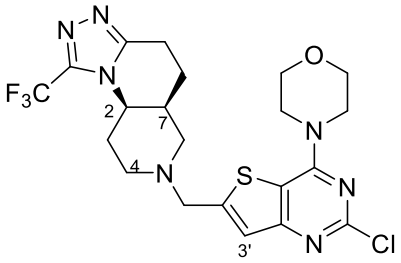
4-(2-chloro-6-(((5aS,9aR)-1-ethyl-4,5,5a,8,9,9a-hexahydro-[1,2,4]triazolo[4,3-a][1,6]naphthyridin-7(6H)-yl)methyl)thieno[3,2-d]pyrimidin-4-yl)morpholine (383)



(26%)

^{1}H-NMR (400 MHz, $CDCl_3$) δ/ppm 7.13 (s, 1H), 4.04-3.93 (m, 5H), 3.84-3.71 (m, 6H), 3.19 (dd, *J*= 5.4, 17.1 Hz, 1H), 3.06-2.95 (m, 2H), 2.87-2.71 (m, 1H), 2.70-2.59 (m, 2H), 2.48-2.37 (m, 2H), 2.22-2.11 (m, 2H), 1.97-1.78 (m, 3H), 1.39 (t, *J*= 7.5 Hz, 3H)

4-(2-chloro-6-(((5aS,9aR)-1-(trifluoromethyl)-4,5,5a,8,9,9a-hexahydro-[1,2,4]triazolo[4,3-a][1,6]naphthyridin-7(6H)-yl)methyl)thieno[3,2-d]pyrimidin-4-yl)morpholine (384)



(48%)

^{1}H-NMR (400 MHz, $CDCl_3$) δ/ppm impurities in aromatic region, 6.94-6.89 (m, H-3', 1H), 4.30 (dt, *J*= 4.2, 11.9 Hz, H-2, 1H), 4.04-3.92 (m, CH_2-morpholine, 4H), 3.84-3.70 (m, CH_2-morpholine, CH_2-thiazole, H-4 or H-6, 7H), 3.26 (dd, *J*= 6.6, 18.1 Hz, H-9, 1H), 3.02-2.96 (m, H-4, H-6, 2H), 2.91-2.79 (m, H-9, 1H), 2.55 (m, H-9, 1H), 2.36-2.29 (m, H-2 or H-6, 1H), 2.2-2.11 (m, H8, H-7, 2H), 2.10-2.03 (m, H-3, 1H), 1.98-1.88 (m, H-3, 1H), 1.86-1.80 (m, H-8, 1H)

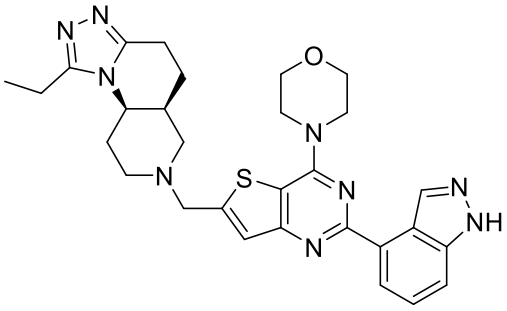
^{13}C-NMR (100 MHz, $CDCl_3$) δ/ppm 162.4, 162.2, 160.3, 157.9, 154.1, 153.4, 149.5, 148.8, 143.2, 142.8, 139.8, 136.7, 132.3, 132.2, 123.6, 123.4, 120.1 (2), 117.6, 117.5, 66.9 (CH_2-morpholin), 66.7 (CH_2- morpholin), 56.9 (2) (CH_2-thiazole), 54.4 (C-4) 52.3 (C-6), 46.5 (C-2), 34. (C-7), 29.7 (C-3), 21.4 (C-9), 20.2 (C-8)

HRMS m/z $C_{21}H_{24}ClF_3N_7OS$ calculated, 514.1398 $[M+H]^+$, found 514.6035.

General procedure for Suzuki coupling

The triazole compounds **383-384** (1.0 eq.) was dissolved in ethanol and sodiumcarbonate (2M, 3 eq.), trans-dichlorobis $(PPh_3)_2$ Pd(II)Cl_2 (0.1 eq.) and the corresponding boronic acid ((3-hydroxyphenyl)boronic acid **385**, (1H-indazol-4-yl)boronic acid **386)** (1.5 eq.) were added to the mixture and heated in the microwave at 140°C for 1h. The reaction mixture was filtered over celite and the filtrate was concentrated under reduced pressure. The crude products were purified by flash chromatography (dichloromethane / methanol 10:1 + 0.2% 7N ammonia in methanol) to yield triazole compounds **381, 387-388**.

4-(6-(((5aS,9aR)-1-ethyl-4,5,5a,8,9,9a-hexahydro-[1,2,4]triazolo[4,3-a][1,6]naphthyridin-7(6H)-yl)methyl)-2-(1H-indazol-4-yl)thieno[3,2-d]pyrimidin-4-yl)morpholine (381)

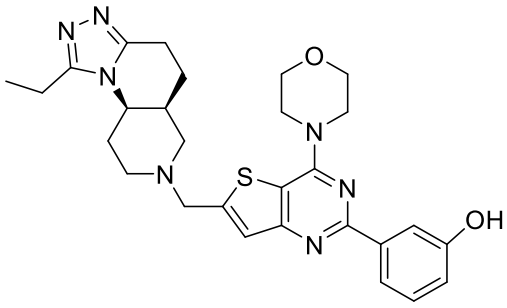


(35 %**)**

^{1}H-NMR (400 MHz, $CDCl_3$) δ/ppm 8.98 (s, 1H), 8.28 (d, *J*= 7.30 Hz, 1H), 7.61 (d, *J*= 8.1 Hz, 1H), 7.50 (d, *J*= 6.9 Hz, 1H), 7.42 (s, 1H), 4.12-3.99 (m, 54H), 3.94-3.85 (m, 6H), 3.25 (dd, *J*= 5.4, 16.5 Hz, 1H), 3.11-3.02 (m, 2H), 2.89-2.78 (m, 1H), 2.75-2.65 (m, 2H), 2.53-2.43 (m, 2H), 2.23 (dt, *J*= 3.1, 11.7 Hz, 1H), 2.14-1.99 (m, 1H), 1.91-1.83 (m, 4H), 1.43 (t, *J*= 7.7 Hz, 3H)

LCMS *m/z* 556.2 $[M+H]^+$, 2.07 min.

3-(6-(((5a*S*,9a*R*)-1-ethyl-4,5,5a,8,9,9a-hexahydro-[1,2,4]triazolo[4,3-a][1,6]naphthyridin-7(6*H*)-yl)methyl)-4-morpholinothieno[3,2-d]pyrimidin-2-yl)phenol (387)

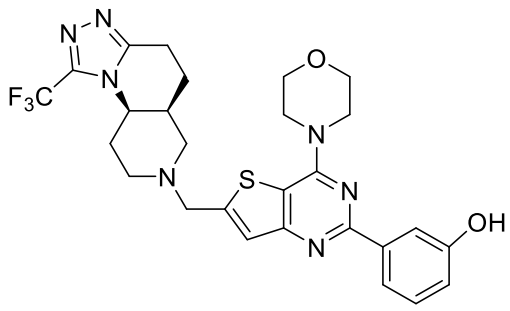


(11 %)

^{1}H-NMR (400 MHz, $CDCl_3$) δ/ppm 7.97-7.94 (s, 2H), 7.35 (s, 1H), 7.31 (t, *J*= 7.8Hz, 1H), 6.98 (dt, *J*= 1.6, 8.1 Hz, 1H), 4.07-3.99 (m, 4H), 3.90-3.85 (m, 4H), 3.79 (q, *J*= 13.7 Hz, 2H), 3.23 (dd, *J*= 6.9, 17.7 Hz, 1H), 3.06 (t, *J*= 11.9 Hz, 2H), 2.86-2.75 (m, 1H), 2.73-2.62 (m, 2H), 2.50-2.40 (m, 2H), 2.27-2.15 (m, 2H), 1.97-1.80 (m, 3H), 1.42 (t, *J*= 7.9 Hz, 3H)

LCMS *m/z* 531.4 $[M+H]^+$, 2.02 min

3-(4-morpholino-6-(((5aS,9aR)-1-(trifluoromethyl)-4,5,5a,8,9,9a-hexahydro-[1,2,4]triazolo[4,3-a][1,6]naphthyridin-7(6H)-yl)methyl)thieno[3,2-d]pyrimidin-2-yl)phenol (388)



(40 %)

^{1}H-NMR (400 MHz, $CDCl_3$) 7.98-7.93 (m, 1H), 7.44 (m, 1H), 7.31 (t, *J*= 9.5 Hz, 1H), 6.95 (ddd, *J*= 1.5, 1.9, 17.1 Hz, 1H), 4.35 (dt, *J*= 4.1, 12.5 Hz, 1H), 4.09-3.98 (m, 4H), 3.94 (m, 1H), 3.88-3.73 (m, 5H), 3.31 (dd, *J*= 7.1, 16.6 Hz, 1H), 3.07-3.00 (m, 1H), 2.96-2.87 (m, 1H), 2.61-2.59 (m, 1H), 2.49-2.43 (m, 1H), 2.30-2.19 (m, 2H), 2.15-1.84 (m, 5H)

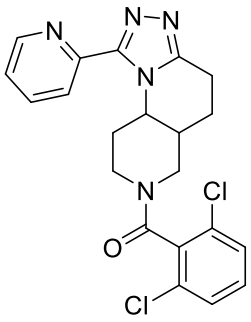
LCMS *m/z* 571.9 $[M+H]^+$, 2.31 min.

10.11 Synthesis of $P2X_7$ analogues

General Procedure for amide coupling

To amine **194** (0.22 mmol, 1.0 eq.) in dichloromethane (1 mL) at 0°C were added triethylamine (0.34 mmol, 1.5 eq.) and the corresponding acid chloride (0.23 mmol, 1.05 eq.) (2-chloro-4-fluorobenzoyl chloride **405**/ 2,6-dichlorobenzoyl chloride **406**) and the reaction mixture was stirred overnight at rt. The reaction mixture was diluted with dichloromethane (10 mL) and water (10 mL) and the mixture was stirred until everything is dissolved. The layers were separated and the aqueous layer was extracted with dichloromethane (3 x 10 mL). The combined organic phases were washed with saturated aqueous $NaHCO_3$ (10 mL) and saturated aqueous NaCl (10 mL) and dried over Na_2SO_4. The solid was filtered and the solvent was evaporated under reduced pressure. The crude product was purified by flash chromatography (dichlormethane/ 7N ammonia in methanol 10:1) or SCX (dichloromethane → methanol →7N ammonia in methanol) to yield amide **376-381** as oils.

(2,6-dichlorophenyl)(1-(pyridin-2-yl)-4,5,5a,8,9,9a-hexahydro-[1,2,4]triazolo[4,3-a][1,6]naphthyridin-7(6H)-yl)methanone (411)

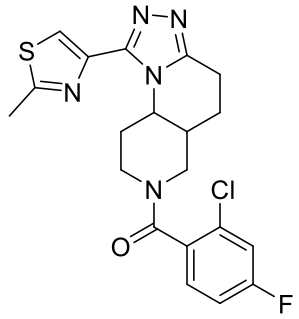


(30%), **HPLC** (t_R= 11.23 min)

^{1}H-NMR (400 MHz, $CDCl_3$) δ/ppm 8.58 (m, 1H), 8.37, 8.34 (2dt, *J*=0.9, 8.1 Hz, 1H), 7.85-7.77 (m, 1H), 7.40-7.26 (m, 4H), 5.65-5.54 (m, 1H), 4.99 (dt, *J*= 2.2, 13.6 Hz, 1H), 3.64-3.18 (m, 4H), 3.10-2.89 (m, 2H), 2.51-2.46 (m, 1H), 2.36-2.24 (m, 1H), 2.21-2.09 (m, 2H), 1.80-1.63 (m, 1H)

HRMS *m/z* $C_{21}H_{20}Cl_2N_5O$ calculated, 428.1039 $[M+H]^+$, found 428.0316.

(2-chloro-4-fluorophenyl)(1-(2-methylthiazol-4-yl)-4,5,5a,8,9,9a-hexahydro-[1,2,4] triazolo[4,3-a][1,6]naphthyridin-7(6H)-yl)methanone (412)

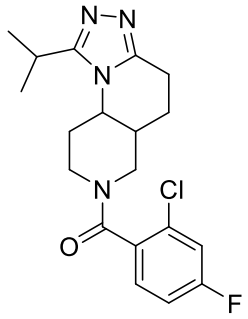


(45 %), **HPLC** (t_R= 12.12 min)

^{1}H-NMR (400 MHz, $CDCl_3$) δ/ppm 7.97, 7.94 (2s, 1H), 7.22-6.98 (m, 3H), 5.37-5.24 (m, 1H), 5.00-4.79 (m, 2H), 4.33-4.22 (m, 1H), 3.58-3.36 (m, 2H), 3.33-2.84 (m, 3H), 2.79-2.66 (m, 3H), 2.48-2.33 (m, 1H), 2.30-2.17 (m, 1H), 2.14-2.06 (m, 1H)

HRMS *m/z* $C_{20}H_{20}ClFN_5OS$ calculated, 432.1056 $[M+H]^+$, found 432.0279.

(2-chloro-4-fluorophenyl)(1-isopropyl-4,5,5a,8,9,9a-hexahydro-[1,2,4] triazolo[4,3-a][1,6]naphthyridin-7(6H)-yl)methanone (408)

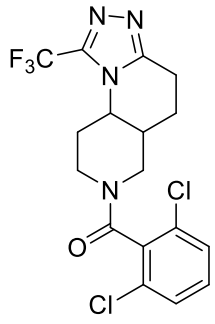


(35 %), **HPLC** (t_R= 10.65 min)

^{1}H-NMR (400 MHz, $CDCl_3$) δ/ppm 7.24-7.14, 7.12-7.03 (m, 3H), 5.09-4.88 (m, 1H), 4.29-4.19 (m, 1H), 3.86-3.76 (m, 0.5H), 3.69-3.58 (m, 0.5H), 3.56-3.44 (m, 1H), 3.29-3.03 (m, 3H), 2.13-1.81 (m, 3H), 1.48 (d, *J*= 6.8 Hz, 1.5H), 1.43 (d, *J*= 6.4 Hz, 1.5H), 1.36 (d, *J*= 6.4 Hz, 1.5H), 1.31 (d, *J*= 6.8 Hz, 1.5H)

HRMS *m/z* $C_{19}H_{23}ClFN_4O$ calculated, 377.1539 $[M+H]^+$, found 377.0994.

(2,6-dichlorophenyl)(1-(trifluoromethyl)-4,5,5a,8,9,9a-hexahydro-[1,2,4]triazolo[4,3-a][1,6]naphthyridin-7(6H)-yl)methanone (409)



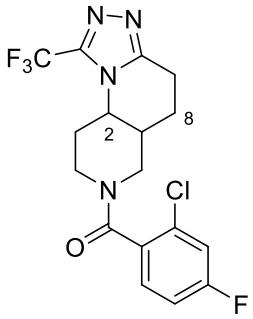
(25%) **HPLC** (t_R= 13.18 min)

^{1}H-NMR (400 MHz, MeOD$_4$) δ/ppm 7.51-7.41 (m, 3H), 4.98-4.89 (m, 1H), 4.26 (tt, *J*= 2.9, 10.8 Hz, 1H), 3.63-3.59 (m, 0.5H), 3.52-3.39 (m, 1.5H), 3.28-3.20 (m, 1H), 3.19-3.06 (m, 1.5H), 3.05-2.96 (m, 0.5H), 2.92 (dd, *J*= 11.6, 12.9 Hz, 1H), 2.72 (dd, *J*= 2.6, 12.6 Hz, 0.5H), 2.55 (dd, *J*= 2.9, 12.2 Hz, 0.5H), 2.17-2.04 (m, 2H), 1.94 (dq, *J*= 4.5, 12.4 Hz, 1H), 1.78 (dq, *J*= 5.8, 13.4 Hz, 1H)

HRMS *m/z* $C_{17}H_{16}Cl_2F_3N_4O$ calculated, 419.0648 $[M+H]^+$, found 418.9954.

(2-chloro-4-fluorophenyl)(1-(trifluoromethyl)-4,5,5a,8,9,9a-hexahydro-[1,2,4]triazolo[4,3-a][1,6]naphthyridin-7(6H)-yl)methanone (407)

(38%), **HPLC** (t_R= 12.07 min)



^{1}H-NMR (400 MHz, CDCl$_3$) δ/ppm 7.23-7.15, 7.12-7.03 (m, 3H), 5.11-4.89 (m, 1H), 4.60-4.51 (m, 0.5H), 4.01-3.90 (m, 0.5H), 3.71-3.62 (m, 1H), 3.57-3.46 (m, 1H), 3.40-2.87 (m, 3H), 2.81-2.68 (m, 1H), 2.57-2.39 (m, 1H), 2.36-2.05 (m, 1H), 2.02-1.74 (m, 2H)

HRMS *m/z* $C_{17}H_{16}ClF_4N_4OCl$ calculated, 403.0943 $[M+H]^+$, found 403.0432.

10.12 Pharmacology

10.12.1 General Material

All general materials used were purchased from Sigma Aldrich unless otherwise mentioned. cAMP reagent was purchased from Promega (E1291), Fluo-4 was obtained from Life Technologies (F14201). G418, Lipofectamine and Optimem were obtained from Invitrogen (Paisley, UK) Pluronic acid F-127 was purchased from ThermoFisher Scientific

10.12.2 Molecular cloning

The competent One Shot TOP10F' *E. coli* was obtained from Invitrogen (C3030-03, C3030-06). The CCR-5 plasmid was obtained from the cDNA.org library (CCR050TN00). The LB agar plates were kindly provided by Richard Proudman.

10.12.3 Transformation of bacterial cells

One vial of the One Shot TOP10F' cells was placed on ice and the transformation was carried out by adding 1 μL of the CCR-5 DNA directly to the competent cells followed by gentle mixing. The vial was incubated for 30 minutes on ice and will be place for 30 seconds at 42°C. Afterwards the vial was shaked for 1h, followed by spreading 50 μL from the transformation vial on a prewarmed LB agar plate containing 100 μg/mL ampicillin. The plates were inverted and incubated at 37°C overnight. Maxi-Preparation of plasmid DNA Preparation

The Maxi preparation of the plasmid DNA was carried out following the procedure by Sigma Aldrich using the GenElute HP Plasmid Maxiprep Kit.

Two times 5 mL of LB media were prepared in a universal and a single colony from the LB agar plate described in section 11.12.3 was chosen and added into each universal, which was incubated at 37^{o}C with agitation for the whole day. After the LB media in the universals was getting cloudy, the whole universal was added to a prepared 500 ml conical flask containing LB media (2g / 100mL) and 100 μg/mLampicillin. This suspension was incubated at 37^{o}C with agitation overnight.

The following morning, the 100 ml bacterial culture was pelleted (4000 rpm for 10 min) and the supernatant discarded. 12 mL of the Resuspension/RNase A solution was added and the pellet was completely resuspended by pipetting up and down. The next step was the lysing of the resuspened cells by adding 12 mL of the Lysis solution and the mixture was inverted 8 times and then left standing for 5 minutes. This is followed by the preparation of a filter syringe by removing the plunge and placing the syringe barrel upright in a rack. The next step in the DNA preparation procedure is the addition of 12 mL of the cooled Neutralization solution to the lysed cells and inverted 6 times, where a white aggregate formed. 9 mL of the binding solution was then added and inverted 2 times and the solution was immediately poured into the barrel of the syringe. The solution was allowed to sit for 5 minutes in the barrel whilst the white aggregate floated to the top. A GenElute Binding column was placed

in a 50 mL collection tube and 12 mL of the column preparation solution was added and centrifuged at 3000 rpm for 2 minutes. The eluate was discarded and in the next step the filter syringe was placed over the binding column and by applying gently pressure through the plunger the lysate (only one third) was added to the column and centrifuged at 3000 rpm for 2 minutes. This procedure was repeated three times and the eluate was discarded after each centrifugation step. This was followed by adding 12 mL of Wash solution 1 to the column and spinning at 3000 rpm for 2 minutes, which was repeated once more by using 12 mL of Wash solution 2 and spinning for 5 minutes. In the final step the column was placed in a 50 mL collection tube and 3 mL of the elution solution was added to the column and centrifuged at 3000 rpm for 5 minutes. And the eluate was divided and stored in two 1.5 ml microcentrifuge tubes at -20C (labelled CCR-5 in pc DNA 3-1, 270 ng/mL, CS, 06/03/2014).

The concentration of the plasmid DNA was determined using a spectrophotometer (Eppendorf) to be 270 ng/mL.

10.12.4 Cell lines used

Human Embryonic Kidney (HEK) 293 cells expressing the Glosensor cAMP biosesnor Glosensor was obtained from Promega (E1261). HEK Glosensor cells expressing the CXCR-4 receptor were kindly provided by Dr. Joelle Goulding. The HEK Glosensor cell line expressing the CCR-5 receptor was generated as part of this work and details can be found in section 11.12.7.

10.12.5 General cell culture

All reagents were obtained from Sigma Aldrich. The culture T75/T25 flasks were obtained from Sarstedt, The 96 well plates back walled, clear bottom were purchased from Costar and the white walled 96 well plates were from Greiner. The 96- well clear compound plates were obtained from costar and the 24 well clear plates and the 6 well clear plates were obtained from Sarstedt. The cells used throughout this study were cultured using Dulbecco's Modified Eagle's Medium D6429 (DMEM), which was supplemented with fetal bovine serum (10%) (complete media), incubated at 37C with 5% CO_2 and all cell culture procedures were carried out in a sterile hood using sterile techniques.

10.12.6 Passaging of cells

The cells were passaged when reaching a confluence of ~80%. The first step was the aspiration of the complete media, followed by washing the cells with PBS (~5 mL). Trypsin/EDTA (1 mL) was added to remove the attached cells (incubation at 37°C, 5% CO_2,

5 min if required). Afterwards 10 mL of the complete media was added and the cell suspension was centrifuged at 1000 rpm for 5 minutes. The supernatant was discarded and the resulting pellet was resuspended using 10 mL of complete media and the corresponding amount (1 mL for 1/10, 0.5 mL for 1/20) was added to a new T75 flask containing 20 mL of complete media and incubated at 37C, 5% CO_2.

10.12.7 Generation of CCR-5 stable cell line

The transfection for the generation of the HEK 293 Glosensor cells expressing CCR-5 was carried out in a sterile hood applying sterile techniques. 3 μg DNA (11.1 μL of CCR-5 DNA), 30 μL Lipofectamine and 330 μL optimem (transfection mix) were combined and incubated for 2 hours in the sterile hood. The confluent ~ 70% T25 flasks of HEK 293 Glosensor cells were washed once with optimem and 3 mL optimem was added to the T75 flask. After the 2 hours incubation the transfection mix was added to the cells in the T75 flasks and incubated for 24h at 37°C, 5% CO_2. After 24h the transfection mix was aspirated and replaced by 10 mL complete media containing 1 mg/mL G418. The media was changed accordingly to the confluence of the cells and 1 mg/mL G418 was added to each new T75 flask.

The cells expressing CCR-5 were passaged as described in chapter 11.12.6 and resuspended in 10 mL complete media and counted using a hemocytometer. To obtain a cell line originating from one cells to ensure homogeneity of expression the following procedure was undertaken. The mixed population of HEK CCR5 cells were passaged as described in chapter 9.10.6, resuspended in 10 mL complete media and the number of cells/mL estimated by counting the cells using a hemocytometer. Then five universals were prepared with the following final concentrations of cells: a) 10 mL complete media containing 10,000 cells/mL, b) 2 x 20 mL complete media containing 200 cells/mL and c) 2 x 20 mL complete media containing 20 cells/mL. Additionally, 100 μL G418 was added in each universal.

For preparation of the universal a) the cells expressing CCR-5 were resuspended using 55 μL of the original 10 mL suspension and were added to the 10 mL of the complete media in universal a). From each of the universals c) 2 mL of the complete media were added to each of the universals b). In the following step 20 μL of the suspension in universal a) were added to each of the universals b). Another 2 mL of the universals b) were transferred into universals c). The cells expressing CCR-5 suspensions in universal b) and c) were seeded at 200 μL/well in a 96 well black walled plate. The cells were fed continuously the next three to

four weeks in which they started growing in the 96 well plates. After reaching ~70% confluence the individual clone was transferred from one well in a 96 well plate into one well in a 24 well plate. Therefore the complete media in the wells was aspirated and the cells were washed with 100 µL of PBS. 50 µL of Trypsin/EDTA was added to each well and the plates were placed in the incubator at 37C, 5% CO_2 for 2 minutes. This was followed by the addition of 1.5 mL complete media in each well of the 24 plate and suspending the cells expressing CCR-5 in a small volume of the complete media and place the cells of each 96 well in one well of the 24 well plate. After 24h the media was replaced with fresh complete media. By reaching ~70% confluence the cells were transferred from each 24 well in one well of the 6 well plate. This was carried out using the above described procedure for transferring the cells into a 24- well plate by changing the amount of PBS and Trypsin/EDTA to 500 µL. And the resuspended cells of each well of the 24 well plate were added in one well of the 6 well plate containing 2 mL complete media. At this stage the individual clones of the HEK293 Glosensor cells expressing CCR-5 were seeded at 200 µL cell suspensions in each well of a 96 well plate following the procedure in chapter 9.10.8 and screened in a Ca^{2+} signaling assay against the agonist MIP-1α to evaluate the quality of the cell line. After reaching ~80% confluence the cells in each well of the 6 well plate were transferred into a T25 flask following the procedure according to chapter 9.10.6 by changing the total volume of complete media to 5 mL/T25 flask.

10.12.8 Seeding of cells

Cells expressing CXCR-4 or CCR-5 were removed from the T75 flask and treated as described in section 9.10.6 and the the resuspended cells were counted using a hemocytometer. The cells suspension was diluted using complete media to achieve a density of 20,000 cells/ µLfor the CXCR-4 expressing cells and 25,000/ µLfor CCR-5 expressing cells by adding 100 µL of the suspension in each well of the 96 well plates. Prior to the addition of the cells into the 96 well plates, the plates were treated using Poly-D-Lysine hydrobromide (50 µL/well of a 0.084 µM sol. in dd H_2O) and incubated for at least 30 min, followed by a complete media (50 µL/well) wash. After addition of the cells, the 96 well plates were incubated for one to two days at 37^{o}C, 5% CO_2 before assaying.

10.12.9 Assays

10.12.9.1 cAMP assay

This assay was carried out using the cells expressing the CXCR-4 receptor and grown in white walled 96-well plates as described in section 9.10.8. The cAMP reagent was prepared by the addition of 300/ 400 µL cAMP reagent (92 mM in 10mM HEPES buffer) was added to 10 mL HBSS complete solution ((1M sol. HBSS composition: 8.460 g NaCl, 0.372 g KCl, 0.246g $MgSO_4$, 2.384 g HEPES, 0.220 g NaPyruvate, 0.126 g $NaHCO_3$, 0.191 g $CaCl_2$ dissolved in 1 L dd H_2O and adjust with 1M NaOH to pH 7.4 and autoclaved) supplemented with 90 mg Glucose and 100 mg BSA/ 50 mL 1x HBSS). 100 µL of the prepared cAMP mix (cAMP in HBSS complete solution) was added in each well of the 96 well plate. The plate was incubated for 2 h at 37°C. In the meantime the concentrations for the concentration response curve of the compounds were prepared (final assay concentrations of 100 µM to 0.1 nM0 in HBSS complete containing 30 µM FSK. 100 µL of each dilution was added in triplicate to the preincubated cells expressing the CXCR-4 receptor to give final assay concentrations of 10 µM to 0.01 nM and the cells were directly screened on the Pherastar (BMG Labtech) at 37°C to measure the luminescence of the cAMP reagent. The luminescence from each well was read every minute for 60 minutes.

10.12.9.2 Ca^{2+} signaling assay

This assay was carried out using the cells expressing the CCR-5 receptor. Therefore 100 µL of HEK 293 Glosensor cells expressing CCR-5 with a density of 2.5 x 10^4 cells/mL were placed in each well of a 96 well black plate and incubated at 37°C, 5% CO_2 for 48h prior to the assay. On the day of experimentthe media was aspirated and replaced with assay buffer. The assay buffer was prepared by adding 90 mg glucose and 50 mg BSA to 50 mL 1 x HBSS (see section 9.10.9.1) and 500 µL of a Probenecid solution (180 mg Probenecid, 1.25 mL 1M NaOH and 1.25 mL assay buffer) (complete assay buffer). 10 mL of the complete assay buffer was supplemented by 23 µL Fluo-4 dye (prepared by adding 23 µL DMSO and 23 µL Pluronic acid 20% in DMSO to Fluo-4 AM) (Fluo-4 buffer). 100 µL Fluo-4 buffer was added to each well of the black walled plate and incubated at 37°C for 45 min. In the meantime the antagonist (compound) solution were prepared by either a single concentration (30 nM, 300 nM, 10 µM in complete assay buffer) or in serial dilutions (100 µM to 0.1 nM in complete assay buffer). The Fluo-4 buffer was aspirated and the cells were washed two times with complete assay buffer. 100 µL complete assay buffer was then added to the wells and 10 µL

of the corresponding concentration of the antagonist was added in triplicate and incubated for 30 min at 37°C to give final concentrations of 3 nM, 30 nM and 1 μM or for the antagonist concentration response curve to give final concentrations of 0.1 mM to 1 nM. In the meantime the agonist concentrations for the dose response curve was prepared by either preparing a single final concentration (300 nM in complete assay buffer) or as serial dilution with final concentrations of 10 μM - 10 nM in half log (MIP-1α) or 100 nM -1 nM in half logs (RANTES). 20 μL of the agonist concentrations were added in triplicate into a clear 96 well plate and were added directly prior to the measurement. The cells were screened on the Flexstation 1 (Molecular Devices) by measuring the intracellular calcium by monitoring the change in fluorescence for 2s every 5 min.

10.12.10 Data analysis

A basal and a FSK control were included in every concentration-response cAMP assay to allow the response of the cell line to be the expressed as of the inhibition of FSK stimulation of cAMP production by normalizing the data to basal and the maximal FSK response. The datapoints showing the peak response of the cAMP. A basal control was included in every concentration-response Ca^{2+} signaling assay to allow the response of the cell line to be the expression of the inhibition of the Ca^{2+} production. Data were normalized to basal and the maximal agonist response. The datapoints monitored for Ca^{2+} were the values for the change (max-min) in fluorescence. Nonlinear regression analysis was carried out using GraphPadPrism 6 (GraphPad Software, San Diego, CA, USA). Concentration response curves were fitted to the following equation:

$$Response = \frac{Emax\ x[A]}{[A]+EC50}$$

where E_{max} is the maximal response, EC_{50} the molar agonist concentration required to generate 50% of E_{max} and [A] is the concentration of agonist. .

Estimated affinity values (pK_D) of **346-348** were calculated from the shift of the dose response curve of the agonist at a single concentration of **346 +348** (30 nM) and **347** (1000 nM) using the following Gaddum equation:

$$K_D = \frac{[B]}{DR-1}$$

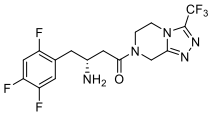
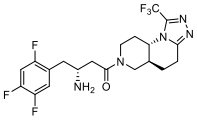
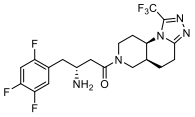
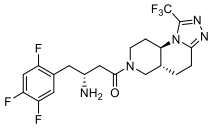
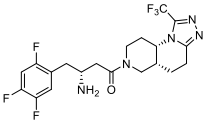
where DR (dose ratio) is the ratio of agonist concentration required to achieve an identical response in the presence or absence of the antagonist [B]. The calculated results were mean values ± SEM mean.

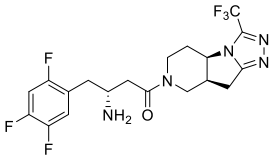
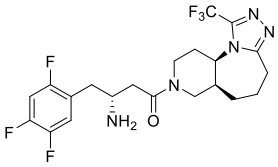
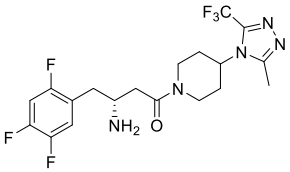
10.13 Molecular Docking studies

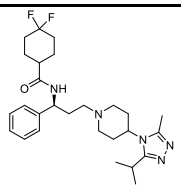
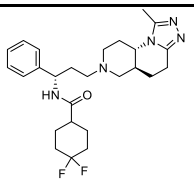
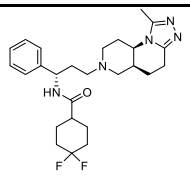
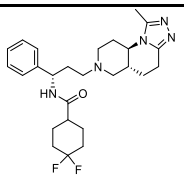
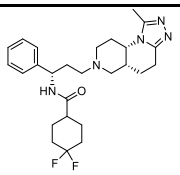
To explain a rationale for the inhibitory activity of compounds **265-268, 332-334**, **344-346** and **381-382** molecular docking studies were performed. The three dimensional coordinates of the co-crystal structure of Sitagliptin in the active site of DPP4, the co-crystal structure of Maraviroc in the active site of the chemokine receptor CCR-5 and the crystal structure of active site of pi3K γ mutant in complex were retrieved from the Protein Data Bank (pdb code 1X70 (DPP4), 4MBS (CCR-5), 4EZL (pi3Kγ mutant)). All non-protein atoms, including water and sugar molecules were removed from the model. Using MAKE RECEPTOR 3.0.0 software (OpenEye Scientific Software) a proper active site used for docking was prepared. A database composed of nine hit compounds and the reference sitagliptin, in the case of DPP4, of four hit compounds and the reference maraviroc for CCR-5 and a database of two compounds for pi3K was processed with the Omega 2.5.1.4 software (OpenEye Scientific Software, Inc.,), in the provided conformation of each compound. Finally, the hit compounds were docked into the prepared DPP4 active site, CCR-4 active site and the pi3Kγ active site using the FRED 3.0.1 software and the Chemgauss4 scoring function (OpenEye Scientific Software, Inc.,). The docking was visualy analysed for the five best scored poses for each provided conformation of the hit compound. The poses were compared with the co-crystalised reference ligand and the best overlaying pose was presented. In most of the cases the highest scored pose was depicted (CCR-5 analogues **344-347**, pi3K analogues **381-382**), but in some cases the second best score was chosen (DPP4 analogues **265-268, 332-334**, including Sitagliptin itself in comparison with the co-crystal structure).

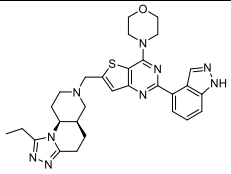
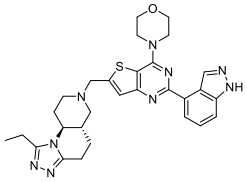
Experimental Part

Table 12 Docking scores for Sitagliptin analogues, Maraviroc analogues and pi3K compounds.

				
256	**268**	**265**	**267**	**266**
-9.99	-10.45	-9.85	-9.41	-8.35
-9.81	-8.63	-9.35	-9.22	-7.94
-9.60	-8.19	-9.16	-9.19	-7.87
-8.84	-7.66	-9.10	-8.29	-7.62
-8.82	-7.62	-8.79	-7.78	-7.29

		
332	**333**	**334**
-8.66	-11.04	-8.25
-8.56	-9.68	-7.71
-8.54	-7.76	-6.68
-8.04	-7.66	-6.51
-7.70	-7.55	-6.39

				
339	**346**	**347**	**345**	**344**
-11.70	-14.25	-13.67	-14.87	-14.17
-11.62	-14.01	-13.37	-14.68	-14.15
-11.57	-13.98	-13.32	-14.61	-13.99
-11.24	-13.93	-12.99	-14.59	-13.70
-11.20	-13.79	-12.93	-14.48	-13.60

	
381	**382**
-13.74	-10.45
-13.31	-8.89
-12.15	-8.60
-10.67	-8.35
	-7.98

12 References

[1] Hughes J.P., Rees, S., Kalindjian, S.B., Philpott, K.L., "Principles of early drug Discovery", *Br. J. of Pharm*., **2011**, *162*, 1239–1249.

[**2**] Graham L. Patrick, "An Introduction to Medicinal Chemistry", 4th edition, *Oxford Press*.

[3] Carroll, F. Y., Houghten, R. A., "From rapid *In Vitro* screening to rapid *In Vivo* screening in the drug discovery process", *Neuropsychopharmacology Reviews*, **2009**, *34*, 251–252.

[4] Gerard J. P., van Westen, J. K., Wegner, A. P., IJzerman, H.,. van Vlijmen, W. T., Bender, A., "Proteochemometric modeling as a tool to design selective compounds and for extrapolating to novel targets", *Med. Chem. Commun*., **2011**, 2, 16.

[5] Carnero A., "High-Throughput Screening in Drug Disovery", *Clin. Transl. Oncol*., **2006**, *8*, 482-489.

[6] Lipinski, C. A., Lombardo, F., Dominy, B. W. & Feeney, P. J., "Experimental and computational approaches to estimate solubility and permeability in drug discovery and development settings", *Adv. Drug Delivery Rev*. **1997,** *23*, 3–25; Leeson P. "Drug Discovery, Chemical Beauty Contest, Box 1: The Lipinski rule of five", *Nature*, **2012**, *481*, 455-456.

[7] Macarron, R., Banks, M.N., Bojanic, D., Burns, D. J., Cirovic, D.A., Garyantes, T., Green, D. V. S., Hertzberg, R. P., Janzen, W. P.,. Paslay, J. W., Schopfer, U., Sittampalam, G. S.; "Impact of high-throughput screening in biomedical research", *Nature Rev. Drug Discovery*, **2011**, *10*, 188.

[8] Dorr. P., Westby, M., Dobbs, S., Griffin, P., Irvine, B., MacCartney, M., Mori, J., Rickett, G., Smith-Burchnell, C., Napier, C., Webster, R., Armour, D., Price, D., Stammen, B., Wood, A., Perros, M., " Maraviroc (UK-427,857), a potent , orally, bioavailable, and selective small-molecule inhibitor of chemokine receptor CCR-5 with broad-spectrum anti human immunodefiency virus type 1 activity", *Antimicr. Agents and Chemotherapy*, **2005**, *49*, 4721-4732.

[9] Szostak, J. W., "Introduction: Combinatorial Chemistry", *Chem. Rev*., **1997**, *97*, 347-348.

[10] Ley, S., Baxendale, R. I., "New tools and concepts for modern organic synthesis", *Nature Rev. Drug Discovery*, **2002**, *1*, 573-586.

[11] Erlanson D. A., McDowell, R. S., O'Brien, T. "Fragment-Based Drug Discovery", *J. Med. Chem*., **2004**, *47*, 3463.

[12] Congreve, M., Carr, R., Murray, C., Jhoti, H., "A 'rule of three' for fragment-based lead discovery?", *Drug Discov. Today*, **2003,** *8***,** 876-877.

[13] Lewell, X. Q., Judd, D.B, Watson, S. P., Hann, M. M, "RECAP ─ Retrosynthetic Combinatorial Analysis Procedure: A Powerful New Technique for Identifying Privileged Molecular Fragments with Useful Applications in Combinatorial Chemistry", *J. Chem. Inf. Comput. Sci*. **1998**, *38*, 511-522.

[14] Erlanson, D.A., Braisted, A. C., Raphael, D. R., Randal, M., Stroud, R. M., Gordon, E. M., Wells, J. A., "Site-directed ligand discovery", *Proc. Natl. Acad. Sci. U.S.A.* **2000**, *97*, 2419-2424. Nakamura, C. E., Abeles, R. H., "Mode of interaction of .beta.-hydroxy-.beta.-methylglutaryl coenzyme A reductase with strong binding inhibitors: compactin and related compounds", *Biochemistry*, **1985**, *24*, 1364-1376. Hajduk, P. J., Dinges, J., Schkeryantz, J. M., Janowick, D., Kaminski, M., Tufano, M., Augeri, D. J., Petros, A., Nienaber, V., Zhong, P., Hammond, R., Coen, M., Beutel, B., Katz, L., Fesik, S. W.,"Novel Inhibitors of Erm Methyltransferases from NMR and Parallel Synthesis", *J. Med. Chem*. **1999**, *42*, 3852- 3859.

Huth, J.R., Sun, C., "Utility of NMR in Lead Optimization: Fragment-Based Approaches", *Comb. Chem. High Throughput Screening*, **2002**, *5*, 631-643; Swayze, E., Jefferson, E., A., Sannes-Lowery, K. A., Blyn, L. B., Risen, L. M., Arakawa, S., Osgood, S. A., Hofstadler, S. A., Griffey, R. H., "SAR by MS: A Ligand Based Technique for Drug Lead Discovery Against Structured RNA Targets", *J. Med. Chem*. **2002**, *45*, 3816-3819.

[15] Frjzo, J., Lepre, C. A., Peng, J. W., Bemis Ajay, G. W., Murcko, M.A., Moore J. M., "The SHAPES strategy: an NMR based approach for lead generation in drug discovery", *Chem. Biol.*, **1999**, *6*, 755-769., Fejzo J1, Lepre, C., Xie, X., "Application of NMR screening in drug discovery", *Curr. Top. Med. Chem*. **2003**, *3*, 81-97.

[16] Shuker, S. B.; Hajduk, P. J., Meadows, R. P., Fesik, S. W., "Discovering high-affinity ligands for proteins: SAR by NMR", *Science*, **1996**, *274*, 1531-1534.

[17] Huc, I., Lehn, J. M., "Virtual combinatorial libraries: Dynamic generation of molecular and supramolecular diversity by self-assembly", *Proc. Natl. Acad. Sci. U.S.A*, **2002**, *99*, 3382-3387. Hochgürtel, M., Biesinger, R., Kroth, H., Piecha, D., Hofmann, M. W., Krause, S., Schaaf, O., Nicolau, C., Eliseev, A. V., "Ketones as Building Blocks for Dynamic Combinatorial Libraries: Highly Active Neuraminidase Inhibitors Generated via Selection Pressure of the Biological Target", *J. Med. Chem*. **2003**, *46*, 356-358.

[18] Kubinyi, H., Mueller, G., *Chemogenomics in Drug Discovery*, Vol. 22, WILEY-VCH, 2004.

[19] Klabunde, T., Chemogenomic approaches to drug discovery: similar receptors bind similar ligands, Br.J. Ph*armacology*, **2007** *152*, 5–7.

[20] Rognan, D., "Chemogenomics approach to rational Drug Design", *Br. J. of Pharm.*, **2007**, *152*, 38-52.

[21] Votano, J. R., Parham, M., Hall, L. H., Kier, L. B., Hall, L. M. "Prediction of aqueous solubility based on large datasets using several QSPR models utilizing topological structure representation" *Chem Biodivers*, **2004**, *1*, 1829–1841; Wallace, A. C., Borkakoti, N., Thornton, Wang, J., Krudy, G., Xie, X. Q., Wu, C., Holland, G., "Genetic algorithm-optimized QSPR models for bioavailability, protein binding, and urinary excretion", *J. Chem. Inf. Model*, **2006**, *46*, 2674–2683. Clark, M. "Generalized fragment-substructure based property prediction method", *J. Chem. Inf. Model*, **2005**, *45*, 30–38.

[22] Weininger, D., "SMILES, a chemical language and information system. 1. Introduction to methodology and encoding rules", *J. Chem. Inf. Comput. Sci*., **1988**, *28 (1)*, 31–36.

[23] Welsch, M., Snyder, S., Stockwell, B., "Privileged scaffolds for library design and drug discovery", *Current opinion in chemical biology*, **2010**, *14*, 1-15.

[24] Evans, B. E., Rittle, K. E., Bock, M. G., DiPardo, R. M., Freidinger, R. M., Whitter, W. L., Lundell, G. F., Veber, D. F., Anderson, P. S., "Methods for drug discovery: development of potent, selective, orally effective cholecystokinin antagonists", *J. Med. Chem.*, **1988**, *31*, 2235.

[25] Evans, B. E., Rittle, K.E., Bock, M. G., DiPardo, R. M., Freidinger, R. M., Whitter, W. L., Lundell, W. L.,Veber, D. F., Anderson, P. S., Chang, R. S. L., Lotti, V. J., Cerino, D. J., Chen, T. B., Kling, P. J., Kunkel, K. A., Springer, J. P., Hirshfieldt., J. "Methods for Drug Discovery: Development of Potent, Selective, Orally Effective Cholecystokinin Antagonists", *J. Med. Chem*. **1988**, *31*, 2235-2246.

[**26]** DeSimone, R. W., Currie, K. S., Mitchell, S. A., Darrow, J. W., Pippin, D. A., "Privileged Structures: applications in drug discovery", *Combinatorial Chemistry & High Throughput Screening*, **2004**, *7*, 473-493; Bemis, G. W., Murcko, M. A., "The Properties of Known Drugs. 1. Molecular Frameworks" *J. Med. Chem*, **1996**, *39*, 2887-2893.

[27] Klabunde, T., Hessler G., "Drug Design Strategies for Targeting G-Protein-Coupled Receptors", *Chembiochem*, **2002**, *3*, 928-944.

[28] Duarte, C. D.; Barreiro, E. J.; Fraga, C. A.M, Privileged Structures: A Useful Concept for the Rational Design of New Lead Drug Candidates, *Mini Reviews in Medicinal Chemistry*, **2007**, *7*, 1108-1119.

[29] Han, C., Zhang, J., Zheng, M., Xiao, Y., Li, Y., Liu, G., "An integrated drug-likeness studyfor bicyclic privileged structures: from physicochemical properties to in vitro ADME properties", *Mol. Divers*., **2011**, *15*, 857-876.

[30] Mueller G., *Drug Discovery Today*, **2003**, *8*, 681-691.

[31] Sheridan, R. P., **"** Finding multiactivity substructures by mining databases of drug like compounds", *J. Chem. Inf. Comput. Sci.*, **2003,** *43*, 1037-1050.

[32] Annadurai, S., Martinez, R., Canney, D. J., Eidem, T., Dunman, P. M., Abou-Gharbia, M., "Design and synthesis of 2- aminothiazole based antimicrobials targeting MRSA", *Bioorg. Med. Chem. Lett*., **2012**, *22*, 7719-7725.

[33] Guo, T., Hobbs, D. W., "Privileged Structure-based combinatorial libraries targeting G protein coupled receptors", *Assay Drug Develop. Technol*. **2003**, *1*, 579, Meng, T., Wang, J., Peng, H., Fang, G., Li, M., Xiong, B., Xie, X., Zhang, Y., Wang, X., Shen, J., "Discovery of benzhydrylpiperazine derivatives as CB1 receptor inverse agonists via privileged structure-based approach", *Eur. J. Med. Chem*. **2010**, *45*, 1133-1139.

[34] Vukovic, N., Sukdolak, S., Solujic, S., Milosevic, T., "Synthesis and Antimicrobial Evaluation of Some Novel 2-Aminothiazole Derivatives of 4-Hydroxy-chromene-2-one", *Arch Pharm*. (Weinheim. Ger), **2008**, *341*, 491-496.

[35] Bondensgaard, K., Ankersen, M., Thøgersen, H., Hansen, B. S., Wulff, B. S., Bywater, R. P. "Recognition of Privileged Structures by G-Protein Coupled Receptors", *J. Med. Chem*,. **2004**, *47*, 888-899.

[36] Filmore D., It's a GPCR world, *Modern Drug Discovery*, **2004,** *November*, 24-28.

[37] Patchett, A. A., Nargund, R. P., Tata, J. R., Chen, M. H., Barakat, K. J., Johnston, D. B., Cheng, K., Chan, W. W., Butler, B., Hickey, G., "Design and biological activities of L-163,191 (MK-0677): a potent, orally active growth hormone secretagogue", *Proc. Natl. Acad. Sci. U.S.A*. **1995**, *92*, 7001-7005.

[38] Labrou, N. E., Bhogal, N., Hurrell,C. R., Findlay, J. B. C., "Interaction of Met297 in the Seventh Transmembrane Segment of the Tachykinin NK2 Receptor with Neurokinin A", *J. Biol. Chem*. **2001**, *276*, 37944-37949, Renzetti, A. R., Catalioto, R.-M., Criscuoli, M., Cucchi, P., Ferrer, C., Giolitti, A., Guelfi, M., Rotondaro, L., Warner, F. J., Maggi, C. A., "Relevance of Aromatic Residues in Transmembrane Segments V to VII for Binding of Peptide and Nonpeptide Antagonists to the Human Tachykinin NK_2 Receptor", *J. Pharmcol. Exp. Ther*. **1999**, *290*, 487-495.

[39] Schnur, D. M., Hermsmeier, M. A., Tebben, A. J., "Are Target-Family Privileged Substructures Truly Privileged?", *J Med. Chem*, **2006**, *49*, 2000-2009.

[40] Patchett, A. A., Nargund, R. P., "Chapter 26. Privileged structures- An update", *Annu. Rep. Med. Chem*., **2000**, *35*, 289-298.

[41] Mason, J. S., Morize, I., Menard, P. R., Cheney, D., L. Hulme, C., Labaudiniere, R. F., "New 4-Point Pharmacophore Method for Molecular Similarity and Diversity Applications: Overview of the Method and Applications, Including a Novel Approach to the Design of Combinatorial Libraries Containing Privileged Substructures", *J. Med. Chem*., **1999**, *42*, 3251-3264.

[42] Hajduk, P. J., Bures, M., Praestgaard, J., Fesik, S. W., "Privileged Molecules for Protein Binding Identified from NMR-Based Screening", *J. Med. Chem*. **2000**, *43*, 3443-3447.

[43] Moroji, T., Okuyama, T., Hagino, Y., Sekiguchi, R., "Neurochemical and behavioral studies on the mode of action of oxypertine", *Arzneimittelforschung*. **1986**, *36(5)*, 804-808.
[44] Ekebergh A., Börje A., Mårtensson J., "Total Synthesis of Nostodione A, a Cyanobacterial Metabolite", *Org Lett*., **2012**, *14* (24), 6274-6277.
[45] Mendgen, T., Steuer, C., Klein C. D., "Privileged Scaffolds or Promiscuous Binders: A Comparative Study on Rhodanines and Related Heterocycles in Medicinal Chemistry", *J. Med. Chem*. **2012**, *55*, 743−753.
[46] Song, Y., Xu, H., Chen, W., Zhan, P., Liu, X., "8-Hydroxyquinoline: a privileged structure with a broad-ranging pharmacological potential", *MedChemComm*. **2015**, *6*, 61-74.
[47] Madonna, S., Béclin, C., Laras, Y., Moret, V., Marcowycz, A., Lamoral-Theys, D., Dubois, J., Barthelemy-Requin, M., Lenglet, G., Depauw, S., Cresteil, T., Aubert, G., Monnier, V., Kiss, R., David-Cordonnier, M-H., Kraus, J.-L., "Structure–activity relationships and mechanism of action of antitumor bis 8-hydroxyquinoline substituted benzylamines", *Eur. J. Med. Chem*. **2010**, *45*, 623-638.
[48] Baell, J. B., Holloway, G. A., "New Substructure Filters for Removal of Pan Assay Interference Compounds (PAINS) from Screening Libraries and for Their Exclusion in Bioassay" *J. Med. Chem*., **2010**, *53*, 2719–2740, Whitty, A., "Growing PAINS in academic drug discovery ", *Future Med. Chem*., **2011**, *3*(7), 797–801.
[49] Baell, J., Walters, M. A., "Chemical con artists foil drug discovery", *Nature*, **2014**, *513*, 481.
[50] Baell, J. B., **"**Observations on screening-based research and some concerning trends in the literature", *Future Med. Chem*., **2010**, *2*(10), 1529–1546.
[51] Recent reviews: a) Davenport, A. J., Hallett, D. J., "Piperazine and aminopyrrolidine compounds as histamine h3 receptor antagonists", *PCT Int. Appl. 2015, WO2015073310 A1*, b) Zeng, Y., Cao, R., Zhang, T., Li, S., Zhong, W., "Design and synthesis of piperidine derivatives as novel human heat shock protein 70 inhibitors for the treatment of drug-resistant tumors", *Eur. J. Med. Chem*., **2015**, 97, 19-31; c) He, X., Jiang, Y., Zhang, Y., Wu, S., Dong, G., Liu, N., Liu, Y., Yao, J., Miao, Z., Wang, Y., Zhang, W., Sheng, C., "Discovery of highly potent triazole antifungal agents with piperidine-oxadiazole side chains", *Med. Chem. Commun*., **2015**, *6*, 653-664., d) Aneja, R., Rashad, A. A., Li, H., Sundaram, R. V. K., Duffy, C., Bailey, L. D., Chaiken, I.,"Peptide Triazole Inactivators of HIV-1 Utilize a Conserved Two-Cavity Binding Site at the Junction of the Inner and Outer Domains of Env gp120", *J. Med. Chem*. **2015**, *58* (9), 3843. e) Kamboj, V. K., Verma, P. K., Dhanda, A., Ranjan, S., "1,2,4-triazole derivatives as potential scaffold for anticonvulsant activity.", *Centr. Nerv. Syst. Agents Med. Chem*. **2015**, *15* (1), 17-22. f) Baumann, M., Baxendale, I. R., "An overview of the synthetic routes to the best selling drugs containing 6-membered heterocycles", *Beilstein J. Org. Chem.* **2013**, *9*, 2265-2319. g) Baumann, M., Baxendale, I. R., Ley, S. V., Nikbin, N., "An overview of the key routes to the best selling 5-membered ring heterocyclic pharmaceuticals", *Beilstein J. Org. Chem.* **2011**, *7*, 442-495.
[52] Martini, E., Di Cesare Mannelli, L., Bartolucci, G., Bertucci, C., Dei, S., Ghelardini, C., Guandalini, L., Manetti, D., Scapecchi, S., Teodori, E., Romanelli, M. N., "Synthesis and Biological Evaluation of 3,7-Diazabicyclo[4.3.0]nonan-8-ones as Potential Nootropic and Analgesic Drugs", *J. Med. Chem.* **2011**, *54*, 2512-2516.
[53] Hubschwerlen, C., Surivet, J.-P., Zumbrunn, A. C., "Spiro antibiotic derivatives",. *PCT Int. Appl., 2008026172*, **2008**; Chen, F., Song, K. S., Wu, Y. D., Yang, D., "Synthesis and Conformational Studies of γ−Aminoxy Peptides", *JACS*, **2008**, *130*, 743-755.
[54] Yoakim, C., Malenfant, E., Thavonekham, B., Ogilvie, W., Deziel, R., Weniger, "Non-nucleoside reverse transcriptase inhibitors", *US*2004/0106791, **2004**; Kozikowski, A. P., Park, P. U. "Synthesis of streptazolin: use of the aza-Ferrier reaction in conjunction with

the INOC process to deliver a unique but sensitive natural product", *J. Org. Chem.* **1990**, *55*, 4668-4682.

[55] Sugg, E. E., Griffin, J. F., Portoghese, P. S., Influence of pseudoallylic strain on the conformational preference of 4-methyl-4-phenylpipecolic acid derivatives, *JOC*, **1985,** *50*, 25, 5032-5037.

[56] Abdel-Magid, A. F., Carson, K. G. , Harris, B. D., Maryanoff, C. A., Shah, R. D., J. "Reductive Amination of Aldehydes and Ketones with Sodium Triacetoxyborohydride. Studies on Direct and Indirect Reductive Amination Procedures", *Org. Chem*. **1996**, *61*, 3849-3862; Borne, R.F., Fifer, E. K., Waters, I. W., "Conformationally restrained fentanyl analogs. 2. Synthesis and analgetic evaluation of perhydro-1,6-naphthyridin-2-ones", *J. Med.Chem.*, **1984**, *27*, 1271-1275; Shah, S. K. Chen N., Guthikonda R. N., Mills S. G., Malkowitz L., Springer M. S., Gould S. L., Demartino J. A., Carella A., Carver G., Holmes K., Schleif W. A., Danzeisen R., Hazuda D., Kessler J., Lineberger J., Miller M., Emini E. A., MacCoss M., "Synthesis and evaluation of CCR5 antagonists containing modified 4-piperidinyl-2-phenyl-1-(phenylsulfonylamino)-butane", *Bioorg & Med. Chem.* **2005**, *15*, 977-982.

[57] Li, Y., Manickam, G., Ghoshal, A., Subramaniam, P., "More Efficient Palladium Catalyst for Hydrogenolysis of Benzyl Groups", *Synthetic Communications*, **2006,** 36:7, 925-928.

[58] Schwehm, C.; Lewis, W.; Blake, A.J.; Kellam, B.; Stocks, M. J., "Preparation and structural analysis of (±)-cis-ethyl 2-sulfanylidenedecahydro-1,6-naphthyridine-6-carboxylate and (±)-trans-ethyl 2-oxooctahydro-1H-pyrrolo[3,2-c]pyridine-5-carboxylate", *Acta Cryst. C70*, **2014,** 1161-1168**.**

[59] Recantini, M., Occhiato, E. G., Ferrali, A., Menchi, G., Guarna, A., Danza, G., Comerci, A., Mancina, R., Serio, M., Garotta, G., Cavalli, A. De Vivo, M., "Synthesis, Biological Activity, and Three-Dimensional Quantitative Structure−Activity Relationship Model for a Series of Benzo[c]quinolizin-3-ones, Nonsteroidal Inhibitors of Human Steroid 5α-Reductase 1", *J. Med. Chem.*, **2004**, *47*, 3546-3560; Scarpi, D., Guarna, G., Lombardi, E., Machetti, F., Occhiato, E. G., "Modification of the Aza-Robinson Annulation for the Synthesis of 4-Methyl-Benzo[c]quinolizin-3-ones, Potent Inhibitors of Steroid 5α-Reductase 1", *J. Org. Chem.*, **2000**, *65*, 8093-8095.

[60] Quan, Z. S., Kwak, K. C., Piao, H. R., Chai, K. Y., Xie, Z. F., "Synthesis and anticonvulsant activity of 7-alkoxyl-4,5-dihydro-[1,2,4]triazolo[4,3-a]quinolines", *Bioorg. Med. Chem. Lett*., **2005**, *15*, 4803.

[61] Borne, R. F., Fifer, E. K., Waters, I. W., "Conformationally restrained fentanyl analogs. 2. Synthesis and analgetic evaluation of perhydro-1,6-naphthyridin-2-ones", *J. Med. Chem.*, **1984**, 27(10), 1271-1275; Renau, P., Schär, P., "Total Synthesis of the Marine Alkaloid (±)-Lepadiformine via a Radical Carboazidation", *Org. Lett.*, **2006**, *8*, 1569-1571.

[62] Bull, S. T., Davies, S. G., Fenton, G., Mulvaney, A. W., Prasad, R. S., Smith, A. D., "Chemoselective debenzylation of *N*-benzyl tertiary amines with ceric ammonium nitrate", *J. Chem. Soc. Pek. Trans 1*, **2000**, 3765-3774.

[63] van den Broek, S., A. M. W., Lemmers, J. G. H., van Delft, F. L., Rutjes, F. P. J. T., "Total synthesis of the monoterpenoid alkaloid (±)-tangutorine", *Org Biomol. Chem*., **2012**, *10*, 945-951.

[64] Liu, L., Ruan, Y.-P., Guo, Z.-Q., Huang, P.-Q., "A General Approach to (5S,6R)-6-Alkyl-5-benzyloxy-2-piperidinones: Application to the Asymmetric Syntheses of Neurokinin Substance P Receptor Antagonist (−)-L-733,061 and (−)-Deoxocassine", *JOC*, **2004**, *69*, 6001-6009.

[65] Chern, C. Y., Huang, Y. P., Kan, W. M., *Tetrahedron Lett*., **2003**, *44*, 1039.

[66] Kawanaka, Y., Kobayashi, K., Kusuda, S., Tatsumi, T., Murota, M., Nishiyama, T., Hisaichi, K., Fujii, A., Hirai, K., Naka, M., Komeno, M., Nakai, H., Toda, M., "Design and synthesis of inhibitors of inducible nitric oxide synthase. Discovery of a new chemical lead with potential for oral bioavailability", *Eur. J. Med. Chem*., **2003**, *38*, 277-288.

[67] Stocks, M. J., Hamza, D., Pairaudeau, G., Stonehouse, J. P., Thorne, P. V., "Concise Synthesis of Novel 2,6-Diazaspiro[3.3]heptan-1-ones and Their Conversion into 2,6-Diazaspiro[3.3]heptanes", *Synlett*, **2007**, *16*, 2587-2589.

[68] Wood, J. L., Stoltz, B. M., Goodman, S. N., "Total Synthesis of (+)-RK-286c, (+)-MLR-52, (+)-Staurosporine, and (+)-K252a", *J. Am. Chem. Soc*., **1996**, *118*, 10656-10657.

[69] Kim, H. S., Choi, B.-S., Kwon, K.-C., Lee, S.-O., Kwak, H. J., Lee, C. H., "Synthesis and antimicrobial activity of squalamine analogue", *Bioorg. & Med. Chem.*, **2000**, *8*, 2059-2065; Dong, Y., Tang, Y., Chollet, J., Matile, H., Wittlin, S., Charman, S. A., Charman, W. N., Tomas, J. S., Scheurer, C., Snyder, C., Scorneaux, B., Bajpai, S., Alexander, S. A., Wang, X., Padmanilayam, M., Cheruku, s. R., Brun, R., Vennerstrom, J. L., "Effect of functional group polarity on the antimalarial activity of spiro and dispiro-1,2,4-trioxolanes", *Bioorg. & Med. Chem*., **2006**, *14*, 6368-6382.

[70] Bayburt, E. K., Daanen, J. F., Gomstsyan, A.R., Latshaus, S. P., Lee. C.H., Schmidt, R. G., "Antagonists of the TRPV1 receptor and uses thereof", *U.S. Pat. Appl. Publ.*, 20080153871, **2008**.

[71] Gustafson, G. R., Beckett, R. P., "Preparation of tetrahydroquinolinones, tetrahydronaphthyridones and derivatives thereof as cannabinoid receptor ligands" *PCT Int. Appl*., 2008079316, 03 Jul 2008.

[72] Brooker, S., Klingele, M. H., „From *N*-Substituted Thioamides to Symmetrical and Unsymmetrical 3,4,5-Trisubstituted 4*H*-1,2,4-Triazoles: Synthesis and Characterisation of New Chelating Ligands", *Eur. J. Org. Chem.*, **2004**, 3422-3434.

[73] Sun, X.Y., Wei, C. X., Kyu, Y. C., "Synthesis and Anti-inflammatory Activity Evaluation of Novel 7-Alkoxy-1-amino-4,5-dihydro[1,2,4] triazole[4,3-a] quinolones" *Arch. Pharm. Chem. Life Sci,*. **2008**, *341*, 288-293.

[74] Glushkov, V. A., Shklyaev, V., Maiora. O. A., Postanogova, G. A., Feshina, E. V., "Investigation of paths for the synthesis of 5,5-dialkyl-3-perfluoroalkyl-5,6-dihydro-1,2,4-triazolo[3,4-a]isoquinolines, *Chem. of Het. Comp*., **2000**, *36*, 319-325.

[75] Dean, D.K., Munoz-Muriedas, J., Sime, M., Steadman, J. G. A., Thewlis, R. E. A., Trani, G., Walter, D. S., "5,6,7,8-tetrahhydro[1,2,4]triazolo[4,3-a]pyrazine derivatives as $P2X_7$ modulators, WO 2010/125102 A1.

[76] Bissantz, C., Goetschi, E., Roetne, R. J., Masciadri, R., Pinard, E., Ratni, H., Evans, M. R., Schnider, P., "Spiro-5,6-dihydro-4h-2,3,5,10b-tetraaza-benzo[e]azulenes", US 20100120751 A1.

[77] Wu, Y., Ma, L.-X., Niu, T.-W., Cui, X.-C., Piao, H. R., "Synthesis and positive inotropic evaluation of N-(1-oxo-1,2,4,5-tetrahydro-[1,2,4]triazolo[4,3-a]quinolin-7-yl)acetamides bearing piperazine and1,4-diazepane moieties", *Bioorg. Med. Chem. Lett*. **2012**, *22*, 4229–4232.

[78] Fan, X., Zhang, H. S., Long, Y. Q., Efficient synthesis and identification of novel propane-1,3-diamino bridged CCR5 antagonists with variation on the basic center, *Eur. J. Med.Chem.*, **2010**, *45*, 2827.

[79] Miyahara, Y. *et al. Synthesis*, **2011**, *3*, 364-366.

[80] Kolb, H. C., VanNieuwenhze, M. S., Sharpless, K. B. "Catalytic asymmetric dihydroxylation", *Chem. Rev.* **1994**, *94*, 2483–2547.

[81] Upadhya, T. T. Sudalai, A., "A short and efficient enantioselective synthesis of cyclohexylnorstatine, a key component of a renin inhibitor", *Tetrahedron: Asymmetry,* **1997**, *8(2*1), 3685-3689.

[82] Hoveyda, A. H., Schrock, R. R., "Catalytic asymmetric olefin metathesis**",** *Chem. Eur. J.,* **2001**, *7*, 945.

[83] Duan, J. J. W., Chen, L., Lu, Z., Xue, C.-B., Liu, R.-Q., Covington, M. B., Qian, M., Wasserman, Z. R., Vaddi, K., Christ, D. D., Trzaskos, J. M., Newton, R. C., Decicco, C. P., "Discovery of b-benzamido hydroxamic acids as potent, selective, and orally bioavailable TACE inhibitors", *Bioorg. Med. Chem. Lett*. **2008,** *18*, 241–246.

[84] Gowda, D. C., Rajesh, B., Gowda, S., "Ammoniumformate catalytic transfer hydrogenation: A convenient method for removal of halogenated and benzyl protected groups in peptide synthesis", *Ind. J. Chem*., **2000**, *39B*, 504-508.

[**85]** Enders *et al*., *Tetrahedron Letters***,** ***17*** (1): 3–6.

[86] "Asymetric Syntheses using the SAMP-/RAMP-hydrazones
method: (S)-(+)-4-methyl-3-heptanone", *Organic Syntheses*, Coll. Vol. 8,.pp. 403 (1993); Vol. 65, p.183 (1987).

[87] Sun, H., Millar, K. M., Yang, J., Abboud, K., Horenstein, B.A., " A new asymmetric route to substitueted piperidines: synthesis of N-alkyl-3,4-dihydroxy-5-alkylpiperidines", *Tetrahedron Lett*., **2000**, *41*, 2801-2804.

[88] Meyers, A. I., Poindexter, G. S., Brich, Z., "Asymetric synthesis of (+) or (-) -2-methyloctanal via the metalloenamines of chiral alkoxy amines", *J. Org. Chem*.,**1978**, *43*, 892-898. Meyers, A.I., Williams, D.R., Druelinger, M., "Enantioselective Alkylation of cyclohexanone via chiral lithio-chelated enamines", *JACS*, **1976**, 3032-3033.

[89] Braun, M., Meier, T., "Palladium-catalysed stereoselective allylic alkylation of lithium enolates", *Synlett*, **2005**, *19*, 2968-2972.

[90] Michael D., McCreary, Daniel W. Lewis, David L. Wernick, George M. Whitesides, Determination of enantiomeric purity using chiral lanthanide shift reagents *J. Am. Chem. Soc*., 1974, 96 (4), 1038–1054.

[91] Parker, D., "NMR determination of enantiomeric purity", *Chem. Rev*., **1991**, *91*, 1441-1457;

[92] Catalano, J. G., Gudmundsson, K. S., Svolto, A., Boggs, S. D., Miller, J. F., Spaltenstein, A., Thomson, M., Wheelan, P. Minick, D. J., Phelps, D. P., Jenkinson, S., " Synthesis of a novel tricyclic 1,2,3,4,4a,5,6,10b-octahydro-1,10-phenanthroline ring system and CXCR4 antagonists with potent activity against HIV-1", *Bioorg. & Med. Chem. Lett*., **2010**, *20*, 2186-2190.

[93] Davis , F. A., Melamed, J. Y., Sharik, S. S., "Total Synthesis of (−)-Normalindine via Addition of Metalated 4-Methyl-3-cyanopyridine to an Enantiopure Sulfinimine", *JOC*, **2006**, *71*, 8761-8766.

[94] Jona, H., Shibata, J., Asai, M., Goto, Y., Arai, S., Nakajima, S., Okamoto, O., Kawamoto, H., Iwasawa, Y., "Efficient and practical asymmetric synthesis of 1-tert-butyl 3-methyl (3R,4R)-4-(2-oxo-2,3-dihydro-1H-benzimidazol-1-yl)piperidine-1,3-dicarboxylate,a useful intermediate for the synthesis of nociceptin antagonists, *Tetrahedron: Asymmetry*, **2009**, *20*, 2439–2446.

[95] IDF *Diabetes Atlas I* Sixth edition, 2013; http://www.who.int/mediacentre/factsheets/fs312/en/

[96] American Diabetes Association. *Living with Diabetes: Insulin Basics*. June 7, **2013**. http://www.diabetes.org/living-with-diabetes/treatment-and-care/medication/insulin/insulin-basics.html. Accessed April 28, 2014.

[97] Gibbson, G. W., "The diabetic foot: amputation and drainage of infections", *Journal of Vascular Surgery*, **1987**, *5*, 791-793.

[98] Thornberry, N. A., Gallwitz, B., "Mechanism of action of dipeptidyl peptidase 4 (DPP-4).", *Best Practice & Research, Clinical Endocrinology & Metabolism*, **2009**, *23*, 479–486.

[99] Drucker, D., Easley, C., Kirkpatrick, P., "Sitagliptin", *Nature Reviews*, **2007**, *6*, 109-110; Drucker, D. J., "The biology of incretin hormones", *Cell Metab.*, **2006**, *3*, 153-165.

[100] Mentlein, R., "Dipeptidyl peptidase IV (CD-26)-role in the inactivation of regulatory peptides", *Regulatory Peptides*, **1999**, *85*, 9-24.

[101] Gault, V.A., Parker, J.C., Harriott, P., Flatt, P.R., O'Harte, F.P.M. "Evidence that the major degradation product of glucose-dependent insulinotropic polypeptide, GIP(3-42), is a GIP receptor antagonist in vivo"., *The Journal of Endocrinology*, **2002**, *175*, 525–533; Knudsen, L.B., Pridal, L., Glucagon-like-peptide-1-(9-36) amide is a major metabolite of glucagon-like-peptide-1-(7-36) after *in vivo* administration in dogs, and it acts as an antagonist on the pancreatic receptor", *Eur. J. Pharm*., **1996**, *318*, 429–435.

[102] Karagiannis, T., Boura, P., Tsapas, A., "Safety of dipeptidyl peptidase 4 inhibitors: a perspective review", *Ther. Adv. Drug. Saf*., **2014**, *5*, 138–146.

[103] Balkan B., Kwasnik L., Miserendino, R., Holst, J.J., Li, X., "Inhibition of dipeptidyl peptidase IV with NVP-DPP-728 increases plasma GLP-1 (7-36 amide) concentrations and improves oral glucose tolerance in obese zucker rats", *Diabetologia*, **1999**, *42*, 1324–1331; Reimer, M. K., Holst, J. J., Ahre´n, B., "Long-term inhibition of dipeptidyl peptidase IV improves glucose tolerance and preserves islet function in mice", *Eur. J. Endocrinology*, **2002**, *146*, 717–727.

[104] Abbott, C. A., Yu, D. M. T., Woollatt, E., Sutherland, G. R., McCaughan, G., Gorrell, M.D., Cloning, expression and chromosomal localization of a novel human dipeptidyl peptidase (DPP) IV homolog, DPP-8, *Eur. J. Biochem*., **2000**, *267*, 6140–6150., Ajami, K., Abbott, C. A., McCaughan, G. W., Gorrell, M. D., "Dipeptidyl peptidase 9 has two forms, a broad tissue distribution, cytoplasmic localization and DPPIV-like peptidase activity", *Biochimica et Biophysica Acta*, **2004**, *1679*, 18–28.

[105] Lankas, G. R., Leiting, B., Roy, R. S., Eiermann, G. J., Beconi, M. G., Biftu, T., Chan, C. C., Edmondson, S., Feeney, W.P., He, H., Ippolito, D.E., Kim, D., Lyons, K. A., Ok, H.O., Patel, R.A., Petrov, A. N., Pryor, K. A., Qian, X., Reigle, L., Woods, A., Wu, J.K., Zaller, D., Zhang, X., Zhu, L., Weber, A. E., Thornberry, N. A., "Dipeptidyl peptidase IV inhibition for the treatment of type-2 diabetes: potential importance of selectivity over dipeptidyl peptidase 8 and 9", *Diabetes*, **2005**, *54*, 2988–2994.

[106] Kim, D., Wang, L., Beconi, M., Eiermann, G. J., Fisher, M.H., He, H., Hickey, G.J., Kowalchick, J. E., Leiting, B., Lyons, K., Marsilio, F., McCann, M.E., Patel, R.A., Petrov, A., Scapin, G., Patel, S. B., Roy, R. S., Wu, J.K., Wyvratt, M. J., Zhang, B. B., Zhu, L., Thornberry, N. A., Weber, A. E., "(2*R*)-4-oxo-4-[3-(trifluoromethyl)-5,6-dihydro[1,2,4]triazolo[4,3-a]pyrazin-7(8*H*)-yl]-1-(2,4,5-trifluorophenyl)butan-2-amine: a potent, orally active dipeptidyl peptidase IV inhibitor for the treatment of type 2 diabetes, *J. Med. Chem*., **2005**, *48*, 141-151. Kim, D., Kowalchick, J. E., Edmondson, S. C., Mastracchio, A., Xu, J., Eiermann, G. J., Leiting, B., Wu, J. K., Pryor, K. A., D., Patel, R. A., He,H.,Lyons, K. A., Thornberry, N.A., Weber, A. E., "Triazolopiperazine-amides as dipeptidyl peptidase IV inhibitors: Close analogs of JANUVIA™ (sitagliptin phosphate)", *Bioorg. & Med. Chem. Lett*., **2007**, *17*, 3373–3377.

[107] Villhauer, E. B., Brinkman, J. A., Naderi, G. B., Burkey, B. F., Dunning, B. E., Prasad, K., Mangold, B. L., Russell, M. E., Hughes, T. E., 1-[[(3-hydroxy-1-adamantyl)amino] acetyl]-2-cyano-(S)-pyrrolidine:a potent, selective, and orally available

dipeptidyl peptidase IV inhibitor with antihyperglycemic properties", J. Med. Chem., 2003, 46, 2774−2789. Juillerat-Jeanneret, L., "Dipeptidyl Peptidase IV and Its Inhibitors: Therapeutics for Type 2 Diabetes and What Else?", *J. Med. Chem*. **2014**, *57*, 2197−2212.

[108] Augeri, D. J., Robl, J. A., Betebenner, D. A., Magnin, D. R., Khanna, A., Robertson, J. G., Wang, A., Simpkins, L. M., Taunk, P., Huang, Q., Han, S.-P., Abboa-Offei, B., Cap, M., Xin, L., Tao, L., Tozzo, E., Welzel, G. E., Egan, D. M., Marcinkeviciene, J., Chang, S. Y., Biller, S. A., Kirby, M. S., Parker, R. A., Hamann L. G., "Discovery and Preclinical Profile of Saxagliptin (BMS-477118): A Highly Potent, Long-Acting, Orally Active Dipeptidyl Peptidase IV Inhibitor for the Treatment of Type 2 Diabetes", *J. Med.Chem*., **2005**, *48*, 5025−5037.

[109] Feng, J., Zhang, Z., Wallace, M. B., Stafford, J. A., Kaldor, S. W., Kassel, D. B., Navre, M., Shi, L., Skene, R. J., Asakawa, T., Takeuchi, K., Xu, R., Webb, D. R., Gwaltney,S. L., "Discovery of alogliptin: a potent, selective, bioavailable, and efficacious inhibitor of dipeptidyl peptidase IV", *J. Med. Chem*. **2007,** *50*, 2297–2300.

[110] Eckhardt, M., Langkopf, E., Tadayyon, M. M. M., Thomas, L., Nar, H., Pfrengle, W., Guth, B., Lotz, R., Sieger, P., Fuchs, H., Himmelsbach, F., "8-(3-(R)-aminopiperidin-1-yl)-7-but-2-ynyl-3-methyl-1-(4-methyl-quinazolin-2-ylmethyl)-3,7-dihydropurine-2,6-dione (BI 1356), a highly potent, selective, long-acting, and orally bioavailable DPP-4 inhibitor for the treatment of type 2diabetes", *J. Med. Chem*. **2007**, *50*, 6450–6453.

[111] Yoshida, T., Akahoshi, F., Sakashita, H., Kitajima, H., Nakamura, M., Sonda, S., Takeuchi, M., Tanaka, Y., Ueda, N., Sekiguchi, S., Ishige, S., Shima, K., Nabeno, M., Abe, Y., Anabuki, J., Soejima, A., Yoshida, K., Takashina, Y., Ishii, S., Kiuchi, S., Fukuda, S., Tsutsumiuchi, R., Kosaka, K., Murozono, T., Nakamaru, Y., Utsumi, H., Masutomi, N., Kishida, N., Miyaguchi, I., Hayashi, Y., "Discovery and preclinical profile of teneligliptin (3-[(2S,4S)-4-[4-(3- methyl-1-phenyl-1H-pyrazol-5-yl)piperazin-1-yl]pyrrolidin-2-ylcarbonyl] thiazolidine): a highly potent, selective, long-lasting and orally active dipeptidyl peptidase IV inhibitor for the treatment of type 2 diabetes", *Bioorg. Med. Chem*. **2012,** *20*, 5705–5719.

[112] Biftu,T., Sinha-Roy, R., Chen, P., Qian, X., Feng,D., Kuethe, J. T., Scapin, G., Duo, Y., Gao, Yan, Y., Krueger, D., Bak, A., Eiermann, G., He, J., Cox, J., Hicks, J., Lyons, K., He,H., Salituro, G., Tong, S., Patel, S., Doss, G., Petrov, A., Wu, J., Xu, S. S., Sewall, C., Zhang, X., Zhang, B., Thornberry, N. A., Weber, A. E., "Omarigliptin (MK-3102): A Novel Long-Acting DPP‑4 Inhibitor for Once-Weekly Treatment of Type 2 Diabetes" *J. Med. Chem*. **2014**, *57*, 3205−3212. Shu, C., Ge, H., Song, M., Chen, J-h., Zhou, H., Qi, Q.,Wang, F., Ma, X.,Yang, X., Zhang, G., Ding, Y., Zhou, D.,Peng, P.,Shih, C-k., Xu, J., Wu, F., "Discovery of Imigliptin, a Novel Selective DPP‑4 Inhibitor for the Treatment of Type 2 Diabetes", *ACS Med. Chem. Lett*. **2014**, *5*, 921−926.

[113] Nabeno, M., Akahoshi, F., Kishida, H., Miyaguchi, I., Tanaka, Y., Ishii, S., Kadowaki, T., "A comparative study of the binding modes of recently launched dipeptidyl peptidase IV inhibitors in the active site", *Biochem. Biophys.Research Commun*., **2013**, *434*, 191–196.

[114] Engel, M., Hoffmann, T., Manhart, S., Heiser, U., Chambre, S., Huber, R., Demuth, H.U., Bode, W., "Rigidity and flexibility of dipeptidyl peptidase IV: crystal structures of and docking experiments with DPPIV", *J. Mol. Biol*., **2006,** *355*, 768–783.

[115] Hansen, K. B., Balsells, J., Dreher, S., Hsiao, Y., Kubryk, M., Palucki, M., Rivera, N., Steinhuebel, D., Armstrong III, J. D., Askin, D. and Grabowski, E. J. J. "First Generation Process for the Preparation of the DPP-IV Inhibitor Sitagliptin", *Organic Process Research & Development* **2005**, *9*, 634-63.

[116] Schwehm, C., Li, J., Song, H., Hu, X., Kellam, B., Stocks, M. J., "Synthesis of new DPP-4 inhibitors based on a novel tricyclic triazole scaffold", *ACS Med. Chem Lett.*, **2015**, *6* , 324–328.

[117] http://www.who.int/mediacentre/factsheets/fs360/en/

[118] Masur, H., Michelis, M. A., Greene, J. B., Onorato, I., Stouwe, R. A., Holzman, R. S., Wormser, G., Brettman, L., Lange, M., Murray, H. W., Cunningham-Rundles, S., "An outbreak of community-aquired *Pneumocystis carinii* pneumonia:initial manifestation of cellular immune dysfunction." *N. Engl. J. Med.*, **1981**, *305*, 1431-1438.

[119] Dorr, P., Stupple, P., Kazmierski W. M., *Antiviral Drugs: From Basic Discovery Through Clinical Trials*, Chapter 9, Discovery and Development of Maraviroc and PF-232798:CCR-5 Antagonists for the treatment of HIV-1 Infection; Huang Xianhai, *Case studies in Modern Drug Discovery and Development*, Chapter 9, Discovery and Development of Maraviroc, Wiley.

[120] Carr, A., "Toxicity of antiretroviral therapy and implications for drug development", *Nat. Rev. Drug Discov.*, **2003**, *2*, 624-634.

[121] Richman, D. D., Morton, S. C., Wrin, T., Hellmann, N., Berry, S., Shapiro, M. F., Bozette, S., "The prevalence of antiretroviral drug resistance in the United States", *AIDS*, **2004**, *18*, 1393-1401; Little, S. J., Holte, S., Routy, J. P., Daar, E. S., Markowitz, M., Collier, A. C., Koup, R. A., Mellors, J. W., Connick, E., Conway, B., "Antiretroviral-drug resistance among patients recently infected with HIV", *N. Engl. J. Med.*, **2002**, *347*, 385-394.

[122] Gudermann, T., Nuernberg, B., Schultz, G., "Receptors and G-proteins as primary components of transmembrane signal transduction. Part 1, G-protein coupled receptors: Structure and function", *J. of Mol. Medicine*, **1995**, *73*, 51-63.

[123] Thelen, M., "Dancing in the tune of chemokines" *Nature Immunology*, **2011**, *2*, 129-134.

[124] Tsibris, A., www.prn.org, Vol.12, 1-9, "Update on CCR-5 inhibitors, scientific rationale, clinical evidence and anticipated uses"

[125] Matthews, T., Salgo, M., Greenberg, M., Chung, J., DeMasi, R., Bolognesi, D., "Enfurvitide: the first therapy to inhibit the entry of HIV-1 into host CD-4 lymphocytes", *Nature Reviews Drug Discovery*, **2004**, *3*, 215-225.

[126] Bleul, C. C., Farzan, M., Choe, H., Parolin, C., Clark-Lewis, I., Sodroski, J. & Springer, T. A." The lymphocyte chemoattractant SDF-1 is a ligand for LESTR/fusin and blocks HIV-1 entry" *Nature*, **1996**, *382*, 829-833., Oberlin, E., Amara, A., Bachelerie, F., Bessia, C., Virelizier, J. L., Arenzana-Seisdedos, F., Schwartz, O., Heard, J. M., Clark-Lewis, I., Legler, D. F., Loetscher, M., Baggiolini, M., Moser, B, " The CXC chemokine SDF-1 a is the ligand for LESTR/fusin and prevents infection by T-cell-line-adapted HIV-1". *Nature*, **1996**, *382*, 833-835.

[127] Qin, L., Kufareva, I., Holden, L. G., Wang, C., Zheng, Y., Zhao, C., Fenalti, G., Wu, H., Han, G. W., Cherezov, V., Abagyan, R., Stevens, R. C., and Handel, T. M., "Crystal structure of the chemokine receptor CXCR4 in complex with a viral chemokine" *Science*, **2015**, *347*, 1117-1122.

[128] Dean, M., Carrington, M., Winkler, C., Huttley, G. A., Smith, M. W., Allikmets, R., Goedert, J. J., Buchbinder, S. P., Vittinghoff, E., Gomperts, E., Donfield, S., Vlahov, D., Kaslow, R., Saah, A., Rinaldo, C., Detels, R. & O'Brien, S. J., "Genetic restriction of HIV-1 infection and progression to AIDS by a deletion allele of the CKR5 structural gene". *Science*, **1996**, *273*, 1856-1862, Huang, Y., Paxton, W. A., Wolinsky, S. M., Neumann, A. U., Zhang, L., He, T., Kang, S., Ceradini, D., Jin, Z., Yazdanbakhsh, K., Kunstman, K., Erickson, D., Dragon, E., Landau, N. R., Phair, J., Ho, D. D., & Koup, R. A., "The role of mutant CCR-5

allele in HIV-1 transmission and disease progression.", *Nature Medicine*, **1996**, *1*, 1240-1243.

[129] Liu, R., Paxton, W. A., Choe, S., Ceradini, D., Martin, S. R., Horuk, R., MacDonald, M. E., Stuhlmann, H., Koup, R. A., Landau, N. R., "Homozygous defect in HIV-1 coreceptor accounts for resistance of some multiply exposed individuals to HIV-1 infection", *Cell*, **1996**, *86*, 367-377., Samson, M., Libert, F., Doranz, B. J., Rucker, J., Liesnard, C., Farber, C. M., Saragosti, S., Lapoumeroulie, C., Cognaux, J., Forceille, C., Muyldermans, G., Verhofstede, C., Burtonboy, G., Georges, M., Imai, T., Rana, S., Yi, Y., Smyth, R. J., Collman, R. G., Doms, R. W., Vassart, G. & Parmentier, M., "Resistance to HIV-1 infection in Caucasian individuals bearing mutant alleles of the CCR-5 chemokine receptor gene" *Nature*, **1996**, *382*, 722-725.

[130] Cocchi, F., Garzino-Demo, A., Arya, S. K., Gallo, R. C., Lusso, P., " Identification of RANTES, MIP-1a, MIP-1b as the major HIV suppressive factors produced by CD8+ T cells ", *Science* **1995**, *270*, 1811-1815.

[131] Alkathib, G., Locati, M., Kennedy, P. E., Murphy, P. M., Berger, E. A., "HIV-1 coreceptor activity of CCR-5 and its inhibition by chemokines: Independence from G-protein signaling and importance of coreceptor downmodulation, *Virology*, **1997**, *234*, 340-348.; Amara, A., Le Gall, S., Schwartz, O., Salamero, J.,Montes, M., Loetscher, P., Baggiolini, M., Virelizier, J.-P., Arenzana-Seisdedos, F., "HIV coreceptor downregulation as antiviral principle: SDF-1α- dependent internalization of the chemokine receptor CXCR-4 contributes to inhibition of HIV replication", *J. Exp. Medicine*, **1997**, *186*, 139-146.

[132] Westby, M., van der Ryst, E., "CCR-5 antagonists,: host targeted antivirals for the treatment of HIV infection", *Antiviral Chemistry&Chemotherapy*, **2005**, *16*, 339-354.

[133] Pugach, P., Marozsan, A. J., Ketas, T. J., Landes, E. L.,Moore, J. P., Kuhmann, S. E., "HIV-1 clones resistant to a small molecule CCR5 inhibitor use the inhibitor-bound form of CCR5 for entry", *Virology*, **2007**, *361*, 212-228., Westby, M., Smith-Burchnell, C., Mori, J., Lewis, M., Mosley, M., Stockdale, M., Dorr, P., Ciaramella, G., Perros, M.J.,"Reduced maximal inhibition in phenotypic susceptibility assays indicates that viral strains resistant to CCR-5 antagonist maraviroc utilise inhibitor bound receptor for entry", *Virol*. **2007**, *81*, 2359-2371.

[134] Ribeiro, R. M., Hazenberg, M. D., Pereleson, A. S., Davenport, M. P., "Naïve and memory cell turnover as drivers of CCR-5-to-CXCR-4 turnover tropism switch in human immunodeficiency virus type-1: implications for therapy", *J. Virol*., **2006**, *80*, 802.

[135] Agrawal, L., Lu X., Quingen J., VanHorn-Ali, J., Nicolescu, I. V., McDermott, D. H., Murphy, P. M., Alkhatib, G., " Role for CCR5Δ32 protein in resistance to R5, R5X4 and X4 human immunodeficiency virus type 1 in primary $CD4^+$ cells", *J. Virol*, **2004**; *78*, 2277-2287.

[136] "Pfizer wins U.S. approval for new HIV drug", Krauskopf, L., 06/08/2007 (Reuters), "Europe gives final approval to Pfizer HIV drug", 24/09/2007 (Reuters), Kuritzkes, D., Kar, S., Kirkpatrick, P., "Maraviroc", Nature reviews Drug Discovery, 2008, 7, 15-16.

[137] Haqqani, A. A., Tilton, J. C., "Entry inhibitors and their use in the treatment of HIV-1 infection."*Antiviral Research,* **2013**, *98*, 158–170.

[138] Emmelkamp, J.M, Rockstroh, J.K., "CCR-5 antagonists: comparison of efficacy, side effects, pharmacokinetics and interactions", *Eur. J. Med. Res,*. **2007**, *12*, 409-417.

[139] Jayaram R. Targat, Julie M Stritzki, Lisa M. Dunkle, Kazmierski Wieslaw M., *Antiviral Drugs: From Basic Discovery Through Clinical Trials*, Chapter 10, Discovery of the CCR5 Antagonist Vicriviroc (SCH 417690/SCH-D) for the treatment of HIV-1 Infection

[140] Wilkin, R. T., Gulick, R. M., "CCR-5 Antagonism in HIV infection: current concepts and future opportunities", *Annu. Rev. Med*. **2012**, *63*, 81-83.

[141] http://www.ncbi.nlm.nih.gov/gene/1565,

[142] Sanguinetti, M. C., Tristani-Firouzi M., "hERG potassium channels and cardiac arrhythmia", *Nature*, **2006**, Vol *440*, 23 March.
[143] Flexner, C.," HIV drug development: the next 25 years", *Nat. Rev. Drug Discovery*, **2007**, *6* (12), 959-66.
[144] Dorr, P., Westby, M., Dobbs, S., Griffin, P., Irvine, B., Macartney, M., Mori, J., Rickett, G., Smith-Burchnell, C., Napier, C., Webster, R., Armour, D., Price, D., Stammen, B., Wood, A., Perros, M. Maraviroc (UK-427,857), a potent, orally bioavailable, and selective small-molecule inhibitor of chemokine receptor CCR5 with broad-spectrum anti-human immunodeficiency virus type 1 activity, *Antimicrob Agents Chemother*. **2005,** 49(11), 4721-32., Abel, S., Back, D. J., Vourhavis, M., " Maraviroc, pharmacokinetics and drug interactions", *Antiviral Therapy*, *14*, 607-618.
[145] Tan, Q., Zhu, Y., Li, J., Chen,Z., Won Han, G., Kufareva, I., Li, T., Ma, L., Fenalti, G., Li, J., Zhang, W., Xie, X., Yang, H., Jiang, H., Cherezov, V., Liu, H., Stevens, R. C., Zhao, Q., Wu, B., "Structure of the CCR-5 chemokine receptor-HIV entry complex inhibitor Maraviroc complex", *Science*, **2013,** *341*, 1387-1390.
[146] Haydock-Lewandowski, S. J., Birch, M., Long, J., Wilder, A., Ahman, J.,"Process research and scale-up of a commercilisable route to Maraviroc (UK-427,857), a CCR-5 receptor antagonist", *Org. Process Research Develop.*, **2008**, *12(6)*, 1094.
[147] Chalard, P., Troin, Y., Eschalier, A., Marchand, F., Plas, A. "Stereoselective synthesis and in vivo evaluation of the analgesic activity of polysubstituted bispidines", *Eur. J. Org. Chem.*, **2012**, 6017; Davies *et al.*," The conjugate addition of enantiomerically pure lithium amides as homochiral ammonia equivalents: scope, limitations and synthetic applications", *Tetrahedron Assymetry*, **2005**,*16*, 2833; Smith, A. D., Prasad, R. S., Mulvaney, A. W., Fenton, G., Davies, S. G., Bull, S. D. *J.*"Chemoselective debenzylation of N-benzyl tertiary amines with ceric ammonium nitrate", *Chem. Soc., Perkin Trans I*, **2000**, 3765-3774.
[148] Flores, H. J., Larraza, M. I., Garcia, G., Ortega, A., Sanchez, I. H. "A general method for the synthesis of N,N dialkylaminobutylamines", *Synthetic Commun.*, **1985**, *15(2)*, 141-149.
[149] Rang, H.P., Dale, M. M, Ritter, J. M., *Pharmacology* 4th edition, **1999**.
[150] http://www.who.int/mediacentre/factsheets/fs307/en/
[151] http://www.who.int/respiratory/copd/en/
[152] Medina-Tato, D. A., Ward, S. G., Watson, M. L.," Phosphoinositide 3-kinase signalling in lung disease: leucocytes and beyond", *Immunology*, **2007**, *121*, 448–461.
[153] Myou, S., Leff, A. R., Myo, S., Boetticher, E., Tong, J., Meliton, A. Y., Liu, J., Munoz, N. M., Zhu, X., " Blockade of inflammation an airway hyperresponsiveness in immune sensitized mice by dominant negative phosphoinositide 3-kinase TAT", *J. Exp. Med.* **2003**, *198*, 1573–82.
[154] Thomas, M., Owen, C.," Inhibition of PI-3 kinase for treating respiratory disease: good idea or bad idea?", *Curr. Opin. Pharmacology*, **2008**, *8*, 267–274.
[155] Samuels, Y., Ericson K., "Oncogenic pi3K and its role in cancer", *Curr. Opin. Oncol*. **2006**, *18*,77-82.
[156] Carson, J. D., Van-a´ aller, G., Lehr, R., Sinnamon, R.H., Kirkpatrick, R. B., Auger, K. R., Dhanak, D., Copeland, R. A., Gontarek, R. R., Tummino, P. J., "Effects of oncogenic p110+α subunit mutations on the lipid kinase activity of phosphoinositide 3-kinase", *Biochem. J*., **2008**, *409*, 519-524.
[157] Jackson, S. P., Schoenwaelder, S. M., Goncalves, I., Nesbitt, W. S., Yap, C. L., Wright, C. E., Kenche, V., Anderson, K. E., Dopheide, S. M., Yuan, Y., "PI 3-kinase p110beta: a new target for antithrombotic therapy", *Nat. Med*., **2005**, *11*, 507-51.
[158] Hirsch, E., Katanaev, V. L., Garlanda, C., Azzolino, O., Pirola, L., Silengo, L.,

Sozzani, S., Mantovani, A., Altruda, F., Wymann, M. P.,"Central role for G protein-coupled phosphoinositide 3-kinase gamma in inflammation", *Science*, **2000**, *287*, 1049-1052; Wang, F., Herzmark, P., Weiner, O. D., Srinivasan, S., Servant, G., Bourne, H. R."Lipid products of PI(3)Ks maintain persistent cell polarity and directed motility in neutrophils", *Nat. Cell. Biol*. **2002**, *4*, 513-518.

[159] Lee, K. S., Park, S. J., Kim, S. R., Min, K. H., Jin, S. M., Puri, K. D., Lee, Y. C."Phosphoinositide 3-kinase-delta inhibitor reduces vascularpermeability in a murine model of asthma", *J. Allergy Clin. Immunol*, **2006**, *118*, 403-409.

[160] Okkenhaug, K., Ali, K., Vanhaesebroeck, B., "Antigen receptor signaling: a distinctive role for the p110δ isoform of the pi3K", *Trends Immunol*. **2007**, *28*, 80-87; Okkenhaug, K., Vanhaesebroeck, B,. "PI3K in lymphocyte development, differentiation and activation", *Nat. Rev. Immunol*., **2003**, *3*, 317.

[161] Workman, P., van Montfort, R. L. M., "PI(3) kinases: Revealing the delta lady", *Nat. Chem. Biol*. **2010**, *6*, 83-82; Berndt, A., Miller, S., Williams, O., Le, D. D., Houseman, B. T., Pacold, J. I., Gorrec, F., Hon, W. C., Liu, Y., Rommel, C., Gaillard, P., Rückle, T., Schwarz, M. K., Shokat, K. M., Shaw, J. P., Williams, R. L.,"The p110 delta structure: mechanism for selectivity and potency for new PI(3)K inhibitors", *Nat. Chem. Biol*. **2010**, *6*, 117-124.

[162] Folkes, A. J., Ahmadi, K., Alderton, W. K., Alix, S. A., Baker, S. J., Box, G., Chuckowree, I. S., Clarke, P. A., Depledge, P. Eccles, S. A., Friedman, L. S., Hayes, A., Hancox, T. C.,Kugendradas, A., Lensun, L., Moore, P., Olivero, A. G., Pang, J., Patel, S., Pergl-Wilson, G. H., Raynaud, F. I., Robson, A., Saghir, N., Salphati, L., Sohal, S.,Ultsch, M. H., Valenti, M., Wallweber, H. J. A., Wan, N. C., Wiesmann, C., Workman, P.,Zhyvoloup, A., Zvelebil, M. J., Shuttleworth, S. J.," The Identification of 2-(1H-Indazol-4-yl)-6-(4-methanesulfonyl-piperazin-1-ylmethyl)-4-morpholin-4-yl-thieno[3,2-d]pyrimidine (GDC-0941) as a Potent, Selective, Orally Bioavailable Inhibitor of Class I PI3 Kinase for the Treatment of Cancer", *J. Med. Chem*. **2008**, *51*, 5522–5532.

[163] Sutherlin, D. P., Bao, L., Berry, M., Castanedo, G., Chuckowree, I., Dotson, J., Folks, A., Friedman, L., Goldsmith, R., Gunzner, J., Heffron, T., Lesnick, J., Lewis, C., Mathieu, S., Murray, J., Nonomiya, J., Pang, J., Pegg, N., Prior, W.W., Rouge, L., Salphati, L., Sampath, D., Tian, Q., Tsui, V., Wan, N.C., Wang, S., Wei, B., Wiesmann, C., Wu, P., Zhu, B. Y., Olivero, A. J., "Discovery of a potent, selective, and orally available class I phosphatidylinositol 3-kinase (PI3K)/mammalian target of rapamycin (mTOR) kinase inhibitor (GDC-0980) for the treatment of cancer.", *J. Med. Chem*. **2011**, *54*, 7579-7587.

[164] Sutherlin, D. P., Baker, S., Bisconte, A., Blaney, P. M., Brown, A., Chan, B. K., Chantry, D. C., Castanedo, G., DePledge, P., Goldsmith, P.,Goldstein, D. M., Hancox, T., Kaur, J., Knowles, D., Kondru, R., Lesnick, J., Lucas, D.D., Lewis, C., Murray, J., Nadin, A. J, Nonomiya, J., Pang, J., Pegg, N., Price, S., Reif, K., Safina, B. S., Salphati, L., Staben, S., Seward, E. M., Shuttleworth, S., Sohal, S., Sweeney, Z. K., Ultsch, M., Waszkowycz, B., Wei, B., "Potent and selective inhibitors of PI3Kd: Obtaining isoform selectivity from the affinity pocket and tryptophan shelf", *Bioorg. Med. Chem. Lett*., **2012**, *22* 4296–4302.

[165] Sugiyama, T., "Role of $P2X_7$ receptors in neuronal death in the retina", *Neural regen. Res*., **2014**, *9*, 579-582.

[166] North, R. A, "Molecular Physiology of P2X receptors", *Physiol. Rev*., **2002**, *82*, 1013-1067.

[167] Lord, B., Aluisio, L., Shoblock, J. R., Neff, R. A., Varlinskaya, E. I., Ceusters, M., Lovenberg, T. W., Carruthers, N., Bonaventure, P.,Letavic, M. A., Deak, T., Drinkenburg, W., Bhattacharya, A., *J. Pharmacol. Exp. Ther*., **2014**, *351*:628–641.

[168] Romagnoli, R., Baraldi, P.G., Cruz-Lopez, O., Lopez-Cara, C., Preti, D., Borea, P.A., and Gessi, S., "The P2X7 receptor as a therapeutic target". *Expert Opin Ther Targets,* **2008**, *12*, 647–661.

[169] Illes, P., Verkhratsky, A., Burnstock, G., Franke, H., "P2X Receptors and Their Roles in Astroglia in the Central and Peripheral Nervous System**",** *The Neuroscientist,* **2012,** *18(5)* 422–438.

[170] Bennett, M. R., "Synaptic $P2X_7$ receptor regenerative-loop hypothesis for depression".*Aust. N. Z. J. Psychiatry* **2007,** *41*, 563–57; Sperlagh, B., Csolle, C., Ando, R. D., Goloncser, F., Kittel, A., Baranyi, M., "The role of purinergic signaling in depressive disorders". *Neuropsychopharmacol Hung* **2012,** *14*, 231–238; Iwata, M., Ota, K.T., Duman, R.S., "The inflammasome: pathways linking psychological stress, depression, and systemic illnesses". *Brain Behav Immun*, **2013,** *31*,105–114.

[171] Virginio, C., Church, D., North, R. A., Surprenant A., "Effects of divalent cations, protons and calmidazolium at the rat P2X7 receptor". *Neuropharmacology*, **1997,** *36*, 1285–1294.

[172] Jiang, L.H., MacKenzie, A. B., North, R. A., Surprenant, A., "Brilliant Blue G selectively blocks ATP-gated rat P2X7 receptors". *Mol Pharmacol*, **2000**, *58*: 82–88.

[173] Nelson, D. W.; Gregg, R. J.; Kort, M. E.; Perez-Medrano, A., Voight, E. A.; Wang, Y.; Namovic, M. T.; Grayson, G.; Donnelly-Roberts, D. L.; Niforatos, W.; Honore, P.; Jarvis, M. F.; Faltynek,C. R.; Carroll, W. A. "Structure-activity relationship studies on a serie sof novel, substituted 1-benzyl-5-phenyltetrazole P2X7 antagonists.", *J. Med. Chem*. **2006**, *49*, 3659–3666.

[174] Letavic, M. A., Lord, M., Bischoff, F., Hawryluk, N. A., Pieters, S., Rech, J. C., Sales, Z., Velter, A. I., Ao, H., Bonaventure, P., Contreras, V., Jiang, X., Morton, K. L., Scott, B., Wang, Q., Wickenden, A. D., Carruthers, N. I., Bhattacharya, A.,"Synthesis and pharmacological characterization of two novel, Brain penetrating $P2X_7$ antagonists", *ACS Med. Chem. Lett*. **2013**, *4*, 419−422.

[175] Baxter, A., Bent, J., Bowers, K., Braddock, M., Brough, S., Fagura, M., Lawson, M., McInally, T., Mortimore, M., Robertson, M., Weaver, R., Webborn, P. Hit-to-lead studies: "The discovery of potent adamantane amide P2X7 receptor antagonists". *Bioorg. Med. Chem. Lett*., **2003**, 4047−4050; Furber, M.; Alcaraz, L., Bent, J. E., Beyerbach, A., Bowers, K., Braddock, M., Caffrey, M. V., Cladingboel, D., Collington, J., Donald,D. K., Fagura, M., Ince, F., Kinchin, E. C., Laurent, C., Lawson, M., Luker, T. J., Mortimore, M. M. P., Pimm, A. D., Riley, R. J., Roberts, N., Robertson, M., Theaker, J., Thorne, P. V., Weaver, R., Webborn, P., Willis, P. "Discovery of potent and selective adamantane-based small-molecule $P2X_7$ receptor antagonists/interleukin-1β inhibitors*." J.Med. Chem*., **2007**, *50*, 5882−5885.

[176] Abberley, L., Bebius, A., Beswick, P. J., Billinton, A., Collis, K. L., Dean, D., Fonfria, E., Gleave, R. J., Medhurst, S. J., Michel, A. D., Moses, A. P., Patel, S., Roman, S. A.,Scoccitti, T., Smith, B., Steadman, J. G. A., Walter, D. S., "Identification of 2-oxo-N-(phenylmethyl)-4-imidazolidinecarboxamide antagonists of the P2X7 receptor", Bioorg. *Med. Chem. Lett*., **2010,** *20,* 6370–6374.

[177] Dean, D.K., Munoz-Muriedas, J., Sime, M., Steadman, J. G.A., Thewlis, R. E. A., Trani, G., Walter, D. S., "5,6,7,8 Tetrahydro[1,2,4]triazolo[4,3-a]pyrazinederivatives as $P2X_7$ modulator, WO 2010/125102 A1.

[178] *Eur. J. Org. Chem*., **2012**, *30*, 6070.